THE UNIVERSITY
of EDINBURGH

Combined wave-current scale model testing at FloWave

Donald Ross Noble

A thesis submitted in partial fulfilment of the requirements for the award of an Engineering Doctorate

The University of Edinburgh

August 2017

IDCORE

This thesis is submitted in partial fulfilment of the requirements for the award of an Engineering Doctorate, jointly awarded by the University of Edinburgh, the University of Exeter, and the University of Strathclyde.

The work presented has been conducted under the industrial supervision of FloWave TT Ltd. as a project within the Industrial Doctoral Centre for Offshore Renewable Energy (IDCORE).

THE UNIVERSITY *of* EDINBURGH

To my parents Ross & Jean, and sister Jenny
*for putting up with me always asking **why?***

Abstract

As part of a global drive to produce renewable electricity, devices are being designed to harness energy from the waves and tidal currents. Physical scale model testing is an important part of the development process for this and other technologies. The *FloWave Ocean Energy Research Facility* at The University of Edinburgh is designed to conduct these tests. Here it is possible to produce multi-directional waves combined with currents in the circular tank, re-creating the complexity of the ocean.

The research was driven by commercial requirements of the facility, aiming to highlight what can be learnt from testing at scale with complex conditions in a controlled environment. To enable this, it was first necessary to extend the characterisation of this new facility. Wave generation and reflections were assessed in a previous project. In this work, flow measurements taken throughout the test volume of the tank, allowed spatial and temporal variations in the currents to be determined. Waves and currents interact in a complex manner, compounded by the method of reproducing them in a tank. The influence of currents on waves in the basin was assessed. This included cases with an oblique angle between them, on which little has been published.

The other part of the project addressed issues to be considered when testing in a combined wave-current basin such as FloWave.

- At many sites of interest for offshore renewable energy, waves are influenced by water depth. Implications of not scaling depth consistently were considered, and design diagrams produced to facilitate understanding and quantification of potential errors.
- At FloWave, waves are generated in still water around the outside of the tank. A process was therefore developed and verified to produce the desired combined conditions in the central test area following their interaction with the current.
- There is a wealth of published guidance on tank testing, for ships, offshore structures, and more recently renewable energy. This has been reviewed and suggestions offered to augment this by including testing in the more advanced conditions possible in a facility like FloWave.
- Tools and guidance have been developed to highlight many of the issues to be considered by clients prior to testing at FloWave. This aims to facilitate planning of a test programme by highlighting potential knowledge gaps and recording decisions made. Flowcharts have been produced to represent this graphically, with a corresponding checklist of questions for clients, which have been trialled in a pilot study.

Outputs from this research are being used to help deliver both academic and commercial client tests at FloWave. The test area in currents was shown to be $>50\,\mathrm{m}^2$ with <10% variation in flow, and the combined wave-current conditions possible have been explored. Results that are important when designing client test plans.

Lay summary

Humans are trying to harness energy from the seas to provide a clean and renewable source of electricity. This energy can be from the flow of the tides or movement of waves. To help with designing these, as well as using computers, small models are often tested in tanks to test new features. This is similar to testing new aeroplane models in a wind tunnel.

This research was carried out at The University of Edinburgh's *FloWave Ocean Energy Research Facility*. Here, a small-scale version of the ocean can be produced in a large circular tank, like a swimming pool. This tank is fitted with paddles that can generate small waves. It also has pumps that can make the water flow like a tidal current in the sea. It is possible to make waves and currents at the same time, at any direction across the tank.

This project was to look at how to test models in the advanced waves and currents possible in the FloWave tank. It also looked at what clients can learn from testing models in waves and currents at the same time.

As a new tank, it is important to check how well the tank works. A previous project checked how well the tank makes waves. This project measured flow across the tank, how the flow varied between different places in the tank, plus changes in flow over time. The research also looked at how the shape of waves are changed by the flow of water. This included cases where there is an angle between the direction the waves and current are travelling in, which has not been studied much before. A way to make the right waves in the middle of the tank, at the same time as a current, was developed and tested. This is useful because the real sea has tidal currents as well as waves, so testing this is important.

The other part of the project looked at some of the problems people testing models in tanks like FloWave need to think about. Many of these have already been thought about before, and are written down in guidance documents. FloWave is different to most other tanks. It is circular and can make very realistic sea conditions. New guidance to cover this is therefore needed and was suggested. A list of questions was also put together, to highlight all the things clients need to think about before testing. This included what is in existing guidance, plus some extra questions about FloWave. These also explain what can be tested in the FloWave tank, and how much time this might take.

Results from this research project show the tank works properly. They show some of what is possible with waves and currents at the same time in the tank. They are also used to help with planning and running tests in the tank for clients.

Acknowledgements

I'd firstly like to acknowledge my supervisors Dr Thomas Davey (FloWave), Prof Tom Bruce (Edinburgh), Dr Helen Smith (Exeter), and Prof Panagiotis Kaklis (Strathclyde) for their input to the project. I'm particularly grateful to Tom & Tom for their guidance and direction throughout the project, without which this research would not have been possible.

Thanks to everyone at FloWave, for making me feel part of the team and assisting with my project. In particular, Jeff Steynor for his crazy antics and helpful insights, Claire Chaperon for her help in translating French reports, and Sam Draycott both for his input on our joint work but also constantly discussing ideas and helping with minor problems.

I also acknowledge the input to my research from discussions with FloWave staff and clients both academic and commercial. Particularly Duncan Sutherland for his contribution to the turbulence measurements, and trying to help me understand that complex subject. Also, Rodrigo Martinez, Penny Jeffcoate, and Anup Nambiar for their time and inputs trialling the test planning tools and guidance.

Through their thorough examination of my thesis and discussions during the viva, my examiners Dr Adam Robinson (Edinburgh), Prof. Guillaume Carpentier (ESTIC-Caen), and Prof. Bas Hofland (Deltares/TU Delft) all improved the quality of my work.

The IDCORE programme has been a great opportunity, during which I have learnt a great deal, developed new skills, and made many friends.

Lastly, I'd like to thank my family and friends for their support, plus everyone in IDCORE and IES who have made the last four years in Edinburgh so enjoyable.

Funding from the following sources is gratefully acknowledged.

- *The Energy Technologies Institute and RCUK Energy programme for funding this research as part of the IDCORE programme (EP/J500847/1).*
- *Nortek UK for supporting the turbulence measurements along with the EPSRC for funding that work under the Impact Accelerator Account.*
- *Funding for FloWave facility was received from the UK Engineering and Physical Sciences Research Council under grant EP/I02932X/1 and from Scottish Enterprise.*

Declaration

I declare that this thesis was composed by myself, that the work contained herein is my own except where explicitly stated otherwise in the text, and that this work has not been submitted for any other degree or professional qualification except as specified.

The following sections were collaborative work, with major contributions noted in the text at the beginning of the section.

- *Section 5.4 Initial characterisation of turbulence, with Dr Duncan Sutherland, then a PhD student at The University of Edinburgh.*
- *Sections 4.2.4 and 6.5 Observation and correction of waves with current,*
- *Section 7.2 Discrepancy in scaled water depth, and*
- *Section 7.4 Recommendations for testing with advanced environmental conditions, all with Dr Sam Draycott, then an IDCORE researcher at FloWave.*

Donald Ross Noble

Contents

Figures

Tables

Nomenclature

Roman letters

A	Wave amplitude [m]
c, C_g	Wave celerity, group celerity [m/s]
C_P, C_T	Coefficients of power and thrust [–]
D	Diameter (or other distance) [m]
E	Energy [J]
E_A	Wave energy per unit horizontal area [J/m^2]
E	Modulus of Elasticity [–]
$f,\ f_p$	Frequency (peak) [Hz]
F	Force [N]
Fr	Froude scale ratio [–] $\left(Fr = U/\sqrt{gD}\right)$
g	Acceleration due to gravity [9.81 m/s^2]
h	Water depth [m]
$H, H_{\max}$	Wave height (maximum) [m]
$H_s, H_{1/3}$	Significant wave height [m] from time domain analysis, average of highest 1/3 of all wave heights
H_{m0}	Significant wave height [m] from spectral moments $H_{m0} = 4\sqrt{m0}$ (frequency domain analysis)
k	Wavenumber ($k = 2\pi/L$) [1/m]
ℓ	Integral lengthscale (of turbulent flow) [m]
L	Wavelength* [m]
m_n	n-th spectral moment [m^{2}Hz^n] $\left(m_n = \int_0^\infty S(f) f^n df\right)$
N	Number of items [–]
p	Pressure [Pa, N/m^2]
P	Power (per unit length) [kW, kW/m]
$r(\Delta t)$	temporal autocorrelation [–]
r	Coefficient of correlation [–]
r^2	Coefficient of determination [–]
R	Radius [m]
Re	Reynolds scale ratio [–] ($Re = DL/\nu$)
s	Wave spreading parameter [–]
S	Wave steepness ($S = H/L$) [–]
$S(f)$	Wave (frequency) spectrum [m^{2}s]
$S(f, \theta)$	Directional wave spectrum [m^{2}s/rad]
$S(k)$	Wavenumber spectrum [m^{2}s]
t	time [s]
T	Period [s]
$\bar{T}, T_E, T_p, T_z$	Mean, energy, peak & zero-crossing wave periods [s]
T_{stat}	Stationarity period (of turbulent flow) [s]
$\mathcal{T}$	Integral timescale (of turbulent flow) [s]
TSR	Tip speed ratio (TSR= $\omega R/U$) [–]
u, v, w	Velocities in streamwise, transverse, & vertical directions [m/s]
U, U_0	Velocity (reference) [m/s]
$\mathcal{U}$	Non-dimensional velocity (wave-current) ($\mathcal{U} = U/\omega h$) [–]
x, y, z	Spatial dimensions [m]
X, Y, Z	Tank coordinates [m]

*. Wavelength is often given the Greek letter λ but this is also used to denote scale factor, thus L is used for wavelength in this document, and D for distances

Greek letters

γ	JONSWAP spectral shape parameter [–]
$\delta f, \Delta F$	Frequency increment [Hz]
Δt	Temporal lag [s]
ε	Error or discrepancy
η	Water surface elevation [m]
θ	Angle (relative to tank) [rad, °]
θ_{rel}	Angle between wave and current propagation directions [rad, °]
κ	Non-dimensional wavenumber ($\kappa = kh$) [–]
λ	Scale factor [–]
ν	Kinematic viscosity [m^2/s]
ρ	Density [kg/m^3]
σ, σ^2	Standard deviation, variance
σ_θ	Wave spreading parameter
τ	Non-dimensional period [–] $\left(\tau = T\sqrt{g/h}\right)$
ω	Rotational (or angular) frequency (relative to fixed bottom) [rad/s]
ω_r	Wave frequency relative to water (intrinsic wave frequency) [rad/s]
Ω	Non-dimensional rotational frequency ($\Omega = \omega_r/\omega$) [–]
ξ, ζ	Horizontal and vertical size of wave orbital [m]

Subscripts

$0, 1$	Regions of still water and current
B	Blocking point for waves
c, w	Relating to currents and waves
f, θ	Relating to frequency and angle
g	Wave gauge in array
i	i-th component
m, p	Relating to model and (full scale) prototype
p	Relating to the spectral peak
r	Relative to a reference frame moving with the current

Acronyms and abbreviations

ASCII	American Standard Code for Information Interchange
ADCP	Acoustic Doppler Current Profiler
ADV	Acoustic Doppler Velocimeter (Velocimetry)
CFD	Computer Fluid Dynamics
DAQ	Data Acquisition
DOF	Degree(s) of Freedom
DSF	Directional Spreading Function
EDL	Edinburgh Designs Ltd.
EM	Electro-Magnetic

EMEC European Marine Energy Centre

EPSRC Engineering and Physical Sciences Research Council

EquiMar Equitable Assessment of Marine Energy Converters (project)

ETI Energy Technologies Institute

EU European Union

EWTEC European Wave and Tidal Energy Conference

FFT Fast Fourier Transform

FOWT Floating Offshore Wind Turbine

FloWTurb Response of Tidal Energy Converters to Combined Tidal Flow, Waves, and Turbulence (project)

HSE Health and Safety Executive (UK Government Dept.)

IEA International Energy Agency

IDCORE Industrial Doctoral Centre for Offshore Renewable Energy

IEC International Electrotechnical Commission

IP Ingress Protection (rating)

IFREMER Institut Français de Recherche pour l'Exploitation de la Mer

InSTREAM In situ Turbulence Replication Evaluation And Measurement (project)

ITTC International Towing Tank Conference

JONSWAP JOint North-Sea WAve Project (spectrum)

LDV Laser Doppler Velocimetry

LOLER Lifting Operations and Lifting Equipment Regulations 1998 (UK legislation)

MARINET Marine Renewables Infrastructure Network for emerging Energy Technologies (project)

MATLAB Matrix Laboratory software by MathWorks

MRE Marine Renewable Energy

MWL Mean Water Level

NI National Instruments

OES IA Implementing Agreement for a co-operative programme on Ocean Energy Systems, framework created by the International Energy Agency

OMAE International Conference on Ocean, Offshore and Arctic Engineering

ORE Offshore Renewable Energy

PIV Particle Image Velocimetry

PM Pierson–Moskowitz (spectrum)

PSD Power Spectral Density

PTO Power Take-Off

PTPD Phase-Time-Path-Difference

R&D Research and Development

RAO Response Amplitude Operator

ReDAPT Reliable Data Acquisition Platform for Tidal (project)

RMS	Root Mean Square
rpm	Revolutions per Minute
SBD	Single Beam Doppler
SDD	Scale Depth Discrepancy
SNR	Signal to Noise Ratio
SPAIR	Single-summation PTPD Approach with In-line Reflection
TI	Turbulence Intensity
TiME	Turbulence in Marine Environements (project)
TRL	Technology Readiness Level
TST	Tidal Stream Turbine
VIV	Vortex Induced Vibration
WEC	Wave Energy Convertor
WES	Wave Energy Scotland (Government body)

Definition of key terms

Regular waves all have the same frequency (monochromatic), whereas an **irregular wave spectrum** is composed of multiple different frequencies (panchromatic).

Long crested waves can be either regular or irregular, but all propagate in one direction (uni-directional), whereas a **short crested spectrum** has a directional spread with waves travelling in multiple directions (multi-directional).

Multi-modal sea states have two or more energy peaks, often corresponding to waves resulting from different weather conditions.

Verical profile of velocity refers to the changing flow speed with depth, also referred to as a 'shear' or 'flow' profile.

Following currents refer to waves propagating in the same direction as the current, whereas **opposing** (or adverse) refers to waves at 180° to the current.

Collinear interactions refer to waves with a following or opposing current. For **non-collinear** cases there is an angle ($0° < \theta_{rel} < 180°$) between waves and current.

The six degrees of freedom (6DOF) for a floating body are translations in x, y, z namely: Surge, Sway, & Heave, and rotations about the x, y, z axes: Pitch, Roll, & Yaw.

FloWave specific terminology is covered in section 4.2.2.

Chapter 1
Introduction

1.1 FloWave Ocean Energy Research Facility

The University of Edinburgh's *FloWave Ocean Energy Research Facility*, or just 'FloWave', is designed to simulate the ocean environment with a high degree of complexity. Combinations of multi-directional waves together with a current from any angle can be re-created in the 25 m diameter circular tank, fig. 1.1.

The facility is mainly used for testing small-scale models, both of devices designed to generate electricity from the waves and tidal currents in the seas, plus other vessels and structures in the marine environment. It is also used for more fundamental academic research into waves, currents, and the combination of these. Commissioned in early 2014, the facility has since been used for a wide range of projects, both academic and commercial.

FloWave was designed to offer an intermediate step between small-scale tank testing at around 1:100 to 1:50 and open water deployment of close to full scale devices, and is therefore optimised for testing at scales of between 1:40 and 1:10 (Davey et al., 2013). Details of how the facility operates are given in section 4.2, including tank co-ordinates and terminology, plus how waves and currents are generated and measured.

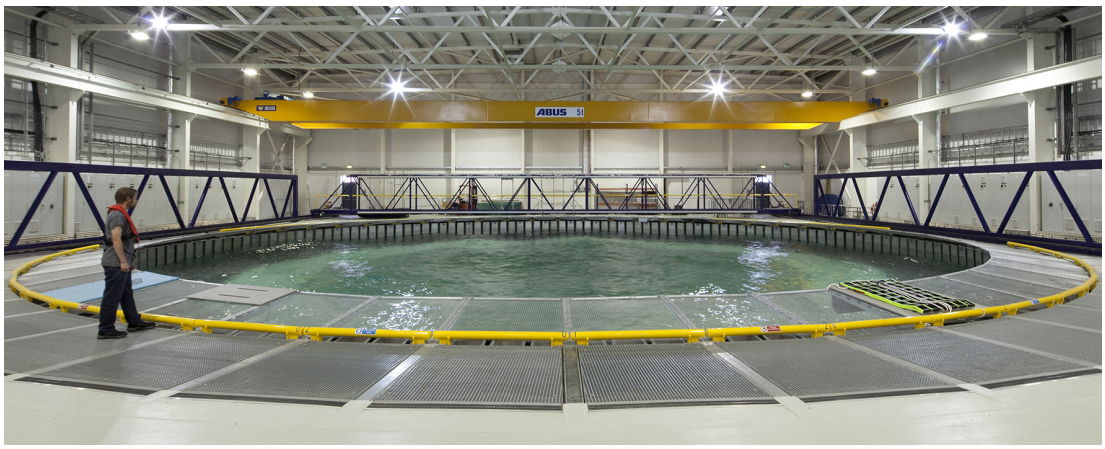

Figure 1.1: Photograph of FloWave tank, generating a realistic sea-state. (Photo: Bennetts Architects).

The measurements and experiments described in this thesis were all carried out in the FloWave facility between June 2014 and August 2017, as part of an Industrial Doctoral Centre for Offshore Renewable Energy (IDCORE) research project.

1.2 Motivation

Energy and electricity demands are increasing as the world develops. The International Energy Agency (IEA) report 3.4% annual increase in global electricity demand over the past 40 years (IEA, 2016*a*). This is projected to continue, mostly due to global economic growth, but also in part due to the uptake of electric vehicles. Global climate targets such as the Paris Agreement will drive the development of renewable electricity generation, to meet the legally binding emission reduction targets introduced under the United Nations Framework Convention on Climate Change (UNFCCC). The IEA project that 60% of new electricity generation capacity will be renewable by 2040, with almost half from wind and solar photo-voltaic (IEA, 2016*b*). Developers are also investigating ways to extract renewable energy from the oceans, a very large and almost untapped, but technically challenging resource.

Scale model testing is an important part of the technological development process in many fields of engineering. It allows investigation into physical phenomena in a controlled, repeatable, and relatively low-cost environment. Tests on small-scale physical models are often used in conjunction with numerical models to validate assumptions. This is explored in more detail in chapters 2 and 3.

Prior to conducting experiments, it is important to understand the behaviour of the facility and the scaled conditions generated. These are the input to the tests conducted, and will have a strong influence on results. For a new facility such as FloWave, it is therefore important to characterise performance in order to understand the results obtained from testing in the tank. Wave generation and absorption capability of the FloWave facility was characterised as part of an earlier IDCORE project (Draycott, 2017). This research project therefore extends this to include flow generation characterisation, and explores the combined wave-current conditions produced in the facility.

Waves and currents interact in a complex non-linear manner. Device motion, foundation and mooring loads, plus power capture performance for Offshore Renewable Energy (ORE) devices could all be affected. To understand this, tests should be undertaken in representative conditions. The only way to accurately reproduce ocean wave properties affected by tidal currents in a test tank is to re-create both the waves and the current simultaneously. A method to produce the desired combined conditions in the tank is therefore required.

1.3 Project aims and objectives

The overall aim of this research is answering the question of *'how to conduct tests for clients in the multi-directional combined wave-current conditions at FloWave?'* This can be split into the two main sections of the research project, with the aims:

1. Extend the characterisation and understanding of the recently constructed FloWave facility, beyond wave generation and absorption.
    a. Firstly, to characterise the generation of currents, focussing on spatial variability but also considering temporal variations including turbulence.
    b. Secondly, investigate the wave-current interactions possible in the facility, including non-collinear cases with waves at oblique angles to the current.
2. Consider guidance, methods, and processes for testing offshore renewable energy devices in a facility such as FloWave, with a combination of multi-directional waves and currents.

To achieve these broad aims, the following objectives are established:

1.a. Assess spatial and temporal variability of currents produced in the tank:
    i. Measure temporal variations, and address repeatability of currents.
    ii. Measure spatial variation in mean flow, across the X, Y, Z dimensions of the test volume, at different input velocities and directions.
    iii. Measure turbulence within the flow, including how this varies spatially through the test volume.
    iv. Disseminate results of the flow measurements to inform the design of other experiments being undertaken at FloWave.
    v. Consider any implications of the spatial variability of currents for testing at FloWave.

1.b. Investigate the range of combined wave-current conditions possible at the facility. This will focus on the impact currents have on waves, for both collinear and non-collinear cases with regular and irregular waves.
    i. Review existing theories for wave-current interactions, and reported experimental studies in combined conditions.
    ii. Assess the generation of combined wave-current conditions at FloWave.
    iii. Measure changes to waves resulting from their interaction with currents (including non-collinear cases) in the FloWave facility.
    iv. Investigate methods to produce the desired waves in the tank after interacting with a current, both for regular waves to characterise the effect and site-specific multi-directional waves to reproduce the full complexity of the ocean.

2. Deliver tools and guidelines for testing in the combined multi-directional wave-current environment at FloWave
   i. Critically review available published guidance for (tank) testing of offshore renewable energy devices, and similar disciplines.
   ii. Define how this applies to testing at FloWave and what limitations exist.
   iii. Recommend extensions to guidance, based on lessons learnt and practices used at FloWave, to make use of the capabilities of the facility.
   iv. Develop and test a process to facilitate client test planning at FloWave.
   v. Deliver metrics to quantify the quality of environmental conditions produced in the tank.

1.4 Thesis outline

The remainder of this thesis is split into a further nine chapters, in four overarching parts. These parts cover (I) background and literature, then (II) tank characterisation and (III) client testing at FloWave — corresponding to the two main aims in section 1.3, followed by a final part (IV) with discussion and conclusions.

Part I: Background and literature

Chapter 2 introduces some of the wide **technical background** on waves, currents, and their interaction. Consideration is also given to the key issues of physical model testing and scaling. This chapter covers well established theories and practice. These are restated here to provide suitable background and context for those less familiar with these subjects.

Chapter 3 reviews recent literature on background challenges plus the three main themes of this thesis. Firstly test facility characterisation at other flow tanks and characterisation of the wave generation and absorption at FloWave. Secondly, on combined waves and currents covering interaction theory, experimental studies, and testing of marine renewable devices. Finally, published guidance for scale model testing for offshore renewable energy is reviewed, with a focus on the advanced environmental conditions that can be produced in facilities such as FloWave.

Part II: Characterising FloWave — currents and wave-current interactions

Chapter 4 The FloWave tank and characterisation methods gives details of how the FloWave facility operates, including co-ordinates and terminology. Procedures and practicalities for running experiments are discussed, along with instrumentation and set-up, plus methods used for data acquisition and analysis of results.

Chapter 5 Flow characterisation describes the experimental measurements conducted to understand the spatial and temporal variability of flow across the FloWave basin. Variation of mean flow throughout the main test volume is assessed, and documented to facilitate testing in the facility. Turbulence within the flow, including spatial variation, is characterised using metrics similar to field measurements. Implications for testing are also considered.

Chapter 6 covers the work on **combined waves and currents at FloWave**, with observation of both regular and irregular wave conditions combined with currents at a range of angles, for both collinear and non-collinear cases. To understand how the tank can be used for testing, the generation of combined wave-current conditions in the facility is also addressed. A method is then developed and tested, for producing the desired wave height in the tank when combined with currents, accounting for the change resulting from the interaction.

Part III: Client testing at FloWave

Chapter 7 Specific technical issues for testing in a combined wave-current environment deals with three particular considerations relating to testing with combined waves and currents, focussing on the FloWave facility. Firstly, consideration is given to the issue of scaled water depth, and the potential errors that may occur if this is not correct. Secondly, an assessment is made of the reproduction quality of conditions in the tank (currents and combined wave-current) using metrics to quantify this subjective process. Finally, recommendations on testing in advanced environmental conditions are offered, to supplement existing guidance.

Chapter 8 details the **guidance and planning tools** developed. Designed to flag issues that should be considered prior to testing, in order to facilitate client tests at FloWave. They provide reasons to test in more advanced conditions (such as non-collinear wave-current) to maximise understanding from the test programme and make the best use of the capabilities of FloWave. The checklist produced also assists with documenting test planning, so that all involved are aware of the drivers and reasoning behind decisions made. Going through this process can highlight gaps in knowledge between the client and tank staff. A description of the tools and guidance is provided, together with development and implementation thereof.

Part IV: Appraisal and closing

Chapter 9 Discussion on characterising currents and wave-current interactions at the new FloWave facility, plus what can be learnt from testing in these conditions.

Chapter 10 Summarises the main **Conclusions** and research contributions.

PART **I**

Background and literature

Chapter 2
Technical background

Chapter summary

- There is a long history of engineering and academic study of the oceans and of physical model scaling. This chapter therefore summaries key areas of established fact, that are useful to understand prior to further research into physical model testing in a combined wave-current environment, focusing on the emerging offshore renewable energy sector.
  - An overview is provided of waves and currents, then their interaction is considered.
  - A brief background is given on physical model testing, scaling, and facilities for undertaking these studies.

2.1 Waves and currents

The real sea is a complex, chaotic, and non-linear system. The free surface boundary is exposed to the atmosphere, and water is driven across the surface by wind, in the form of waves. Interplanetary gravitational forces drive the movement of water around the planet, visible in the familiar rise and fall of the tides. Below the surface, the sea-bed is undulating on many scales, adding complexity and turbulence to the currents.

While real sea waves are inherently complex, useful predictions can be made from simplifications. The most basic of these is small amplitude wave theory (also known as linear, or Airy, wave theory), summarised in section 2.1.2. More complex, non-linear, wave motions can be described using Stokes or Cnoidal wave theories amongst others. Building on regular wave theory, random waves can be modelled as a summation of many individual waves with varying phase, amplitude, and period, as discussed in section 2.1.3.

2.1.1 Wave properties

Waves vary in both space and time, denoted x and t. Figure 2.1 shows key parameters, defined below. The coordinate system has the origin at Mean Water Level (MWL), with z positive upwards, x positive in the direction of wave propagation, and water depth h.

Celerity c the speed at which an individual wave propagates.

Zero-crossing is a point where the (instantaneous) water surface η crosses MWL.

Wavelength L taken as the horizontal distance between successive peaks, troughs, or zero-crossing points.

Wavenumber k defined as $k = 2\pi/L$, the (angular) wavenumber refers to the spatial frequency and is often used in calculations.

Wave height H usually defined as the difference in water surface elevation between a crest and the preceding trough, which can be determined in the time domain from a zero-down-crossing analysis, as recommended by The IAHR Working Group on Wave Generation and Analysis (1989). For regular linear sinusoidal waves $H = 2A$, where A is wave amplitude. In real sea waves, the wave crest height is usually greater than trough depth, relative to MWL.

Significant wave height H_s, H_{m0} is a common measure used to describe the size of irregular (random) waves. Defined from time- or frequency-domain analysis.

Steepness defined as H/L which it should be noted is not the water surface slope. Note that steepness is sometimes defined as kA, which differs by a factor of π.

Breaking occurs in water waves when the steepness exceeds a critical value, of around 14%. Various formulae have been developed to calculate the breaking point, of which Miche (1944, 1951) is commonly used. This is reproduced as eq. (2.1), where H_B and L_B are the wave height and length at the breaking point respectively, and h the water depth.

$$H_B = 0.142 L_B \tanh \frac{2\pi h}{L_B} \tag{2.1}$$

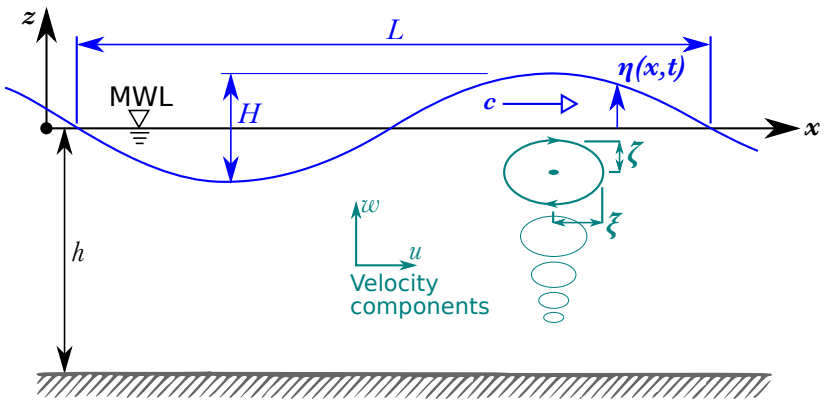

Figure 2.1: Definition sketch of a wave, with water surface shown in blue, and indicative wave orbitals in teal. (Adapted from Dean and Dalrymple, 1991).

Wave orbital motion Particles in the water below a wave move in elliptical orbits, as shown in fig. 2.1, with horizontal and vertical displacements and velocities ξ, ζ and u, w respectively. The size of these orbital motions decays exponentially with depth below MWL, as discussed below.

2.1.2 Small amplitude wave theory

Small amplitude wave theory uses sinusoidal waves that vary in space and time. The theory strictly only applies to non-breaking waves, and where the amplitude is small compared to both the wavelength and water depth; but this theory offers good approximation for many situations. It is also necessary to first understand this before considering more complex theories (Andersen et al., 2014).

There are many texts that describe the formulation and application of small amplitude wave theory including Chakrabarti (2005); Dean and Dalrymple (1991); Holthuijsen (2007); Wright et al. (1999).

Small amplitude wave theory states that the water surface elevation η of a regular wave varying in one dimension of space plus time (x and t) can be described by eq. (2.2),

$$\eta(x,t) = A\sin(kx - \omega t) \tag{2.2}$$

where A, k, and ω are the amplitude, wavenumber and angular frequency respectively. The wavenumber and angular frequency can be expressed in terms of the wavelength L and period T as eq. (2.3),

$$k = \frac{2\pi}{L}; \quad \omega = \frac{2\pi}{T} \tag{2.3}$$

The speed, or celerity, defined as the time for a wave passing to fixed point in space, is given by eq. (2.4),

$$c = \frac{L}{T} = \frac{\omega}{k} \tag{2.4}$$

The *dispersion relationship* links frequency and wavenumber, as a function of water depth h and gravitational acceleration g. This can be derived from a velocity potential function φ and appropriate boundary conditions, as given in Dean and Dalrymple (1991). It can be expressed in various forms, based on the relationships defined in eqs. (2.3) and (2.4), as eq. (2.5),

$$\omega^2 = gk\tanh(kh), \quad \text{or} \quad L = \frac{gT^2}{2\pi}\tanh\left(\frac{2\pi h}{L}\right), \quad \text{or} \quad c = \sqrt{\frac{gL}{2\pi}\tanh\left(\frac{2\pi h}{L}\right)} \tag{2.5}$$

There is a unique wavenumber for any particular combination of wave frequency and water depth. Therefore knowing one of k, ω, L, T it is possible to determine the other

three quantities, provided the (relative) depth is also known, see Wave orbital velocity and influence of water depth below.

Wave groups

As shown above, the speed of a wave is a function of wavelength divided by period. Longer period waves travel faster than those of shorter period for a given water depth. Thus waves of different frequencies tend to separate, or disperse, hence the name 'dispersion relationship'.

The speed at which a group of waves travels is known as 'group velocity' or 'group celerity' C_g, eq. (2.6),

$$C_g = \frac{1}{2}\sqrt{\frac{gL}{2\pi}\tanh\left(\frac{2\pi h}{L}\right)}\left[1 + \frac{4\pi h}{L\sinh\left(4\pi h/L\right)}\right] \tag{2.6}$$

Wave orbital velocity and influence of water depth

Particles in a water wave move in elliptical orbits. These are almost circular in relatively deep water. The diameter at the surface equates to wave height, but this decays exponentially with depth, becoming negligible below about half the wavelength (Wright et al., 1999). The particle velocity is proportional to diameter, as the period is fixed.

Using linear wave theory, the wave orbital motions ξ, ζ and velocities u, w can be calculated by eqs. (2.7) and (2.8) for the horizontal and vertical directions respectively. The final $(kx - \omega t)$ term in each equation is the periodic motion. Removing this gives solutions for the maximum displacements and velocities, which are proportional to wave height, within the limits of linear wave theory.

$$\xi = \frac{-H}{2}\frac{\cosh k(h+z)}{\sinh kh}\sin(kx - \omega t) \qquad u = \frac{\pi H}{T}\frac{\cosh k(h+z)}{\sinh kh}\cos(kx - \omega t) \tag{2.7}$$

$$\zeta = \frac{H}{2}\frac{\sinh k(h+z)}{\sinh kh}\cos(kx - \omega t) \qquad w = \frac{-\pi H}{T}\frac{\sinh k(h+z)}{\sinh kh}\sin(kx - \omega t) \tag{2.8}$$

As noted above, water depth is a factor in the dispersion relationship, therefore wavelength, celerity, and other parameters are affected by the water depth, but simplifications can sometimes be applied.

Water depth can broadly be split into three regions, noting that the hyperbolic tangent function is asymptotic at small and large numbers. For small values of x, $\tanh(x) \approx x$, and for large x, $\tanh(x) \approx 1$, corresponding to shallow and deep water respectively. Note that these terms are not absolute, and depend on the properties of the wave. The finite depth equations can thus be simplified when dealing with deep water or for shallow

water, as shown in table 2.1, although the full equation will give a similar, but more exact, result. It is also noted that many conditions of interest to Offshore Renewable Energy (ORE) developers are classified as intermediate depth, and thus these simplifications cannot be applied.

Table 2.1: Small amplitude wave theory equations with deep & shallow water simplifications.

Item	Finite depth	Deep water	Shallow water
Limiting criteria	—	$kh > \pi$, $h/L > 1/2$	$kh < \pi/10$, $h/L < 1/20$
Approximation	—	$\tanh(kh) \approx 1$	$\tanh(kh) \approx kh$
Wavelength	$L = \frac{gT^2}{2\pi} \tanh(kh)$	$L = \frac{gT^2}{2\pi}$	$L = T\sqrt{gh}$
Wave celerity	$c = \sqrt{\frac{gL}{2\pi} \tanh\left(\frac{2\pi h}{L}\right)}$	$c = \sqrt{\frac{gL}{2\pi}}$	$c = \sqrt{gh}$
Group celerity	$C_g = \frac{c}{2}\left(1 + \frac{2kh}{\sinh 2kh}\right)$	$C_g = \frac{c}{2}$	$C_g = c$

Assumptions of Small Amplitude Wave Theory

There are a number of assumptions implicit in small amplitude wave theory, which are set out in Wright et al. (1999) and others. Namely:

- The wave shape is sinusoidal, and is symmetrical about the mean water level.
- The wave height is very small in comparison with both wavelength and water depth.
- The effects of surface tension and viscosity of the water, plus the Coriolis force, are all negligible and can be ignored.
- The water is of uniform depth with no local changes in bathymetry, and the water is not constrained by obstructions such as land masses or structures in the sea.
- That three-dimensional waves (which vary in x, y, and z) behave in a similar way to the simplified two-dimensional waves (which only vary in x and z).

Despite these limitations, which are often not strictly applied, small amplitude wave theory offers good predictions of real waves in many situations. Other theories need to be applied in special circumstances, such as breaking waves, or waves in shallow water close to the coast, etc.

Small amplitude wave theory does not represent non-linearities present in real sea waves. Alternative theories have therefore been developed to better describe these mathematically. Two main theories to model the non-linear effects of steady waves, are Stokes and Cnoidal theories, which are appropriate for deep and shallow water respectively, as set out in Fenton (2013); Holthuijsen (2007) and others.

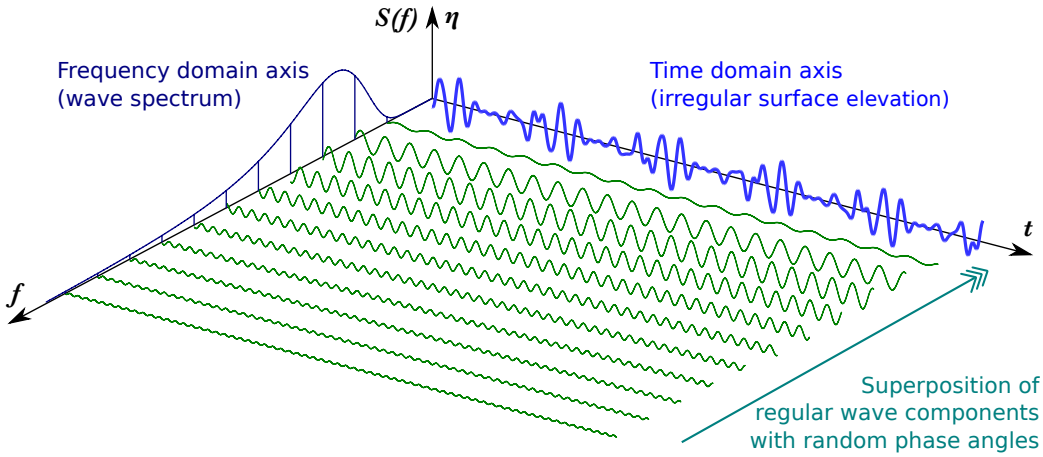

Figure 2.2: Graphical representation of an irregular wave (blue) comprised of many individual regular waves (green), with frequency spectrum shown on left (dark-blue). (Adapted from Holmes, 2015; Faltinsen, 1993).

2.1.3 Random wave spectra

Real sea states are made up of random waves, primarily driven by the wind (Fenton, 2013). This can be a combination of locally generated wind waves, and swell that has travelled hundreds of miles.

A random sea state can be represented numerically as the summation of a series of N regular waves, each with a different period, phase and amplitude, eq. (2.9). To facilitate analysis, these can be represented in the frequency domain as a spectrum $S(f)$. This is shown graphically in fig. 2.2. When specifying an irregular sea in this manner, a uniform distribution of phase angles should be used to prevent all component being in phase at the start. For realistic sea conditions, multiple wave directions should also be considered.

$$\eta(x,t) = \sum_{i=1}^{N} A_i \sin(kx_i - \omega_i t) \tag{2.9}$$

Spectral formulations

There are three commonly used formulations for wave spectra in ocean engineering, with increasing complexity and number of parameters (Holmes, 2009; Holthuijsen, 2007). There are also different formulations of these, depending on the parameters used to describe the waves. These can either be related to the wind-wave generation processes, or more usually for device testing, based on summary sea state parameters, e.g. H_{m0}, T_p.

1. **Pierson–Moskowitz** (one parameter: T_p) eq. (2.10), representing a fully-developed sea state, i.e. where the wind is in equilibrium with the waves.

2. **Bretschneider** (two parameters: H_{m0} and T_p) eq. (2.11), which can model spectra other than fully-developed.
3. **JONSWAP** (five parameters: T_p, α, γ, σ_a and σ_b) eq. (2.12), based on measurement from the JOint North-Sea WAve Project, therefore it is appropriate for describing fetch-limited seas. The parameter γ is a 'peak enhancement factor', typically taken as 3.3. With $\gamma = 1$ this equates to a PM spectra.

$$S(f)_{\text{PM}} = \frac{\alpha g^2}{(2\pi)^4} \frac{1}{f^5} \exp\left[\frac{-5}{4}\left(\frac{f_p}{f}\right)^4\right] \tag{2.10}$$

$$S(f)_{\text{B}} = \frac{5}{16} \frac{H_{m0}^2}{f} \left(\frac{f_p}{f}\right)^4 \exp\left[\frac{-5}{4}\left(\frac{f_p}{f}\right)^4\right] \tag{2.11}$$

$$S(f)_{\text{JONSWAP}} = \frac{\alpha g^2}{(2\pi)^4} \frac{1}{f^5} \exp\left[\frac{-5}{4}\left(\frac{f_p}{f}\right)^4\right] \left(\gamma^{\exp\left[\frac{-(f-f_p)^2}{2\sigma^2 f_p^2}\right]}\right),$$

$$\sigma = \begin{cases} 0.07, & f \leq f_p \\ 0.09, & f > f_p \end{cases}, \quad \alpha = 0.0081, \text{ or } \alpha = 0.076\widehat{F}^{-0.22} \tag{2.12}$$

Maximum and significant wave height

In a random wave spectrum, several terms are used to summarise the wave heights including the 'significant wave height' H_s or $H_{1/3}$, and the maximum wave height $H_{\max}$. For a recorded group of N waves, ordered by height, then $H_{1/3}$ is the mean height of the largest 1/3 waves, and $H_{\max}$ is the single largest wave height (Dean and Dalrymple, 1991). The distribution of wave heights can be represented by a Rayleigh distribution (Massel, 1996; Holthuijsen, 2007), therefore these parameters will vary both with the random set of waves, but also the number of waves N in the sample. Due to the skewness of the Rayleigh distribution, the ratio of $H_{\max}$ to H_s increases with record length, an example for this is given in The Rock Manual (CIRIA et al., 2007), reproduced as table 2.2.

The significant wave height can also be determined in the frequency domain from spectral moments using eq. (2.13) although this is not strictly equal to $H_{1/3}$.

$$H_{m0} = 4\sqrt{m0} \qquad \text{where} \qquad m_0 = \int_0^\infty S(f)df \tag{2.13}$$

Table 2.2: Mean values of wave height distribution in a sea state composed of N waves following a Rayleigh distribution of wave heights (from CIRIA et al., 2007)

Number of waves N	100	200	500	1000	2000	5000	10 000
$(H_{\max}/H_s)_{\text{mean}}$	1.61	1.72	1.84	1.94	2.02	2.13	2.21

2.1.4 Currents and turbulence

Water currents in coastal seas are primarily driven by tides and from rivers discharging into estuaries. There are also ocean currents driven by temperature and salinity gradients, but these are not so relevant to marine renewable energy devices*. The motion of waves also drives the net movement of water, especially in shallow water, in a process known as 'Stokes Drift'. In this case, the water particle motions are no longer closed loops, as assumed for linear wave theory.

Water flowing from rivers into the sea will not create large currents, but can change wave dynamics especially in high river flow events. Large rivers and estuaries are also being considered as a location for in-stream hydro-kinetic turbines, that will act in the same manner as those driven by tidal currents.

Tides

Tides are caused by the gravitational interaction between the bodies in the solar system, principally the Moon and the Sun. Rotation of the combined Earth-Moon system about the common centre of mass causes a tidal bulge to form on both sides of the planet, facing towards and away from the Moon, and similarly for the Sun. Rotation of the Earth about its axis beneath the tidal bulge causes high tide to move relative to the land masses (Wright et al., 1999).

The tide progresses as a depth limited wave, which is affected by the coastal bathymetry, altering the timing of the tides. Resonant amplification in estuaries can locally increase the tidal range, and constrictions such as channels and headlands can lead to faster tidal currents. These sites are attractive to renewable energy devices, as power is proportional to the cube of velocity.

The timing of tides is deterministic, based on planetary motion. Most European waters have semi-diurnal tides, with successive high tides approximately 12 hours 45 minutes apart. The tidal range varies over the course of a month, with two spring–neap cycles of larger and smaller tides over a 29.5 day period. Tides are not completely predictable, as weather systems can affect the tidal height in a non-deterministic way. For example, storm surges caused by low-pressure systems can increase MWL by half a metre or more.

---

*. Power generation from deep ocean circulation is being considered, however this is an early concept and not discussed further. Similarly, generation from tidal range using barriers or lagoons is not included in this study. It is unlikely that any of these technologies would be tested at FloWave, due to the design and constraints of the facility.

Turbulence

The flow of water through energetic tidal channels of interest for electricity generation is often highly turbulent. This has implications for predicting loading on blades and submerged structures.

The study of turbulence is a complex field, the subject of significant ongoing research, particularly in the field of ORE. Three recent key projects are In situ Turbulence Replication Evaluation And Measurement (InSTREAM), Reliable Data Acquisition Platform for Tidal (ReDAPT), and Turbulence in Marine Environements (TiME).

As part of the TiME project (Clark, 2015), a working definition of turbulence was established as:

> *A turbulent flow is both chaotic (highly unstable, sensitive to changes in initial conditions) and dissipative (governed ultimately by viscous effects).*

Clark (2015) also notes that most turbulent flows exhibit the property of 'coherence', and gives the definition from Robinson (1991).

> A coherent structure is defined as: "A three-dimensional region of the flow over which one fundamental flow variable exhibits significant correlation with itself or with another variable over a range of space and/or time that is significantly larger than the smallest scales of the flow"

Sources of turbulence within the flow were also considered by the TiME project. These were listed as the inflow conditions, bed roughness and channel shape, stratification in temperature and/or density, and finally wind shear applied to the surface (Clark, 2015).

2.1.5 Wave-current interactions

Currents change the physical form of waves, but the waves also have an impact on the current, as discussed by Peregrine (1976); Hedges (1987) and others. This is a complex and non-linear interaction, although simplifications such as small amplitude wave theory (section 2.1.2) can be used to give an approximate solution.

Although the wave period remains constant, waves become steeper when they encounter an opposing current; a combination of both the wave height increasing and wavelength decreasing. Wave breaking will occur as the steepness approaches a critical limit, and faster currents may prevent upstream wave propagation completely, i.e. wave blocking. With a following current the converse occurs and waves become less steep, therefore breaking is not an issue.

A summary of the basic equations for wave-current interactions is presented below, based on the work of Peregrine (1976); Peregrine and Jonsson (1983); Jonsson (1990), using notation consistent with this document. Details of reported experimental tests on

combined waves and currents, together with more recent theoretical developments, are given in section 3.3.

To assist with solving the problem, a number of assumptions and simplifications are made, including those for small amplitude wave theory, section 2.1.2. In addition, the current is assumed to be horizontally and vertically uniform. This allows a reference frame moving at the current velocity to be defined, simplifying the analysis, as only the wave motion need be considered in this frame.

The general case can be described by a Doppler shift, eq. (2.14).

$$\omega = \omega_r + \vec{u} \cdot \vec{k} \tag{2.14}$$

where ω is wave frequency in a fixed frame of reference, ω_r wave frequency in a reference frame moving with the current, $\vec{u}$ is current velocity vector, and $\vec{k}$ wave number vector (magnitude $k = 2\pi/L$ in the direction of wave propagation).

Wave properties can be calculated in this moving reference frame using the dispersion relation, eq. (2.5) and the relevant wave frequency ω_r, to give eq. (2.15)

$$\omega_r^2 = gk \tanh kh \,. \tag{2.15}$$

Combining eq. (2.15) with the Doppler relation, eq. (2.14), gives eq. (2.16)

$$\left(\omega - \vec{u} \cdot \vec{k}\right)^2 = gk \tanh kh \,. \tag{2.16}$$

then equating eqs. (2.15) and (2.16) gives eq. (2.17)

$$\omega - kU = \pm\omega_r = \pm\sqrt{gk \tanh kh} \,. \tag{2.17}$$

There can be up to four solutions to eq. (2.17), shown graphically in fig. 2.3. Solution E relates to still water, or no current in the direction of wave propagation, which is the standard solution to the dispersion relation. With a current, solutions B and D refer to waves propagating in the same direction (i.e. a following current), whilst A and C are for waves opposing the current. Solutions A and B are most of interest to coastal engineering, representing waves that have propagated from still water upstream or downstream respectively. The other two solutions, C and D represent short waves that would have to be generated on the current. With increasing current velocity, solutions A and C converge at F, which represents the blocking point, and corresponding blocking velocity U_B. There are no solutions for situations with faster currents for the specified frequency ω, indicating that these waves cannot physically exist.

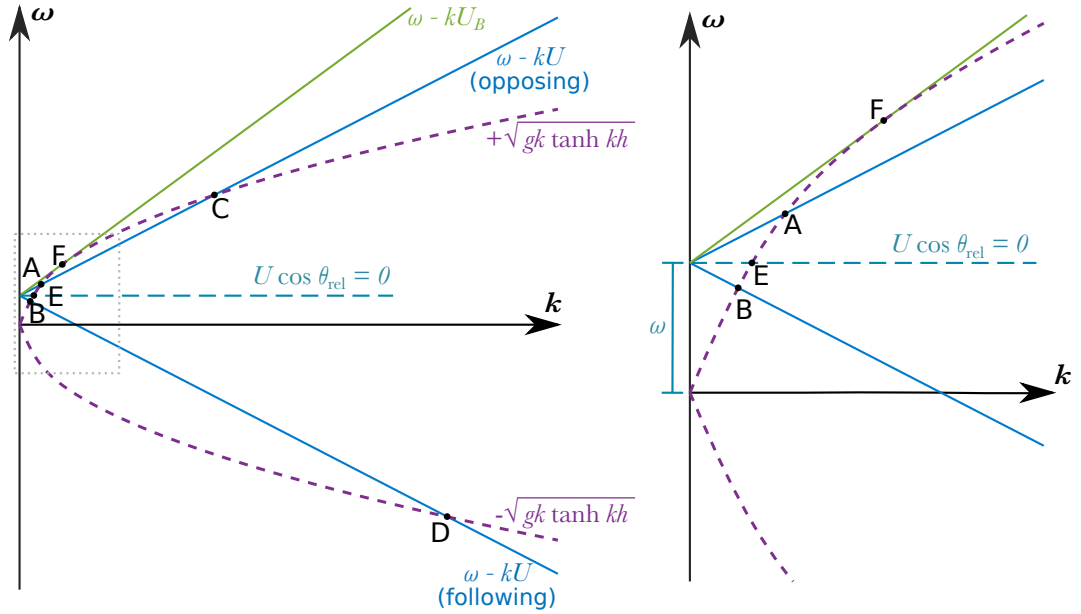

Figure 2.3: Graphical solutions to the dispersion relation with collinear waves of given frequency and various currents. Line slope represents the magnitude of current velocity. Plot on right shows detail of solutions ABEF (Adapted from Jonsson, 1990).

Hedges et al. (1993) note the first paper to correctly consider the interaction of waves and currents, including energy transfer between them, was Longuet-Higgins and Stewart (1961). This used the term 'radiation stress' to describe the mean excess momentum-flux due to the presence of waves. Subsequently, Bretherton and Garrett (1968) introduced the term 'wave action' for the quantity that is conserved during the interaction between waves and currents. Wave action is defined as wave energy divided by rotational frequency, E/ω_r. This term allows the mathematics of interaction between waves and currents to be simplified, allowing the energy exchange to be accounted for without explicit calculation (Hedges et al., 1985).

The modified wave height can be calculated as shown below, using conservation of wave action eq. (2.18), where C_{gr} is the group velocity relative to a moving reference frame.

$$\frac{\partial}{\partial x}\left(\frac{E(C_{gr}+U\cos\theta_{\text{rel}})}{\omega_r}\right)=0 \tag{2.18}$$

Change in wave height and wavelength caused by currents

Wave properties, particularly height and length, will change as a result of interaction with a current. Consider a wave propagating from a region of still water (denoted by subscript $_0$) to one with a current (subscript $_1$). The wavelength can be calculated from the dispersion relation, using the appropriate wavenumber for that region. Firstly, in still water,

$$\omega = \sqrt{g k_0 \tanh k_0 h}, \qquad L_0 = 2\pi/k_0 \tag{2.19}$$

and with a collinear current U,

$$\omega - k_1 U_1 = \sqrt{g k_1 \tanh k_1 h}, \qquad L_1 = 2\pi/k_1 \,. \tag{2.20}$$

Assuming the wave height in still water H_0 is known, wave height in the region with current H_1 can be calculated using eq. (2.21), as outlined by Smith (1997) and others.

$$H_1 = H_0 \sqrt{\left(\frac{C_{g0}}{C_{gr1} + U}\right)\left(\frac{1}{1 + U/C_{gr1}}\right)} \tag{2.21}$$

$$\text{where} \quad \omega_r = \sqrt{g k_1 \tanh k_1 h} \tag{2.22}$$

$$\text{and} \quad C_{gr1} = \frac{1}{2}\frac{\omega_r}{k_1}\left(1 + \frac{2k_1 h}{\sinh 2k_1 h}\right) \tag{2.23}$$

In the above equations, C_g refers to the wave group velocity, and the subscript r denotes quantities relative to a reference frame moving at the same velocity as the current. For a wave spectrum, the modification in amplitude for each wave component can be considered in a similar way, as demonstrated in section 6.5. This formulation is correct only to first order, based on linear wave theory for uniform collinear currents.

As a first estimate where waves are propagating at an oblique angle to the current, the interaction might be expected to vary in proportion to the current speed in the direction of wave propagation eq. (2.24), where θ_{rel} is the angle between the two,

$$H \propto U \cos \theta_{\text{rel}} \tag{2.24}$$

More accurately however, there is also refraction of wave direction by the current, see fig. 2.4, and the current field is also affected by the waves (Zaman and Baddour, 2011). These more advanced theories are reviewed in section 3.3.

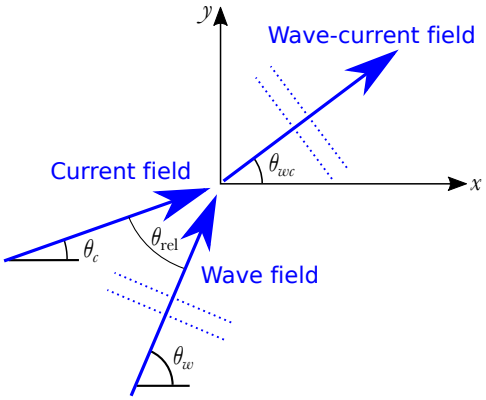

Figure 2.4: Definition sketch showing relative non-collinear directions of wave-free current, current-free wave, and combined wave-current fields (Adapted from Zaman and Baddour, 2011).

Change in currents resulting from waves

The interaction between waves and currents also affects the vertical structure of the flow field. Although not the focus of this research, it is an important consideration, particularly when testing Tidal Stream Turbine (TST) or looking at coastal morphology and sediment transport.

The wave driven change in the current profile has been extensively studied (e.g. Peregrine, 1976; Jonsson, 1990; Soulsby et al., 1993) however there is no simple formulation to describe or calculate the interaction. Groeneweg (1999) presents a method to solve the wave-induced mean motion over the flow cross-section (i.e. a 2D case) using a generalised Lagrangian mean based approach. Groeneweg also provides a comprehensive review of literature on the subject.

2.1.6 Power available in waves and currents

The power available in waves and currents is obviously extremely important to the developers of wave and tidal stream energy devices. Both in terms of understanding the resource available at particular sites, and also performance of their device . It is common to consider power for waves or currents alone, as in the following formulations. These do not include for any interaction between waves and currents in the combined case, which as shown in section 6.5.2 could be significant.

The amount of useful extractable power will obviously depend on the type of device used, and conversion efficiencies etc., which is beyond the scope of this research.

Waves

The power available in waves P_w is a function of height, period, and wavelength. This is therefore influenced by water depth in coastal regions, as discussed in section 2.1.2. The International Towing Tank Conference (ITTC) give incident wave power per unit length of wave crest in kW/m for regular, long crested irregular, and short crested irregular waves respectively as eqs. (2.25) to (2.27). Wave power can also be expressed as $P_w = E_A C_g$, where E_A is wave energy per unit horizontal area (Méhauté, 1976).

$$P_w = \frac{1}{2}\rho g A^2 C_g\,, \qquad c_g = \frac{1}{2}\frac{\omega}{k}\left(1 + \frac{2kh}{\sinh 2kh}\right) \tag{2.25}$$

$$P_w = \rho g \int_0^\infty C_g(f) S(f)\, df \tag{2.26}$$

$$P_w = \rho g \int_0^\infty \int_{\theta_0-\pi/2}^{\theta_0+\pi/2} C_g(f) S(f,\theta)\, d\theta df \tag{2.27}$$

Tidal currents

The power available in tidal currents P_c can also be represented by the energy flux per unit area of turbine (Garrett and Cummins, 2004). This is proportional to the velocity cubed, as shown in eq. (2.28) where ρ is the density of (sea) water and U a characteristic current speed,

$$P_c = {}^1/_2 \rho U^3 \tag{2.28}$$

The extractable power in a real tidal channel will depend on many other factors, including turbulence and local velocity variations from the bathymetry, boundary effects from bed and surface, interaction between multiple devices in an array, etc.

2.2 Physical model testing and scaling

2.2.1 Background and history

There is a long history of physical model testing using scale models to determine the properties of a full sized device. One of the pioneers was William Froude (1810–1879), who constructed a long tank to tow model ships, and developed the law of similitude named after him (table 2.3).

Early tanks for tow-testing ships were long and relatively narrow, primarily used to understand resistance to motion, and thus required power. Rectangular basins were later developed to test seakeeping performance of vessels. To simulate waves, various types of paddles or ‘wavemakers’ were then added to these tanks and basins.

The University of Edinburgh also has a long history of developing and operating wave tanks over the past forty years. These were used by Prof. Salter and the Wave Power Group in the 1980's to develop the Edinburgh Duck, one of the pioneering Wave Energy Convertors (WECs).

- The rectangular 'Wide Tank' was operational from 1977–2001. This had a bank of wavemakers along the long edge, to maximise the test area and minimise reflections from side walls (Davey et al., 2012).
- The first computer-controlled force-feedback wavemaker paddles were installed at either end of the 'Narrow Tank' in 1984 (Taylor et al., 2003).
- The successor to the wide tank was the smaller 'Curved Tank' constructed in 2002, and still operational today. To make use of the limited space, but still allow the generation of multi-directional waves, a novel design with 48 wavemakers installed in a 90° arc was constructed, as described in Taylor et al. (2003).
- Most recently, the circular FloWave facility was constructed in 2013. This has wavemakers around the entire circumference removing directional limitations from the wave generation (section 4.2).

A spin-off company was established based on the research of developing the Wide Tank. Edinburgh Designs Ltd now design and install test tanks worldwide, including the Curved Tank and FloWave.

When conducting scale model tests, it is important to understand the various relationships between the model and full size device, so called 'scale effects', as discussed in the following section. For any test, there will also be unwanted 'model effects', for example resulting from incorrect representation of the full scale features (Heller, 2011). In addition, conducting the same test in multiple facilities will produce varying results (e.g Gaurier et al., 2015). Termed 'lab effects', this is a result of differing equipment and practices in each laboratory.

2.2.2 Scaling for physical model testing

Scaling is simply the ratio of a parameter on the full sized device (or prototype) to that same parameter on the model being tested (Hughes, 1993). This can then be used to translate the behaviour of the model, or of forces acting on it, to that of the full sized prototype.

Three main areas where similitude between the model and prototype is required are given by Chakrabarti (1998, 2005); Hudson et al. (1979); Hughes (1993); Steen (2014) and others. These are the geometry of the device or structure, the fluid flow around it, and the interaction between these two. Similitude is therefore required in geometry, kinematics, and dynamics.

For the geometry of the structure to be similar, it is usual to scale every linear dimension by a constant factor λ, such that $\lambda = D_p/D_m$, where D_p and D_m denote the same reference dimension of the full sized prototype and the model respectively. If all dimensions are scaled by this factor, the shape of the model remains the same as the prototype. It can also be seen that areas and volumes, with dimensions $[D]^2$ and $[D]^3$, scale with λ^2 and λ^3 respectively.

To achieve kinematic similarity, all motions in the model must be similar to the prototype. This refers to both the device motion and also the motion of the surrounding fluid particles. And in this case motions refer to differentials of length with respect to time, i.e. velocities and accelerations. The exact relationship will be determined by the scaling law used.

For dynamic similarity, there must be a constant ratio for masses and forces between the model and prototype, which arises from Newton's second law of motion. The forces typically of interest in hydrodynamic model testing are: inertial force F_i (i.e. mass × acceleration), gravitational force F_g, viscous force F_μ, surface tension force F_σ, elastic compression force F_e, and the pressure force F_{pr}, which can be expressed as eq. (2.29).

$$F_i = F_g + F_\mu + F_\sigma + F_e + F_{pr} \tag{2.29}$$

Of these, the first three are of comparable interest when considering the physical interaction between fluids and solids (Payne et al., 2009).

For overall dynamic similarity, the ratio of inertial forces between model and prototype has to equal the ratio of the vector sum of active forces. For perfect similitude, all force ratios between model $(F)_m$ and full scale prototype $(F)_p$ must be equal, eq. (2.30), so that the relative influence of each force is independent of scale and remains in proportion.

$$\frac{(F_i)_m}{(F_i)_p} = \frac{(F_g)_m}{(F_g)_p} + \frac{(F_\mu)_m}{(F_\mu)_p} + \frac{(F_\sigma)_m}{(F_\sigma)_p} + \frac{(F_e)_m}{(F_e)_p} + \frac{(F_{pr})_m}{(F_{pr})_p} \tag{2.30}$$

All but one of these force ratios are taken as independent quantities. In hydraulic model testing it is usual to take the pressure ratio as dependent, and determine this after the other ratios are established (Warnock (1950) cited in Hudson et al. (1979); Hughes (1993)).

It is not possible to simultaneously satisfy every requirement of eq. (2.30) for a model scale other than unity. This would require the viscosity, surface tension, and elastic modulus, to be scaled from the fluid used for the full scale prototype to that for testing the model. A single important force ratio must therefore be selected from an understanding of the physical process, with justification for neglecting the others.

There exist a number of dimensionless ratios between quantities that are useful in offshore model testing, that are summarised in table 2.3. It is important to understand the physical phenomena, to ascertain which are of greatest importance, as typically only one can be met (Chakrabarti, 2005). When investigating flow phenomena there will always be an inertial reaction, so the inertial force needs always to be considered in combination with the other force of interest. The first two ratios, Froude and Reynolds, are commonly used in scaling models for tank testing. It is noted that Reynolds similarity can be difficult to obtain for small models due to the high velocities required.

As Froude scaling is used for many problems involving surface gravity waves, the scaling factors for typical parameters used in tank testing are given in table 2.4. There often a density difference between the full-scale device deployed in sea water and the fresh water used for the model tests, represented by the $\frac{\rho_p}{\rho_m}$ term. The effect of Froude scaling on these parameters is illustrated in table 2.5 for a range of typical scales used at FloWave. It is clear that the effects are exacerbated when using a smaller scale such as 1:100.

Table 2.3: Common dimensionless quantities in offshore engineering. (Adapted from Chakrabarti, 2005; Steen, 2014).

Dimensionless number	Symbol	Force Ratio	Definition
Froude number	Fr	Inertia/Gravity	$\frac{U}{\sqrt{gD}}$
Reynolds number	Re	Inertia/Viscous	$\frac{UD}{\nu}$
Euler number	Eu	Inertia/Pressure	$\frac{p}{\rho U^2}$
Cauchy number	Ch	Inertia/Elastic	$\frac{pU^2}{E}$
Mach number	Mn	Inertia/Elastic	$\frac{U}{\sqrt{E_v/\rho}}$
Keulegan-Carpenter number	KC	Drag/Inertia	$\frac{uT}{D}$
Strouhal number	St	Eddy/Inertia	$\frac{f_e D}{u}$

Where: U is characteristic velocity, D characteristic length or cylinder diameter, T wave period, g gravity, ν kinematic viscosity, ρ density, p pressure, E modulus of elasticity, E_v volume elasticity, f_e vortex (eddy) shedding frequency, and $\sqrt{E_v/\rho}$ the speed of sound in water.

Table 2.4: Table of Froude scaled parameters. (Adapted from McCombes et al., 2012).

Variable	Symbol	Units	Scale Factor
All linear dimensions/displacements	D	[m]	λ
Time or period	t	[s]	$\lambda^{0.5}$
Frequency	f	[Hz]	$\lambda^{-0.5}$
Fluid or structure velocity (linear)	u	[m/s]	$\lambda^{0.5}$
Fluid or structure acceleration (linear)	$\dot{u}$	[m/s^2]	1
Angular dimensions/displacements	θ	[rad]	1
Angular velocity	ω	[rad/s]	$\lambda^{-0.5}$
Angular acceleration	$\dot{\omega}$	[rad/s^2]	λ^{-1}
Structure mass	m	[kg]	λ^3
Force	F	[N]	λ^3
Moment or torque	M	[Nm]	λ^4
Pressure or stress	σ	[N/m^2]	λ
Power	P	[W]	$\frac{\rho_p}{\rho_m}\lambda^{3.5}$
Wave power (per unit crest length)	P	[kW/m]	$\frac{\rho_p}{\rho_m}\lambda^{2.5}$
Section moment of inertia (important for stiffness)	I	[m^4]	λ^4
Structure displacement volume	V	[m^3]	λ^3
Spring constant	K	[N/m]	λ^2
Gravity	g	[m/s^2]	1
Fluid density	ρ	[kg/m^3]	1
Fluid kinematic viscosity	ν	[m^2/s]	1
Turbulent Kinetic Energy & Reynolds Stresses		[m^2/s^2]	λ
Turbulence Dissipation Rate		[W/kg]	$\frac{\rho_p}{\rho_m}\lambda^{0.5}$
Reynolds number	Re	[-]	$\lambda^{1.5}$
Keulegan-Carpenter number	KC	[-]	1

Table 2.5: Effect of scale size on Froude scaled model parameters. Quantities given are factor between model and prototype for each given scale and parameter.

Factor	Parameters	Scale:	1:10	1:20	1:25	1:30	1:50	1:100
λ^{-1}	Angular acceleration		0.1	0.05	0.04	0.033	0.02	0.01
$\lambda^{-0.5}$	Frequency, Angular velocity		0.316	0.224	0.2	0.183	0.141	0.1
λ^0	Acceleration, Angular displacements		1	1	1	1	1	1
$\lambda^{0.5}$	Time, Period, Velocity		3.16	4.47	5	5.48	7.07	10
λ^1	Length, Pressure		10	20	25	30	50	100
$\lambda^{1.5}$	Reynolds Number		31.6	89.4	125	164	354	1000
λ^2	Areas, Spring constant		100	400	625	900	2500	1.00E4
$\lambda^{2.5}$	Wave power per metre *		324	1833	3203	5052	1.81E4	1.03E5
λ^3	Volume, Mass, Force		1000	8000	1.56E4	2.70E4	1.25E5	1.00E6
$\lambda^{3.5}$	Power *		3240	3.67E4	8.01E4	1.52E5	9.06E5	1.03E7
λ^4	Moment, Torque, Stiffness		1.00E4	1.60E5	3.91E5	8.10E5	6.25E6	1.00E8

* includes 2.5% allowance for density difference between sea-water and fresh water.

The effect of scaling on two of these quantities in particular warrants further discussion.

- Power is scaled by $\frac{\rho_p}{\rho_m}\lambda^{3.5}$, therefore testing a 1:25 scale model of a 1.0 MW device would result in a maximum power output of just 12.5 W, which might be difficult to measure accurately.
- Time is scaled by $\lambda^{0.5}$, meaning that things happen faster at model scale than in real life. Five times faster for the 1:25 scale example. High-frame-rate (slow-motion) video is therefore required to produce realistic sequences. This scaling may also cause issues with actively controlled models, as the model control system must run faster than that on the full-scale device.

2.2.3 Types of physical model testing facilities

Facilities for undertaking physical model testing of marine renewable energy devices can also be split into three broad categories†, although the boundaries between these are not that well defined.

Towing tanks These are long tanks primarily designed for testing ships by towing a model through the water. They often have a wavemaker situated at one end, and an absorbing beach at the other. These can be used to test WECs in uni-directional waves, and TSTs by towing them through the still water.

Flumes, water channels, and cavitation tunnels In this type of facility, the water is moved by pumps, either around a re-circulating channel, or between sumps and header tanks. In terms of shape, these tend to be slightly longer than wide. These may have a free surface and wave making facilities, or they may be completely filled and have the facility to reduce the ambient pressure for cavitation testing. As cavitation tunnels have historically been used to test ship propellers they are often well suited for testing tidal turbines, as these act on a similar principle, and have similar testing requirements (McCombes et al., 2010*a*).

Wave basins These tend to have more equal plan dimensions, and have wavemakers along one or more sides, with the ability to generate multi-directional waves. Equipment may be installed to create currents and/or wind over all, or part, of the facility.

To give an indication of how the FloWave facility compares to other hydrodynamic test facilities of interest to renewable energy device developers, key details for selected European facilities are given in table 2.6.‡

---

†. In addition to these, there are many basic tanks that can be used for testing simple parameters, plus facilities where the pressure, temperature, and/or chemical composition can be varied for performance testing of materials and components, however these fall outside the scope of this study.

‡. Sources: MARINET (2014); Collins et al. (2013); de Jesus Henriques et al. (2014); Deltares (2017*a*,*b*); Galloway et al. (2014); Gaurier et al. (2015); HR Wallingford (2017); IH Cantabria (2017); MARINTEK (2011); Plymouth University (2017)

Table 2.6: Summary details of selected hydrodynamic test facilities.

Organisation, tank name, and location Size [m]	Depth [m]	Wavemaker type	Max. $H(H_s)$ [m]	Current generation	Max. U [m/s]
University of Edinburgh FloWave Ocean Energy Research Facility, Edinburgh, UK					
25 ⌀	2	168 active-absorbing flap-type	0.45 (0.35)	28 impellers	1.2
University of Edinburgh Curved tank, Edinburgh, UK					
14×9	1.2	48 flap-type in 90° arc	0.22	—	0
Aalborg University Deep water wave basin, Aalborg, DK					
15.7×5.5	0.75	10 piston-type paddles	(0.2)	—	0
Has $4.5 \times 2.1 \times 3$ m pit					
Cantabria Coastal and Ocean Basin (CCOB), Santander, ES					
44×30	0.2–3.4	64 flap-type	1.0	12×0.9m⌀ mixers capable of generating a flow of up to $18\,m^3/s$	0.2
Has 6 m⌀ × 8 m deep pit					
CNR-INSEAN Towing tank 2, Rome, IT					
220×9	3.5	Single flap-type	0.45	Carriage	10
CNR-INSEAN Circulating water channel, Rome, IT					
10×3.6	2.25	—	—	2 four-bladed axial-flow impellers	5
Can control absolute pressure in test section: 3–101kPa, and adjust water depth to have free surface or not.					
Deltares Atlantic Basin, Delft, NL					
75×8.7	0–1	8.7m long cradle-type	0.45(0.25)	Pumps totalling $3.0\,m^3/s$	~
Angle between flow and wave direction 0° or 180°					
Deltares Pacific Basin, Delft, NL					
30×22.5	0.25–1	14m long cradle-type	0.4(0.21)	8 pumps totalling $1.8\,m^3/s$	~
Angle between flow and wave direction 45°–90°					
HR Wallingford Fast-Flow Facility, Wallingford, UK					
70×4	0.8–2	10 paddle flap-type	(0.5)	Reversible pumps	2
Has $16\,m^2$ pit 1 m deep for sediment studies, and secondary (return) channel 50×2.6 m.					
IFREMER Deep wave basin, Brest, FR					
50×12.5	10	Uni-directional wavemaker	0.45	Carriage	1.5
Has 12.5 m section near beach 20 m deep					

Table 2.6: Summary details of selected hydrodynamic test facilities.

Organisation, tank name, and location Size [m]	Depth [m]	Wavemaker type	Max. $H(H_s)$ [m]	Current generation	Max. U [m/s]
IFREMER Towing tank, Brest, FR					
50 × 4	3	—	—	Carriage	4.5
IFREMER Hydrodynamic water tunnel, Boulogne sur Mer, FR					
18 × 4	2	8 surface mounted paddles	0.3	2 recirculating pumps	2.2
Plymouth University COAST Ocean basin, Plymouth, UK					
32.4 × 15.6	0–3	24 flap-type wave-makers	0.32	Multi-pump recirculating hydraulic system	0.5
Mean U of 0.3 m/s at 2 m water depth. Recirculating current both in-line with, and transverse to the waves.					
Queens University Belfast Shallow water wave tank, Portaferry, UK					
18 × 16	0.65	24 top-hinged sector-carrier paddles	0.55	Cross-currents only	0.25
SINTEF (Formerly MARINTEK) Ocean basin, Trondheim, NO					
80 × 50	0–10	144 flap type (on long edge)	0.4(0.2)	Pumps	0.25
		5 double-flap (on short edge)	0.9(0.5)	Carriage	5
Maximum flow of 0.25 m/s at 2 m water depth, or 0.18 m/s at 5 m.					
SINTEF Towing tank I, Trondheim, NO					
175 × 10.5	5.6	—	—	Carriage	8
SINTEF Towing tank III, Trondheim, NO					
85 × 10.5	10	Double flap	0.9	Carriage	0.5
Can combine tanks I & III to create a 260 m long tank					
Southampton Solent University Wave-towing tank, Southampton, UK					
60 × 3.7	1.8	Flap type wavemaker		Carriage	4
UCC/HMRC National Ocean Wave Basin, Cork, IE					
25 × 18	1	40 flap type	(0.16)	—	0
University of Liverpool Recirculating water channel, Liverpool, UK					
3.7 × 1.4	0.76	Surface mounted flap		Axial flow impeller	6
University of Strathclyde Kelvin Hydrodynamics Laboratory towing tank, Glasgow, UK					
76 × 4.6	0.5–2.5	4 flap type	0.5	Carriage	5

Wave generation and absorption

Wave generation in test tanks is achieved via some means of wavemaker paddle. These can be fitted along one or more edges of the tank. Modern wavemakers are computer controlled, either by position or using force-feedback. They can produce a range of regular waves which are combined to generate irregular sea states. The phase angles for each wave component can either be random, or deterministic pseudo-random, with pros and cons of each method given in Guillouzouic (2014).

In long narrow tanks, particularly towing tanks, only long crested waves can be produced (McCombes et al., 2010*a*). Short waves with directional spreading, representative of real sea conditions, can only be modelled in wider basins. A greater range of wave directions can be created by having wavemakers on more than one side of the wave basin.

Waves generated in a tank will be reflected from the sides, which may lead to standing waves or other wave inaccuracies within the test area. The impact of reflection can be more problematic in smaller tanks and flumes, where there could be reflections present during even short tests (Holmes, 2009). In larger tanks, the time taken for reflected waves to return to the test area is longer. Reflections will be greatest from solid walls, so to limit this, absorbing beaches are typically used along one or more sides of the tank. The form and shape of these beaches can vary significantly between facilities, but all have the same purpose. Active absorption using force-feedback paddles is also possible, using the wavemakers to both generate and absorb waves in the tank. This latter case is used in the circular FloWave basin.

CHAPTER 3

On physical model testing for offshore renewable energy

Chapter summary

- Background is provided on some challenges involved in the field of physical scale model testing for Offshore Renewable Energy (ORE), and comparison of facilities used to undertake these tests.
- Published material on characterising wave and current test facilities is reviewed. This focuses on measuring currents, as a precursor to chapter 5. Previous work on characterising waves in the FloWave basin is also reviewed, as this is of relevance to chapter 6.
- Recent publications on wave-current interactions relevant to their study in a facility such as FloWave are summarised. This includes experimental studies and the impact on ORE. The development of interaction theory for regular waves is also considered as this is used for comparison with observations at FloWave.
- The body of existing guidance for tank testing ORE devices is reviewed. Key limitations are highlighted, particularly for testing in advanced environmental conditions such as multi-directional waves combined with currents.

3.1 Background

3.1.1 Diversity of device concepts

One of the challenges in producing guidance for marine renewable energy testing is the shear diversity of device concepts. A three level device classification template for wave and tidal energy converters is given by Myers et al. (2010). This categorises devices based on the general form, the power take-off subsystem, plus the reaction and control subsystems. For each level, there are a number of standardised descriptors, giving many thousands of possible device concept permutations. Technology reviews, such as Falcão (2010); Yuce and Muratoglu (2015), identify more than 100 wave and tidal energy concepts in various stages of development, and suggest that there are fewer concepts

being abandoned than there are new ones being developed. In addition, whilst wave and tidal energy are often grouped together, they are very different problems, apart from the common purpose of extracting power from the harsh marine environments.

Although there is some standardisation of devices, particularly for Tidal Stream Turbines (TSTs) where horizontal-axis three-bladed turbines are emerging as a favoured design, there are also many novel devices including underwater kites and other rotor configurations. The 'novelty' of a device is described by Bahaj et al. (2008) as *"the extent to which the design of the subsystem components represents a significant departure from the body of existing knowledge within the offshore, marine, and wind industries."* A tidal stream energy stakeholder perception study (McLachlan, 2010) agreed there was consolidation of designs for TST, but also noted that the similarity of this concept to the more established wind industry might help investment.

3.1.2 Evaluation of model testing methods

Models can be grouped into three broad types: computer numerical models, small-to-medium scale physical models in dedicated (indoor) facilities, and large-to-full scale prototype testing in sheltered waters. There is always a trade-off between the strengths and weaknesses of each type of testing, which needs to be considered throughout the development process. It should also be highlighted that a composite test programme of numerical modelling and tank testing can offer more than either individually, as discussed by Sutherland and Barfuss (2011) and others.

Vyzikas et al. (2014) suggest that physical model testing does not require parameterisation nor simplification through assumptions and equations as it implicitly includes the physical processes involved. There are however downsides to physical scale model testing. Primarily these are the inclusion of (adverse) effects of scaling and facility specific constraints such as blockage or reflections; although these can often be mitigated through experiment design (Holmes and Nielsen, 2010). As discussed in section 2.2.2, it is not possible to scale all parameters consistently, and some effects may become disproprtionately important when modelled at scale. Scaling of turbulent flow is one particularly complex area (see e.g. Hughes, 1993; Pope, 2000), although maintaining the correct turbulent flow-regime is often considered sufficient. Two other related drawbacks are, that it is not possible to record and visualise the outcome throughout the whole test domain, only at specific measurement points (Vyzikas et al., 2014). Also these physical measurements may impact upon the result being measured.

Undertaking this testing in a laboratory environment provides a controlled, repeatable, and low-risk environment where technological concepts and operational techniques may be developed (Ingram et al., 2011). The alternative of full-scale operations at sea is subject to the vagaries of the weather, is significantly more difficult, and is likely to be

at least an order of magnitude more expensive. Holmes and Nielsen (2010) note that specified conditions can be created, and *just as importantly stopped*, on demand when working in dedicated test facilities.

An alternative viewpoint is suggested by Peter Fraenkel, former director of Marine Current Turbines Ltd., that *model testing is not robust enough.* To properly understand how a device operates requires testing at sea, in harsh conditions (Discussed with P Fraenkel during IDCORE group design project, March 2014; Gupta, 2014).

3.1.3 Physical model testing facilities

When deciding to undertake a programme of physical model testing, the type of facility used (section 2.2.3) is important. Each has particular strengths and weaknesses, often complimented by another type of facility. Multiple facility types may be advantageous or required during the development of a project, to test different stages or aspects of the device.

It is highlighted in McCombes et al. (2010*a*) that for both towing tanks and flumes, the device model may take up a significant proportion of the channel cross-sectional area. This could result in a measurable influence of the boundary effects at the walls and/or floor, which is unlikely to be representative of the real world situation. For TSTs the full-scale device could occupy a significant proportion of the water column, and therefore the bed and surface boundary effects are real. There may also be horizontal constraint on the flow through arrays of TSTs, but this is not the same as wall boundary effects in a tank, and needs to be accounted for.

Scaling of turbulence is problematic, and it is not entirely clear as to how this can be done in a rigorous manner (McCombes et al., 2010*b*). The uncertainty of both measuring and re-creating complex real-world turbulent tidal flows was highlighted as an issue in Germain (2008), and this still remains an area with little published guidance. Recent studies, such as those conducted under the Reliable Data Acquisition Platform for Tidal (ReDAPT) project (Sellar et al., 2015), are providing promising site specific information based on spatially rich, high-resolution velocimetry, that may in future be used to define test conditions.

McCombes et al. (2010*a*) highlight that in circulating current flumes and tunnels, there is usually a velocity profile over the depth of the tank which may or may not not be representative of the real site. Additionally, the profile may vary along the length of the facility. In contrast, where the device is being towed through stationary water there is no boundary layer development from the motion of the water relative to the bed. It is also likely that the ambient turbulence levels will be too low, especially when the carriage has been stationary for a period. The wake, and wake recovery, observed downstream will

also be incorrect because of the lack of turbulence (Myers and Bahaj, 2010; Salvatore et al., 2014)

The maximum duration of a single test run in a towing tank is a function of the tank length and velocity required, accounting for carriage acceleration and deceleration. This duration can often be relatively short, unless a very long (and likely expensive) facility is used. In comparison, testing in recirculating tunnels, tanks, or flumes has the advantage that the flow speed can be kept constant for a long duration (Kimball, 2010), and the flow speed is not necessarily proportional to the size of the facility.

In narrow and/or shallow facilities, it may not be possible to accurately model spread moorings to scale, given the space constraints. Alternative arrangements may be required, such as using springs to model moorings. Holmes (2009) points out that towing tanks have an advantage in that relatively long devices can be accommodated, albeit subject to other space constraints such as blockage and mooring footprint.

Many facilities (including FloWave) operate using first-order wavemaker control (see e.g. Dean and Dalrymple (1991) for details). This however results in spurious free waves, harmonics of the desired waves. A second-order control signal, such as Schäffer (1996), can be implemented to suppress these. This only applies for wavemeker paddles operated in position control; facilities using paddles controlled by the force on them instead require empirical calibration to develop a tank-transfer function (Masterton and Swan, 2008). According to Spinneken and Swan (2009*a*), dry-back force-controlled wavemakers (such as those installed at FloWave) seem to introduce very little spurious harmonic content, and also absorb waves well, so have been implemented at many facilities worldwide. Spinneken and Swan (2009*a*,*b*) have now developed a second-order wavemaker theory for paddles using force-feedback control.

3.1.4 Comparison of testing between facilities

Gaurier et al. (2015) conducted a comparative study of different facilities for testing a tidal turbine as part of the Marine Renewables Infrastructure Network for emerging Energy Technologies (MARINET) project. Comparisons are made between four facilities: two towing tanks and two recirculating flumes. The authors considered differences between using a towing tank and a recirculating flume for testing a model tidal turbine, plus differences in operating procedures at each facility. To minimise difference resulting from operational practices in each lab, measurements were made using the same equipment under guidance from IFREMER staff.

Similar results were generally found for average power and thrust coefficients C_P, C_T once corrected for blockage. The biggest discrepancies were found for the time-varying fluctuations of C_P, C_T. Attributed to differences in both the level of turbulence between

towing-tanks and flumes, but also lack of detailed characterisation of the turbulent flow beyond just Turbulence Intensity (TI).

A similar round-robin test of a Wave Energy Convertor (WEC) was planned as part of MARINET, comparing the performance between six facilities (Holmes, 2015). Unfortunately this does not appear to have been published. It is understood that further round-robin testing for both WEC and TST will be undertaken and reported on as part of the ongoing MARINET2 project, which runs from 2017–2021.

3.2 Test facility characterisation

There is a limited amount of published work on the characterisation of facilities for testing ORE devices, and most cover only the measurement and characterisation of waves *or* currents in a facility, rather than combined wave-current. It can be speculated the paucity of information may be partly attributable to the commercial nature of operation at some facilities, but this cannot be substantiated.

There is also a lack of guidance on how to characterise these facilities for testing ORE devices. This is noted in Collins et al. (2013), citing proposals for the MARINET project, in relation to testing WECs.

More has been published on characterising waves and wavemakers, but this less relevant to the present study, which focuses on currents and combined conditions.

The following subsections consider methods to characterise flow in test facilities as a precursor to chapter 5, review the limited information on characterising wave-current facilities, and summarise the characterisation of wave generation and absorption at FloWave.

3.2.1 Characterising currents in flumes and tanks

There are a few published flow characterisation studies for recirculating flumes and cavitation tunnels designed primarily for naval testing, such as ship propellers. In addition, baseline flow conditions for experimental studies in other facilities have also been reported.

Hydrodynamic characterisation of the US Navy 'William B. Morgan' Large Cavitation Channel, Memphis, Tennessee, is reported in Park et al. (2002, 2005); Derradji-Aouat et al. (2007). Using Laser Doppler Velocimetry (LDV) and hot-film anemometry, three key characteristics of tunnel velocity were measured: temporal stability, spatial uniformity, and turbulence. For the velocity calibration, both linear and power-law fits were used, with the accuracy assessed by plotting the residuals to these fits. Temporal stability of

the flow was assessed over a period of several hours, with resulting flow variation within ±0.2%. Mapping the 3D velocity field in the test section was achieved by splitting the LDV measurements into two-component pairs. Firstly axial and lateral (X–Y) velocities were measured through the top window, then axial and vertical (X–Z) from the side.

Flow characteristics of the Chilworth flume, Southampton, UK were measured using a Nortek Acoustic Doppler Velocimeter (ADV) at 50 Hz (Myers and Bahaj, 2010). This was part of a study to investigate wake effects of TST at small scale using porous disks. Results are only presented for cases with the model installed, so this is not a facility characterisation, however it is interesting to note that the measurement methods used are similar to those used for characterising other facilities. Myers and Bahaj also discuss the conflict inherent in scaling for TSTs, and highlight the lack of data from full-scale deployment sites.

3.2.2 Characterising combined wave-current facilities

Some initial performance results for the Coastal, Ocean, and Sediment Transport (COAST) laboratory at Plymouth University are presented in Collins et al. (2013). Although the ocean basin has the ability to generate currents in addition to waves, no details are given on the measurement of current in the facility, nor anything on combined wave-current characterisation. It also appears that nothing further has been published on the characterisation of this facility.

Removable wavemakers and beach have been retrofitted to the IFREMER hydrodynamic water tunnel at Boulongne-sur-Mer, France (see table 2.6 for key parameters). This facility is often used for testing ORE devices, as it is possible to create combined wave-current conditions, although only for collinear cases (i.e. waves with either following or opposing currents). Whilst not presenting a full characterisation of the facility, Germain et al. (2007) give an example of using LDV to confirm the flow stability and performance of the flume, amongst other discussion on testing marine current energy converters.

Characterisation of the combined wave-current capability is presented in Bacchetti et al. (2010). When installed, the wavemaker and beach sit within the top 0.5 m of the 2.0 m deep flume. This impacts on the vertical flow profile, reducing velocities in the upper water column but increasing them in the lower part. The magnitude of effect is also dependent on the generation direction, i.e. waves following or opposing the current (Bacchetti et al., 2010, Fig. 3.3). The flow in the flume is therefore less similar to the power-law or logarithmic profiles typically used to model channels.

The change in wave height and length as a result of interaction with the current was considered using four different wave frequencies from 0.5 Hz to 1.0 Hz and six velocities up to ±0.8 m/s. Comparison is made to theory, presumably a linear interaction although

this is not stated. Bacchetti et al. (2010) note the relative amplitude of lower frequency waves on a following current is smaller than predicted by theory. This is also the case for higher frequency waves with an opposing current, but other waves were found to be close to the theoretical value. The measured relative length was similar to theory, and not particularly sensitive to frequency.

Bacchetti et al. (2010) also consider the impact of waves on the current profile and the mean wave orbital velocity. The waves considered of 0.5 Hz and 0.6 Hz do not cover the whole operational range of the facility, but two amplitudes are used for each frequency. There is some discussion of flow uniformity for the cases with waves, but a case without waves is not provided for reference in this paper. One interesting point noted is that the larger waves opposing the current were asymmetrical, and overtopped the basin on one side but not the other.

Germain et al. (2010) considers some implications for the testing of TST in the flume at Boulongne-sur-Mer, including comparison to a numerical model of the turbine blades. LDV measurements of the wake are presented, together with some discussion on the effects of turbulence, noting that the facility can operate with nominal TI levels of 3% and 15%, with and without flow conditioning.

3.2.3 Characterisation of wave generation and absorption at FloWave

Characterisation of the wave generation and absorption capability of the FloWave facility was undertaken as part of an earlier IDCORE project (Draycott, 2017). This began in mid 2012 as construction of the facility was nearing completion.

Details of the FloWave basin, including the method of wave generation, are covered in section 4.2, and it is shown diagrammatically in fig. 4.1.

A programme of measurements were carried out across the 15 m⌀ test area of the tank, by Draycott. This comprised a set of regular waves plus uni- and multi-directional spectra. Five frequencies from 0.3 Hz to 0.9 Hz at 1%, 2%, and 4% steepness values were used, corresponding to the tank generation specifications.

Assessment of regular waves generated by the tank show these closely match Stokes' 2nd order theory, with $r^2 > 0.99$ for all test cases. Maximum deviation in the water surface elevation from the theoretical value were around 3% of wave height for the example given, a 0.9 Hz, 4% steepness regular wave. The commonly used assumption of linear wave theory was also found to perform adequately, with $r^2 > 0.98$. Draycott notes that the difference between theories is insignificant in the context of other errors involved in tank testing, justifying the use of linear wave theory in spectral formulation.

Due to the circular nature of the FloWave facility, it was important to demonstrate that through careful timing of individual paddle motion, accurate generation of 'straight'

long-crested waves is achieved. This was done using an array of gauges perpendicular to the wave propagation direction. Wave curvature and skewness (correctness of angle) was inferred from the measured phase difference between gauges for the initial wave crest. The lag was < ±0.5% of the wave period for the vast majority of measurements, close to the limiting resolution imposed by the 128 Hz sample frequency. This confirms that truly long crested waves are generated in the facility over a range of frequencies, which is visually apparent in the facility.

Wave reflection analysis

One of the key features of FloWave is the circular design, with wavemakers around the whole circumference. This removes any directional generation limitations from the facility, but it requires the wavemakers also absorb wave energy at the opposite side due to the absence of beaches to dissipate energy. Any imperfections and/or non-uniformity in the wavemaker absorption will lead to the build up of reflections. In a tank, reflections lead to spatial variability of wave heights across the basin, with a pattern of 'hot' and 'cold' spots where the waves interfere constructively and destructively respectively.

To understand this behaviour in the FloWave facility a frequency domain reflection analysis was conducted by Draycott (2017). This included spatial and temporal variability of the wave field across the tank. For regular waves, the frequency domain method of Zelt and Skjelbreia (1992) was used. For irregular waves in a tank, knowledge of the generated wave component directions enables more accurate reconstruction of the directional spectra. Draycott et al. (2015*b*) shows that a Phase-Time-Path-Difference (PTPD) approach can effectively be used to measure directional spectra in tanks where waves are generated using a single summation method, as at FloWave (section 4.2.4). Capitalising on this, the Single-summation PTPD Approach with In-line Reflection (SPAIR) methodology was developed in Draycott et al. (2016). It uses a PTPD approach to calculate wave component directions, but includes in-line reflection analysis similar to Zelt and Skjelbreia (1992). This allows incident and reflected directional spectra to be isolated. This SPAIR method was used by Draycott (2017) to analyse all the irregular sea states measured, allowing comparison whilst resulting in better understanding of reflections for directionally spread conditions.

Paddle absorption effectiveness was found to be greater at lower frequencies, attributed to the paddle shape characteristics (Draycott, 2017). Additionally, absorption effectiveness was reduced for low steepness waves compared to steeper waves. This is explained by the force-feedback system not accurately measuring the smaller forces from the lower height low-steepness waves. The rate at which the wave force is changing is also smaller for lower steepness waves, which may exacerbate the control problem.

The absorption effectiveness was also found to decrease rapidly for higher frequency wave components, above around 1 Hz. The amount of directional spreading did not have a significant impact on reflections.

Temporal and spatial variability of the wave field

To understand how waves progress across the tank and reflections build up, Draycott (2017) created a database of wave height interpolated across the test area over the 128 s test length for a range of regular waves. This shows the first wave moving across the tank, a function of the frequency dependent wave speed C_g, eq. (2.6). Following this, reflections build up from the absorbing paddles. This is shown to be stable after 64 s to 128 s dependent on frequency, with low frequency waves stabilising more quickly.

The reflections are shown to be curved, a function of the circular tank geometry. Focussing of the waves leads to greater variability in the wave conditions close to the reflecting boundary, the absorbing paddles. Draycott suggests the ideal location for testing is therefore located far from these paddles, a few meters from the tank centre towards the generating paddles. It may also be advantageous to position the model off-centre with regards to the wave propagation direction. This is only possible for uni-directional or low-spread sea states, where all tests have a similar direction.

3.3 Wave-current interactions

Much published literature on wave-current interactions relates to the currents generated by the presence of waves, particularly in shallow coastal waters, which is important for sediment transport. The impact of a current on wave properties is of more interest when considering tank testing at FloWave, where waves are generated in still water and then interact with a current in the test area.

3.3.1 Development of wave-current interaction theory

Interacting waves and currents influence each other in a complex manner. The general formulation for wave-current interactions based on a Doppler shift, presented in section 2.1.5, does not include all of this complexity.

A method developed by Baddour and Song (1990*a*) allows for changes in the mean water depth and mean current speed as a result of the wave-current interaction. This is achieved by solving the dispersion relation with equations for mass, momentum, and energy transfer, allowing calculation of wave length, height, current velocity, and water depth from their pre-interaction values. A series of non-dimensional constants are introduced to facilitate computation, using Newton's method. The calculation is correct to

second order, albeit still using small amplitude (linear) wave theory, and is only valid for collinear waves and currents.

This method was extended in Baddour and Song (1990*b*) to consider second-order wave theory. A further extension to this method by Zaman and Baddour (2011) was to include non-collinear waves-current interactions, i.e. where there is an angle θ_{rel} between the wave and current propagation directions. A computational procedure is described, in terms of the same non-dimensional variables introduced in Baddour and Song (1990*a*). The parameters of the combined wave-current field are found by simultaneously solving the dispersion relation together with equations for conservation of mass, momentum, and energy. The conservation relations are expressed both normal and perpendicular to the combined direction of propagation, allowing the resulting angle to be calculated.

3.3.2 Experimental studies

Much published literature on wave-current interactions relates to the currents generated by the presence of waves, focusing on sediment transport and coastal processes. This is not however something that can be studied in the FloWave facility. Several experimental studies have been published on the influence of currents on waves, mostly focusing on the collinear case with waves on a following or opposing current.

Early studies including Thomas (1981); Kemp and Simons (1982, 1983) used hydraulic flumes to investigate collinear wave-current interaction for regular waves. The main focus was the influence of waves and bed roughness on the current profile, although modification of wave height and wavelength by the current was also included.

This experimental work on regular waves was extended to consider wave uni-directional JONSWAP spectra in deep water with collinear currents by Chakrabarti and Johnson (1995). A good match to theory was found for all cases observed. To account for the current generated in the tank not being uniform throughout the depth, an equivalent current was calculated using the method of Hedges and Lee (1992). This aims to maintain the correct wavelength and was calculated for the spectral peak, although it was noted the wavelength will not be correct at other frequencies. Guedes Soares et al. (2000) conducted similar tests, and compared the results to theoretical formulations of Huang et al. (1972); Hedges (1981). Reasonable approximation was found, but for both following and opposing currents the theoretical formulations underestimated the change in the spectral shape.

Adding more complexity, Nwogu (1993) looked at the influence on directional JONSWAP spectra of currents following and opposing the mean wave direction With following currents, good agreement was found between the measured frequency spectra and theory. The degree of directional spreading ($s = 1, 3, 6$) did not significantly affect the

resulting spectra. For opposing currents, the spectrum was slightly larger than predicted by theory, and tests with regular waves showed greater amplification than predicted for the shorter waves. Mean wave directions of 15°, 30°, and 45° relative to the current were also tested by Nwogu, although any modification of the frequency spectra is not reported.

3.3.3 Impact on marine renewables

The influence of wave-current interactions on the power availability at sites has been discussed in a number of papers. The effects were generally found to be considerable, but it is noted this interaction is often neglected in resource assessment studies.

The wave energy resource for the north-west European shelf was investigated by Hashemi et al. (2014), using a coupled SWAN–ROMS model and also using a simplified analytical approach. Hashemi et al. highlight that even for the idealised case, wave power is a function of five variables: water depth, wave period, tidal amplitude and velocity, plus the phase relationship between tidal elevations and currents. The numerical modelling showed the impact on wave power resource could exceed 10% at a site with tidal currents of 1.5 m/s. The effect is most prominent for shorter period (higher frequency) waves. Zodiatis et al. (2015) consider the impact of currents on the wave power resource of the Eastern Mediterranean Sea. The third-generation wave model WAM was used to consider two cases, with and without sea-surface currents. The overall conclusion was that currents need to be included when modelling wave power potential, as the effect is non-trivial. The most extreme results showed reductions in peak period of 20% and reduction in wave energy of 24%. Other studies, such as Saruwatari et al. (2013), suggest the effect of wave-current interaction on the wave resource could be as much as 60% in currents of 3 m/s, although this study does not appear to include the current-induced changes in wavelength and group velocity discussed in section 6.5.2, which leads to an overestimate of the effect.

The impact of waves on the tidal stream resource is investigated in Hashemi et al. (2015), looking at a site to the north-west of Anglesey in the Irish Sea, using a TELEMAC2D model. This shows a reduction in tidal energy, with more effect when the wind is opposing the current. Two interesting points are highlighted by Hashemi et al. Firstly, that 2D models are depth averaged, so cannot accurately determine the impact at turbine hub height. Secondly, the availability of wave data in strong tidal sites is limited, due to operational difficulties in positioning wave buoys at these sites.

3.3.4 Tank testing in combined waves and current

Experimentally testing the impact of wave current interactions on model TSTs is reported in a number of studies as discussed below. Tank testing the impact of currents on waves and a WEC does not appear to have been reported on however.

Most of these studies were carried out by pulling a model turbine in a towing tank. A small model, with a 250 mm rotor diameter was tested by Barltrop et al. (2006) at the Strathclyde tank, Faudot and Dahlhaug (2012) tested a 1.475 m⌀ model in the 260 m tank in Trondheim, and Galloway et al. (2014) tested a 0.8 m⌀ model at Southampton.* For these cases, the model was towed into various wave cases, modelling an opposing current. Faudot and Dahlhaug note that in a long tank, the wave profile is not constant, so wave gauges are mounted on the carriage close to the rotor to confirm the actual wave profile. A different approach was taken by de Jesus Henriques et al. (2014), testing a 0.5 m⌀ model in the Liverpool recirculating water channel. This is fitted with a surface wavemaker, but only wave propagating in the same direction as the current were tested, i.e. a following current case.

All these studies were primarily concerned with the performance and loading on the particular model turbine, rather than the effect of the wave-current interaction. No baseline cases without waves were presented for comparison.

It is noted by Barltrop et al. (2006) that linear wave-current theory does not accurately describe the forces experienced, particularly in steep waves, which are encountered in combined conditions, highlighting the need for model tests.

3.4 Guidance for scale model testing of marine renewable energy systems

3.4.1 Availability of guidance

Historically, there has been only limited guidance available relating specifically to scale model testing of marine renewable energy systems. This situation has improved over the last decade however, as the offshore renewables industry has developed towards commercialisation. A chronological list of published guidance relating to model testing of marine renewable energy devices is given in table 3.1.

This historical lack of published practice was highlighted by Germain (2008). Device developers previously have had to make use of guidance for the model testing of ships and offshore structures, such as that produced by the ITTC, one of the key organisations

*. See table 2.6 for key parameters of the facilities discussed here.

Table 3.1: Chronological list of published marine renewable tank testing guidance documents.

Organisation	Date	Applicability	Title & Reference
ITTC	2005		Recommended Procedures for Floating Offshore Platform Experiments (ITTC, 2005*b*).
IFREMER	2008	TST	Marine current energy converter tank testing practices (Germain, 2008).
OES IA	2008	TST	Tidal-current Energy Device Development and Evaluation Protocol (Bahaj et al., 2008).
Uni.Edin.	2009	WEC	Best Practice Guidelines for Tank Testing of Wave Energy Converters (Payne et al., 2009).
EMEC	2009	WEC	Tank Testing of Wave Energy Conversion Systems (Holmes, 2009).
OES IA	2010	WEC	Guidelines for the development & testing of wave energy systems (Holmes and Nielsen, 2010).
EquiMar	2009-2011	General	EquiMar Protocol II.A Tank Testing (Ingram et al., 2011), plus various work package deliverable reports.
ITTC (26th)	2011	General	Recommended Procedures and Guidelines Seakeeping Experiments (ITTC, 2011*a*).
		WEC	Recommended Guidelines, Wave Energy Converter Model Test Experiments (ITTC, 2011*b*).
MARINET	2012-2015	WEC	Wave Instrumentation Database (Lawrence et al., 2012). Collation of Wave Simulation Methods (Guillouzouic, 2014). Standards for Wave Data Analysis, Archival and Presentation (Cândido et al., 2015). Best Practice Manual for Wave Simulation (Holmes, 2015).
		TST	Collation of Tidal Test Options (McCombes et al., 2012).
		FOWT	Collation of Offshore Wind-Wave Dynamics (Bredmose et al., 2012). Best Practice Protocol for Offshore Wind System Fluid-Structure Interaction Testing (Brand et al., 2015).
ITTC (27th)	2014	General	Specialist Committee on Hydrodynamic Testing of Marine Renewable Energy Devices (ITTC, 2014*d*).
		WEC	ITTC Recommended Guidelines - Wave Energy Converter Model Test Experiments (ITTC, 2014*a*).
		TST	ITTC Recommended Guidelines - Model Tests for Current Turbines (ITTC, 2014*c*).
		FOWT	ITTC Recommended Guidelines - Model Tests for Offshore Wind Turbines (ITTC, 2014*b*).
ITTC (28th)	2017	General	ITTC Recommended Guidelines - Laboratory Modelling of Waves: regular, irregular and extreme events (ITTC, 2017*b*).
		General	ITTC Recommended Guidelines - Laboratory Modelling of Multidirectional Irregular Wave Spectra (ITTC, 2017*a*).
		WEC	ITTC Recommended Guidelines - Wave Energy Converter Model Test Experiments (ITTC, 2017*d*).
		TST	ITTC Recommended Guidelines - Model Tests for Current Turbines (ITTC, 2017*f*).
		FOWT	ITTC Recommended Guidelines - Model Tests for Offshore Wind Turbines (ITTC, 2017*e*).

involved in tank testing of ships and offshore structures. More recently guidance specific to marine renewable energy has been published by OES IA, EMEC, and ITTC, plus the EU funded projects EquiMar and MARINET, as detailed in table 3.1 and discussed below. These guidance documents are still somewhat generic however,as it is difficult to go into specifics for such a broad field with a very diverse range of concepts being tested, as discussed in section 3.1.1. The published guidance is predominantly segregated by technology types, with a slight bias towards guidance on WECs. This bias may be due to similarities between tank testing of WECs to the more established procedures for testing ships and oil platforms.

Recommendations of best practice learned from tank testing of marine renewable energy devices were published almost a decade ago by IFREMER (Germain, 2008) and the University of Edinburgh (Payne et al., 2009), covering TSTs and WECs respectively. Additional guidance was published after this by the EMEC (Holmes, 2009) and OES IA (Holmes and Nielsen, 2010).

The established Recommended Procedures for Floating Offshore Platform Experiments (ITTC, 2005*b*) were extended to cover WEC model testing (ITTC, 2011*b*). Three main differences from floating platforms and challenges specific to wave energy are given as:

- the inclusion of Power Take-Off (PTO),
- testing at various stages of development, from concept validation onwards, and
- testing multiple devices (or multi-body devices), including their interactions.

Hydrodynamic testing of marine renewable energy devices was further considered by a specialist ITTC committee (ITTC, 2014*d*). The guidance on WECs was updated, and new guidance for testing of FOWT and TST produced (ITTC, 2014*c*,*b*,*a*). A review of these ITTC guidelines is undertaken by Day et al. (2015), as part of a wider assessment of hydrodynamic modelling. Following their 28th conference, many of the recommended procedures and guidance documents were updated, including those for testing ORE devices (ITTC, 2017*f*,*e*,*d*). As part of the MARINET2 programme, Noble et al. (2018) produced a summary of standards, guidance, and test recommendations for testing ORE devices, including an analysis of perceived gaps in guidance.

The International Electrotechnical Commission (IEC) had initially planned to release guidance on scale testing of WECs (IEC/TS 62600-103) and tidal stream energy systems (IEC/TS 62600-202) in 2015, but this has now been delayed until 2019 (IEC, 2018).

3.4.2 Structured device development programmes

Model testing has become an established part of a structured development process for ORE devices, as in other technologies and processes. Similar multi-stage development plans for WECs and TSTs are outlined in published guidance. These all relate to the widely used Technology Readiness Level (TRL) concept, developed initially by NASA (Mankins, 1995), suggesting increasingly complex testing as the device technology matures. At each stage the developer is aiming to maximise understanding of the device performance with the minimum of risk and outlay. The stages can broadly be defined as per table 3.2, although there is likely to be overlap between stages in reality. The development might be an iterative process, particularly for subsequent revisions to the device concept, going back to tank test improvements to the design following open water deployment.

Some of the first guidance specifically relating to ORE devices outlined similar multi-stage development plans for tidal-current devices (Bahaj et al., 2008) and for wave energy systems (Holmes, 2009; Holmes and Nielsen, 2010). More recent guidance issued by ITTC (2014*c*,*b*,*a*) also suggests similar stages. While this guidance is technology specific, they have commonality and wider applicability, linking back to the same TRL. The stages can broadly be defined as per table 3.2, although there is likely to be overlap between stages in reality.

Table 3.2 also gives typical infrastructure used for testing of marine renewable energy devices. Tank testing usually fits into the early development stages, proving preliminary concepts with small scale models and refining design with bigger models, before moving onto open water testing. As noted in section 4.2, the FloWave facility is designed for models around 1:40 to 1:10 scale, and so can be used for both concept and design validation, depending on the device specifications.

Model tests can be used to firstly validate the concept with simplified small scale models. Larger scale models are then used to further investigate and verify the design (Holmes

Table 3.2: Five stages of development, for marine renewable energy devices. (Adapted from Bahaj et al., 2008; Holmes, 2009; Holmes and Nielsen, 2010).

Stage	TRL	Nominal scale*	Typical infrastructure
1. Concept validation	1–3	Small scale (circa 1:50)	Small university laboratory
2. Design validation	3–5	Larger scale (circa 1:25–1:10)	Industrial scale laboratory
3. Systems validation	5–6	Sub-prototype size (circa 1:4)	Benign test site
4. Device validation	7–8	Approaching full size (circa 1:1)	Exposed test site
5. Economics validation	9	Full size, small arrays	Commercial site

*. Scales refer to WEC & TST models, for FOWT smaller scales are typically used at each stage given the larger size of the prototypes.

and Nielsen, 2010), looking at seaworthiness and survivability, development and optimisation of control strategies and power take off, plus investigating the mooring/anchorage subsystem. It is noted that scale and laboratory effects may be more significant at smaller scales, particularly that excessive hydrodynamic damping may result from sharp corners. Conversely, larger models offer the opportunity for on-board sensors which should offer less interference with floating vessels.

A similar incremental process is also recommended for resource assessment in Davey et al. (2010), using available data from existing atlases and wide area models for early development stages. Once projects progress further, more money can be spent on collecting actual site measurements for detailed assessment.

3.4.3 Increasing the complexity of test conditions

This incremental approach is also recommended in guidance for the selection of environmental conditions for tank testing, as discussed below. Initial tests should be made with simple conditions, before adding increased complexity. By adopting an incremental approach, it should be easier to obtain more general results from simplified early tests. Later, more advanced cases can be used to give additional understanding of device performance.

WECs and floating devices

The need for testing in both regular and irregular waves during WEC development was highlighted in Payne et al. (2009). Regular waves are useful to obtain an understanding of the device performance with a minimum of parameters to consider, just height, period, and possibly angle. They are commonly used to determine Response Amplitude Operator (RAO) and for validation of numerical models. To account for non-linear wave response, which may be easier to characterise with regular waves (Payne et al., 2009), it is also recommended that several wave heights should be checked at selected wave periods (ITTC, 2005*a*).

As regular waves do not capture the complexity of a real ocean, it is also important to test irregular (polychromatic) seas to better characterise device performance. This should include consideration of multi-directional seas and energy spreading, both of which may impact how much of the available energy a particular device can absorb. Even when testing more advanced models, it is good practice to use regular waves to check the response of the new model is similar to previous models (Holmes and Nielsen, 2010). Not all devices will respond to regular and irregular waves in the same manner, e.g. coastal structures such as perforated caissons and potentially some WECs, so it is important to test both regular and irregular waves.

For concept design stage, it is usual to test with long-crested waves to simplify the test design and analysis. Initially from a single direction, then considering waves at an oblique angle to the device. Short-crested waves with directional spreading should be considered later in the development process to obtain accurate estimates of power production, especially where WEC power production may depend on incident wave direction (ITTC, 2014*a*).

As well as understanding device performance, it is important to test survivability limit conditions prior to sea trials (ITTC, 2014*a*). This should consider the performance of both the hull(s) and moorings in extreme waves (Holmes, 2009). Given the limitations of facilities to generate large waves, it may be appropriate to adapt the smaller stage 1 model for testing survivability at stage 2 (Holmes and Nielsen, 2010). For devices in finite depth water, the difference in water depth resulting from astronomical tides, storm surge, etc. may change the shape of extreme waves, and thus water depth is an important paramter to consider. Inconsistent depth scaling is explored in more detail in section 7.2.

Tidal stream turbines

Whilst there is an obvious progression in the specification of waves for testing, this is not so straightforward when considering tidal currents, and is not covered in existing guidance.

An additional complexity is that the environmental conditions at tidal sites can be difficult to fully characterise, see section 3.4.4. For early stage devices, this may be compounded by the fact that deployment sites may not have been identified or licensed (ITTC, 2014*c*).

During more advanced tank tests for higher TRL devices, it is recommended that extreme tidal conditions should be tested (McCombes et al., 2010*a*). An example given is by adding large scale high intensity turbulence to the flow, although it is noted that scaling turbulence is problematic.

3.4.4 Specification of environmental conditions

A wealth of guidance exists on how environmental conditions in the ocean can be specified. Either specific to the marine renewable sector (such as Venugopal et al., 2011), or from other related sectors published by organisations such as the International Standards Organisation (ISO), American Petroleum Institute (API), and Det Norske Veritas (DNV), see table 3.3 (Ricci et al., 2009). These full scale conditions need to be translated and simplified to a matrix of tank scale conditions for testing, which will depend on the type of condition.

Table 3.3: Standards on physical environmental data description (Ricci et al., 2009).

Standard	Year	Description
DNV-RP-C205	2007	Recommended practices for environmental conditions representation
DNV-OS-J101	2007	Standard for offshore turbines. Recommendations on wave modelling
API RP 2A	2000	Design of fixed offshore platforms: Indications on waves and current representation
API RP 2T	1997	Tension Leg Platforms: Indications on waves and current representation. Wind spectrum description
ISO 19901-1	2005	Requirements for offshore structures. Recommendations on use of oceanographic data
ISO 21650	2007	Determination of wave and current actions on coastal structures

Waves

It is possible to generate both irregular and regular wave equivalents of the desired parameters in test tanks accurately. Historically, only uni-directional waves were possible, but most ocean basin facilities are now able to generate waves across multiple directions, providing realistic conditions for model testing.

It is common to test a range of regular waves, defined by height and period. These are often specified as a matrix, to tie up with industry standard power matrices (Holmes, 2009). Tests with regular waves can be quite short, allowing wide range of conditions to be tested in a relatively short time. A minimum run length of 10 cycles is given in ITTC guidelines (ITTC, 2005*a*), however some longer tests may be considered.

When testing irregular sea states, the test duration should be long enough to give a statistically representative sample. ITTC guidelines and procedures recommend a minimum length of 20–30 minutes (at full scale), or approximately 500–1000 waves, a well-established benchmark in tank testing (McCombes et al., 2010*a*). For survivability conditions, a three hour (full-scale) storm duration should be simulated. As mentioned in section 2.1.3, it should be noted that the maximum wave height is statistically a function of the number of waves, so longer tests will tend to give more extreme conditions.

For the creation of short-crested sea states, a cosine squared ($\cos^{2s}\theta$) spreading function is often used to describe the directional spread of the waves (ITTC, 2014*a*). Methods to estimate the spreading parameter s from site data are given in Payne (2008).

Currents

There is uncertainty of both the real-world flow field dynamics in energetic tidal channels where TSTs will be deployed, as well as how to reproduce these in test facilities once the flow is characterised. The local bathymetry of tidal channels can be complex and lead to localised conditions that may not be captured effectively (ITTC, 2014*c*).

The flow conditions that can be generated is specific to the type of facility, e.g. towing tank, cavitation tunnel, offshore basin, etc. ITTC (2014*c*) advises these conditions should be documented, including:

- Flow speed and direction;
- Spatial uniformity, including blockage effects and vertical flow profile;
- Steadiness and turbulence characteristics.

Turbulence is commonly described by a single 'turbulence intensity' parameter, but length scales are also important to characterise small and large scale fluctuations within the flow. Many facilities are only able to change the mean flow velocity, but cannot easily adjust turbulence or change the vertical flow profile. Generation of small scale turbulence may be possible in some facilities by introducing a grid or other structure upstream of the turbine (ITTC, 2014*c*).

Combined Conditions

There is limited guidance on the specification of combined wave-current conditions, however ITTC guidance for floating platforms (ITTC, 2005*b*) recommends that the wave spectrum is calibrated in the presence of current, i.e. the combined conditions are recreated.

The presence of waves will alter the flow field and impact on submerged device loadings. A wave-current tank should be used to study this, although may present challenges for scaling TSTs (ITTC, 2014*c*). It is possible to test with waves in a tow-tank or apply an oscillatory motion to the device foundation, however this will not produce the correct distribution of velocities across the rotor plane (ITTC, 2014*c*).

Directionality

The influence of directionality of the environmental conditions should be considered for all devices that are not rotationally symmetrical. The moorings/foundation for the device should be considered when assessing symmetry as these are usually sensitive to direction. For example, the moorings of an axi-symmetric point absorbing WEC may still be sensitive to the predominant wave direction (Holmes and Nielsen, 2010).

3.4.5 Key Limitations of Guidance

As noted above, existing published guidance does not offer detailed recommendations for testing in the advanced environmental conditions now possible in facilities such as FloWave. These include multi-directional multi-modal waves, as well as combined waves and currents at various relative directions.

Although the issue of directionality is mentioned in guidance, it may not be given sufficient importance when developing test plans. This may result in discrepancy between predicted and observed performance when devices are deployed at sea. Directional spectra have increased complexity in terms of documenting, generating, analysing, and interpreting model results (ITTC, 2005*a*), which may partially account for directionality being neglected.

The uncertainty of both measuring and re-creating complex real-world turbulent tidal flows was highlighted as an issue in Germain (2008), and this still remains an area with little published guidance. Recent studies, such as those conducted under the ReDAPT project (Sellar et al., 2015), are providing promising site specific information based on spatially rich, high-resolution velocimetry, that may in future be used to define test conditions.

PART **II**

Characterising FloWave — currents and combined wave-current

CHAPTER 4

The FloWave tank and characterisation methods

Chapter summary

- Specifications of the FloWave facility, including terminology and coordinate systems, plus how waves and currents are generated and measured in the tank.
- Details of the instruments used for wave and current measurements at FloWave, and an outline of instrument set-up used for this project.
- Summary of test procedures and practicalities for running experiments at FloWave, including data acquisition and analysis of results.

4.1 Introduction

This chapter summarises the methods and instruments used for the tank characterisation part of the project. Each test had specific requirements based on what was being measured, but was also dictated the availability of instrumentation. A general description of the facility and methods used is given in this chapter, with further details, results, and discussion in the following two.

In order both to characterise the facility and to gain meaningful output from model tests, it is required to measure the relevant properties of interest. To characterise the tank capability, these are primarily wave height/water surface elevation and current velocity. There is also a wide range of other instrumentation including Qualisys motion capture, load cells, etc. available and used for the test programmes undertaken in the facility. Further discussion of their use is outwith the scope of this project.

Data used to characterise the current and wave-current interactions came from two main sources. Firstly, a number of measurement campaigns were designed specifically to collect data for particular aspects of the current characterisation and exploration of wave-current interactions in the tank. Additionally, data from other test campaigns was used opportunistically where possible. These included a PhD on oblique wave and current loading on a Tidal Stream Turbine (TST), plus other internal FloWave projects.

4.2 The FloWave Ocean Energy Research Facility

4.2.1 About the facility

The FloWave Ocean Energy Research Facility is a circular combined wave and current test tank. Located at the King's Buildings campus of The University of Edinburgh, it was opened in 2014.

The tank is optimised for waves of around 2 s period, and is capable of generating currents of 1.6 m/s. This offers the ability to model metocean conditions for most renewable energy devices at typical scales around 1:20 to 1:40 (Ingram et al., 2014). The unique design features of the facility remove any inherent limitation on both wave and current direction, enabling the recreation of complex directional sea states in combination with current. Generation of these conditions is discussed in the following sections. Having control over wave and current directions means that a model does not need to be repositioned to test different angles.

There are 168 active-absorbing force-feedback hinged wavemaker paddles around the entire circumference of the tank, as shown in fig. 4.1. These are able to generate regular and irregular waves, both long-crested and multi-directional, as well as complex multimodal sea states with waves from multiple directions.

Currents are generated by 28 impeller units mounted in the plenum chamber below the test floor. Turning vanes mounted below and in front of the wavemakers direct current across the tank, as shown in fig. 4.1, but allow the wavemakers to operate in a zone of relatively still water (Robinson et al., 2015*a*).

There is a 15 m diameter buoyant floor in the centre of the basin, which notionally represents the test area. This floor can be raised to just above the water level to facilitate model installation and reconfiguration as required, then submerged to working depth. It is only possible to generate waves or currents with the floor in the fully lowered position, so it is not possible to adjust the water depth in the test section.

The water depth in the test area is 2.01 m ±0.01 m with the wavemakers powered on. When testing with only currents, the wavemakers are generally powered down and rest on their backstops, with the paddle face approximately 20° from vertical. This results in the water level in the tank dropping by 84 mm, to 1.93 m.

Water temperature during the tests was approximately 17 °C, varying slightly by season.

The tank machinery, including wavemakers, drive units, and control system were supplied and installed by Edinburgh Designs Ltd. (EDL). The wavemakers and control system are based on a standard EDL components, albeit modified for the unique circular arrangement at FloWave. The design of the current drive system and turning vanes is based on research at The University of Edinburgh (Robinson et al., 2015*a*,*b*).

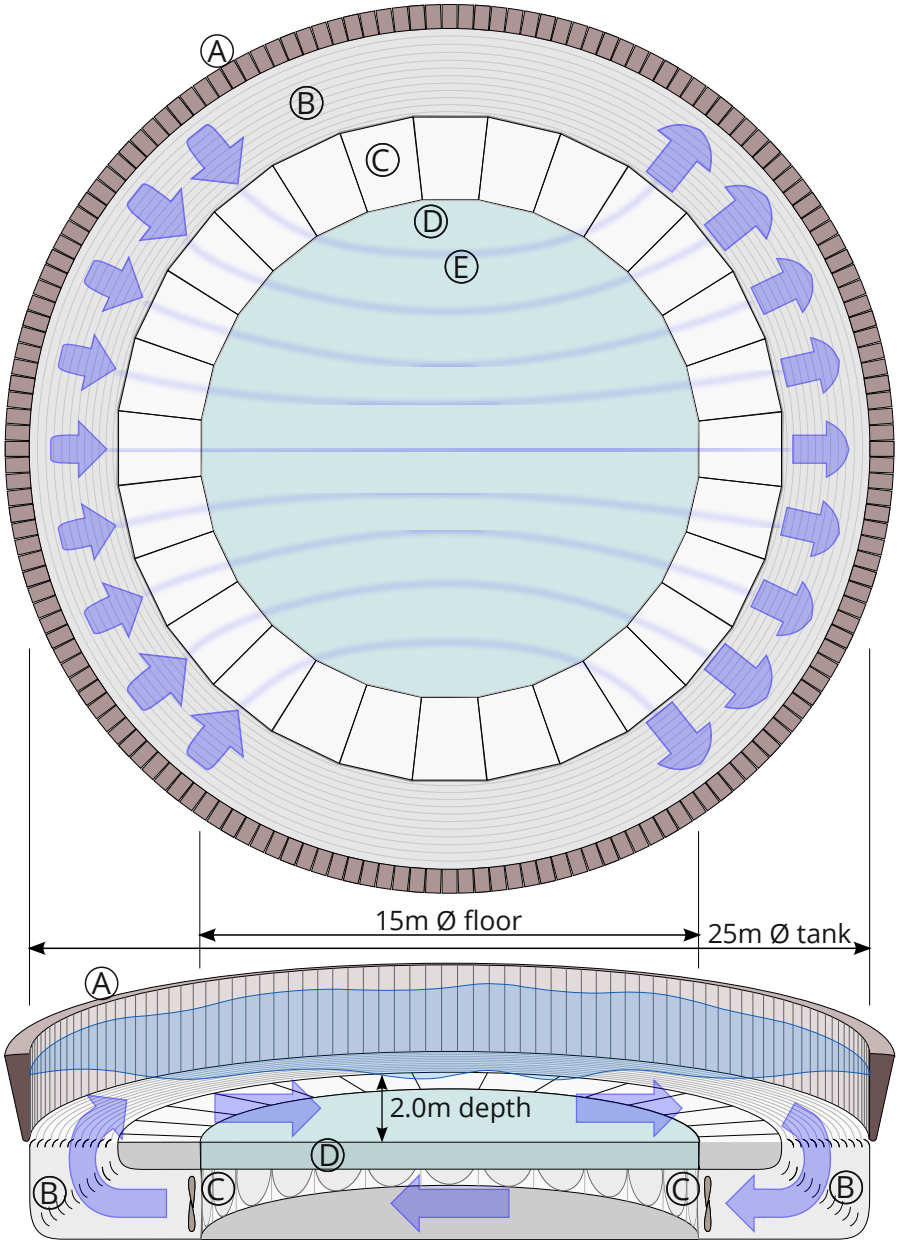

Figure 4.1: Schematic of FloWave in plan and oblique section showing:
- (A) Wavemaker paddles around circumference (168 Nr)
- (B) Turning vanes and flow conditioning filters
- (C) Current drive impeller units (28 Nr)
- (D) Buoyant raisable floor (15 m⌀) below test area
- (E) Idealised streamlines of flow across tank floor.
  Indicative flow recirculation shown by blue arrows.

4.2.2 FloWave terminology and coordinates

The FloWave building consists predominantly of the 'tank hall'. At the west end of the building office accommodation is located on the first floor, with workshop and plant facilities below. The tank can be operated from either of two control desks, one located in the office, or more generally when running tests from a computer at tank side.

The tank coordinate system is Cartesian, as shown in fig. 4.2. The origin is located at tank centre on the test floor with $+Z$ positive upwards. The $+X$ axis is defined from the tank centre towards the back of the building, away from the office and control desks. Rotations are positive anti-clockwise. Coordinates are subsequently referred to in short as (X, Y) or (X, Y, Z).

Waves and current directions are specified positive in the propagation direction, as opposed to the nautical convention of waves coming from a direction. Currents flow from 'upstream' to 'downstream', with left and right assuming a viewpoint looking downstream in the direction of the current. The tank is rotationally symmetrical, meaning the 'centreline' is the diameter in line with the direction of wave or current propagation.

A movable instrument and access gantry spans across the full width of the tank, which can traverse along the tank X-axis, supported by trusses on either side of the tank. This is used to provide access onto the raisable floor for model installation, as shown in fig. 4.3. The gantry is fitted with aluminium sections top and bottom on both sides, which are used to affix instruments etc. It is also possible to fit a movable carriage that can traverse

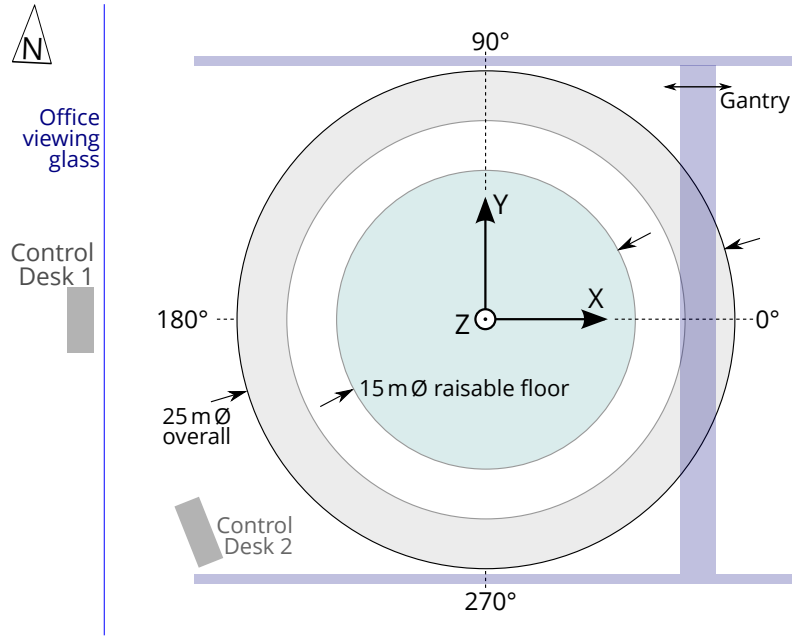

Figure 4.2: Tank reference coordinates.

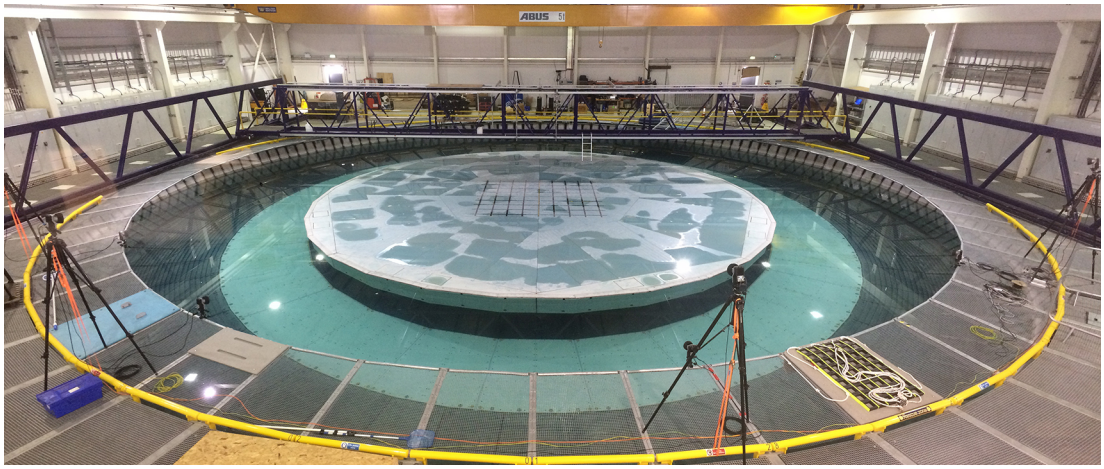

Figure 4.3: Photograph of tank with floor up, looking from office control desk, and showing: 5 tonne gantry crane at back of tank hall; Access and instrumentation gantry towards rear of the tank with temporary ladder onto floor; Edge protection cantilevered over the tank inside circular yellow bump rail; and Qualysis motion capture cameras are mounted on the four tripods in the foreground.

the tank Y-axis. The gantry underside is approximately 1 m above the water surface, 3 m above the test floor. The facility is also fitted with a 32 m span 5 tonne capacity gantry crane that can be used to move models and other equipment around the tank hall.

There is a pattern of attachment points spaced across the raisable floor, to which models, instruments, or cables can be bolted. These are covered when not in use, to maintain uniform flow. For testing loads on bed mounted devices, a 6-DoF load cell can be installed within the floor with the top surface flush to limit the hydrodynamic impact. This can be positioned at two locations in the tank, $(-1.6, -0.5)$ and $(1.6, 0.5)$.

Above the wavemakers and level with the tank hall floor is the 'edge protection', fabricated from framed steel mesh. This frame is occasionally used as an attachment point during testing, e.g. for mooring lines.

4.2.3 Generation of currents at FloWave

Currents across the FloWave basin are generated by a subset of the 28 drive units. Each of these units contains a single 1.7 m diameter low-solidity 5-bladed symmetrical impeller driven by a 48 kW motor, sitting within a flow diffuser (Edinburgh Designs Ltd, 2014). Turning vanes mounted below and in front of the wavemakers direct current across the tank, with the flow returning via the plenum chamber as shown in fig. 4.1. These turning vanes incorporate porous screens to provide flow conditioning and prevent debris ingress to the plenum chamber.

As described in Robinson et al. (2015*a*), the inlet turning vanes were designed both to allow the wavemakers to operate in a region of relatively still water, and to produce a

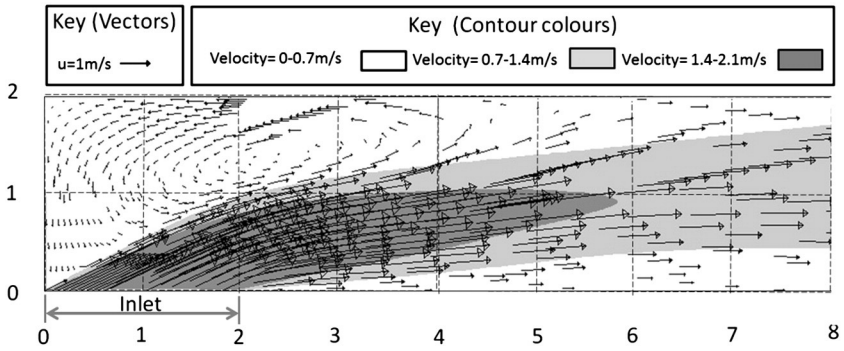

Figure 4.4: Design stage CFD model of inlet vanes, showing higher velocity jet and recirculation zone. Vector and contour map around the inlet for a 25° isolating inlet flume simulation (Case 2E). Velocity is proportional to vector length and contour colour. (from: Robinson et al., 2015*a*). Note that geometry shown does not match final FloWave design.

developed flow profile with low turbulence over a short distance. To achieve this, a jet of higher velocity water is directed at an angle through the turning vanes, which develops into the desired flow profile in the tank centre. As the tank floor is constructed from smooth plastic, the flow profile is predominantly generated by the turning vane geometry rather than through bed roughness.

The developing jet can clearly be seen on both the design stage Computer Fluid Dynamics (CFD) modelling, fig. 4.4, and measurements of the constructed FloWave tank, see section 5.3. Another consequence this jet of water has is the formation of a recirculation zone above the inlet, which can affect the wave-current generation (section 6.2).

Creating a horizontally uniform current in a circular tank is a non-trivial matter, requiring precise control of the individual impellers (Robinson et al., 2015*b*). In summary, the impeller units on either side of the required current direction on both upstream and downstream sides of the tank are driven at varying speeds. A transfer function sets each individual drive motor rpm, based on the input rpm from the control software and flow direction in the tank. Drives at ~45° to the flow direction are driven at 100% of the input rpm set in the control software. Those in line with the flow direction are driven at a reduced rate, and drives to the sides not driven, as described in Robinson et al. (2015*b*). This is shown indicatively by the flow arrow size on fig. 4.1, and by flow velocities at each drive on the design stage CFD modelling, fig. 4.5. The relative rpm for each drive is not changed for different conditions, with only one transfer function used.

Assessment and modification of the motor transfer function was outside the scope of work for this project, but may be considered in future.

The control system for the impellers incorporates feedback to ensure the desired rpm is reached. It also includes the facility to change current direction during a test, either to an arbitrary angle or rotating by a set angle every minute. This capability allows for the

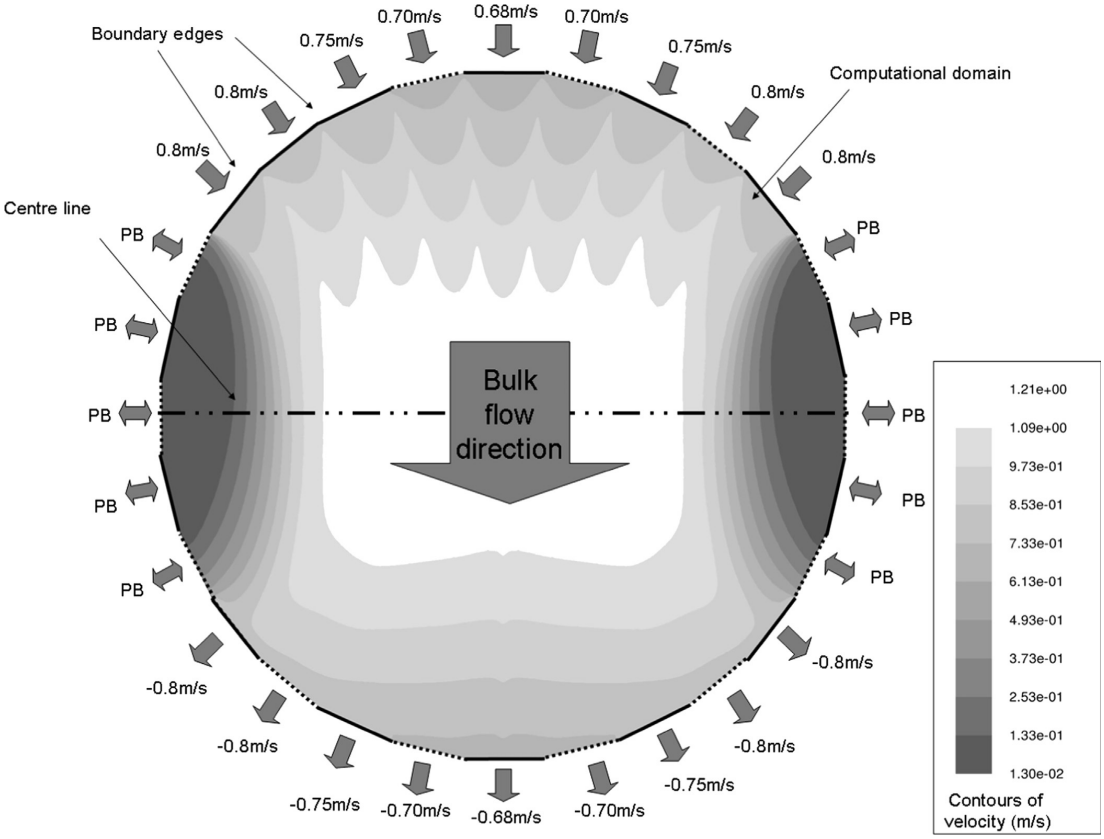

Figure 4.5: Design stage CFD model of motor control, showing individual drive velocities and predicted variation across tank. Computational domain superimposed on contours of velocity magnitude plot, the ideal array test area is the white contour at the centre of the tank. (from: Robinson et al., 2015*b*). PB refers to a pressure boundary, i.e. an unpowered drive unit. Note that geometry shown does not exactly match the final FloWave design.

simulation of cross-currents, or a tidal ellipse, without having to reposition the device model. The flow characterisation presented in chapter 5, shows that a predominantly straight flow can be achieved in any direction across the central test area, and the flow is rotationally symmetrical.

4.2.4 Wave generation and absorption at FloWave

Waves are generated by 168 hinged paddles around the 25 m diameter tank. These produce deterministic waves, providing a very high degree of repeatability in the wave conditions (Ingram et al., 2014). More complex waves are created by superposition of waves as discussed in section 2.1.3. A series of regular wave 'fronts' of the desired amplitude are produced with unique frequency and direction, each at a pseudo-random phase, combining together to produce the required sea state. Using this pseudo-random phase (i.e. deterministic wave generation) means that a particular sea state is repeatable in the tank by choosing the same seed number.

Unlike more traditional tanks, FloWave does not have any 'beaches' to dissipate wave energy, instead relying on the paddles to absorb the waves. This is done by generating an inverse wave, effectively cancelling out the incoming wave. The paddle control software is based on a combination of force-feedback and position control (Edinburgh Designs Ltd, 2014). The paddles are told what wave conditions to expect based on a simulation of the tank, but also respond to measured water pressure on the paddle. Reflections may occur when waves travelling across the tank are not fully absorbed by the paddles on the opposing side of the tank, as characterised by Draycott (2017), see section 3.2.3.

The reflected waves may be re-reflected across the tank multiple times in the worst case. The paddle absorption effectiveness was found to decrease for waves $\gtrsim 1$ Hz, and the circular geometry of the paddles leads to curved reflections (Draycott, 2017). The tank typically reaches an acceptably quiescant state, where the reflections have decreased sufficiently, after a period of around one to five minutes. Methods to expediate dampening of reflections in the tank are being considered at FloWave, as part of ongoing research. The presence of a current can alter the time it takes for reflections to dissipate significantly. Higher frequency reflections can be blocked by, or become trapped in, an opposing current. Conversly, a following current may sweep reflected waves away from the test area, reducing the time for the tank to settle.

The control input for each individual paddle is generated by the Edinburgh Designs 'Njord runtime' software*. This is based on wave conditions that can be programmed in the 'Njord wave synthesiser' (Edinburgh Designs Ltd, 2016*b*). These can be regular waves specified by T, H, θ, or irregular waves spectra such as JONSWAP with T_p, H_{m0}, γ, s, θ. The Njord runtime software also has the capability to run a number of wave conditions sequentially in batch mode, with a defined wait time between to allow the tank to settle back to a calm state. An empirical 'tank transfer function' relates the control software input to the wave height produced in the tank. For best performance, individual sea states are calibrated by measuring the conditions actually generated in the tank and adjusting the input accordingly, based either on the total or incident wave spectra.

Directional Sea State Generation

Directional wave spectra are generated at FloWave using a deterministic approach. As explained in Draycott et al. (2016), a single-summation rather than double-summation method is used. This avoids a phenomenon called phase-locking (Miles and Funke, 1989), whereby waves with the same frequency but different directions interact and cause spatial patterns, resulting in a non-ergodic wave field. To avoid phase-locking, initial frequency increments ΔF can be split further, into sub-frequency increments $\delta f = \Delta F / N_\theta$

*. The Njord software is named after the Norse god of the sea Njörðr

(Pascal, 2012), shown in fig. 4.6. These new frequency increments, within the original frequency bins, each have a unique wave propagation direction. When analysing results in the frequency domain, each measured component amplitude $A_i(f_i, \theta_i)$ can thus be identified and operated on individually, although only if the FFT bins match the generation frequencies. Using a single-summation generation approach therefore facilitates measurement of the sea state, and is key for implementation of the correction method described in section 6.5.

As an example, the directional sea states used for the wave-current observation and correction (sections 6.3 and 6.5) have a repeat time T of 2048 s, defining the sub-frequency increments δf to be $1/2048$ Hz. In order to achieve the desired frequency increments, the scaled spectrum was interpolated to create 64 frequency bins between 0 Hz and 1 Hz, and 32 directional bins from 0 to π, covering the region with significant energy content in the directional spectrum ($N_f = 64,\ N_\theta = 32$). Re-defining the directional spectrum for use in the single-summation method gives the required frequency increments of:

$$\delta f = \frac{\Delta F}{N_\theta} = \frac{1}{N_f N_\theta} = \frac{1}{T} = \frac{1}{2048}[\text{Hz}] \tag{4.1}$$

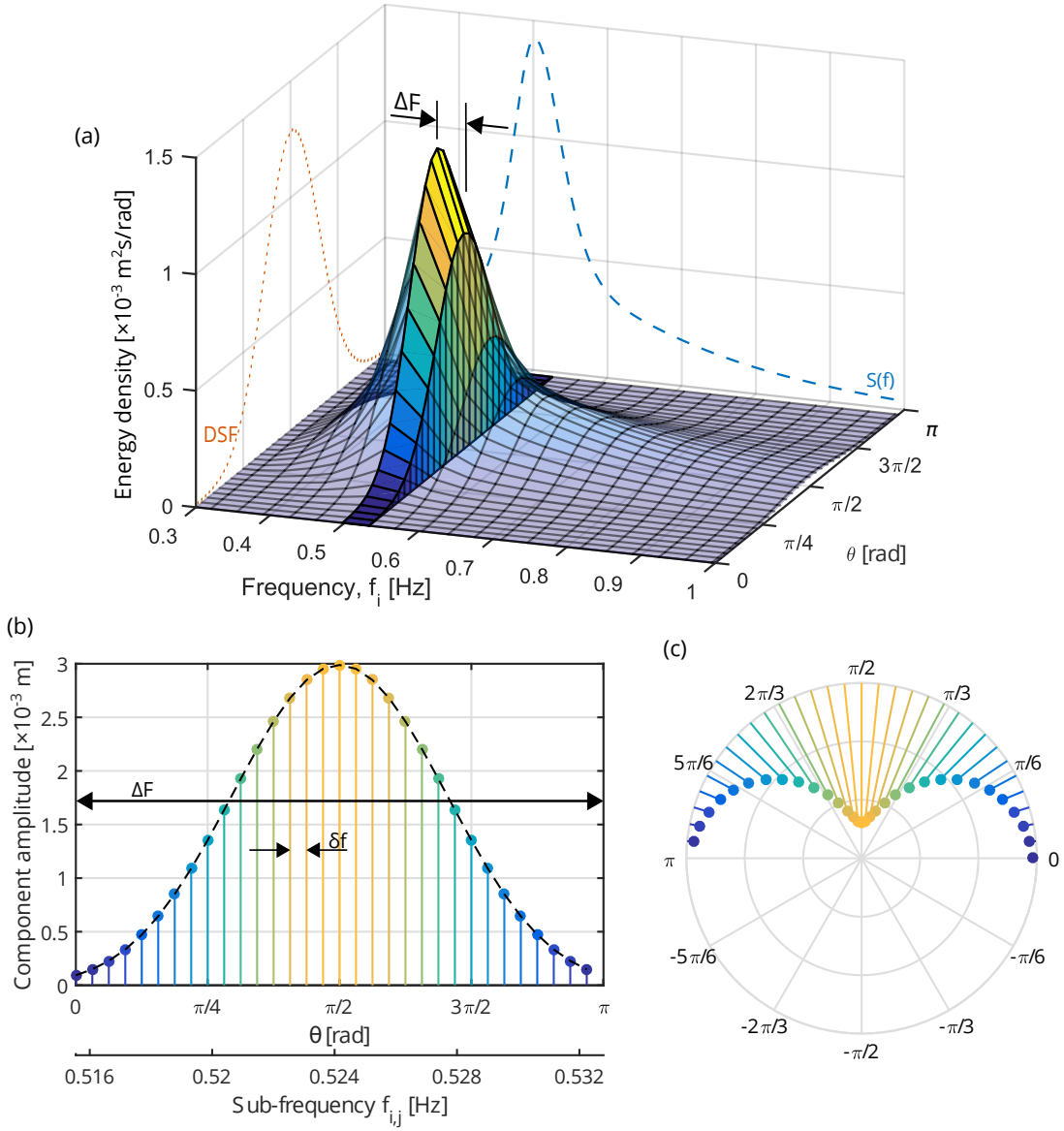

Figure 4.6: Schematic discretisation of a directional spectrum using the single summation method and subsequent recreation in the tank. Panels show (a) the directional spectrum highlighting the frequency bins ΔF, with frequency spectrum $S(f)$ and directional spreading function DSF shown, (b) how the sub-frequency bins δf are split across direction for each ΔF frequency bin, and (c) indicative representation of how this directional spread is created in the tank.

4.2.5 Tank limits and performance constraints

There are physical limits on the waves and currents that can be generated in the tank. There are also operational 'soft limits' on those conditions typically generated, within the physical limits, that are based on operational experience. For waves or currents alone, these are relatively well-defined, and are discussed below. For combined wave-current conditions, the tank limits are more complex and were not fully understood at the beginning of this research project. Generation of combined conditions is considered in more detail in section 6.2.

As part of this research project, quality metrics have been developed to quantify the tank performance for different conditions. This is discussed further in section 7.3.

Wave generation and absorption

At FloWave, the nominal wavemaker generation range is 0.2 Hz to 2.0 Hz (0.5 s to 5 s period). There is no specific physical limit on the lowest paddle frequency, although the maximum wave amplitude that can be generated is a function of how much water is moved by the wavemaker. This imposes a practical limit on the waves that can be produced. At high frequencies, the physical limitation is based on the paddle motion and how quickly they can respond. Although the upper generation limit is 2.0 Hz, in practice however, the wavemakers do not reliably absorb waves of $\gtrsim$1 Hz (Draycott, 2017). A low pass cut-off is often employed on frequency spectra to limit the build-up of unwanted reflections in the tank. The 'soft' operational limits for the wavemakers are shown in fig. 4.7 for regular and long-crested irregular waves. These limits are based on wave steepness, and represent the nominal range of waves that can be well gener-

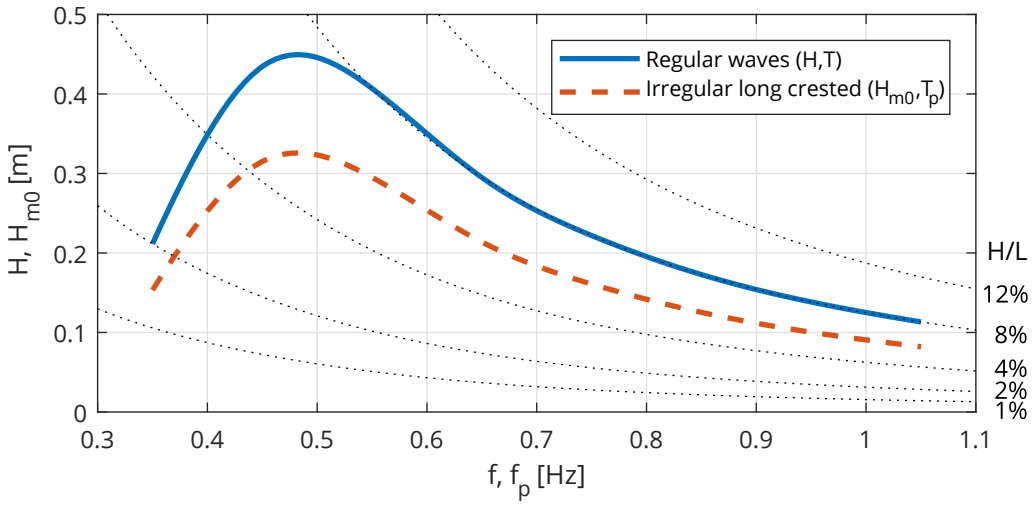

Figure 4.7: FloWave wavemaker operational limits (March 2016). Dotted lines are contours of constant wave steepness H/L.

ated and absorbed by the tank. The limits were set on a precautionary principle, with the envelope of waves run increasing as more is learnt about the performance of the facility. For conditions close to or outside this nominal operating envelope, it is possible to incrementally increase wave height, checking at each stage that the tank can safely generate and absorb those waves. This is particularly important for combined wave current conditions where the tank performance is less well understood.

As discussed in section 3.2.3, the wavemaker characterisation (Draycott, 2017) found reflections in the tank to be curved, focussed by the circular geometry of the tank. The reflections lead to the formation of standing waves in the tank, with patterns of constructive and destructive interference.

In addition to reflections from the absorbing paddles, there may also be reflections radiating from any model(s) in the tank. It may be advantageous to measure these reflections in order to understand device performance.

Current and turbulence

The design specification for FloWave was to produce a 0.8 m/s current. Specifications for the drive units allowed for additional flow conditioning to be added if required. They are therefore capable of generating much faster flows, of up to ~1.8 m/s in the tank centre. At higher velocities (particularly $\gtrsim$1.2 m/s), the flow becomes less suitable for conducting tests. A soft limit of 1.2 m/s is therefore usually applied when testing with currents only.

The method of generating currents in a circular tank creates spatial variation in the flow as shown by the characterisation in chapter 5. This is discussed further in section 5.5, including implications for testing.

At present, it is not possible to control the level of turbulence in the tank independently of flow velocity. There is variation in the flow characteristics throughout the test volume. It may be possible to take advantage of this, although noting there are many other constraints on testing, as discussed in chapter 8. Future research may investigate methods of controlling and/or introducing turbulence within the FloWave basin, however this is not planned at present.

4.3 Measurement instrumentation

4.3.1 Wave measurement

Wave measurements at FloWave are made using multiplexed resistance-type wave gauges (Edinburgh Designs Ltd, 2016*a*). These are arranged in various array layouts depending on test requirements. A maximum of 16 gauges can be connected via two control boxes. Data from the wave gauges is recorded by the tank control software, at either 32 Hz, 64 Hz or 128 Hz depending on the test requirements.

Two methods of mounting wave gauges are typically used at FloWave, depending on the array requirements:

1. Mounted directly onto instrumentation gantry, with locations and spacing between gauges set for each specific test.
2. Mounted on an adjustable array frame, described in Draycott (2017). For most tests where directional measurements were required, a standard wave gauge array layout (WA1, fig. 4.8) was used (Draycott, 2017, §3.4). This can be located at different points in the tank, although it was located at the tank centre for all tests described here.

Where directional wave measurement was not required, the gauge spacing was typically equidistant (WA2, WA3, fig. 4.8) or based on a Goloumb ruler (WA4, WA5). The marks on a Goloumb ruler are such that the distances between every pair of marks is unique (Weisstein, 2017), which is useful for wave reflection analysis. Although analysis of reflections was not required for this project, results from tests using these arrays were used in other studies necessitating this type of array.

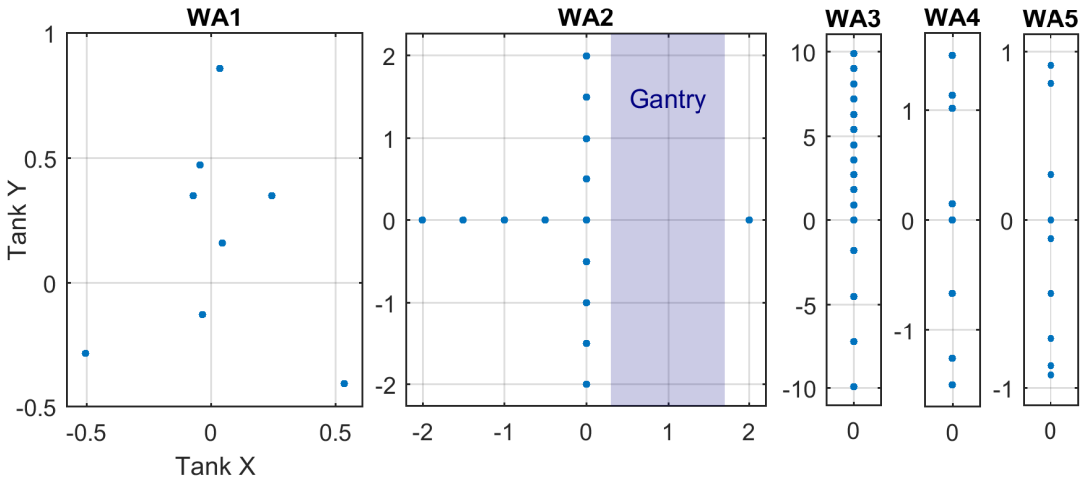

Figure 4.8: Wave gauge array layouts used in testing, (WA1) directional array (Draycott, 2017), (WA2, WA3) equidistant spaced cross and long array, (WA4, WA5) linear reflection arrays.

In all cases, the gauges were set such that still water level was approximately mid depth on the probe. Results were monitored to check that no clipping had occurred, e.g. the wave crest over-topped the gauge. The x, y locations of each gauge were recorded relative to tank coordinates for every set-up.

Directional Wave Measurement

Using the directional wave gauge array, a Phase-Time-Path-Difference (PTPD) approach (Fernandes et al., 2000; Esteva, 1977) is used to calculate component angles and directional spectra. Draycott et al. (2016) has shown this method to be a highly effective approach for measuring directional spectra when combined with the single-summation wave generation used in FloWave. For measuring directional wave characteristics in currents, this approach has also found to be much more effective, as discussed in section 6.5.

4.3.2 Flow measurement

Flow measurements in the tank were primarily undertaken with two types of point measurement instruments, Electro-Magnetic (EM) current meters and Acoustic Doppler Velocimeters (ADVs), based on instrument availability and what was being measured.

Electro-Magnetic (EM) current meters

The flow of water can be measured using the phenomenon of electro-magnetic induction, using EM current meters. These instruments generate an electro-magnetic field using a wire coil, in which a voltage is induced by water moving past it. According to Faraday's principle, the induced voltage is the vector product of the velocity and the magnetic field (Kanwisher and Lawson, 1975; Shercliff, 1987). The flow can therefore be determined by measuring this voltage.

A key advantage of EM current meters over other techniques including ADV and Particle Image Velocimetry (PIV) is that they measure the water movement directly, rather than the motion of suspended particles which must be assumed to move with the water.

Valeport EM current meters were used for some of the early flow measurements, with both single-axis (model 801) and dual-axis (model 802) instruments used. For tests with the Valeport 801 EM current meter, a flat-type sensor head was used which has a cylindrical sensing volume approximately 20 mm$\varnothing$ × 10 mm high (Valeport, 2011*a*). The 2 Hz raw ASCII text output from the Valeport control display unit was logged directly to a laptop for further processing. The Valeport 802 EM current meters were fitted with a 32 mm discus-type sensor head, for which the sensing volume is a cylinder of approximately 32 mm$\varnothing$ × 16 mm high (Valeport, 2011*b*). The raw ASCII text output was again

Figure 4.9: [Photographs of example EM meter mounting, showing (left) Valeport 801 and (right) two Valeport 802 sensors for the horizontal variation tests.

logged, either at 8 Hz or 16 Hz, although this can also be logged through the data acquisition system.

The EM sensors were mounted to the gantry, using a height- or position-adjustable bracket made from square profiled aluminium section, see fig. 4.9. The sensor cable was tucked into the section profile or helically wrapped around the supporting pole to try reduce effects of vortex induced vibration. A small degree of lateral vibration was observed during some tests, with the sensor head moving by approximately ±10 mm at around 1–2 Hz, however it is not anticipated that this will affect the averaged inline velocity calculated from the data.

Acoustic Doppler Velocimeters (ADV)

Nortek Vectrino ADVs were also used to measure flow velocities in the tank. These operate by emitting a single acoustic pulse into the water. This pulse is reflected by particulate (termed back-scatters) in the water, assumed to be moving with the same flow speed, and the reflected pulse is detected by four angled transducers. The pulse is Doppler shifted according the flow velocity, and the four transducers allow the measurements of four flow components which can be transformed into a Cartesian u,v,w coordinate system (Nortek, 2013).

Table 4.1: Vectrino settings used for each measurement campaign.

Test campaign	Sample rate [Hz]	Velocity range [m/s]	Cell size [mm]	Pulse length [mm]	Nr. cells
Rotational symmetry	100	1.4–1.7	4.0	4.0	1
Turbulence measurements	100	0.8–1.6	0.3	0.3	5

For the majority of measurements, including the turbulence characterisation (section 5.4), a Nortek Vectrino Profiler was used. This instrument is capable of sample rates up to 100 Hz and can also measure at multiple cells within a space of 30 mm (Nortek, 2013).

Settings for an ADV are a trade off between minimising bad data and maximising resolution. One key metric in assessing data quality is the pulse to pulse correlation. The minimum pulse length and cell volume were selected to keep a mean correlation >95%. The velocity range was also monitored in order to keep it to the minimum value without velocity wrapping occurring due to high velocity spikes. Settings for the various measurement campaigns are given in table 4.1.

For the ADV measurements to be accurate, it is important that the water contains a sufficient quantity of back-scatters. Low particle density will result in weak signal returns with low associated correlation values and high uncertainty. The tank was initially tested unseeded, and correlations found to be $\lesssim$70% which was deemed unacceptable. Glass micro-beads of nominally neutral buoyancy were added to the tank until average correlation on all four beams was >95%. When the facility had not been operated for an extended period, e.g. overnight, it was found that correlation dropped. Running the tank at a medium-high velocity with the flow rotating through ~45° angle redistributed the seeding effectively, and correlation rose back to acceptable levels. The correlation was monitored throughout testing and where this dropped too far, further seeding was added or the velocity increased for a period to mix up seeding present. Signal to Noise Ratio (SNR) is a measure of the acoustic signal strength relative to the background noise level. For the Vectrino Profiler, SNR should be ~30 dB in the central region of the profile, dropping to ~20 dB at the extremities (Nortek, 2018). During tests, SNR was also monitored, with typical values of 25 dB to 35 dB, although occasionally dropping as low as 20 dB. The adaptive ping algorithm was used to minimise accoustic interference, as recommended by Nortek guidance.

For most tests with the ADV, including the turbulence measurements, it was attached to the gantry via an adjustable support frame, made from 45 mm square aluminium section. The support frame was mounted vertically, fixed to the gantry at two points 2 m apart, as shown in the schematic fig. 4.10. The instrument was typically mounted so that the ADV data used the same coordinate system as the tank where velocities u, v and w correspond to directional vectors X, Y and Z.

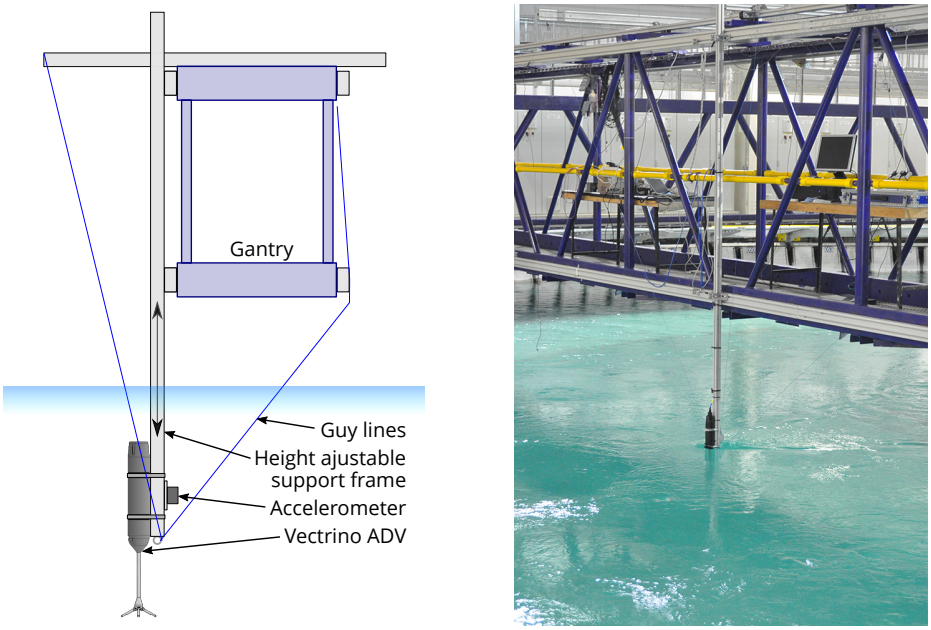

Figure 4.10: (left) Vectrino mounting schematic (not to scale), showing ADV with associated supports, accelerometer and instrumentation gantry. (right) Photo during testing with Z=1.4m.

4.3.3 Calibration

For the velocity measurement instruments, EM and ADV, the calibration is pre-set. The instruments are returned to the manufacturer periodically for checking and re-calibration, with no significant discrepancies identified during the research period.

Resistance-type wave gauges are simple and robust, but require recalibration as the measurement is susceptible to changes in the conductivity of water, a function of temperature (Lawrence et al., 2012; Clayson, 1989). Fryer and Thomas (1975) state that conductance in fresh water changes by about 2% per °C change in water temperature. Measurement of the FloWave tank shows fluctuation in water temperature of order 0.1 °C over the course of a day.

Calibration of the wave gauges at FloWave is typically undertaken every day prior to taking measurements. This allows any long term drift in the gauges to be corrected for. The vertical position of the wave gauge is adjusted vertically by set amounts, altering the immersed length. The electrical resistance is measured at each point, and used to set a transfer function. A software check is undertaken on the linearity of measurements, which should pick up instances of bad calibration, e.g. due to user error in setting elevation points. For most tests at FloWave, a three-point wave gauge calibration is used. If greater accuracy is desired, a five or seven point calibration may be undertaken. Where the gauges have to be fixed in place, a two-point calibration is used, making use of the 84 mm water level increase when the wavemakers are powered on (section 4.2). A comparison between the two and three point calibration showed $< 0.5\%$ difference.

4.4 Conducting and analysing tests

4.4.1 Test practicalities and procedures

There are a number of practicalities that need to be considered when running tests in any facility. Many of these are specific to the tank and its associated infrastructure, but are covered by wider tank testing guidance, as discussed in section 3.4.

Considerations for testing with different environmental conditions

Individual test length is often set as an integer power of two seconds ($t = 2^n$) to facilitate generation and/or analysis using Fast Fourier Transform (FFT). Additional time may be allowed at the start of a test to allow waves to propagate across the tank and reach a steady state.

Sufficient time is also required between wave tests, for reflections to die down and the tank return to an acceptably quiescent state. This is a function of frequency and amount of energy in the sea state. Typically at FloWave, settling time between tests is 3 to 5 minutes. It can be 10 minutes or more however, if there are specific requirements for a very still tank at the start of each test.

When testing with currents, sufficient time needs to be allowed for the current to stabilise in the tank after changing flow velocity or direction. If the flow velocity is not actively being monitored during the test, then a conservative estimate is allowed. This is typically 10 minutes, based on the temporal stability analysis (section 5.2.2).

There are additional considerations when running combined wave-current conditions. Primarily it is important that the tank can safely run with the desired conditions. The other key consideration is whether the combined conditions can physically exist, and the waves do not break or become blocked as a result of the current, as discussed further in section 6.1.

Potential sources of error in wave gauge measurements

There are potential sources of error in all measurements that should be considered. As an example, the wave gauge measurements are considered below. As noted in section 4.3.3, resistance-type gauges are sensitive to the conductivity and temperature of water. With a large volume in a below-ground-level basin, the water temperature in FloWave is fairly stable. This error is thus likely to be ~0.2%. To limit the impact of water surface meniscus, it is best-practice to wet the wave probe before use.

To maintain correct spacing between the two rods of the wave gauge, and to limit bending of the gauges, they are constructed from stiff metal rods with a larger diameter used

for longer gauges. Using the wave gauges in currents can result in bending of the gauge, plus run-up of water on the upstream side with a drop on the opposing side. The deflected angle is small, therefore the immersed length does not change significantly.

Positioning

Positions of instruments such as wave gauges of velocity meters are recorded relative to the global tank coordinates, section 4.2.2. The location of the instrumentation gantry (tank X) is measured using a laser range finder. Although it is not possible to pre-set a desired location for the gantry, it is possible to position it to ±10 mm of the desired location, with this position measured ±1 mm. Measurements along the gantry (tank Y) are made from a point in the centre at $Y = 0$. Positioning of model mooring points etc. on the tank floor is via an array of fixing points with known coordinates.

Instrument positions in the tank were recorded with ±1–2 mm accuracy in X, Y, Z. As the measured quantities vary relatively slowly with position, this position discrepancy will not result in significant error in the measurement value. The largest change in the spatial variation of velocity measurements (section 5.3) was ~0.01 m/s over 50 mm when measuring a flow of ~0.8 m/s, or ~0.025% per mm offset. For the wave reflection analysis (Draycott, 2017), the measured change in wave height is a function of both frequency and location in the tank relative to the reflecting boundary. For a typical 0.6 Hz wave in the central region of the tank, the maximum discrepancy in wave height due to reflections may be ~±15% over a distance $L/4 = 1.1$ m. This is of similar order (0.03% per mm offset) to the velocity measurements.

Where very accurate measurement of instrument position is required, or the location and orientation of a device model is important, a Qualysis motion capture system can be used to record this during set-up and tests. Qualysis measurements were not used for any of the tests used for this research.

Data acquisition

Several Data Acquisition (DAQ) systems are used to log measurements in the tank.

- The tank control software is used to log the tank trigger(s), wave gauge data, and diagnostic information on paddle response.
- A National Instruments (NI) DAQ is used to log voltage or current output from instruments, such as load cells or accelerometers.
- Some instruments, such as the Vectrino ADV or Qualisys motion capture cameras, record data separately through a proprietary software interface.

Where different DAQ systems are used, synchronisation of the various instruments is required. When running tests with waves, the tank control system sends a trigger pulse

on starting the test. This can be used to start logging data through the NI DAQ, trigger the Vectrino software, or suchlike. For tests with current only, the tank trigger pulse can be sent manually to synchronise other recordings.

4.4.2 Analysis and interpretation of results

To facilitate processing and analysis of results, a number of MATLAB functions are used at FloWave. These include standard MATLAB toolboxes, code from the MATLAB Central File Exchange, plus functions developed in-house.

Data import scripts FloWave code to import ASCII wave gauge data, split up multiple tests run in batch mode, etc.

Wave analysis scripts Implemented in Draycott (2017), these were used for the spectral analysis of uni- and multi-directional waves.

Zero-crossing analysis Implemented in Davey et al. (2008), this applies MATLAB polynomial interpolation to identify crests, troughs, and zero-crossing points, outputting wave parameters including height and length.

Despiking toolbox Implemented in Mori et al. (2007) based on the method of Goring and Nikora (2002), this toolbox is used to remove outlier spikes from ADV data.†

Theoretical wave-current interaction To assist with understanding the wave-current interactions observed in the tank, an analytical interaction model was implemented in MATLAB as part of this project. Based on a method outlined by Smith (1997), it uses linear wave theory and implements the Doppler shift discussed in section 2.1. This method only considers collinear interaction, i.e. waves on following and opposing currents, but not those at an oblique angle. Example results provided in Smith (1997) were used to check the method was implemented correctly.

†. Note than an alternative approach was used for the turbulence measurements, as discussed in Sutherland et al. (2017), see Appendix B.

Chapter 5
Flow characterisation

Chapter summary

- To characterise temporal and spatial variability of flows throughout the test area of the tank, a series of flow measurements were conducted.
  - Drive motor rpm was calibrated against velocity in the tank centre.
  - Temporal stability and repeatability of flows is assessed.
  - Spatial variability of flows in plan, vertical profile, and direction also evaluated.

  These focus on mean flow, but turbulence within the flow is also investigated.
- Implications for testing resulting from spatial variability of flow in the tank are considered.
- A tool for specifying the drive motor rpm to get the required velocity at any point in the tank has been developed, which is used when running tests.

5.1 Flow characterisation methodology

5.1.1 Rationale

As part of the commissioning and characterisation process for the FloWave facility, it was important to investigate the performance characteristics of the waves and current generation capability. These were initially considered separately, before investigating their combined interaction. Analysis and calibration of the wave generation capability was carried out under a separate IDCORE project (Draycott, 2017), see section 3.2.3.

This chapter presents measurements to characterise the flow field in the tank. This substantiates the design stage Computer Fluid Dynamics (CFD) modelling and facilitates client testing. Although the characterisation is now sufficiently complete to permit the facility to operate effectively, this is also an ongoing process, refining understanding of how the tank operates.

An ideal test tank would have a spatially and temporally uniform current, flowing straight across the whole tank. Due to the method employed for creating combined waves and currents from any direction in a circular tank, there is some spatial variability in the

flow across the tank. This work shows that a central test region exists where the flow is considered acceptably straight and uniform for undertaking tests. To facilitate testing is important to understand the shape and size of this test area over a range of flow conditions. It is also important to compare the flow generated in the tank with measurements of real conditions that are being replicated.

5.1.2 Experimental method overview

Time constraints limit the extent of characterisation that can be undertaken. Ideally every point in the tank should be characterised at every velocity, but this quickly becomes unmanageable. Fully describing currents in the FloWave facility is a complex multi-dimensional problem, with many variables including:

- reference velocity magnitude U_{ref}, related to drive input rpm,
- streamwise/transverse/vertical components of velocity u, v, w,
- spatial variation across the test area X, Y,
- vertical (shear) profile of velocity Z,
- different input current direction in the tank θ,
- mean temporal variations in current, and
- turbulence within the mean flow.

To simplify the characterisation, it was broken down to a series of tests with one or two variables, and these used to characterise the facility. This is common practice when characterising facilities (section 3.2.1). The characterisation tests were conducted with only the required measurement equipment in the tank, to avoid potential distortion of flow around a device model.

The flow characterisation was split into three sections, firstly calibrating the velocity relationship of the drive motors and demonstrating temporal stability. The main part of the characterisation considered spatial variability of flow throughout the basin, focusing on the central test region. Finally, measurements were taken of turbulence within the flow, including assessing spatial variation.

As noted in section 4.2, when testing with only current, the wavemakers are generally powered down and rest on their backstops. This configuration was used for all tests, with a water depth in the test section of 1.93 m. Both Electro-Magnetic (EM) current meters and Acoustic Doppler Velocimeters (ADVs) (section 4.3.2) were used for the flow characterisation.

Table 5.1: Tank input rpm and nominal velocity used for flow characterisation tests.

Input rpm	Nominal velocity [m/s]
25	0.20
46	0.42
54	0.50
61	0.58
82	0.80

Flow velocities

A set of nominal velocities, table 5.1, were used for much of the flow characterisation to facilitate comparison between tests. These were the tank's design velocity specification of 0.8 m/s, a typical low end test velocity of 0.2 m/s, and three additional intermediate velocities. For a typical test at 1:20 Froude scale, this design specification corresponds to a peak current of 3.6 m/s in 39 m water depth, which corresponds with typical Tidal Stream Turbine (TST) deployment sites currently being proposed.

The drive motor rpm was set based on preliminary calibration undertaken during the commissioning process*. Although the nominal velocity was not obtained in all cases, using the same input rpm allowed comparison between tests.

5.2 Generation of steady currents

5.2.1 Drive motor calibration (rpm–velocity)

The initial calibration of velocity in the tank against primary control motor rpm was used to set input velocities for early tests in the tank. Subsequently, porous screens were fitted to the turning vanes to provide additional flow conditioning. This changed the flow dynamics of the tank slightly. A revised calibration of drive motor rpm to velocity was undertaken with a Vectrino ADV in the tank centre at $(0.0, 0.0, 1.4)$. The primary drive motor was increased in steps of 20 rpm up to a maximum of 120 rpm. Data from the vertical profiles at three additional rpm steps were also used. A 600 s data sample was taken at each rpm step, once the velocity had stabilised. Results for each velocity component are shown in fig. 5.1. Linear regression was used to determine fit coefficients, with details in table 5.2.

*. The initial calibration was undertaken by FloWave staff, prior to the start of the research project.

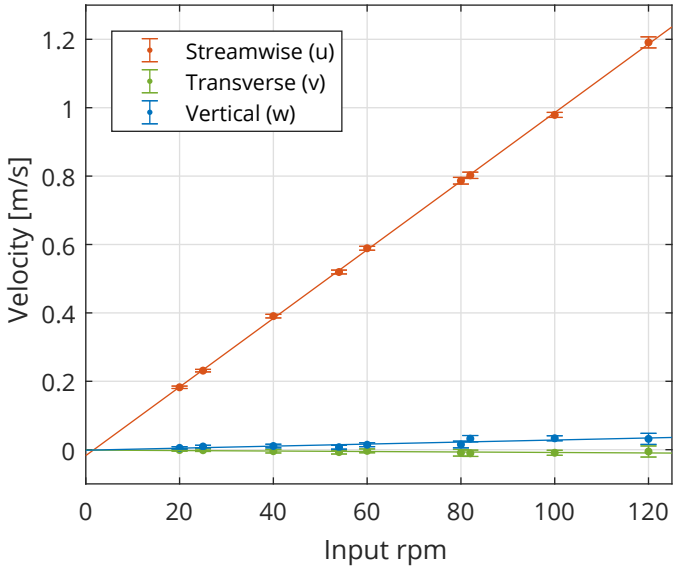

Figure 5.1: Calibration of velocity at (0.0,0.0,1.4) against drive input rpm. For each velocity dots shown mean velocity with $\pm 1\sigma$ error bars, and solid line of best linear fit.

Table 5.2: Details of linear regression fit for velocity–rpm calibration in fig. 5.1.

Velocity vector	Gradient $\times 10^{-3}$ [m/s/rpm]	Intercept $\times 10^{-3}$ [m/s]	r^2 Fit
Streamwise (u)	10.03	-17.25	1.00
Transverse (v)	-0.07	-1.12	0.48
Vertical (w)	0.30	-1.51	0.77

5.2.2 Temporal stability of flow generation

For effective testing, mean flow in the tank needs to be steady. This relates to timescales of minutes, while at shorter timescales, turbulence within the flow will dominate. Turbulence characterisation is covered in more detail in section 5.4. It is also important to understand how long the tank takes to respond to changes in flow input. The current usually needs to reach a steady equilibrium prior to commencing a test.

Temporal stability was assessed using two tests. Firstly a 20 minute test, with an EM current meter, then a longer 60 minute duration was measured with an ADV as part of the turbulence characterisation (section 5.4). An upper water column location was chosen for both these tests to minimise disturbance and vibration resulting from an instrument mounting bracket in the water.

As a first measure of the temporal stability of the tank, the current ramp-up from rest and the subsequent stable flow was measured for a period of 20 minutes using a 2-axis EM meter. The measurement was taken in the tank centre at $Z = 1.5$ m, with the primary drive motor set to 50 rpm, a nominal velocity of 0.48 m/s. Figure 5.2 shows that velocity increases asymptotically, to within 10% of target after approximately 2 minutes, and

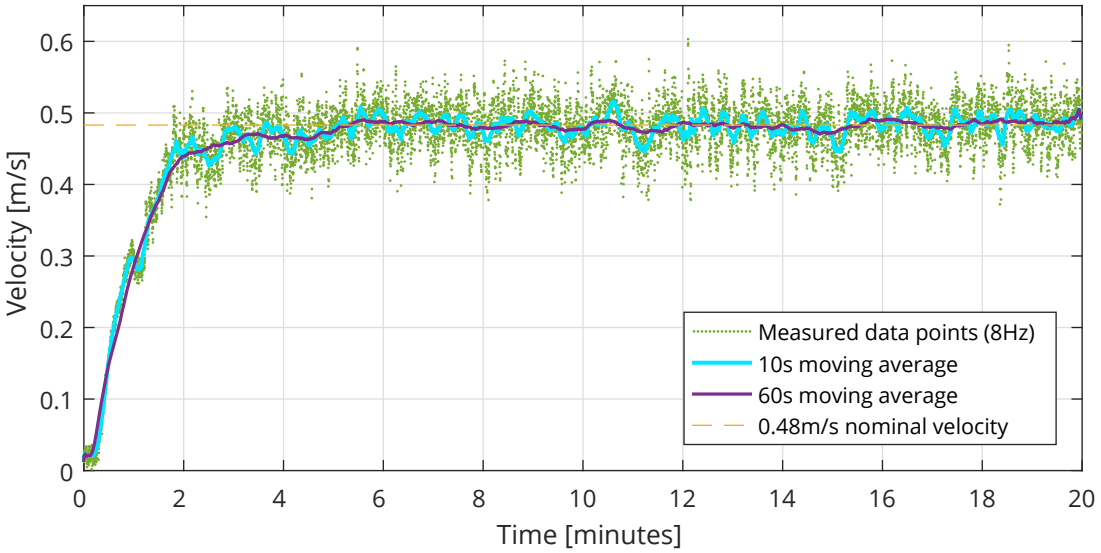

Figure 5.2: 20 minute temporal stability velocity measurement with EM meter, at tank centre 1.5 m above floor, 50 rpm (nominally 0.48 m/s).

reaches a stable velocity after 5 or 6 minutes. This is similar across the range of velocities used at FloWave, and also applies to changes in flow direction. The flow remains stable thereafter, with only minor fluctuations.

This test was repeated for a longer 1 hour duration using a Vectrino ADV at 100 Hz sample rate. The instrument measurement volume was located at $Z = 1.4$ m above the floor and the primary drive motor set to 82 rpm, a nominal velocity of 0.8 m/s. The ADV gives u, v, w components, i.e. streamwise, transverse, and vertical velocities, permitting assessment of all three velocity components, as shown in fig. 5.3.

It is interesting to note that the streamwise velocity measurements are not normally distributed about the mean, but negatively skewed, i.e. the median velocity is faster than the mean. It is not equally likely to have velocities faster or slower than the mean, presumably as higher velocities have proportionally more energy. The transverse and vertical velocity components are normally distributed around nominally zero flow. There is however similar variance in each of the three components about their mean value.

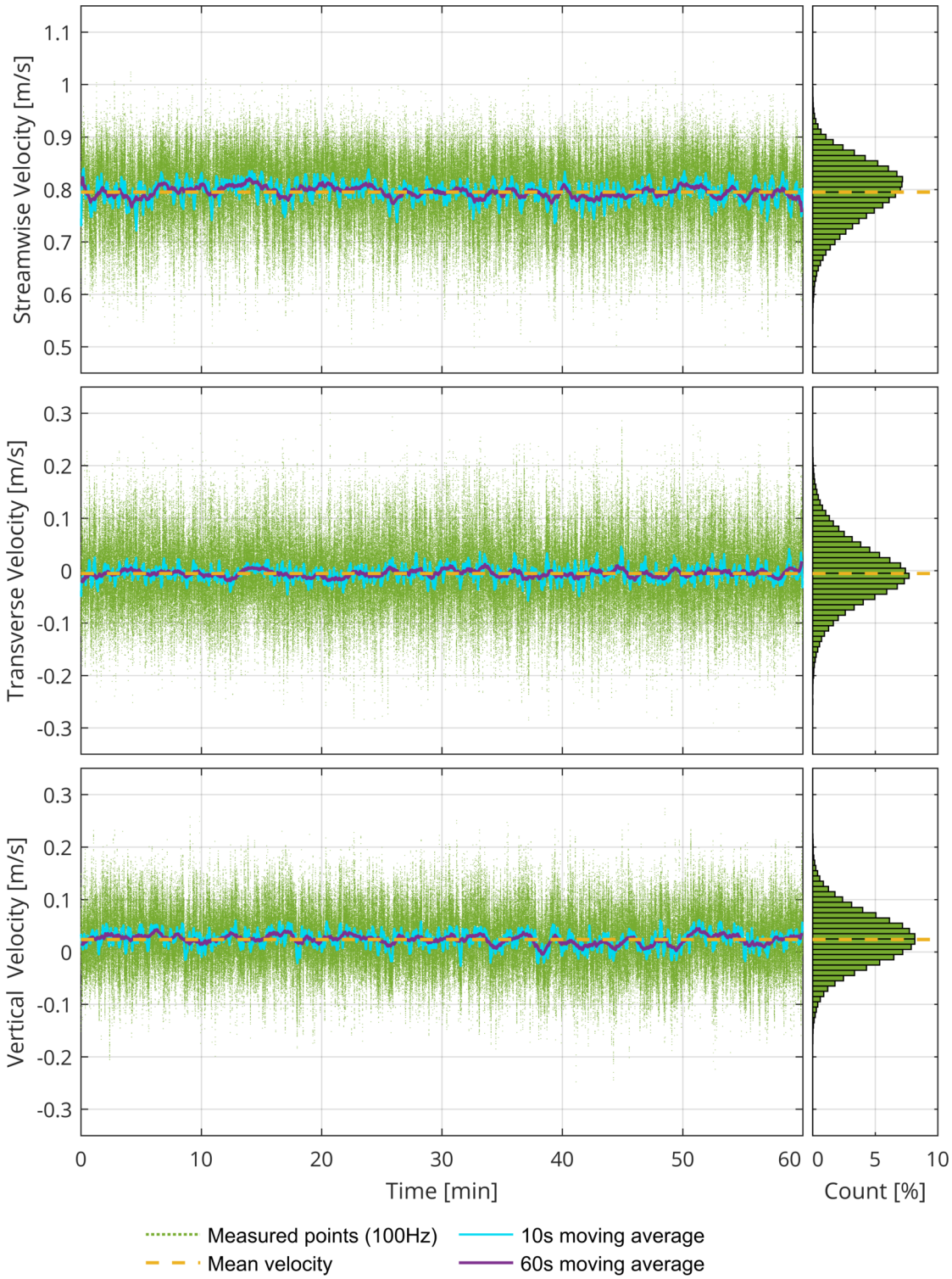

Figure 5.3: 60 minute temporal stability velocity measurement with Vectrino, at tank centre 1.4 m above floor, 82 rpm (nominally 0.8 m/s), for u, v, w velocity components. Right panels show histograms with 0.01 m/s bins.

5.3 Spatial variability of mean flow

To characterise the tank, spatial variability of mean flow (magnitude and direction) was assessed across the X, Y, Z dimensions of the central test area. A series of vertical profiles were measured at different velocities and a small number of X, Y locations. Additionally, a series of point measurements were made at one depth and three velocities, to give more detail on a horizontal section covering the test floor.

For the turbulence characterisations (section 5.4), measurements were taken at the same spatial positions and velocities to facilitate comparison. Two additional profiles to the side of tank centre increased spatial coverage of the flow characterisation.

5.3.1 Vertical profile

Boundary effects, particularly bed friction, have an impact on the vertical profile of flowing water. The flow close to the bed is slowed by bed roughness, which can be considerable in the sea. This vertical profile is also referred to as a 'shear' or 'flow' profile. Although not necessarily representative of real sites, it is commonly represented by a power law, eq. (5.1), where z is the height above bed, h total water depth, and n the exponent often taken as seven. The reference velocity U_{ref} can be either a depth averaged or a surface velocity depending on the definition.

$$U = \left(\frac{z}{h}\right)^{1/n} U_{\text{ref}} \tag{5.1}$$

To assess the spatial variability of flow in the tank, a series of vertical profiles were measured. The (X, Y) coordinates and tank input rpm for each profile measured are given in table 5.3. For all tests flow across the tank was at 0°. Initial measurements were made with single-axis EM meter at 2 Hz, taking mean flow over a 60 s period at 38 vertical points with 0.05 m spacing. Repeat measurements were later made with an ADV for a subset of these tests, measuring both mean flow and turbulence at 100 Hz. For these a 600 s sample was recorded at 11 points above the floor (0.1 m, 0.2 m, 0.3 m, 0.4 m, 0.6 m, 0.8 m, 1.0 m, 1.2 m, 1.4 m, 1.6 m, and 1.8 m). The coarser vertical resolution kept the overall time-scale manageable given the longer sample time at each point.

Table 5.3: Details of vertical profiles measured, with X, Y coordinates and drive motor rpm noted for each instrument type used. See main text for Z positions measured

	Tank rpms recorded with each instrument	
(X, Y) [m]	EM	Vectrino
$(-7.5, 0.0)$	82	—
$(-5.0, 0.0)$	82	82
$(-2.5, 0.0)$	82	82
$(0.0, 0.0)$	25,46,54,51,82	25,54,82
$(2.5, 0.0)$	82	82
$(5.0, 0.0)$	82	82
$(7.5, 0.0)$	82	—
$(0.0, 2.5)$	—	82
$(0.0, 5.0)$	—	82

Variation of vertical profile with mean velocity

At the tank centre, the change in vertical profile with increasing mean velocity was assessed for the five input rpms in table 5.1, as shown in fig. 5.4.

The shape of the velocity profile in the tank is almost independent of average velocity, as shown by the similarity between normalised velocity plots in fig. 5.5(a). This is most closely described by a 1/15th power law, fig. 5.5(b). It is reasonably similar to other profiles used within the industry, such as the 1/7th or 1/10th power laws and the profile described in the UK Health and Safety Executive (HSE) guidance (HSE, 2002).

Variation of vertical profile across tank

To assess the change in vertical profile across the tank, the vertical profiles measured across the tank in line with the current direction are compared in figs. 5.6 and 5.7. The profiles perpendicular to the current direction are shown in fig. 5.8.

The flow profile 5 m to the side of centre in fig. 5.8 shows a noticeable velocity deficit at mid depth, 0.2 m to 1.2 m above the floor. This is not apparent in any other profiles measured. It is less representative of typical deployment sites, and so marks a boundary for the testing area for normal use.

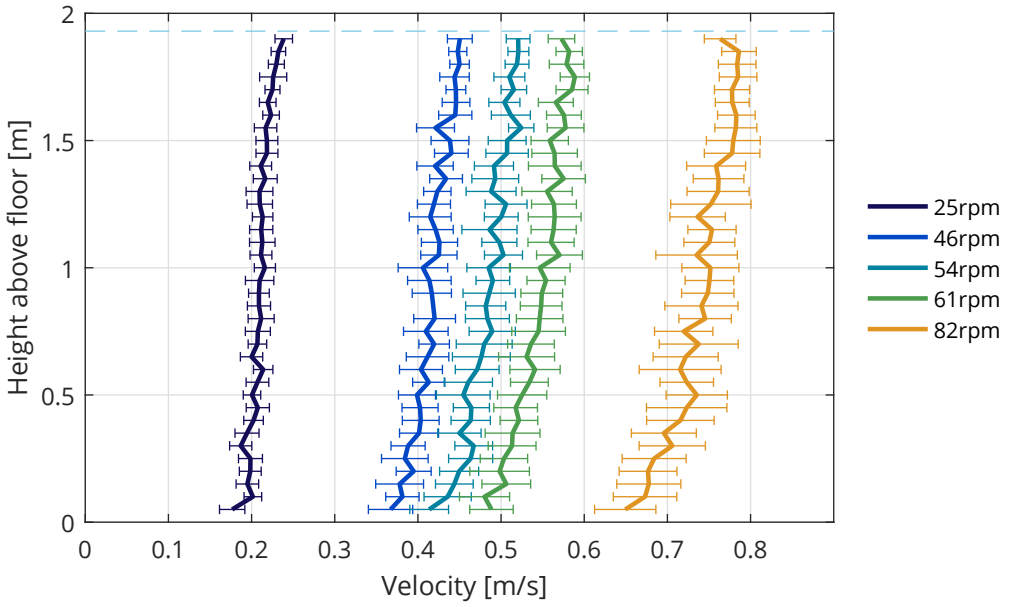

Figure 5.4: Vertical velocity profiles measured at tank centre for 5 input drive motor rpms. Error bars show $\pm 1\sigma$ deviation of 2 Hz samples, and water surface at 1.93 m shown dashed light blue.

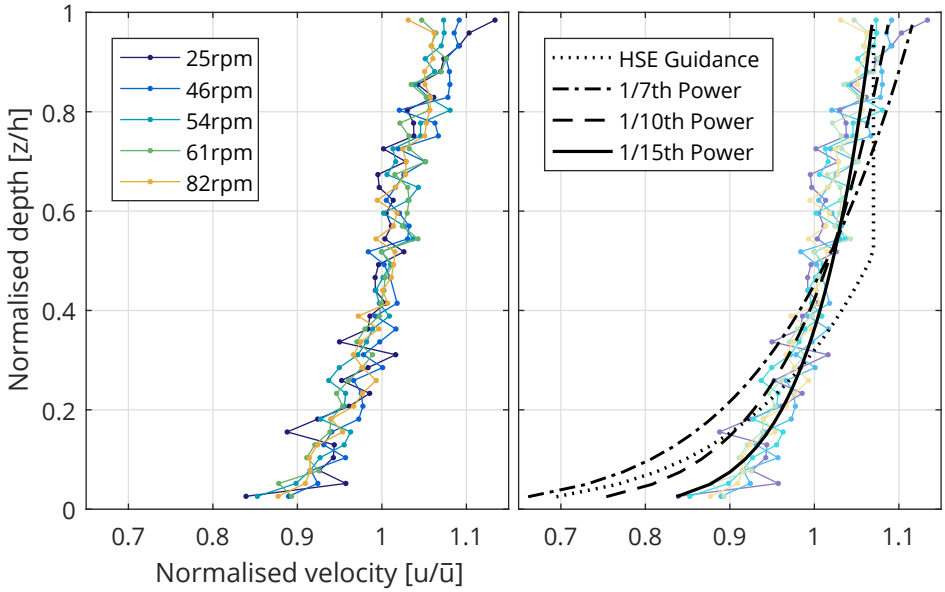

Figure 5.5: Normalised vertical velocity profiles measured at tank centre. Sub-panels show (left) 5 input drive motor rpms, and (right) these profiles overlain with various theoretical models.

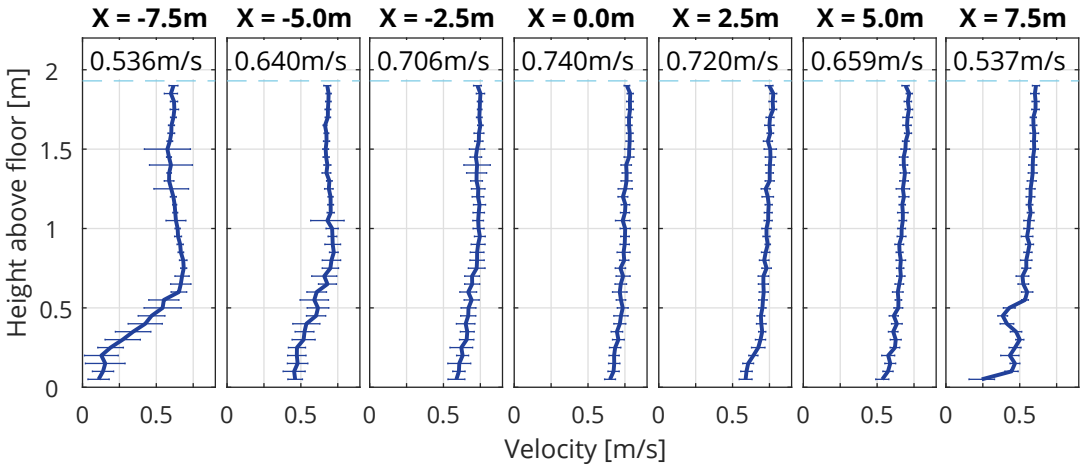

Figure 5.6: Vertical velocity profiles across the tank in line with flow, measured using EM meter at X coordinates noted. Input 82 rpm (nominally 0.8 m/s), with measured depth averaged velocity given for each profile location. Error bars show $\pm 1\sigma$ deviation of 2 Hz signal. Water surface shown dashed light blue.

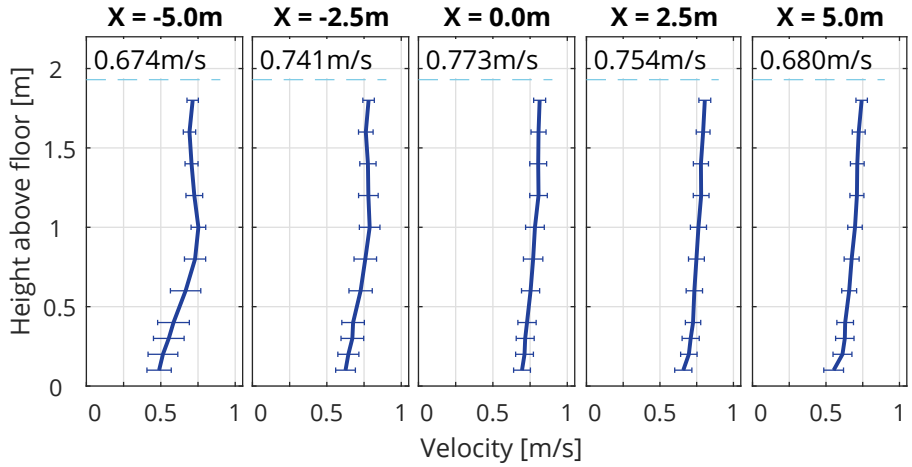

Figure 5.7: As fig. 5.6, but measured using Vectrino Profiler ADV at 100 Hz.

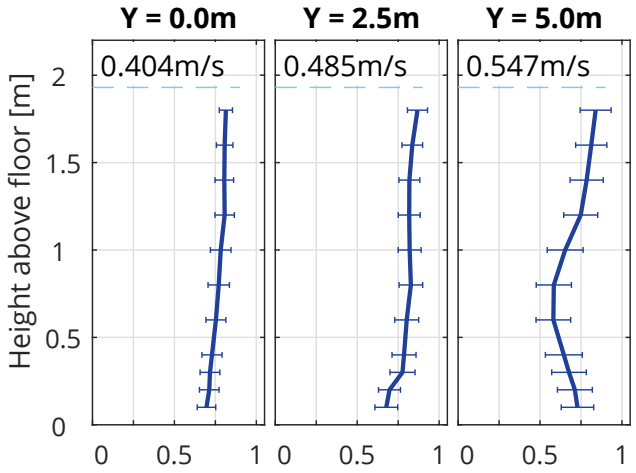

Figure 5.8: As fig. 5.7. Points transverse to flow direction at Y coordinates shown and X=0.

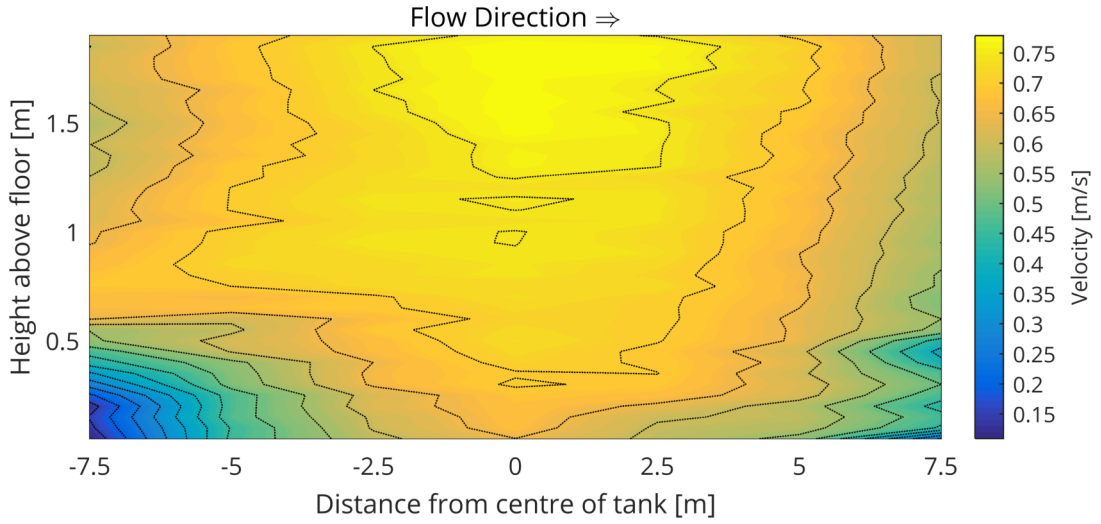

Figure 5.9: Interpolated variation in velocity for vertical section across the tank in line with flow, based on profiles in fig. 5.6. Flow direction left to right, for 82 rpm input.

To help visualise the flow velocity magnitude along a vertical slice through the tank centre, the data in fig. 5.6 was interpolated to give fig. 5.9. This shows an increase in flow speed towards the centre of the tank, a result of the converging nature of the flow in this region that is required to create uniform flow in a circular tank, as discussed in section 4.2.

There is a significant velocity deficit in the lower part of the water column at the extreme 'upstream' edge of the floor $X = -7.5$. Above this is a jet of higher velocity flow, approximately 0.6 m to 1.0 m above the floor. Both of these features are also apparent in the vertical profile fig. 5.6, and the design stage modelling discussed in section 4.2.3. They are a result of the current rising at an angle from the turning vanes.

Close to the centre of the tank, in the middle of test area, is a relatively uniform section of flow. This covers approximately $X = -2.5$ m to $X = +5.0$ m in the lower part of the water column, and $X = \pm 5.0$ m in the upper half of the water column. At the 'downsteam' edge of the floor ($X = +7.5$ m) the velocity throughout the water column reduces, as a result of the flow diverging into the tuning vanes around that half of the tank.

5.3.2 Spatial variation in plan

To determine the planar extents of the usable test area and the variation in velocity therein, flow measurements were made on a number of horizontal transects across the tank. This was conducted using two dual-axis EM meters, at 25 rpm, 54 rpm, and 82 rpm. Locations of the measurement points are shown in fig. 5.10, with separate markers for each of the instruments used. Five locations along $Y = 0$ were measured with both instruments to confirm there were no discrepancies between them.

All measurements were conducted at 1.5 m above the floor, 0.43 m below the water surface, to characterise the upper part of the water column. At this level the immersed length of support structure was kept to a minimum, reducing the impact on flow measurements, and guy lines were not required for stability.

The mean u and v horizontal velocity components, plus the horizontal velocity vector $\overrightarrow{U}$, were calculated. The measured data points were interpolated to a regular 0.1 m grid in MATLAB using a triangulation-based natural neighbour approach.

The spatial variation in flow across the central section of the tank, roughly corresponding to the raisable floor, is shown in figs. 5.11 and 5.12. These show the velocity magnitude to be broadly symmetrical about the current flow direction. It is also relatively consistent (around ±10% or ±0.05 m/s) across a test area approximately 8 m to 10 m wide and 6 m long, which is offset about 1 m downstream of the tank centre. This is an approximate region to be considered for testing, but the specifics should be considered for each test, as discussed in chapter 8.

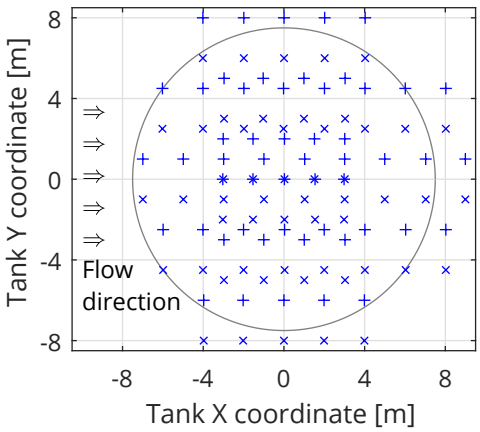

Figure 5.10: Measurement locations for XY spatial variability tests, all at z = 1.5 m. The symbol (x+) corresponds to which of two identical instruments used. Flow direction left to right, 15 m diameter raisable floor shown as a grey circle.

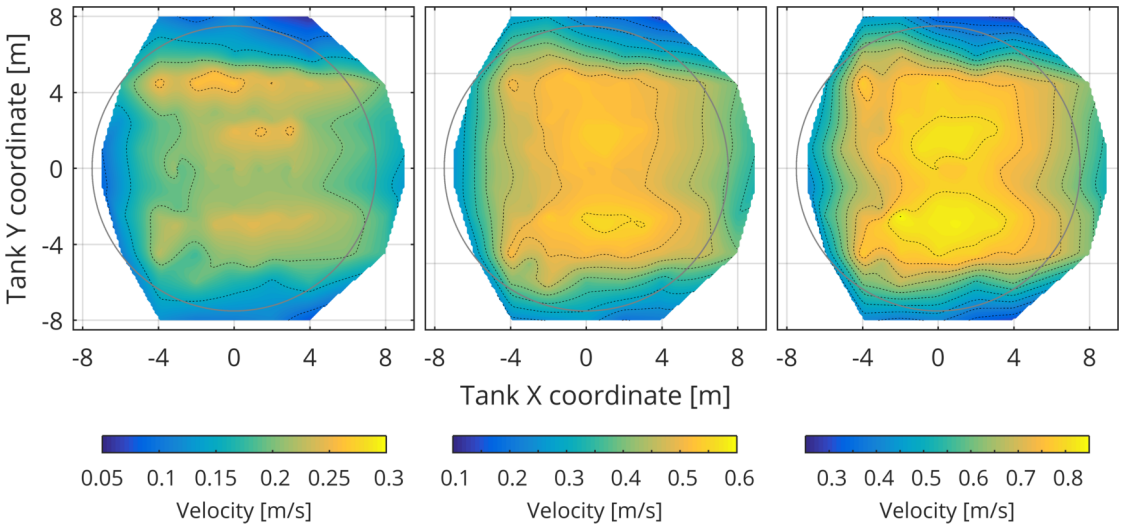

Figure 5.11: Interpolated variation in velocity across test area for horizontal plane 1.5 m above floor. Subplots show from left (a) 25 rpm (0.2 m/s), (b) 54 rpm (0.5 m/s), and (c) 82 rpm (0.8 m/s), with flow direction from left to right. 15 m diameter raisable floor shown as a grey circle.

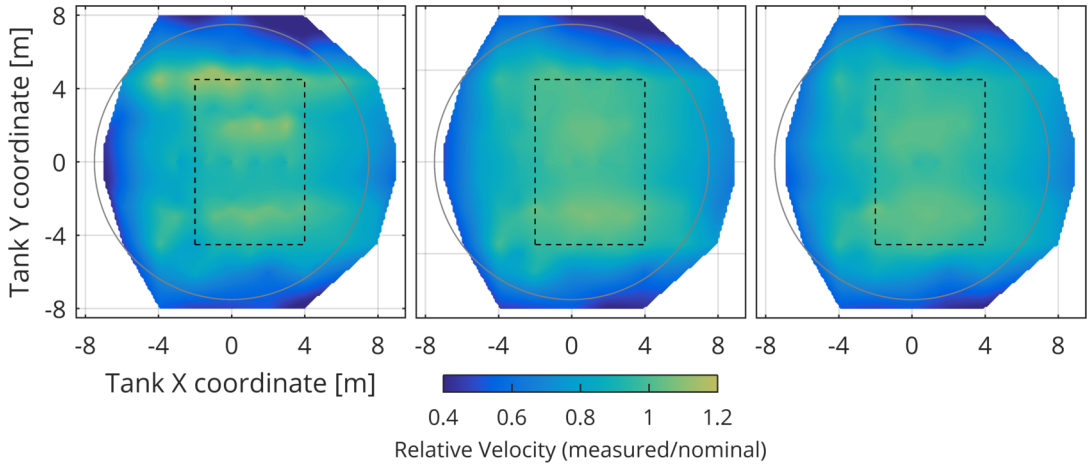

Figure 5.12: As fig. 5.11, but for velocity deviation relative to the nominal velocity. Nominal test area shown by dashed black rectangle.

The measurements show a slight asymmetry in the velocity magnitude, with marginally faster flows (<5%) on the right hand side of the flow. There is also marginally slower flow (≈5%) along the current centreline near the middle of the tank.

5.3.3 Uniformity of flow direction

In addition to minimising spatial variability of flow magnitude, ideally the flow direction would also be uniform across the tank, with negligible transverse and vertical flow, i.e. $u = U_{\text{ref}},\ v \approx 0,\ w \approx 0$.

Taking the EM flowmeter data (section 5.3.2) the horizontal current direction can be calculated across the tank test area. Figure 5.13 shows that an acceptable horizontally uniform flow can successfully be created in the circular tank, with only a slight directional bias towards the outside of the raisable floor, 7.5 m from the tank centre.

The vertical profile measurements using the ADV (section 5.3.1) give u, v, w components of velocity. This can be used to show how the vertical velocity component varies across the test area of the tank, fig. 5.14. The vertical component of velocity is small, although with a slight upward trend in the upstream half of the tank.

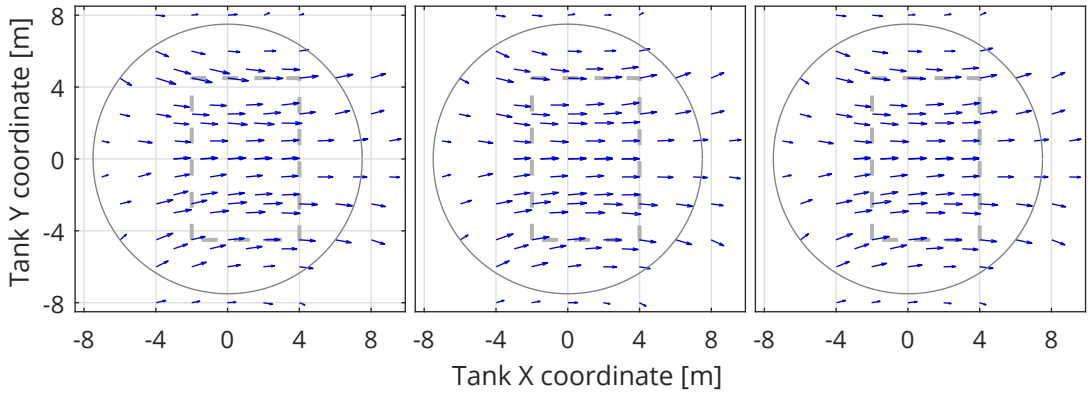

Figure 5.13: Velocity vectors in plan (u, v) across test area for three nominal input velocities: (a) 25 rpm (0.2 m/s), (b) 54 rpm (0.5 m/s), and (c) 82 rpm (0.8 m/s). Vector length is proportional to velocity at measurement point (tail) relative to input velocity. Flow direction from left to right. Nominal test area shown by grey dashed rectangle, 15 m⌀ raisable floor shown as a grey circle.

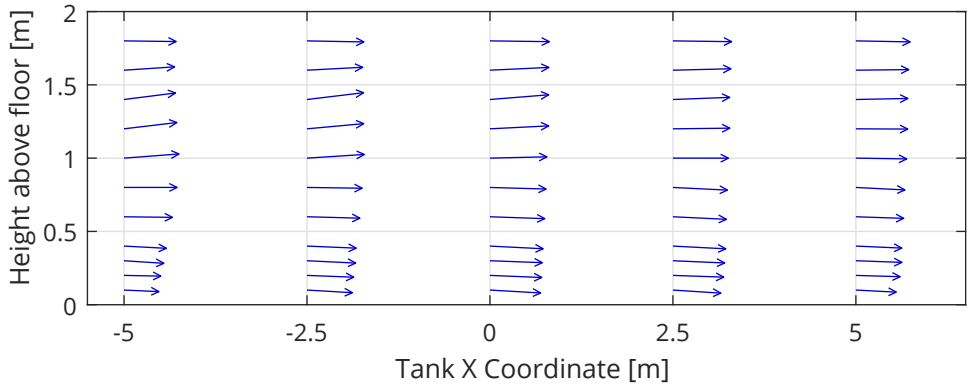

Figure 5.14: Velocity vectors in cross section (u, w) from vertical profiles measured with Vectrino. Vector length is proportional to velocity at measurement point (tail). Vertical axis exaggerated 2×. Input velocity 82 rpm (0.8 m/s).

5.3.4 Rotational symmetry of flow generation

The FloWave facility is designed to be rotationally symmetrical, including both wave and current generation. It was demonstrated by Draycott (2017) that the wave generation and absorption is rotationally symmetrical. A similar analysis is therefore required for currents in the facility.

Rotational symmetry allows more flexible use of the tank. For example, the ability to rotate the flow and/or waves through 90° permits more flexible use of the gantry, allowing the single axis of motion to be aligned either in-line or transverse to the propagation direction. Being able to freely rotate the wave and current generation is also useful when testing device models.

To test the assumption of rotational symmetry, the flow was measured using a Vectrino Profiler at 100 Hz sample rate for 600 s per measurement. The instrument was mounted with the measurement volume located at $Z = 1.5$ m, to keep the device mounting frame out of the water. Alignment of the instrument was such that the x, y, z axes lined up with tank X, Y, Z.

Two sets of tests were conducted. Firstly, considering the effect of input angle on flow at tank centre $(0, 0, 1.5)$. All four cardinal directions were measured, plus input angle was varied in steps of 15° from −30° to +60°. To investigate the possible influence of the drive motors and turning vanes which are spaced at $^{28}/_{360} = 12.86°$, input angles of 6.4°, 12.9°, 19.3°, and 25.7° were also measured. Secondly, spatial variation was assessed for flow at the cardinal directions, using five measurement points as shown in fig. 5.15 and table 5.4. This allowed comparison of points relative to the rotated flow direction, e.g. point 3 with flow at 90° equates to point 2 with flow at 0°.

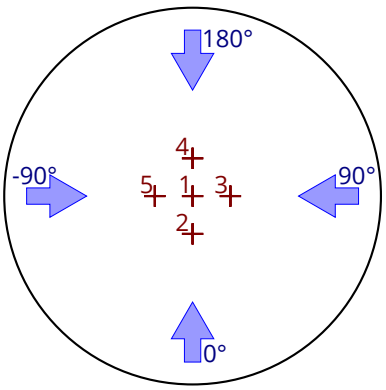

Figure 5.15: Measurement points and flow directions for rotational symmetry tests.

Table 5.4: Measurement point coordinates for rotational symmetry tests.

Point	Location	(X,Y,Z) [m]
1	Centre	(0, 0, 1.5)
2	Upstream	(-2.5, 0, 1.5)
3	Right	(0, -2.5, 1.5)
4	Downstream	(2.5, 0, 1.5)
5	Left	(0, 2.5, 1.5)

Recorded u, v velocity components were transformed to polar coordinates U, θ and rotated by input angle θ_c to permit comparison. Normalised probability distributions for directional spread $\Delta\theta$ and velocity magnitude U were calculated. The data was partially analysed in 10 sub-samples of 60 s to also assess temporal stability.

Results of the rotational symmetry analysis are shown over the following pages for the following cases:

1. Cardinal flow directions $0^\circ, 90^\circ, 180^\circ, -90^\circ$, with a repeated test at 90°, shown in figs. 5.16 and 5.17.
2. 15° increments between -30° and 60°, shown in figs. 5.18 and 5.19.
3. Increments based on 12.86° drive motor spacing, shown in figs. 5.20 and 5.21.
4. Spatial variation across the central test area, shown in fig. 5.22.

There is a relatively good match between the flows recorded at different angles, showing the tank can be considered rotationally symmetrical. However the case with flow at -90° on fig. 5.17 apears to be a slight anomily. For all cases, the mean direction is misaligned by approximately -2°. This may be due to instrument misalignment, or it may be a real effect.

It can be seen from the box-plots (figs. 5.17, 5.19 and 5.21) that the turbulent flow in the tank varies from minute to minute. There is no trend in the directional spread over time, showing that the tank had reached a steady state prior to measurement. The turbulent flow variation is a similar order of magnitude to the variance resulting from rotational asymmetry, meaning it is difficult to separate these effects.

There is a larger discrepancy in flow where there is a misalignment between the input direction and the drive motors at multiples of $^{28}/_{360} = 12.86^\circ$. This can be seen in figs. 5.18 and 5.20 with reference to tables 5.5 and 5.6. It is particularly obvious in fig. 5.20 where the directional spread for the recorded cases with input direction exactly half-way between two drive units is more widely spread compared with those cases directly aligned. Where the input direction was altered in steps of 15°, the distribution of directional spread is clearly related to the misalignment from the drive units. The distribution of velocity magnitude does not appear to be correlated with misalignment from drive motors in the same manner.

Some of the discrepancy can be attributed to the manufacture and installation tolerances of the turning vanes. These are large metal components, and individual units may not be identical. Placement of these units ±10 mm results in variable gaps between them, which may have an influence the flow across the tank. This is a likely source for the discrepancy visible in the -90° flow case on fig. 5.17, howeve this is something that could be investigated in future flow characterisation work.

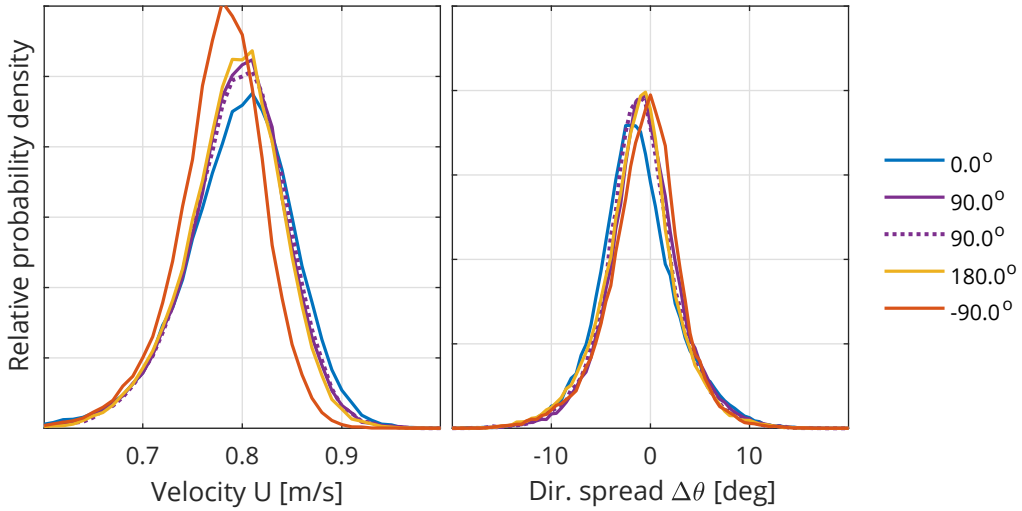

Figure 5.16: Rotational symmetry for cardinal directions at tank centre. Plots compare relative probability densities of velocity magnitude U (left) and directional spread $\Delta\theta$ (right) for whole test length at each input direction.

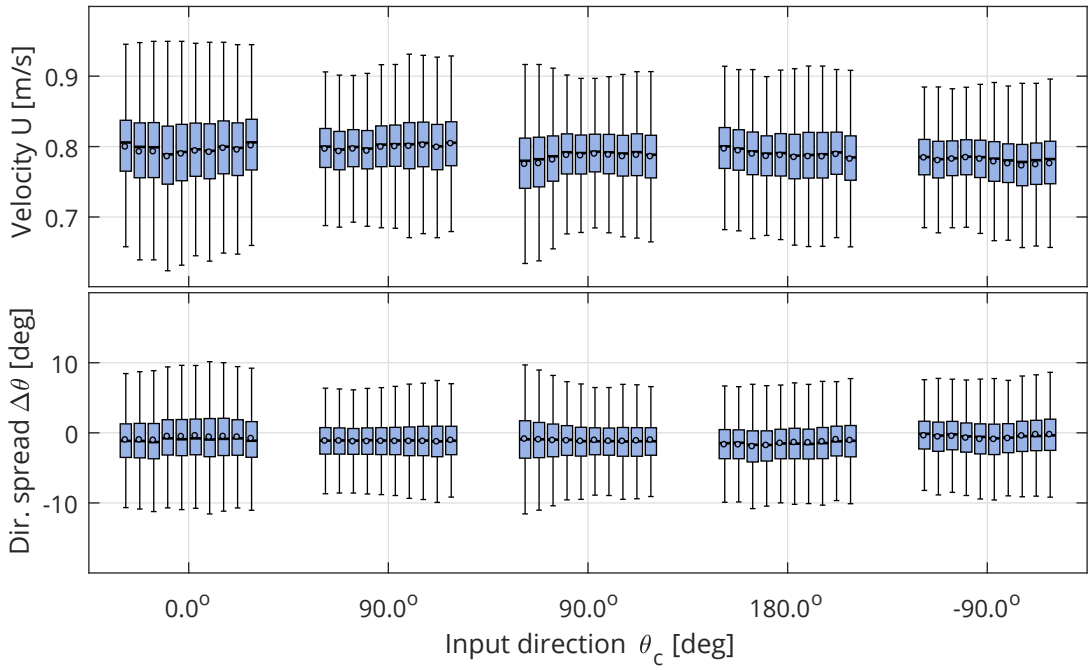

Figure 5.17: Rotational symmetry for cardinal directions at tank centre. Box and whiskers plots show quartiles of velocity magnitude U (top) and directional spread $\Delta\theta$ (bottom) for 60s subsamples at each input direction.

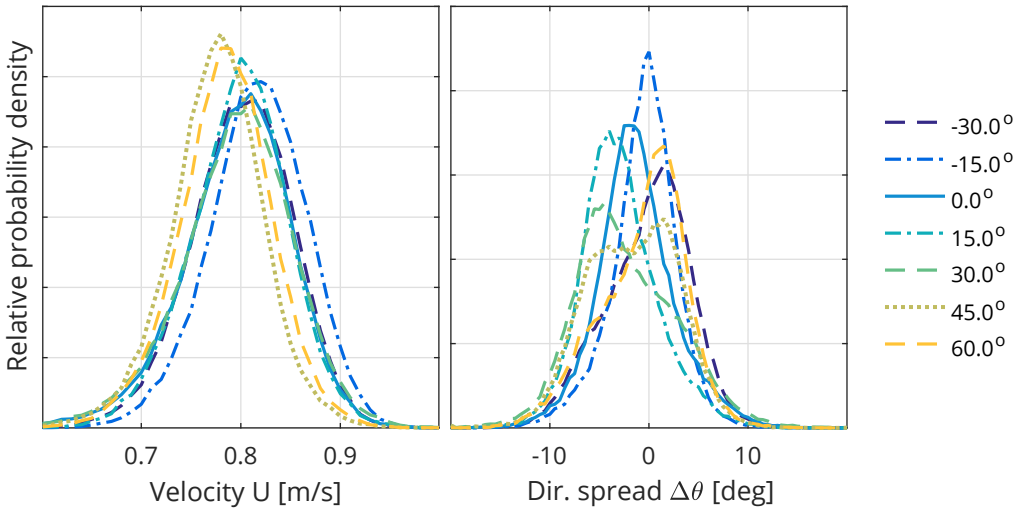

Figure 5.18: As fig. 5.16 but for 15° increments. Line style relates to misalignment, see table 5.5.

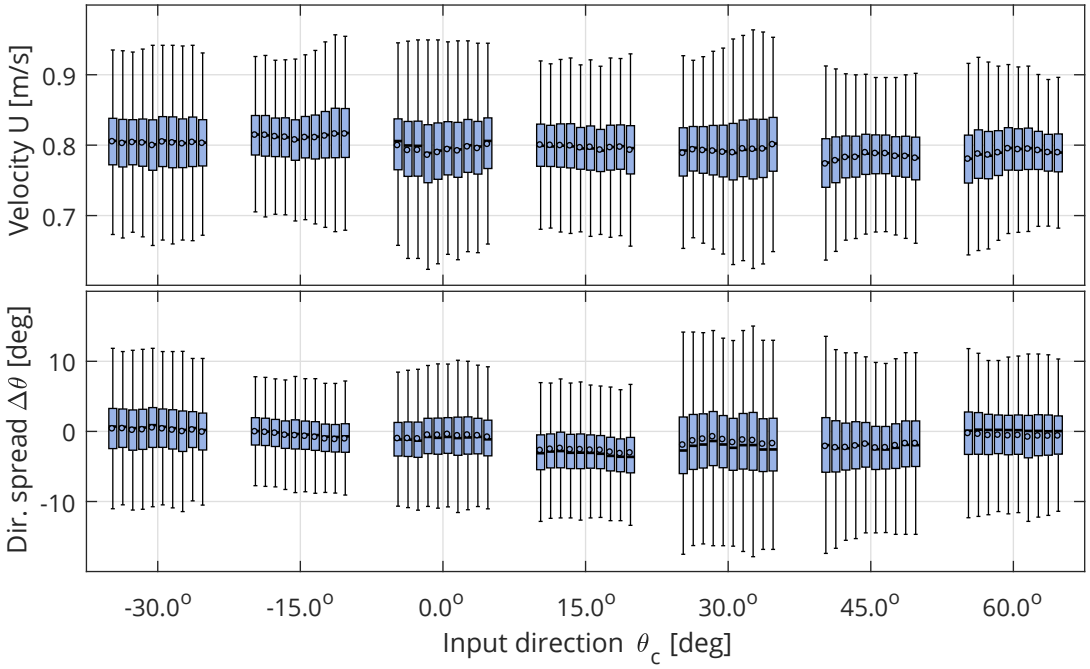

Figure 5.19: As fig. 5.17 but for 15° increments.

Flow angle	Misalignment from drive unit
−30.0°	−4.3°
−15.0°	−2.1°
0.0°	0.0°
15.0°	2.1°
30.0°	4.3°
45.0°	±6.4°
60.0°	−4.3°

Table 5.5: Misalignment between measured input flow angles and drive units.

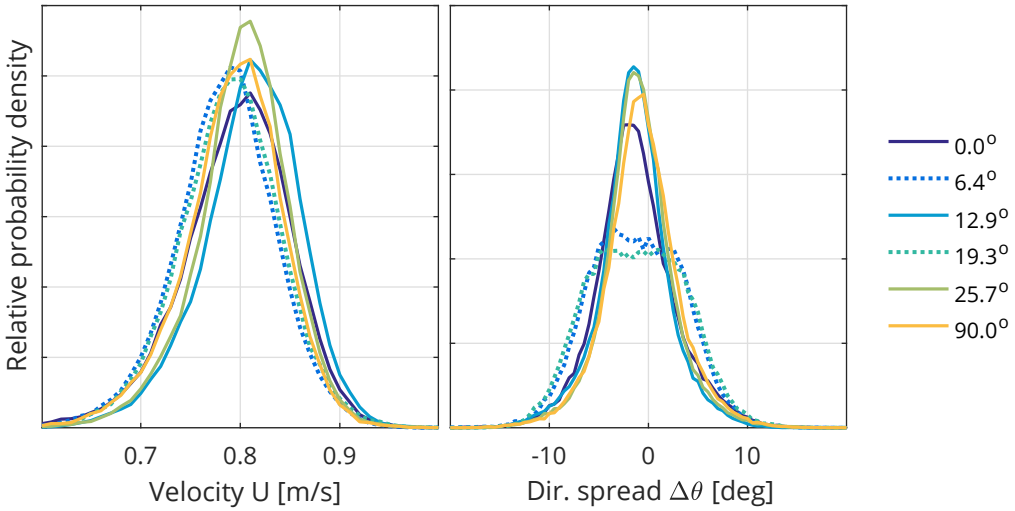

Figure 5.20: As fig. 5.16 but for increments based on drive spacing. Solid lines relate to flow directly in line with drives, dotted lines are half-way between 2 drives, see table 5.6.

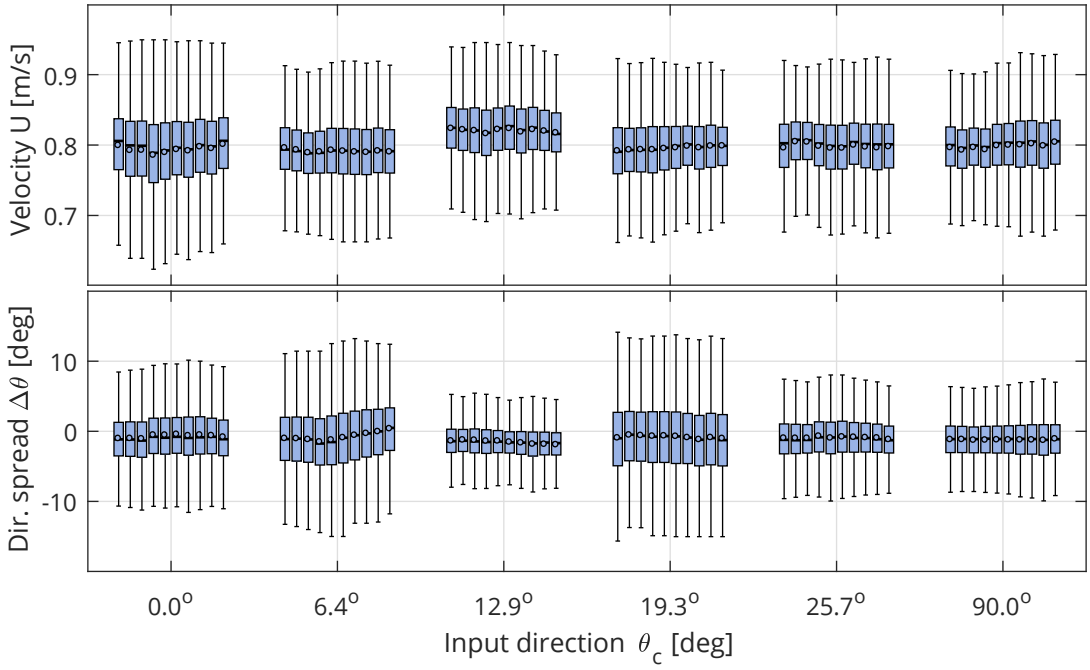

Figure 5.21: As fig. 5.17 but for increments based on drive spacing.

Flow angle	Alignment relative to drive units
0.0°	Inline with drive unit
6.4°	½ way between 2 drive units
12.9°	Inline with drive unit
19.3°	½ way between 2 drive units
25.7°	Inline with drive unit
90.0°	Inline with drive unit

Table 5.6: Alignment of measured input flow angles and drive units.

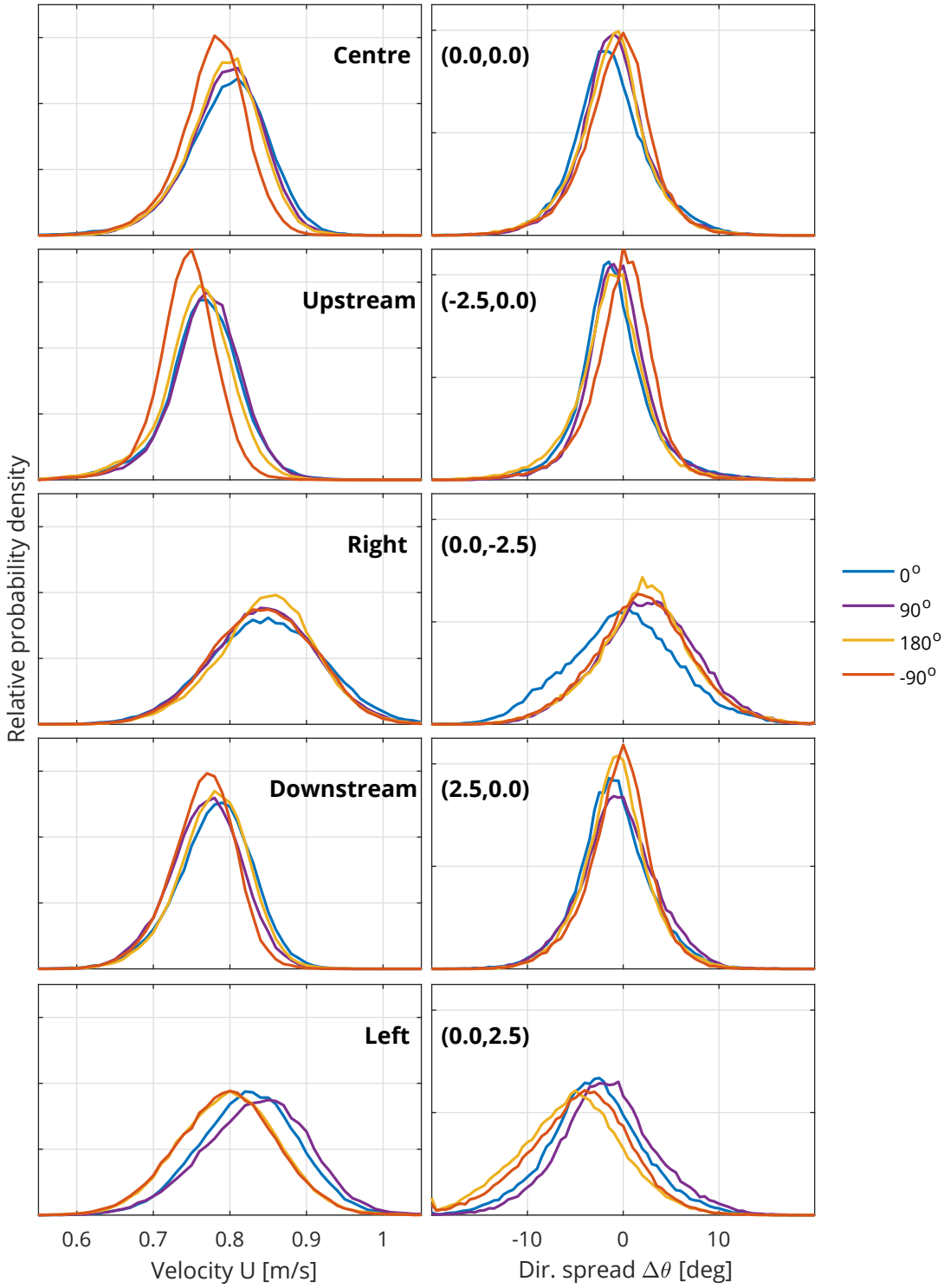

Figure 5.22: Spatial assessment of rotational symmetry for cardinal directions. Plots compare relative probability densities for whole test length at each direction, with velocity magnitude U (left) and directional spread $\Delta\theta$ (right). Row are measurement points relative to flow direction, as given in fig. 5.15 and table 5.4. Top row shows the same data as fig. 5.16.

5.4 Initial characterisation of turbulence

As well as spatial variability of mean flow, turbulence within the flow is an important consideration, particularly when testing TSTs. The level of detail required will depend on user need. Some clients may only require an overview of the turbulence, described by metrics such as Turbulence Intensity (TI). More advanced clients may wish to understand the turbulent flow in great detail, and possibly even look at methods to alter the flow field. For this project, initial characterisation of the turbulent flow was undertaken, considering spatial variation of key metrics. Characterising turbulence and the impact on devices such as TSTs is an ongoing research area at FloWave.

The turbulence measurements described here were collaborative work with Dr Duncan Sutherland, then a PhD student at The University of Edinburgh. Test planning, conducting the measurement campaign, and writing the resulting paper was a joint effort. Dr Sutherland was responsible for the turbulence characterisation and calculation of the metrics, based on his previous experience with the ReDAPT project. A paper describing this work was published in Ocean Engineering (Sutherland, Noble et al., 2017), see Appendix B, which has been incorporated in into this section, focusing on my contribution to the work.

5.4.1 Turbulent flow parameters

A range of parameters were calculated to describe the turbulent flow in the tank, as discussed below. The metrics used were chosen to be in-line with those used in field measurement campaigns (Sellar et al., 2015; Thomson et al., 2012). To understand tank performance, spatial variation of the metrics was assessed through a series of vertical profiles at a number of locations in the tank, as discussed in section 5.4.3. Measurements were made using a Vectrino Profiler ADV (section 4.3.2) at the maximum 100 Hz sample rate. Further details on the data quality control and other metrics including Reynolds stresses are given in Sutherland et al. (2017), see Appendix B.

Temporal stability and stationarity period

The tank is stable over timescales of minutes, as discussed in section 5.2.2. To calculate mean or turbulent parameters of the flow a period of stationarity must be defined. This is taken as the period over which flow measurements have stable mean $\overline{u}$ and variance σ_u^2 (Thomson et al., 2010).

The first stage of turbulent flow parametrisation is to assess an appropriate stationarity period based on the variation of σ_u^2 and $\overline{u}$. This was done utilising the 1 hour sample at tank centre, $(0.0, 0.0, 1.4)$ with input rpm of 82. The resulting time series was then subdivided into a range of T_{stat} periods from 1 s to 120 s in 1 second increments, with the mean σ_u^2 and $\overline{u}$ values across each sample calculated.

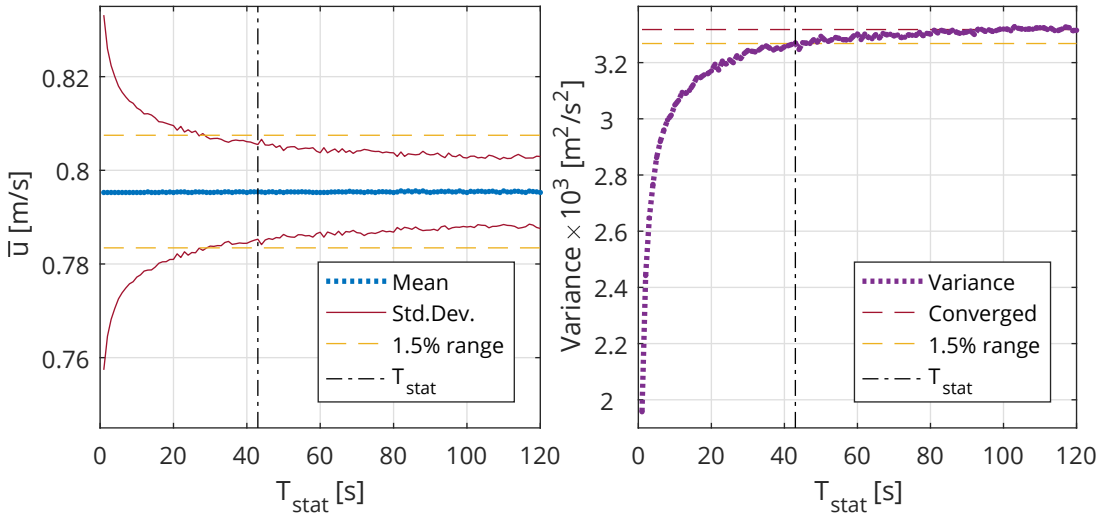

Figure 5.23: Derivation of stationarity period. (a) Variation of mean and standard deviation of $\overline{u}$ with T_{stat}. (b) Variation of streamwise velocity variance with T_{stat} showing convergence to within 1.5% of the long term mean value.

Figure 5.23(a) illustrates that the mean of $\overline{u}$ remains constant as would be expected, while the standard deviation of the mean values slowly decreases with increasing T_{stat}, and appears to be nearing an asymptotic value. A target for standard deviation of $\overline{u}$ to be less than 1.5% of the total mean value was set, which gave T_{stat} of under 1 minute.

Figure 5.23(b) shows the variance increasing towards an asymptotic value. Defining the asymptote as the mean of values over the 100 s to 120 s range, the period at which the variance was within 1.5% of this value was found to be 43 s. The first value where both the mean and standard deviation of $\overline{u}$ were within the 1.5% threshold was selected as the stationarity period. This period relates to a standard deviation in mean values of 0.010 m/s in fig. 5.23(a).

Turbulence spectrum

The turbulence spectrum of the tank is plotted as a Power Spectral Density (PSD) in fig. 5.24. To smooth the random fluctuations due to noise, the PSD was calculated for each T_{stat} long sub-sample and the mean value taken. The turbulent energy cascade is clearly evident, following the $f^{-5/3}$ law proposed by Kolmogorov (Pope, 2000). At higher frequencies, instrument noise tends to dominate the signal. The mean PSD in fig. 5.24 is asymptotically approaching the noise floor for $f > 50$ Hz. In this test, a small vibrational frequency is present in the mean PSD signal at 41.7 Hz. This is likely to be a result of the mounting arrangement, thus dependent on cantilever length and guy line tension for the specific test (section 4.3.2). The vibration was not of particular concern, as the frequency and magnitude were close to the instrument noise.

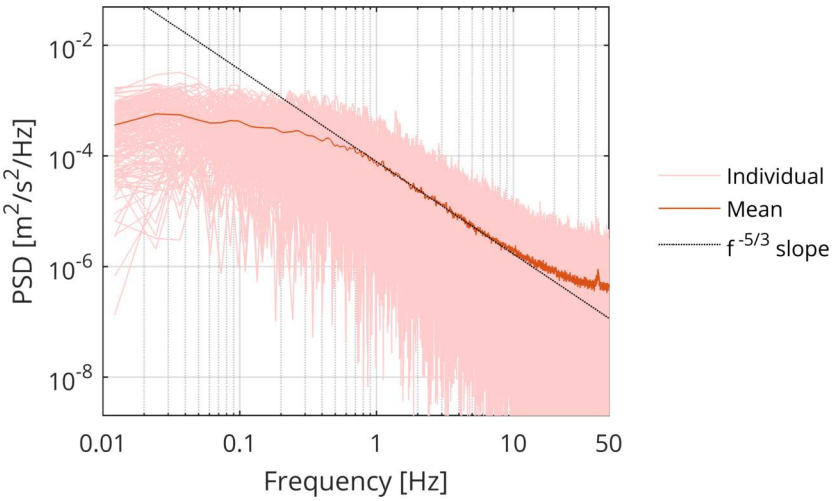

Figure 5.24: Example turbulence PSD from the 1 hr test, with all the individual PSD for each T_{stat} time series and the mean PSD. A small vibrational frequency is present at 41.7 Hz in the mean signal.

Turbulence intensity

One metric commonly used to quantify the magnitude of turbulence is the 'turbulence intensity' I, also referred to as TI. This term is adopted from the wind industry as a measure of the magnitude of fluctuation as a percentage of the mean flow velocity. It is defined as the RMS velocity perturbations divided by the mean velocity over a period of stationarity.

For this work, an anisotropic environment was assumed. Individual components of I for each Cartesian direction are calculated using eq. (5.2). The measured velocity u is a combination of mean velocity $\overline{u}$, turbulent fluctuation u', and a noise component n, eq. (5.3),

$$I_u = \frac{\sqrt{\langle u'^2 \rangle}}{\overline{u}} \times 100\% \tag{5.2}$$

$$u = \overline{u} + u' + n \tag{5.3}$$

Integral lengthscale

The integral lengthscale is defined qualitatively as the average size of the largest eddies in a turbulent flow (Pope, 2000). There are several methods of estimating this value. Here the temporal autocorrelation method is utilised as it was deemed the most appropriate for the this measurement data (Sutherland, 2015; O'Neill et al., 2004). This method utilises the integral timescale $\mathcal{T}$ of turbulence which is calculated from the time based autocorrelation function given by eq. (5.4), where Δt is a temporal lag, $r(\Delta t)$ is the correlation coefficient, t is a point in time, and σ_u^2 is the variance of the velocity (Pope, 2000). The area under the $r(\Delta t)$ curve between $\Delta t = 0$ and where $r(\Delta t)$ crosses the Δt

axis gives the integral timescale. Assuming a frozen field of turbulence (Taylor, 1938), this can be multiplied by the mean streamwise velocity to give an estimate of the integral lengthscale, eq. (5.5).

$$r(\Delta t) = \frac{\langle (u_t - \overline{u})(u_{t+\Delta t} - \overline{u}) \rangle}{\sigma_u^2} \tag{5.4}$$

$$\ell_x = \overline{u} \cdot \mathcal{T} = \overline{u} \cdot \sum_{\Delta t=0}^{r(\Delta t)=0} r(\Delta t)\, \mathrm{d}\Delta t \tag{5.5}$$

5.4.2 Measurements and calculation of turbulence metrics

Two sets of measurements were conducted as part of this work. Firstly, to assess the impact of mean velocity on turbulence metrics, at the tank centre $(0, 0, 1.4)$ for a range of input rpms. Secondly, to map out the spatial variation across the tank, at a single velocity (82 rpm, nominally 0.8 m/s) over a range of X, Y, Z locations in the tank (table 5.3). For each measurement point a 600 s sample was recorded once the flow had stabilised. This was subdivided into T_{stat} long periods for calculation of the metrics.

Variation with mean velocity

Variation in turbulent flow metrics with input velocity was assessed at the tank centre. Figure 5.25 shows the variation in turbulence intensity I and integral lengthscale ℓ for increasing input velocity. There is no clear trend for I, but ℓ increases slightly with velocity.

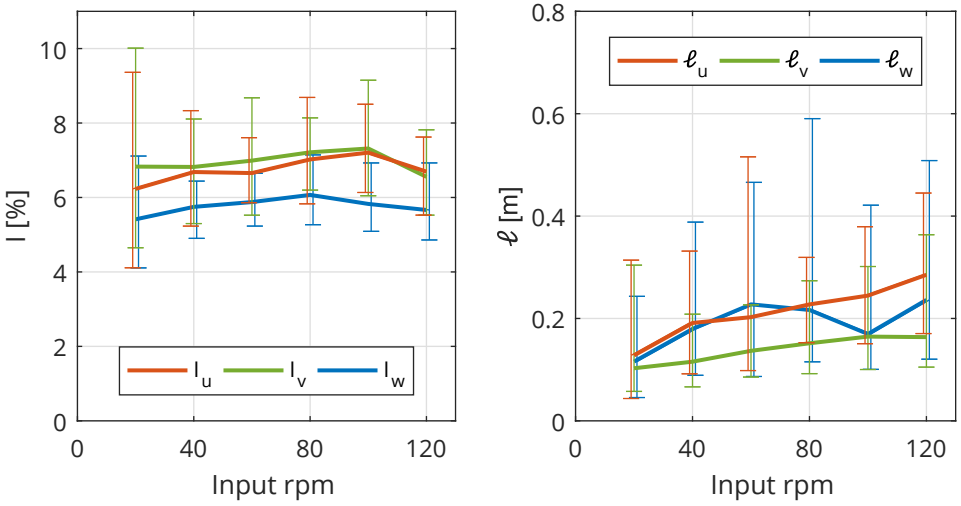

Figure 5.25: Variation in turbulence intensity I (left) and integral lengthscale ℓ (right) for increasing input rpm from nominally 0.2 m/s to 1.2 m/s at tank centre. Lines show mean values in streamwise u, transverse v, and vertical w directions, and bars indicate range of values recorded (with a small horizontal offset added for clarity).

5.4.3 Spatial variation of turbulence

To assess the spatial variation of turbulence in the tank, vertical profiles were measured at seven (X, Y) locations in the tank, chosen to line up with previous characterisation, section 5.3.2 and Noble et al. (2015). Vertical profiles of three key metrics, velocity, TI, and lengthscales are given in figs. 5.26 to 5.28. For clarity, these have been split into profiles upstream, downstream, and to the side of tank centre, with the central profile shown in each. Typical parameter values are given in table 5.7.

Transverse and vertical velocity components along the flow centreline ($X = 0$) are negligible, <10% of streamwise velocity. There is a slight negative bias to the transverse components, although this may be a result in a minor misalignment of the instrument.

Turbulence intensity in each axis is generally below 10% within the test area. The upstream profile $(-5, 0)$ has significantly higher TI, particularly in the lower half of the water column. This is the location closest to the inlet turning vanes, and so the flow profile is not fully developed by this point. Similarly, the profile 5 m to the side of tank centre $(0, 5)$ has higher TI, indicating a boundary of the better quality testing region.

Table 5.7: Typical mean turbulence parameter values.

Metric	Symbol	Typical Values
Turbulence intensity	I_x	5–11%
Integral lengthscale	ℓ_u	0.18–0.41 m

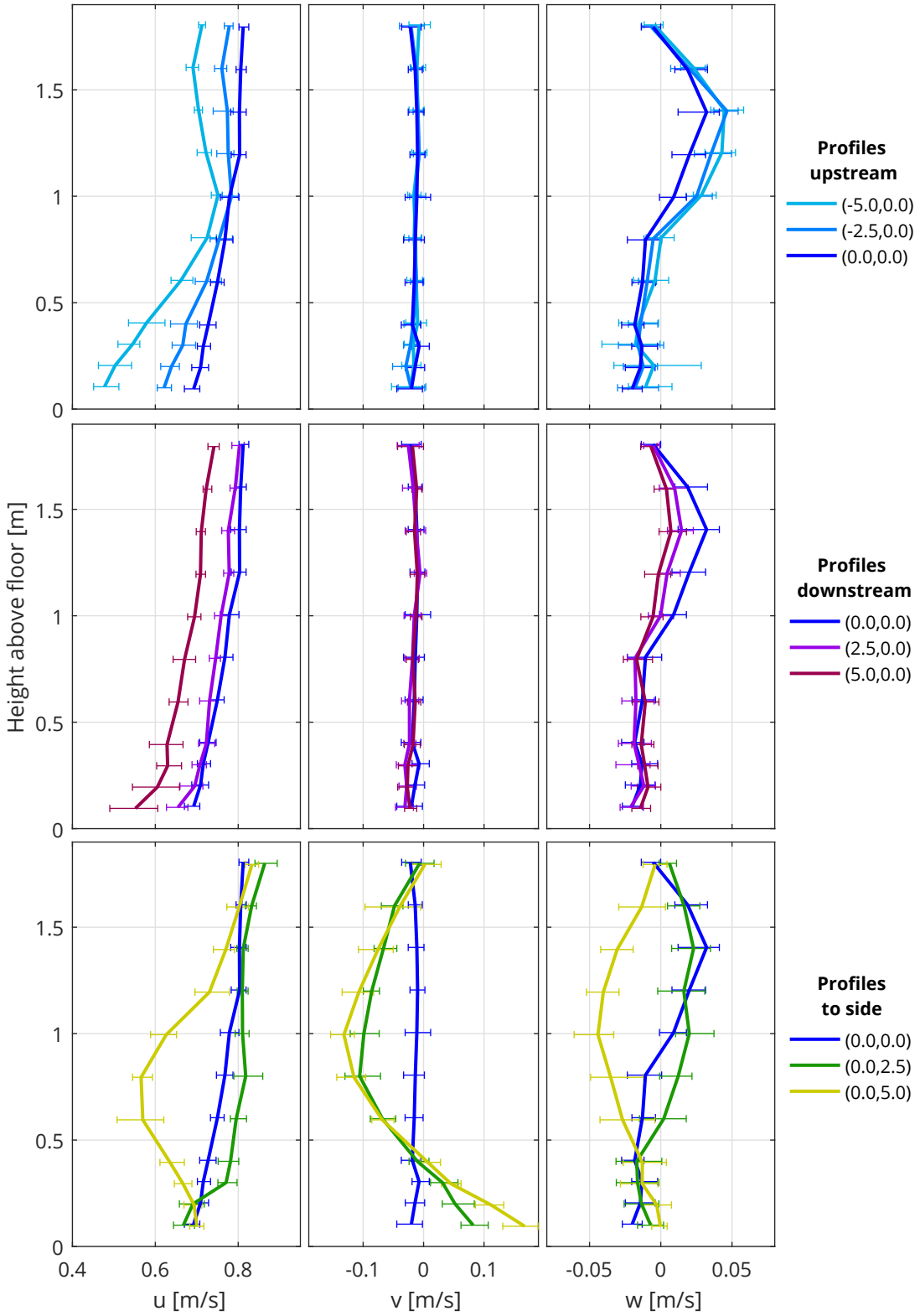

Figure 5.26: Spatial variation of turbulence metrics in the tank. Sub-panel columns show velocities in streamwise u, transverse v, and vertical w directions, rows are profiles upstream, downstream, and to side of tank centre at (X, Y) coordinates shown. Lines show mean value and bars indicate range of values recorded (with a small vertical offset added for clarity).

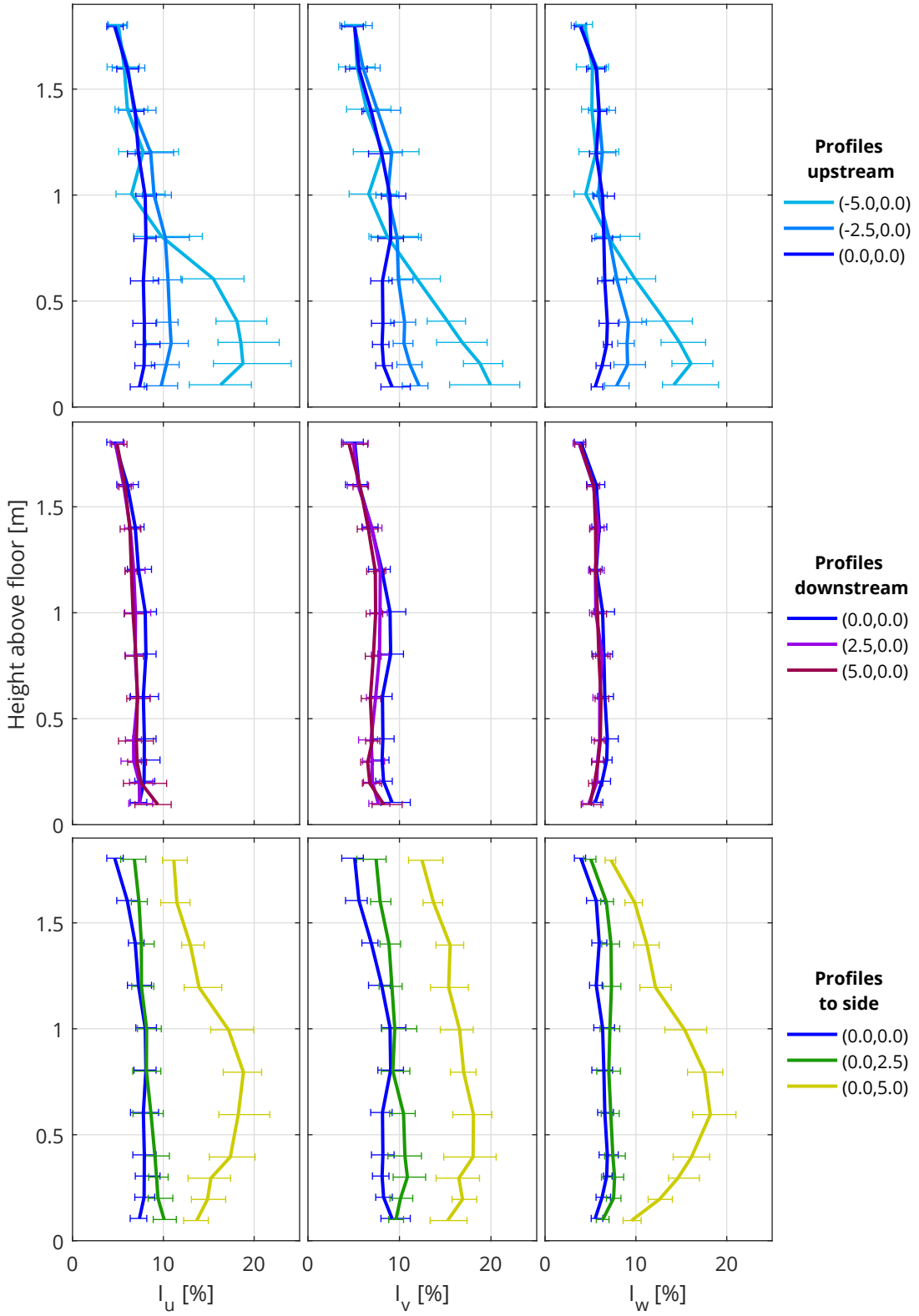

Figure 5.27: As fig. 5.26, but turbulence intensities in streamwise I_u, transverse I_v, and vertical I_w directions.

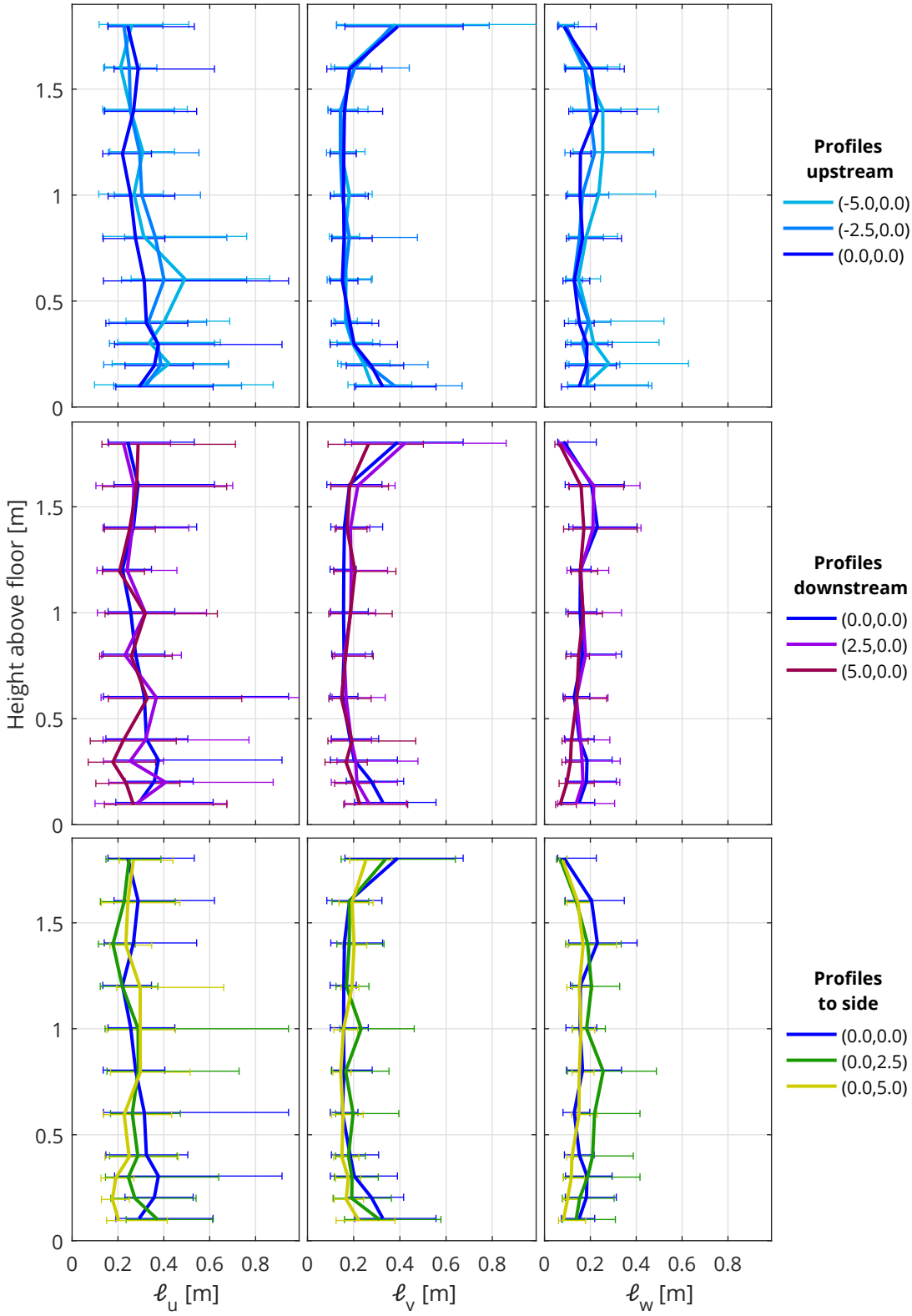

Figure 5.28: As fig. 5.26 but turbulent lengthscales in streamwise ℓ_u, transverse ℓ_v, and vertical ℓ_w directions.

5.5 Discussion on characterisation

5.5.1 Usable test area

Although there is spatial variability in mean flow across the tank, there is a central test area that is relatively uniform. The size of this area depends on the level of spatial variability that can be tolerated, as shown in table 5.8. For many tests, a variation of ±10% in flow velocity and ±10° in flow direction may be acceptable. This is based on typical requirements for client tests, but should be clarified on a case-by-case basis.

The wavemaker generation and absorption characteristics introduce additional constraints, including the spatial distribution of reflections. This is particularly important for combined wave-current conditions (section 6.2.1), where the usable test area becomes a function of at least four parameters ($H, T, U, \theta_{\text{rel}}$).

To help communicate the usable test area and conditions, quality metrics have been developed as discussed in section 7.3.

Table 5.8: Usable test area for different flow criteria.

Usable test area [m^2]		Variation in flow velocity			
		—	±20%	±10%	±5%
Variation in flow angle	—		136	92	59
	±20°	167	119	89	59
	±10°	103	77	64	50
	±5°	57	43	36	29

5.5.2 Implications of spatial variability

The test area in the tank is around 50 m^2, which is large enough for testing small arrays of devices. Whilst there is some variation in velocity over this area, it is only around 10% in plan and in depth. Knowing this baseline variation allows a reference velocity to be calculated at any point in the tank, or device in an array. Theoretical forces can then be predicted with a computer model and compared to those measured, for example. In addition, velocity measurements are typically made at a point close to the model during testing.

The tests undertaken show that across the test area, the flow is acceptably straight and horizontally uniform. This allows consistent testing over a large area of the tank, for example, to investigate impacts between small arrays of devices. It is noted that the configuration of a circular tank with circumferential wavemakers and impeller drive units below the floor by necessity leads to non-uniformities in the current flow field,

particularly around the turning vanes. The extent of non-uniform flow is limited through careful design of the turning vanes and drive motor control.

The spatial variation in flow speed and direction has implications for the generation of combined wave-current conditions in the tank, as discussed in chapter 6.

Full characterisation of the variation in flow field allows for a greater variety of flow conditions to be modelled in the tank, making use of the velocity gradients that exist in specific locations away from the central test area. There are likely be other constraints that need to be considered when locating a test location in the tank, as discussed in chapter 8.

A velocity transfer function was developed to translate input rpm to measured velocity at an X, Y, Z point in the tank, and vice-versa. This is described in more detail in section 5.6, and allows a good estimate of the flow conditions to be calculated. For tests requiring more accuracy in flow velocity, measurement and calibration of velocity at the point(s) of interest is undertaken.

5.5.3 Repeatability of currents

The flow generation in the tank is highly repeatable. Running separate tests with the same input rpm will result in the same mean flow for a given location in the tank.

As discussed in section 5.2.2, the current takes a few minutes to reach equilibrium. Thereafter, the mean flow velocity remains constant. Measurement of turbulence within the flow shows that the stationarity period T_{stat} is approximately 1 minute (section 5.4.1). This is defined as the period over which the turbulent flow has a stable mean and variance. For turbulence measurements to be repeatable, this gives a minimum record length that must be sampled.

There is a slight asymmetry in currents from different directions (section 5.3.4) but this is of a similar order of magnitude to turbulent fluctuations in the flow, and can be corrected through measurement and calibration at the point(s) of interest if required.

5.5.4 Comparison with design specifications

The design specification for the current generation at FloWave was a 0.8 m/s flow from any direction, with TI of ~10% (Davey et al., 2013). The central test area was envisaged as nominally 15 m diameter, to be large enough for testing small arrays of devices.

The drive motors are easily capable of creating flows of 1.2 m/s in the central test area (section 5.2.1), exceeding the design requirements. For typical test conditions, TI is around 5% to 10% (section 5.4.3), again matching or exceeding the design requirements.

The geometry of published numerical and physical modelling undertaken during the design stage (including Robinson et al., 2015*a*,*b*) does not necessarily match the final specification for FloWave. Additionally, the 3D volume of the tank was also represented numerically in two 2D models of XY and XZ dimensions respectively. Nevertheless, measured spatial variability of flow compares well with the design stage work.

The spatial extent of the test area with uniform current is an area approximately 6 m × 8 m transverse to the flow direction (section 5.3.2). Although this is smaller than the nominal 15 m diameter proposed, it is still large enough for testing multiple devices.

5.6 Velocity specification tool

To facilitate testing at FloWave, a velocity specification tool was developed in Microsoft Excel, as shown in fig. 5.29. It uses the flow characterisation data in this chapter, and was designed to be a stand-alone tool that is quick to use and does not require MATLAB.

The tool takes user input parameters specifying X, Y, Z position in the tank plus required flow velocity and calculates the primary control motor input rpm required, this can then be entered into the tank control software. As many clients relate their test programme to full scale units, the tool incorporates scaling using either the Froude or Reynolds relationship. Currents can also be specified in m/s or knots.

Selection of either a depth-averaged or tank-specific velocity profile is possible, and the change in water depth with wavemaker paddles resting on their backstops is also accounted for. The current angle is used to determine rotated X', Y' coordinates, the tank being assumed to be rotationally symmetrical.

Notifications and warnings are offered to users for input parameter combinations outside the well calibrated X, Y, Z, U region. The underlying model can also be updated as more calibration data become available. The calculation process is as follows:

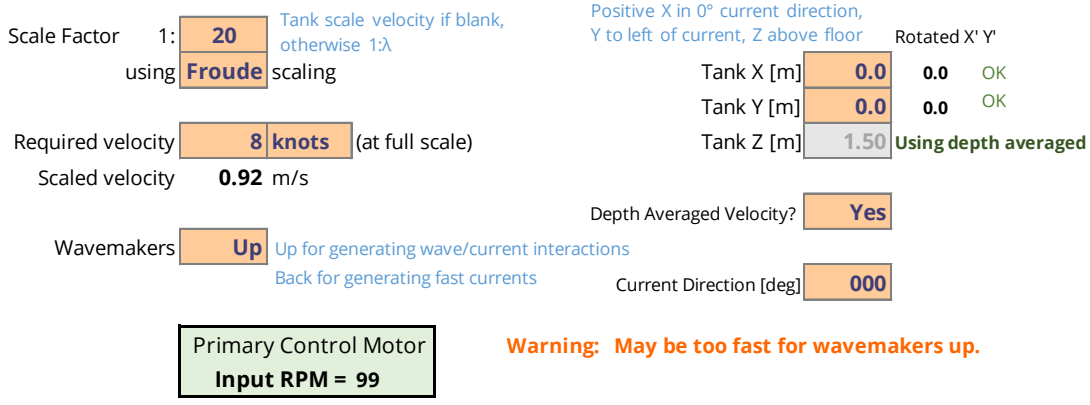

Figure 5.29: Screenshot of velocity transfer tool with user input cells highlighted orange.

1. Look up from horizontal spatial variability data the velocity relative to nominal at required X, Y coordinates .
2. Calculate velocity multiplier based on position of wavemakers, and depth-averaged velocity or Z coordinate.
3. Calculate control rpm from calibration of drive motors, based on a depth-averaged velocity.
4. Perform error checks, display warnings and rounded result.

5.7 Chapter conclusions

To carry out tests in the recently conducted FloWave facility, it was important to understand the flow generation performance. A series of experiments were therefore undertaken to characterise the current, considering both spatial and temporal variability of the mean flow. Initial characterisation of turbulence within the flow was also undertaken, including spatial variation of key metrics.

A revised calibration of the control drive motor rpm versus velocity in the tank was undertaken, and is now used to set the required flow speed for testing. Following a ramp-up period of 2–10 minutes, the flow is shown to remain stable and repeatable. Flow generation in the tank is rotationally symmetrical, albeit with a slight influence from the drive motors at $^{28}/_{360} = 12.86^{\circ}$ increments.

Measurements of spatial variation in the mean flow show that the vertical profile can be approximated as a $^{1}/_{15}$th power law. They also demonstrate there is a sufficiently large area where the flow is acceptably straight and uniform for the testing of small arrays of devices. The spatial variability, both in plan and vertical section through the tank, is close to design-stage modelling.

Measurements from the characterisation across the test volume can be used as a first estimate to set the required motor rpm. A tool has been developed to facilitate this in user-friendly way. These measurements can be refined with additional data if required for specific purposes.

The work presented in this chapter is used to enable commercial operation of the facility. For some client tests, flow velocity in the tank is specified directly based on the drive motor calibration and spatial characterisation undertaken. For other tests, where velocity is more critical or where there a model in the tank affects the flow, the characterisation is used as a starting point for measurement and correction of the required input.

CHAPTER 6

Combined waves and currents at FloWave

Chapter summary

- An overview of wave-current interactions considering their impact on Offshore Renewable Energy (ORE). This includes physical limits of waves combined with currents (wave breaking and blocking).
- Methods of generating combined conditions in a tank, focusing on FloWave. Physical constraints of a circular wave-current facility are considered, as is the repeatability and spatial variation of combined wave-current conditions produced at FloWave.
- Observations of the influence of currents on the properties of waves, including both collinear and non-collinear interaction cases.
- A methodology to produce waves of the 'correct' height in the tank when combined with a current is developed and tested.

6.1 Summary of wave-current interactions

Water waves and currents both have an effect on, and are affected by, each other in a complex manner, as discussed in section 2.1.5. This can be simplified into two main cases in terms of tank testing.

1. The changes to waves as a result of interaction with currents, primarily of interest for floating devices and Wave Energy Convertors (WECs). The observed influence of currents at an angle to waves is also of more general interest, as there are few published experimental results with waves at oblique angles to currents (section 3.3.2).
2. The impact of waves on the current and turbulence, important for understanding loading on Tidal Stream Turbines (TSTs) and subsurface structures.

The work in this chapter only considers the former case. The latter is being investigated as part of the Supergen Marine grand challenge *'FloWTurb: Response of Tidal Energy Converters to Combined Tidal Flow, Waves, and Turbulence'* (EP/N021487/1) lead by The University of Edinburgh, which includes tank testing at FloWave.

Over 30 years ago, Peregrine and Jonsson (1983) noted:

> In engineering practice, the importance of wave-current interaction has often been poorly understood. In some cases, the fact that both the waves and currents are simultaneously important is not recognized. In other cases, where both waves and currents are understood to be important at the same time, the importance of the interaction between the waves and currents is not recognized. Even when both the waves and the currents are known, their interaction may produce a significantly different effect from that obtained by simply adding the effect of the waves and the currents considered separately.

This is possibly still true today, especially in the field of ORE. A summary of wave-current interaction effects particularly of relevance to ORE is therefore provided below.

- There is a change in wave steepness, with height increasing and length decreasing on an opposing current, and vice-versa with following currents. Fast currents opposing the waves will result in wave breaking as the steepness increases past a critical value, and will eventually lead to blocking.
- The intrinsic wave period T (as measured by a stationary observer) does not change, but the period *relative* to the moving mass of water T_r does.
- There is also a change in wave power, resulting from the change in wave height and group velocity, discussed further in section 6.5.2.
- Turbulence generally increases with current speed, and the interaction with wave orbital motion is a complex subject. Wave motion is often considered separately to turbulence, then the two superimposed. Strictly speaking, the passage of a wave may stretch turbulent eddies, altering their form (Clark, 2015). These eddies can also alter the shape of individual waves.
- Loads on submerged structures and floating device moorings will typically increase, as a result of both current drag and also the change in wave loading.

The relative angle between current and wave propagation directions is taken as θ_{rel}. A 'following' current is defined as one flowing in the direction of wave propagation, i.e. $\theta_{\text{rel}} = 0^\circ$, and an 'opposing' current is the opposite, i.e. $\theta_{\text{rel}} = 180^\circ$.

Change in wavelength and height with breaking and blocking limits

To illustrate the change in wavelength and wave height occurring from the interaction with a current, theoretical values have been calculated using linear interaction theory for a typical range of wave conditions used in the tank, as shown in fig. 6.1. This includes conditions where wave breaking and blocking may be an issue, with these criteria marked. Waves are blocked for conditions to the left of blocking criteria lines in fig. 6.1(b), highlighting that this is primarily an issue for high-frequency (short period)

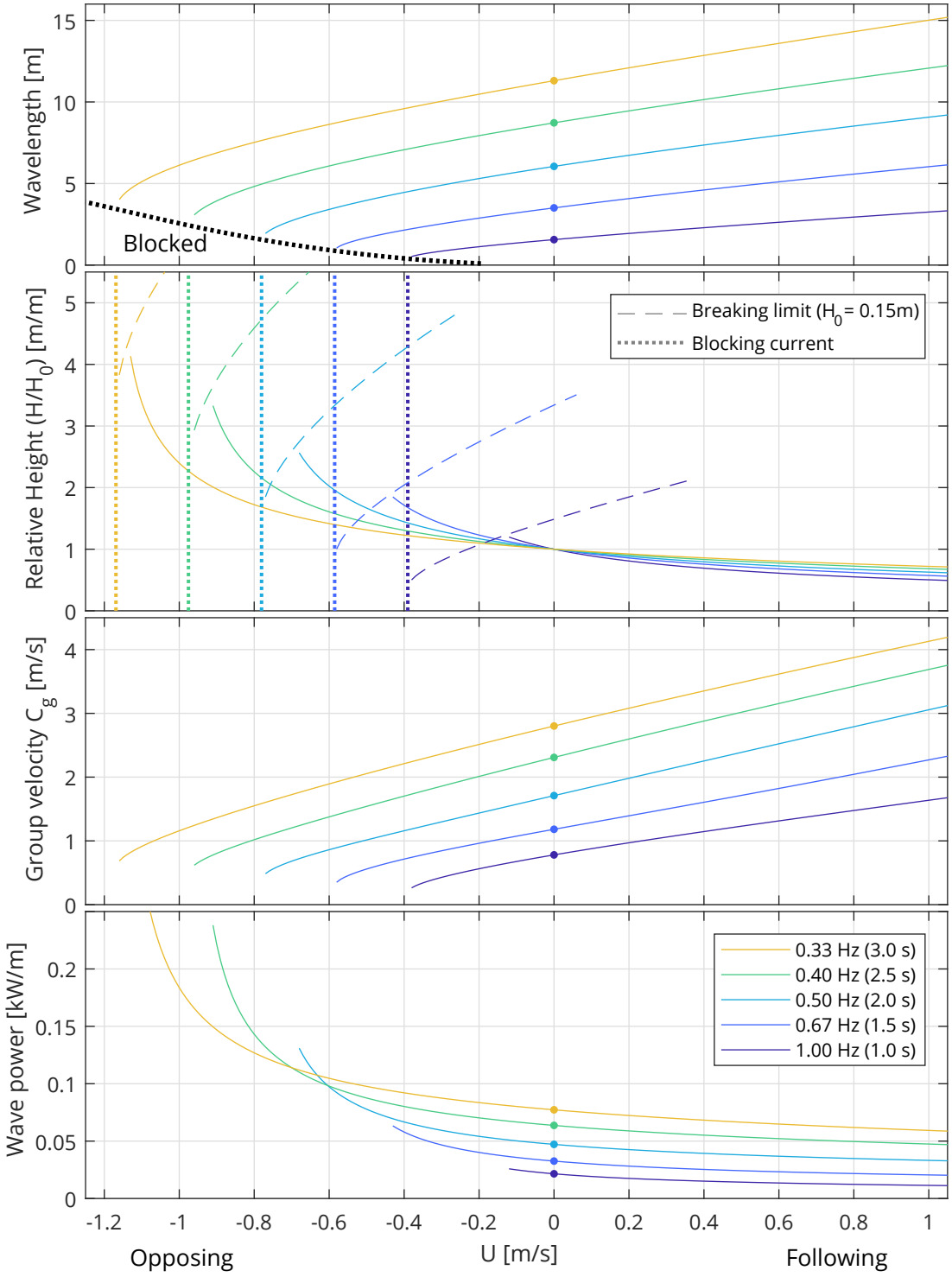

Figure 6.1: Change in parameters with collinear current for typical wave conditions at tank scale, based on linear interaction theory. Plots show from top:
(a) Change in wavelength L, proportional to celerity c. Wavelength without current L_0 marked by point for each period. Blocking limit shown by black dotted line.
(b) Change in relative wave height as solid lines. Breaking criteria for H_0 = 0.15 m shown by dashed lines. Blocking velocities U_B shown by vertical dotted lines.
(c) Change in group velocity C_g. (d) Change in wave power per unit crest length P_w for H_0 = 0.15 m.

waves propagating against relatively fast currents. Corresponding change to group velocity C_g and wave power per unit crest length P_w are also shown, illustrating that wave power is not conserved. The breaking limit and wave power are a function of wave height, and for these examples are based on a 0.15 m high wave prior to interaction with the current.

This theoretical approximation is based on linear wave theory, assuming infinitely long plane waves on a uniform current. The waves generated in the tank however, have a finite crest length and interact with a current that is varying both spatially and temporally as discussed in chapter 5, so observations in the tank may not match theory.

While comparison is made in this chapter to a linear theoretical model of wave-current interaction, this is purely to improve understanding of the results, and illustrate the effects observed. It is not the aim of this project to validate these theories, nor to develop or use a complex numerical model of the tank.

Calculation of wave blocking current

As noted in section 2.1, wave blocking occurs when the current velocity exceeds the group velocity of the wave, $C_g + U \leq 0$. This blocking point is marked on fig. 2.3, where there is exactly one solution to eq. (6.1).

$$\omega - kU = \pm\sqrt{gk \tanh kh} \tag{6.1}$$

This can be solved using the non-dimensional variables introduced by Suastika (2012), $\kappa = kh$, $\mathcal{U} = U/\omega h$, $\Omega = \omega_r/\omega$, and simultaneously solving eqs. (6.2) and (6.3).

$$(1 - \kappa\mathcal{U}) \pm \sqrt{\frac{g}{\omega^2 h}\kappa \tanh \kappa} = 0 \tag{6.2}$$

$$\frac{d}{d\kappa}(1 - \kappa\mathcal{U}) - \frac{d}{d\kappa}\left(\omega - \kappa\mathcal{U}\sqrt{\frac{g}{\omega^2 h}\kappa \tanh \kappa}\right) = 0 \tag{6.3}$$

6.2 Generating combined wave-current conditions at FloWave

In the FloWave facility, waves are generated in a region of relatively still water around the circumference of the tank and then interact with the current which is injected through the floor, as discussed in section 4.2. Waves propagate across the tank, interacting with the current in the central region. To produce the desired wave height in the central test area of the tank in the presence of a current, a correction factor must be applied to the wave generated in still water, discussed further in section 6.5.

6.2.1 Combined wave-current generation limits

There are physical generation limits on flow velocity and on the maximum wave height that can be produced at any given frequency (section 4.2.5). The envelope of combined wave-current conditions that can be generated sits within these limits. The wavemaker limits apply in still water, and those waves are then transformed by the current. An added complication is the envelope becomes a function of four parameters: $H, T, U, \theta_{\text{rel}}$.

There are also fundamental constraints on water waves that can physically exist, e.g. steep waves will tend to break. In fast opposing currents, wave steepness increases and breaking becomes more likely. Waves may also be blocked by sufficiently fast opposing currents as discussed in section 6.1.

The capability to generate currents, or to generate and absorb waves, is relatively well understood for each condition independently. Combined conditions however are more complex and less well understood, therefore need to be approached differently. There has been a process of understanding what waves can safely be generated and absorbed by the tank machinery when produced in combination with currents, incrementally increasing the envelope of possible conditions.

Although the wavemakers operate in a zone of relatively still water (section 4.2) there is some re-circulation of the current. This is clearly visible on the design stage numerical modelling, fig. 4.4. Particularly when producing faster currents, this leads to increased force on the wavemaker paddles. To limit this impact when running combined conditions, the current velocity is usually capped at ~0.9 m/s (at the time of writing). The envelope of wave height/frequency conditions run is also reduced compared with waves in still water (fig. 4.7).

Both the magnitude and spatial distribution of reflections in the tank are affected by the presence of a current. It has also been found that the paddle absorption efficiency decreases in combined wave-current, for some conditions more that others. Additionally, there may be tank-specific generation effects influencing the waves produced in combination with current. These are a function of at least four-parameters ($H, T, U, \theta_{\text{rel}}$), and work is ongoing at FloWave to characterise this. As part of this, methods are being developed to measure wave reflections in the presence of a current (Draycott et al., 2018).

When generating waves on a following current in the central test area, reflections will meet an opposing current. In this case high frequency components may be blocked, improving the quality of conditions in the test area. Conversely, reflected waves may be swept into the central test area for opposing current cases.

The spatial variation in mean flow across the tank also affects the distribution and curvature of waves, as discussed in section 6.2.3.

6.2.2 Repeatability of combined wave-current conditions

Before testing with combined wave-current conditions, it is important to understand the tank performance and repeatability, both for the combined conditions but also for waves or currents alone.

The temporal stability and repeatability of currents generated in the tank is discussed in section 5.5.3. Short term turbulent fluctuations are averaged out for samples of ~1 minute or more. Turbulence within the flow can alter the shape of individual waves in the tank, as in the real ocean. As turbulence is a chaotic process, this will reduce the repeatability of combined wave-current conditions.

As noted in section 3.2.3, Draycott (2017) showed that without currents, wave generation at FloWave is highly repeatable as expected. A good demonstration of the controllability and repeatability of wave generation at FloWave is the 'concentric spike' wave (FloWave Ocean Energy Research Facility, 2015, 0:47). For this, all paddles create a focused wave group from 360° which meet in the tank centre, causing a 5 m high wave.

Method

To assess the repeatability of waves, both with and without current, five repeat runs were measured of the waves in table 6.1.

The first set of waves (a) correspond to a client test of a TST operating in waves combined with a 0.8 m/s hub-height current, at multiple relative angles. The measurements used here were conducted without the model in the tank, as a baseline case. The next two sets of waves (b,c) are defined by steepness, and tie in with those used for the wave characterisation. Additionally, a focussed wave group (PM spectrum) that breaks in the tank was also measured, set (d). The latter three were all for the still water case only.

For the tests without current, an eight gauge linear reflection array (WA4, section 4.3.1) was set up on the gantry along the direction of wave propagation. The tests with current used only two gauges, 0.7 m apart, centred on (−2.1, −0.5) where the turbine blades were located in subsequent tests. An Acoustic Doppler Velocimeter (ADV) was also used to measure the current and turbulence at five points in the water column for the client.

A cross-correlation matrix of the water surface elevation measurements between repeats was calculated using the MATLAB `xcorr` function. Excluding the five auto-correlations and noting by symmetry $r_{1,2} = r_{2,1}$ etc., this gives ten pairs of repeats with which to assess the repeatability, at each gauge location. The coefficient of determination r^2 was then used as a comparator to assess repeatability.

Table 6.1: Test parameters for wave and wave-current repeatability tests.

Set	f, f_p [Hz]	T, T_p [s]	H, H_{m0} [m]*	Steepness	Velocity [m/s]
(a) Long crested regular waves for 160 s test length. Run with no current and with 0.8 m/s current at various angles to wave propagation direction					
	0.33	3.0	0.087	~	0, 0.8
	0.40	2.5	0.092	~	0, 0.8
	0.50	2.0	0.103	~	0, 0.8
(b) Long crested regular waves, for 128 s test length					
	0.30	3.33	0.130	1%	—
	0.45	2.22	0.145	2%	—
	0.60	1.67	0.086	2%	—
	0.75	1.33	0.056	2%	—
	0.90	1.11	0.039	2%	—
(c) Long crested JONSWAP spectrum ($\gamma = 3.3$), for 512 s test length					
	0.30	3.33	0.130	1%	—
	0.45	2.22	0.145	2%	—
	0.60	1.67	0.086	2%	—
	0.75	1.33	0.056	2%	—
	0.90	1.11	0.039	2%	—
(d) Long crested focused breaking wave group, for 64 s test length					
	0.55	1.8	0.240	~	—

*. All wave heights relate to that in still water, but are altered by interaction with the current.

Results

The high level of repeatability for waves alone is shown in fig. 6.2, with $r^2 > 0.97$ for all cases. The irregular sea states and the higher frequency waves have a slightly lower coefficient of determination, which is likely due to increased reflections in the tank. Even the breaking wave group was highly repeatable.

When combined with a current the repeatability of waves in the tank reduces, as shown in fig. 6.3, with $0.7 < r^2 < 1$. Turbulence within the flow affects wave orbital motion, and thus timing of wave crests in a random manner. Only one set of wave-current conditions are presented here, but they are representative of other observations made at FloWave.

The tendency for lower repeatability with higher frequency waves is still apparent, although not as clear because the highest frequency tested was 0.5 Hz. The quality of waves in the tank at 135° and 155° to the current was visibly poorer, leading to a reduction in repeatability apparent in fig. 6.3. It is unclear why the quality of 0.4 Hz waves at 0° and 20° was so low, but this is may be a result of spatial variation in reflections. For most other waves tested, the repeatability was found to be relatively high, with $r^2 > 0.95$.

These measurements represent only one position in the tank, but the quality should be representative of the central test region. Considerable spatial variability of the combined wave-current field was however observed visually during testing, particularly around

the perimeter of the tank. This is a combination of spatial variation in the current (section 5.3) and wave reflections (Draycott, 2017).

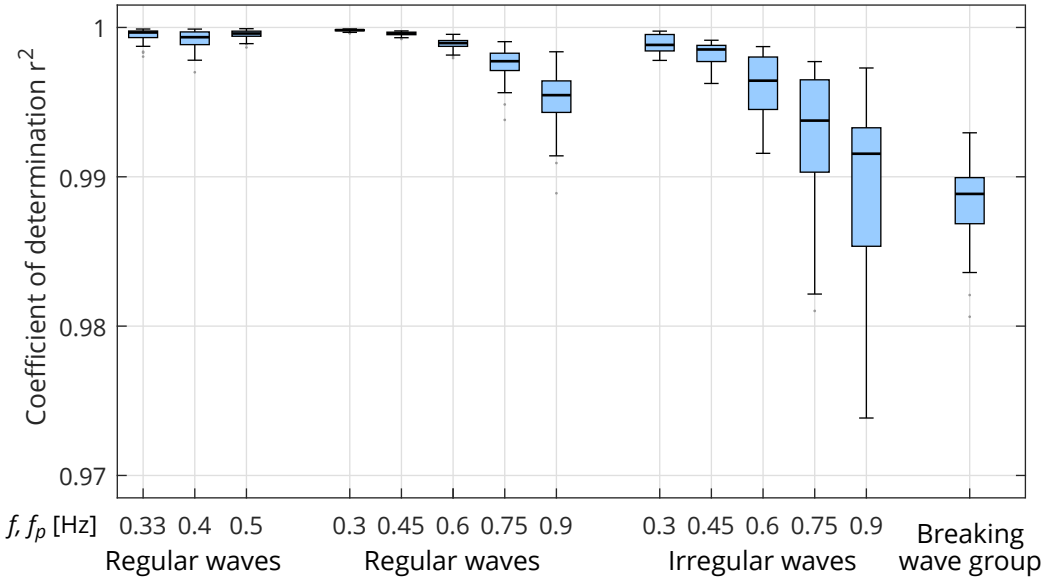

Figure 6.2: Repeatability of waves without current for four sets of waves with varying frequency and height, see table 6.1 for wave properties. Box and whiskers show quartiles of r^2.

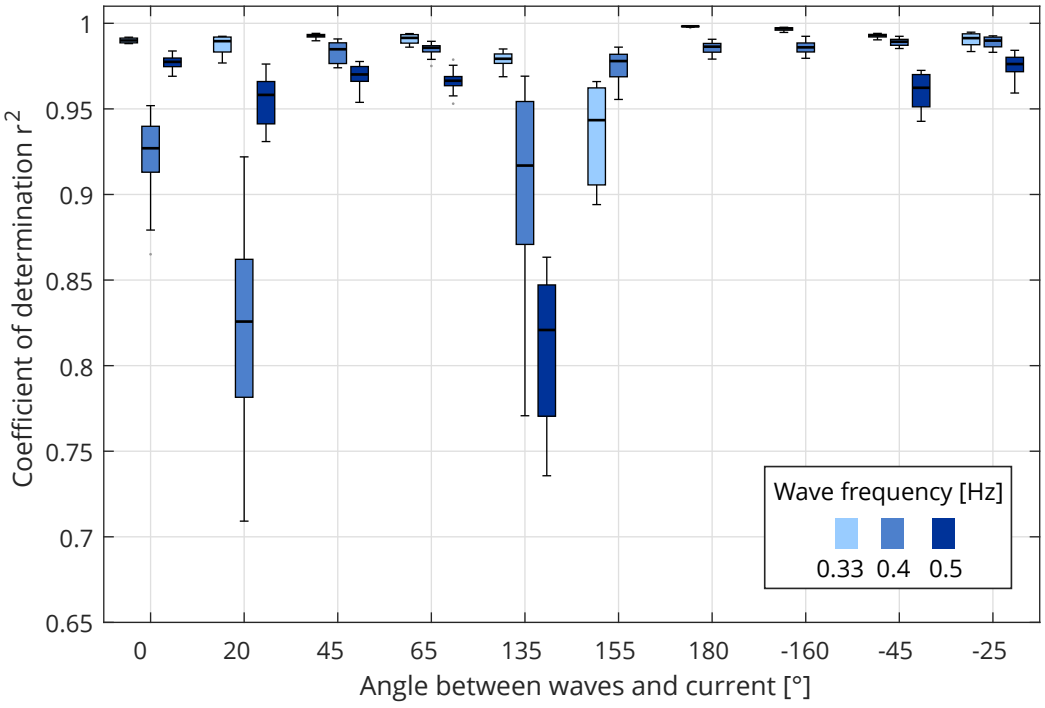

Figure 6.3: Repeatability of regular waves of varying frequency and height, with a 0.8 m/s current at various relative angles. Box and whiskers show quartiles of r^2. Note that 0.5 Hz wave was not run at 155°, 180°, or -160° due to partial blocking.

6.2.3 Wave curvature as a result of non-uniform current

The method of flow generation at FloWave results in a non-uniform flow field across the test area with faster flow near the tank centre. Characterisation of this variation is shown in section 5.3.2. When combined wave-current conditions are generated, this non-uniform flow results in a curvature of the wave crest, due to the central section of the wave interacting with a faster current than at the tank edges. This effect is particularly noticeable for long-crested regular waves, where any discrepancy is easy to spot. Irregular and short-crested waves will also be affected to the same degree, but it is not visually as apparent being masked by the variability of the underlying waves.

Method

To measure the effect, a wave gauge array (WA3, section 4.3.1) was set up along the gantry perpendicular to the wave propagation direction. This used 12 gauges at 0.9 m spacing covering half of the tank. An additional four gauges were used to check symmetry of the wave crests about the flow direction. To limit the build-up of reflections, waves were only generated for 32 s. Data was recorded at the maximum 128 Hz sample rate for a 64 s period, to include time taken for the waves to propagate across the tank.

A series of five regular waves of varying frequency from 0.3 Hz to 0.9 Hz were used, table 6.2, chosen to match previous wave characterisation work (Draycott, 2017). The waves were generated at 0° and 180°, in still water and with currents at 0° in steps of nominally 0.1 m/s up to a maximum of 0.5 m/s, to give following and opposing cases.

The temporal lag Δt at each wave gauge relative to the tank centre was calculated using cross-correlation. A short sub-sample was used for the calculation, with an integer number of waves over approximately 12 s. The start time was based on the expected time for the first wave crest to reach the wave gauges, a function of distance and relative group velocity C_{gr}, eq. (2.23).

Table 6.2: Wave parameters for wave-current curvature observations. Long crested regular waves, for 32 s test length, measured using wave gauge array WA3.

f [Hz]	T [s]	H [m]	Steepness
0.3	3.33	0.130	1%
0.45	2.67	0.145	2%
0.6	1.67	0.086	2%
0.75	1.33	0.055	2%
0.9	1.11	0.039	2%

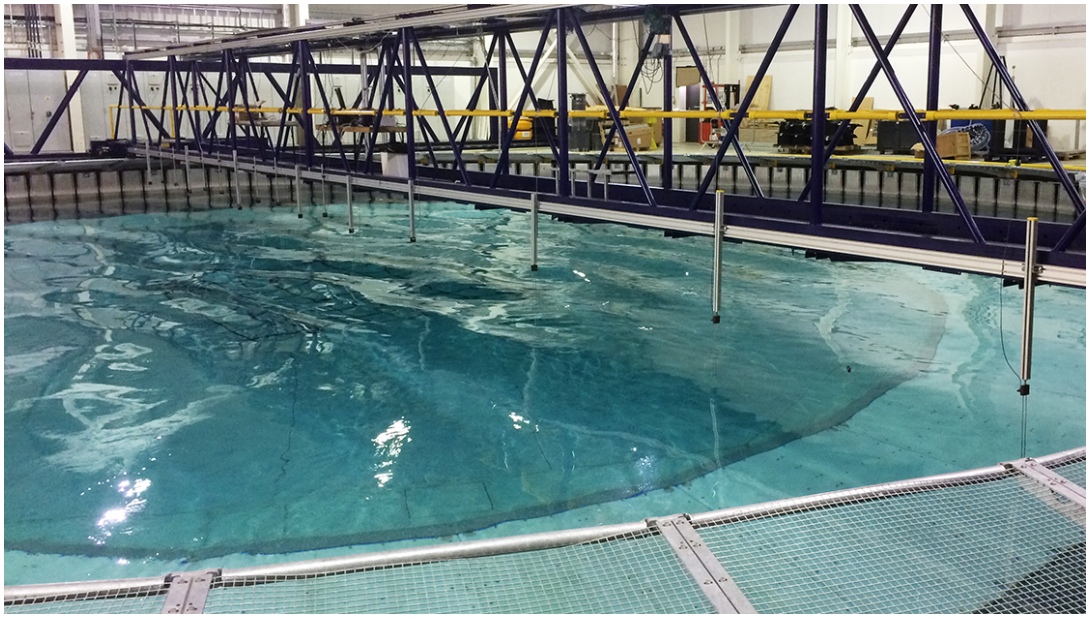

Figure 6.4: Photo showing lack of spatial coherence in combined wave-current. Regular 0.9 Hz wave crests splitting with a 0.2 m/s opposing current. Wave gauge array WA3 installed on gantry.

The signal was first smoothed by 5 samples (0.04 s) to reduce the influence of any high-frequency vibrations. It was then up-sampled by a factor of 5 to give a finer temporal resolution and thus reduce quantisation of the results.

Results

The results of these tests are presented in fig. 6.5. The lag is shown relative to the wave period (i.e $\Delta t/T$) as this corresponds to what is observed, i.e. a fraction of a wavelength. As the water velocity and wave celerity relative to the moving water are not known, it is not possible to calculate the lag in terms of a distance, therefore curvature shown in the figure does not accurately represent geometrical distortion.

As expected, the effect increases with distance from tank centre, current velocity, and frequency, as shown in fig. 6.5. For waves on a following current the maximum absolute lag is around 0.1 s to 0.5 s. Waves opposing the current show a larger effect, with lags from 0.3 s to 1 s or possibly more. For some conditions, particularly higher frequency waves with faster opposing currents, the cross-correlation fails. It appears to correlate with the wrong wave crest, but this is not clear when examining the recorded timeseries. For these conditions, the wave crests are no longer uniform. Instead, there is a loss of spatial coherence, with the crest tending to split up along its length, as shown in fig. 6.4. The effect of wave curvature is symmetrical about the wave and current propagation direction. This is slightly masked by the increased number of wave gauges on one side shown in fig. 6.5.

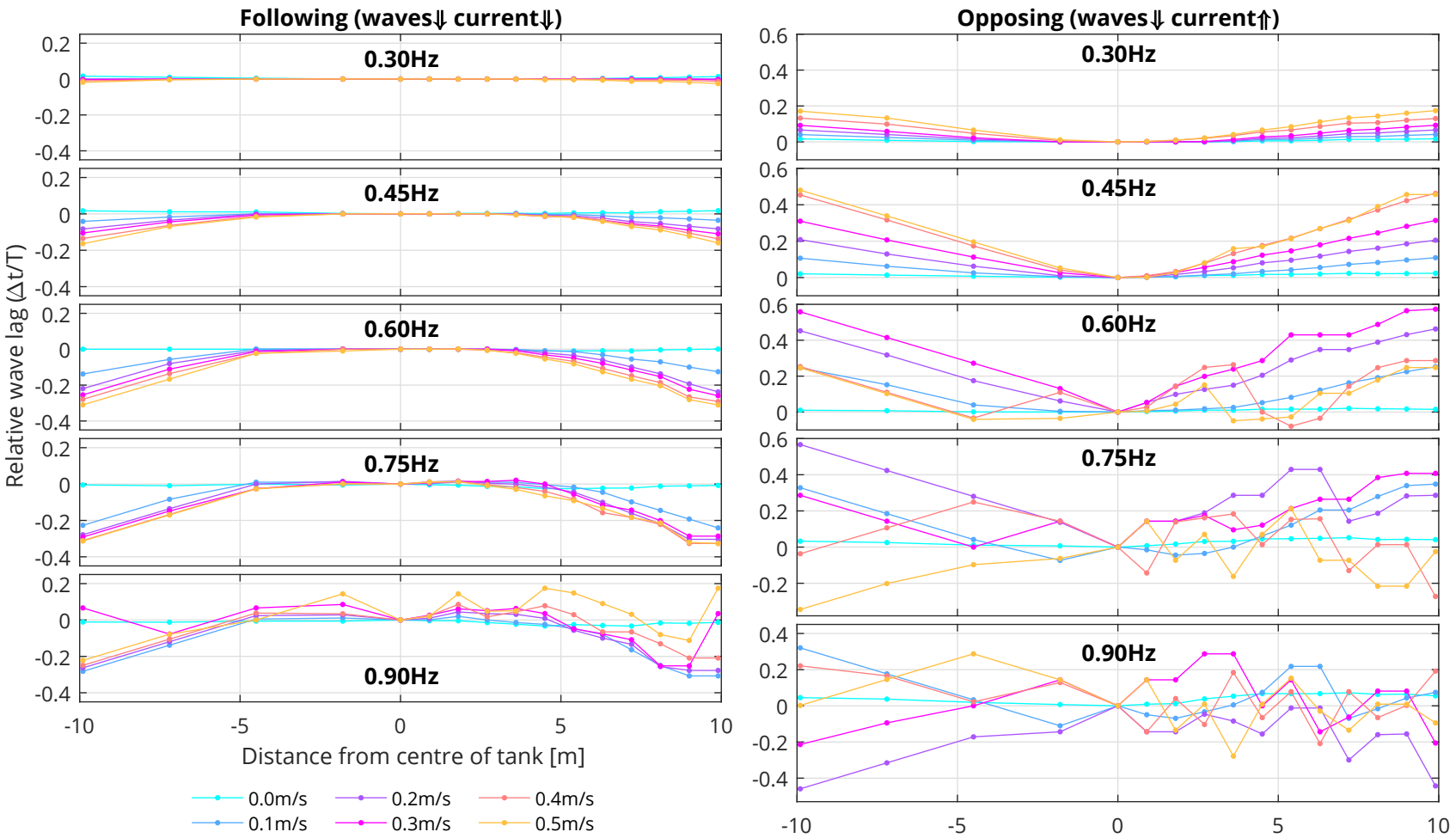

Figure 6.5: Wave curvature in the time domain as a result of non-uniform current. Subplots show the five wave frequencies with following and opposing currents. Aliasing between waves apparent for higher frequency waves in faster currents, particularly for the opposing case. Note that curvature shown does not accurately represent geometrical distortion.

6.3 Methods for characterising combined wave-current conditions at FloWave

To facilitate testing in combined conditions, it is important to understand how waves and currents interact within the circular FloWave basin. This includes non-collinear interactions with waves at oblique angles to currents, something that is not possible at many other facilities.

It is not intended that this project will characterise the full complexity of wave-current interactions at every point in the basin, nor consider all possible combinations of waves and currents. This would be a very time-consuming and complex project, occupying the tank for considerable periods. A limited number of cases have therefore been investigated as discussed below to give an overview. It is envisaged that future tests in combined wave-current conditions will expand this envelope.

6.3.1 Test plans

A series of experiments were conducted to record the influence of currents on waves, particularly focussing on the change in wave height and wavelength. Four sets of waves were observed with current, of which some were also corrected (section 6.5). Details of the test matrix are given in table 6.3, where the wave height refers to that in still water prior to interaction with the current.

Regular waves with four frequencies and three steepness values (a), although not every permutation was tested. These waves were propagating over current velocities up to 0.5 m/s, at nine relative angles to the current direction between following and opposing.

Two complimentary irregular sea states were also used: (b) a parametric uni-directional JONSWAP spectrum, and (c) a non-parametric directional sea state (fig. 6.6) derived in Draycott et al. (2015*a*) from data recorded at the EMEC Billia-Croo test site. Due to test length limitations, only five relative angles were tested for the irregular seas. Tank limits (section 6.2.1) capped the current velocity to 0.2 m/s for the 0.3 Hz waves.

Finally, long-crested Pierson–Moskowitz (PM) spectra with varying height and frequency (d) were tested with following and opposing currents up to 0.3 m/s. These sea states were specified, without current, for client testing during the Wave Energy Scotland novel WEC funding call, and thus used to demonstrate typical test conditions. Test length for these was set to give 512 s of data with a 33 s period for the waves to reach a steady state.

All of these wave conditions were recorded without current to provide a baseline measurement. Velocity was specified as a depth averaged value at tank centre based on the tank calibration for all these tests. No velocity measurements were made during these tests, partially to simplify the tests, but also due to instrumentation issues.

Table 6.3: Test parameters for wave-current interaction observations (all conditions, section 6.4) and for correction of wave height (marked ‡, section 6.5).

Set	f, f_p [Hz]	T, T_p [s]	H, H_{m0} [m]*	Steepness	Current velocities [m/s]
(a) Long crested regular waves, at 9 relative angles 0–π in $\pi/8$ increments, for 128 s test length, using wave gauge array WA1					
	0.3	3.33	0.130 ‡	1%	0.05, 0.1, 0.2
	0.3	3.33	0.259	2%	0.05, 0.1, 0.2
	0.4	2.5	0.087	1%	0.05, 0.1, 0.2, 0.3, 0.4, 0.5
	0.4	2.5	0.174	2%	0.05, 0.1, 0.2, 0.3, 0.4, 0.5
	0.4	2.5	0.349	4%	0.05, 0.1, 0.2
	0.5	2.0	0.121	2%	0.05, 0.1, 0.2, 0.3, 0.4, 0.5
	0.6	1.67	0.086	2%	0.05, 0.1, 0.2, 0.3, 0.4, 0.5
(b) Long crested JONSWAP spectrum (γ=3.3), at 5 relative angles 0–π in $\pi/4$ increments, for 512 s test length, using WA1					
	0.3	3.33	0.130 ‡	1%	0.05, 0.1, 0.2
(c) Non-parametric directional sea state derived from EMEC Billia Croo site data, at 5 relative angles 0–π in $\pi/4$ increments, for 2048 s test length, using WA1					
	0.266	3.76	0.128 ‡	~	0.05, 0.1, 0.2
(d) Long crested PM spectra, with following/opposing currents, for 545 s test length, using WA5					
	0.26	3.92	0.08	~	0.1, 0.2, 0.3
	0.35	2.82	0.10	~	0.1, 0.2, 0.3
	0.43	2.35	0.18	~	0.1, 0.2, 0.3
	0.49	2.03	0.18	~	0.1, 0.2, 0.3
	0.58	1.72	0.13	~	0.1, 0.2, 0.3

*. All wave heights relate to that in still water, but are altered by interaction with the current.

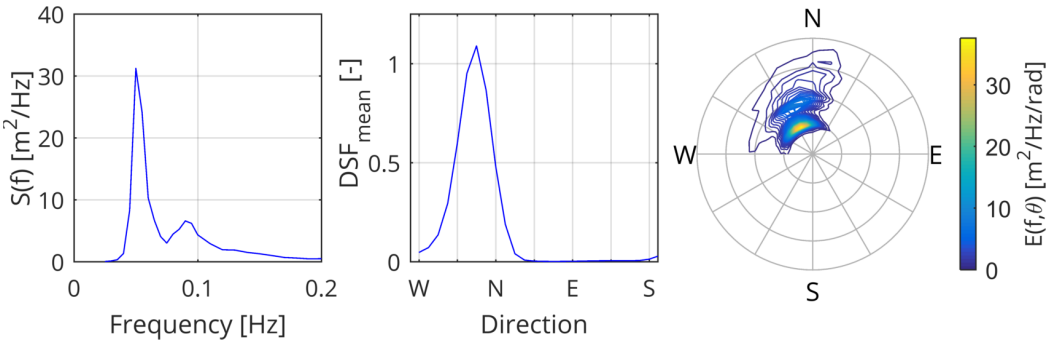

Figure 6.6: Non-parametric directional sea state derived from EMEC Billia Croo site data (Draycott et al., 2015*a*), which was measured and corrected with current. Subplots show spectral density $S(f)$, weighted mean directional spreading function DSF_{mean}, and directional spectrum $E(f, \theta)$. Full-scale values are: H_{m0} 3.53 m, T_p 20 s, and P 87.6 kW/m

6.3.2 Measurement of interaction

For test conditions (a,b,c) in table 6.3, the standard directional wave gauge array was used in the centre of the tank (WA1, section 4.3.1). A cross-shaped array (WA5) was used for test (d). The data sample rate was 32 Hz for the regular wave tests (a), and 128 Hz for the irregular sea states (b,c,d).

To reduce the test matrix for conditions (a,b,c), waves in still water were only measured at one angle, corresponding to a perpendicular current. For the tests with current, waves in the tank were generated at various angles, with the current kept at a constant direction to optimise timings. To provide a steady-state test, current in the tank was allowed to stabilise for a period of at least 10 minutes prior to taking any measurements, and the wave spectra were calculated over the full 512 s or 2048 s measurement duration.

Determining regular wave height

Due to the build-up of reflections, recorded wave height in the tank is not always constant over the whole test duration, especially when considering combined wave-current conditions where temporal variations in the current also affect the waves. As noted section 6.2.1, reflections in the tank are more problematic when running combined condition. This can lead to the build-up of 'hot' and 'cold' spots, where there is constructive and destructive interference respectively, between the incoming and reflected waves. Where a reflected wave interfers completely with the incident wave to become a standing wave, the points of destructive interference where there is no vertical movement of the water surface are referred to as 'nodes', with 'antinodes' in between where there is constructive interference causing a double amplitude wave.

For any point in the tank, there is a short period after the first waves reach this point, but before the reflected waves return, where only the incident wave crest is present. As the celerity of a water wave is frequency dependent (section 2.1.2) so to is the timing and duration of this period with only incident waves, although this is affected by the current.

Wave height for the regular waves, table 6.3(a), was calculated at each gauge in the time domain using a zero-down-crossing analysis (section 4.4.2). To avoid spurious small waves resulting from vibration of the gauges or high frequency reflections, a seven-sample (0.22 s) moving average smoothing function was applied to the input for the zero-crossing analysis. Calculated wave height was interpolated to produce a time series showing how wave height H, rather than water surface elevation η, changed throughout the test. The standard deviation of wave height measured across all N_g wave gauges for the time period of interest (from t_1 to t_2 samples) was taken as a proxy for wave quality, eq. (6.4).

$$\varepsilon = \frac{1}{t_2 - t_1} \sum_{t=t_1}^{t_2} \sqrt{\frac{1}{N_g - 1} \sum_{g=1}^{N_g} |H_{g,t} - \bar{H}_t|} \tag{6.4}$$

It was observed that there is generally a period of 'good quality' waves at the start of each test, followed by a build-up of reflections. When this period starts depends on how fast the first wave propagates across the tank, a function of current velocity U and wave group velocity C_g. The duration of this period is more complex, based on the tank response and reflections, both of which are frequency dependent. Figures 6.7 and 6.8 show the time-domain analysis for two example wave-current conditions with low and high deviation between gauges respectively. There are few reflections with the low-frequency waves in fig. 6.7, shown by the low standard deviation between wave heights measured at individual gauges. Reflections are much greater for the steeper higher-frequency waves, fig. 6.8. The lowest dotted lines on fig. 6.8 show wave gauges close to a partial node, and the highest dotted line is close to a partial antinode, although it is important to note that the reflections do not produce a full standing wave. The gauge array is also located at an overall cold spot, where destructive interference reduces mean wave height after 20–30 s.

Calculating a single value of wave height from the mean of all gauge data will likely lead to an underestimate, as it will include the period where the first waves are travelling across the tank. This would also be affected by the build-up of reflections, potentially giving a spurious result for the interaction. To overcome this, the mean height for each test was calculated from a short sample near the start of each test. A 5 s sample was found to work for most tests, starting 2 s after the first wave height measurement to avoid any spurious peaks, as shown in fig. 6.8.

Determining regular wavelength

Wavelength was calculated for the regular waves, table 6.3(a), using cross-correlation between recorded water surface elevation data at pairs of gauges. A sub-sample of the wave gauge data was used for the cross-correlation, using the first few waves to give a reliable estimate of their length. The start time for this was a function of C_g. Sample length was an integer multiple of the wave period, with six waves found to perform well.

For each of the nine wave directions tested, in-line separation ΔD between each pair of gauges in the array was calculated. The largest five separations were used for the analysis, taking a mean of these estimates. Wavelength was calculated using eq. (6.5) where T is wave period and Δt the computed lag between signals.

$$L_{\text{xcorr}} = T \frac{\Delta D}{\Delta t} \tag{6.5}$$

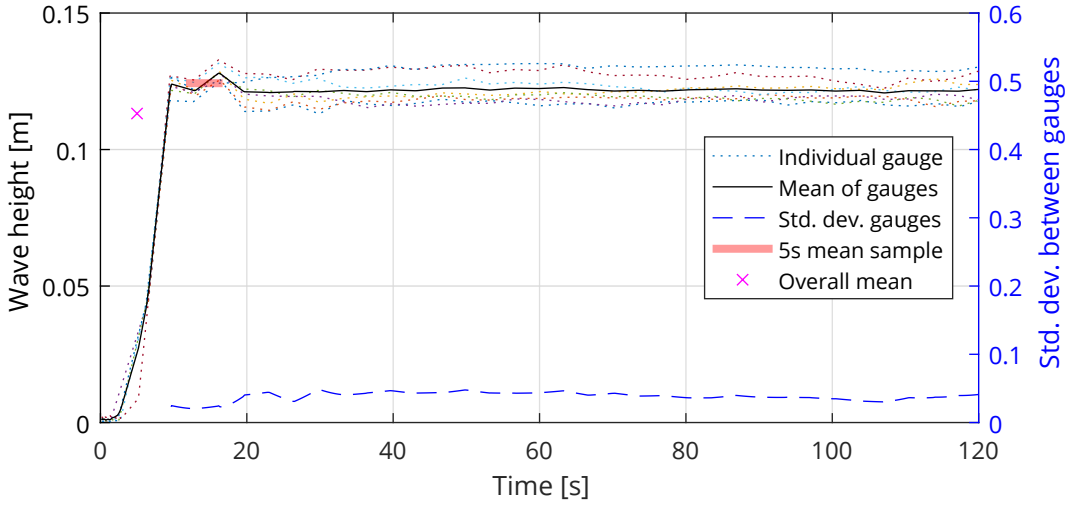

Figure 6.7: Example of time-domain wave-height calculation for conditions with low deviation, namely 0.3 Hz 1% steepness wave with 0.2 m/s following current. Interpolated time series of wave height from individual gauges shown dotted, with mean shown by solid black line, and standard deviation by blue dashed line (right axis scale). Mean of 5 second sample shown by think pink line, and mean of all data by magenta cross.

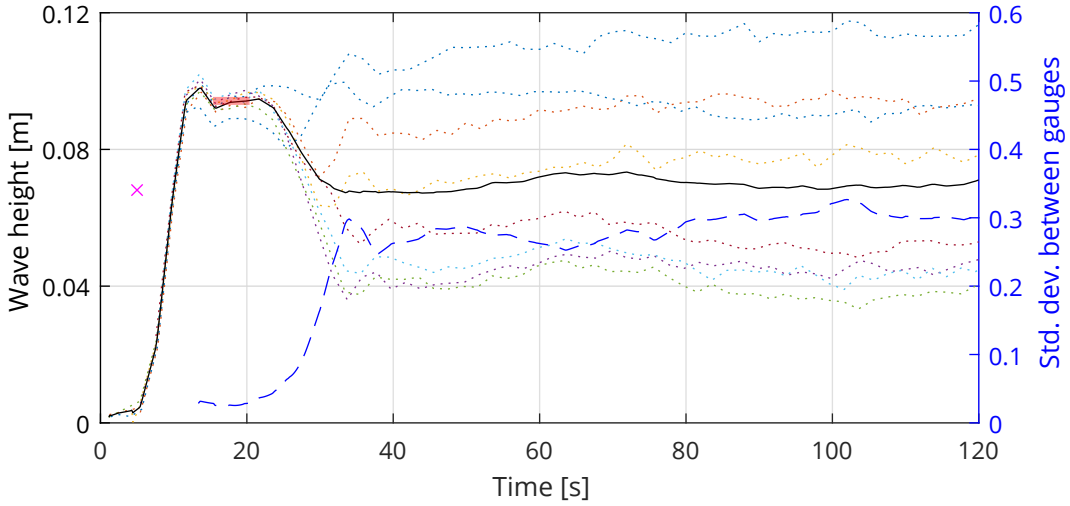

Figure 6.8: As fig. 6.7, but for conditions with high deviation, namely 0.6 Hz 2% steepness wave with 0.2 m/s following current, showing large discrepancy between gauges, and overall reduction in wave height once reflections build up at about 30 s.

6.4 Observed influence of currents on waves

The change in wave height H/H_0 and wavelength L/L_0 resulting from interaction with currents in the tank are considered below, firstly for waves on following and opposing currents, then considering the impact of angle. Wave height H and wavelength L were calculated as described in section 6.3.2 above. The conditions in still water (H_0 & L_0) were measured using the same method, but only for waves at one angle in the tank, corresponding to the direction of waves perpendicular to the current.

6.4.1 Collinear cases

A first step is to consider collinear interaction between waves and currents, i.e. ignoring the impact of angle, looking just at waves propagating in the same direction and directly opposing the current. These cases have been investigated in several previous studies, as discussed in section 3.3.2.

Regular wave height

For regular waves the change in height relative to the no current case H/H_0 with following and opposing currents is shown in figs. 6.9 and 6.10 respectively.

The change in wave height shouldn't be affected by the wave steepness, at least to a first order approximation. This is shown by the results where multiple steepness values were tested, namely 0.3 Hz and 0.4 Hz.

For the higher frequency waves, 0.5 Hz and 0.6 Hz, on a following current there is an offset between the measured and theoretical values in fig. 6.10. This may result from H_0 being measured incorrectly. The gradient of measured data with currents of 0.05 m/s to 0.5 m/s matches theory relatively closely.

Waves on a following current become lower and thus more similar to the assumptions of linear wave theory. Conversely, waves opposing the current become higher, steeper, and more non-linear, which can be seen in the recorded data.

Regular wavelength

The change in wavelength compared to the theoretical still water case, i.e L/L_0, is shown in figs. 6.11 and 6.12 for increasing following and opposing currents respectively.

Separations between gauges for WA1 (section 4.3.1) were relatively small (0.1 m to 1.3 m) compared with the wave celerity, table 6.4. This requires short lag times to be computed, typically 0.2 s to 0.5 s. Measurement of wavelength is therefore more sensitive to error than that of wave height. Small discrepancies in timing or gauge position can have a significant impact, particularly for lower frequency waves that travel faster.

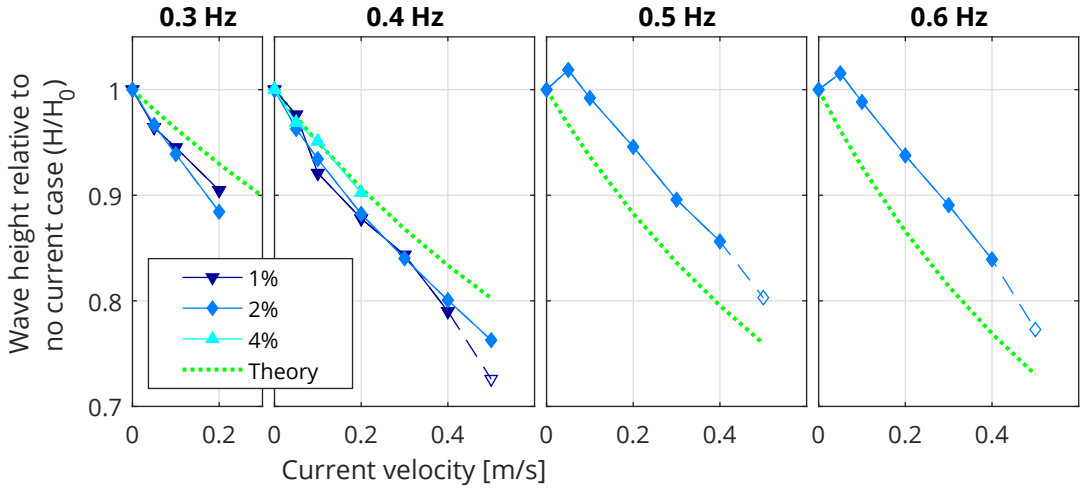

Figure 6.9: Variation in wave height relative to the no-current case, for increasing following current. Panels show different frequencies tested. Data points with greater uncertainty shown with dashed lines and open symbols. See main text for discussion on offset in 0.5Hz and 0.6Hz subplots.

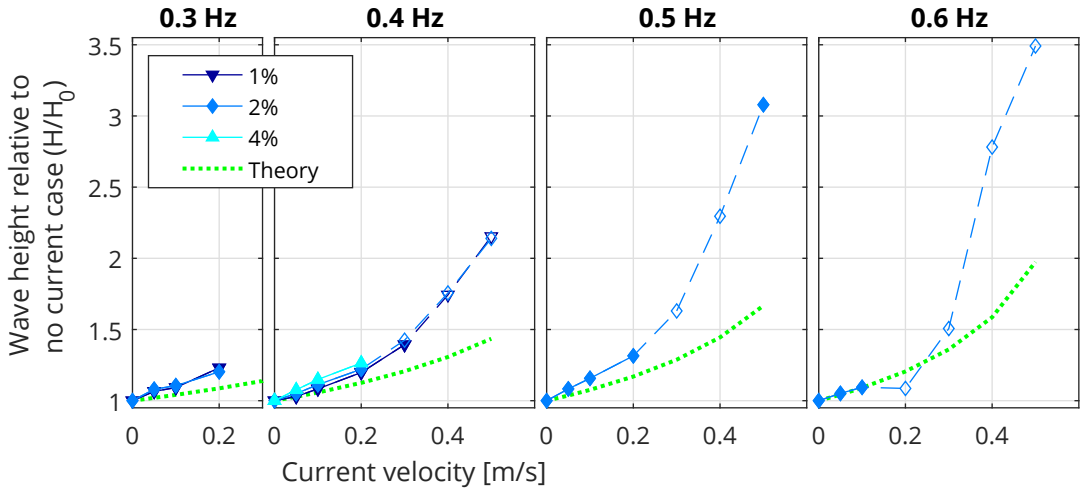

Figure 6.10: As fig. 6.9 but for opposing current.

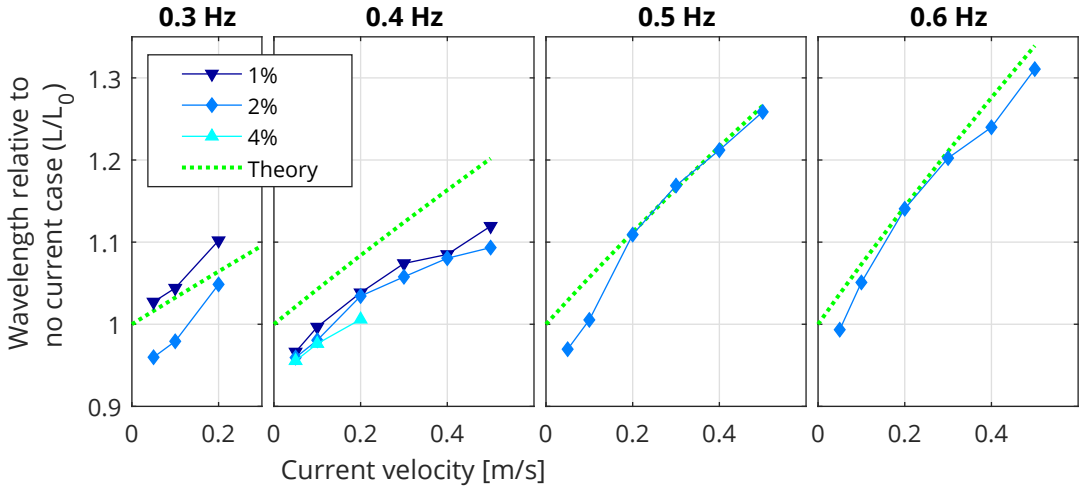

Figure 6.11: Variation in wavelength relative to the theoretical no-current case, for increasing following current. Panels show different frequencies tested. See main text for discussion on uncertainty.

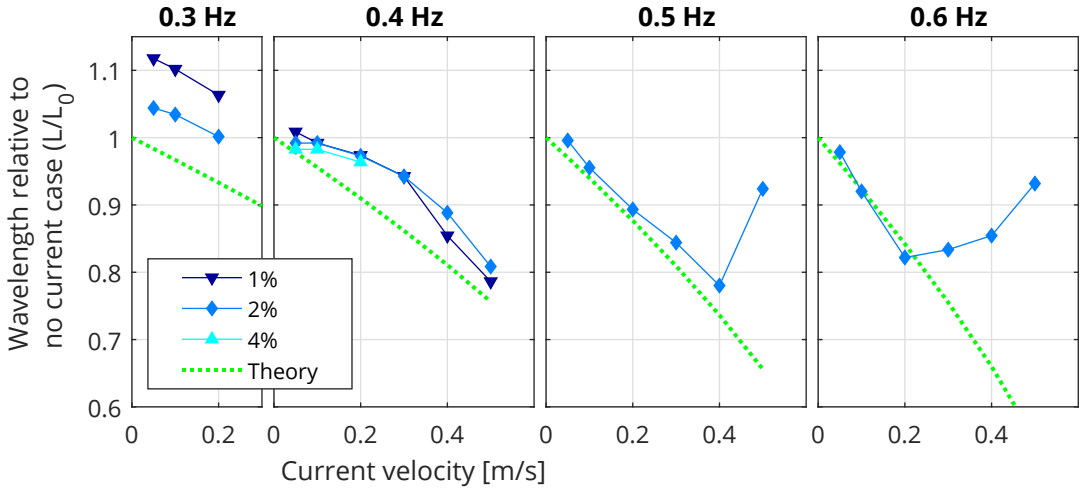

Figure 6.12: As fig. 6.11 but for opposing current.

Table 6.4: Theoretical wave properties in still water.

Frequency [Hz]	L_0 [m]	c [m/s]	C_g [m/s]
0.3	12.97	3.89	3.06
0.4	8.72	3.49	2.31
0.5	6.05	3.03	1.71
0.6	4.31	2.59	1.34

Waves were generated in the tank at a range of directions, relative to the current which was kept fixed. Measurements of wavelength at each angle therefore used different pairs of gauges, and any discrepancy in the gauge position would affect each angle differently. This may be compounded by only measuring L_0 at one angle inthe tank.

There is a discrepancy in the measured wavelength compared with theory, particularly for the lower frequency waves 0.3 Hz and 0.4 Hz. The *change* in wavelength with increasing current matches theory well in most cases however. For the higher frequency waves opposing faster current, the results are uncertain. This is similar to the cases considered in section 6.2.3, where there is aliasing between the spilt wave crests for high frequency waves on fast opposing currents.

Irregular wave spectra

The changes to wave spectra in the tank, when combined with following or opposing currents of up to 0.3 m/s, are illustrated in fig. 6.13 using five PM spectra, table 6.3(d). These show similar patterns to the regular waves, with increasing height for opposing currents, and decreasing on following.

The frequency dependant change in wave height is also apparent. Different frequencies of the spectrum are affected to varying degrees, which can cause the peak frequency to shift. A theoretical example shows this effect more clearly than the measured data. The current induced change to a PM spectrum has been calculated using linear interaction theory. The peak frequency can be seen to change with current velocity in fig. 6.14, moving to a lower frequency with following currents and vice-versa.

The spectra measured with current include significant unwanted noise, particularly at higher frequencies. This can partially be attributed to increased reflections, but tank-specific generation effects may also be present (section 6.2.1).

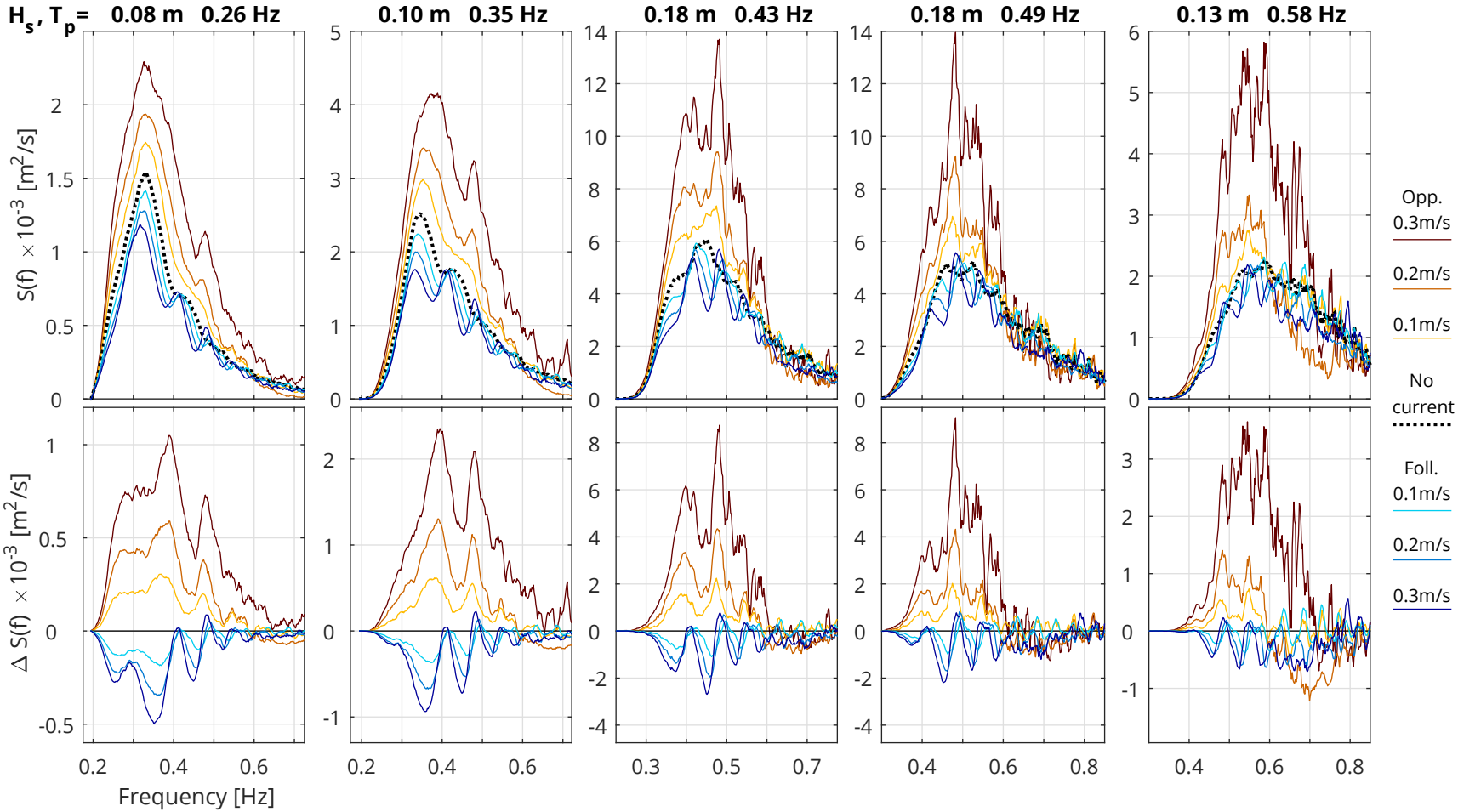

Figure 6.13: Measured change to example PM spectra with following (foll.) and opposing (opp.) currents. Top row shows absolute change, and bottom row difference from no current case. Note that plots are to varying scales based on input wave conditions.

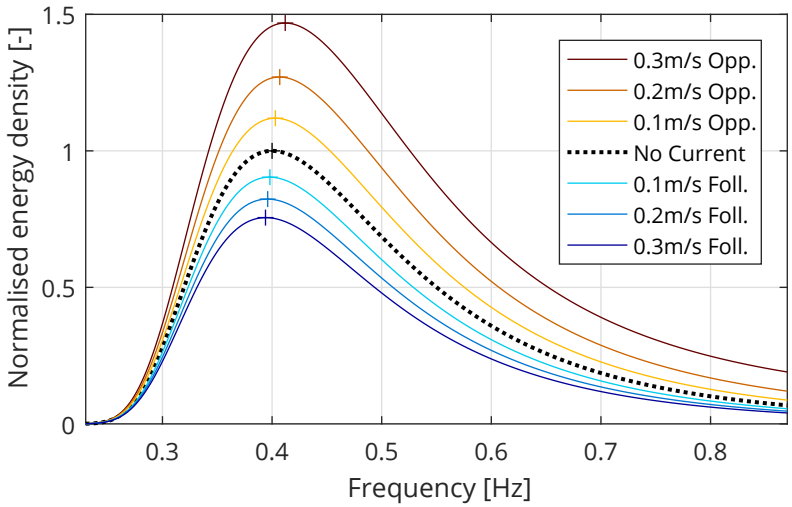

Figure 6.14: Theoretical change to example PM spectra (H_s=0.2m, f_p=0.4Hz) with following (foll.) and opposing (opp.) currents. Based on linear wave-current interaction theory. Peak frequency marked + highlighting change with current velocity.

6.4.2 Non-collinear cases

Regular wave height

The change in regular wave height as a result of interaction with a non-collinear current is shown in fig. 6.15. This includes all 297 test cases considered in table 6.3(a). Change in wave height H/H_0 is plotted against relative angle θ_{rel} between the waves and currents for each wave frequency and steepness measured. Measurement points with greater uncertainty are marked. This is based on the analysis of wave height (section 6.3.2), taking cases with mean deviation between individual wave gauge measurements $> 5\%$.

There is a clear trend of increasing interaction with current velocity. As before there is less certainty in the high frequency waves opposing faster currents. As was seen for the collinear cases, the magnitude of change is much greater for the opposing cases. This can only partially be explained by the reciprocal definition of relative wave height, suggesting non-linear interaction, tank-specific generation effects, or both.

Wave heights decrease when propagating on a current between $\theta_{\text{rel}} = 0$ and $\theta_{\text{rel}} = \pi/2$, i.e. following to perpendicular currents. Conversely, wave heights increase when propagating against a current at $\theta_{\text{rel}} = 3\pi/4$ to $\theta_{\text{rel}} = \pi$. For the intermediate case with a slightly opposing but mostly perpendicular current $\theta_{\text{rel}} = 5\pi/8$ no clear pattern was observed, with some waves decreasing in height and some increasing. For waves propagating on a non-collinear current, the spatial variation in flow velocity (section 5.3) will influence the observed interaction in the tank.

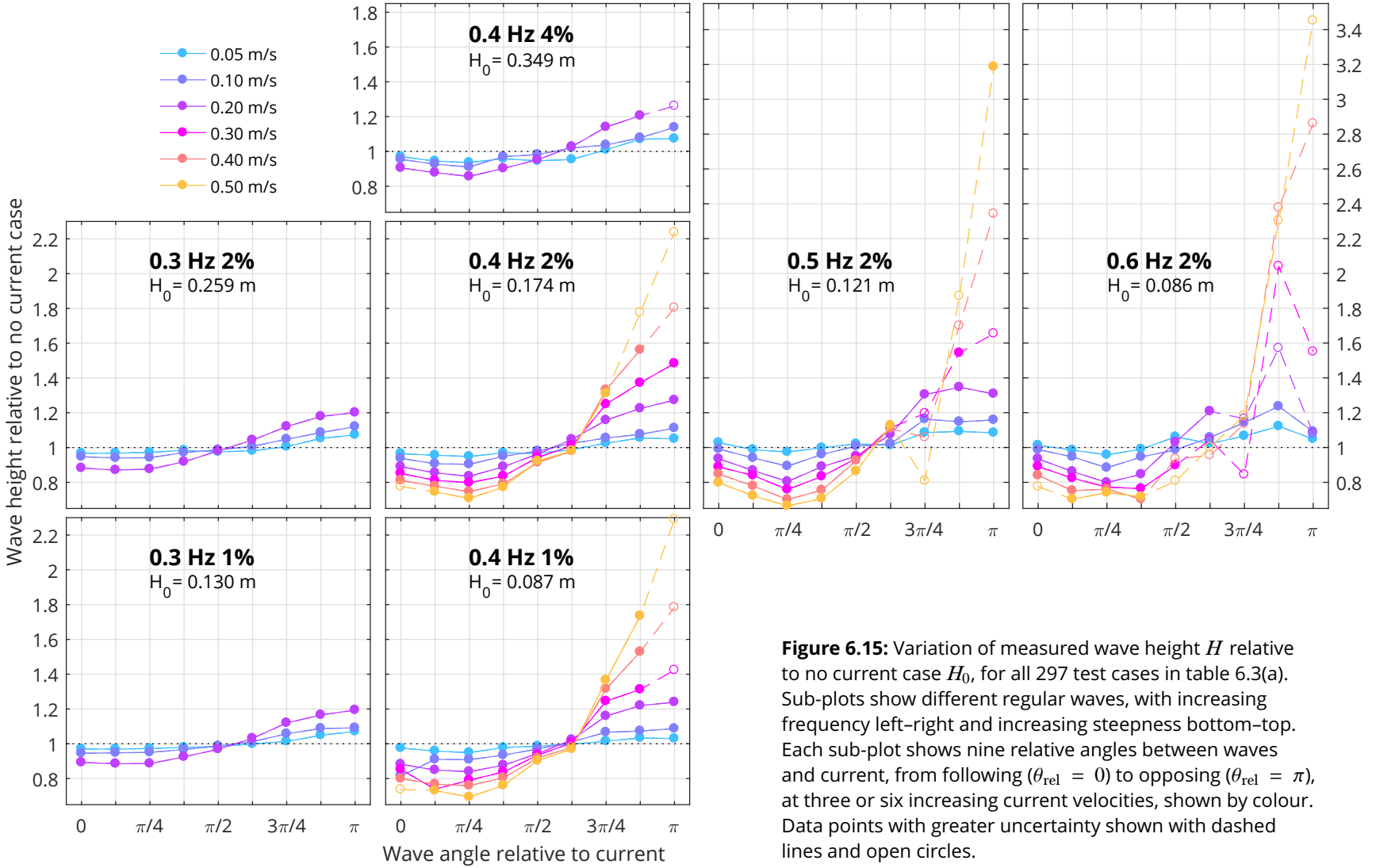

Figure 6.15: Variation of measured wave height H relative to no current case H_0, for all 297 test cases in table 6.3(a). Sub-plots show different regular waves, with increasing frequency left–right and increasing steepness bottom–top. Each sub-plot shows nine relative angles between waves and current, from following ($\theta_{\text{rel}} = 0$) to opposing ($\theta_{\text{rel}} = \pi$), at three or six increasing current velocities, shown by colour. Data points with greater uncertainty shown with dashed lines and open circles.

Unfortunately it is not possible to produce an equivalent plot to fig. 6.15 showing change in wavelength, as those measurements appear to be influenced by angle, as discussed in section 6.4.1.

For waves propagating across a perpendicular current, a reduction in wave height is observed fig. 6.16. A simple theoretical analysis assuming $H \propto U \cos\theta_{\text{rel}}$ would suggest no change. A critical assumption of linear wave theory is two-dimensional waves, with infinitely long wave crests. This is not the case in the tank, where the crests have a finite length, and water is recirculated under the test floor. This could result in a net loss of energy as the wave propagates across the tank, reducing wave height. Measured change in wavelength with perpendicular currents, fig. 6.17, shows no clear trends.

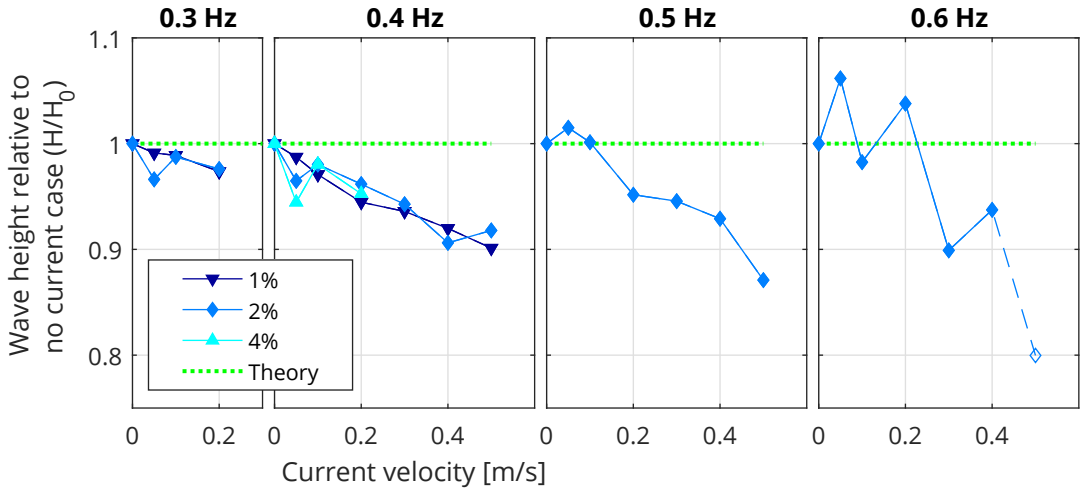

Figure 6.16: Variation in relative wave height, as fig. 6.9 but for a perpendicular current.

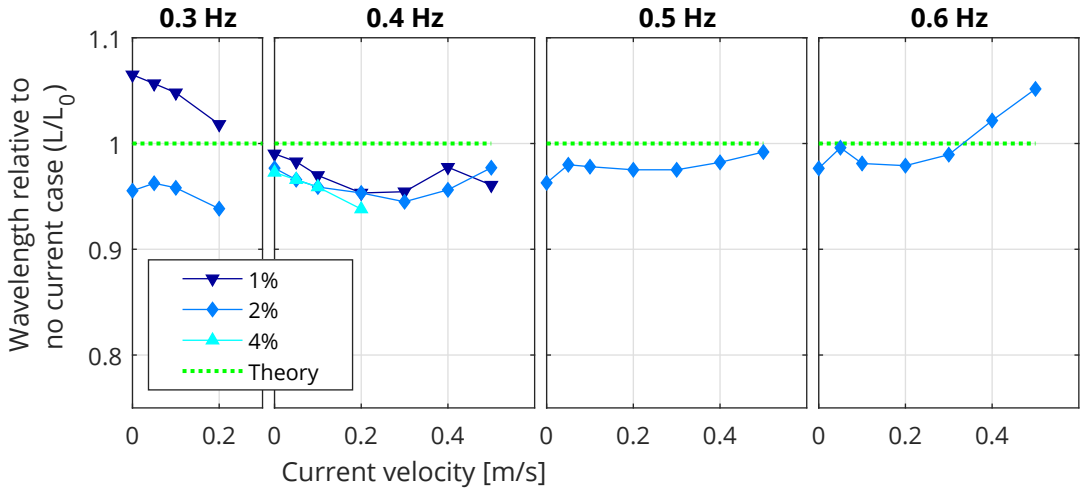

Figure 6.17: Variation in relative wavelength, as fig. 6.11 but for a perpendicular current.

Irregular wave spectra with non-collinear current

Observations of parametric and non-parametric wave spectra interacting with collinear and non-collinear currents are shown in section 6.5 as part of the correction process.

6.5 Correction of waves with current

This section includes joint work with fellow IDCORE researcher at FloWave, Sam Draycott. This has been published as a paper in Ocean Engineering (Draycott, Noble et al., 2017), see Appendix B, which has been amended and incorporated into the following section.

Test design and planning, implementation, and writing the resulting paper was a joint effort. Dr. Draycott lead on the application of his previous research, including directional sea state measurement and analysis, plus implementation of correction procedures. He was also largely responsible for the theoretical analysis on changes to wavenumber spectra, power and steepness. The work built on my research into wave-current interaction theory, implementation of analytical models, and preliminary tank tests.

6.5.1 Motivation for correction of combined conditions

There are two contrasting methods to specify combined wave-current conditions:

1. Wave properties can be defined in still water, before they interact with a known current. This is how combined conditions are produced in the tank at FloWave.
2. They can also be specified as a combined field, i.e. waves of a certain height and period propagating over a fixed current velocity. Field measurements of conditions, e.g. at a deployment site, would be recorded and thus specified in this manner.

Obviously there is a mismatch between these. To reproduce a recorded combined wave-current condition in the tank requires the wave properties in still water be determined, as this is used as the wavemaker input. A correction factor is required to the wavemaker input, where the waves are generated in still water, so that the desired conditions are produced in the tank centre following interaction with the current.

Another key issue is that for recorded data, the current velocity may not be known. It is common only to measure wave properties without the corresponding currents, as these are often considered insignificant. The effect of currents on wave properties may not be insignificant however, and the implications of ignoring them are discussed below.

6.5.2 Change to the wave field resulting from interaction with a current, including power and steepness

For waves in the absence of current, the wavenumber k for each frequency can be obtained from the dispersion relation, eq. (2.5). The corresponding wavenumber spectrum $S(k)$ and group velocities $C_g(f)$ can be calculated from the measured frequency spectrum $S(f)$ using eq. (6.6). The total power in a wave spectrum P can be obtained by integrating component wave power using eq. (6.7).

$$S(k) = \frac{S(f)C_g(f)}{2\pi} \qquad \text{where} \quad C_g(f) = \frac{1}{2}\frac{\omega}{k}\left(1 + \frac{2kh}{\sinh 2kh}\right) \tag{6.6}$$

$$P = \int P(f)df \qquad \text{where} \quad P(f) = \rho g S(f) C_g(f) \tag{6.7}$$

Significant steepness S_p^* is calculated as significant wave height H_{m0} divided by the wavelength associated with the peak of the wavenumber spectrum L_p^*, eq. (6.8). This version of peak wavelength is used, rather than the wavelength associated with peak frequency, for two reasons. Firstly, the wavelength associated with the peak of the wavenumber spectrum does not always equal that obtained from f_p, as discussed in Plant (2009). The peak energy lies at the wavelength associated with the wavenumber peak so using this value provides a more representative figure for the true steepness of a sea state. Secondly, this definition allows for a consistent comparison of steepness between cases with and without current.

$$S_p^* = \frac{H_{m0}}{L_p^*} \tag{6.8}$$

Transformation of the frequency spectrum can be calculated using a slightly modified version of the method presented in section 2.1.5. Using a linear superposition, the amplitudes of each frequency component $A(f)$ are given by eq. (6.9). The change in component amplitudes resulting from interaction with the current can be calculated from eq. (6.10), which is equivalent to eq. (2.21).

$$A(f) = \sqrt{2S(f)\delta f} \tag{6.9}$$

$$A_1 = A_0\sqrt{\left(\frac{C_{g,0}}{C_{gr,1} + U\cos\theta_{\text{rel}}}\right)\left(\frac{1}{1 + U\cos\theta_{\text{rel}}/C_{gr,1}}\right)} \tag{6.10}$$

The transformed frequency spectrum can then be reconstructed using eq. (6.9), taking $A_1(f)$ to get $S_1(f)$. This results in the same transformation as that formulated in Chakrabarti and Johnson (1995). The wavenumber spectra, power available, and wave steepness in the presence of a current can be calculated via eqs. (6.6) to (6.8), using the relevant terms with current as appropriate.

Power and steepness assumed if wavelength and group velocity change omitted

Power and steepness calculated for waves in the presence of a current will give incorrect results if the wavenumber transformation is not also included. This situation could arise when using measurements from a wave buoy where there is no knowledge of the current, and thus the wavelength change. The measured transformed spectrum $S_1(f)$ has associated wavenumbers $k_1(f)$. With the assumption of no current, wavenumbers $k_0(f)$ are calculated using the standard dispersion relation eq. (6.11), rather than using the modified version eq. (6.12) to get $k_1(f)$. This assumption leads to incorrect calculation of group velocities and wavenumber spectra, hence the power and steepness will also be incorrect.

$$\omega = \sqrt{g k_0 \tanh k_0 h} \tag{6.11}$$

$$\omega - k_1 U \cos\theta_{\text{rel}} = \sqrt{g k_1 \tanh k_1 h} \tag{6.12}$$

To demonstrate the effect of current on both the transformed and assumed spectra, a full-scale PM spectrum with H_{m0} of 5 m and T_p of 8 s is used to show the effect over a wide range of frequencies. This has been analysed with both opposing and following current velocities of 0.25 m/s, 0.5 m/s, and 1.0 m/s. The significant wave height is found to increase 27.6% with 1 m/s opposing current, and decrease 17.2% for 1 m/s following current.

The transformation of frequency and wavenumber spectra are shown in fig. 6.18, along with the wavenumber spectrum that would be assumed without the knowledge of the current present. In opposing flow, waves increase in steepness and thus spectral magnitude increases, with associated reduction in wavelength shown as a shift to higher wavenumbers. The opposite is true of the following current conditions.

For the assumed case with no current there is no shift in wavenumber, hence the steepness change will be underestimated. In addition, the group velocity is unaltered with resulting overestimation of the change in power. This is shown in fig. 6.19, where the maximum discrepancy is the 1 m/s opposing case, underestimating steepness by 18.6% and overestimating power by 26.9%. This demonstrates the importance of measuring currents at a site in order to obtain a realistic resource assessment and site characterisation.

When tank testing with realistic site conditions the associated current should be included, so that conditions mimic the site, and results inferred from the testing are representative. The correct wavenumber for each frequency component cannot be attained without the current, but are implicitly correct if the current and scaled depth are accurately reproduced. It is important the frequency spectrum is correct in order to obtain the desired wavenumber spectra, power and steepness. At FloWave this requires a correction procedure as a result of the current transformation, so input amplitudes must be altered.

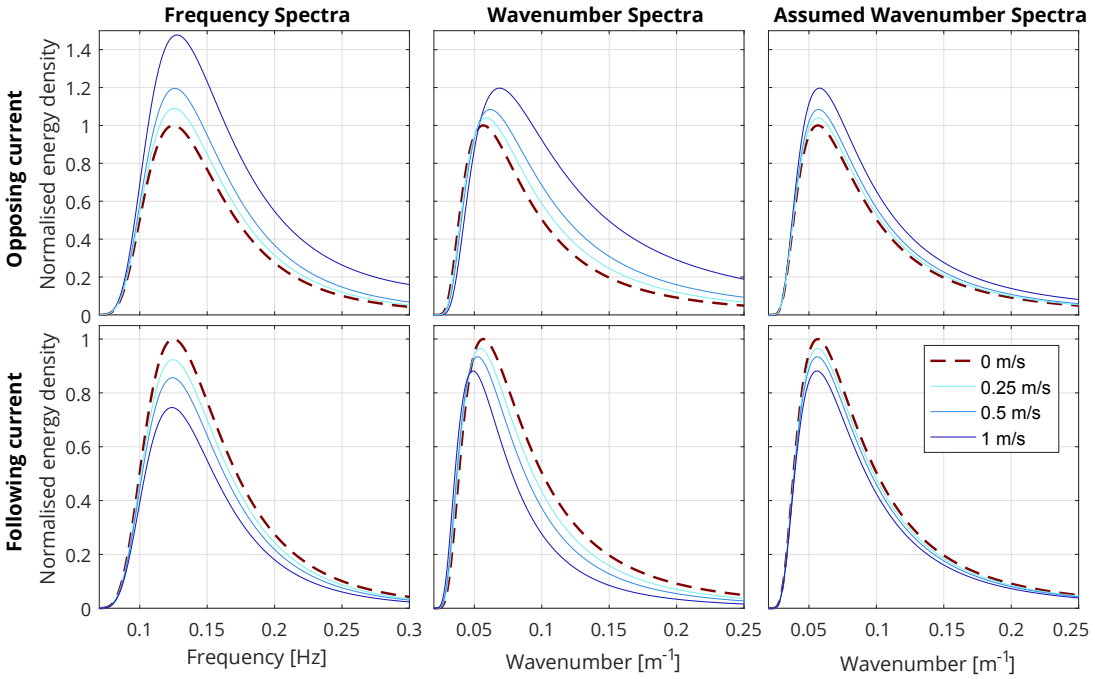

Figure 6.18: Change in frequency and wavenumber spectra in the presence of opposing and following currents, using an example PM spectrum (H_{m0} = 5 m, T_p = 8 s). Panels show the real frequency and wavenumber spectra, along with the wavenumber spectra assumed without knowledge of the change in wavelength resulting from the interaction with current.

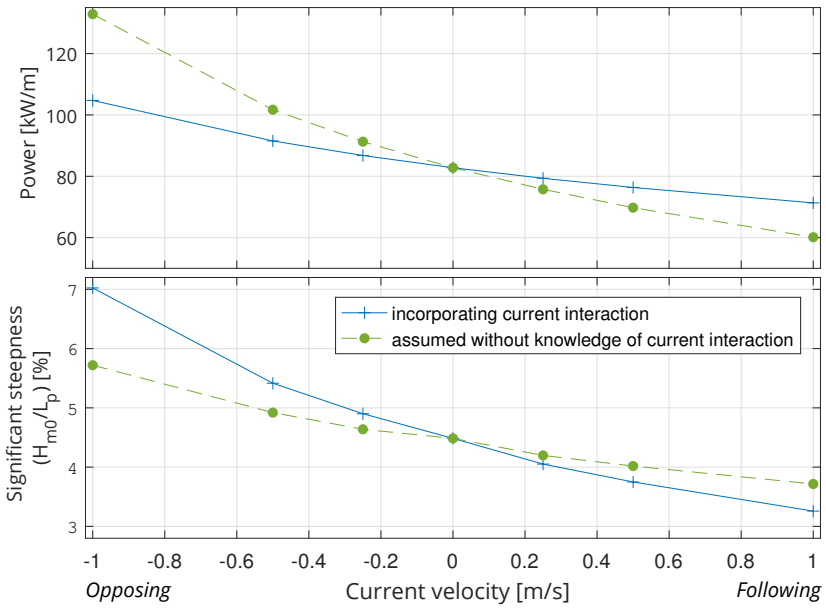

Figure 6.19: Change in power and significant steepness in the presence of opposing and following currents for cases incorporating wavelength change and that assumed without knowledge of the interaction with current Based on example full-scale PM spectrum (H_{m0} = 5m, T_p = 8s).

6.5.3 Theoretical and empirical correction methods

Several approaches were considered and trialled to correct wave height in the tank when combined with a current:

1. Purely theoretical calculation,
2. A hybrid theoretical–empirical method,
3. An empirical only approach.

The process used for these three approaches can be summarised as fig. 6.20. The empirical part of the correction process is described in section 6.5.4, and is the same for approaches 2 and 3.

It was found that the purely theoretical calculation was not suitable. This approach does not account for any reflections, tank-specific generation effects, and is based on a first-order linear approximation of a non-linear process.

To compare the relative performance of the purely empirical and combined theoretical–empirical correction procedures, these were tested with an example sea state. A long-crested JONSWAP spectrum, table 6.3(b), was run at 135° to the current direction and corrected using the two methods.

Both approaches were found to have acceptably low errors (<5%) after just one iteration, as shown in figs. 6.21 and 6.22. Either methodology can therefore be effectively applied to produce the desired output. As the theoretical–empirical approach requires an extra step for little benefit, the purely empirical approach was adopted.

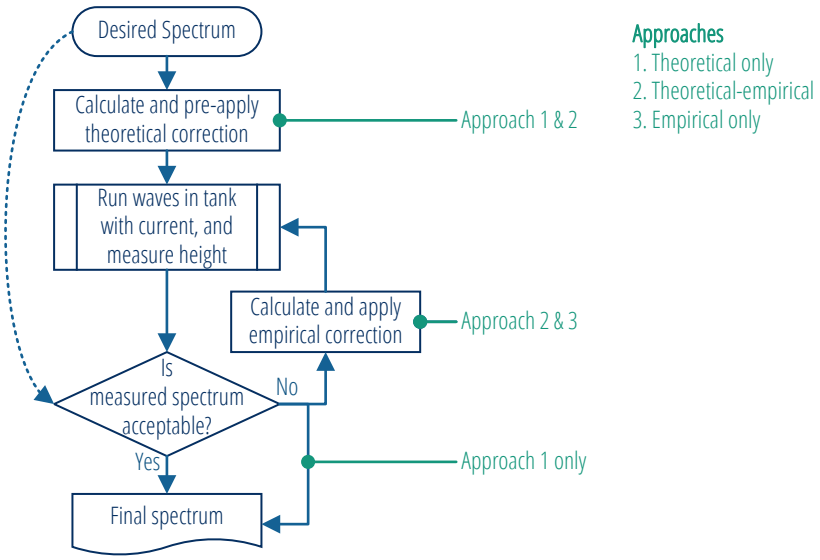

Figure 6.20: Flowchart of wave-current correction processes trialled.

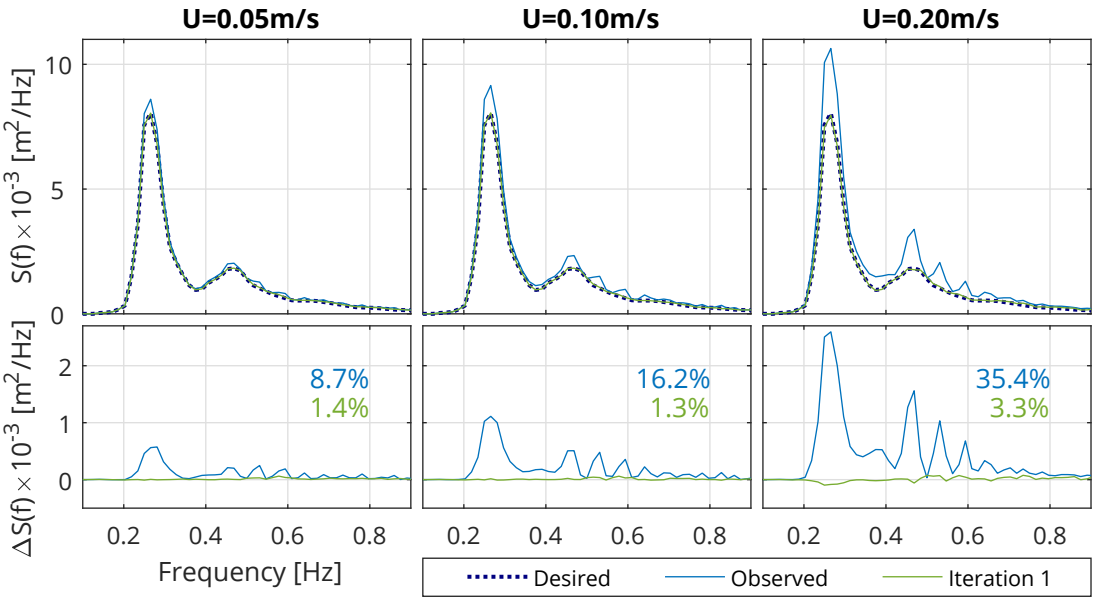

Figure 6.21: Example measured spectra with the purely empirical correction procedure for the 3 current velocities, with deviations displayed below. Mean errors shown as a percentage.
Note that the observed case is with no correction factor applied.

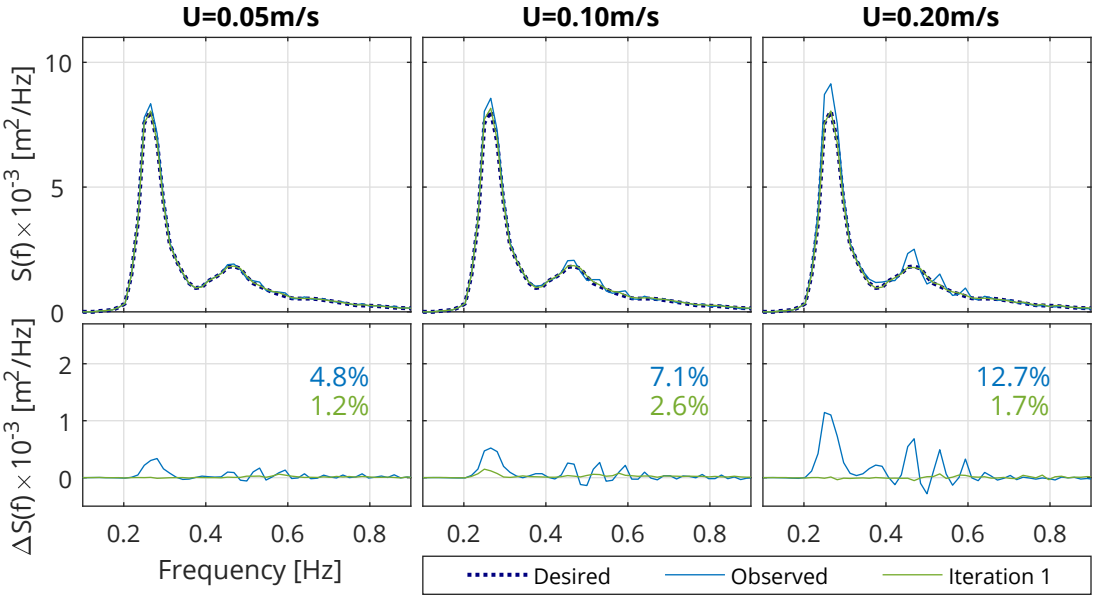

Figure 6.22: As fig. 6.21 but for theoretical–empirical correction procedure.
Note that the observed case is with a theoretical correction factor pre-applied.

6.5.4 Empirical correction procedure

To produce waves of a specified height in combination with a current, an amplitude based correction factor needs to be applied to the wavemaker input. For a directional spectrum, it is necessary to determine this correction factor for every frequency and direction component. As a result of using a single summation method to generate waves in the tank (section 4.2.4) the amplitude of each wave component with unique frequency and direction $A_i(f_i, \theta_i)$ can be corrected. These correction factors are assumed linear, taken as the inverse of the change in component amplitude as a result of the interaction with the current field, and are calculated empirically.

The input wave spectrum is generated in the tank with current, measured, and the resulting component amplitudes compared with those desired, eq. (6.13). The correction is based on observed discrepancy between desired and measured directional spectra, and is multiplicatively applied to the input spectrum. This process is repeated iteratively as necessary until the measured spectrum is acceptably correct, defined in this case as a mean spectral error $\varepsilon < 5\%$, eq. (6.14).

$$CF_{\text{empir}}(f_i, \theta_i) = \frac{A_i(f_i, \theta_i)_{\text{desired}}}{A_i(f_i, \theta_i)_{\text{measured}}} \tag{6.13}$$

$$\varepsilon = \frac{\sum_{i=1}^{N_f} \left| S_i(f_i, \theta_i)_{\text{measured}} - S_i(f_i, \theta_i)_{\text{desired}} \right|}{\sum_{i=1}^{N_f} S_i(f_i, \theta_i)_{\text{desired}}} \tag{6.14}$$

Measurement of the spectra, $S(f), S(f, \theta)$, used directional array WA1 (section 4.3.1). This was analysed using the Phase-Time-Path-Difference (PTPD) method (Fernandes et al., 2000; Esteva, 1977) to calculate frequency spectra, and Directional Spreading Function (DSF) if appropriate. The PTPD method uses triads of gauges to determine frequency at each direction, without knowledge of any underlying current. The approach used was found to work well with the conditions tested.

For conditions where wave phase is important, such as time-series data or focused wave groups, the correction method of Fernández et al. (2013) may be used. This extra step was not necessary to correct purely spectral inputs.

6.5.5 Correction results

To demonstrate and validate the correction method, three types of wave conditions were tested: regular waves, a parametric uni-directional spectrum, and a non-parametric directional sea state. Details of these are given in table 6.3 marked ‡.

Regular waves

The error in wave height following empirical correction is shown in fig. 6.23(c), with fig. 6.23(b) showing the *apparent* angular change. For all velocities and relative angles, the resulting measured wave heights were within 0.7% of the desired. The measured angular change is also relatively small, yet displays no obvious pattern with respect to relative angle and current velocity. The presence of a current reduces measurement accuracy (through gauge vibrations, bending etc.) making it difficult to isolate small refraction effects from this increased error. It is evident that any refraction effects are very small at these velocities and so have not been corrected for any of the sea states.

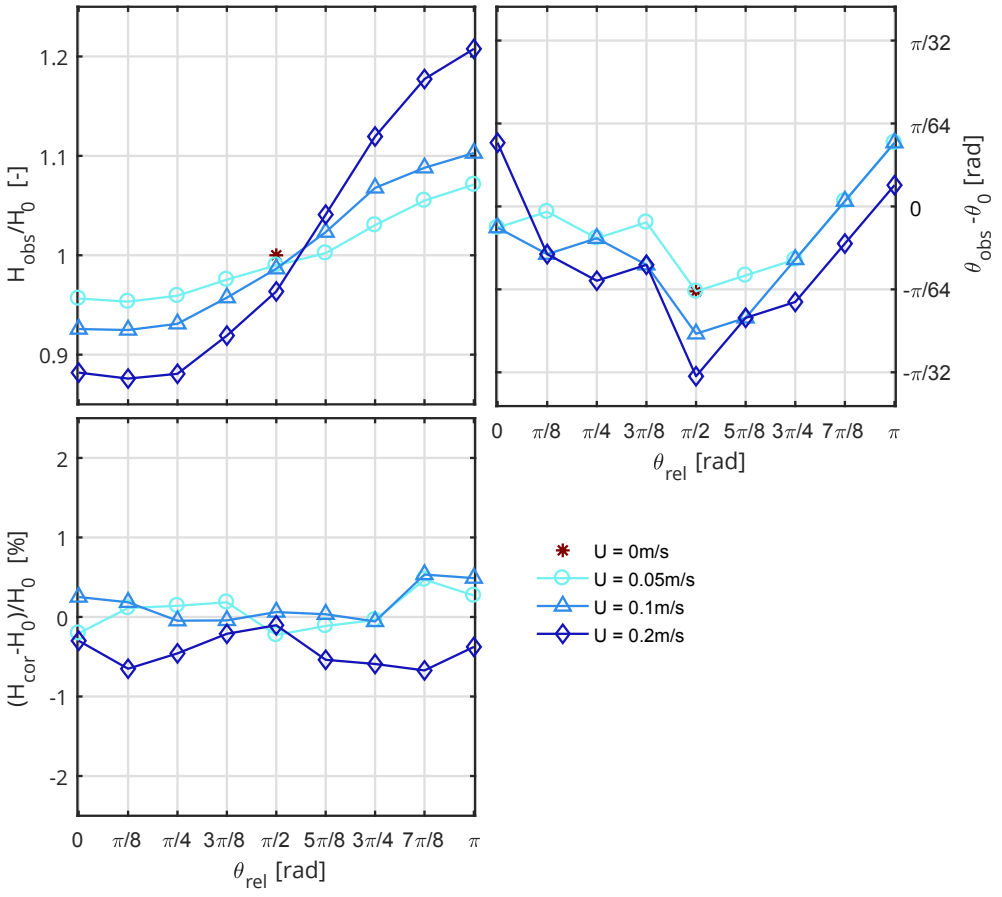

Figure 6.23: Observation and correction of regular waves at 9 measured angles to the current direction and 3 velocities. Panels show (a) observed change in wave height, (b) observed change in wave direction, (c) observed error in wave height once corrected.

Uni-directional parametric spectrum

The observed transformation of the parametric spectra is shown in fig. 6.24, along with the deviation in energy density compared to the desired before and after correction. Clearly the same trend is seen as with the regular waves, with larger transformations in the presence of larger currents, and larger wave heights with increasing angle.

Analysing this change in energy density, it can be inferred that although the majority of the change is a result of wave-current interaction, there is also significant variation due to reflections, particularly affecting the higher frequencies. The magnitude of these variations are a function of the reduced absorption effectiveness in the presence of larger currents. The reason for this 'spiky' variation at higher frequencies is due to incident and reflected wave components at a given frequency being in or out of phase at the gauge array location.

Regardless of the source of the frequency dependent variation, the corrected deviation shows that the spectrum has been effectively corrected using a linear approach in a single iteration. All wave-current-angle scenarios were corrected to give a final weighted error of less than 3%.

Non-parametric directional spectrum

Similar to the parametric outputs found in fig. 6.24, the frequency spectrum transformation and correction for the non-parametric EMEC derived sea state are shown in fig. 6.25. Despite this sea state having significant directional spreading, a similar magnitude of transformation is observed to the parametric case, along with analogous influence of reflections. The corrected frequency spectra are also all within 3% of the desired, demonstrating that the linear correction procedure applied to the sub-frequency angular components is just as effective.

The final corrected sea states are shown in fig. 6.26. Frequency spectra along with the weighted DSFs are shown, for the three velocities and five relative angles tested. The final directional spectrum output using the PTPD approach is shown for the base 0.1 m/s case, noting that the 0.05 m/s and 0.2 m/s results appear very similar.

These re-iterate that the frequency spectra have been effectively corrected for all velocity-angle combinations, and in general so have the directional spectra and mean DSF. Directional errors are larger with increasing current velocity which is clear when assessing the weighted DSF errors. With zero current the weighted DSF error was 6.95%, whereas in 0.05 m/s, 0.1 m/s, and 0.2 m/s current the mean errors over all angles are 13.3%, 14.3%, and 18.5% respectively. Although this is a significant increase it is felt that the majority of this is not refraction induced and instead is a product of increased measurement error combined with the way the error is calculated. Performance of the correction procedure, potential sources of error, and implications for testing are discussed in section 6.5.6.

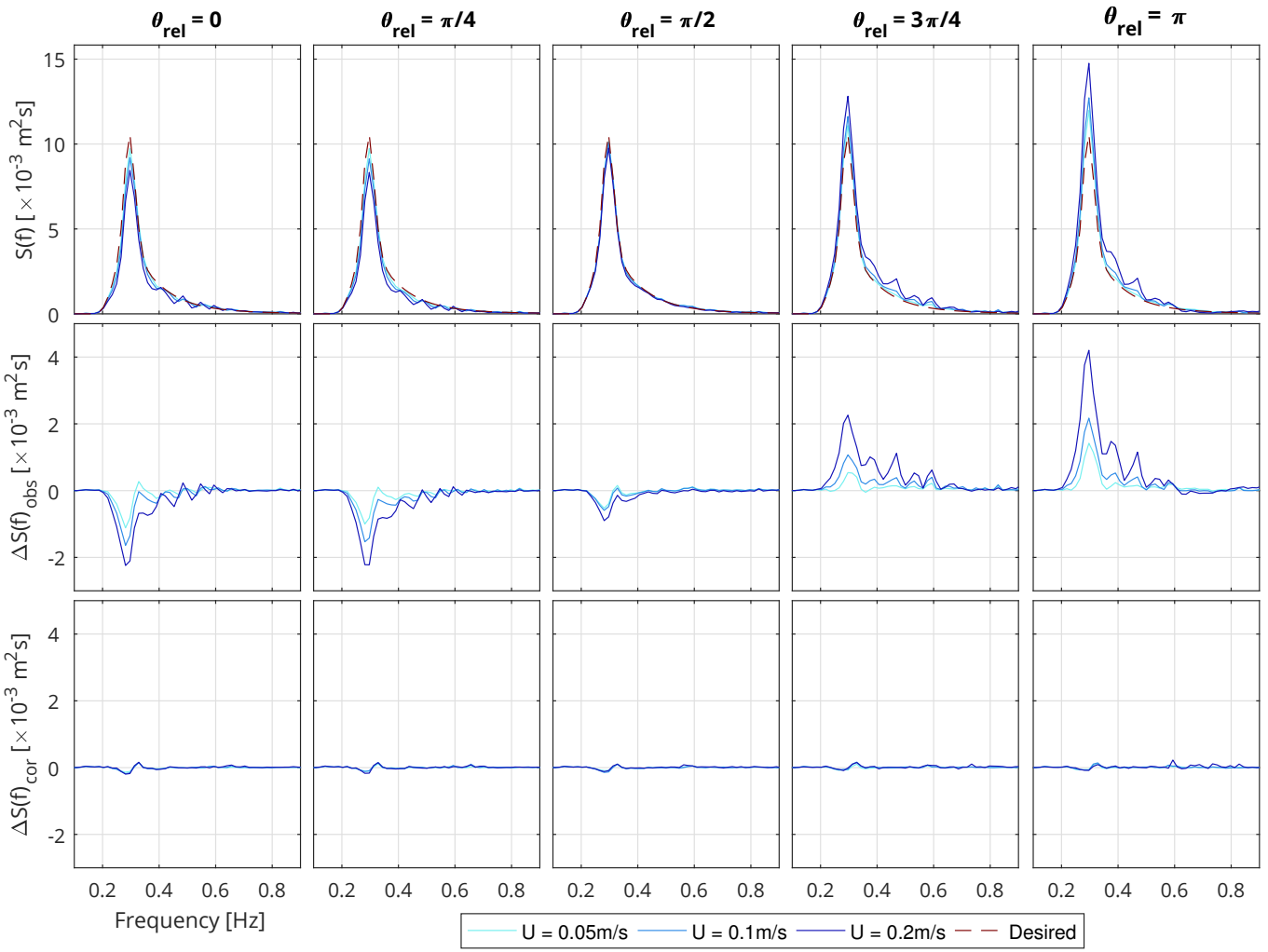

Figure 6.24: Observation and correction of parametric spectrum at 5 relative angles to current. Top row shows observed spectral density, middle row observed deviation from desired prior to correction, and bottom row deviation following correction.

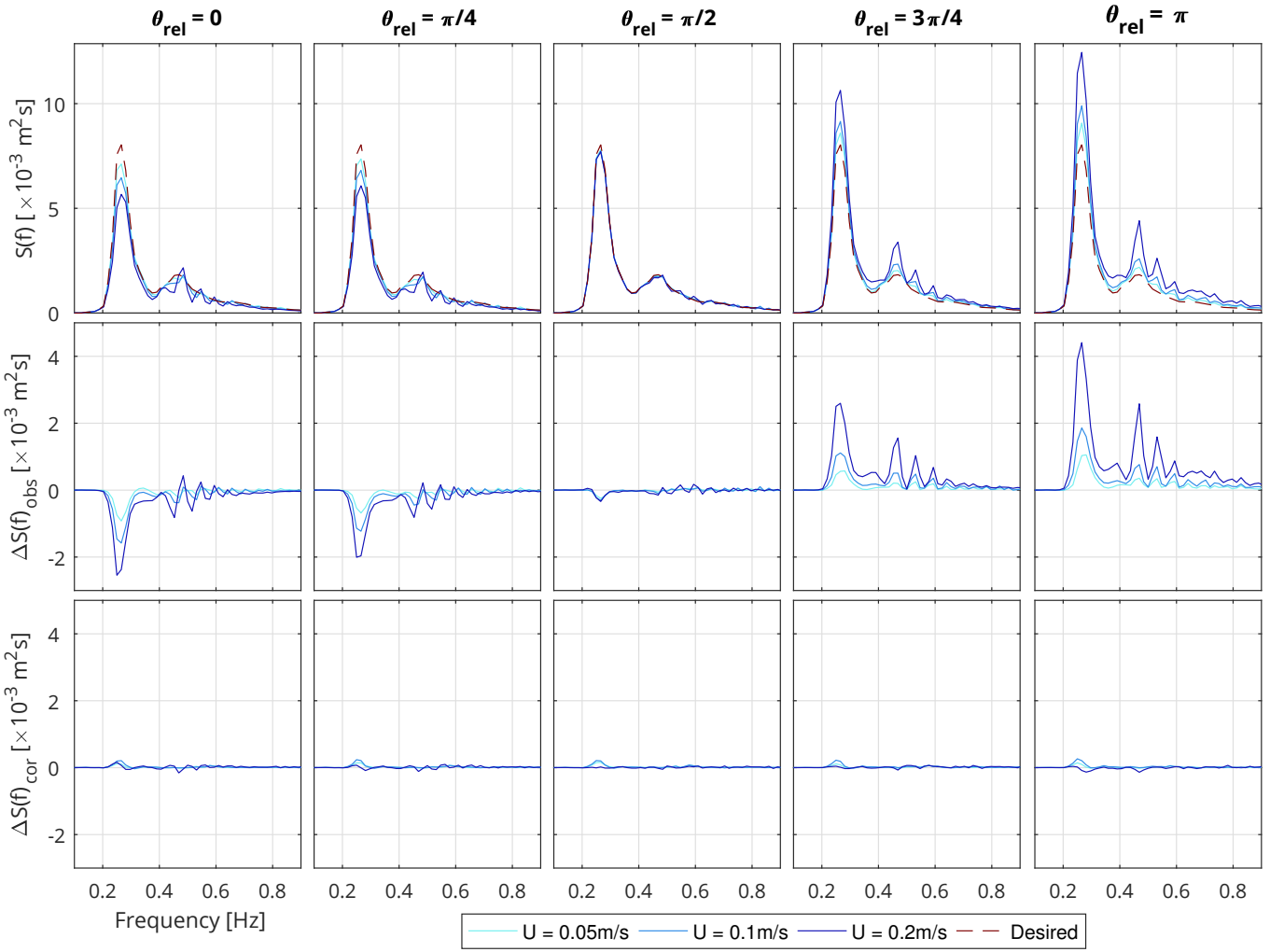

Figure 6.25: Observation and correction of non-parametric EMEC spectrum at 5 relative angles to current. Top row shows observed spectral density, middle row observed deviation from desired prior to correction, and bottom row deviation following correction.

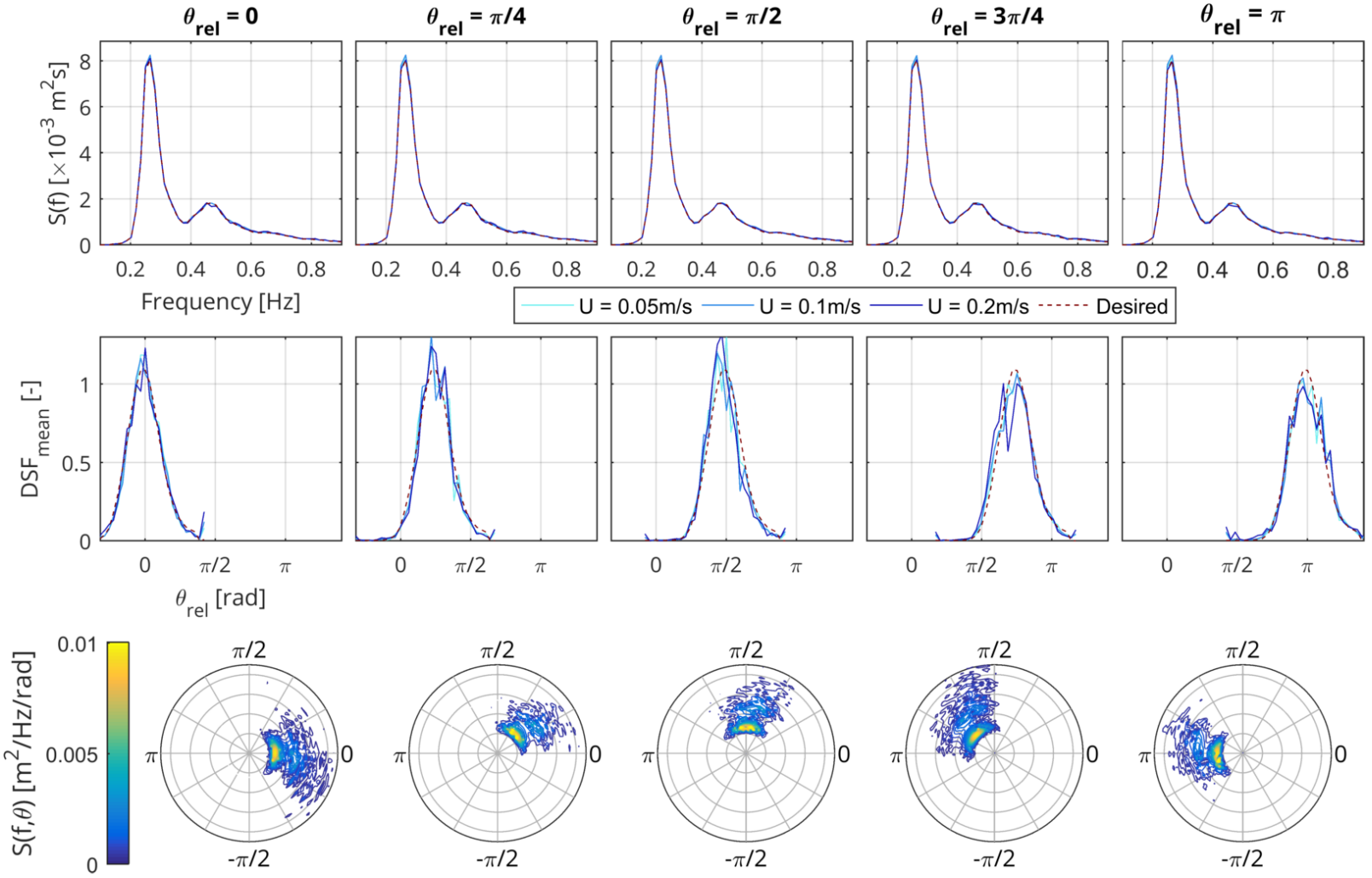

Figure 6.26: Final non-parametric EMEC spectra following correction, at 5 relative angles to current. Top row shows spectral density $S(f)$, middle row weighted mean directional spreading function DSF_{mean}, and bottom row directional spectra $S(f,\theta)$ for 0.1 m/s current.

6.5.6 Discussion on correction procedure

Further discussion on the measurement of wave directionality, including the relative performance of the PTPD method is given in Draycott et al. (2017), see Appendix B.

Assessment of correction procedure

The amplitude correction procedure applied has proven to be effective for all sea states and velocity combinations tested, providing frequency spectrum errors of less than 3% in all cases. The tank-scale conditions tested (table 6.3) had $f, f_p \approx 0.3\,\mathrm{Hz}$, combined with currents of up to $0.2\,\mathrm{m/s}$ at a range of relative angles, from following through perpendicular to opposing the waves.

The resulting wave heights were consequently found to be very close to desired. For the regular, uni-directional parametric, and non-parametric EMEC sea states, the mean wave height discrepancy over all velocity-angle combinations were found to be 0.27%, 0.42%, and 0.91% respectively (maximum errors of 0.67%, 1.11%, and 1.38%).

The correction factor, although assumed linear, includes a number of different factors of which the proportional influence remains unknown. Namely:

1. Superposition of wave and current fields,
2. Energy transfer between wave and current fields,
3. Increased reflections with larger currents, which is relative to the array location,
4. Spatial variation of current in the tank, and
5. Paddle response to presence of current.

The favourable results show that, although current effects on the wave field at FloWave are inherently complex and non-linear, the variation in relative wave deformation as a result of a modest change in input wave amplitude can effectively be approximated as a linear process. This is a useful output from this work, although limits to the validity of this will need to be identified through additional testing with steeper waves and higher current velocities. Wave-current interaction theories do not include all of these factors, which may account for the observed discrepancies. The linear theory only accounts for the first, while the non-linear theory also partially accounts for the second. Factors 3–5 are facility specific, and thus cannot be dealt with by general theories.

Application and implications for physical testing

The wave amplitude spectrum is corrected for the average height measured across the gauge array. The array should therefore be placed at the location proposed in the tank for model deployment during testing.

When re-creating site conditions for tank testing, including measured or representative currents can help explore the envelope of expected responses. This will in turn provide more insightful and realistic device and mooring loads, including both those incurred through the presence of the current directly as well as those resulting from the influence of the current on the wave field. If combined conditions are specified, then the input spectrum will need to be corrected so that the desired spectrum is obtained at the device location, thus appropriately representing the power available. With the current included, the correct wavenumber spectrum will also be obtained, ensuring that wave amplitudes, along with wavelength, steepness and celerity match those at the site.

Due to the potentially significant effect current can have on perceived power and assumed wavelengths, it is clearly advantageous to measure current velocities when carrying out resource assessment. This is also the case when carrying out full scale testing as it enables true context to be placed on the results. For example, if characterising a WEC performance by H_{m0} and T_e, a device sensitive to wavelength and steepness will respond very differently in the presence of current despite having comparable H_{m0}, T_e values. Additionally, the available power will be misinterpreted.

The level of sea state complexity generally increases as a concept advances through Technology Readiness Levels (TRLs) as discussed in section 3.4.3. Early stage testing is typically limited to regular waves of varying frequency and height before advancing to standard parametric spectra (both long and short crested). The ability to produce combined wave-current sea states, especially with non-parametric spectra, will usually apply more to devices at advanced TRLs where a particular deployment site has been identified. As such, this ability to produce site-specific combined sea states has the potential to extend and complement established development paths.

6.6 Chapter conclusions

Wave-current interactions are complex, and often not fully understood by developers of ORE devices. This can lead to the situation where clients request combined wave-current test conditions that cannot physically exist, e.g. blocked waves. Expectations of wave quality may also be unrealistically high, as the influence of chaotic turbulent currents on individual wave shape is ignored.

For many devices, particularly WECs and other floating vessels, the implications of interaction with a current should be considered when assessing wave power resource or device performance in the tank. The wave power resource is altered by currents, but this change will not be apparent if the current is not measured and reproduced.

An initial characterisation of the FloWave tank performance when producing a subset of possible combined conditions has been completed. This includes repeatability of waves on currents, plus the straightness of long-crested waves interacting with the non-uniform current field.

A series of observations were made, investigating the change to wave properties resulting from the interaction with a current in the FloWave facility. This includes cases with currents at an oblique angle to the waves, on which little has been published. Caution is required when comparing these results with theory however, as it has not been possible to separate tank-specific generation effects from the pure underlying interaction.

Finally, a method has been developed to produce waves of the required height in the tank following interaction with a current, even though the waves are generated in still water and are then transformed by the current. This has already been used to facilitate client testing in combined wave-current conditions at FloWave.

Part **III**

Client testing at FloWave

Chapter 7

Specific technical issues for testing in a combined wave-current environment

Chapter summary

- There are many issues that should be considered when testing scale models in a combined wave-current environment. This is largely covered in existing guidance, standards, and other research. Three considerations particularly relevant to FloWave are addressed in more detail in this chapter:
- Discrepancies resulting from producing waves in inconsistently scaled water depth, as a result of testing with a fixed water depth.
- The quality of scaled environmental conditions (currents and combined wave-current) that can be generated in the basin, using metrics to quantify this subjective process.
- Recommendations are suggested for testing using advanced environmental conditions, augmenting existing guidance on test planning.

7.1 Introduction

There are many issues that should be considered when testing scale models, for Offshore Renewable Energy (ORE) and other sectors. The general aspects have been widely covered by previous research, and are reported in existing guidance and standards, as discussed in section 3.4. These general issues are also considered further in chapter 8 in relation to test planning.

Three specific aspects of relevance when testing at FloWave were considered as part of this research project, and are discussed in this chapter.

1. Firstly, the discrepancies that result from generating waves in a water depth that is inconsistently scaled from full scale. This is important for ORE devices, as these are often deployed in 'intermediate depth' coastal environments where the waves are influenced by the water depth. It is also a particular consideration at FloWave, due to the fixed water depth.

2. Secondly, metrics were developed to highlight the quality of the scaled environmental conditions (waves, currents, and combined) that can be generated in the FloWave basin. It is important to understand and quantify this, but also to disseminate the information to clients.
3. Finally, recommendations are offered for testing using advanced environmental conditions, like multi-directional wave-current, possible in facilities such as FloWave. This can increase understanding of device performance in the lower-cost controlled environment of a tank, before deployment at sea. These recommendations augment existing guidance on test planning.

7.2 Discrepancy in scaled water depth

This section includes joint work with fellow IDCORE researcher at FloWave, Sam Draycott. The discrepancy was initially identified by Dr Draycott. I expanded upon this work to make it more general including producing the design diagrams. A paper on this work has been published in the International Journal of Marine Energy (Noble et al., 2017a), see Appendix B, which has been incorporated into the following section.

There are numerous design considerations for wave and current basins, many of them conflicting. For the FloWave tank, one practical limitation of the design chosen is that the tank has a fixed water depth. This is of particularly relevance when testing intermediate depth waves that are impacted by the water depth.

This section therefore explores the impacts of testing in a constant depth tank. It is also of relevance where the water depth is not, or cannot be, scaled consistently for whatever reason.

7.2.1 Background and theory

Whilst it is common knowledge that the wavelength of a water wave is a function of water depth, there has been little published regarding the incorrect scaled reproduction of wavelength resulting from inconsistent depth scaling. This issue was mentioned in Draycott et al. (2015*a*), and expanded upon in Draycott (2017), but there do not appear to be any other published discussions.

A number of authors, including Holmes (2009); Holmes and Nielsen (2010), highlight the issue of scaling water depth when tank testing in the context of modelling mooring systems. These do not, however, highlight the consequences for wavelength error. Water depth scaling in relation to distorted hydraulic models is discussed in Méhauté (1976), noting that these models cannot be used for the study of water waves, as wavelength

depends on water depth. For similitude in waves, the horizontal and vertical scales must be the same.

As discussed in chapter 2, when re-creating waves in a test tank, the Froude scaling law is normally used to match the ratio of inertial to gravitational forces that dominate this problem. The ratio of depth at the site of interest to the tank depth is important because gravity waves in water of finite depth can only be correctly re-created when the water depth is also scaled. The properties of water waves are related by the dispersion relation, eq. (2.5), which gives a unique relationship between the three quantities of wavelength, period, and depth. This fact is widely known and well understood. When tank testing, if the water depth is not scaled consistently, then wavelength will also be incorrect for a given Froude scaled period. This has implications for testing, as discussed below.

The wavelength at a site L_{site} can be calculated from wave period and depth the dispersion relation, expressed here in terms of wavelength and period at the site, eq. (7.1).

$$L_{\text{site}} = \frac{g T_{\text{site}}^2}{2\pi} \tanh\left(\frac{2\pi h_{\text{site}}}{L_{\text{site}}}\right) \tag{7.1}$$

Using Froude scaling, where λ is the scale factor, these properties at tank scale should thus be as eq. (7.2), giving eq. (7.3).

$$T_{\text{tank}} = T_{\text{site}}\sqrt{\lambda}\,, \quad h_{\text{tank}} = h_{\text{site}}\lambda\,, \quad L_{\text{tank}} = L_{\text{site}}\lambda \tag{7.2}$$

$$L_{\text{tank}} = \frac{g T_{\text{site}}^2 \lambda}{2\pi} \tanh\left(\frac{2\pi h_{\text{site}}\lambda}{L_{\text{tank}}}\right) \tag{7.3}$$

However, if the tank depth is not correctly scaled, $h_{\text{tank}} \neq h_{\text{site}}\lambda$, the (incorrect) wavelength in the tank $L_{\text{tank}*}$ will instead be given by eq. (7.4), assuming the period is correctly Froude scaled.

$$L_{\text{tank}*} = \frac{g T_{\text{site}}^2 \lambda}{2\pi} \tanh\left(\frac{2\pi h_{\text{tank}}}{L_{\text{tank}*}}\right) \tag{7.4}$$

The error in wavelength ε_L is taken as the ratio of wavelength actually generated in the tank $L_{\text{tank}*}$ to the correctly scaled wavelength $L_{\text{tank}} = L_{\text{site}}\lambda$.

$$\varepsilon_L \equiv \frac{L_{\text{tank}*}}{L_{\text{tank}}} \tag{7.5}$$

The group velocity of a wave C_g is a more complex function of wavelength and water depth, given by eq. (7.6).

$$C_g = \frac{1}{2}\sqrt{\frac{gL}{2\pi}\tanh\left(\frac{2\pi h}{L}\right)}\left[1 + \frac{4\pi h}{L\sinh\left(4\pi h/L\right)}\right] \tag{7.6}$$

The error in group velocity can be computed in the same manner, by calculating $C_{g,\text{tank}*}$ based on the wavelength actually generated in the tank, and $C_{g,\text{tank}}$ from the correctly scaled wavelength. The error is simply the ratio between these, eq. (7.7)

$$\varepsilon_{Cg} \equiv \frac{C_{g,\text{tank}*}}{C_{g,\text{tank}}} \tag{7.7}$$

The speed, or celerity, of an individual wave is given by $C = L/T$, and steepness by $S = H/L$. Provided the period and height are correctly Froude scaled, the corresponding relative errors in celerity and steepness will thus equal the error in wavelength. As wave power $P_w = E_A C_g$, where E_A is wave energy per unit horizontal area (Méhauté, 1976), the relative error in power will equal that of group velocity. Any discrepancy in wave power is particularly important in tank testing wave energy converters, as wave power (kW/m) is scaled by $\frac{\rho_p}{\rho_m}\lambda^{2.5}$ (section 2.2.2) magnifying the projected full scale power discrepancy.

As discussed in section 2.1.1, wave orbital motions ξ, ζ and velocities u, w can be calculated by eqs. (7.8) and (7.9) for the horizontal and vertical directions respectively.

$$\xi = \frac{-H}{2}\frac{\cosh k(h+z)}{\sinh kh}\sin(kx-\omega t) \qquad u = \frac{\pi H}{T}\frac{\cosh k(h+z)}{\sinh kh}\cos(kx-\omega t) \tag{7.8}$$

$$\zeta = \frac{H}{2}\frac{\sinh k(h+z)}{\sinh kh}\cos(kx-\omega t) \qquad w = \frac{-\pi H}{T}\frac{\sinh k(h+z)}{\sinh kh}\sin(kx-\omega t) \tag{7.9}$$

Assuming wave height H and period T are correctly scaled in the tank the initial terms cancel, and the final $(kx - \omega t)$ term for periodic motion can be neglected when calculating the maxima. The error in horizontal and vertical wave orbitals $\varepsilon_{\text{hor}}, \varepsilon_{\text{vert}}$ respectively can thus be calculated using eqs. (7.10) and (7.11).

$$\varepsilon_{\text{hor}} \equiv \frac{\xi_{\text{tank}*}}{\xi_{\text{tank}}} \qquad \text{where} \qquad \xi \propto \frac{\cosh k(h+z)}{\sinh kh} \tag{7.10}$$

$$\varepsilon_{\text{vert}} \equiv \frac{\zeta_{\text{tank}*}}{\zeta_{\text{tank}}} \qquad \text{where} \qquad \zeta \propto \frac{\sinh k(h+z)}{\sinh kh} \tag{7.11}$$

7.2.2 Design diagrams for graphical visualisation of errors

Whilst the theory covered in section 7.2.1 is not new knowledge, a method to calculate and visualise these discrepancies has been developed in order to assist with test design and aid understanding of this potential source of error. This method utilises a new term 'scale depth discrepancy' (*SDD*), defined as eq. (7.12), and shown graphically in fig. 7.1.

$$SDD \equiv \lambda\frac{h_{\text{site}}}{h_{\text{tank}}} \tag{7.12}$$

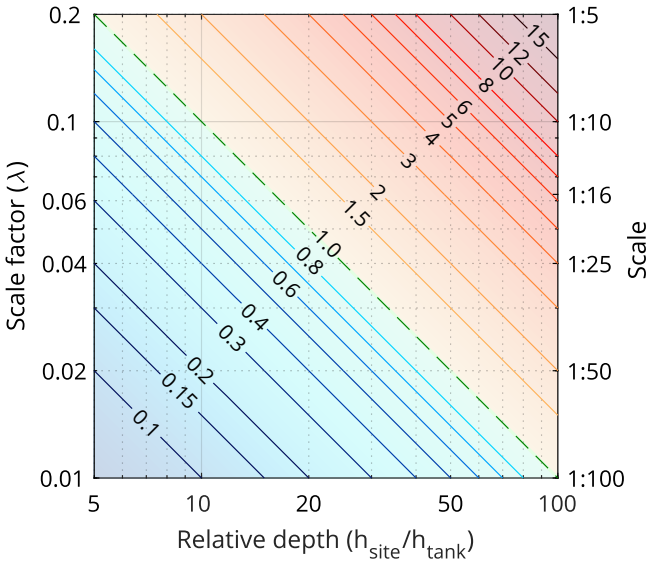

Figure 7.1: Contours of scale depth discrepancy (SDD) shown for a range of relative depths (site to tank) and scale factors (scale being the reciprocal of scale factor).

This term aggregates the scale factor plus relative water depths between deployment site and tank into one variable. A value of SDD less than unity corresponds to the tank being too deep for the scaled site depth, resulting from a relatively shallower deployment site and/or a smaller model scale.

The frequency dependent errors resulting from this discrepancy can then be plotted over the range of SDD and non-dimensional tank-scale period, eq. (7.13).

$$\tau_{\text{tank}} = T_{\text{tank}}\sqrt{g/h_{\text{tank}}} = T_{\text{site}}\lambda\sqrt{g/h_{\text{tank}}} \tag{7.13}$$

The non-dimensional period is only the same in the tank as at the site when the depth is scaled consistently, i.e. $SDD = 1$. Discrepancy in wavelength, steepness, or celerity is shown in fig. 7.2, noting that these are of the same magnitude, whilst the discrepancy in group velocity or power is shown in fig. 7.3.

A deep water simplification is often used in offshore engineering, based on the fact that $\tanh(kh) \to 1$ for large kh (section 2.1.2). This simplification is usually applied for $kh > \pi$ where the discrepancy is <0.4% (Dean and Dalrymple, 1991). Expressed in terms of depth and wavelength, this limit equates to $h/L > 1/2$. For situations where both the deployment site and test tank can be considered deep water, i.e. below both dashed lines in fig. 7.2, the error in wavelength is negligible and correct depth scaling is not required. It is interesting to note that the errors in wavelength are compounded when calculating the group velocity, resulting in a discrepancy for $C_g \approx 2\%$ at the deep water limit, although this is still likely to be acceptable when tank testing.

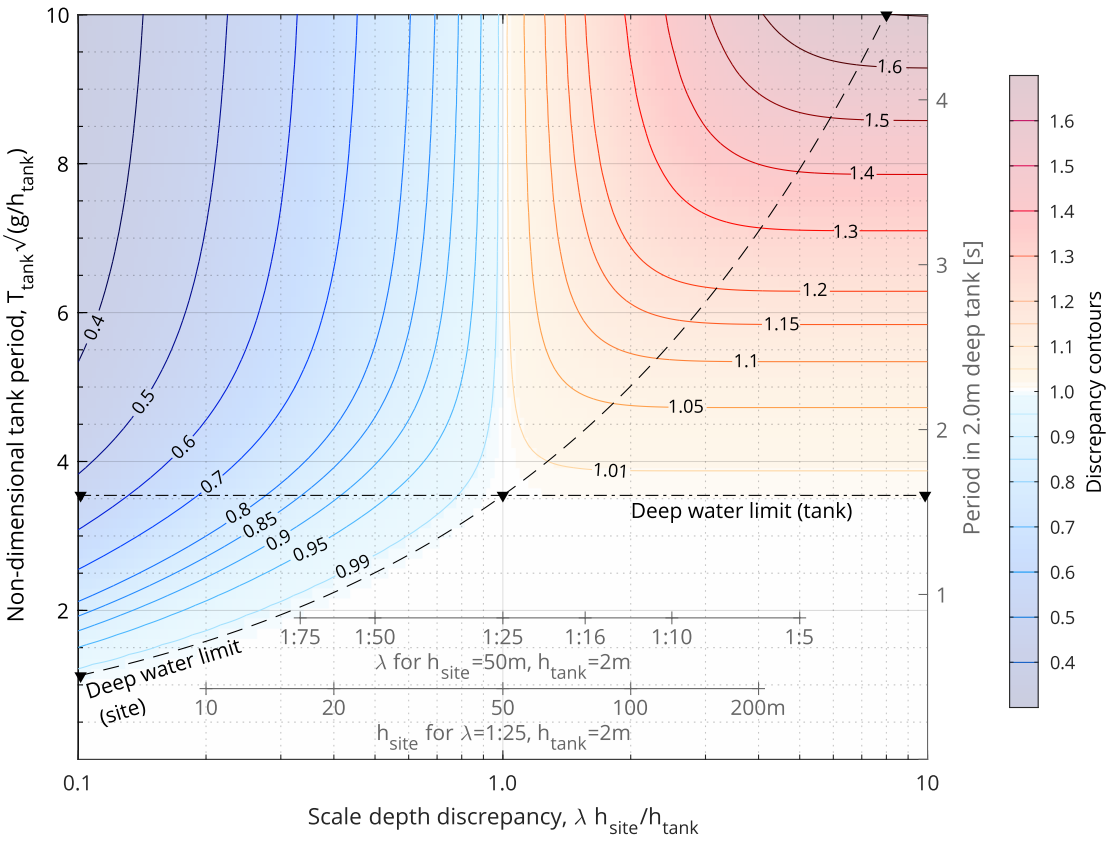

Figure 7.2: Contours of relative error in wavelength or steepness or celerity for a range of scaled depth discrepancies and non-dimensional periods. Sub-axes show example scale factor and site depth for other parameters fixed. Dashed and dash-dot lines show deep water limits for site and tank respectively.

Wave energy converters typically operate in wave periods of 3 s to 15 s, and depths around 20 m to 80 m, which equates to full-scale non-dimensional periods of about 1 to 10. At tank scale, this should be similar, providing the *SDD* is close to unity. Typical model scales for testing model renewable energy devices are between 1:100 and 1:10, tested in tanks 0.5 m to 5 m deep, although large models are unlikely to be tested in small tanks and vice versa. This may result in scaled depth discrepancies in the order of 0.3 to 3, obviously depending on the specifics of model, device, and tank. Therefore, errors in the wavelength/steepness/celerity of up to around ±30% may be experienced in testing. This results in a corresponding ±20% discrepancy in wave power and group velocity.

To facilitate understanding of figs. 7.2 and 7.3, examples are shown on the secondary axes with a 1:25 scale model, 50 m deep site, and 2 m deep test facility. A 12 s full-scale wave of interest to a wave-energy device would have non-dimensional period $\tau_{\text{tank}} = 5.3$. If the site depth was 40 m or 100 m instead of 50 m, as shown on the lower secondary x-axis, the wavelength/steepness/celerity (fig. 7.2) would be wrong by a factor ε_L of 0.95

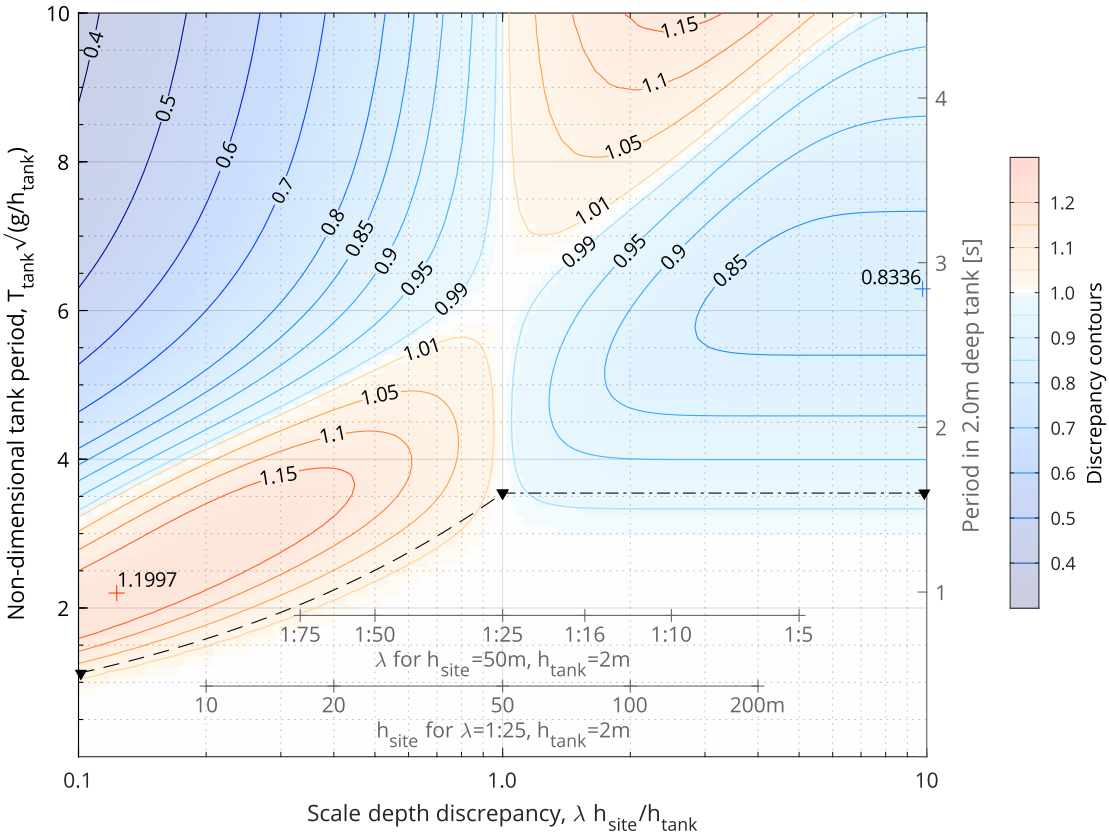

Figure 7.3: As fig. 7.2 but showing contours of relative error in group velocity or wave power.

or 1.09 respectively, and group velocity/wave power (fig. 7.3) would be wrong by a factor ε_{Cg} of 1.13 or 0.88, as shown in table 7.1 along with additional examples.

Potential errors in wave orbital motions from incosistant depth scaling are shown on fig. 7.4. At the water surface ($z = 0$, MWL), the discrepancy in horizontal motions/velocities ε_{hor} is the reciprocal of the wavelength error ε_L, and there is no error in the vertical motions/velocities, $\varepsilon_{\text{vert}} = 0$. Below the water surface, it is not possible to obtain the correct wave orbtal motion if the water depth is not scaled consistently between the site

Table 7.1: Example discrepancies in a 12 s full-scale wave, for wavelength/steepness/celerity ε_L (fig. 7.2) and for group velocity/wave power ε_{Cg} (fig. 7.3).

Scale	h_{site} [m]	h_{tank} [m]	SDD	τ_{tank}	ε_L	ε_{Cg}
1:25	50	2	1	5.31	1	1
1:25	40	2	0.8	5.31	0.95	1.13
1:25	75	2	1.5	5.31	1.07	0.93
1:50	50	2	0.5	3.76	0.92	1.13
1:16	50	2	1.56	6.64	1.13	0.98
1:25	50	3	0.67	4.34	0.94	1.08

and the tank. This error increases with depth below the surface, shown by the sub-plots vertically on fig. 7.4. It should be noted that the large error shown is a function of how $\varepsilon_{\text{hor}}, \varepsilon_{\text{vert}}$ are defined; where the wave orbital size is small, division can result in a large relative error even though the absolute difference in orbital magnitudes is small. This is shown by the contours of wave orbital size relative to wave height ($\xi/H, \zeta/H$), which are just a function of wave period. For example, a 0.1 m 0.35 Hz wave in a 2 m deep tank has $\tau_{\text{tank}} \approx 2.9$; at mid depth ($z/h = -0.5$) both the horizontal and vertical orbital size are about 5% of the wave height, i.e. 0.005 m. Another point to note is that the discrepancies have been calculated using small amplitude wave theory, and are not strictly accurate for higher-order waves.

7.2.3 Discussion

For marine renewable energy devices, such as Wave Energy Convertors (WECs) or Floating Offshore Wind Turbines (FOWTs), wave steepness can be particularly important as this affects floating device response. Loads and responses on foundations and moorings will be affected by wave orbital motion. It is also beneficial to understand how the power of waves is scaled and what errors may be present when modelling a device to extract this power. The method presented here is designed to be an aid to tank test planning, allowing the range of discrepancies to be quantified when selecting a facility and model scale. It will also be of benefit when correlating tank test measurements to real site deployment where the scaled depth ratio is not unity, which is a likely scenario.

This issue of incorrect depth scaling may not have received much attention previously, as it is less critical for other applications of tank testing. For coastal models where water depth is paramount, the bathymetry is usually re-created in the test facility, removing any depth error and corresponding wavelength issues. When testing ships, there is not a unique depth in which they operate, and this can often be classified as 'deep water' reducing the importance of understanding this depth scaling discrepancy. Oil platforms also typically operate in deep water relative to the waves experienced.

While the errors presented here have been calculated using linear wave theory, ε_L and ε_{Cg} also hold for second order Stokes waves, where although the wave shape is different the dispersion relation remains the same (Dean and Dalrymple, 1991). A correction to the dispersion relation is required for third and higher orders. The errors in wave orbitals $\varepsilon_{\text{hor}}, \varepsilon_{\text{vert}}$ are correct only for first order linear waves.

Discrepancies in wave spectra are frequency dependent, and can be visualised as vertical sections through the contoured surfaces shown in figs. 7.2 and 7.3. For wavelength, steepness, or celerity the error has the same direction as the scale depth discrepancy, i.e. $\varepsilon_L < 1$ for $SDD < 1$. For group velocity or wave power it is possible to have both errors smaller and larger than unity for a given SDD.

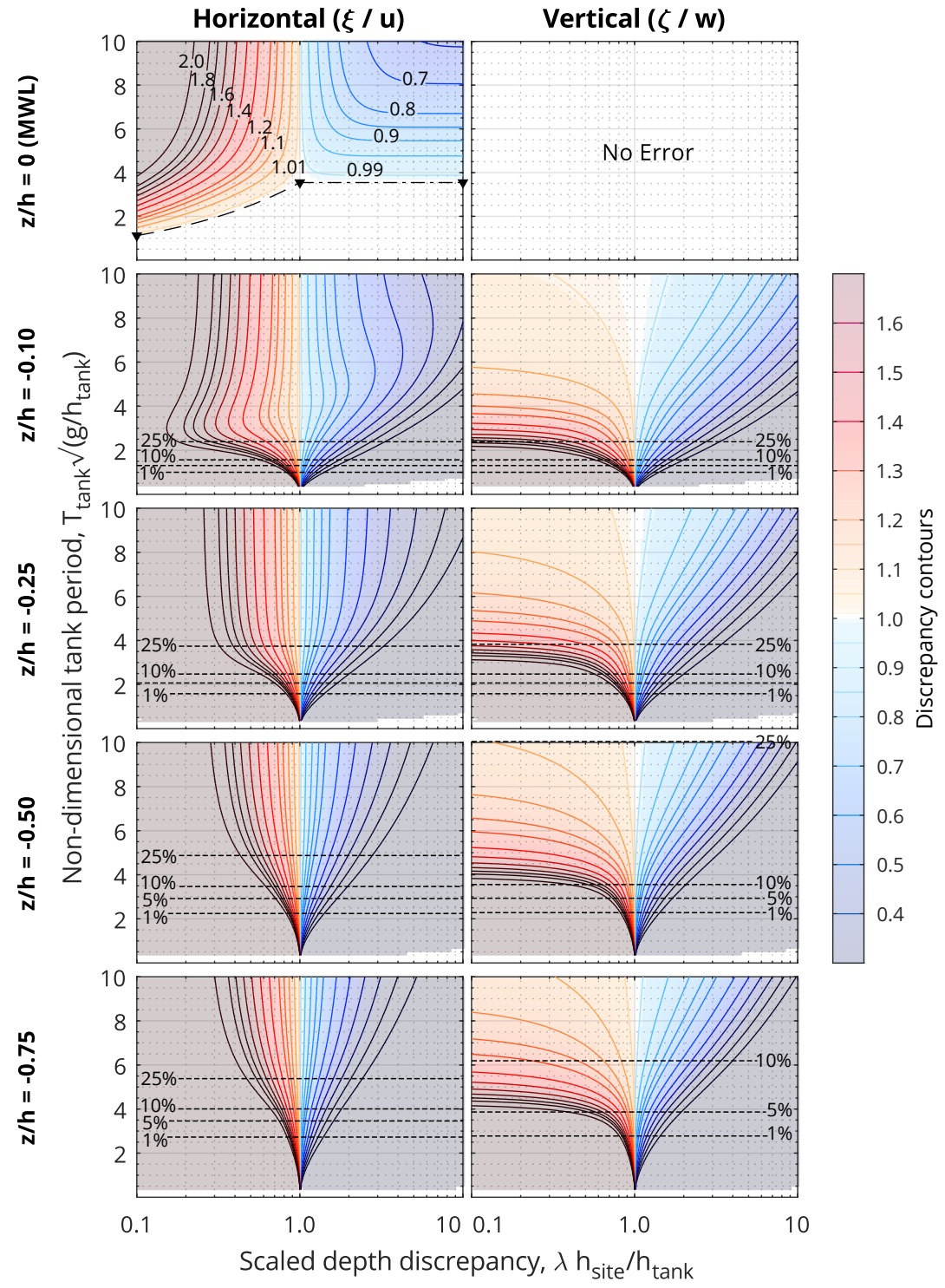

Figure 7.4: Contours of relative error in horizontal and vertical wave orbitals (size and velocity), for a range of scaled depth discrepancies and non-dimensional periods. Sub plots from top to bottom show different vertical positions in the water column. Dashed and dash-dot lines on z/h=0 plot show deep water limits for site and tank respectively. Short dashed lines on other plots show contours of wave-orbital size relative to wave height (ξ/H, ζ/H of 1%,5%, 10%, 25%).

Scale dependencies are routinely accounted for in the analysis of test results. For example, when using Froude scaling in tank testing, time is scaled by $\sqrt{\lambda}$. It is also common to test in fresh water which is approximately 2.5% less dense than typical sea water. In the same manner, the design methods presented here could also be applied to any discrepancy in the scaled water depth.

7.3 Quality metrics

7.3.1 Use and requirements

Quality metrics have been developed to convey how well various conditions can be generated in the FloWave facility. These can be used to provide an overview of complex data, highlighting trends albeit at the expense of obscuring details and potentially amplifying small differences close to the boundaries.

There are two main uses for the quality metrics:

1. For assessing tank performance, what conditions can be generated, and how well those conditions can be produced in the tank. This may be used to plan and prioritise future upgrades to the control system and/or tank hardware. Importantly, the quality metrics could then be used to monitor if these upgrades are successful for the conditions of interest.
2. The quality metrics will also be useful for communicating with clients how well the tank performs over a range of conditions. This is particularly the case for those clients less familiar with tank testing and associated limitations. It is important to be aware however, that there are different types of clients using the facility, with varying expectations and experience. An academic with a meticulously planned experiment investigating minor discrepancies in non-linear wave theories is likely to have quite different quality expectations to a developer looking to gain a rough understanding of device behaviour.

Note that for any classified analysis, there is a trade-off between the granularity of variance and ease of understanding the data. Studies such as Padilla et al. (2017) suggest that binning of continuous 2D scalar data can facilitate comprehension and improve performance accuracy. A subjective judgement is required on the quantity and magnitude of levels used in splitting data into bins. More categories give an 'information rich' view of the data, although potentially at the expense of legibility (Harrower and Brewer, 2003).

Quality metrics have been produced for two key areas of tank characterisation undertaken. Spatial variability of mean flow, and also quality of wave-current conditions produced in the facility. It would also be possible to produce similar figures for parameters such as wave reflections, based on the work of Draycott (2017).

7.3.2 Spatial variability of flow generation

Figure 7.5 shows a simplified view of the data presented in section 5.3, highlighting areas where flow is nominally the same as at the tank centre. This is particularly useful for clients planning tests with either large devices, or with arrays of multiple turbines.

Similarly, fig. 7.6 highlights points where the flow direction is close to desired. Although it is possible to interpolate between the measurement points for flow direction, this does not work so well as a quality metric. The eye is drawn more to artefacts around the periphery where flow direction switches from positive to negative angles. Coloured flow vectors are therefore used instead.

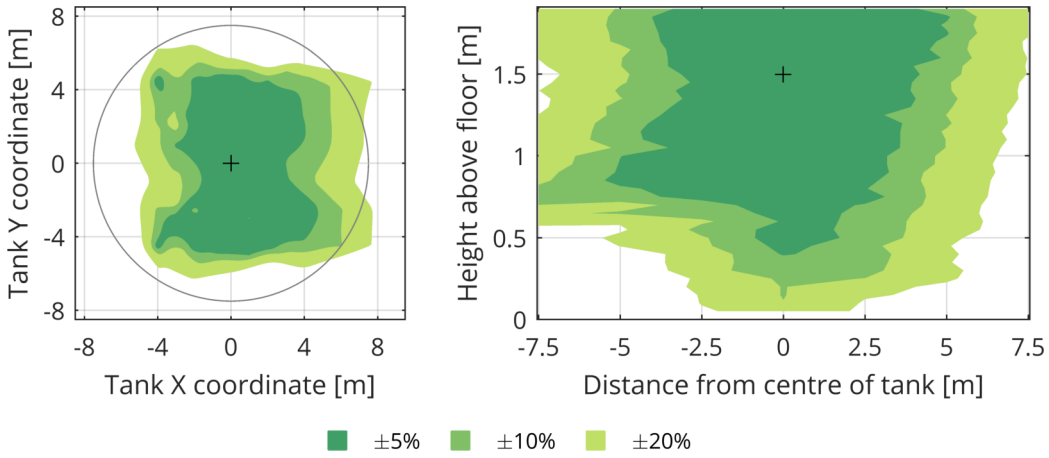

Figure 7.5: Quality metric for spatial variability of mean flow generation, for nominally 0.8 m/s. Percentage variation in mean flow relative to tank centre (0,0,1.5) shown by 3 colours. Subplots show plan view (left) and vertical section (right), (cf. figs. 5.11(c) and 5.13(c)).

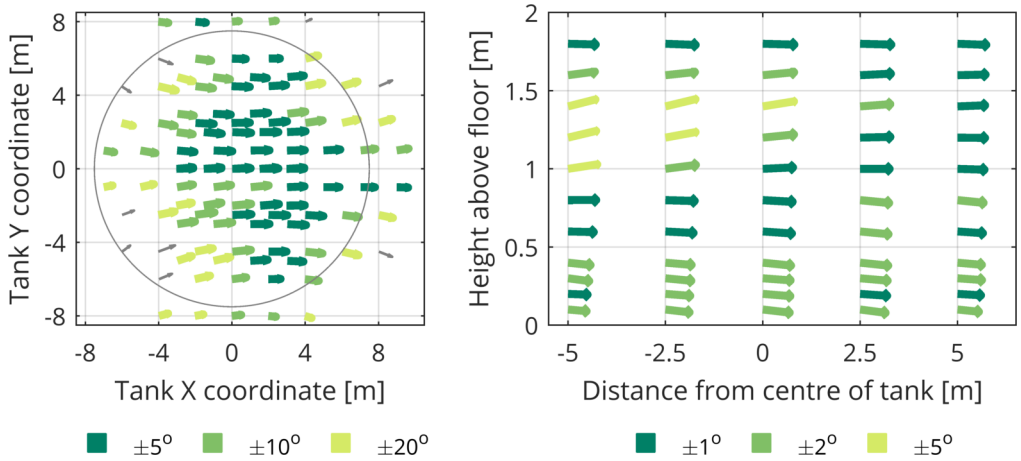

Figure 7.6: Quality metric for spatial variability of flow direction, for nominally 0.8 m/s. Absolute misalignment from desired direction shown by 3 colours. Subplots show plan view (left) and vertical section (right), (cf. figs. 5.13(c) and 5.14).

Similar plots could be produced for other velocity conditions and/or spatial points in the tank, to understand the usable test area for the conditions of interest.

7.3.3 Quality of combined wave-current conditions

To quantify the quality of combined wave-current conditions produced in the tank, a proxy of variance in measured wave height across the wave gauge array has been used, as in section 6.3.2, eq. (6.4). This has been applied to the set of regular waves run at various relative angles to current velocities up to 0.5 m/s given in table 6.3(a).

The quality metric has been calculated for the whole test (i.e. including the build-up of reflections) shown in fig. 7.7. It was also calculated for a short 5 s sub-sample where no reflections are present to understand the quality of just the incident wave generation, shown in fig. 7.8. Again, this method could be expanded to other wave-current conditions once these have been measured and analysed.

The plots concisely document a complex multi-dimensional phenomenon, where the quality of waves produced in combination with current is a function of $T, H, U, \theta_{\text{rel}}, t$. One of the data simplifications required is to exclude spatial variability across the tank, which may be important and should be checked. The metrics instead represent the conditions averaged over the measurement array, indicative of a model test location.

Combined conditions with higher wave quality in the FloWave tank are apparent on figs. 7.7 and 7.8, namely slower velocities, lower frequency, and to a lesser extent perpendicular currents.

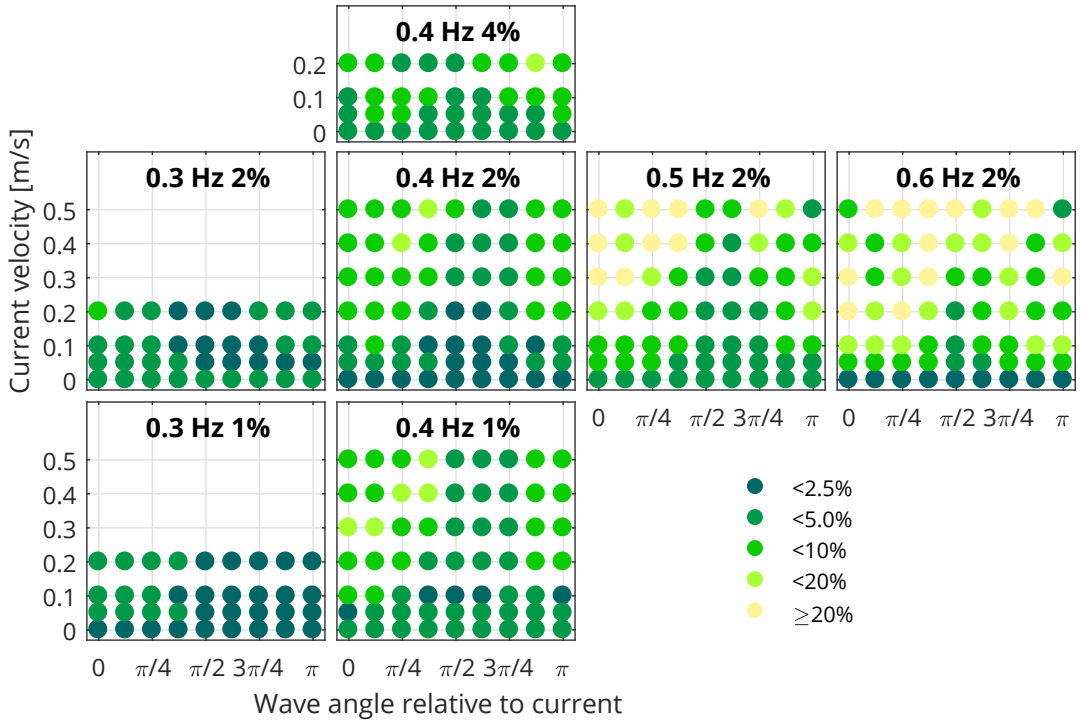

Figure 7.7: Quality metric for combined wave-current conditions, covering the whole length of the test. Sub-plots show different regular waves, with increasing frequency left–right and increasing steepness bottom–top. Each sub-plot shows nine relative angles between waves and current, from following ($\theta_{\mathrm{rel}} = 0$) to opposing ($\theta_{\mathrm{rel}} = \pi$), at three or six increasing current velocities on the y-axis. Quality of the conditions generated is represented by 5 colours, using percentage variation in wave height between wave gauges in the array as a proxy.

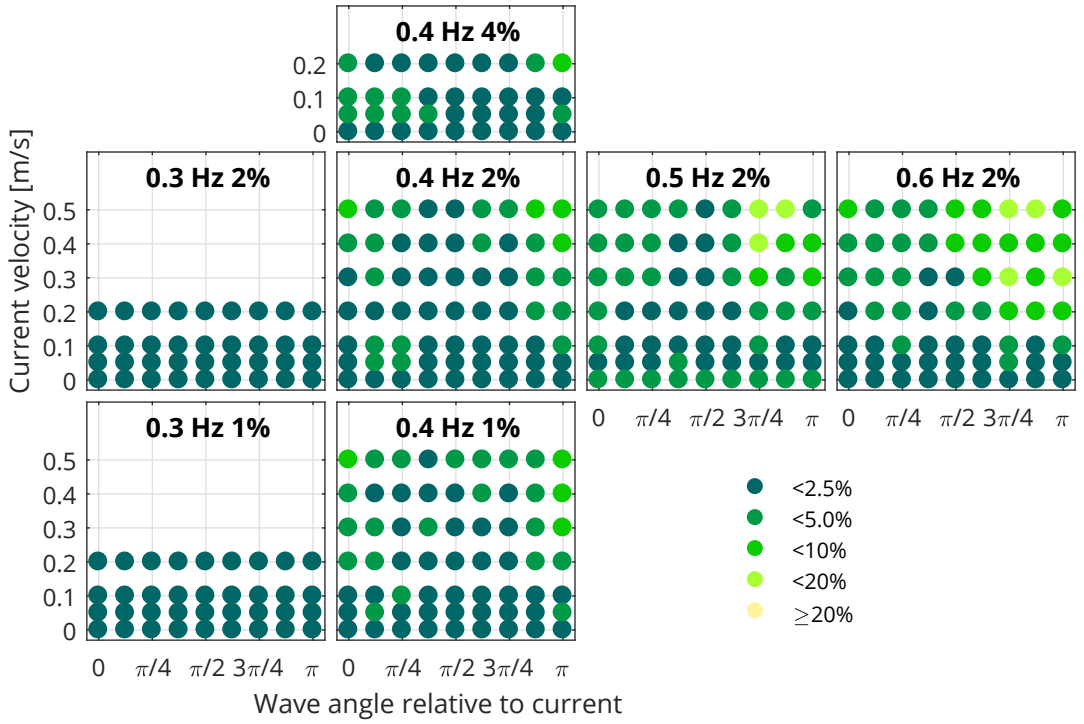

Figure 7.8: As fig. 7.7 but for short 5s sub-sample of just incident waves.

7.4 Recommendations for testing with advanced environmental conditions

This section is based on a paper presented at the 36th International Conference on Ocean, Offshore and Arctic Engineering (Noble et al., 2017b), see Appendix B. The discussion on advanced waves is partially based on issues highlighted in Draycott (2017) with additional input from Dr Draycott on the resulting conference paper.

7.4.1 The test process and existing guidance

Tank testing is an important process in the development of marine renewable energy devices. The use of structured development plans is an established part of this process, as set out in guidance, with an incremental approach recommended. Initial tank tests should be undertaken at small scale with relatively simple input conditions, before moving on to larger and more complex tank tests, then open water deployment. At each stage the developer is aiming to maximise understanding of their device and its performance, with the minimum of risk and financial outlay. Published guidance for ORE development and testing outlines the process and gives details for general aspects of tank testing. Recommendations for advanced test conditions are more limited however. The knowledge and experience of those working in test-tanks is invaluable when testing, and critical for a successful outcome. Documenting and publishing this experience will facilitate sharing of knowledge, improving testing throughout the sector.

A key challenge for combined wave-current basins such as FloWave is the limitations of existing guidance, specifically on testing in more advanced conditions such as multi-directional waves and combined wave-current, as discussed in section 3.4.5. These can be summarised as:

- Not enough emphasis on directional sensitivity.
- Little guidance on testing with advanced wave conditions, such as multi-directional and multi-modal sea states.
- More guidance required on the implications of combined wave-current conditions, and how this should be incorporated in to test-plans.

Initial recommendations are therefore given in the following sections, that mirror the limitations identified. These recommendations are used to inform the tests taking place in the FloWave facility. Since opening in 2014, numerous clients have made use of the facility to test ORE devices, measurement instrumentation, and other devices. This has included several tests assessing performance and loading on Tidal Stream Turbines (TSTs) and WECs with combined wave-current at multiple angles, as well as WEC performance in site specific wave conditions.

It is envisaged that these advanced environmental conditions would be used towards the end of stage 2 tank testing, for devices at mid TRL. They are offered in addition to and consistent with existing guidance on developing test plans. They are based on documenting the ongoing research plus lessons learnt during testing conducted at FloWave.

Realistic waves, and wave-current interactions particularly, are complex non-linear processes that can be difficult to model numerically, and thus developers may benefit from the increased learning carried out in controlled conditions on a relatively inexpensive model, prior to conducting real-world tests in the ocean.

The advanced test conditions proposed all have potential to affect both the power capture performance and loading on devices. These should therefore be considered when testing wave energy converters, tidal stream turbines, and floating offshore wind turbines, although the applicability of particular conditions will depend on the specifics of device and deployment site.

7.4.2 Consider directional sensitivity

When assessing the directional sensitivity of the device, this should apply to all environmental conditions being tested: wind, wave, current, and combined; unless there is strong justification not to do so. Wind is likely only to be significant for FOWT tests, as most TSTs and WECs do not protrude significantly above the sea surface. Directional considerations for combined wave-current conditions are discussed further in section 7.4.4.

- For devices that do not weathervane to face the incoming conditions, the effect of off-axis waves or currents (as appropriate) on power capture and foundation/mooring loads should be assessed.
- Some WECs are designed to face into the prevailing wave direction to maximise power capture. The presence of cross-currents or multi-modal waves could affect this orientation, potentially increasing the mooring loadings and decreasing power capture. This was highlighted as an important consideration in lessons learnt from the Pelamis WEC (Retzler, 2015).
- Particularly for sites at headlands, the tidal flow may exhibit asymmetry rather than being purely rectilinear, with corresponding directional loading on the TST and foundation.
- TSTs are also likely to be affected by wave loading which is unlikely to always be aligned with the current direction, except perhaps in narrow channels.

Where there is symmetry in the device, either mirror or rotational, this can be used to reduce the size of the test matrix. Many devices will have bilateral symmetry although this is worth confirming with a few test cases, especially where the device has rotating turbine(s) that may impart asymmetry. Where the worst case direction(s) for mooring

loads can readily be identified, this can also be used to minimise the test matrix size, as noted in ITTC (2014*b*).

7.4.3 Use of advanced wave conditions

While regular waves and parametric spectra are useful for understanding device motions and performance, they do not capture the full complexity of the real ocean. This may be particularly relevant for WECs. Additional understanding of device performance can be obtained by testing with increased complexity sea conditions. These include multi-modal and multi-directional waves, either specified parametrically or from the characterisation and re-creation of recorded sea conditions. Multi-modal waves may be important for understanding directional performance, as discussed above.

Dynamic response of devices is dependent on spectral form (Mansour and Ertekin, 2003), hence it is the frequency and directional spectral shapes that determine the device response, rather than proxy statistical parameters such as H_{m0} and T_E. It is suggested by Holmes (2009) that using site specific spectral shapes be used for testing in order to assess devices in more realistic wave conditions, however methodologies for extracting meaningful test cases from the vast amount of data are not detailed. This has been explored in Draycott et al. (2015*a*); Draycott (2017), and it is noted that in order to make use of recorded site data in the tank within a realistic time-frame, a small number of representative sea states are required. These should embody the various characteristics of the site, such as:

- Significant wave height H_{m0}, energy period T_E, and wavelength L;
- Wave energy frequency and directional spectra, $S(f)$ and $S(f,\theta)$ respectively;
- Mean direction $\bar{\theta}$, spectral width ν, and directional spreading e.g. s, $\bar{\sigma_\theta}$.

The relative importance of these variables is somewhat subjective, and will depend on site, device, and test purpose. Data can be partitioned using classical binning techniques applied to statistical parameters, (e.g. Ingram et al., 2011; Pitt, 2009), however more advanced clustering algorithms can be used to classify spectral and other high-dimensional data (Hamilton, 2010; Draycott et al., 2015*a*; Draycott, 2017). These sorts of clustering and binning approaches can be used to partition the data into distinct groups, from which representative sea states can be extracted and used for testing. Using such sea states will increase test realism, providing an understanding of real-world-like performance. For subsequent test plans, at higher TRL, insight may also be gained by comparing the performance of model and prototype in the 'same' sea-conditions, in order to improve future testing.

7.4.4 Combined waves and currents

Testing in combined wave-current conditions is important for floating and mid-water-column devices. As discussed in section 6.1, currents change the shape of waves and the impact of wave orbitals propagate well below the surface, particularly for longer period waves. Both waves and currents are present throughout the oceans, and they interact in a complex non-linear way. While the frequency or period of the wave remains constant under the assumptions of small-amplitude wave theory (section 2.1), the wave height and length are altered.

Considerations for floating devices and WECs

For devices that are floating on the sea surface, and/or aim to capture the power of waves, it is important to model the combined wave-current properties correctly. Even low currents have an impact on wave height and length, changing the relationship between period and wavelength, as demonstrated in section 6.4.

The dynamic response of every WEC is different, and beyond the scope of this research to investigate. The underlying change in wave length and height from interaction with a current is considered and illustrated in section 6.1. For waves on opposing currents, length L shortens, while height H increases, and vice-versa for following currents.

The steepness of an individual wave is given by $S = H/L$, the speed (or celerity) by $C = L/T$, and group celerity by eq. (7.14), where h is water depth and g gravitational acceleration. Wave power P_w can be expressed as eq. (7.15)

$$C_g = \frac{1}{2}\sqrt{\frac{gL}{2\pi}\tanh\left(\frac{2\pi h}{L}\right)}\left[1 + \frac{4\pi h}{L\sinh\left(\frac{4\pi h}{L}\right)}\right] \tag{7.14}$$

$$P_w = \frac{1}{8}\rho g H^2 C_g \tag{7.15}$$

All of these parameters ($H,\ L,\ S,\ C,\ C_g,\ P_w$) are affected by the interaction of waves with currents. Therefore, the only way to properly test waves where a current is present at the site is to reproduce that current at scale in the test facility. A method to reproduce a combined wave-current field in the FloWave is presented in section 6.5.

The change in wave shape as a result of the interaction with a current will affect floating device motion and mooring loads, and is highly likely to impact WEC power capture efficiency. In addition to the change in wave shape, the 'apparent' power in a wave calculated ignoring wave-current interaction will be different to the true wave power (Draycott et al., 2017), see section 6.5.2. This may be higher or lower than the correct value, depending on the relative direction of the current. If this change in wave power

is not accounted for, device performance will be misrepresented, affecting economic assessment and comparison with real-world performance.

As well as in tank testing, it is important to consider the potential effect of tidal currents in resource assessment for wave energy sites, as the wave power will be altered. Wave-current interactions should also be included when determining the environmental conditions for floating device deployment. If the current is not included, the wave shape will not match that expected, with implications on power capture and device motion that may be significant. This is explored in more detail in section 6.5.2 with an example given in figs. 6.18 and 6.19.

Impact of waves on currents

The influence of waves on a tidal current is also important for the design of near surface structures and turbine blades, as wave orbital velocities can introduce significant additional cyclic loading. Wave orbital size decreases exponentially with depth, but may still result in considerable cyclic velocities at mid depth where turbines are typically located. This is particularly true for sites that are not 'deep water' as defined by eq. (7.16) where h is water depth, T wave period, and g gravitational acceleration. These waves are influenced by the bed as wave orbital size at this depth is not insignificant.

$$h > \frac{gT^2}{4\pi} \tag{7.16}$$

Surface gravity waves also impact on the flow, increasing turbulence and changing the shape of the vertical profile (Klopman, 1994). This may have implications for TSTs, particularly on differential blade loading for horizontal-axis turbines.

Although tidal currents are predictable, and may propagate through a channel with approximately 180° between ebb and flood, potentially removing the need to assess directionality, the waves will not be predictable and might come from any direction. In narrow channels predominant wave directions may be limited, but still may not necessarily be aligned with the tidal flow. Understanding impact of off-axis waves on a device could be important for device loading and performance, and is something that has been studied in the FloWave facility on behalf of external clients.

Chapter 8

Guidance and planning tools for FloWave

Chapter summary

- Facility specific guidance and planning tools have been developed for FloWave, to flag both issues that should be considered and gaps in knowledge of the client and FloWave staff. It highlights reasons to test in more advanced wave-current conditions, to make use of FloWave's capabilities.
- This interlinking process brings together knowledge on tank testing into six aspects: 1. Research questions; 2. Environmental conditions; 3. Tank capability and performance; 4. Model and instrumentation; 5. Timings and budgets; plus 6. Other issues.
- Development and implementation of the tools and guidance is covered, including client beta tests and a pilot study showcasing the benefit of highlighting these issues to clients.

8.1 Introduction

Test planning is a complex process with many issues that should be considered. There are overlapping areas of knowledge held by FloWave, the client, and published in relevant guidance, as shown in fig. 8.1. This includes new outcomes from this research covered in chapters 5 to 7. The goal for a successful test campaign is for all parties involved to be aware of all the issues.

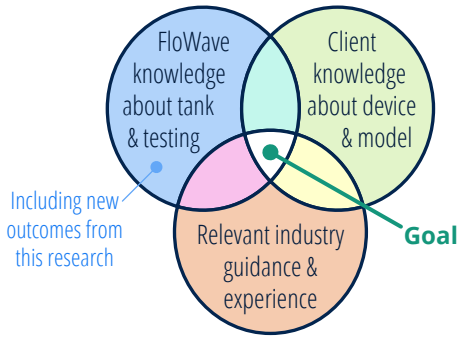

Figure 8.1: Venn diagram highlighting overlap between areas of knowledge.

Detailed guidance and planning tools have therefore been developed to facilitate test planning at FloWave. These are to be used by FloWave staff when discussing tests with a (potential) client. They are intended to flag up common issues when testing, identify gaps in knowledge sharing (fig. 8.1), and assist with optimising the test programme. They are also designed to highlight the more advanced capabilities of the FloWave facility, such as multi-directional waves at an oblique angle to a current.

A series of flowcharts have been produced along with a checklist questionnaire. These flowcharts visually represent linkages between the many issues to be considered when tank testing. The checklist is designed to provide a record of discussions, decisions, and outstanding actions. These are detailed in section 8.2.3, and are based on published guidance plus experience of testing at FloWave over the past three years.

This facility specific guidance gathers together for the first time a comprehensive set of issues that should be considered prior to testing in a facility such as FloWave. Many of these issues will be well-known and understood by those involved in tank testing. It is noted however, that *not all these issues will necessarily be known and understood* by the wide range of clients interested in testing at FloWave, illustrating the business need to collate and explain them.

8.1.1 Requirements for the test planning tools and guidance

The test planning tools and guidance should be device agnostic as far as possible, due to the wide range of devices that are tested at FloWave. There is also a wide range of clients, ranging from purely academic projects to commercial developers with devices at different Technology Readiness Levels (TRLs), plus there are various collaborative arrangements in between. The tools and guidelines developed concentrate on wave and tidal energy devices, as these are what is most commonly tested at FloWave. They also focus on the more advanced combined wave-current generation capabilities of the FloWave facility, as this is often a key reason for developers and academics to test in this specific tank.

The tools developed have been designed to assist with decisions on how both the overall test programme and individual tests should be set up. It is noted however, that some parameters may be fixed prior to initial client contact with FloWave. For example, where there is an existing model, this will limit choice of scale, and potentially other parameters, so this needs to be accounted for in the process. It is also common for device developers to compare results of tank tests to their numerical models of the device. Some parameters of the physical model tests may therefore be constrained to overcome software limitations, even if these tests are possible in the tank.

Financial aspects of test planning are not considered in detail, as this is considered outside the scope of this work. Most of the decisions made when planning a test will have an economic impact of some description, which could often be significant, and so must be considered by both the client and FloWave.

It is acknowledged that the guidance and planning tools will not be exhaustive, and so are live documents that should continue to be developed as lessons are learnt from testing and additional guidance is published. Comments and feedback were obtained from FloWave staff and clients during development, beta testing, and the pilot study, as discussed in section 8.3.1.

Selection of model scale

Selection of the model scale is not a single issue in the test planning process, rather it is influenced by and has influence on a number of factors. This can be one of the key issues driving the iterative nature of the planning tool.

There may be specific drivers that force the selection of model scale, such as having an existing model. The selection of model scale may therefore have been made in advance of the client approaching FloWave, which is a relatively common situation. Having a fixed scale may limit the choices when considering other issues, simplifying the process in some respects. It is however worth still considering all of the issues as they may highlight the need to use a different model at a revised scale.

Constraints and flexibility

Highlighting specific issues that are particularly fixed or flexible can assist with developing the test plan, and save needless iterations. For example, where there is an existing model the scale of the tests will be fixed and other parameters need to fit around that.

Conversely, some parameters may be particularly flexible and can easily be adjusted to optimise the tests. One recent example of this at FloWave was a client testing a floating device in combined waves and currents. The original test plan called for conditions that were close to the wave blocking point, and so were not reproduced well in the tank. It transpired the specific wave frequencies were not that critical, and could be adjusted as required to obtain more useful test results. Early knowledge of this flexibility could have saved a day or two of pre-test engineering, and improved another aspect of the tests.

To capture this, the test planning tool checklist contains a field to highlight any specific parameters that are either fixed or flexible. It is noted that most test parameters can be changed to some degree, so these are relative terms. The prompt of querying flexibility may highlight those parameters of lower importance that can be changed to obtain better results without (too much) sacrifice.

8.1.2 Terminology and key to symbols

In order to clarify the flowcharts and documentation, the following terminology has been adopted:

Client Individual or organisation wishing to test at FloWave. Commonly this will be a device developer or an academic project.

FloWave Refers to both the tank and staff running the facility.

Model What is being tested in the tank, usually a small scale version of a larger device or prototype, but not exclusively. Note that some academic and internal tests may not include a model, instead focusing on wave and/or current phenomena.

Device The full scale technology being developed by the client. This may be generic for an academic project or very detailed for an advanced commercial client. Some tests may be focussed only on the performance of a specific device component.

Mooring Means of securing device to the seabed, including cabling for communication and power export as appropriate. For fixed devices, this may be some type of piled or gravity foundation.

Test plan All details of the proposed tests including set-up that needs to be developed prior to testing, so the tests are successful.

Test campaign An overarching term that includes all stages of the tests, including planning, execution, and analysis. This may be split over several visits FloWave if appropriate.

A key to the symbols used in the planning tool flowchart diagrams is given in fig. 8.2. Some key links between processes are highlighted on the charts. Many more cross-linkages between the issues are however not shown for clarity.

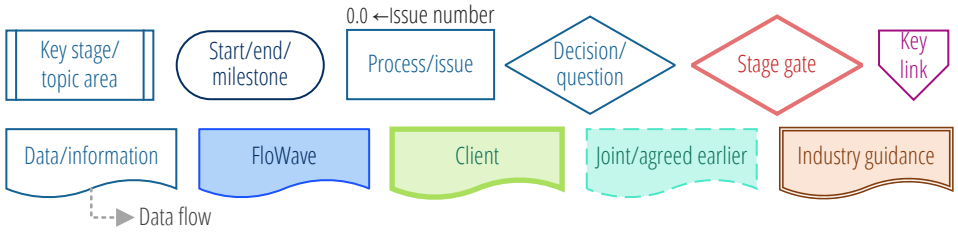

Figure 8.2: Key to flowchart symbols used in this chapter.

8.2 Test planning tool

8.2.1 Staged development and agreement

For clients interested in testing at FloWave, there are a number of discussion stages prior to testing. Between these are stage gates where the process could be stopped if there are unresolvable issues, as shown in fig. 8.3. This dialogue will usually start with high level discussions regarding test aspirations and tank capability. Following a period of discussion regarding scope and technicalities of both tests and contracts, the test contract can be produced. Once this is agreed, detailed planning of specifics related to the test programme can continue prior to the test plan start. In reality, these stages may have some degree of overlap.

Each of these stages will consider a broadly similar range of aspects, although obviously in increasing detail. It is not possible to highlight the aspects that will be most significant at the early stages, as these will be specific to that particular test. Something such as wave shape may be critical to a Wave Energy Convertor (WEC) developer, but not of any interest to another client testing a tidal turbine in currents only.

After determining whether FloWave will be suitable to conduct the proposed tests, there will be a period of discussion regarding the test scope. This can be a high level pass over the planning tool, with the client providing details, flagging the status and importance of each issue, plus highlighting the flexibility of parameters. This will give a rough scope of the test plan and will highlight areas that need further investigation. Having a draft test plan at this early stage can facilitate discussions, even if it is completely revised during the remainder of the planning process.

Contract negotiations can be conducted in parallel with this first pass. Once the contract is agreed, the detailed pre-test engineering can commence, which will be a more detailed pass through the test design procedure to confirm and finalise outstanding issues.

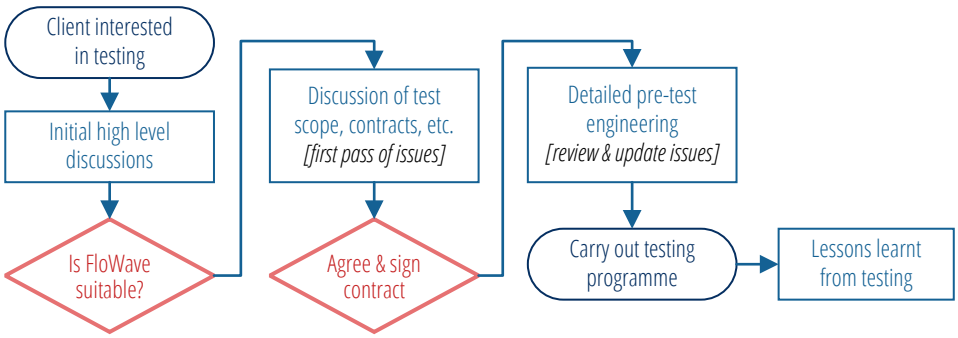

Figure 8.3: Flowchart showing the high-level process prior to testing.

8.2.2 Overall framework

As with any complex process, many of the test design choices will impact on other areas, and thus an iterative process is required, converging on a refined test plan. This planning tool has been split in to six aspects.

A1. Identification of research question and constraints.
A2. Specification of environmental conditions for testing.
A3. Tank capability and performance to generate scaled environmental conditions.
A4. Issues relating to the model, instrumentation, and data acquisition.
A5. Budget and timings for both individual tests and overall test plan.
A6. Other issues not covered above.

A 'first pass' route is suggested in this linearised order, as shown in fig. 8.4, with sections 8.A1 to 8.A6 detailing each of the six aspects. In practice however, it is unlikely that this sequential path will be followed rigidly, and issues may be considered in parallel. Reviewing one issue may flag up something that should be considered elsewhere in the framework. Additionally, some issues will not be applicable for all types of devices or tests, in which case they can be skipped after reviewing they are not applicable.

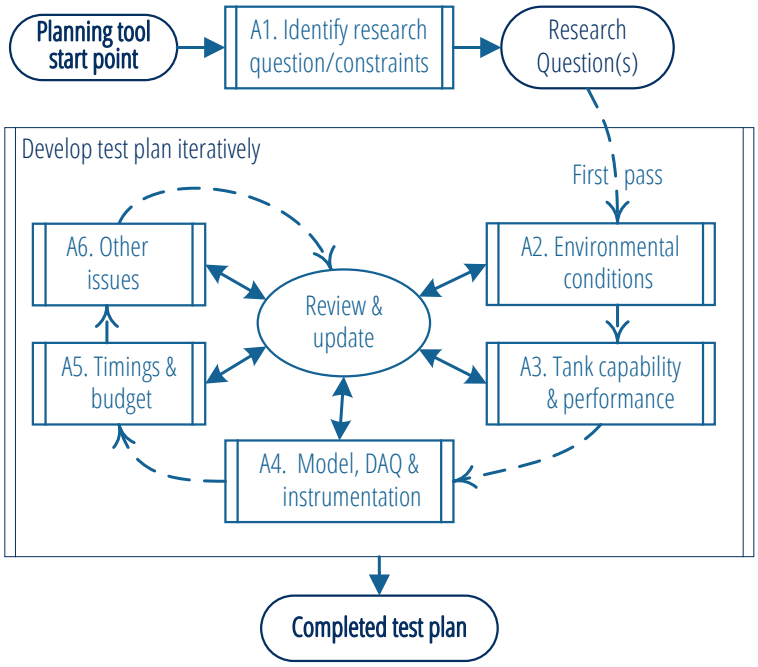

Figure 8.4: Flowchart showing planning tool overall framework with six aspects to be considered.

8.2.3 Flowcharts and issues checklist questionnaire

The test planning tool includes a series of flowcharts to visually represent the linkages between the many issues to be considered when tank testing, these are incorporated in to the relevant sections of this chapter. A checklist questionnaire has also been developed, to elaborate on the flowcharts and provide a record of discussions, decisions, and outstanding actions. The top section of this is shown in fig. 8.5 with the complete checklist of issues in Appendix A, along with all flowcharts grouped together.

When completing the checklist, each of the issues/questions should be reviewed, although not all will be applicable for every test.

- Some issues have multiple-choice select answer boxes, e.g. type of environmental conditions: waves; current; combined. Depending on the answers chosen, certain later issues are faded out if they are no longer relevant. This can be overruled by changing the later issue status as appropriate.
- Green shaded boxes in the client comments column denote answers that should be completed in all instances, however comments can be added to all issues.
- The importance and flexibility columns permit issues where this is particularly high or low (relative to other issues) to be flagged, as discussed in section 8.1.1.

1. Consider each of the Issues/questions below. Complete "Select" and "Client comments" columns, green shaded boxes denote required answers, but can add comments to all.
2. Select importance, flexibility, review status, and actions as appropriate.
3. Review with FloWave, particularly any flagged issues, unknowns, and high priority issues still to be completed.

Nr.	Issue/question	Select Answer:	Client Comments
1.	**Identify research question and constraints**		
1.1.	*What is the client looking to learn from these tests?*		
1.1.1.	**Provide details** of the type(s) of test envisaged e.g.: concept validation and basic performance testing; validating and refining numerical models; estimation of the full scale device performance; comparison of the model with full scale observations; etc.		
1.1.2.	Also **provide details** of the type(s) of conditions of interest, such as: energy production,device deployment, survivability, assessing fatigue limits, etc.		
1.1.3.	Has a successful outcome from the tests been defined yet **(Y/N?)**	No	
1.1.3.1.	*If so* ***provide details***		
1.1.3.2.	If not this should be considered		
1.1.4.	How well defined are the objectives of the test at this stage? **Rate as Loosely->Well defined**	Somewhat defined	

TOTALS:					Actions		
4 High	2 Fixed	0 Yes, To Do			3 Client	Today:	20-Jul-17
1 Medium	0 Medium	0 In Progress			2 FloWave	plus	14 days
2 Low	*1 Flexible*	0 Complete			0 Other	Soon:	3-Aug-17
Note that these are relative		1 N/A			7 with date	***Overdue:***	***2***
		0 Unknown	3			**Due soon:**	**3**
Importance for test	**Flexibility in parameter**	**Review Status**	**Flagged issues**	**Review Comments**	**Action for**	**Staff Initials**	**Due by Date**

Figure 8.5: Screenshots showing first part of test planning tool checklist. (top) columns 1–4 with issues and required client input boxes in green. For full checklist see Appendix A.
(bottom) status columns to right of issues, with summary totals at top for each status.

- The status of each issue can be set as one of five values: Yes this issue applies but still to be done; In progress; Complete; Not applicable; or Unknown.
- Some combinations of issues are flagged in the tool, such as having an existing model but not setting the scale as a fixed parameter, or if there are conflicting answers to some questions.
- There are also fields to note additional comments following review, and to record actions for the client/FloWave/other with initials and due date. Issues with a date that is either overdue or due soon are highlighted in orange, the latter date being a user configurable number of day in the future.

There are many possible scenarios to consider when planning tests. The visual layout of the flowcharts does not therefore follow exactly the same order as the checklist, but equivalent hierarchical issue numbers are used in both, linking them together. The issue numbers are noted in the following text with figure reference and issue number (e.g. 0.0) in the margin where appropriate, as shown here.

fig. 8.2
0.0

8.A1 Aspect 1: Research questions and key constraints

The first part of the process is to identify the research questions that the tests are aiming to answer, as shown in fig. 8.A1. If the purpose of the tests is not clear, it will be difficult to plan and conduct them effectively. Key constraints should also be identified at this stage as these can have a major influence on the test plan.

The research questions prompting testing are likely to be quite different for academic versus commercial clients. Projects with an more academic nature are more likely to focus on generic devices or the underlying physical phenomena, such as wave-current-turbulent interactions. Conversely, commercial developers generally consider their specific device or a particular aspect thereof.

It is important for FloWave to understand what the client is looking to learn from the test campaign. There are a number of common campaign types undertaken at facilities such as FloWave. These include:

fig. 8.A1
1.1

- Concept validation and basic performance testing,
- Validation and refinement of numerical models,
- Estimation of the full scale device performance, and
- Comparison of the model with full scale observations.

In conjunction, there are multiple different types of conditions that may be of interest, including: energy production, device deployment, survivability, and fatigue limit assessment. Understanding the testing requirements and operation of the device will help with designing the tests to make the best use of the tank capabilities.

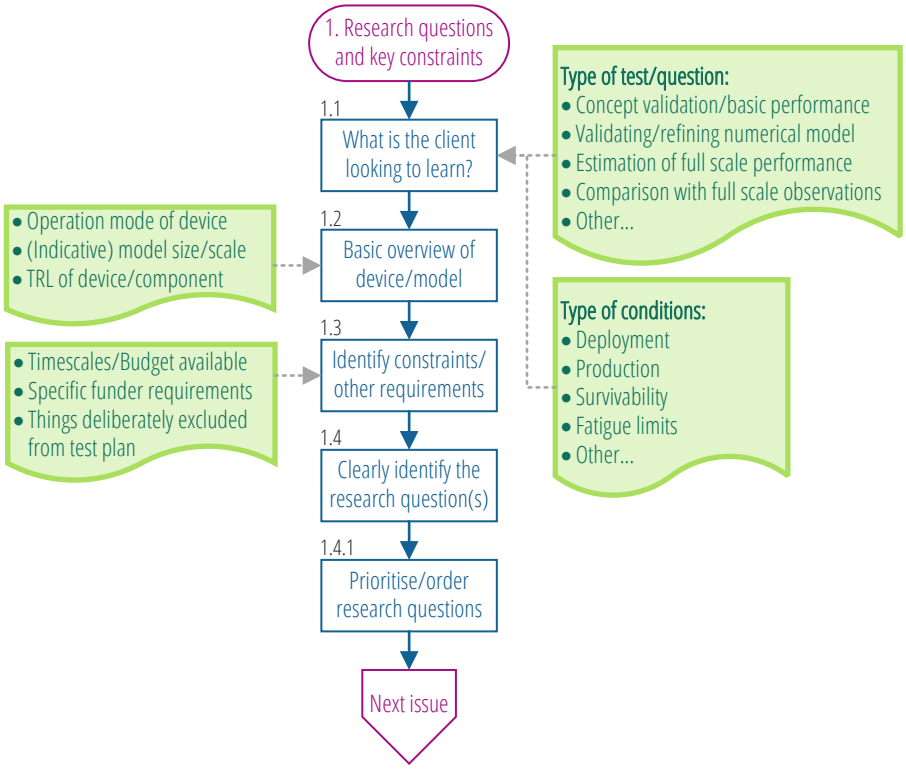

Figure 8.A1: Aspect 1 flowchart, identifying the research question and key constraints.

1.1.3 It is worth defining what the successful outcome from the test programme is, and how this can be measured. Also, for some campaigns the objectives may be well-defined early in the planning stage, but for others they may only be loosely defined when the client first approaches FloWave. This should be recorded on the checklist, and can be updated as the planning progresses.

1.2 For tests of a device or model, the client should provide an overview of the device to be tested and model if it exists, including size and (indicative) scale for testing. This overview should cover the proposed mooring solution, and device operational mode(s), such as how it captures power.

As discussed in sections 3.4.2 and 3.4.3, the type of testing is likely to depend upon the development stage, or TRL, of the device/component being tested. As developers may not like to think of their device concept being not well developed (at an early TRL) this is also phrased in terms of 'stage 1' and 'stage 2' testing, which may be less controversial and is consistent with other guidance (section 3.4.3). Understanding the device development level will assist with selection of other parameters, such as the environmental conditions, and is used by the tool to flag particular issues.

1.3 Key constraints, including budgetary and timescale, should be identified and outlined by the client. Timescales may be dictated to meet funding sources and/or lead times for

model build. There may also be specific requirements imposed by a funding agency. An example of this was the standardised sea conditions to be tested for the Wave Energy Scotland 'Novel Wave Energy Converter' project call (WES, 2015). To simplify testing, the client may deliberately wish to exclude certain elements from the test plan, e.g. wave loading on turbine blades, or current loading on moorings. This might just be for this stage of testing, and assessed in later tests.

Once all of these areas have been considered, it should be possible to state the research questions clearly. Being clear of the drivers will help everyone involved in planning the tests. Where there are multiple research questions, some sort of priority should be given to them, to help focus the test planing. 1.4

8.A2 Aspect 2: Environmental conditions

While considering the environmental conditions, fig. 8.A2, the tank generation capability envelope for waves and currents should be included as appropriate (section 4.2.5). The real conditions that can be simulated in the tank obviously depend on the model scale, so it is useful to have an indication of this early on. Additional checks on scaling the environmental condition, tank performance, and calibration of conditions are discussed in section 8.A3.

For devices at an early concept stage of development specific deployment sites may not have been identified. The environmental conditions should therefore be based on a range of typical or generic parameters. For devices at a more advanced stage, it is likely that either deployment site(s), representative conditions, or both will have been identified. If this is not the case, then the client should consider whether this needs to be undertaken prior to planning tank testing, so that the results are representative. It is standard practice to test with simple conditions in addition to more advanced conditions, to facilitate understanding of the device performance. For these, the parametric environmental conditions should be selected based on the identified deployment site where possible. fig. 8.A2 2.1 2.1.1

Where a deployment site has been identified, clients at a more advanced development stage may wish to make use of the complex realistic site conditions that can be generated at FloWave (sections 4.2 and 6.5.5). As shown in fig. 8.A2b, whether to use site-specific environmental conditions or not will often be related to the availability of data. The additional time and effort to simulate and analyse these conditions will also be major consideration. 2.3 fig. 8.A2b 2.3.2 2.3.1

In both cases, parametric and site-specific, the decision trees (figs. 8.A2 and 8.A2b) prompt about the influence of combined wave-current conditions, making use of the

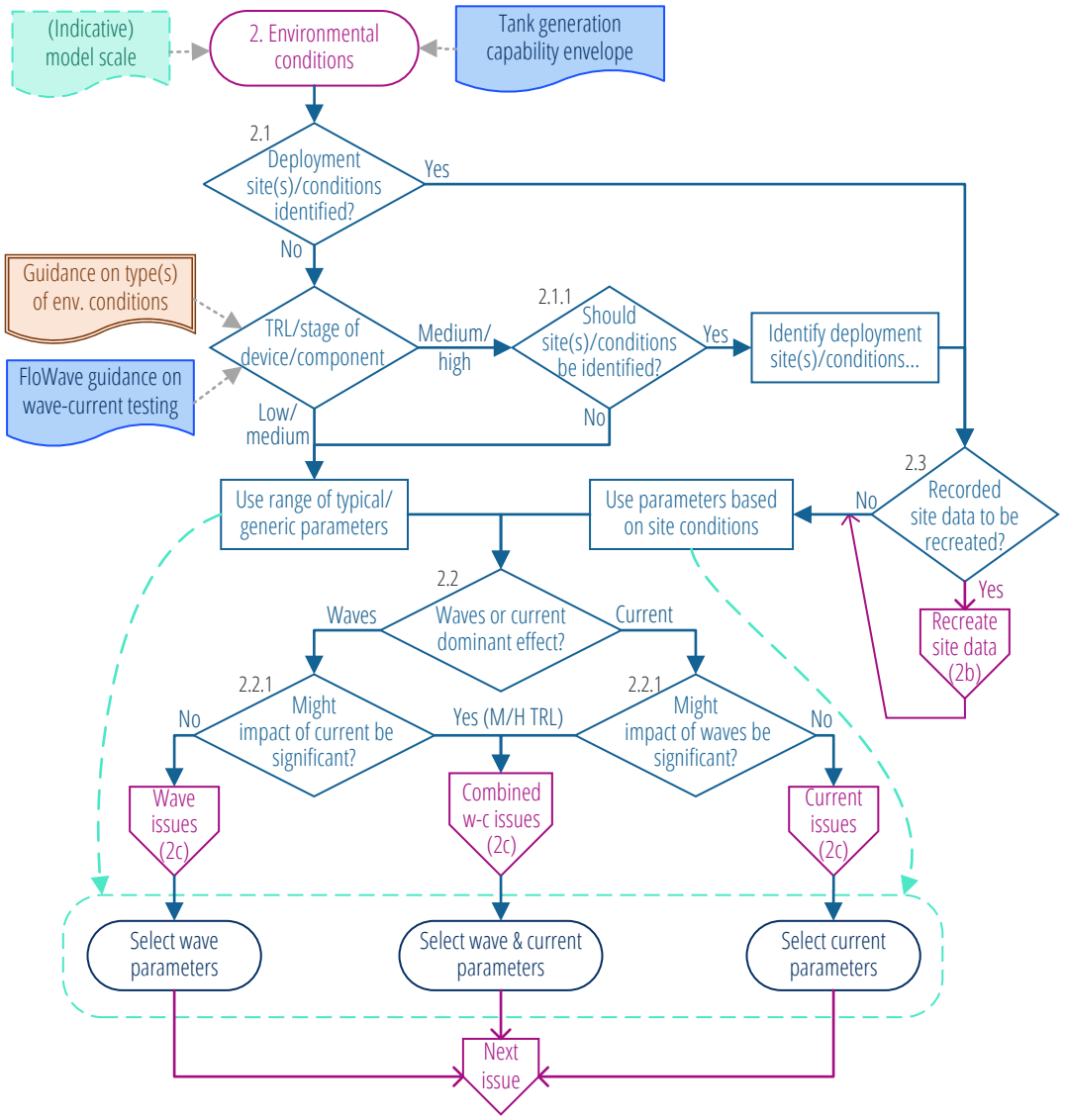

Figure 8.A2: Aspect 2 flowchart, considerations for environmental conditions and parametric specification.

capabilities at FloWave. As discussed in section 7.4, the influence of combined wave-current conditions could be significant. When reproducing site-specific conditions if suitable data are not available, then current velocities or wave parameters may need to be modelled or otherwise estimated.

To facilitate generation of the tank scale wave conditions these should be specified using the 'FloWave Sea Generation' Excel worksheet. Regular waves are specified by height and period, parametric spectra by type (PM, JONSWAP, etc.) and H_s, T_p, γ. Particular care is required with the specification of period, as there are several similar definitions, e.g. $T_p, T_E, T_z, \bar{T}$. Wave direction(s) need to be defined for long-crested waves, or the mean

direction(s) and spreading function(s) for short-crested waves. If other wave conditions such as focused wave groups are to be used these should be documented separately.

Currents are easier to specify in the tank, as the only controllable parameters are velocity magnitude and direction. Again clarity is required in specification of velocity, whether this is depth averaged value, surface current, or for specified point in the water column, and whether this is with or without a model installed. Additional parameters such as depth profile, turbulence intensity, etc. cannot be controlled in the tank at present, but it may be possible to select the best matching point in the tank based on spatial characterisation and quality metrics (sections 5.3 and 7.3).

8.A2.b Specifying site-specific environmental conditions

Where site-specific environmental conditions are to be used in testing, four main pathways are identified to recreate these in the FloWave tank, as given below and in fig. 8.A2b.

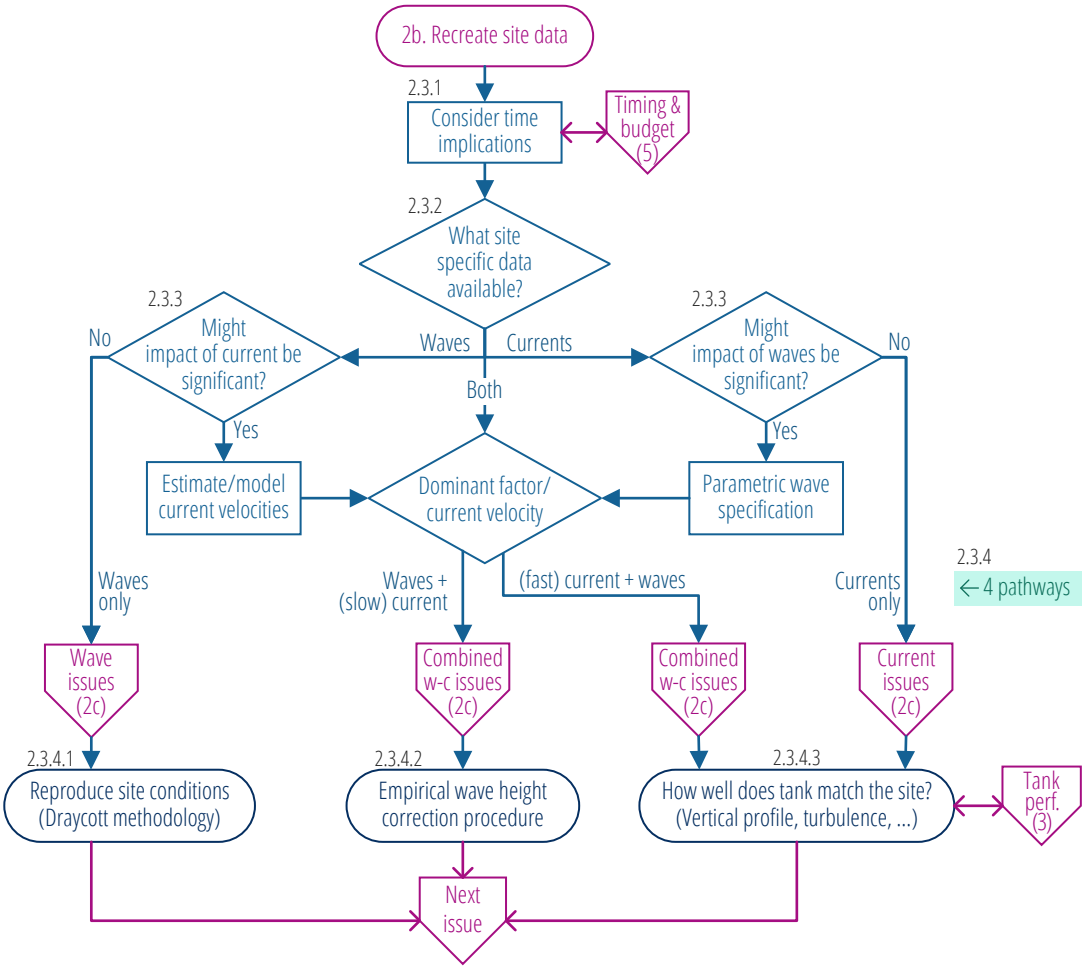

Figure 8.A2b: Aspect 2b flowchart, reproducing site specific environmental conditions.

2.3.4.1 1. Wave data available and currents are not significant. In this instance, the methods developed by e.g. Draycott (2017) can be used to simplify the data into a suitable test-plan.

2.3.4.2 2. Wave data available and there are relatively low current velocities ($\lesssim$0.2 m/s in the tank, $\lesssim$1 m/s at full scale) e.g. a WEC deployment site. The combined conditions should be reproduced in the tank, using the iterative correction method developed at FloWave (section 6.5).

2.3.4.3 3&4. For relatively fast currents in combination with waves, or for currents where wave loading is not an issue, the process is the same at present. There is less control over current and turbulence produced in the tank than there is for waves. It is therefore a case of considering how well the desired conditions can be generated in the tank, and how well these represent the full scale site data. This may change in the future, with the potential to adjust the flow profile and/or turbulence in the tank to simulate a tidal channel.

8.A2.c Further issues to be considered on environmental conditions

Once the types of conditions have been identified, there are a number of issues to check, shown by the grid in fig. 8.A2c. These are grouped into three rows, with four columns of issues dependent on the type of conditions used (all tests, waves only, current only, and combined wave-current where all the issues need to be considered).

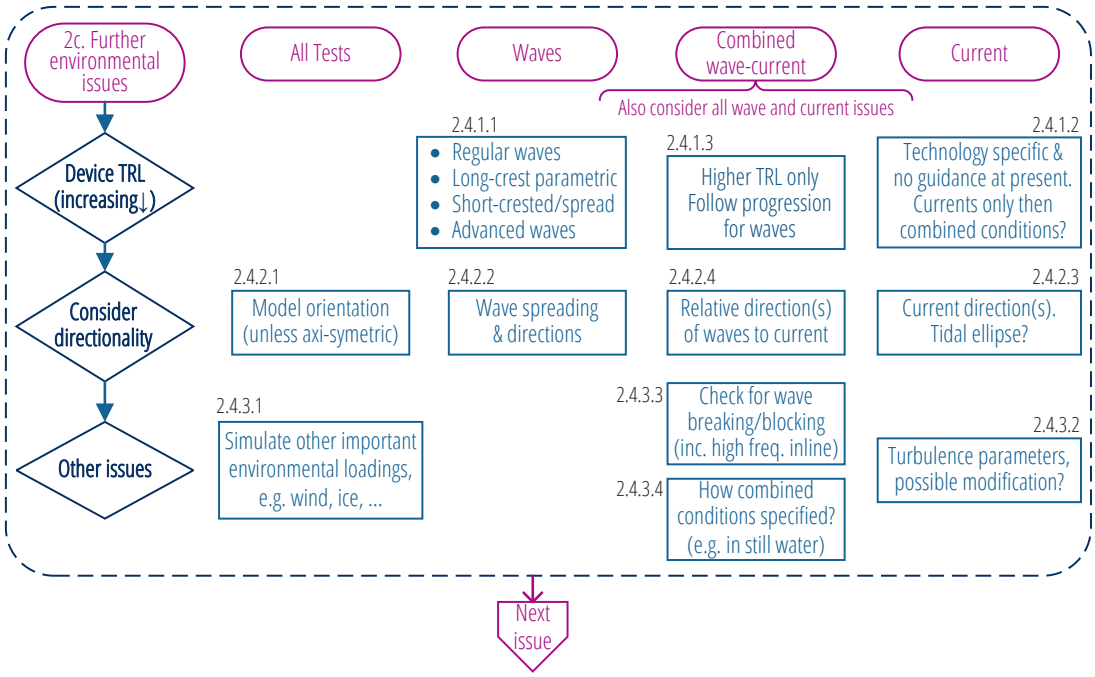

Figure 8.A2c: Aspect 2c flowchart, grid of issues to be considered when testing with waves, currents, or combined conditions.

1. Firstly, the development level is important for all tests, as discussed earlier. More complex conditions are normally used for devices further through the development process.
    - For testing with waves only, the progression is relatively clear and well established, as outlined in various guidance documents (section 3.4.3). This can be broadly summarised as: regular waves, long-crested parametric spectra, short-crested parametric spectra, and finally complex recorded spectra. fig. 8.A2c 2.4.1.1
    - For devices in tidal currents, there is not such a clear progression, and this is likely to be technology specific. Initial tests may consider flow alone, before adding the complexity of combined wave-current conditions, with waves following a similar progression to that above. It may be that different facilities are used at each stage, e.g. towing tank with no turbulence, flume, flume with collinear waves, wave-current basin with multi-directional waves. 2.4.1.2
    - Combined wave-current conditions are likely only to be used for higher TRL devices, as they lead to complex conditions and analysis. All issues above for wave or current only should also be considered. 2.4.1.3
2. Next the issue of directionality should be addressed.
    - The model orientation with respect to the waves and/or currents needs to be considered for all tests, unless the device (including moorings) is not directionally sensitive (Holmes and Nielsen, 2010). Although FloWave is rotationally symmetrical, with the ability to generate waves and current from any direction, it is important to consider the incident direction relative to the model. 2.4.2.1
    - Where short crested waves are planned, the spreading function(s) should be determined. 2.4.2.2
    - Consider and note if oblique currents or multiple directions required, e.g. to simulate loading at different times in a tidal ellipse. 2.4.2.3
3. Finally, there are a few other issues that may need to be considered.
    - There may be additional environmental conditions, such as wind loading, that are sufficiently important to consider simulating their effect during the model testing. This would need to be discussed with FloWave, and is likely to add significant complexity. 2.4.3.1
    - Turbulence parameters and flow profile(s) for the deployment site should be summarised by the client where known, and this should be discussed with FloWave. Although it is not possible at the present time to change these at FloWave, it may be possible to select a location in the tank to best match the scaled site flows, while accounting for any impact the model has on flow in the tank (see section 8.A3 issue 3.3). 2.4.3.2
    - For combined wave-current conditions there are a number of additional issues to be considered. Firstly, the relative direction(s) of the waves to the current, 2.4.2.4

2.4.3.3 and how these relate to the model orientation. It is also important to check for wave breaking and blocking (section 6.1) as some waves cannot physically exist when propagating against a current. It is also necessary to check high frequency waves following the current, as these may break on the recirculating flow in front of the wavemaker paddles at FloWave.

2.4.3.4 • Wave-current conditions can be specified in two different ways. As a combined field, i.e. waves of a certain height and period propagating over a fixed current velocity. Alternatively, the wave properties can be specified in still water, before they interact with a defined current. The latter is how waves are generated in the FloWave facility (section 4.2) and may have implications of the range of conditions that can be tested (section 6.2.1).

8.A3 Aspect 3: Tank capability and performance

The capability of every test facility to generate scaled environmental conditions will have limits, both physically and in terms of quality. It is important to check first that the required conditions can be generated, but also that they are of sufficiently high quality for useful testing. Figure 8.A3 shows this process.

fig. 8.A3 As discussed in section 2.2.2, environmental conditions are usually Froude scaled. The
3.1 first step is therefore to calculate a representative envelope of the conditions at tank
3.2 scale. This should initially cover upper and lower bounds in terms of wave height, frequency, and current velocities as appropriate. A more detailed review will be required at a later point, where the actual conditions to be used are scaled and checked. Any conditions close to tank limits (section 4.2.5) need to be reviewed with FloWave staff, as the limits are for guidance only, particularly for combined wave-current. If the scaled conditions are outside the physical limits that can be generated by the tank, it may be possible to adjust the scale to permit reproduction of the conditions.

3.3 Providing the required conditions can physically be generated in the tank, how well these are generated at the model deployment location should then be assessed. This is a subjective process, so quality metrics (section 7.3) have been developed to assist with this. Additional calibration measurements will be required to assess quality for a non-standard test or location in the tank. When testing a device in current, the installed model will likely change the flow in the tank. The impact of this must be considered, with adjustment to the flow speed and additional calibration as required. As more devices are tested in the tank over time, it will be possible to develop an understanding of their impact on the flow conditions in the tank. Using an alternative position in the tank may provide better quality reproduction of the environmental conditions,

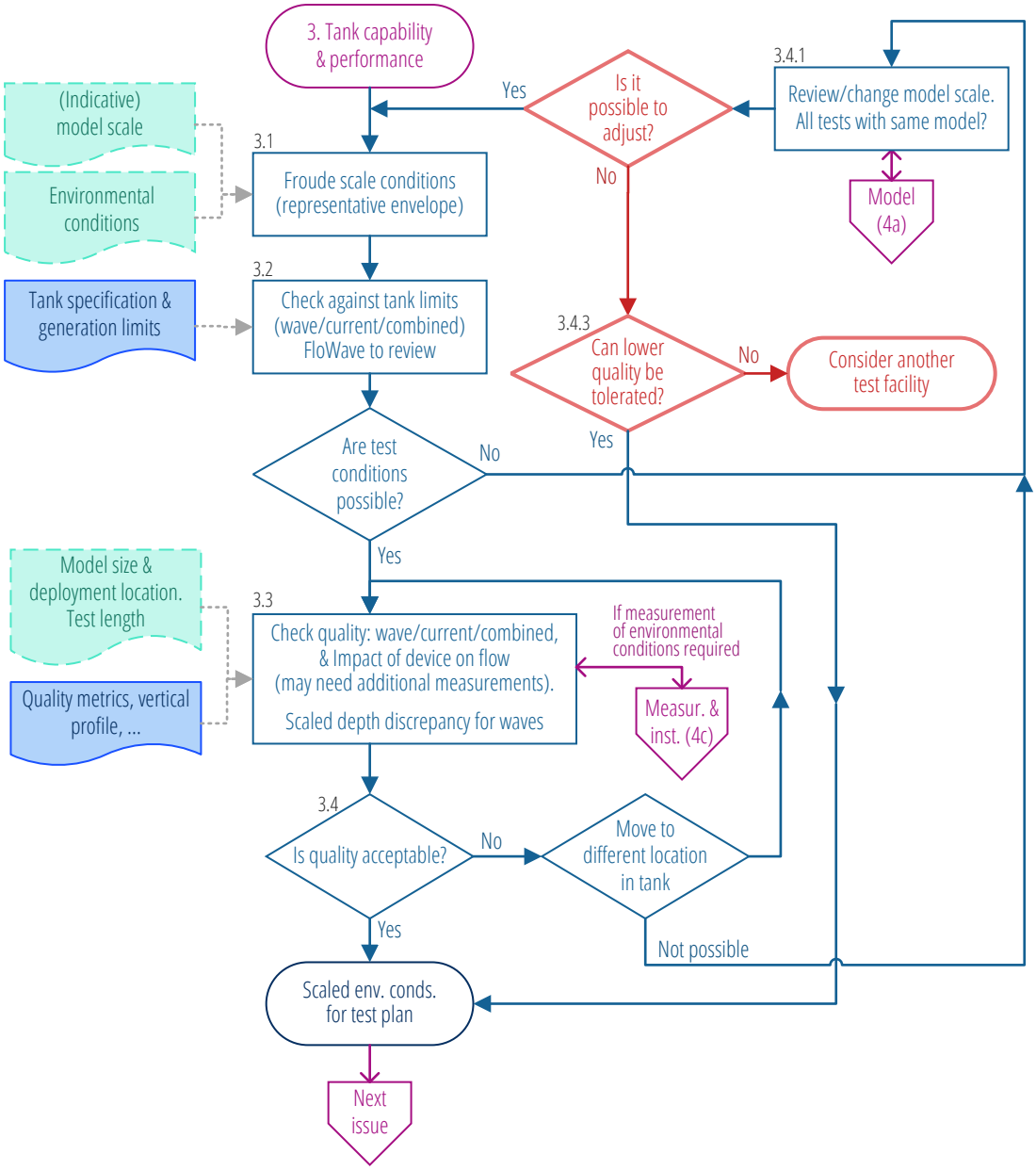

Figure 8.A3: Aspect 3 flowchart, tank capability and performance considerations.

with less influence of reflections for example, however there may be limitations on model placement due to mounting arrangements etc. Again, a different model scale may be considered if the quality is not deemed to be acceptable.

As part of the check on wave quality, wavelength errors resulting from a scale depth discrepancy (section 7.2) should be considered, especially where the device is sensitive to wave steepness. This may not be an issue for the particular device or environmental conditions of interest, and/or it may be possible to deal with any discrepancy in the analysis stage, but it is something that should be considered. 3.3

3.4.1 If it is not possible to generate the scaled environmental conditions, or the reproduction quality is not considered good enough in the tank, then the proposed model scale should be reviewed. It may be possible to adjust the model scale (smaller or larger) so that the required conditions can be recreated (at a higher quality). This may require the use of more than one model scale if there are large differences between the environmental conditions, e.g. using a smaller scale model to assess extreme survivability conditions (ITTC, 2014*a*). If the model scale is changed, then obviously all other constraints on model scale will need to be reviewed again. If it is not possible to rescale
3.4.3 such that the conditions can be generated at an acceptable quality, the use of a different test facility may be considered.

8.A4 Aspect 4: Model and instrumentation

As the majority of testing at FloWave for clients involves some form of model, the tools and guidance have been written on this basis. For those tests without, the corresponding sections can be ignored. Moving components have been grouped with the Power Take-Off (PTO) subsystem, as these have many similar issues.

8.A4.a Device model

fig. 8.A4a Consideration of issues relating to the device model, fig. 8.A4a, will depend on whether
4.2 there is an existing model available or not. For the latter, issues identified should be used in scoping and developing the model. If a model already exists, the suitability of this for the proposed tests shall be considered when developing the test plan, reviewing against these issues to check for potential problems. While an existing model might not be ideal in all respects, it may be considered 'good enough' given other constraints. If too many compromises are required, consideration should be given to developing a new model.

The starting point should then be the design (or concept) for the scaled device model, based on the (indicative) model scale and full scale device details, as shown in fig. 8.A4a. This will normally be Froude scaled, although other relationships may be required for some elements or situations.

4.3.1 Most models can be categorised as fixed or floating, which will impact on how they are mounted/anchored in the tank. For fixed devices, the mounting solution will normally involve the bolt points on the floor, or the 6-DOF load cell. Models may also be fixed to the tank sides, to the gantry, or some combination of these. Most floating devices will require mooring, and similar mounting constraints apply to the anchor points. Additional factors include the size and spread of the mooring, as well as the water depth. It also

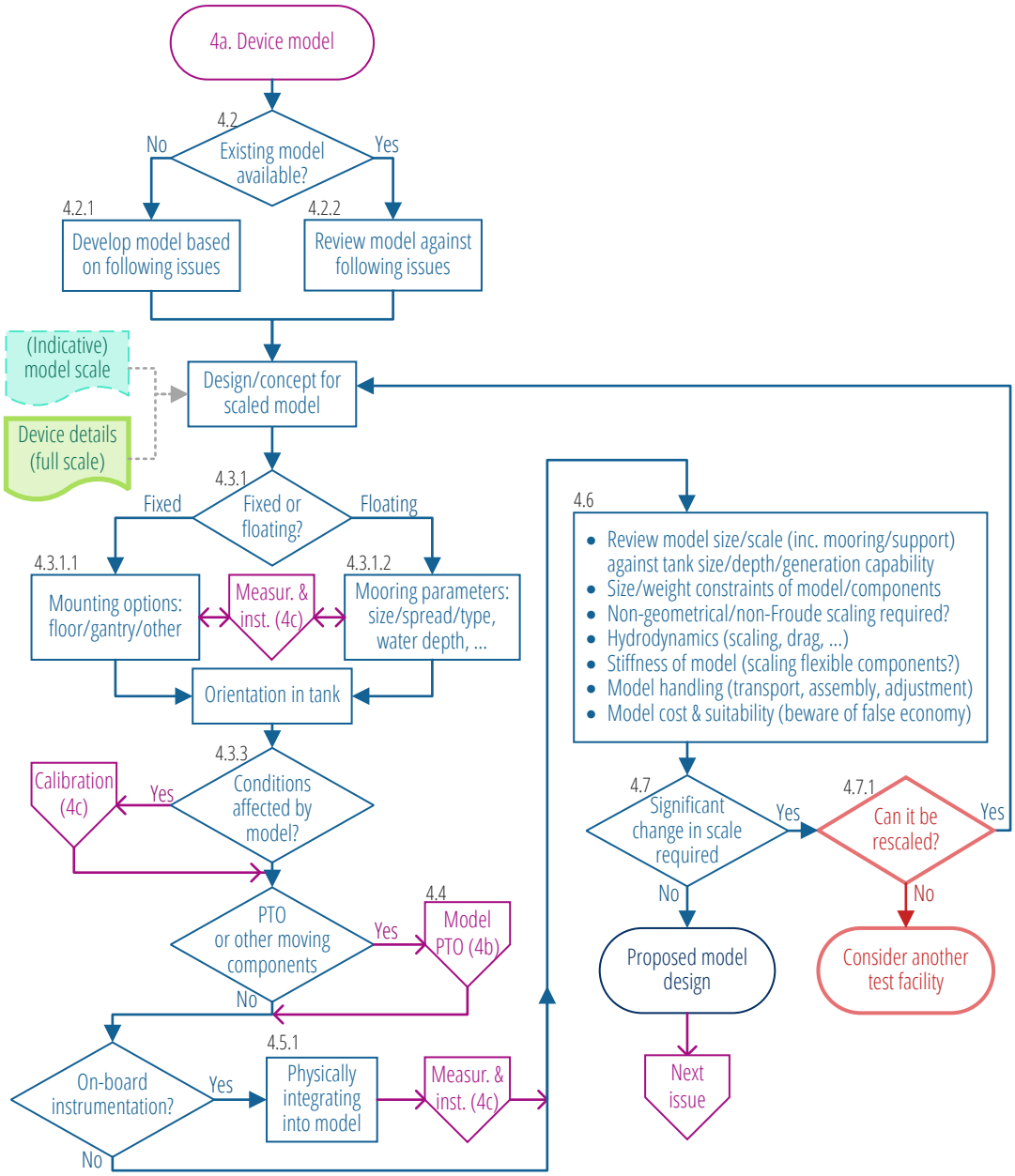

Figure 8.A4a: Aspect 4a flowchart, considerations for device model.

may not be possible and/or desirable to model the entire geometrically scaled mooring solution, requiring a scaled or partial mooring to be implemented.

The presence of a model in the tank will change the environmental contitions. This is particularly critical for larger Tidal Stream Turbines (TSTs) that may change the flow in the tank significantly. Where a specific inflow to the model is desired, additional calibration of flow in the tank with that device model installed will therefore be required. ITTC guidance (2017*c*) recommends calibrating wave conditions at the model location, i.e. without a model in the tank. 4.3.3

4.6 The following issues relating to the device model should also be addressed.

- The model size and scale needs to be appropriate for the tank, including any moorings and support structure. The fixed 2 m water depth plus wave and current generation limits may impact this, as discussed in sections 7.2 and 8.A2.
- There may be size and/or weight constraints imposed by the materials or components used to construct the model. These include for example, prefabricated sections like tubes used to construct the model, size of PTO motors or blades available, and providing sufficient space for on-board instrumentation. This may be less of an issue with bespoke manufacturing, but at a price.
- Some form of non-geometrical scaling may be required to overcome scaling law mismatches, or to reduce size of mooring footprint. This may be particularly relevant for turbine blades, where matching C_p vs. TSR in a similar Reynolds regime can be more important than scaling the geometrical shape.
- The model hydrodynamics needs to match that of prototype, however direct geometrical scaling of every component may result in increased drag, particularly for small details (ITTC, 2014*a*).
- The stiffness of flexible components can be difficult to scale accurately. Smaller models tend to be proportionately more rigid than the full-scale prototype (tables 2.4 and 2.5). This is often not a concern, unless flexure of the model is critical for the test, or impact loads to be tested/quantified.
- It is also important to think about model handling. The model may need to be disassembled for transportation and reassembled prior to testing with implications for both strength and for test plan timing, section 8.A5.b. Consideration should also be given as to how the model will be lifted into the tank, and how minor adjustments will be made to the model during testing, e.g. raising the tank floor, access by boat, or by lifting the model out of the water.
- The model needs to be fit for purpose. Cheap models can be a false economy. While the cost of repairing broken or leaking parts may not be that significant, the consequential delay might be expensive if it puts a stop to testing. This may also mean the test plan has to be reduced or the test programme extended. Low quality components may also increase uncertainty in the results, reducing the overall effectiveness of the testing. Sufficient budget should therefore be allowed to construct a suitably high quality model, as highlighted by Doherty (2015); Sutherland (2017).

The issues above may flag up that the model size or scale needs to be changed significantly. Assuming this is possible, the whole test design procedure will need to be reviewed with the revised model, to check for impacts on other parameters. If it is not possible to change the model size or scale for whatever reason an alternative test facility may need to be considered.

8.A4.b Model PTO and moving parts

Where the model has some form of Power Take-Off (PTO), the following issues should be considered, as shown in fig. 8.A4b. Many of these issues are also relevant for other moving parts of the model, so should also be considered in this respect.

fig. 8.A4b

How the PTO is represented in the scale model is important, and one of the main challenges with tank testing renewable energy converters (ITTC, 2011*b*). The method chosen will depend on the type of device, model size, and technology level. It is common to represent the PTO using an energy sink or idealised damper, which may be actively or passively controlled (Day et al., 2015). For early development stages, and small scale models, passive control is often used. Typically, this can be via perforated 'actuator disks' to represent tidal turbines, or an orifice plate to simulate an air turbine at small scale on a WEC. For these cases, consideration needs to be given as to how the power generation of the device will be estimated or quantified.

4.4.2

4.4.2.1

Larger models for later stages are more likely to use bladed turbines with a motor/generator to regulate torque, or similar. The active control system implementation will vary between devices, and may influence the test plan. Some developers may have developed advanced control systems as part of their device, in which case the Data Acquisition (DAQ) interface needs addressing. Consideration is again required as to how power generation will be quantified.

4.4.2.2

There are a range of different issues that should be considered for each type of PTO or other moving part, some of which are highlighted below.

- For electro-mechanical systems, friction losses from moving parts are significant in scale models, as friction does not scale linearly with size. The friction experienced by a model will therefore be disproportionately large, which could have a knock on impact on power measurements. Electrical losses are also critical. Power output is Froude scaled by a factor of $\lambda^{3.5}$ (section 2.2.2), which requires very low voltages or currents to be measured. Voltage drop should therefore be considered. Electrical safety is also paramount when working near or in water, particularly with mains voltages or powerful capacitors/batteries.

4.4.5

- If pneumatic systems are used, issues arise regarding scaling of air stiffness (Weber, 2007). To overcome this, it may be necessary to include an oversized pressure vessel, which may have a negative impact on floating device motions, although is less of a concern for fixed devices.

4.4.6

- For situations where the hydrodynamics are critical, e.g. tidal turbines, the mismatch between the Froude and Reynolds scaling laws is important, and may require non-geometric scaling of turbine blades (e.g. Payne et al., 2017).

4.4.7

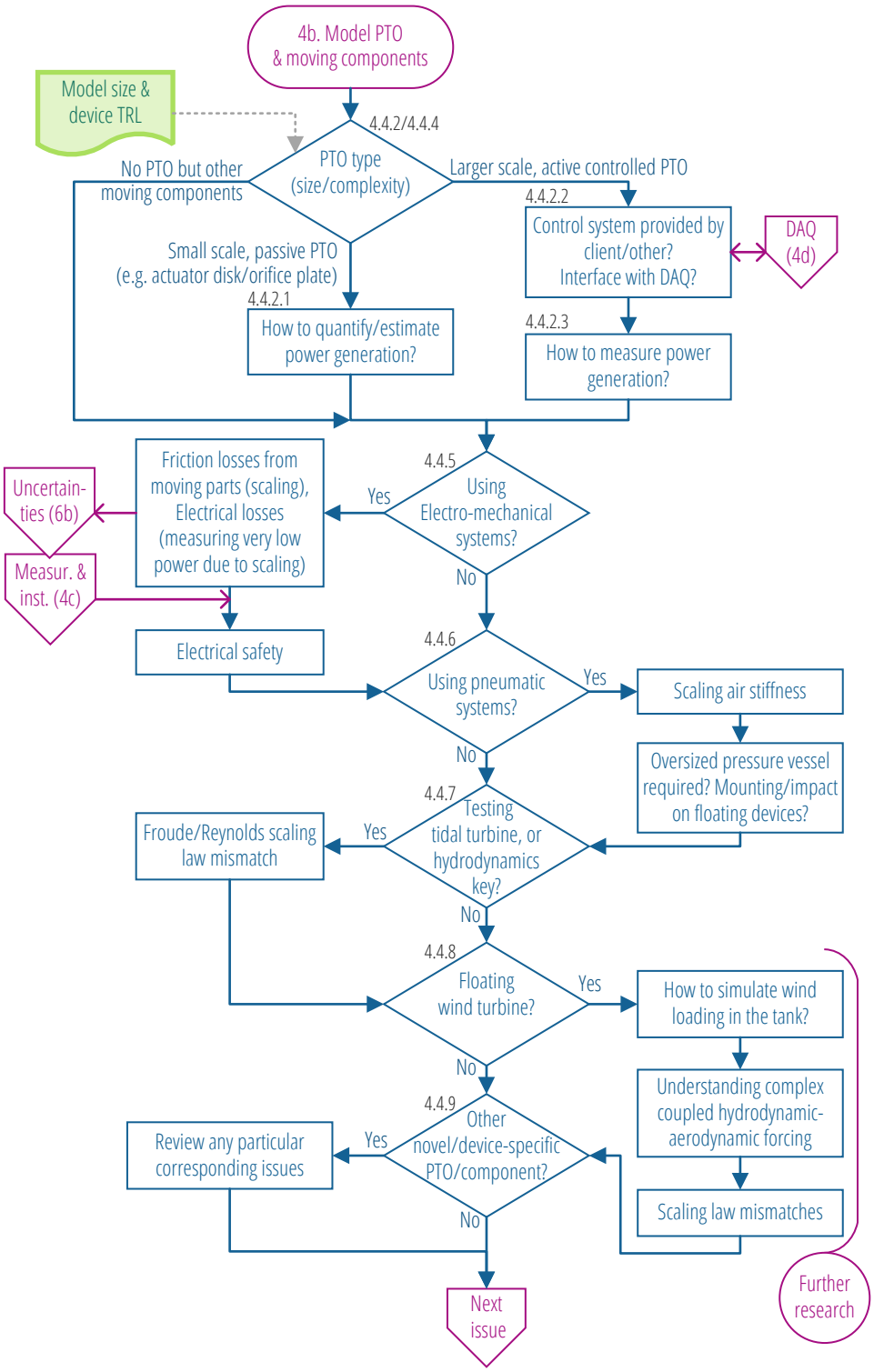

Figure 8.A4b: Aspect 4b flowchart, model PTO and moving part considerations.

- Floating wind turbines have another level of complexity, and how to test these at scale is ongoing research. Some key issues include how to simulate the wind loading in the tank, understanding the complex coupled hydrodynamic-aerodynamic forcing, and the scaling law mismatches. 4.4.8
- Other innovative or device-specific methods of PTO are likely to have particular issues relating to them. These should be addressed individually during test planning. 4.4.9

8.A4.c Instrumentation and measurements

What can and should be measured is driven by the research question(s), but also be the availability of instruments to make measurements and the capability thereof. Some considerations are shown in fig. 8.A4c. fig. 8.A4c 4.8.1

For most tests, the environmental conditions in the tank are measured, either during the test, and/or as a calibration in advance of the testing, see also section 8.A5 on timings. What is measured will largely depend on what is of interest to the client. To record waves or water surface elevation, the number of gauges, the wave gauge positions and array types should be considered. When setting the gauge locations it is important to consider what is (most) important for the test, e.g. waves radiated from the model, reflections in the tank, and/or directional waves. Measurement of current and turbulence is more limited by the instruments available. Only point measurements of flow are presently possible at FloWave, therefore repeat tests are required to understand spatial variability. 4.8.2

Models with on-board instrumentation can present particular challenges. Physically fitting the instruments inside the device, within a suitable waterproof enclosure if required, but without impacting the hydrodynamics can be challenging. Additional concerns include: weight distribution and influence of connecting cables on device motion for floating devices; and how to instrument rotating parts on tidal turbines. Bigger models make this easier, which is another advantage of working at a larger scale. fig. 8.A4a 4.5.1

The size and measurement range of the instruments required will depend on the expected range of values to be recorded, and it may not be possible to record all tests accurately with the same instrument, or even using the same model scale. It may also be the case that a client supplies additional instruments to measure particular variables of interest during the test, which will need to be linked in with the DAQ, see below. fig. 8.A4c 4.8.1.2

While some properties can be recorded remotely, such as device motion, many others will require direct measurement. Any intrusive measurements will affect the testing, and this needs to be considered. Two examples are the extra drag from load sensors 4.8.4

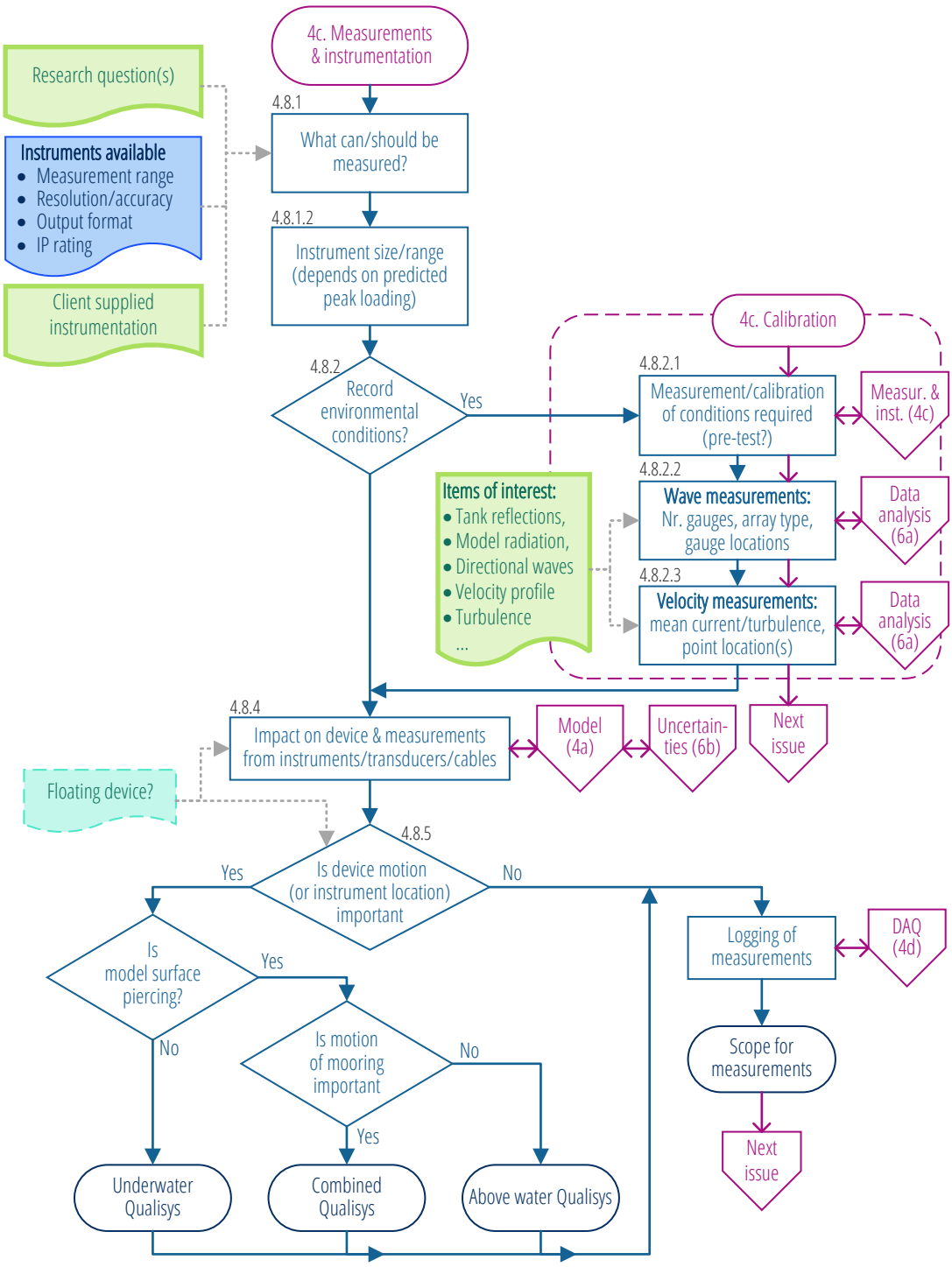

Figure 8.A4c: Aspect 4c flowchart, instrumentation and measurement considerations.

on mooring lines, or the impact of power/sensor cables connected to a floating device constraining motion in a way non representative of the full scale device.

Where device movements are important, such as a floating body, it is possible to track this using motion-tracking systems such as Qualisys. It is also possible to use this system to track accurate locations of measurement instruments, such as wave gauges, that are being moved during testing. The FloWave facility has both above and under-water camera systems, that can be combined if required. As the above water system is non-intrusive and easier to calibrate, it should preferentially be used where possible, such as on devices that are surface piercing. If motion of submerged components such as moorings is important, or the device is completely submerged, then underwater Qualisys cameras will be required. As well as being more complex to set-up and calibrate, the underwater camera housings are quite large and may have an adverse impact on flows. 4.8.5

8.A4.d Data acquisition

When planning the data acquisition, fig. 8.A4d, the first step is to list all required measurements. This includes data being logged by the client on their own DAQ system. There are a number of practical issues relating to recording data that should be addressed prior to commencing testing. These issues are well documented in existing guidance. fig. 8.A4d 4.9.1

- Appropriate sample frequency should be considered. Recording data at a higher sample frequency gives more points for analysis, albeit at the expense of larger data files and an increased potential for errors or bad data. It is also important to consider aliasing, between recorded signals, and with the 50 Hz power supply. 4.9.2
- Signal amplification and filtering may be required for some instruments, ideally as close to the sensor as possible. 4.9.3
- Synchronisation of the measurement system(s) with the wave and current generation so that these can later be analysed as one. At FloWave, this synchronisation is usually triggered by the tank clock (section 4.4.1). It may not be possible to trigger all types of system, and so relying on time-stamps may be required for synchronisation, although this can be subject to difficulties. 4.9.4
- Unique identifiers are required for each test. Standardised file naming conventions are used at FloWave to deal with multiple instruments and tests. These are recorded in a test log, detailing what was actually run and when. This log should link back to the test plan, including client test references if applicable. It should also record any issues that arose during the test. 4.9.5
- Video and photographs are routinely collected during the testing, often on personal cameras/mobile phones. A means of collating and correlating these back to the test log should be set-up. 4.9.6

4.9.8

- Agreement on test data provided to the client after testing is finished, possibly including interim results during the test programme. This should specify in what format(s) and what level of processing is required. Plans should be made for data storage and transfer, especially where large file sizes are anticipated.

In addition, how this all links to the client's proposed data analysis should be given some consideration during the planning stage, as discussed in section 8.A6.a

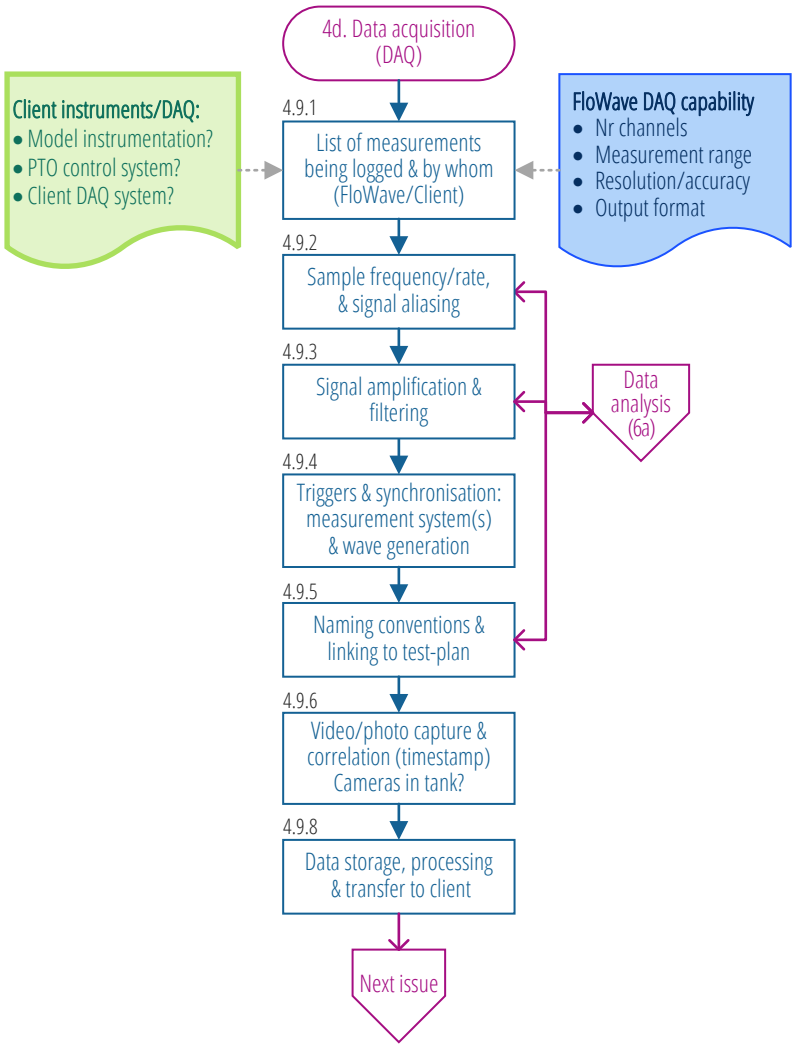

Figure 8.A4d: Aspect 4d flowchart, logging and data acquisition considerations.

8.A5 Aspect 5: Timings and budget

An initial idea of the timescales can be obtained 'bottom up' from the list of tests to be run and 'top down' from the budget available. At least initially, there is likely to be a mismatch between these two estimates, and further consideration will be required to resolve/correlate. When planning the test campaign, it is important to have a realistic understanding of how long the whole testing process will take and how much can be accomplished within the test programme. This includes proper experimental design and cognisance of timings, as shown in fig. 8.A5. fig. 8.A5 5.1

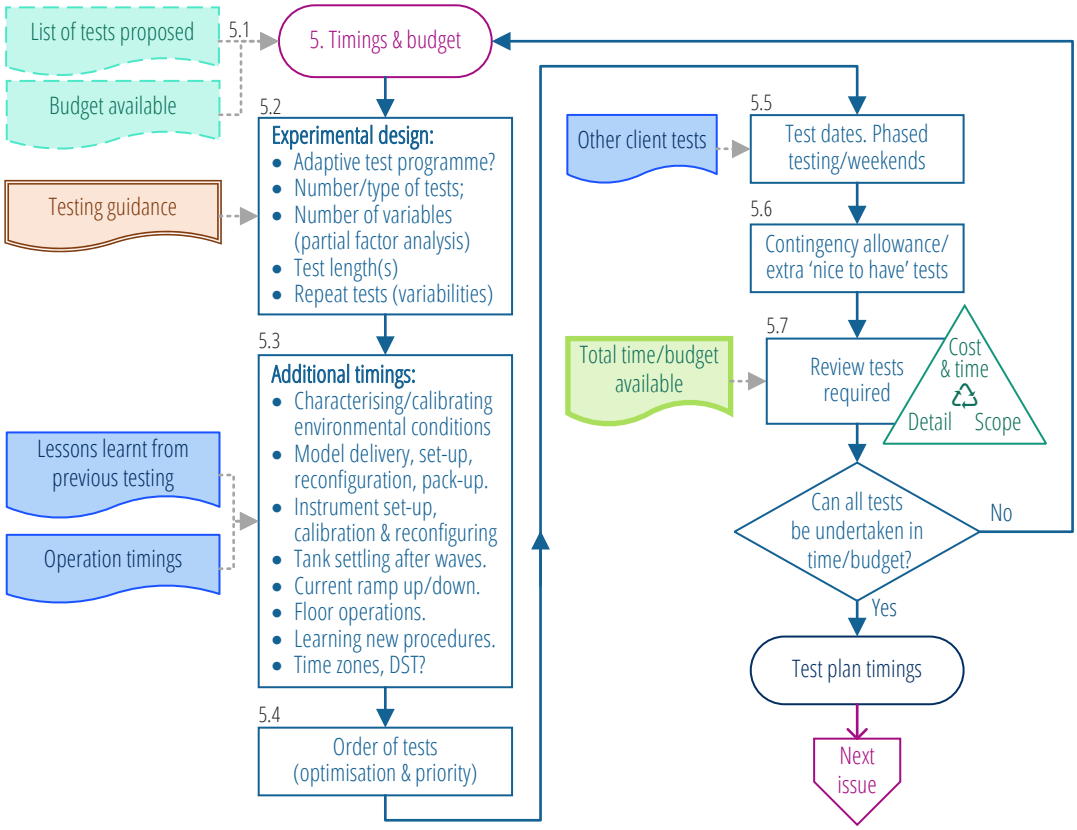

Figure 8.A5: Aspect 5 flowchart, considerations relating to timings and budget.

8.A5.a Experimental design

There is a wealth of guidance available on experimental design for tank testing, as discussed in section 3.4.1. 5.2

Some test campaigns may use an 'adaptive test programme', where results from initial tests are used to inform selection of the remaining test programme. An example of this might be testing three concepts, with more detailed tests on just the most favourable concept. This allows both a wide range of options to be considered, but also provide

specific detail on the areas of most interest. Prior agreement of what results and data analysis are required, and by when, is therefore required to permit this. Plans should also be made for the analysis, section 8.A6.a.

The number of tests required will be a function of the number of variables of interest. It may be advantageous to do a partial factor analysis, rather than running every combination of tests (Ingram et al., 2011).

The length of individual tests will depend on the type of conditions. For regular waves, a small number may be sufficient, requiring perhaps a 60 s test. Guidance for irregular sea states is usually to have 500–1000 waves to be statistically representative including extremes (McCombes et al., 2010*a*,*b*). Although as mentioned in section 2.1.3, the maximum wave height is statistically a function of the number of waves, so longer tests will tend to give more extreme conditions. If a frequency domain analysis is planned, it may be important that the sample rate and test length give frequency bins that match those of the wavemaker control, therefore test lengths are often set as a multiple of 2^n seconds. This may require extended tests, the time implications of which can mount up over many runs. It is also worth noting, particularly for short tests, that it can take around 30 s for the initial waves to reach the central test area at FloWave, and this should be included when setting the test length. The length of test to properly quantify a complex directional sea-state will typically need to be greater than for a uni-directional spectrum, given the number of wave components being measured. There may be a trade-off between the length of individual tests and the number of tests that can be completed in a given time.

Consideration should be given to conducting repeats of nominally identical tests. This can help with understanding the inherent variabilities in the tank, model, and experimental processes. Running these at different times of the day may flag issues with calibration drift for example. This research has demonstrated that the repeatability of combined wave-current conditions in the tank is lower than for waves alone (section 6.2.2), highlighting the need to characterise this when testing.

The test order should be considered at the detailed planning stage. Priority of each test outcome should be accounted for, so that the important tests can be completed early. As part of the test design, randomisation of the test order may be considered (Ingram et al., 2011). It may also be possible to optimise the programme by running the tests in a particular order to minimise the time spent on additional tasks, as discussed below.

8.A5.b Timings and dates

It can be easy to underestimate the time require for model set-up and calibration, and thus be over-optimistic about how much can be achieved within a test programme. Knowledge of previous tests are a useful benchmark when determining how long these processes will take. As a first estimate based on experience at FloWave, a 50% utilisation rate of good test data to overall test campaign length is reasonable, although this depends on test complexity, plus the length of individual tests and overall campaign. Additional time should be allowed for more complex models or novel devices, as well as when using additional measurement instruments. 5.3

When planning tests, time should be allowed for the following aspects that are sometimes omitted, or insufficient time allowed. A spreadsheet-based tool is used internally at FloWave to develop detailed test plan timings including all these additional tasks, but a simple allowance can be made at early planning stages.

- Characterising and/or calibrating environmental conditions for the tests without a model in the tank, as required. It may be possible to do this prior to the first day of testing, as part of pre-test engineering.
- Client familiarisation with FloWave, including safety briefings and induction (typically ½ to 1 hour)
- Time for model delivery, unpacking, and set-up, plus disassembly and pack-up at the end of test campaign. This is typically ½ to 1 day for set-up plus ¼ to ½ day for pack-up, but this very much depends on the model size and complexity.
- Instrument set-up and calibration, both at the start of test campaign and every morning (as required), which will depend on type/number of instruments.
- Sufficient time should be allowed for the tank to settle between wave tests, or for the current to reach a steady state (typically 2 minutes to 10 minutes).
- Time also needs to be included for tasks such as raising/lowering the floor (c. 10 minutes each), and model reconfiguration (timing depends on its complexity).
- When testing new set-ups/procedures, additional time should be allowed, as the staff/client will not be familiar with how best to do these, and some learning may be required.

Some clients may wish to split testing into more than one visit, for example to allow a period of analysis in between two sets of tests. This has to be weighed up against the increased set-up and set-down, which has both time and cost implications. Setting up subsequent tests may not take as long as the first time, as issues may have been resolved the first time, and the client will be more familiar with protocol and procedures at FloWave. It may also be possible to schedule testing across multiple weeks, giving time at weekend(s) for analysis. This does however put additional pressure on staff, which may not be acceptable. 5.5

Finally, a small point to be aware of is issues relating to time zone(s) including changes from daylight savings time. This was highlighted by a client following personal experience with previous testing.

8.A5.c Development and review of test plan

5.6 A contingency allowance should be included in case of problems with the testing or other unforeseen delays. Alternatively, lower priority tests could be dropped. It is also worthwhile having a list of additional 'nice to have' tests for when the testing all goes smoothly, or if some of the planned tests cannot be run for whatever reason. This will make best use of time in the facility, rather than being forced under time pressure to decide which tests are most important.

5.7 As the draft test plan is developed, it should be reviewed against the total time and budget available. It will usually be a trade-off between the cost and time, the amount of detail covered, and the overall scope of the tests. If all of the tests cannot be undertaken in the time available, they will need to be reviewed, excluding the lower priority tests or revisiting the order to optimise the test programme.

8.A6 Aspect 6: Other issues

fig. 8.A6 6.1 There are many other issues can affect test planning. Some key ones are given here, as shown in fig. 8.A6, which should be reviewed if not already done so. This list is not exhaustive however, and it is not possible to fully document every issue for every type of test that might be undertaken at FloWave.

8.A6.a Plans for analysis

6.2.1 6.2.2 Plans for the analysis should be, at least partially, developed while planning the testing in order to make the best use of the time available at the test tank. This includes a list of all quantities to be recorded and data requirements of the measurements made, such as sample frequency and record length.

6.2.3 If an adaptive test programme is being used, where subsequent tests depend on results from initial tests, code to analyse and compare the outcomes should ideally be ready to process the test results as soon as these are available. FloWave may be able to provide example test results to show data formats, so that this code can be checked beforehand. For all test campaigns, analysis of results during the tests may also flag up faults with sensors before too much time is lost (Doherty, 2015).

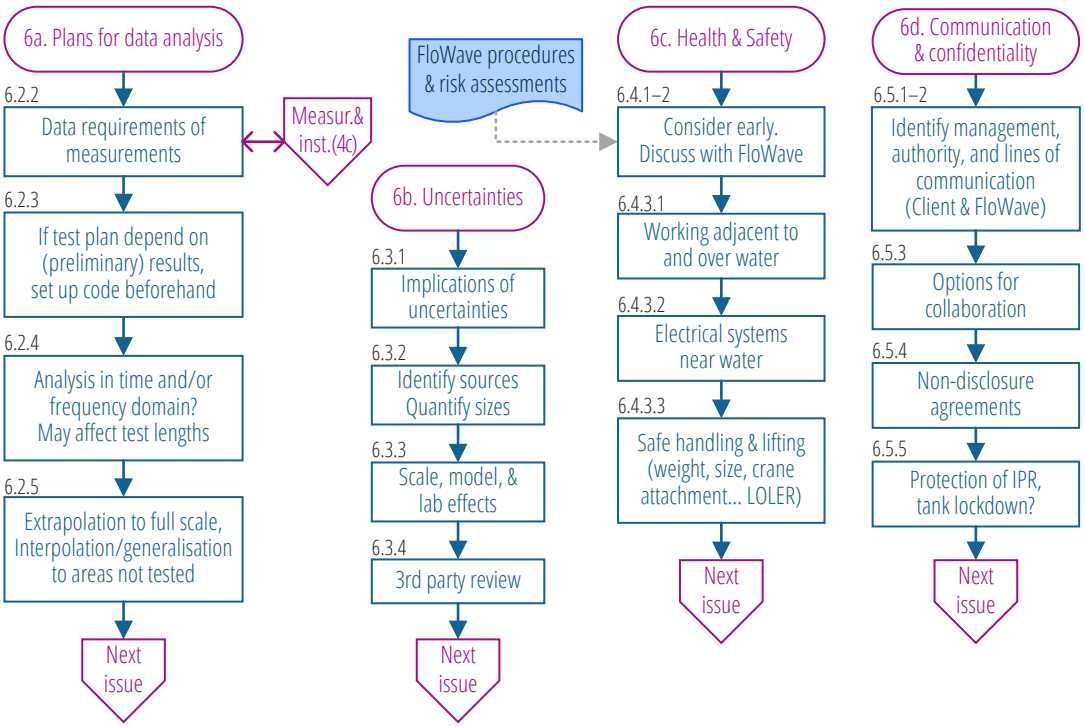

Figure 8.A6: Aspect 6 flowcharts, highlighting some other key considerations.

Consideration should be given to whether the analysis will be conducted in the time and/or frequency domain, as this may affect test lengths chosen, as discussed in section 8.A5.a. 6.2.4

Where the model represents a full-scale device, consideration should be given to how model results will be scaled-up. In addition, it may be worthwhile thinking about how the results can be interpolated to areas or cases not covered in the test plan, and whether sufficient data points will be collected to adequately describe the device behaviour. 6.2.5

8.A6.b Uncertainties

While uncertainties by their nature cannot be removed, they should at least be acknowledged. Physical model testing will also involve unwanted scale, model, and lab effects as noted in section 2.2. Getting a third party to review the test plan may help identify other potential sources of uncertainty (the ‘unknown unknowns’). 6.3

Considering possible implications of these uncertainties prior to testing may flag up specific areas for concern. Some of these may be ameliorated by amending the test programme or the experimental set-up in some way. Thinking about these issues early may reduce the cost associated with any changes to the test plan. 6.3.1

8.A6.c Health and safety

6.4.1 It is important to consider how to conduct the test programme safely early in the planning stages, because resolving issues at a later date may involve significant reworking and additional costs. FloWave procedures for how to operate tank and conduct tests, plus risk assessment for common tasks undertaken in the facility, will be used to inform the development of a new test plan. Three areas particularly of note are:

6.4.2

6.4.3.1 • Working adjacent to and over water in the lab is covered by FloWave risk assessments and procedures. The most dangerous situation is when currents are being generated, as the recirculation could potentially drag someone down towards the turning vanes mounted in the floor.

6.4.3.2 • Electrical systems require proper design and implementation, particularly where mains voltages or powerful capacitors/batteries are involved. This should be done in line with FloWave risk assessments, including suitable emergency stop and isolation protection.

6.4.3.3 • Safe handling and lifting of the model and instrument rigs needs to be addressed. Some models, or components, may be light and small enough to manhandle safely. If not, suitable lifting points shall be identified and a method statement developed for the lifting operations, in line with the Lifting Operations and Lifting Equipment Regulations 1998 (LOLER).

Sufficient time shall be allowed in the test plan to undertake all tasks in a safe manner. Accidents are most likely to happen when people are rushing around following poor planning.

8.A6.d Communication and client confidentiality

6.5.1 At the start of the test planning process, FloWave shall specify points of contact for different aspects of development and execution of the test programme. To avoid issues where conflicting requests are being made to FloWave personnel running experiments, the client shall specify who is responsible for authorising changes to the test plan during the test campaign. This is especially important where the client involves several partners or subcontractors.

6.5.3 There may be options for collaboration, whereby a small amount of extra work can give better results for all those involved. As part of this, FloWave may be able to provide additional pre-test engineering, tank time, or analysis of results, however this will depend on the project specifics.

6.5.4 A significant amount of the testing carried out at FloWave relates to novel devices that may be commercially sensitive. This can normally be covered by a non-disclosure agreement between FloWave and the client, including respective employees. Any visits to

the FloWave facility shall normally be agreed with the client in advance. In particular circumstances, to further protect intellectual property rights, access to the facility can be restricted further, e.g. to just members of staff.

8.3 Development and implementation

The planning tools were developed to provide a structured means of listing the multitude of aspects that should be considered when testing in a facility such as FloWave. Initially this was based around scaling and scale issues, but it became apparent there were many other considerations that need to be reviewed with appropriate guidance.

This has been developed with reference to client and internal tests undertaken at FloWave over the past three years. It has been discussed with FloWave project engineers involved with the technical aspects of delivering tests, as well as those on the commercial and business-development side of the company. It aims to build on the solid foundation of testing guidance (section 3.4) plus address those limitations identified for testing in more advanced conditions (section 7.4). Knowledge on how the tank produces currents and combined wave-current conditions (chapters 5 and 6) is also incorporated.

Test planning is an inherently complicated process, with a vast permutation of issues to consider. It is envisaged that the test planning tool will be completed in multiple stages, as it requires input from the client as well as joint discussions. Some issues in the checklist may not be fully self-explanatory and will warrant further discussion, however which issues this is will depend on the test requirements plus the client's knowledge and specific areas of expertise.

8.3.1 Trialling with clients

To improve the process and understand how well it works, a number of beta-tests have been conducted with FloWave staff and clients. Early drafts of the tools and guidance were discussed with FloWave staff on various occasions. Feedback has been incorporated into revised versions of the tools and guidance. A number of clarifications were made to the flowcharts and issues. The checklist format was also revised, altering the wording to form more specific questions for the developer/client to answer. Aspect and issue numbering was added to the flowcharts, to make these easier to follow and better link them to the checklist spreadsheet.

As a first trial, a retrospective review was undertaken of the test plan developed by a PhD candidate for their tests at FloWave. These were to assess the impact of off-axis non-collinear wave and current loading on a nominally 1:20 scale TST (Martinez et al., 2017; Payne et al., 2017). The review used the checklist and flowcharts to go through all

issues. As this was retrospective, it was not possible to change the test plan, but it was still considered useful by the client.

The tools were then reviewed with the developer of a floating TST platform during testing of their device at FloWave. This was at a high level, primarily discussing the flowcharts and issues, rather than going through the checklist-spreadsheet line-by-line. Again, no revisions were made to the client's test plan as a result of the review, but the issues discussed may be incorporated when planning future test campaigns.

Parts of the accompanying draft guidance were also used to assist when planning tests with other clients at FloWave.

Pilot study of test planning tools and guidance with a client

A pilot study of the tools and guidance was undertaken prior to joint testing for the academic projects FloWTurb and SupergenTEC. These are investigating turbulent loading and network integration for TSTs, using the same nominal 1:20 scale model as the PhD project discussed above.

There had been a change of staff working on the project, so the opportunity was taken to review the test plan using the checklist as a prompt. This was approximately one month before the tests, allowing some time for issues raised by the planning tools to be resolved before testing commenced.

A follow-up discussion during the test campaign revealed a couple of particular issues highlighted by going through the test planning process. Firstly, as understanding was gained into the complexity of selecting combined wave-current conditions that can be produced well in the tank. This lead to further discussion with FloWave on the range of conditions to be tested. Secondly, timings for tank settling, floor operations, etc. were included in the draft test plan. This allowed a better idea of the number of tests that could be undertaken within the allocated time. It was also noted that due to other time constraints, there was not sufficient time to take stock of the findings, so in an ideal world the test planning process should have been reviewed earlier.

8.3.2 Limitations of test planning tool

The test planning tool should form a live document for FloWave, and be updated with additional issues as these are highlighted by specific tests or new guidance. There are a number of issues that are not fully addressed at present, including:

- Technical aspects of selecting and specifying instrumentation set-up, such as choosing a wavegauge array and/or locations of gauges in the tank.

- Rationale behind the selection of particular environmental parameters, such as types of sea states, JONSWAP parameters, phase seeds for irregular sea states, etc. This is largely covered in the body of existing guidance.
- Testing survivability of devices in 'extreme' sea states, using techniques such as focused wave groups.
- Testing arrays of devices, to quantify interactions between them. These are more complex tests typically undertaken at later stages of development.

8.4 Chapter conclusions

A comprehensive collection of issues to be considered when tank testing has been collated. Tools and guidance have been developed and implemented to assist with test planning at FloWave. These aim to flag up common issues when testing plus identify gaps in knowledge shared between the client (typically a device developer), FloWave staff, and the body of published guidance on tank testing. They are also designed to highlight the more advanced capabilities of the FloWave facility, and what can be learnt from testing in these conditions.

Many of the issues covered are well-known and understood by those involved in tank testing. This is not necessarily the case for the wide range of clients that test at FloWave. There is therefore a requirement to assist clients when planning tests to make the most from testing. By flagging up potential issues prior to testing, these may be resolved, ameliorated, or at the very least expectations managed, leading to a better outcome from the test campaign.

A checklist of questions has been prepared, for the client to complete in consultation with FloWave. This can also provide a record of discussions, decisions, and outstanding actions, to be updated during the planning process. To illustrate some of the interlinking complexities of test planning, a series of flowcharts have also been developed.

It is acknowledged that the tools and guidance cannot cover every possible test scenario for FloWave. These should be live documents, updated to incorporate future lessons learnt from testing and additional published guidance.

The effectiveness and potential benefit of the tools and guidance was demonstrated in a pilot study. Clients involved in the beta testing also expressed the opinion that had these been used for planning their tests, they would have improved the test outcomes.

PART **IV**

Appraisal and closing

Chapter 9
Discussion

9.1 Characterising the new FloWave facility

As a new and novel facility, it was important to understand the FloWave tank performance. Firstly, how well currents are generated in the circular tank. Secondly, what combined wave-current conditions can be produced in the facility, including non-collinear cases. The characterisation serves a number of purposes:

- To understand how the facility operates, providing a baseline calibration of flow generation and combined wave-current conditions to facilitate client testing.
- To demonstrate that the novel circular tank can produce acceptably uniform flow for testing, validating the design stage modelling.
- Highlighting the range of advanced conditions such as multi-directional waves with non-collinear currents that can be produced in this facility, and what can be learnt from testing with these.

9.1.1 Spatial and temporal variability of currents

To fulfil objective 1a. of this research project, the spatial and temporal variability of currents in the FloWave basin have been characterised. As noted in section 5.1, characterising currents in FloWave is a multi-dimensional problem, with at least six variables: $U_{\text{ref}}, X, Y, Z, \theta, t$. Demonstrating the rotational symmetry (section 5.3.4) and long-term temporal stability (section 5.2.2) reduced this to a four-dimensional problem for mean flow in the tank.

One of the challenges in measuring spatial variability of flow throughout the basin was that only point measurements of velocity were possible with the instruments available*. Multiple measurements were therefore required, a sample at every X, Y, Z location of interest, meaning the test programme can quickly become unmanageably large. Balance was therefore required between spatial coverage, resolution, and duration of the test

*. The Vectrino Profiler can measure multiple samples simultaneously, but only within a limited measurement volume 30 mm long (Nortek, 2013), which is effectively a point on the scale of the tank.

campaign. Over 1000 velocity point measurements were made to characterise the flow. This required around four weeks of tank time, split up to fit around client testing in the tank. The measurement campaigns focused on the central test volume of the tank, nominally defined by the 15 m⌀ floor, as this is of most interest for client tests.

While the detail and resolution of the characterisation could always be improved with further data, results from this work are comprehensive. They are already used when planning and conducting tests at the facility. Using techniques such as Particle Image Velocimetry (PIV) it is possible to obtain spatial distribution of velocity measurements, however there are practical difficulties of implementing this in a large basin and there is not currently funding to install PIV at FloWave. Acoustic tomography may offer an alternative, but this is still at the R&D stage (Li et al., 2016, 2017).

The circular design of the tank results in non-uniform flow across the tank. The flow characterisation undertaken has validated the design stage modelling, showing there is a central test area with usably straight and uniform flow. The shape and size of this area depends on the flow velocity and the uniformity desired, but for a typical test may be 8 m to 10 m wide and 5 m long. Due to the flow development, this is offset slightly downstream of tank centre, away from the inlet turning vanes. This area is large enough to test small arrays of devices, one of the original drivers for the facility. As an example, one proposed test will investigate Tidal Stream Turbine (TST) array effects with three 1.2 m⌀ turbines. The front two will be at 3⌀ spacing and a centrally located turbine 1⌀ downstream, requiring a test area approximately 5 m × 3 m for the turbines.

The vertical flow profile in this central test area can be represented as a 1/15th power law. This is somewhat more uniform than the 1/7th power law often used to model channels although without much basis as real tidal flow can be very complex and not match this (Gunn and Stock-Williams, 2013; Polagye et al., 2010). Characterising tidal flow in complex real-world channels is also still an area of ongoing research (e.g. Creech and Jackson, 2017; Sellar et al., 2015). If the site conditions are not fully known, it is not possible to understand how well the tank can represent them.

Further discussion on the implications for testing of the variability in currents across the tank is given in section 5.5.

Turbulence within the flow is inherently chaotic, so conditions with currents are not as repeatable as waves in still water. Alternatively, the conditions require averaging over a longer period to obtain repeatable results. This is particularly an issue for faster flows with higher turbulence, and for wave-current interactions as discussed below. The turbulence characterisation (section 5.4) defined a stationarity period T_{stat} of 43 s, where the mean and standard deviation of the flow were <1.5%. This gives a minimum sample

period for flow measurements in the tank to be representative. Based on this, flow measurements in the tank are typically taken over a period of 1 minute or longer.

The limited control over the generation of currents in the tank means that, at present, it is not possible to *replicate* a tidal site in the same way as the wave climate for a specific site can be. There is no way to control the level of turbulence I or turbulent lengthscales ℓ in the tank independently of bulk flow velocity U. It is also not possible to alter the vertical profile of the flow, although due to the spatial variability it may be possible to select the best matching location in the tank, subject to other constraints. For tidal stream tests, conditions similar to those required should be generated in the tank, measured, and compared to site data where this is available. An approach similar to this was used for the InSTREAM project tests at FloWave (Clark et al., 2017). Additionally, numerical models could be calibrated against the tank then used to relate to real site characteristics.

The next stage in the flow characterisation will be to investigate dynamic control of the tank, in order to produce time-varying flows, e.g. a tidal ellipse, as discussed in section 9.4.

9.1.2 Wave-current interactions

The envelope of combined wave-current conditions that can be generated in the tank has been explored, starting with a set of lower steepness waves on slower currents where tank performance is better understood. Quantifying combined conditions has multi-dimensional layers of complexity. Even for regular waves, the conditions are a function of the wave properties T, H, current velocity $U_{\text{ref}}, \theta_{\text{rel}}$, tank position X, Y, Z, and time t, i.e. an 8-dimensional problem. More complex waves, e.g. parametric or non-parametric spectra potentially with directional spreading, will increase complexity of the combined conditions with additional dimensions. This can result in an impractically large measurement campaign to characterise fully.

The interaction between waves and currents in the tank has been studied, focusing on the influence of currents on waves. This interaction is complex and non-linear. There are no analytical models for 2nd or higher order waves interacting with non-collinear currents. Measurements were therefore compared with a linear wave-current interaction theory to help understand what is happening in the tank. This has also been used to quantify potential impacts for Offshore Renewable Energy (ORE) devices, highlighting why they should be tested in combined wave-current conditions.

A set of regular waves from 0.3 Hz to 0.6 Hz were observed interacting with currents of up to 0.5 m/s at nine relative angles from following to opposing, giving 297 cases in total. This included non-collinear wave-current cases, on which little has been published

(section 3.3). Additionally, several parametric JONSWAP spectra, plus a non-parametric multi-modal spectrum derived from site data, were observed in the tank interacting with collinear and non-collinear currents.

Separating any non-linear wave-current interaction from potential tank-specific generation effects is difficult. It is acknowledged there are a number of issues that affect the conditions generated in the tank, not all of which are representative of the real sea.

- Turbulent fluctuations within the current will result in individual waves interacting with a slightly different current, in the tank as in the sea. This leads to less repeatable conditions and complicates the analysis. A stationarity period T_{stat} has been calculated for the tank as 43 s. This is considerably longer than wave periods of interest, typically 1–3 s. Over this timescale, standard deviation in flow velocity is around ±3%, with greater fluctuations over shorter timescales.
- Spatial variation of the current throughout the tank will affect conditions generated. Methods have been developed to deal with a vertical flow profile by defining an equivalent uniform current (e.g. Hedges and Lee, 1992). At FloWave however, the current also varies spatially in X, Y (chapter 5). Waves interact with a current varying from ~0 at the wavemaker paddles to $\sim U_{\text{ref}}$ in the central test area, over a distance of order L for some waves of interest. It is therefore unknown if the interaction has reached a steady-state where the measurement is made.
- The horizontal variation in current across the tank leads to curvature of wave crests (section 6.2.3). This curvature is a function of wave frequency, current velocity, and relative direction. The effect is greater for high frequency waves, and for faster and opposing currents. In extreme cases this leads to a loss of spatial coherence, with wave crests splitting along their length. It is also likely that the spatial variation in current direction will result in varying degrees of refraction for non-collinear waves at different angles to the mean current direction. Both may influence the non-collinear wave-current interaction measurements (section 6.4.2). Accurate measurement of the wave direction was found to be difficult with the directional wavegauge array used for the observation tests, see Draycott et al. (2017, §5.3) in appendix B for further details. This meant it was not possible to assess accurately the refraction of wave direction as a result of non-collinear currents, any effect was close to the measurement tolerance. Despite this, it was possible to develop a method to re-create in the tank site conditions where waves interact with currents, as discussed in section 9.2.2.
- Although the wavemaker paddles operate in a zone of relatively still water, there is some recirculation of current above the inlet turning vanes, visible when the tank is generating currents. This was predicted in the design stage modelling (Robinson et al., 2015*a*) and does not appear to have a significant effect on most of the conditions generated. High frequency waves with a following current may not actually reach

the central test area however, as they can break on the adverse recirculation close to the water surface in front of the paddles. This has been observed in the tank for a number of combined wave-current cases. For a 0.8 m/s following current in the tank centre, a 0.75 Hz 0.06 m wave was breaking in the recirculation zone, with blocking at around 0.9 Hz. Linear interaction theory gives a blocking velocity of 0.4 m/s for this frequency, suggesting the recirculating current is of order 50% of the velocity in the test area. Additional measurements to characterise the current directly in front of the wavemaker paddles would be required to quantify this accurately.

- Further work is also required to fully understand the paddle response in combined wave-current conditions. The wave absorption effectiveness may be reduced for some cases. This can lead to increased build-up of reflections in the tank. This mainly occurs with currents $\gtrsim$0.4 m/s and higher frequency waves, meaning this may be more of an issue when testing TSTs in combined wave-current conditions.

9.1.3 Quality metrics

For waves or current alone, it is relatively straightforward to understand the generation envelope and quality of conditions produced. Currents are a function of U_{ref} plus variability in X, Y, Z, t. Waves are generally specified in terms of H, T to tie up with industry standard power matrices, with tank variability in X, Y, t. Individually, these are therefore 5-dimensional problems. Combined wave-current conditions encapsulate all this variability, plus the relative angle between waves and currents. A means of displaying this multi-dimensional characterisation data is therefore required. Quality metrics were developed (section 7.3) to give a high-level overview of the data. Particular environmental conditions of interest can then be reviewed in more detail as required.

The wave-current quality metric highlights the combined conditions that can be generated with higher wave quality in the FloWave tank. These are generally lower frequency waves with slower velocities. If a client test can therefore be directed towards these conditions, without affecting the learning outcomes significantly, uncertainty can be reduced and better results obtained.

For proposed tests with similar environmental conditions (waves, currents, or combined) to those that have been undertaken before, there will already be an understanding of how the facility operates and the quality of conditions produced. For other environmental conditions and/or locations in the tank, additional characterisation may be required. An initial estimate can be obtained by interpolating existing results, although this can be problematic with sparse multi-dimensional data, especially where the underlying trends are not fully understood.

9.2 Testing with advanced wave-current conditions at FloWave

9.2.1 Test planning tools and guidance

The overall aim of this research is to consider how to conduct client tests at FloWave in the multi-directional combined wave-current conditions that can be generated in this facility. Part of this is highlighting to clients what they can and should test, showcasing the capabilities of FloWave. The use of more advanced environmental conditions, in addition to those typically used in tank testing, can reveal additional insights into device performance in 'real world' like conditions.

It is also important to show how these tests can be undertaken, and what clients need to consider when planning tests. This includes issues that they are perhaps not (fully) aware of. To assist with this, test planning tools and guidance were developed (chapter 8).

These have been developed based on what clients are testing in the tank, but also on what they are *not* testing or don't understand. They build on the established body of published guidance on tank testing (section 3.4). As previously discussed, this guidance has to be quite generic to cover the wide range of devices and environmental conditions involved in the field of ORE. There are therefore limitations in published guidance, particularly covering testing in the more advanced environmental conditions that are possible in facilities such as FloWave, but are not typically included in testing. Finally, knowledge of the conditions that can be generated in the tank (waves, currents, and combined; section 3.2.3, plus chapters 5 and 6) has also been incorporated when developing the test planning tools and guidance.

The tools should guide the client towards a better test plan, rather than just being yet another data gathering exercise. This can be done by highlighting key drivers to all involved and flagging potential issues early in the planning stages, which the test planning process has been designed to do. Identifying and hopefully resolving these issues early in the planing stages should improve the test plan, thus allowing the client to make the best use of their time at FloWave. It is also important to flag constraints as early as possible, because there can be long lead times on items such as instrumentation, or for model construction. If the model scale is fixed prior to properly planning the tests, this may limit the scope of testing and the facilities it can be conducted in, reducing the effectiveness of the testing.

The tools and guidance include issues that some of the clients testing at FloWave did not fully understand or appreciate the importance of, such as specifying wave-current test conditions that cannot physically exist. If the tools had been available and were reviewed prior to the client testing, they should have flagged this issue and offered guidance.

For the pilot study of the planning tools, going through this process at an early stage flagged up the complexity of what combined wave-current conditions can be generated well at FloWave. More guidance was therefore sought from FloWave on the most suitable conditions to be tested, to meet both the test objectives and also the tank generation capability. This resulted in less time spent on running conditions that could not be well generated in the tank, and so improved the overall quality of data recorded during the test campaign.

9.2.2 Testing with combined wave-current conditions

Over the past three years, client tests at FloWave with combined conditions have primarily been for TSTs with a few Wave Energy Convertors (WECs). Both fixed and floating TST have been tested, investigating influence of waves on device loading and power capture for the former, and on motion and mooring loads for the latter. The fixed TST have typically been physically larger models, allowing more on-board instrumentation to measure quantities such as thrust and torque to quantify power generation. A small number of the WEC tests conducted have considered the influence of currents on device motion, mooring loading, and power capture.

It is apparent that the interaction between waves and currents is not necessarily well understood by clients and developers of ORE devices. This can lead to requests for combined conditions that physically cannot exist or do not represent reality, based solely on linear superposition rather than correctly accounting for the interaction. This lack of understanding may also result in developers excluding combined conditions from their test plans, as they are not aware of the potential impact wave-current interaction can have on properties such as wave shape and power.

To address this lack of understanding, plots were produced to highlight the changes to typical waves in the tank resulting from interaction with a current (section 6.1). These show the change in wave height and length, together with frequency dependant breaking and blocking limits. The effect on C_g and power is also demonstrated. Both wave breaking and power are a function of wave height as well as frequency and water depth. For clarity, only one wave height is shown on the plots. A simple extension to these plots that may be of interest to developers, who often think in terns of full-scale values, would be an interactive version — plotting the interaction of full-scale waves and currents at the water depth for their deployment site. This could also incorporate scaling the water depth from site to tank, and highlight any resulting discrepancies.

While it is possible to plot quantities in non-dimensional terms, this additional level of abstraction can reduce comprehension, which should be (and has been) avoided for this less well understood subject.

Replicating real world sites with waves and currents in FloWave

As noted previously, the research focus was on how to utilise the conditions possible at the FloWave facility for testing ORE devices. One key use case is a WEC in combined wave-current. This was therefore explored in more detail.

Wave buoys record the combined (post-interaction) conditions. This is also how ITTC guidance (for floating platforms) recommends wave-current conditions are specified (ITTC, 2005*b*). At FloWave however, waves are generated in still water prior to interaction with the current. An iterative correction method was therefore developed (section 6.5) to produce the desired waves in the central test area. This was validated with different types of waves, including a complex non-parametric spectrum, to demonstrate that *real-world-like* conditions can be replicated in the tank, one of the key drivers for FloWave.

It was found that theoretical interaction models cannot account for all process in a tank. Wave generation, reflections, and spatial variability of the current are all specific to the facility. An empirical measurement-correction process was therefore required to account for these in addition to the wave-current interaction.

It is interesting to note that even though wave-current interactions are an inherently non-linear process, a single-step linear correction factor was found to work satisfactorily for slow to moderate currents ($\lesssim$0.2 m/s in the tank, $\lesssim$1 m/s at full scale). This is typical of those likely at a WEC deployment site. Because it takes only a single step, correction of combined wave-current conditions in the tank is a relatively quick process. This also gives an understanding of the time required to calibrate combined conditions prior to a client test, i.e. a similar time to calibrating waves alone, for each current velocity to be tested. Knowledge of the interaction at a similar velocity or frequency range may assist with correcting the spectra in a similar manner to the theoretical-empirical correction procedure trialed, however measurement is still required to confirm that acceptably correct conditions are generated in the tank.

9.2.3 Testing with inconsistently scaled water depth

One practical constraint of the FloWave facility is the fixed water depth. For many ORE applications, devices are mounted in a fixed location which is often classified as intermediate depth water. Wave shape and power are critical for testing WECs, both of which are affected by the scaled water depth. It is therefore of utmost importance to understand the potential discrepancies that could be introduced when testing with inconsistently scaled water depth (section 7.2).

Implications of not scaling depth consistently were considered, and design diagrams produced to facilitate understanding and quantification of potential errors (Noble et al.,

2017*a*). The discrepancy introduced from scaling the water depth inconsistently may be up to ±30% for wavelength/steepness, and up to ±20% for power. If the discrepancy in scaled water depth is smaller, these errors will reduce.

Although tank testing inherently encapsulates the physical phenomena, compromises are always introduced. These include effects resulting from incorrect scaling of small details, testing in fresh rather than salt water with differing density, and not being able to scale all phenomena at once. Provided these compromises are understood however, they can be accounted for in the analysis of results.

As discussed in section 7.2.3, the issue of inconsistently scaled water depth may not have received much attention previously as it is less critical for other tank testing applications. Typically, the bathymetry is modelled for coastal scenarios, or the conditions are in deep water relative to the wavelength. Having the correct tank water depth to accurately represent a WEC deployment site at the chosen model scale was highlighted in lessons learnt from Aquamarine Power (Doherty, 2015) as one of the most important constraints when tank testing. This report was however not publicly available until July 2017 (WES, 2017).

9.3 Envelope of combined wave and current conditions

As discussed earlier, the envelope of wave and current conditions possible in the tank is a multi-dimensional problem, with particular complexity for combined conditions. As a new facility, there was also a learning process; incrementally understanding what conditions could be created in the tank, starting from relatively benign cases then adding energy and complexity. The envelope of conditions generated in the tank continues to be expanded by FloWave, beyond the work described in chapters 5 and 6, and Draycott (2017) which do not represent the physical limitations of what can be generated.

The work undertaken by Draycott characterised wave generation and absorption in the tank over a range of typical conditions. As noted in section 3.2.3, a consistent set of waves was used for much of this work, defined by a matrix of frequency and steepness. The directional sea states had a runtime of 2048 s (34 min each), so time constraints limited the number of conditions that could be tested, with a focus on lower steepness waves. For consistency and to facilitate comparison, these wave conditions were adopted for some of the combined-wave current characterisation presented in chapter 6.

It is acknowledged that there is a requirement in some studies to include steeper waves, close to the breaking point. This is particularly true for coastal regions, where the changing bathymetry leads to ‘shoaling’ – an increase in wave steepness as waves propagate into shallower water.

The steepness of regular waves that can be generated in the tank is a function of the paddle dynamics, as discussed in section 4.2.4, and is typically limited to ~8%. For some tests at FloWave, although not part of this research, focused wave groups have been used to study steep and breaking waves. In an extreme case, it was possible to create breaking 'freak' waves ~0.8 m high in the tank centre.

The maximum flow velocity that can be generated in the central region of the tank is ~1.8 m/s, although for currents $\gtrsim$1.2 m/s the flow becomes less homogeneous, with vertical shear layers visible downstream of the boundaries between drive units, and larger scale turbulent eddies are prominent on the water surface. At present combined wave-current conditions are limited to $\lesssim$0.9 m/s, although it may be possible to increase this slightly with improvements to the tank control software.

Re-creating real word conditions

The envelope of real-world conditions that can be generated in the tank is a function of scale. The fastest currents in UK waters are around 4 m/s (ABP MER, 2012), which are amongst the fastest worldwide. At 1:25 and 1:16 Froude scale, this equates to 0.8 m/s and 1.0 m/s respectively, so it possible to represent these conditions in the tank. It should be noted however, that the velocity profile may not match specific site data, as discussed in chapter 5.

The range of wave conditions that can be generated at scale in the tank was considered by Draycott (2017). The tank limits (section 4.2.5) impose upper and lower bounds on the wave frequencies that can be generated, with a frequency dependent height limit. For any sea-state to be generated in the tank, it is important not to exclude too much energy content by these limits, although it may be acceptable to curtail low-energy high-frequency components for example. It is also important to consider the depth ratio between site and tank, as discussed in section 7.2.

Combined wave-current conditions

The envelope of combined conditions that can be generated in the tank is a function of both the wave and current parameters $U, T, H, \theta_{\text{rel}}$. It is also directly influenced by the way currents are generated in the tank.

In combined conditions, it is easily possible to generate breaking waves on an opposing current, by selecting conditions within the generation envelope that are close to the blocking point, as discussed in chapter 6. The maximum steepness wave that can be generated on a following current is limited by wave breaking before entering the central test region, either when leaving the paddles or in the recirculation zone above the inlet turning vanes. To generate steeper waves on a following current it would be necessary

to generate waves in the current, which is not possible at FloWave, where the waves are generated in a zone of still water as explained in section 4.2.3.

For waves on a following current, the operational envelope of wave height (fig. 4.7) reduces with increasing current, due to the interaction. Wave height in the tank centre increases on an opposing current, although it is not possible to predict exactly by how much, as the interaction is non-linear and subject to tank-specific effects, as discussed in chapter 6.

As discussed in section 9.1.2, it is not known whether the wave-current conditions reach a steady state in the tank centre, as the current varies spatially over this distance. Despite this, it is possible to generate waves in the test area of the desired height when combined with currents from any direction by using the single-step iterative correction method demonstrated in section 6.5.

9.4 Recommendation for further work

Recommendation for further work building on this research are given below, split into three main topics:

1. Improve understanding of the tank performance, both for waves and currents alone, and for combined conditions.
2. Investigate options to improve the tank performance.
3. Continue to develop the tools and guidance for testing in a facility like FloWave initially formulated as part of this research.

There is also a continuous programme of research and development at FloWave. This includes options to improve tank performance, such as installing some form of physical filters to reduce reflections and settling time. Improved measurement techniques and technologies, including Laser Doppler Velocimetry (LDV), are also being considered.

Improve understanding of tank performance

The characterisation of environmental conditions generated in the FloWave facility to date is comprehensive. However, as this is a complex multi-dimensional problem, further measurements will assist with both understanding tank performance and quantifying the effectiveness of any improvement to the control systems. Project specific requirements may dictate future measurements, but the following should also be considered.

- Further measurement and analysis of currents and turbulence in the tank should include velocities faster than the nominal 0.8 m/s design specification characterised in this work.

- With further testing of device models, particularly TSTs, in the tank it should be possible to build up an understanding of how the flow conditions are affected by those models, and thus better understand the requirement for flow recalibration.
- Improved measurement of the spatial variability of the flow shouldn't be limited to the central test area, although better detail here is likely to be beneficial for future client testing. Measurement of currents in recirculation zone, above the turning vanes and in front of wavemakers, would allow the limitations for the generation of combined condition in the tank to be considered in more detail.
- The wave characterisation (Draycott, 2017) and wave-current characterisation undertaken for this project focused largely on lower steepness waves, which are closer to the assumptions of linear wave theory. Tank performance to generate and absorb higher steepness waves outside the envelope already characterised should therefore be further quantified.
- Similarly, the capability of the tank to generate and effectively absorb waves with faster currents should be explored, a process that is already underway at FloWave. As part of this, methods are being developed to measure wave reflections in the presence of a current (Draycott et al., 2018). As this is a complex multi-dimensional problem, requiring significant tank time to characterise fully, it will likely have to be broken down into multiple stages, building on the exploratory work presented in chapter 6.

Options to improve the tank performance

- Investigate dynamic control of the tank, to produce time-varying flows, e.g. a tidal ellipse. This is another large piece of work, building on this research project. To implement dynamic control, it will be important to understand and account for inertia in the tank. Changing the velocity of the 2000 tonnes of water in the tank requires time and a significant input of energy. Predicting exactly how much will require further measurement, analysis, and modelling to develop the control strategy.
- Investigate how best to make spatially distributed flow measurements in the tank, addressing the practical difficulties of implementing this. High quality spatial measurement of flow would both reduce the time to collect data and improve the resolution thereof, with clear benefit both for clients and for further characterisation of the FloWave facility.
- Explore ways to integrate the wave and current generation systems to achieve higher performance with combined conditions. This includes improving the effectiveness of the wavemaker absorption capability in currents. Discussions are ongoing between FloWave and Edinburgh Designs regarding this.

- Options to reduce flow variability in the tank by tweaking the motor control distribution from the design stage parameters could be considered. This would likely involve revisiting the Computer Fluid Dynamics (CFD) models, tweaking these based on actual flow measurements in the tank. Quantifying any change to the control system would require significant measurement effort, so this is likely to be a longer term goal, and may depend on the implementation of spatial flow measurement techniques at FloWave.

Continued development of tools and guidance

- The tools and guidance produced in this work to facilitate testing in a facility like FloWave should continue to be developed. These are live documents which should be amended and improved, both as additional lessons are learnt through testing at FloWave, and as updates/additions to testing guidance and standards are published.
  - The MARINET2 project is continuing to address testing of Marine Renewable Energy (MRE) devices at all stages of development. This includes 'round-robin' testing of the same device in several facilities, and lessons learnt through this should be addressed.
  - The International Electrotechnical Commission (IEC) is drafting Technical Standards for tank testing WECs and TSTs (IEC TS 6200-103 and IEC TS 6200-202 respectively), which are now due to be published in 2019. While it is not expected these will deviate significantly from the body of published guidance, these nevertheless need to be reviewed and incorporated into the operation of the FloWave facility.
- An interactive tool could be produced for device developers to explore wave-current interactions and scaling considerations, expanding on fig. 6.1 to show both full-scale and tank-scale parameter values, and incorporating any potential errors from inconsistently scaling the water depth (section 7.2).

Chapter 10
Conclusion

10.1 Conclusions

FloWave is a state-of-the-art test-tank for conducting research on combined multi-directional waves and currents, with no inherent limitations on direction in the circular tank. As a new facility, it is important to characterise and understand the generation of waves, currents, and combined conditions in the facility. Wave generation and absorption was characterised by Draycott (2017), and this research builds on that work.

Conclusions made earlier in the thesis are collated in the following sections under the three key objectives.

10.1.1 Characterisation of flow (objective 1a)

- Currents in the novel circular FloWave tank have been well characterised throughout the test volume. It was demonstrated that after a ramp-up period, the flow is temporally stable, and repeatable between tests. Calibration of input drive motor rpm against velocity in the test area was updated.
- Flow across the central test area of the tank has been assessed using a map of flow measurements. Although there is spatial variability, this has been characterised in terms of magnitude and direction. It matches design-stage modelling, both in plan and a vertical section along the flow direction. The vertical flow profile can be approximated as a 1/15th power-law near the tank centre, with some variation towards the test area perimeter.
- An initial characterisation of turbulence within the flow has been undertaken, including spatial variation, using similar metrics to field measurement campaigns. Typical values for streamwise turbulence intensity I_x and integral lengthscale ℓ_u in the central test area are 5–11% and 0.18–0.41 m respectively.
- As it is not presently possibly to control the flow profile or turbulent flow parameters, and there is spatial variation of these across the tet area, one outcome of this work is suggesting that it may be possible to select the best matching location in the tank to represent a specific site. Other considerations regarding the test set-up still need to be satisfied however, as discussed in chapter 8.

- Results of the flow characterisation were presented at the European Wave and Tidal Energy Conference (EWTEC) (Noble et al., 2015). The turbulence characterisation was then published in Ocean Engineering (Sutherland et al., 2017). See appendix B for both. This information can then be used by clients planning tests at FloWave.
- A tool has also been developed to calculate required primary drive motor rpm for the desired velocity and location in the tank. This can be used directly to set test parameters, or as a first step in a velocity calibration where there is a model in the flow for example. It is based on the flow characterisation measurements conducted, but this tool could easily be updated as additional data become available.

10.1.2 Wave-current interactions (objective 1b)

- Literature on wave-current interaction theory has been reviewed, and summarised to assist clients testing at FloWave. The full complexity of wave-current interactions may not be well understood by Offshore Renewable Energy (ORE) device developers. This can lead to requests for combined wave-current conditions that cannot physically exist, or conditions that are not representative of the deployment site.
- A linear interaction theory has been implemented in MATLAB, and used to help understand combined conditions generated in the tank. It was also used in the theoretical and theoretical–empirical correction procedures trialled.
- The generation of combined wave-current conditions in the FloWave basin has been assessed. Due to interaction with chaotic turbulence within the flow, repeatability of waves on currents is lower than for waves alone. The spatial variability of flow velocity across the tank also results in curvature of waves in the tank with a current. This is particularly noticeable for long-crested regular waves, but will affect all types of waves.
- Changes to waves resulting from their interaction with a current have been studied in the FloWave basin. This includes both collinear and non-collinear cases, noting that little has been published to date on the latter. For these conditions, tank performance has also been rated, facilitating future wave-current experiments and helping to direct any tank control improvements.
- Waves in the FloWave facility are generated in still water around the tank circumference then interact with a current in the central test area. Producing waves of the desired height therefore requires a correction to the wavemaker input. A method has been developed based on an empirical correction factor. This has been trialled with regular waves, a long-crested JONSWAP spectrum, and a complex non-parametric multi-directional spectrum based on data recorded at EMEC to demonstrate that *real-world-like* conditions can be recreated in the tank.

10.1.3 Tools and guidelines for testing at FloWave (objective 2)

- A method has been developed to quantify and visualise the errors that may arise while tank testing if the scaled water depth is not correct (Noble et al., 2017*a*, see appendix B). This issue may be of particular relevance to marine renewable energy, where devices sensitive to wavelength and power are moored in finite depth water conditions. For typical model tests, this may result in wavelength/steepness errors of up to ±30%, and up to ±20% in wave power.
- Published guidance for tank testing ORE devices has been reviewed. This addresses the many aspects that should be considered, however three key limitations were identified for testing in the advanced environmental conditions possible at facilities such as FloWave. Initial recommendation to augment guidance, mirroring these limitations, are therefore suggested. These are based on ongoing research and lessons learnt during testing at FloWave.
  1. Consider directional sensitivity for all devices that are not rotationally symmetrical. Direction may not be given sufficient importance when developing test plans, resulting in discrepancy between predicted and observed loading or performance when devices are deployed at sea.
  2. Test with complex waves, to increase understanding of real sea performance. While regular waves and parametric spectra are useful for understanding general device motions and performance, they do not capture the full complexity of the real ocean. Behaviour in multi-directional/multi-modal sea states may be quite different, with implications on mooring loadings or Wave Energy Convertor (WEC) power capture.
  3. Perhaps most importantly, include combined wave-current conditions if these may occur at the deployment site. Even low tidal currents can impact wave parameters (H, L, S, C, C_g, P_w). The only way to accurately re-create waves where a current is present at the site is to reproduce that current at scale in the test facility. The influence of waves on a tidal current is also important for the design of near surface structures and turbine blades, as wave orbital velocities can introduce significant additional cyclic loading.

  These recommendations were presented at the 36th International Conference on Ocean, Offshore and Arctic Engineering (OMAE2017) (Noble et al., 2017*b*, see appendix B).
- Tools and guidance have been developed and implemented to assist with test planning at FloWave. These show the many issues that should be considered when developing the test plan. Reviewing them may highlight gaps in knowledge shared between the client (typically a device developer), FloWave staff, and the body of published guidance on tank testing. They also showcase the range of advanced environmental

conditions that can be generated in the facility, and what can be learnt from testing with these. The checklist tool also serves as a record of decisions made during test planning, which should help those involved in conducting the test. A pilot study with an academic client demonstrated the benefit of this process. Particular issues with generating combined wave-current conditions were highlighted, and guidance was offered on how the test plan should be developed.

10.2 Main research contributions

The main outcomes of the research can be summarised as:

- Currents in the FloWave basin have been comprehensively characterised, including temporal and spatial variations. This is used, both directly and as a starting point for further calibration, to enable commercial operation of the facility.
- The envelope of combined wave-current conditions that can be generated in the tank has been explored. This includes non-collinear interactions with an angle between wave and current, on which little has been published.
- A method has also been developed to produce the desired waves in combination with low currents in the central test area of the tank. This is used for client testing of WECs and other floating devices.
- Potential discrepancies resulting from tank testing with inconsistently scaled water depth have been highlighted and quantified. Design diagrams were produced to aid understanding of this issue when testing.
- Limitations of published guidance have been identified when considering testing in the type of advanced conditions now possible at a facility such as FloWave. To address this, recommendations were suggested to augment existing guidance.
- Finally, to tie all of these together, tools and guidance have been developed to assist with test planning at FloWave. These are designed to flag the many issues and constraints that should be considered, and ideally addressed, prior to testing.

10.3 Commercial impact

The Engineering Doctorate should deliver commercial impact for the host company plus the wider offshore renewable energy sector. This encompasses tangible benefits as well as those intangibles that are more difficult to quantify but are nevertheless important.

Flow characterisation undertaken in this project is directly used to enable commercial operation of the FloWave facility, delivering a clear benefit for both the tank and the wider industry testing there. Having a well characterised tank can save in the order of

1–2 days of pre-test measurements per test campaign of typically two weeks duration. It also permits quick and confident responses to enquiries about the tank capability, potentially attracting new clients.

The tools and guidance developed for FloWave highlight some of the complexities involved in tank testing, particularly in using multi-directional combined wave-current conditions. They also offer knowledge transfer to clients less familiar with all aspects of tank testing, helping them to get the most from testing at FloWave, and offering further benefit to the wider industry.

Using these tools when developing test plans makes efficient use of staff time. The tools and guidance should help flag potential issues and problems early in the planning process, avoiding rework and allowing test parameters to be aligned with the tank capability where possible, improving test outcomes. Specifics are not given for client confidentiality reasons, but for several test plans with combined wave-current, up to 25% of the conditions requested could not physically exist or were not well generated in the tank. Over a typical 2-week test programme at c.£50 k, the cost of running conditions that do not generate good quality data soon mounts up.

On a more technical level, a method has been developed to re-create site conditions with multi-directional waves combined with a current from any direction in the FloWave tank. This showcases the technical capabilities of the facility and is beneficial to clients looking to understand floating device performance in real sea conditions. The potential errors of neglecting the impact of tidal currents has also been quantified. Incident wave power may be assumed up to 20% different to the true value if the effects of wave-current interaction are not considered and re-created in the tank. This would obviously have significant implications for WEC performance testing. Similarly, potential discrepancies for tests with inconsistently scaled water depth of up to 20–30% have been quantified through design diagrams, improving knowledge of this issue.

Testing ORE devices in multi-directional waves with currents can improve understanding of real-world behaviour and performance, leading to gains for the wider industry. This research contributes to that process — by providing characterisation, tools, and guidance to conduct these tests at the FloWave Ocean Energy Research Facility. It also demonstrates the importance of considering wave-current interactions, even in comparatively low flows.

Bibliography

ABP MER (2012), Pentland Firth and Orkney Waters Strategic Area : Marine Energy Resources, Technical Report November, The Crown Estate.

Andersen, T. L., Frigaard, P. B. and Burcharth, H. F. (2014), *Lecture notes for the course in water wave mechanics*, 3 edn, Aalborg University, Aalborg, Denmark.

Bacchetti, T., Facq, J.-V., Gaurier, B. and Germain, G. (2010), Essais combinés houle-courant – Caractérisation des conditions générées au bassin de Boulogne-sur-Mer (in French) [Trials of combined wave-current – Characterisation of conditions at the Bologne-sur-mer tank], Technical report, Département Recherche et Développement Technologique Service Hydrodynamique et Océano-Météo.

Baddour, R. E. and Song, S. W. (1990*a*), 'On the interaction between waves and currents', *Ocean Engineering* **17**(1/2), 1–21. doi: 10.1016/0029-8018(90)90011-T.

Baddour, R. E. and Song, S. W. (1990*b*), 'Interaction of higher-order water waves with uniform currents', *Ocean Engineering* **17**(6), 551–568. doi: 10.1016/0029-8018(90)90023-Y.

Bahaj, A. S., Blunden, L. and Anwar, A. A. (2008), Tidal-current Energy Device Development and Evaluation Protocol, Technical report, University of Southampton, Southhampton.

Barltrop, N., Varyani, K. S., Grant, A. D., Clelland, D. and Pham, X. (2006), 'Wave-current interactions in marine current turbines', *Proceedings of the Institution of Mechanical Engineers, Part M: Journal of Engineering for the Maritime Environment* **220**(4), 195–203. doi: 10.1243/14750902JEME45.

Brand, A. J., Peeringa, J. M., Marino, E., Cappietti, L. and Pecora, M. L. (2015), D2.10 Best Practice Protocol for Offshore Wind System Fluid-Structure Interaction Testing, Technical report, MARINET.

Bredmose, H., Larsen, S. E., Matha, D., Marino, E. and Saettran, L. (2012), D2.4 Collation of offshore wind-wave dynamics, Technical report, MARINET.

Bretherton, F. P. and Garrett, C. J. R. (1968), 'Wavetrains inhomogeneous moving media', *Proceedings of the Royal Society of London A* **302**(1471), 529–554. doi: 10.1098/rspa.1983.0054.

Cândido, J., Finn, M., Dampney, K., Lawrence, J. and Margheritini, L. (2015), D2.9 Standards for Wave Data Analysis, Archival and Presentation, Technical report, MARINET.

Chakrabarti, S. K. (1998), Physical model testing of floating offshore structures, *in* 'Proc. Int. Symp. Dynamic Positioning Committee'.

Chakrabarti, S. K., ed. (2005), *Handbook of Offshore Engineering*, Elsevier. doi: 10.1016/B978-0-08-044381-2.50002-3.

Chakrabarti, S. K. and Johnson, J. (1995), Random wave-current interaction – Theory and experiment, *in* 'Proceedings of the 14th International Conference on Offshore Mechanics and Arctic Engineering (OMAE1995)', Copenhagen, Denmark.

CIRIA, CUR and CETMEF (2007), *The Rock Manual. The use of rock in hydraulic engineering*, CIRIA.

Clark, T. H. E. (2015), Turbulence in Marine Environments (TiME): A framework for understanding turbulence and its effects on tidal devices ., *in* 'Proceedings of the 11th European Wave and Tidal Energy Conference (EWTEC2015)', Nantes, France.

Clark, T. H. E., Lueck, R., Hay, A., Davey, T., Stern, P., Horwitz, R. and Pearson, N. (2017), InSTREAM: Measurement, Characterisation and Simulation of Turbulence from Test Tank to Ocean, *in* 'Proceedings of the 12th European Wave and Tidal Energy Conference (EWTEC2017)', Cork, Ireland.

Clayson, C. H. (1989), Survey of Instrumental Methods for the Determination of the High Frequency Wave Spectrum, Technical report, Natural Environment Research Council, Wormley, Surrey.

Collins, K., Iglesias, G., Greaves, D., Toffoli, A. and Stripling, S. (2013), The New Coast Laboratory at Plymouth University : A World-Class Facility for Marine Energy, *in* 'ICE Breakwaters 2013'.

Creech, A. and Jackson, A. (2017), Developing Fluidity for high-fidelity coastal modelling, Technical report. URL: `https://www.archer.ac.uk/community/eCSE/eCSE05-07/eCSE05-07_Technical_Report.pdf`

Davey, T. A. D., Brown, S., Bryden, I. G., Ingram, D. M., Robinson, A. and Wallace, A. R. (2013), The All-Waters Test Facility – The Role of a New Facility in Physical Modelling for Marine and Coastal Engineering, *in* 'ICE Breakwaters 2013'.

Davey, T. A. D., Bruce, T. and Allsop, W. (2008), 'Getting more from physical modelling – measuring extreme responses using importance sampling', *Proceedings 31st International Conference on Coastal Engineering* .

Davey, T. A. D., Bryden, I. G., Ingram, D. M., Robinson, A., Sinfield, J. L. and Wallace, A. R. (2012), The All-Waters Test Facility – a new resource for the marine energy sector, *in* 'Proceedings of the 4th International Conference on Ocean Energy (ICOE2012)', Dublin.

Davey, T. A. D., Venugopal, V., Girard, F., Smith, H. C. M., Smith, G. H., Lawrence, J., Cavaleri, L., Bertotti, L., Prevosto, M. and Holmes, B. (2010), D2.7 Protocols for wave and tidal resource assessment, Technical report.

Day, A. H., Babarit, A., Fontaine, A., He, Y.-P., Kraskowski, M., Murai, M., Penesis, I., Salvatore, F. and Shin, H.-K. (2015), 'Hydrodynamic modelling of marine renewable energy devices: A state of the art review', *Ocean Engineering* **108**, 46–69. doi: 10.1016/j.oceaneng.2015.05.036.

de Jesus Henriques, T., Tedds, S., Botsari, A., Najafian, G., Hedges, T. S., Sutcliffe, C., Owen, I. and Poole, R. J. (2014), 'The effects of wave-current interaction on the performance of a model horizontal axis tidal turbine', *International Journal of Marine Energy* **8**, 17–35. doi: 10.1016/j.ijome.2014.10.002.

Dean, R. G. and Dalrymple, R. A. (1991), *Water Wave Mechanics for Engineers and Scientists*, World Scientific.

Deltares (2017*a*), 'Atlantic Basin'. URL: `https://www.deltares.nl/en/facilities/atlantic-basin-3/` [Accessed: 2017-07-20]

Deltares (2017*b*), 'Pacific Basin'. URL: `https://www.deltares.nl/en/facilities/pacific-basin-2/` [Accessed: 2017-07-20]

Derradji-Aouat, A., Park, J. T. and Sparkes, D. (2007), LDA Experiments – Flow Characterization of the NRC-IOT Cavitation and Water Re-circulating Tunnel, *in* '8th Canadian Marine Hydromechanics and Structures Conference', St. John's, NL.

Doherty, K. (2015), WES Knowledge Capture Report WP5 – Tank Testing of WECs, Technical report, Wave Energy Scotland, Inverness.

Draycott, S. (2017), On the Re-creation of Site-Specific Directional Wave Conditions, Engineering doctorate, The University of Edinburgh.

Draycott, S., Davey, T. A. D., Ingram, D. M., Day, A. H. and Johanning, L. (2016), 'The SPAIR method: Isolating incident and reflected directional wave spectra in multidirectional wave basins', *Coastal Engineering* **114**, 265–283. doi: 10.1016/j.coastaleng.2016.04.012.

Draycott, S., Davey, T. A. D., Ingram, D. M., Lawrence, J., Day, A. H. and Johanning, L. (2015*a*), Applying Site-Specific Resource Assessment : Emulation of Representative EMEC seas in the FloWave Facility, *in* 'Proceedings of the Twenty-fifth International Ocean and Polar Engineering Conference (ISOPE2015)', ISOPE, Kona, Big Island, Hawaii, USA, pp. 815–821.

Draycott, S., Davey, T. A. D., Ingram, D. M., Lawrence, J., Day, A. H. and Johanning, L. (2015*b*), Using a Phase-Time-Path-Difference Approach to Measure Directional Wave Spectra in FloWave, *in* 'Proceedings of the 11th European Wave and Tidal Energy Conference (EWTEC2015)'.

Draycott, S., Noble, D., Davey, T., Bruce, T., Ingram, D., Johanning, L., Smith, H., Day, A. and Kaklis, P. (2017), 'Re-creation of site-specific multi-directional waves with non-collinear current', *Ocean Engineering* **152**, 391–403. doi: 10.1016/j.oceaneng.2017.10.047.

Draycott, S., Steynor, J., Davey, T. and Ingram, D. M. (2018), 'Isolating incident and reflected wave spectra in the presence of current', *Coastal Engineering Journal* . doi: 10.1080/05785634.2017.1418798.

Edinburgh Designs Ltd (2014), User Manual For University of Edinburgh, Flowave, Technical report, Edinburgh, UK.

Edinburgh Designs Ltd (2016*a*), 'Edinburgh Designs Wave Gauges'. URL: `http://www.edesign.co.uk/product/wavegauges/` [Accessed: 2017-03-16]

Edinburgh Designs Ltd (2016*b*), 'Wave Generating Software'. URL: http://www.edesign.co.uk/product/wave-generating-software/ [Accessed: 2017-03-16]

Esteva, D. (1977), Wave Direction Computations with Three Gage Arrays, *in* 'Coastal Engineering 1976', American Society of Civil Engineers, New York, NY, pp. 349–367. doi: 10.1061/9780872620834.020.

Falcão, A. F. d. O. (2010), 'Wave energy utilization: A review of the technologies', *Renewable and Sustainable Energy Reviews* **14**(3), 899–918. doi: 10.1016/j.rser.2009.11.003.

Faltinsen, O. (1993), *Sea Loads on Ships and Offshore Structures*, Cambridge University Press, Cambridge.

Faudot, C. and Dahlhaug, O. G. (2012), 'Prediction of Wave Loads on Tidal Turbine Blades', *Energy Procedia* **20**, 116–133. doi: 10.1016/j.egypro.2012.03.014.

Fenton, J. D. (2013), *Coastal and Ocean Engineering (lecture notes)*, TU Wien, Institut für Wasserbau und Ingenieurhydrologie.

Fernandes, A. A., Sarma, Y. V. B. and Menon, H. B. (2000), 'Directional spectrum of ocean waves from array measurements using phase/time/path difference methods', *Ocean engineering* **27**(4), 345–363. doi: 10.1016/S0029-8018(99)00024-4.

Fernández, H., Schimmels, S. and Sriram, V. (2013), 'Focused Wave Generation by Means of a Self Correcting Method', *Proceedings of the Twenty-third International Offshore and Polar Engineering (ISOPE2013)* **9**, 917–924.

FloWave Ocean Energy Research Facility (2015), 'FloWave Exhibition Video 2014'. URL: https://www.youtube.com/watch?v=WffR6HrEqTA [Accessed: 2017-04-05]

Fryer, D. K. and Thomas, M. W. (1975), 'A linear twin wire probe for measuring water waves', *Journal of Physics E: Scientific Instruments* **8**(5), 405–408. doi: 10.1088/0022-3735/8/5/021.

Galloway, P. W., Myers, L. E. and Bahaj, A. S. (2014), 'Quantifying wave and yaw effects on a scale tidal stream turbine', *Renewable Energy* **63**(2014), 297–307. doi: 10.1016/j.renene.2013.09.030.

Garrett, C. and Cummins, P. (2004), 'Generating Power from Tidal Currents', *Journal of Waterway, Port, Coastal, and Ocean Engineering* **130**(3), 114–118. doi: 10.1061/(ASCE)0733-950X(2004)130:3(114).

Gaurier, B., Germain, G., Facq, J. V., Johnstone, C. M., Grant, A. D., Day, A. H., Nixon, E., Di Felice, F. and Costanzo, M. (2015), 'Tidal Energy "Round Robin" Tests Comparisons between towing tank and circulating tank results', *International Journal of Marine Energy* **12**(2015), 87–109. doi: 10.1016/j.ijome.2015.05.005.

Germain, G. (2008), Marine current energy converter tank testing practices, *in* 'Proceedings of the 2nd International Conference on Ocean Energy (ICOE 2008)', Brest, France.

Germain, G., Bahaj, A. S., Huxley-Reynard, C. and Roberts, P. (2007), Facilities for marine current energy converter characterization, *in* 'Proceedings of the 7th European Wave and Tidal Energy Conference (EWTEC2007)', Porto, Portugal.

Germain, G., Maganga, F., Gaurier, B., Facq, J. V., Bacchetti, T., Pinon, G., Rivoalen, E. and Etancelin, J. M. (2010), 'Vers une Caracterisation Realiste des Conditions de Fonctionnement des Hydroliennes (in French) [Towards a Realistic Characterisation of the Operational Conditions of Marine Current Turbines]', *12èmes Journées de l'Hydrodynamique* .

Goring, D. G. and Nikora, V. I. (2002), 'Despiking Acoustic Doppler Velocimeter Data', *Journal of Hydraulic Engineering* **128**(1), 117–126. doi: 10.1061/(ASCE)0733-9429(2002)128:1(117).

Groeneweg, J. (1999), Wave-current interactions in a generalized Lagrangian mean formulation, Phd thesis, TU Delft. URL: https://repository.tudelft.nl/islandora/object/uuid:b1e7558c-3ae7-4edd-a58f-bb6caba0541e

Guedes Soares, C., Rodriguez, G., Cavaco, P. and Ferrer, L. (2000), Experimental study on the interaction of wave spectra and currents, *in* 'Proceedings of the ASME 19th International Conference on Offshore Mechanics and Arctic Engineering (OMAE2000)'.

Guillouzouic, B. (2014), D2.12 Collation of Wave Simulation Methods, Technical report, MARINET.

Gunn, K. and Stock-Williams, C. (2013), 'On validating numerical hydrodynamic models of complex tidal flow', *International Journal of Marine Energy* **3-4**, e82–e97. doi: 10.1016/j.ijome.2013.11.013.

Gupta, R. (2014), 'Peter Fraenkel: "Tank test models and an artist's impressions aren't enough. It definitely demands patience for something successful to come through"'. URL: http://analysis.newenergyupdate.com/tidal-today/peter-fraenkel-tank-test-models-and-artists-impressions-arent-enough-it-definitely [Accessed: 2017-05-19]

Hamilton, L. J. (2010), 'Characterising spectral sea wave conditions with statistical clustering of actual spectra', *Applied Ocean Research* **32**(3), 332–342. doi: 10.1016/j.apor.2009.12.003.

Harrower, M. and Brewer, C. A. (2003), 'ColorBrewer.org: An Online Tool for Selecting Colour Schemes for Maps', *The Cartographic Journal* **40**(1), 27–37. doi: 10.1179/000870403235002042.

Hashemi, M. R., Neill, S. P., Davies, A. G. and Lewis, M. J. (2014), The Implications of Wave-Tide Interactions in Marine Renewables within the UK Shelf Seas, *in* 'Proceedings of the 2nd International Conference on Environmental Interactions of Marine Renewable Energy Technologies (EIMR2014)', Stornoway, Scotland.

Hashemi, M. R., Neill, S. P., Robins, P. E., Davies, A. G. and Lewis, M. J. (2015), 'Effect of waves on the tidal energy resource at a planned tidal stream array', *Renewable Energy* **75**, 626–639. doi: 10.1016/j.renene.2014.10.029.

Hedges, T. S. (1981), Some effects of currents on wave spectra, *in* 'Proceedings of the First Indian Conference in Ocean Engineering', pp. 30–35.

Hedges, T. S. (1987), 'Combinations of waves and currents: an introduction', *ICE Proceedings* **82**(3), 567–585. doi: 10.1680/iicep.1987.319.

Hedges, T. S., Anastasiou, K. and Gabriel, D. (1985), 'Interaction of random waves and currents', *Journal of Waterway, Port, Coastal, and Ocean Engineering* **111**(2), 275–288. doi: 10.1016/0198-0254(85)92681-0.

Hedges, T. S. and Lee, B. (1992), 'The equivalent uniform current in wave-current computations', *Coastal Engineering* **16**, 301–311. doi: 10.1016/0378-3839(92)90046-W.

Hedges, T. S., Tickell, R. and Akrigg, J. (1993), 'Interaction of short-crested random waves and large-scale currents', *Coastal Engineering* **19**(3-4), 207–221. doi: 10.1016/0378-3839(93)90029-8.

Heller, V. (2011), 'Scale effects in physical hydraulic engineering models', *Journal of Hydraulic Research* **49**(3), 293–306. doi: 10.1080/00221686.2011.578914.

Holmes, B. (2009), Tank Testing of Wave Energy Conversion Systems, Technical report, Orkney.

Holmes, B. (2015), D2.8 Best Practice Manual for Wave Simulation, Technical report, MARINET.

Holmes, B. and Nielsen, K. (2010), Guidelines for the development & testing of wave energy systems, Technical report, Hydraulics Maritime Research Centre, UCC, Cork, Ireland.

Holthuijsen, L. H. (2007), *Waves in Oceanic and Coastal Waters*, Cambridge University Press.

HR Wallingford (2017), 'Fast Flow Facility Contact Key features of the Fast Flow Facility'.

HSE (2002), Environmental considerations, Technical report, Health & Safety Executive, London.

Huang, N. E., Chen, D. T., Tung, C.-C. and Smith, J. R. (1972), 'Interactions between Steady Non-Uniform Currents and Gravity Waves with Applications for Current Measurements', *Journal of Physical Oceanography* **2**(4), 420–431. doi: 10.1175/1520-0485(1972)002<0420:IBSWUC>2.0.CO;2.

Hudson, R. Y., Herrmann, F. A. J., Soger, R. A., Whalin, R. W., Keulegan, G. H., Chatham, C. E. J. and Hales, L. Z. (1979), *Coastal hydraulic models*, U.S. Army, Corps of Engineers Coastal Engineering Research Center, Fort Belvoir, VA.

Hughes, S. A. (1993), *Physical models and laboratory techniques in coastal engineering.*, World Scientific, Singapore.

IEA (2016*a*), Key Electricity Trends – Excerpt from Electricity Information, Technical report, International Energy Agency.

IEA (2016*b*), World Energy Outlook 2016 (Executive Summary), Technical report, International Energy Agency, Paris, France.

IEC (2018), 'TC 114 Marine energy – Wave, tidal and other water current converters –Work programme'. URL: http://www.iec.ch/dyn/www/f?p=103:23:10705541553692::::FSP_ORG_ID,FSP_LANG_ID:1316,25

IH Cantabria (2017), 'IHLab Hydro – Wave Basins'. URL: http://www.ihcantabria.com/en/ihlab-menu/ihlab-hidro/item/697/697 [Accessed: 2017-07-26]

Ingram, D. M., Smith, G. H., Bittencourt-Ferreira, C. and Smith, H. C. M. (2011), Protocols for the Equitable Assessment of Marine Energy Converters, Technical report, Edinburgh.

Ingram, D. M., Wallace, A. R., Robinson, A. and Bryden, I. G. (2014), The design and commissioning of the first, circular, combined current and wave test basin., *in* 'Proceedings of Oceans 2014 MTS/IEEE', Taipei, Taiwan.

ITTC (2005*a*), Recommended Procedures and Guidelines: 7.5-02-07-01.1 Laboratory Modelling of Multidirectional Irregular Wave Spectra, Guideline, International Towing Tank Conference.

ITTC (2005*b*), Recommended Procedures and Guidelines: 7.5-02-07-03.1 Floating Offshore Platform Experiments, Procedure, International Towing Tank Conference.

ITTC (2011*a*), Recommended Procedures and Guidelines: 7.5-02-07-02.1 Seakeeping Experiments, Procedure, International Towing Tank Conference.

ITTC (2011*b*), Recommended Procedures and Guidelines: 7.5-02-07-03.7 Wave Energy Converter Model Test Experiments, Guideline, International Towing Tank Conference.

ITTC (2014*a*), Recommended Procedures and Guidelines: 7.5-02-07-03.7 Wave Energy Converter Model Test Experiments, Guideline, International Towing Tank Conference.

ITTC (2014*b*), Recommended Procedures and Guidelines: 7.5-02-07-03.8 Model Tests for Offshore Wind Turbines, Procedure, International Towing Tank Conference.

ITTC (2014*c*), Recommended Procedures and Guidelines: 7.5-02-07-03.9 Model Tests for Current Turbines, Procedure, International Towing Tank Conference.

ITTC (2014*d*), Specialist Committee on Hydrodynamic Testing of Marine Renewable Energy Devices. Final Report and Recommendations to the 27th ITTC, *in* 'Proceedings of the 27th International Towing Tank Conference', Vol. II, International Towing Tank Conference, Copenhagen, Denmark, pp. 680–725.

ITTC (2017*a*), Recommended Procedures and Guidelines: 7.5-02-07-01.1 Laboratory Modelling of Multidirectional Irregular Wave Spectra, Guideline, International Towing Tank Conference.

ITTC (2017*b*), Recommended Procedures and Guidelines: 7.5-02-07-01.2 Laboratory Modelling of Waves: regular, irregular and extreme events, Guideline, International Towing Tank Conference.

ITTC (2017*c*), Recommended Procedures and Guidelines: 7.5-02-07-03.1 Floating Offshore Platform Experiments, Procedure, International Towing Tank Conference.

ITTC (2017*d*), Recommended Procedures and Guidelines: 7.5-02-07-03.7 Wave Energy Converter Model Test Experiments, Guideline, International Towing Tank Conference.

ITTC (2017*e*), Recommended Procedures and Guidelines: 7.5-02-07-03.8 Model Tests for Offshore Wind Turbines, Procedure, International Towing Tank Conference.

ITTC (2017*f*), Recommended Procedures and Guidelines: 7.5-02-07-03.9 Model Tests for Current Turbines, Procedure, International Towing Tank Conference.

Jonsson, I. G. (1990), Wave-current Interactions, *in* B. LeMehaute and D. M. Hanes, eds, 'The Sea, Ocean Engineering Science', Vol. 9, Wiley-Interscience publications, New York, chapter 7, pp. 65–120.

Kanwisher, J. and Lawson, K. (1975), 'Electromagnetic flow sensors', *Limnology and Oceanography* **20**(March), 174–182.

Kemp, P. H. and Simons, R. R. (1982), 'The interaction between waves and a turbulent current: waves propagating with the current', *Journal of Fluid Mechanics* **116**(-1), 227–250. doi: 10.1017/S0022112082000445.

Kemp, P. H. and Simons, R. R. (1983), 'The interaction of waves and a turbulent current: waves propagating against the current', *Journal of Fluid Mechanics* **130**, 73–79. doi: 10.1017/S0022112083000981.

Kimball, R. (2010), Power Performance Measurements of Electricity Producing Hydrokinetic Turbines: Laboratory Scale Models, Technical report, U.S. Department of Energy.

Klopman, G. (1994), Vertical structure of the flow due to waves and currents: laser-Doppler flow measurements for waves following and opposing a current., Technical report, Delft Hydraulics.

Lawrence, J., Holmes, B., Bryden, I. G., Magagna, D., Torre-Enciso, Y., Rousset, J.-M., Smith, H. C. M., Paul, M., Margheritini, L. and Cândido, J. (2012), D2.1 Wave Instrumentation Database, Technical report, MARINET.

Li, G., Ingram, D., Kaneko, A., Chen, M., Gohda, N. and Polydorides, N. (2017), 'Vertical underwater acoustic tomography in an experimental basin', *The Journal of the Acoustical Society of America* **141**(5), 3656–3656. doi: 10.1121/1.4987918.

Li, G., Ingram, D., Kaneko, A., Gohda, N. and Polydorides, N. (2016), 'The application of coastal acoustic tomography to a large experimental wave/current basin', *The Journal of the Acoustical Society of America* **140**(4), 3183–3183. doi: 10.1121/1.4970007.

Longuet-Higgins, M. S. and Stewart, R. W. (1961), 'The changes in amplitude of short gravity waves on steady non-uniform currents', *Journal of Fluid Mechanics* **10**(04), 529. doi: 10.1017/S0022112061000342.

Mankins, J. C. (1995), 'Technology readiness levels', *White Paper, April* pp. 4–8.

Mansour, A. E. and Ertekin, R. C. (2003), Report of technical committee I.1 environment, *in* 'Proceedings of the 15th international ship and offshore structures congress', Vol. 1.

MARINET (2014), 'Transnational Access - Facilities Available [no longer online]'. URL: `http://www.marinet.eu/access_facilities-available_category-view.html` [Accessed: 2014-11-27]

MARINTEK (2011), 'Hydrodynamic Laboratories'. URL: `https://www.sintef.no/globalassets/marintek/publikasjoner/brosjyrer/hydrodynamic-laboratories.pdf`

Martinez, R., Payne, G. and Bruce, T. (2017), Preliminary results on the effects of oblique current and waves on the loadings and performance of tidal turbines, *in* 'Proceedings of the 12th European Wave and Tidal Energy Conference (EWTEC2017)', Cork, Ireland.

Massel, S. (1996), *Ocean surface waves: their physics and prediction.*

Masterton, S. R. and Swan, C. (2008), 'On the accurate and efficient calibration of a 3D wave basin', *Ocean Engineering* **35**(8-9), 763–773. doi: 10.1016/j.oceaneng.2008.02.002.

McCombes, T., Iyer, A. S., Falchi, M., Elsäßer, B., Scheijgrond, P. and Lawrence, J. (2012), D2.2 Collation of Tidal Test Options, Technical report, MARINET.

McCombes, T., Johnstone, C. M., Holmes, B., Myers, L. E., Bahaj, A. S. and Kofoed, J. P. (2010*a*), D3.3 Assessment of current practice for tank testing of small marine energy devices, Technical report.

McCombes, T., Johnstone, C. M., Holmes, B., Myers, L. E., Bahaj, A. S. and Kofoed, J. P. (2010*b*), D3.4 Best Best practice for tank testing of small marine energy devices, Technical report.

McLachlan, C. (2010), Tidal stream energy in the UK: Stakeholder perceptions study, Technical report, Tyndall Centre for Climate Change Research, Manchester.

Méhauté, B. L. (1976), *An introduction to hydrodynamics and water waves*, Springer, New York.

Miche, A. (1944), 'Mouvements ondulatoires de la mer en profondeur croissante ou décroissante. Forme limite de la houle lors de son déferlement. Application aux digues maritimes. Deuxième partie. Mouvements ondulatoires périodiques en profondeur régulièrement décroissante', *Annales des Ponts et Chaussées* .

Miche, A. (1951), 'Le pouvoir réfléchissant des ouvrages maritimes exposés à l'action de la houle', *Annales des Ponts et Chaussées* .

Miles, M. D. and Funke, E. R. (1989), 'A Comparison of Methods for Synthesis of Directional Seas'. doi: 10.1115/1.3257137.

Mori, N., Suzuki, T. and Kakuno, S. (2007), 'Noise of Acoustic Doppler Velocimeter Data in Bubbly Flows', *Journal of Engineering Mechanics* **133**(1), 122–125. doi: 10.1061/(ASCE)0733-9399(2007)133:1(122).

Myers, L. E. and Bahaj, A. S. (2010), 'Experimental analysis of the flow field around horizontal axis tidal turbines by use of scale mesh disk rotor simulators', *Ocean Engineering* **37**(2-3), 218–227. doi: 10.1016/j.oceaneng.2009.11.004.

Myers, L. E., Bahaj, A. S., Retzler, C. H., Pizer, D., Gardner, F., Bittencourt-Ferreira, C. and Flinn, J. (2010), D5.2 Device classification template, Technical report.

Noble, D., Draycott, S., Ordonez Sanchez, S., Porter, K., Johnstone, C., Finch, S., Judge, F., Desmond, C., Santos Varela, B., Lopez Mendia, J., Darbinyan, D., Khalid, F., Johanning, L., Le Boulluec, M. and Schaap, A. (2018), D2.1 Test recommendations and gap analysis report, Technical report, MaRINET2.

Noble, D. R., Davey, T. A. D., Smith, H. C. M., Kaklis, P., Robinson, A. and Bruce, T. (2015), Spatial variation in currents generated in the FloWave Ocean Energy Research Facility, *in* 'Proceedings of the 11th European Wave and Tidal Energy Conference (EWTEC2015)', Nantes, France.

Noble, D. R., Draycott, S., Davey, T. A. D. and Bruce, T. (2017*a*), 'Design diagrams for wavelength discrepancy in tank testing with inconsistently scaled intermediate water depth', *International Journal of Marine Energy* **18**, 109–113. doi: 10.1016/j.ijome.2017.04.001.

Noble, D. R., Draycott, S., Davey, T. A. D. and Bruce, T. (2017*b*), Testing marine renewable energy devices in an advanced multi-directional combined wave-current environment, *in* 'Proceedings of the ASME 36th International Conference on Ocean, Offshore and Arctic Engineering (OMAE2017)', Vol. Volume 7B:, ASME, Trondheim, Norway, p. V07BT06A020. doi: 10.1115/OMAE2017-62052.

Nortek (2013), 'Vectrino Profiler Technical Specification'. URL: `http://www.nortek-as.com`

Nortek (2018), 'How do I enhance Correlation and SNR ?'. URL: `https://www.nortekgroup.com/faq/how-do-i-enhance-correlation-and-snr` [Accessed: 2018-04-25]

Nwogu, O. (1993), Effect of Steady Currents on Directional Wave Spectra, *in* '12th Intl Conf on Offshore Mechanics & Arctic Eng', ASME, Glasgow, UK.

O'Neill, P., Nicolaides, D., Honnery, D. and Soria, J. (2004), Autocorrelation Functions and the Determination of Integral Length with Reference to Experimental and Numerical Data, *in* '15th Australasian Fluid Mechanics Conference', Vol. 1.

Padilla, L., Quinan, P. S., Meyer, M. and Creem-Regehr, S. H. (2017), 'Evaluating the Impact of Binning 2D Scalar Fields', *IEEE Transactions on Visualization and Computer Graphics* **23**(1), 431–440. doi: 10.1109/TVCG.2016.2599106.

Park, J. T., Cutbirth, J. M. and Brewer, W. H. (2002), Hydrodynamic Performance of the Large Cavltatlon Channel (LCC), Technical Report December 2002, Naval Surface Warfare Center, Carderock Division, West Bethesda, MD.

Park, J. T., Cutbirth, J. M. and Brewer, W. H. (2005), 'Experimental Methods for Hydrodynamic Characterization of a Very Large Water Tunnel', *Journal of Fluids Engineering* **127**(November 2005), 1210–1214. doi: 10.1115/1.2060740.

Pascal, R. (2012), Quantification of the influence of directional sea state parameters over the performances of wave energy converters, Phd, The University of Edinburgh, Edinburgh. URL: `https://www.era.lib.ed.ac.uk/handle/1842/7653`

Payne, G. S. (2008), Guidance for the experimental tank testing of wave energy converters, Technical report, SuperGen Marine, Edinburgh, UK.

Payne, G. S., Stallard, T. and Martinez, R. (2017), 'Design and manufacture of a bed supported tidal turbine model for blade and shaft load measurement in turbulent flow and waves', *Renewable Energy* **107**, 312–326. doi: 10.1016/j.renene.2017.01.068.

Payne, G. S., Taylor, J. R. M. and Ingram, D. M. (2009), 'Best Practice Guidelines for Tank Testing of Wave Energy Converters', *Journal of Ocean Technology* **4**(4), 38–70.

Peregrine, D. H. (1976), Interaction of Waves and Currents, *in* 'Advances in Applied Mechanics', Vol. 16 of *Advances in Applied Mechanics*, Elsevier, pp. 9–117. doi: 10.1016/S0065-2156(08)70087-5.

Peregrine, D. H. and Jonsson, I. G. (1983), Interaction of Waves and Currents., Technical report, U.S. Army, Corps Of Engineers. Coastal Engineering Research Center, Fort Belvoir, VA.

Pitt, E. (2009), Assessment of Wave Energy Resource, Technical report.

Plant, W. (2009), 'The ocean wave height variance spectrum: Wavenumber peak versus frequency peak', *Journal of Physical Oceanography* . doi: 10.1175/2009JPO4268.1.

Plymouth University (2017), 'Coastal, Ocean And Sediment Transport (COAST) laboratory'. URL: `https://www.plymouth.ac.uk/research/institutes/marine-institute/coast-laboratory` [Accessed: 2017-07-20]

Polagye, B. L., Epler, J. and Thomson, J. (2010), Limits to the predictability of tidal current energy, *in* 'Oceans 2010 MTS/IEEE Seattle', IEEE, Seattle, WA. doi: 10.1109/OCEANS.2010.5664588.

Pope, S. B. (2000), *Turbulent Flows*, Cambridge University Press, Cambridge. doi: 10.1017/CBO9780511840531.

Retzler, C. H. (2015), Critique of potential future work, Technical report, Wave Energy Scotland, Inverness, UK.

Ricci, P., Villate, J. L., Scuotto, M., Zubiate, L., Davey, T. A. D., Smith, G. H., Smith, H. C. M., Huertas-Olivares, C., Neumann, F., Stallard, T., Ferreira, C. B., Flinn, J. and Sorensen, H. C. (2009), D1.2 Recommendations from other sectors, Technical report.

Robinson, A., Ingram, D. M., Bryden, I. G. and Bruce, T. (2015*a*), 'The effect of inlet design on the flow within a combined waves and current flumes, test tank and basins', *Coastal Engineering* **95**, 117–129. doi: 10.1016/j.coastaleng.2014.10.004.

Robinson, A., Ingram, D. M., Bryden, I. G. and Bruce, T. (2015*b*), 'The generation of 3D flows in a combined current and wave tank', *Ocean Engineering* **93**, 1–10. doi: 10.1016/j.oceaneng.2014.10.008.

Robinson, S. K. (1991), 'Coherent Motions in the Turbulent Boundary Layer', *Annual Review of Fluid Mechanics* **23**(1), 601–639. doi: 10.1146/annurev.fl.23.010191.003125.

Salvatore, F., Iyer, A., Day, A. H. and Felice, F. D. (2014), D2.23 Review of Tow Tank Limitations, Technical report, MARINET.

Saruwatari, A., Ingram, D. M. and Cradden, L. (2013), 'Wave-Current Interaction Effects on Marine Energy Converters', *Ocean Engineering* **73**, 106–118. doi: 10.1016/j.oceaneng.2013.09.002.

Schäffer, H. A. (1996), 'Second-order wavemaker theory for irregular waves', *Ocean Engineering* **23**(1), 47–88. doi: 10.1016/0029-8018(95)00013-B.

Sellar, B., Harding, S. and Richmond, M. (2015), 'High-resolution velocimetry in energetic tidal currents using a convergent-beam acoustic Doppler profiler', *Measurement Science and Technology* **26**(8), 085801. doi: 10.1088/0957-0233/26/8/085801.

Shercliff, J. A. (1987), *The theory of electromagnetic flow-measurement*, Cambridge University Press.

Smith, J. M. (1997), Coastal Engineering Technical Note One-dimensional wave-current interaction (CETN IV-9), Technical report, US Army Engineer Waterways Experiment Station, Coastal Engineering Research Center, Vicksburg, MS.

Soulsby, R., Hamm, L., Klopman, G., Myrhaug, D., Simons, R. and Thomas, G. (1993), 'Wave-current interaction within and outside the bottom boundary layer', *Coastal Engineering* **21**(1-3), 41–69. doi: 10.1016/0378-3839(93)90045-A.

Spinneken, J. and Swan, C. (2009*a*), 'Second-order wave maker theory using force-feedback control. Part I: A new theory for regular wave generation', *Ocean Engineering* **36**(8), 539–548. doi: 10.1016/j.oceaneng.2009.01.019.

Spinneken, J. and Swan, C. (2009*b*), 'Second-order wave maker theory using force-feedback control. Part II: An experimental verification of regular wave generation', *Ocean Engineering* **36**(8), 549–555. doi: 10.1016/j.oceaneng.2009.01.019.

Steen, S. (2014), *Experimental Methods in Marine Hydrodynamics (lecture notes)*, NTNU, Trondheim, Norway.

Suastika, K. (2012), 'Nonlinear-Dispersion Effects in Modeling of Blocking of Stokes Waves', *Journal of Coastal Research* **283**(4), 829–842. doi: 10.2112/JCOASTRES-D-10-00112.1.

Sutherland, D. R. J. (2015), Assessment of mid-depth arrays of single beam acoustic doppler velocity sensors to characterise tidal energy sites, Phd, The University of Edinburgh. URL: `http://hdl.handle.net/1842/19559`

Sutherland, D. R. J. (2017), Tank Testing of Tidal Turbine Arrays, *in* 'IES Seminar Series', Edinburgh, UK.

Sutherland, D. R., Noble, D. R., Steynor, J., Davey, T. and Bruce, T. (2017), 'Characterisation of current and turbulence in the FloWave Ocean Energy Research Facility', *Ocean Engineering* **139**, 103–115. doi: 10.1016/j.oceaneng.2017.02.028.

Sutherland, J. and Barfuss, S. (2011), Composite Modelling, combining physical and numerical models, *in* '34th IAHR World Congress, Brisbane, Australia', Brisbane, Australia.

Taylor, G. (1938), 'The spectrum of turbulence', *Proceedings of the Royal Society A: Mathematical, Physical and Engineering Sciences* **164**(919), 476–490. doi: 10.1098/rspa.1938.0032.

Taylor, J. R. M., Rea, M. and Rogers, D. (2003), The Edinburgh curved tank, *in* 'Proceedings of the 5th European Wave and Tidal Energy Conference (EWTEC2003)'.

The IAHR Working Group on Wave Generation and Analysis (1989), 'List of Sea-State Parameters', *Journal of Waterway, Port, Coastal, and Ocean Engineering* **115**(6), 793–808.

Thomas, G. P. (1981), 'Wave-current interactions: an experimental and numerical study. Part 1. Linear waves', *Journal of Fluid Mechanics* **110**(1981), 457. doi: 10.1017/S0022112081000839.

Thomson, J., Polagye, B. L., Durgesh, V. and Richmond, M. C. (2012), 'Measurements of Turbulence at Two Tidal Energy Sites in Puget Sound, WA', *IEEE Journal of Oceanic Engineering* **37**(3), 363–374.

Thomson, J., Polagye, B., Richmond, M. and Durgesh, V. (2010), Quantifying turbulence for tidal power applications, *in* 'MTS/IEEE Seattle, OCEANS 2010', number 4, Ieee. doi: 10.1109/OCEANS.2010.5664600.

Valeport (2011*a*), 'Model 801 Electromagnetic Flow Meter Datasheet'. URL: `http://www.valeport.co.uk/Portals/0/Docs/Datasheets/Valeport_Model801_v2a.pdf`

Valeport (2011*b*), 'Model 802 Electromagnetic Flow Meter Datasheet'. URL: `http://www.valeport.co.uk/Portals/0/Docs/Datasheets/Valeport_Model802_v2a.pdf`

Venugopal, V., Davey, T. A. D., Smith, H. C. M., Smith, G. H., Holmes, B., Barret, S., Prevosto, M., Maisondieu, C., Cavaleri, L., Bertotti, L., Lawrence, J. and Girard, F. (2011), D2.2 Wave and Tidal Resource Characterisation, Technical report.

Vyzikas, T., Greaves, D., Simmonds, D., Maisondieu, C., Smith, H. C. M. and Radford, L. (2014), Application of numerical models and codes Task 3.4.4 of WP3 from the MERiFIC Project A, Technical report, University of Plymouth, MERiFIC, Plymouth, UK.

Warnock, J. (1950), 'Hydraulic similitude', *Engineering hydraulics* pp. 136–176.

Weber, J. (2007), Representation of non-linear aero-thermodynamic effects during small scale physical modelling of OWC WECs, *in* 'Proceedings of the 7th European Wave and Tidal Energy Conference (EWTEC2007)'.

Weisstein, E. W. (2017), '"Golomb Ruler" From MathWorld–A Wolfram Web Resource.'. URL: `http://mathworld.wolfram.com/GolombRuler.html` [Accessed: 2017-04-12]

WES (2015), Novel Wave Energy Converter Competition Tank Testing Guidance, Technical report, Wave Energy Scotland.

WES (2017), 'Wave energy information to be shared online'. URL: `http://www.waveenergyscotland.co.uk/news-events/wave-energy-information-to-be-shared-online/` [Accessed: 2017-08-07]

Wright, J., Colling, A. and Park, D. (1999), *Waves, tides, and shallow-water processes*, Pergamon Press, Oxford.

Yuce, M. I. and Muratoglu, A. (2015), 'Hydrokinetic energy conversion systems: A technology status review', *Renewable and Sustainable Energy Reviews* **43**, 72–82. doi: 10.1016/j.rser.2014.10.037.

Zaman, M. H. and Baddour, R. E. (2011), 'Interaction of waves with non-colinear currents', *Ocean Engineering* **38**(4), 541–549. doi: 10.1016/j.oceaneng.2010.11.015.

Zelt, J. and Skjelbreia, J. E. (1992), Estimating Incident and Reflected Wave Fields Using an Arbitrary Number of Wave Gauges, *in* 'Proceedings of the 23rd International Conference on Coastal Engineering', American Society of Civil Engineers, Venice, Italy, pp. 777–789. doi: 10.1061/9780872629332.058.

Zodiatis, G., Galanis, G., Kallos, G., Nikolaidis, A., Kalogeri, C., Liakatas, A. and Stylianou, S. (2015), 'The impact of sea surface currents in wave power potential modeling', *Ocean Dynamics* **65**(11), 1547–1565. doi: 10.1007/s10236-015-0880-4.

APPENDICES

Appendix A
Test Planning Tools — Flowcharts & Checklist

The collated test planning flowcharts are included over the following four A3 pages, with the checklist spreadsheet of all issues over the subsequent 10 pages.

Venn diagram of knowledge areas

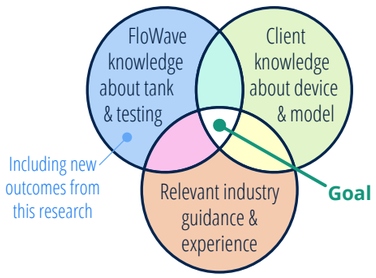

High level process

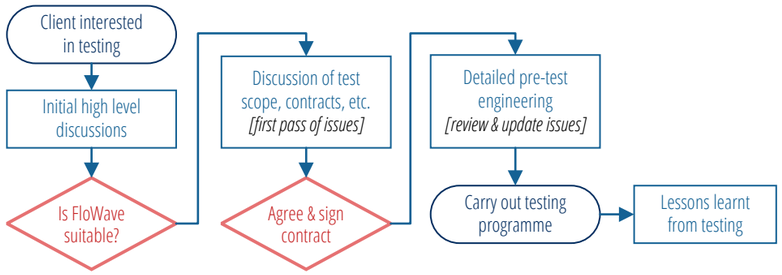

Key to symbols

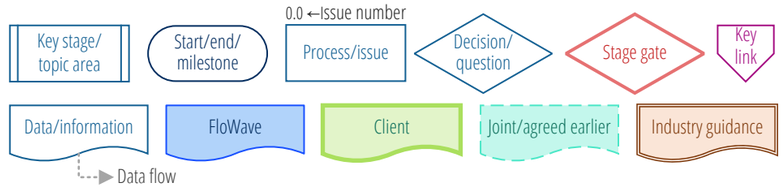

Overall framework showing 6 aspects

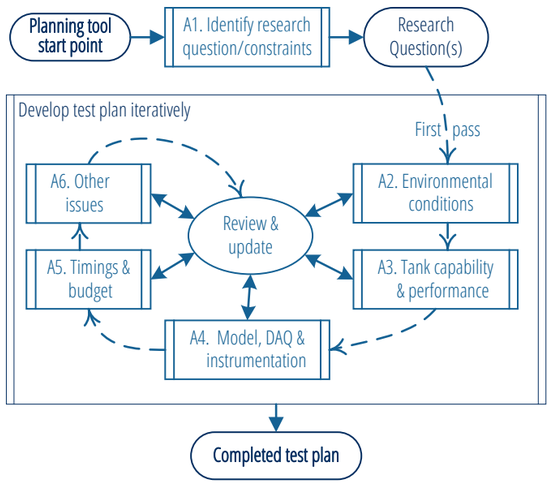

Aspect 1

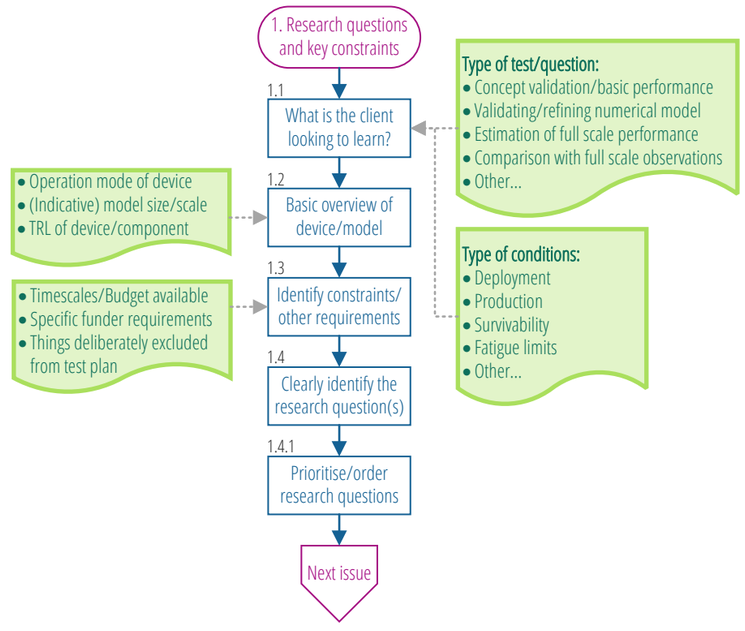

Aspect 2

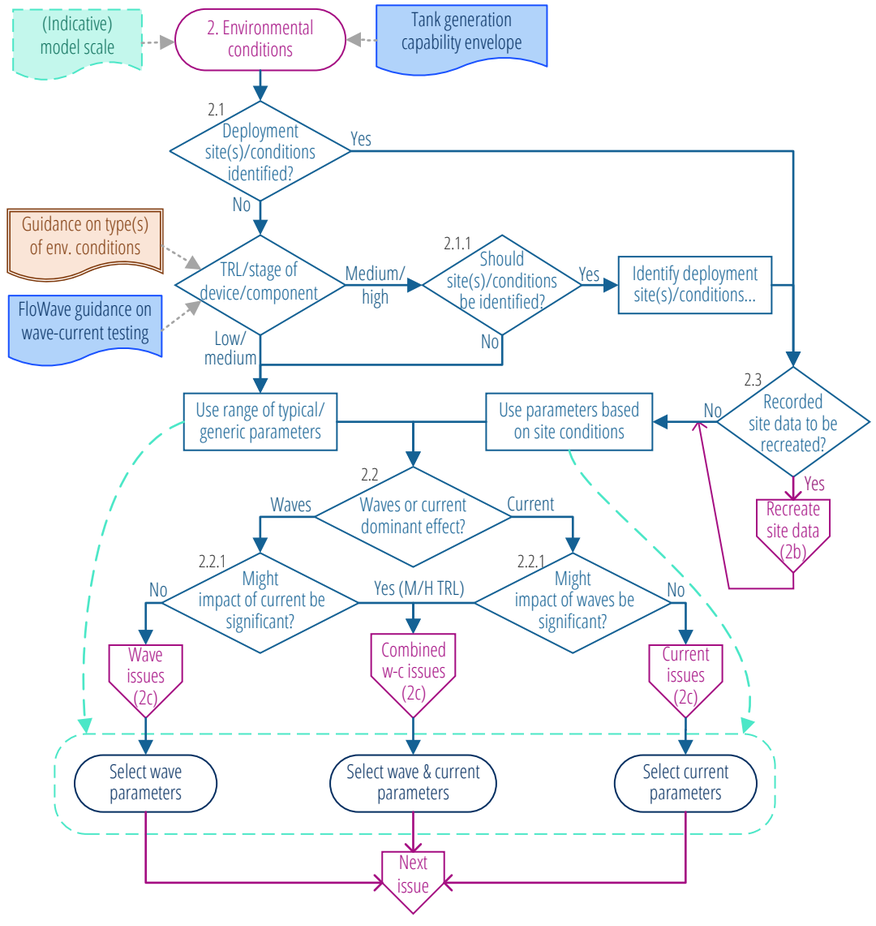

Aspect 2b

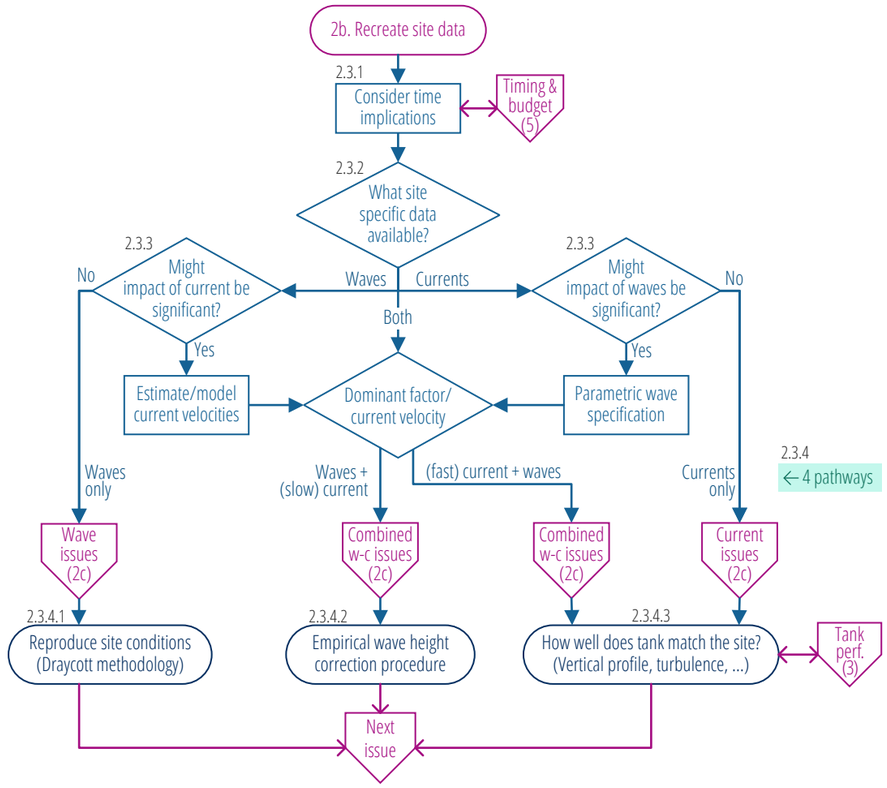

Aspect 2c

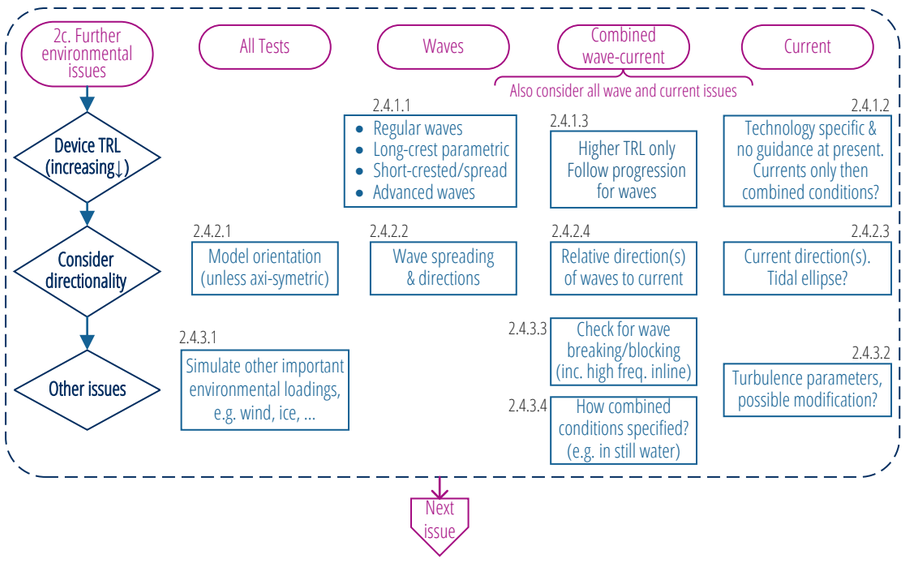

Aspect 3

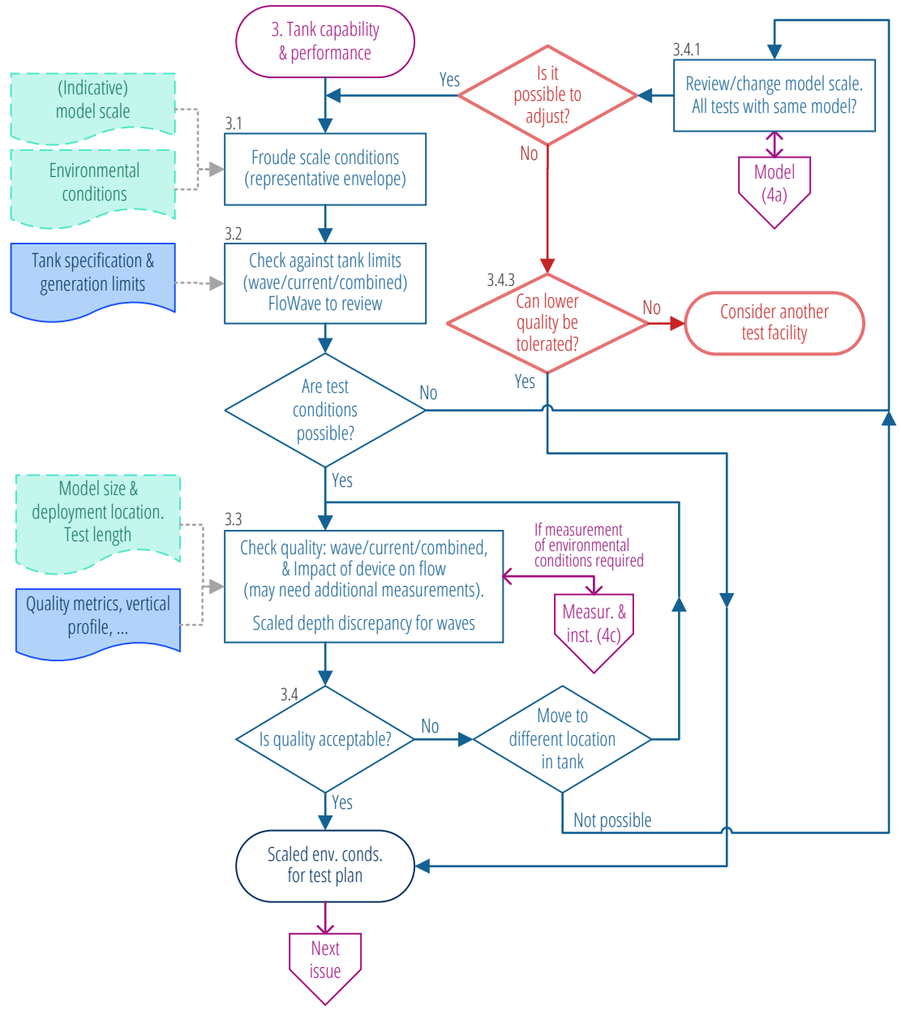

Aspect 4a

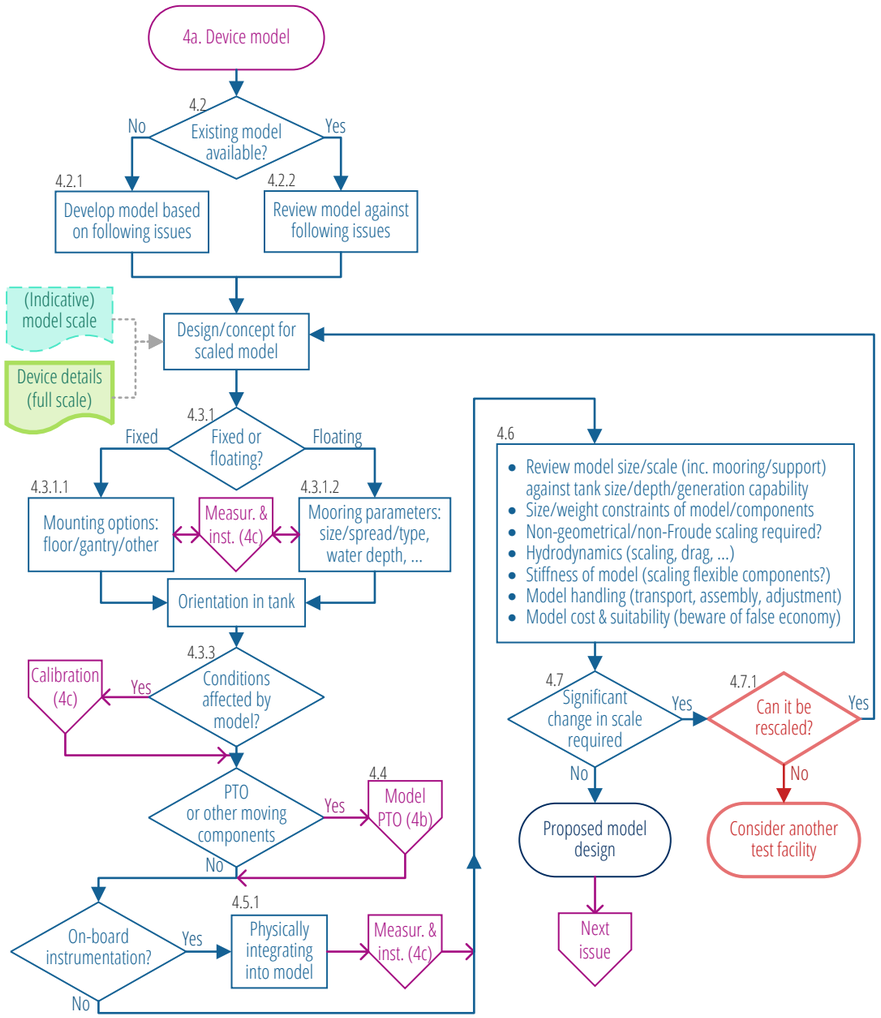

Aspect 4b

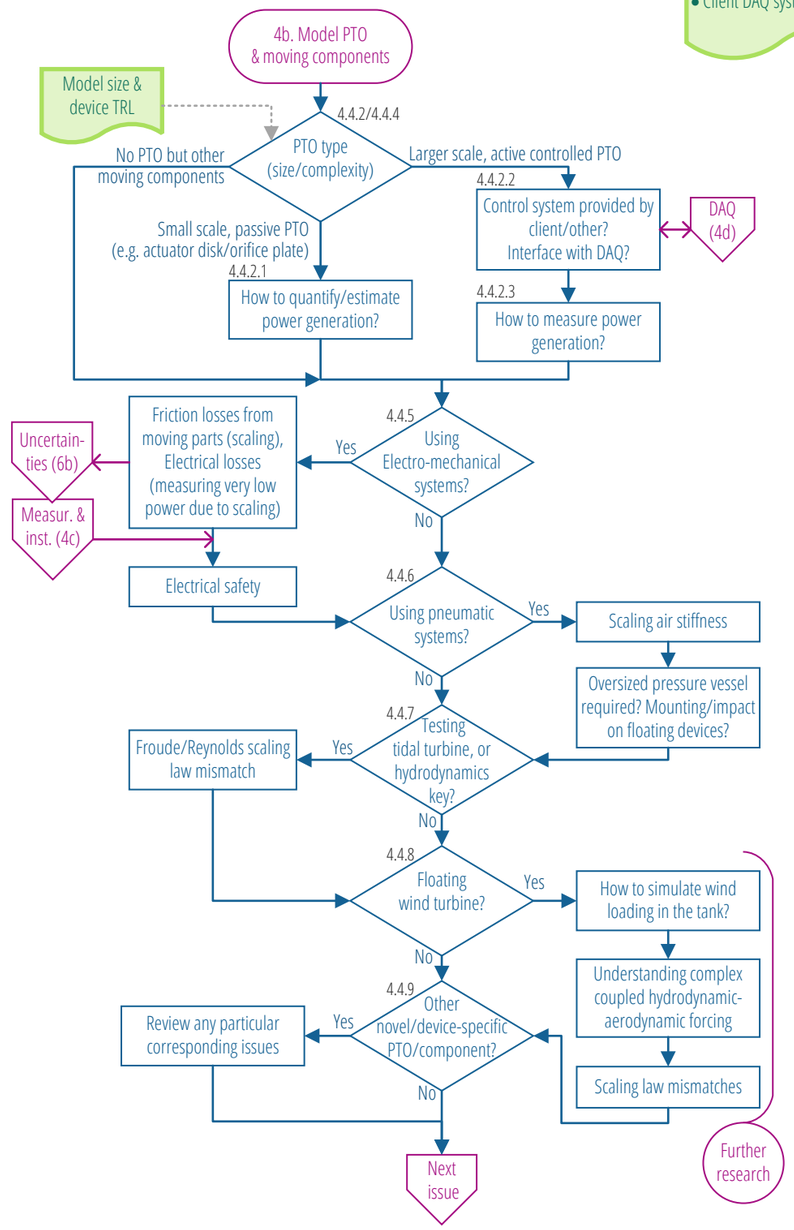

Aspect 4d

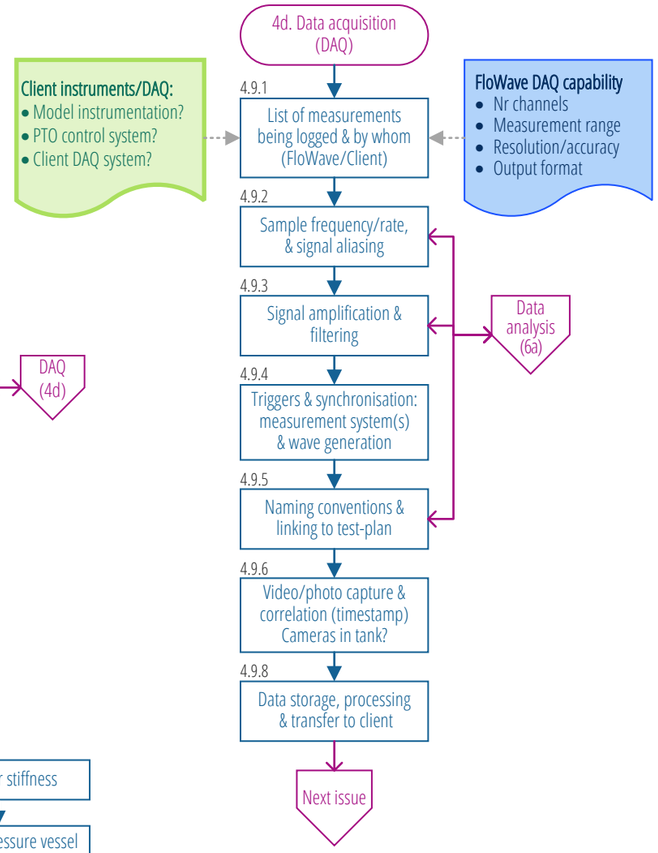

Aspect 4c

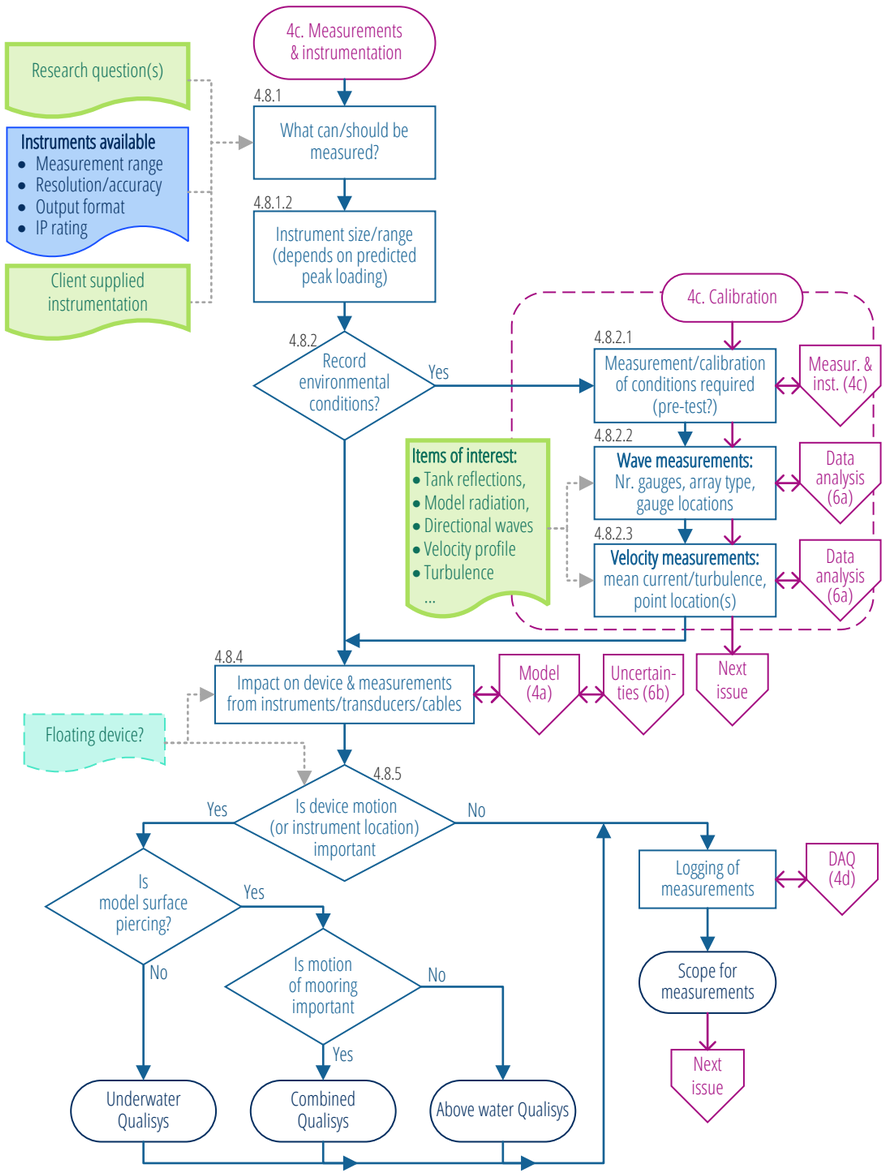

Aspect 5

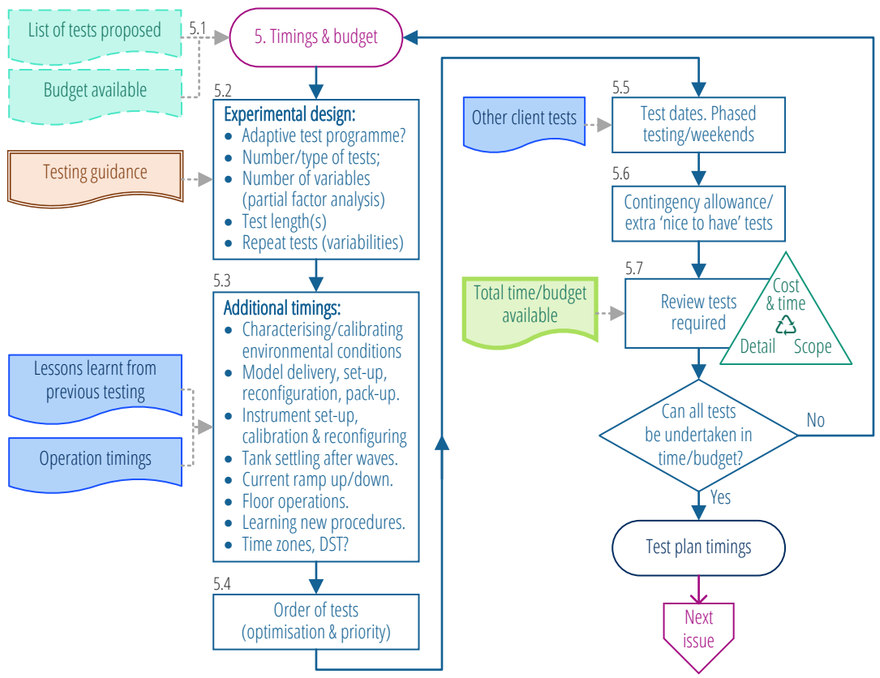

Aspect 6

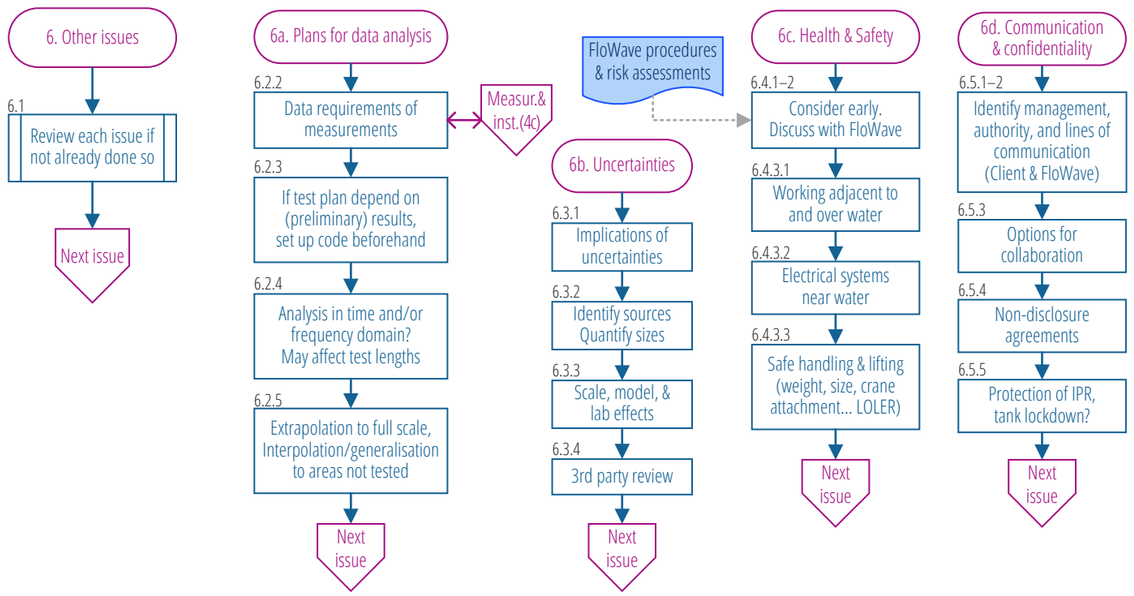

1. Consider each of the Issues/questions below. Complete "Select" and "Client comments" columns, green shaded boxes denote required answers, but can add comments to all.
2. Select importance, flexibility, review status, and actions as appropriate.
3. Review with FloWave, particularly any flagged issues, unknowns, and high priority issues still to be completed.

Aspect Nr.	Issue/question	Select Answer:	Client Comments
1.	**Identify research question and constraints**		
1.1.	*What is the client looking to learn from these tests?*		
1.1.1.	**Provide details** of the type(s) of test envisaged e.g.: concept validation and basic performance testing; validating and refining numerical models; estimation of the full scale device performance; comparison of the model with full scale observations; etc.		
1.1.2.	Also **provide details** of the type(s) of conditions of interest, such as: energy production, device deployment, survivability, assessing fatigue limits, etc.		
1.1.3.	Has a successful outcome from the tests been defined yet **(Y/N?)**	No	
1.1.3.1.	*If so* **provide details**		
1.1.3.2.	If not this should be considered		
1.1.4.	How well defined are the objectives of the test at this stage? **Rate as Loosely->Well defined**	Somewhat defined	
1.2.	Is there a model/device/instrument to be tested **(Y/N?)**	Yes	
1.2.1.	**Provide an overview** of the operation mode of the device, including how it is moored/mounted, how it moves (and generates power if applicable), etc.		
1.2.2.	Is there an existing model **(Y/N?)**	Yes	
1.2.2.1.	If yes: **provide details** of the physical size and scale.		
1.2.2.2.	*If not:* **provide details** of expected physical size and range of scales being considered		
1.2.3.	What is the development stage/TRL of device/component being tested as this influences other issues later on. **(H/M/L?)**	Medium	
1.2.3.1	Low = early stage concepts at TRL1-4, testing in simplified conditions (typically stage 1 testing).		
1.2.3.2.	Medium/High = (more) advanced concepts at TRL 3+, in more advanced conditions (typically stage 2 testing)		
1.3.	*The key constraints and requirements need to be identified:*		
1.3.1.	**Provide an outline** of timescales/budget available (indicative)		
1.3.2.	**Provide details** of any specific requirements from an external body (e.g. funders)		
1.3.3.	**Provide details** of any things deliberately excluded from the test plan (at this stage) in order to simplify it (e.g. wave loading on turbine blades, current loading on moorings)		
1.3.4.	**Provide details** of any other key constraints or requirements		
1.4.	The research question(s) shall be clearly identified, so that everyone involved in planning the tests is aware of the drivers.		
1.4.1.	If there are multiple research questions, these should be prioritised.		
1.4.2.	**Clearly state** the research question, or a prioritised list of research questions.		
2.	**Environmental Conditions**		
	[see guidance on development stage progression & high level tank generation envelope]		
2.1.	Has a specific deployment site, or conditions typical of deployment sites, been identified? **(Y/N?)**	No	
2.1.1.	If not, the client should consider if this is appropriate at this stage in the development of the device, particularly for medium/high TRL devices (Q.1.1.3.), and identify site(s) if required.		
2.2.	What type of environmental conditions will be used in the tank? **Select: Wave/Current/Combined**	Combined	
2.2.1.	*For wave or currents alone,* **consider the impact of a combined case**. The effect of wave-current interactions could be significant, either at the site or on the model performance. [Link to more details]		

Aspect Nr.	Issue/question	Select Answer:	Client Comments
2.2.2.	Representative current velocities and/or wave parameters should be estimated/modelled as required.		
	2(b) Site-specific environmental conditions		
2.3.	Will recorded site data be recreated in the tank as part of the test programme? **(Y/N?)** (normally at medium/high TRL only)	Yes	
2.3.1.	Consider the time implications for recreating site data.		
2.3.2.	**Provide a summary** of what data are available to be used, in terms of waves/currents/combined conditions? (e.g. summary statistics, multiple years of recorded data)		
2.3.3.	Again the impact of combined wave-current should be considered (Q.2.2.1.)		
2.3.4.	Methods to recreate recorded environmental conditions in the tank can be split into four pathways, depending on the presence/dominance of waves and currents: 1) Waves only 2) Current only 3) Waves with relatively slow currents 4) Faster currents with wave impact. This should be **discussed with FloWave**		
2.3.4.1.	*For waves only: the site data should be characterised and a representative set of tests developed (may already have been done). Methods outlined by FloWave (Draycott 2017), or others, may be used to assist with this.*		
2.3.4.2.	For waves with relatively slow currents: (≲0.2m/s in the tank, ≲1m/s at full scale, e.g. a wave energy device deployment site), the combined conditions should be reproduced in the tank using the iterative correction method developed by FloWave (Draycott, Noble, et al. 2018).		
2.3.4.3.	For currents only, or for faster currents with waves: how well the tank matches the full scale site data should be considered. It is not possible to control the current profile or turbulence produced in the tank at present, although this may change in future with further research.		
	2(c) Further issues to be considered on environmental conditions		
2.4.	The following issues **should be reviewed** depending on the type of environmental conditions (wave/current/combined) to be tested.		
2.4.1.	*Issues relating to development level:*		
2.4.1.1.	WAVES) The progression for wave-energy device is relatively clear and defined by guidance, broadly summarised as: regular waves; long-crested parametric spectra; short-crested parametric spectra; complex recorded spectra. This can also be applied to other floating devices.		
2.4.1.2.	CURRENTS) For devices in tidal currents, there is no defined progression in guidance. This is likely to be technology specific, with possible considerations being; one/multiple velocities, velocity changing over time, and matching the flow profile/turbulence of a site as best possible.		
2.4.1.3.	COMBINED) Combined waves and current is likely only to be used for higher TRL devices, as it leads to complex conditions and analysis.		
2.4.2.	*Issues concerning directionality:*		
2.4.2.1.	ALL) Model orientation with respect to the tank, plus waves and/or currents should be considered and discussed with FloWave, unless device (including moorings) is not directionally sensitive.		
2.4.2.2.	WAVES) Where short crested waves are planned, the spreading function(s) and range(s) shall be determined. These **should be specified in Q2.5.1.**		
2.4.2.3.	CURRENTS) Clients may wish to model oblique currents and/or (part of) the tidal ellipse if appropriate.		
2.4.2.4.	COMBINED) Relative direction(s) of waves to currents shall be determined with respect to the model orientation. This may affect waves that can be run, see Q2.4.3.4.		
2.4.3.	*Other issues:*		
2.4.3.1.	ALL) The client may wish to review other environmental conditions, such as wind loading, that are sufficiently important to consider simulating their effect during the model testing. **Provide comments** on any to be discussed with FloWave.		

Aspect Nr.	Issue/question	Select Answer:	Client Comments
2.4.3.2.	CURRENTS) Turbulence parameters and flow profile(s) for the deployment site should be summarised where known, for discussion with FloWave. Although it is not possible to change these at FloWave, it may be possible to select a location to best match the scaled flow, subject to other constraints.		
2.4.3.3.	COMBINED) Wave properties are altered by interaction with a current. A check shall be conducted on wave breaking and blocking [[link to explanation]] as some waves cannot physically exist when propagating against a current. It is also necessary to check high frequency waves following the current, as these may break on the recirculating flow in front of the wavemaker paddles.		
2.4.3.4.	COMBINED) The client shall specify how the waves and currents are defined. Wave-current conditions can be specified either as a combined field, (i.e. waves of a given height and period propagating over a fixed current velocity), or alternatively, the wave properties can be specified in still water before they interact with a defined current. The latter is how waves are generated in the FloWave Facility, and may have implications of the range of conditions that can be tested.		
2.5.	*A range of parameters to describe waves and current should be selected as appropriate.*		
2.5.1.	WAVES) Typical wave conditions should be **specified using FloWave Sea Generation Excel sheet**		
2.5.1.1.	Regular waves are specified by height and period (amplitude/frequency to be converted, specifying by steepness requires calculation)		
2.5.1.2.	Parametric spectra by type (JONSWAP/ITTC/etc.) and Hs/Tp/gamma (nb Pierson-Moskowitz is JONSWAP with gamma=1). Care required with specifying correct version of parameters, Tp, Te, Tz, etc.		
2.5.1.3.	Wave direction(s) to be defined for long-crested waves, or mean direction(s) and spreading function(s) for short-crested waves.		
2.5.1.4.	Other wave conditions, such as focused wave groups, to be included in test plan need to be documented as appropriate (not in sea generation spreadsheet)		
2.5.2.	CURRENTS) Should be specified as velocity(s) including direction(s) and any changes desired.		
2.5.2.1.	Define if velocity is depth averaged value, surface current, or for specific depth, and whether this is with or without the model installed		
2.5.2.2.	Additional parameters such as depth profile, turbulence intensity, etc. cannot be controlled in the tank at present, but it may be possible to select the best matching point in the tank. This should be discussed with FloWave		
3.	**Tank capability and performance**		
3.1.	Input environmental conditions should usually be Froude scaled to tank scale, to maintain ratio between inertial and gravitational forces, which are dominant in free surface waves.		
3.1.1.	A representative envelope of conditions to be used if final test conditions not known at this stage		
3.2.	**Check** the scaled conditions against physical tank generation limits (for wave/current/combined as appropriate) [[link]].		
3.2.1.	Any points close to the limits shall be reviewed with FloWave.		
3.2.2.	**Select whether** any of the scaled conditions are close to or outside the physical tank generation limits	Close to tank limits	
3.2.2.1.	**Review with FloWave any conditions close to the limits, as these may be possible.**		
3.2.2.2.	If it is not possible to generate the scaled environmental conditions, see Q.3.4.		
3.3.	How well the scaled conditions can be reproduced in the tank should be **reviewed with FloWave**.		
3.3.1.	This is subjective, so quality metrics [[link]] have been produced to assist.		
3.3.2.	Additional calibration measurements will be required to assess quality for a non-standard test or location in the tank. When testing a device in current, the installed model will change the flow in the tank. The impact of this must be considered, with adjustment to the flow speed and additional calibration as required.		

Aspect Nr.	Issue/question	Select Answer:	Client Comments
3.3.3.	Using an alternative position in the tank may give higher quality metrics, e.g. with less influence of reflections, however there may be limitations on model placement due to mounting etc. and reflections are frequency dependent. This should be reviewed if appropriate.		
3.3.4.	As part of the check on wave quality, wavelength errors resulting from a scale depth discrepancy should be considered [[Noble et al 2017]], especially where the device is sensitive to wavelength or steepness.		
3.3.5.	The quality of conditions in the tank may depend on model location and test length(s), as these can affect wave reflections.		
3.4.	Are scaled environmental conditions possible and at a reasonable quality? **(Y/N)**	No	
3.4.1.	**The proposed model scale should be reviewed** if not**.** It may be possible to adjust the model scale (smaller or larger) so that the required conditions can be recreated (at a higher quality). This may require the use of more than one model scale if there are large differences between the environmental conditions, e.g. using a smaller scale model to assess extreme survivability conditions.		
3.4.2.	*If the model scale is changed, all other constraints on model scale shall be reviewed again for knock on changes.*		
3.4.3.	If it is not possible to rescale such that the conditions can be generated at an acceptable quality, the use of a different test facility may be considered, unless lower quality conditions can be tolerated.		
4.	**Model and instrumentation**		
4.1.	Is a model/device to be tested **(Y/N?)**	Yes	
4.2.	Is there an existing model available? (see Q.1.1.2.)	Yes	
4.2.1.	YES) the following issues should be reviewed to check existing model is suitable for the proposed tests, and is a reasonable scale for the FloWave tank.		
4.2.2.	*NO) the following issues may provide guidance when developing the model.*		
4.2.2.1	*The starting point should be the design or a concept for the scaled device model, normally Froude scaled, although the exact model scale may not be known during the early stages. Details of the model shall be provided to FloWave (when known).*		
4.3.	*Mounting/mooring options*		
4.3.1.	**Provide details** of the proposed arrangement/concept for mounting/mooring the model, to be discussed/agreed with FloWave. Alternatively describe the full scale device. Note if it is fixed (i.e. bed mounted), floating, or other.	Fixed	
4.3.1.1.	For fixed devices, the mounting solution will normally involve the bolt points on the floor, or the 6-DoF load cell. Models may also be fixed to the tank sides, to the gantry, or some combination of these.		
4.3.1.2.	*Most floating devices will require mooring, and similar mounting constraints apply to the anchor points. Additional factors include the size and spread of the mooring, as well as the water depth. It may not be possible and/or desirable to model the entire geometrically scaled mooring solution.*		
4.3.1.3.	The mounting/mooring solution may be influenced by requirements for instrumentation (such as load cells, or Qualisys) and my determine model orientation in tank relative to gantry (see also Q.4.8 measurements and instrumentation)		
4.3.2.	Following discussion with FloWave, has a mounting/mooring solution been identified **(Y/N?)**	No	
4.3.3.	The presence of a model in the tank will change the environmental conditions in the tank, which should be considered and outcome noted		
4.3.3.1.	WAVES) ITTC guidance for floating platforms, recommends calibrating wave conditions at the model location, i.e. without a model in the tank.		
4.3.3.2.	CURRENTS) Flow in the tank may be particularly affected by larger TST models. Where a specific inflow is desired, additional calibration with the model in the tank will be required to achieve this. (see Q.4.8.2.)		
4.4.	***4(b) Model power take-off (PTO) & other moving components***		

Aspect Nr.	Issue/question	Select Answer:	Client Comments
4.4.1.	How the PTO is represented in the scale model is important, and one of the main challenges with tank testing renewable energy convertors. Many of the points below are also applicable to other moving parts in the model.		
4.4.2.	Does the model include some form of PTO? If so what type? **Select** For early development stages, and small scale models, it is common to represent the PTO using an energy sink or some other passive device. Larger models for later stages are more likely to use bladed turbines with a motor/generator to control the torque, or similar.	Active control	
4.4.2.1.	*For a passive control PTO representation, consider how to estimate/quantify the power generation of the device.*		
4.4.2.2.	The implementation of the control system will be device specific, details to be provided to FloWave including who is responsible for the control system, including interface with DAQ systems, etc. (see Q.4.9.)		
4.4.2.3.	For active control PTO. How will power generation be measured/quantified?		
4.4.3.	Are there any other moving components on the model **(Y/N?)**	No	
4.4.3.1.	*If so, these should be described (or sumarised if already covered in Q.1.1.1.)*		
4.4.4.	*Issues relating to PTO type or other moving components:*		
4.4.5.	Are electro-mechanical systems used **(Y/N?)**	Yes	
4.4.5.1.	Have friction losses from moving parts been addressed?		
4.4.5.2.	Electrical losses may be critical. Power output is Froude scaled by a factor of λ^3.5, which requires low voltages or currents to be measured. Voltage drop should also be considered.		
4.4.6.	Are pneumatic systems used **(Y/N?)**	No	
4.4.6.1.	*Consider the scaling of air stiffness. May require larger reservoir volumes, how this is incorporated especially important for floating devices*		
4.4.7.	Are hydrodynamics critical (e.g. tidal turbine) **(Y/N?)**	Yes	
4.4.7.1.	Consider mismatch between the Froude and Reynolds scaling laws (this may require non-geometric scaling of turbine blades or other components).		
4.4.8.	Testing floating wind turbine(s) **(Y/N?)**	No	
4.4.8.1.	*These are significantly more complex, and how to test these at scale is ongoing research, beyond scope of this guide. Some key issues include how to simulate the wind loading in the tank, understanding the complex coupled hydrodynamic-aerodynamic forcing, and the scaling law mismatches*		
4.4.9.	Other novel or device-specific PTO component **(Y/N?)**	Yes	
4.4.9.1.	These are likely to have particular issues relating to them, that should be addressed individually during the planning stage.		
4.5.	Does the model have on-board instrumentation **(Y/N?)**	Yes	
4.5.1.	Consider how this will be physically integrated into the model without adversely affecting motions/performance (see Q.4.8.)		
4.5.2.	Also consider measurement & instrumentation (see Q.4.8.)		
4.6.	The following common potential issues with models **should be considered**		
4.6.1.	Model size and scale needs to be appropriate for the tank, including moorings and support structure. The fixed 2m water depth and the wave/current generation limits may affect this (see Q.2.).		
4.6.2.	Are there any size or weight constraints imposed by the materials/components used to construct the model, e.g. tube sections, PTO motors/blades, instrumentation? This becomes less of an issue with bespoke manufacturing.		
4.6.3.	Is non-geometrical scaling required? E.g. to overcome scaling law mismatches, or to reduce size of mooring footprint?		
4.6.4.	The model hydrodynamics needs to match that of prototype, however direct geometrical scaling of every component may result in increased drag, particularly for small details, which should be considered		
4.6.5.	Stiffness of flexible components can be difficult to scale accurately; smaller models tend to be proportionately more rigid. Particularly important if flexure of the model is critical for the test, or impact loads to be tested/quantified		
4.6.6.	*Model handling:*		

Aspect Nr.	Issue/question	Select Answer:	Client Comments
4.6.6.1.	Will the model be disassembled for transportation and reassembled? (see also Q.5.3. on timings)		
4.6.6.2.	How will the model be lifted into the tank? (see Q.6.3. H&S)		
4.6.6.3.	How will minor adjustments be made to the model during testing? This should be discussed with FloWave, but note preliminary thoughts. E.g. raising tank floor, access by boat, lifting model out of water, etc. (again Q.5.3. on timings)		
4.6.7.	Model needs to be fit for purpose (Cheap models can be a false economy).		
4.6.7.1.	Delays caused by repairing broken or leaking parts can be expensive and mean the test plan has to be reduced.		
4.6.7.2.	Low quality components may also increase uncertainty in the results, reducing the effectiveness of the testing.		
4.6.7.3.	**Consider** if the budget is sufficient to get a suitably high quality model.		
4.7.	Do any of these issues above require the model size/scale to be changed significantly? **(Y/N?)**	No	
4.7.1.	*If so, can the model be rescaled?* **(Y/N?)** Go back and review issues with revised scale.	*Yes*	
4.7.2.	*If not possible to rescale, might need to consider an alternative test facility.*		
4.8.	***4(c) Measurements and instrumentation:***		
4.8.1.	The first question to ask is what can and should be measured?		
4.8.1.1.	This will be driven by the research question(s), but also be the availability of instruments to make the measurements and the capability thereof.		
4.8.1.2.	The size and measurement range of the instruments required will depend on the expected range of values to be recorded, and it may not be possible to record all tests accurately with the same instrument.		
4.8.2.	Are the environmental conditions in the tank (waves, currents) to be measured? **(Y/N?)**	Yes	
4.8.2.1.	Is this during the test and/or as a pre-calibration of the conditions? Additional time may be required to calibrate the conditions to exactly those desired, alternatively if the exact conditions are not critical the wave height and/or current velocity can be recorded during the test.		
4.8.2.2.	*For wave measurements:* Consider number of gauges, gauge positions, and array type. When setting the locations, it is important to consider what variables are (most) important, such as radiated waves from the model, reflections in the tank, and directional waves. This should be discussed with FloWave, but **note requirements**		
4.8.2.3.	*Measurement of current and turbulence:* This is more limited by the instruments available. Only point measurements of flow are presently possible at FloWave, therefore repeat tests are required to understand spatial variability. This has an impact on test duration (see Q.5. timings). This should be discussed with FloWave, but **note requirements**		
4.8.2.4.	The requirements for measurement arrays on the gantry may determine orientation of the test in tank (see also Q.4.3. mounting/mooring). This should be discussed with FloWave.		
4.8.3.	Are there any on board instruments as part of the model? (see Q.4.5.)	Yes	
4.8.3.1.	**Provide details**, including how these are physically integrated into the model, and connected/interfaced to the DAQ (see Q.4.9)		
4.8.4.	Has the impact on the model and/or the measurements from the measurement instruments themselves (including cables and frames etc.) been considered? Also think about mass distribution and scaling? (See Q.6.2. uncertainties).		
4.8.5.	Is device motion (or the location of instrumentation) important, and should this be measured with the motion capture system?	No	
4.8.5.1.	*As the above water system is easier to calibrate, it should preferentially be used where possible, such as on devices that are surface piercing.*		
4.8.5.2.	*If the motion of submerged components such as moorings is important, or the device is completely submerged, then underwater Qualisys cameras will be required.*		
4.8.5.3.	*It is also possible to use the two systems combined, however this has additional set-up time.*		

Aspect Nr.	Issue/question	Select Answer:	Client Comments
4.8.5.4.	*Qualisys can be used to track accurate positions of measurement instruments, such as wave gauges, that are being moved during testing.* **Note requirements**		
4.9.	***4(d) Data acquisition (DAQ)***		
4.9.1.	**List all parameters** being logged during testing. This includes data logged by client on their own DAQ system.		
4.9.2.	At what sample frequency should data be recorded? Higher sample frequency gives more data for analysis, albeit at the expense of larger data files and an increased potential for errors or bad data. It is also important to consider aliasing between signals.		
4.9.3.	Is signal amplification and filtering required? Consider details.		
4.9.4.	Discuss with FloWave how the measurements system(s) will be synchronised with the wave (and current) generation so that these can later be analysed as one. This is usually triggered by the tank clock but it may not be possible to synchronise all systems accurately, so may have to rely on timestamping or some other system.		
4.9.5.	Unique identifiers are required for each test, linked to the test log of what was actually run and when, recording any issues that arose during the test. FloWave has standardised file naming conventions to deal with multiple instruments and tests, but there may also be other identifiers used, such as Client references, sea-state or PTO configuration, etc. It is important to document these clearly, especially if there are any issues when testing.		
4.9.6.	Video and photographs are routinely collected during the testing, often on individual cameras/mobile phones. A means of collating and correlating these back to the test plan should be set-up beforehand.		
4.9.7.	Should cameras be mounted in or around the tank to film the experiment? Provide details of what requires filming.		
4.9.8.	Agree what test data to be provided to the client after the test. This includes file format(s), data processing, and timing.		
4.9.9.	Plans should be made for data storage and transfer, especially where large file sizes are anticipated.		
5.	**Timings and budget**		
5.1.	An initial idea of the timescales can be obtained 'bottom up' from the list of tests to be run and 'top down' from the budget available, however there is likely to be a mismatch.		
5.2.	**Consider** the experimental design, using available guidance including:		
5.2.1.	Is an 'adaptive test programme' proposed, i.e. where the results from initial tests are used to inform selection of the remaining test programme?	No	
5.2.1.1.	*If so discuss with FloWave what results and analysis are needed and when. (See also Q.6.2.)*		
5.2.2.	*The number and type of tests to be run:*		
5.2.2.1.	This will be a function of variables of interest, and the measurements to be made.		
5.2.2.2.	It may be advantageous to look at partial factor analysis, rather than running every combination of tests. [[see Equimar protocols]]		
5.2.3.	The length of individual tests will depend on the device and type of conditions.		
5.2.3.1.	For regular waves, a small number may be sufficient, requiring perhaps a 60s test.		
5.2.3.2.	Guidance for irregular sea states is usually to have 500-1000 waves to be statistically representative. [[see Equimar D3.3,D3.4]]		
5.2.3.3.	It is worth noting, particularly for short tests, that it can take around 30s for initial high frequency waves to reach the test area at tank centre, and this should be included when setting test length. Additional considerations are repeat/run times, and recording data after wavemakers stop generating.		

Aspect Nr.	Issue/question	Select Answer:	Client Comments
5.2.3.4.	For current and turbulence measurements, the period over which the flow can be assumed stationary is approximately 1 minute. [[link to details. Sutherland et al 2017]]		
5.2.3.6.	Consider trade-off between individual test length and number of tests that can be completed in a given time.		
5.2.3.7.	Consider conducting repeats of nominally identical tests, to help understand inherent variabilities in the tank, model, and experimental processes. Running these at different times of the day may flag issues with calibration drift for example.Particularly important for combined wave-current conditions with lower repeatability.		
5.3.	When determining timings need to **account for the following**. These additional aspects are often omitted or insufficient time allowed:		
5.3.1.	Characterising/calibrating the environmental conditions (if required). It may be possible to do this as part of pre-test engineering.		
5.3.2.	Client familiarisation with FloWave, including safety briefings and induction (typically ½–1hour)		
5.3.3.	Time for model delivery, unpacking, and set-up, plus disassembly and pack-up at the end of the test campaign. (Typically ½–1 day set-up plus ¼–½ day pack-up, but depends on model size and complexity)		
5.3.4.	Instrument set-up and calibration, both at the start of the test campaign and every morning (as required), which will depend on type/number of instruments.		
5.3.5.	Sufficient time should be allowed for the tank to settle between wave tests, or for the current to reach a steady state (typically 2–10 minutes).		
5.3.6.	Time also needs to be included for tasks such as floor operations (c.10 min each), and model/instrument reconfiguration between tests as required.		
5.3.7.	Additional time needs to be allowed when testing new set-ups/procedures, as staff/client will not be familiar with how best to do these, and some learning may be required		
5.3.8.	A minor point to be aware of is timing issues relating time zone(s) including changes for daylight savings time.		
5.4.	The **order of tests should be considered** at the detailed planning stage,		
5.4.1.	This should account for the priority of each test, so that the important tests can be completed early on in the test programme, in case of unforeseen problems.		
5.4.2.	As part of the test design, randomisation of the test order may be considered.		
5.4.3.	It may also be possible to optimise the programme by running the tests in a particular order to minimise the time spent on additional tasks, see Q5.3.		
5.5.	Dates for testing campaign shall be **agreed with FloWave**		
5.5.1.	This will obviously depend on the tank availability and other clients testing.		
5.5.2.	Some clients may wish to split testing into more than one visit, for example to allow a period of analysis in between two sets of tests. This has to be weighed up against the increased set-up and set-down, which has both time and cost implications, although unlikely to be double. It may also be possible to schedule testing across multiple weeks, giving time at weekend(s) for analysis.		

Aspect Nr.	Issue/question	Select Answer:	Client Comments
5.6.	**A contingency allowance should be included**		
5.6.1.	It can be easy to underestimate the time require for model set-up and calibration, and thus be over-optimistic about how much can be achieved within a test programme. Knowledge of previous tests are a useful benchmark when determining how long these processes will take. As a first estimate based on experience at FloWave, a 50% utilisation rate of good test data to overall test campaign length is reasonable, although this depends on test complexity, plus the length of individual tests and overall campaign.		
5.6.2.	Additional allowance should be allowed for more complex models or novel devices, as well as for using additional measurement instruments.		
5.6.3.	This contingency might be a list of 'nice to have' tests, that can be run at the end if all goes well, or if some of the planned tests cannot be run for whatever reason.		
5.7.	Once the list of tests and their timings are ascertained, **review against the total time and budget available.**		
5.7.1.	There will usually be some trade-off between the time/cost of the testing, the amount of detail covered, and the overall scope covered by the tests.		
5.7.2.	It may be necessary to review which tests are highest priority if not all are possible within the time/budget available.		
6.	**Other issues**		
6.1.	Many other issues can affect test planning. Some key ones are given here, which **should be reviewed** if not already done so. However this list is not exhaustive.		
6.2.	***6(a) Data analysis***		
6.2.1.	Plans for the analysis should be developed, at least partially, to make best use of the time available at the tank and make sure the correct data is collected.		
6.2.2.	List all the parameters to be recorded and data requirements of the measurements, such as sample frequency and record length, and who is responsible.		
6.2.3.	If the tests to be run depend on (preliminary) results from the testing (e.g. test 3 concepts, then further testing on best), ideally have code ready to process these results. FloWave may be able to provide example test results to show data formats, so that this code can be checked.		
6.2.4.	If a frequency domain analysis is planned, it is important that the sample rate and test length give frequency bins that match those of the wavemaker control, therefore test lengths are often set as a multiple of 2^n seconds. However it may also important to account for the initial wave ramp-up (see Q.5.2.2.3.)		
6.2.5.	Where the model represents a full-scale device, consideration should be given to how the model results will be scaled and extrapolated. In addition, it may be worthwhile thinking about interpolation and generalisation of the results to areas or cases not covered by the test plan and measurements, in case the test plan or measurements need to be revised.		
6.3.	***6(b) Uncertainties***		
6.3.1.	Considering possible implications of uncertainties prior to testing may flag up specific areas for concern. Some of these may be ameliorated by amending the test programme or the experimental set-up in some way.		
6.3.2.	Identify as many sources of uncertainty as possible, and estimate their likely size (even if this is qualitative).		
6.3.3.	These can be split into scale, model, and lab effects:		
6.3.3.1.	Effects resulting from testing at reduced scale, such as mismatch between scaling ratios, friction not scaling, etc.		
6.3.3.2.	Model effects, such as increased hydrodynamic damping from sharp corners, instrumentation cables affecting motion, etc.		
6.3.3.3.	Lab effects, resulting from the particular procedures of one facility versus another.		
6.3.4.	Getting a third party to review this may help identify other potential sources of uncertainty (the "unknown unknowns").		
6.4.	***6(c) Health & safety***		

Aspect Nr.	Issue/question	Select Answer:	Client Comments
6.4.1.	It is important to consider early on in the development how to conduct the test programme safely, as resolving issues later may involve significant reworking and additional costs.		
6.4.2.	This should be **discussed with FloWave**. Existing FloWave procedures for how to operate tank and conduct tests, as well as risk assessment for common tasks undertaken in the facility, shall be used to inform the development of a new test plan. Sufficient time shall be allowed to undertake all tasks safely.		
6.4.3.	*Three areas particularly of note are:*		
6.4.3.1.	Working adjacent to and over water. The most dangerous situation is when currents are being generated, as the recirculation could potentially drag someone who fell in the tank down towards the floor.		
6.4.3.2.	Electrical systems require proper design and implementation, particularly where mains voltages or powerful capacitors/batteries are involved. This should be done in line with FloWave risk assessments, including suitable emergency stop and isolation protection.		
6.4.3.3.	Safe handling and lifting of the model. Some models, or components, may be light and small enough to manhandle safely. If not, suitable lifting points shall be identified and a method statement developed for the lifting operations, in line with LOLER regulations.		
6.5.	***6(d) Communication and client confidentiality***		
6.5.1.	FloWave shall specify points of contact for different aspects of the test programme development and execution		
6.5.2.	The client shall specify who is responsible for authorising changes to the test plan during the test campaign. This is especially important where the client involves several partners or subcontractors.		
6.5.3.	There may be options for collaboration, whereby a small amount of extra work can give better results for all those involved. This can be discussed with FloWave.		
6.5.4.	Confidentiality will normally be dealt with by appropriate non-disclosure agreement between FloWave and the Client, including respective employees.		
6.5.5.	Any visits to the FloWave facility shall normally be agreed with the client in advance. In specific circumstances, to protect intellectual property rights further, access to the facility can be restricted further if required.		
	Remember this list is not exhaustive. Note any other issues/questions/remarks that arose during the discussion.		

Appendix **B**
Publications

Journal and conference publications resulting from this research project are included in chronological order over the following pages.

B.1. Noble, D. R., Davey, T. A. D., Smith, H. C. M., Kaklis, P., Robinson, A. and Bruce, T. (2015), Spatial variation in currents generated in the FloWave Ocean Energy Research Facility, *in* 'Proceedings of the 11th European Wave and Tidal Energy Conference (EWTEC2015)', Nantes, France. [8pp]

B.2. Sutherland, D. R. J., Noble, D. R., Steynor, J., Davey, T. and Bruce, T. (2017), 'Characterisation of current and turbulence in the FloWave Ocean Energy Research Facility', *Ocean Engineering* **139**, 103–115. doi: 10.1016/j.oceaneng.2017.02.028. [13pp]

B.3. Noble, D. R., Draycott, S., Davey, T. A. D. and Bruce, T. (2017*b*), 'Design diagrams for wavelength discrepancy in tank testing with inconsistently scaled intermediate water depth', *International Journal of Marine Energy* **18**, 109–113. doi: 10.1016/j.ijome.2017.04.001. [5pp]

B.4. Noble, D. R., Draycott, S., Davey, T. A. D. and Bruce, T. (2017*a*), Testing marine renewable energy devices in an advanced multi-directional combined wave-current environment, *in* 'Proceedings of the ASME 36th International Conference on Ocean, Offshore and Arctic Engineering (OMAE2017)', Trondheim, Norway. [9pp]

B.5. Draycott, S., Noble, D. R., Davey, T. A. D., Bruce, T., Ingram, D. M., Johanning, L., Smith, H. C. M., Day, A. H. and Kaklis, P. (2017), 'Re-creation of Site-Specific Multi-Directional Waves with Non-Collinear Current', *Ocean Engineering.* **152**, 391-403. doi: 10.1016/j.oceaneng.2017.10.047. [13pp]

Spatial Variation of Currents Generated in the FloWave Ocean Energy Research Facility

Donald Noble*[1], Thomas Davey*[2], Helen Smith†[3], Panagiotis Kaklis‡[4], Adam Robinson§[5], and Tom Bruce§[6]
*FloWave Ocean Energy Research Facility, University of Edinburgh, UK
†College of Engineering, Mathematics and Physical Sciences, University of Exeter, Penryn Campus, UK
‡Naval Architecture, Ocean and Marine Engineering, University of Strathclyde, UK
§Institute for Energy Systems, School of Engineering, University of Edinburgh, UK
[1]D.Noble@ed.ac.uk [2]Tom.Davey@ed.ac.uk [3]H.C.M.Smith@exeter.ac.uk
[4]Panagiotis.Kaklis@strath.ac.uk [5]Adam.Robinson@ed.ac.uk [6]Tom.Bruce@ed.ac.uk

***Abstract*—FloWave is a state of the art test facility which can produce combined waves and currents from any direction in a circular tank. Characterisation of this new facility is ongoing, with initial results from the flow generation measurements presented. This is a complex problem, considering different input velocities, 3D spatial variability of the flow in the X, Y, & Z directions, as well as temporal stability of the flow. In a circular tank, production of uniform flow is a non-trivial problem, however this has been achieved across a large test area using precise control of the individual drive units and specially designed turning vanes. This allows the testing of device models and small arrays, in controlled realistic sea conditions, prior to deployment at sea.**

***Index Terms*—Tank testing, tidal current, vertical flow profile, spatial variation, measurement, characterisation**

I. Introduction

Physical scale model testing is an essential element in the development of marine renewable technologies and techniques. Laboratory testing provides a repeatable, controlled, low-risk environment where technological concepts and operational techniques may be developed [1].

FloWave is a state of the art ocean energy research facility, designed to provide large scale physical modelling services to the tidal and wave energy sector. It has the unique ability to provide complex multi-directional waves combined with currents from any direction in the 25 m diameter circular tank.

As part of the commissioning and characterisation process for this new facility it is important to investigate the performance characteristics of the waves and current generation capability, both individually and in combination. It is also important to understand the shape and size of the usable test area. The focus of this paper is on the generation of currents, and specifically looking at spatial variation thereof.

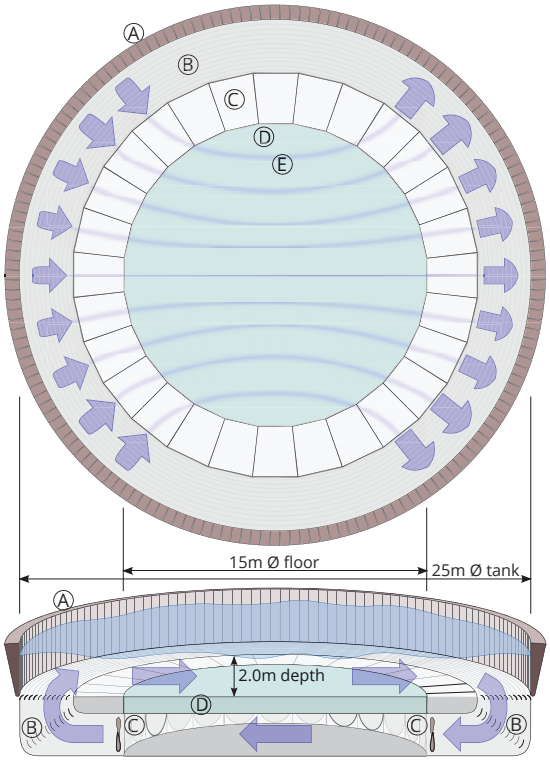

Fig. 1. Schematic of FloWave in plan and oblique section showing:
(A) Wavemaker paddles around circumference (168 Nr)
(B) Turning vanes and flow conditioning filters
(C) Current drive impeller units (28 Nr)
(D) Buoyant raisable floor (15 mØ) below test area
(E) Idealised streamlines of flow across tank floor

A. About the facility

FloWave is a circular combined wave and current test tank. Wavemakers are located around the entire circumference, with impellers to drive the current recirculation mounted in a plenum chamber below the test area, as shown in Fig. 1.

The tank is optimised for waves of around 2 s period, and is capable of generating currents upwards of 1.6 m/s. This offers the ability to model metocean conditions for most renewable energy devices at a typical scale of between 1:20 and 1:40 [2].

There is a 15 m diameter buoyant floor in the centre of the tank, which notionally represents the test area. This floor can be raised above the water level to facilitate model installation and reconfiguration as required, then submerged to the 2 m working depth.

Around the circumference of the tank there are 168 active-absorbing hinged wavemakers. These are able to generate regular and irregular waves, both long-crested and multi-directional, as well as complex multi-modal sea states with waves from multiple directions.

Currents are generated by 28 impeller units mounted in the plenum chamber below the test floor. Each of these contains a single 1.7 m diameter low-solidity 5-bladed symmetrical impeller, driven by a 48 kW motor. Turning vanes mounted below and in front of the wavemakers direct the current across the tank [3], as shown in Fig. 1. These turning vanes incorporate porous screens to provide flow conditioning and prevent debris ingress to the plenum chamber.

Creating a horizontally uniform current in a circular tank is a non-trivial matter, requiring precise control of the individual impellers [4]. In summary, the impeller units on either side of the required current direction on both the upstream and downstream side of the tank are driven at varying speeds to produce the required current corresponding to the desired test velocity. The control system for the impellers includes the facility to change the direction of the current during the test, either to an arbitrary angle or rotating by a set angle every minute. This capability allows for the simulation of cross-currents, or a tidal ellipse, without having to reposition the device model.

B. Device Testing and Scales

The development of new technologies generally follows an iterative process, refining and developing the initial concept, towards the goal of producing a viable product. A five-stage structured development plan has been developed for for wave energy systems [5], and this can be related to the Technology Readiness Level (TRL) concept developed by NASA [6]. With appropriate modifications, this process is also applicable for other marine renewable energy devices plus the supporting infrastructure, as captured by the EquiMar Protocols [1]. The development stages are reproduced in Table I, together with typical scales for marine renewable energy device testing. It is important to note that development is not a linear 'once-through' process, and that multiple loops through the different stages are typical.

Tank testing usually fits into the early development stages, proving preliminary concepts with small scale models and refining designs with larger models that are more detailed or more representative, before moving onto open water testing. As noted above, the FloWave facility is optimised for models around 1:40 to 1:20 scale, and so can be used for both concept and design validation. Depending on the specifics of the device and the constraints of the tank, both physical as well as the wave and current generation, it is possible to test at a broader range of scales.

It is not possible to accurately scale all physical phenomena by the same factor when undertaking physical model testing at a scale other than unity [7]. Given that gravitational forces are likely to be dominant in problems involving a free surface with waves, Froude scaling is used for most of the testing at FloWave. This is one of two dimensionless scaling factors commonly used in tank testing, the Froude and Reynolds numbers, respectively the ratios between inertia/gravity forces and inertia/viscous forces. In tank testing, both the small scale model and full scale prototype are immersed in the same fluid and are subject to the same gravitational force, therefore it is not possible to satisfy both relationships simultaneously.

Testing closer to full scale reduces the impact of these scaling effects, resulting in more accurate and representative testing. It is also difficult to include power take off and control systems in small models. Therefore testing physical models at a larger scale is a valuable stage in the development process between small scale models and open water testing.

Most marine renewable energy devices are intended to be installed in arrays, with multiple devices in close proximity. Therefore modelling inter-array effects is an important part of the design process, e.g. assessing the impact on power capture. The physical size of the facilities used to test marine renewable energy devices will place limits the number of individual units that can be tested in an array configuration. This is typically in the region of 2 to 7, but will depend on the shape and size of both the device and the test facility.

The results from physical model testing can then be used to validated computer numerical models. These computer models are typically used to simulate either performance at the level of an individual component or device, or the interactions between multiple devices which can be extended to cover large arrays of devices in a variety of different conditions, subject to sufficient computational resource.

II. Experimental Method

A series of tests were conducted to characterise the performance of currents generated in the facility. These were conducted with only the required measurement equipment in the tank, to avoid potential distortion of flow around a device model.

TABLE I
FIVE STAGES OF DEVELOPMENT, FOR WAVE AND TIDAL ENERGY DEVICES

Stage	TRL	Nominal scale	Typical infrastructure
1. Concept Validation	1-3	Small scale (c. 1:100-1:25)	University laboratory
2. Design Validation	3-5	Larger scale (c. 1:25-1:10)	Industrial scale laboratory
3. Systems Validation	5-6	Sub-prototype size (c. 1:4)	Benign test site
4. Device Validation	7-8	Approaching full size (c. 1:1)	Exposed test site
5. Economics Validation	9	Full size, small arrays	Commercial site

TABLE II
SIX DIMENSIONS OF VARIABILITY IN VELOCITY WITHIN THE FACILITY

Dimension of velocity variability	Symbol
Reference velocity magnitude	U_0
Spatial variation across the test area	X, Y
Vertical (shear) profile of velocity	Z
Different current directions	θ
Temporal variations in current	t

For effective testing, controlled steady flows need to be provided in the tank, with a vertical profile representative of real sites. It is also important to understand any variation in velocity throughout the test volume, so that the correct velocity can be specified for any model position.

As part of previous commissioning work, a calibration of velocity in the tank against primary control motor rpm was undertaken. This showed a linear relationship, and was used to set input velocities for these tests.

A. Test Plan

An initial measurement and characterisation program focusing on the performance of generating currents in the tank was developed, concentrating on the test volume at the tank centre. Characterisation of the FloWave facility is a complex multi-dimensional problem, as illustrated in Table II.

The first phase of testing, presented here, considers the spatial variability of the generated current over a range of baseline velocities. Measurements were made of the vertical profiles of velocity, and of the spatial variation of velocity across the plan area of the tank. These cover the horizontal components of velocity for the vertical plane ($X - Z$) and horizontal plane ($X - Y$) for different input velocities (U_0). The tank is designed to be rotationally symmetrical, and therefore current direction is not discussed here. Measurement of temporal variation and turbulence is ongoing, but initial results showing the temporal stability of the facility are presented.

1) Tank Coordinates and Terminology: The tank coordinate system is Cartesian, as shown in Fig. 2, with the origin at the centre of the tank on the test floor, and Z positive upwards. Waves and currents are specified as positive in the direction of the vector, as opposed to the nautical convention of waves coming from a direction. Currents flow from upstream to downstream, with left and right assuming a viewpoint looking downstream in the direction of the current.

B. Test method

All tests were run with a current direction of 0°, i.e. flow in the $+X$ direction. At least 10 minutes was allowed for the current to fully stabilise following changes in velocity before taking measurements of the steady state condition. The results from the temporal stability test, Section III-A, demonstrates that this is sufficient.

For testing with only current, the wavemakers are powered down and rest on their backstops. This results in the water level in the tank dropping by approximately 80 mm. This

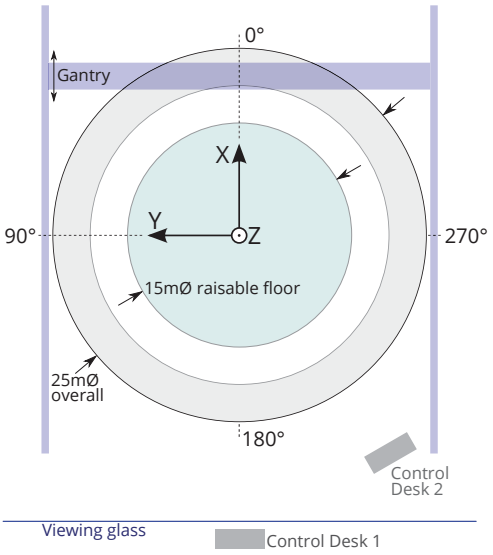

Fig. 2. Tank reference coordinates

configuration was used for all tests, with a water depth in the test section of 1.93 m. Water temperature during the tests was approximately 15°C.

1) Measurement of vertical profiles: Vertical profiles of velocity were measured to determine both the variation in velocity with depth and input velocity ($U_0 - Z$) and also the spatial variation in velocity profiles across the tank ($X - Z$).

Tests were undertaken at a range of nominal target velocities, specified for the centre of the tank 1.5 m above the floor. These were the tank's design velocity specification of 0.8 m/s, a typical low end test velocity of 0.2 m/s, and three additional intermediate velocities of 0.42 m/s, 0.5 m/s, and 0.58 m/s. The preliminary calibration of velocity in the tank against primary control motor rpm was used to set these velocities. The variation in the vertical profile with input velocity was measured at the tank centre throughout the whole water column.

The development of the vertical profile, from the turning vanes across the usable test area, was characterised by a vertical slice along the flow direction. A series of seven velocity profiles were measured at 2.5 m horizontal spacing along the direction of current, covering the full diameter of the raisable floor. Velocity measurements were taken throughout the whole depth of the water column at each location.

For these tests, a Valeport model 801 single-axis electromagnetic (EM) current meter with a flat-type sensor head for which the sensing volume is a cylinder of approximately 20 mm Ø $\times$ 10 mm high. [9]. This was mounted to a height-adjustable bracket fixed to the gantry across the tank, with the sensor cable helically wrapped around the supporting pole to reduce the effects of vortex induced vibration. The raw ASCII output from the Valeport control display unit was logged directly to a laptop for further processing.

To measure each vertical profile, the sensor was lowered to the base of the tank (Z = 0.05 m), and data logged at 2 Hz for 60 seconds. It was raised by 0.05 m to the next measurement position, and the process repeated. In total 38 measurements were taken for each profile (Z = 0.05 m to Z = 1.90 m). Repeat measurements confirmed the temporal stability over the time taken to measure each profile. Vertical position was measured with a 0.5 mm graduated scale fixed to the height adjustable bracket. The gantry position was measured with a laser range finder. A small degree of lateral vibration was observed during some tests, with the sensor head moving by approximately $\pm$10 mm at around 1-2 Hz, however it is not anticipated that this will affect the averaged inline velocity.

2) Measurement of spatial variability in plan: To determine the planar extents of the usable test area, plus any variation in velocity therein, the velocity was measured on a number of horizontal transects across the tank, both along and transverse to the flow direction. This was conducted at three nominal velocities, 0.2 m/s, 0.5 m/s, and 0.8 m/s.

These tests used two separate 2-axis EM current meters, Valeport model 802 fitted with a 32 mm discus-type sensor head, for which the sensing volume is a cylinder of approximately 32 mm Ø $\times$ 16 mm high [10]. The two sensors were fixed 2 m apart onto a carriage mounted frame that could be moved along the gantry to set the Y-position in the tank. The X-position in the tank was adjusted using translation of the gantry as before. The sensor height was fixed at 1.5m above the floor for all tests (i.e. 0.43 m below the water surface), with the supporting frame mostly above the water level.

At each data point the raw ASCII output was recorded at 8 Hz over a 60 s period. The mean u and v horizontal velocity components, plus the horizontal velocity vector $\vec{U}$, were then calculated. The measured data points were interpolated to a regular 0.1 m grid in MATLAB using a triangulation-based natural neighbour approach.

3) Measurement of long duration temporal variation: As a first measure of the temporal stability of the tank, the current ramp-up from rest and the subsequent stable flow was measured for a period of 20 minutes. The measurement was taken at the tank centre at 1.5 m above the floor, with a nominal velocity of 0.48 m/s at 50 rpm.

This longer duration temporal variation test was undertaken in a similar manner to the spatial plan tests, with a single Valeport 802 discus-type sensor. At the start of the test the primary drive motor was increased to 50 rpm in 5 steps over approximately 1 minute, and then held at this speed throughout the test.

III. Results

A. Temporal variability

Conditions in the tank need to be consistent over the duration of the test and repeatable between tests, in order to undertake useful model tests. The normalised velocity profiles in Section III-B show that conditions in the tank are self-similar and scaleable between different velocities.

As an example of the temporal stability of the tank, Fig. 3 shows a test where the motors were ramped up to 50 rpm and held at that speed for 20 minutes. During this test, velocity in the centre of the tank increases asymptotically, to within 10% of target after approximately 2 minutes, and reaches a stable velocity after 5 or 6 minutes. The flow remains stable thereafter, with only minor fluctuations.

B. Variation of Vertical Profile with Velocity

Vertical profiles of velocity were measured at the centre of the tank for five nominal input velocities, shown in Fig. 4. The drive motors have a linear relationship between rpm and flow, which is confirmed by these tests, the depth-averaged velocity increases in a linear manner with nominal velocity, see Fig. 5. The depth-averaged standard deviation increases as a power law, with an exponent just below unity.

The shape of the vertical profile of velocity in the tank is almost independent of average velocity, as shown by the similarity between the normalised velocity plots in Fig. 6a. This is most closely described by a 1/15th power law, Fig. 6b, although it is not dissimilar to other profiles used within the industry.

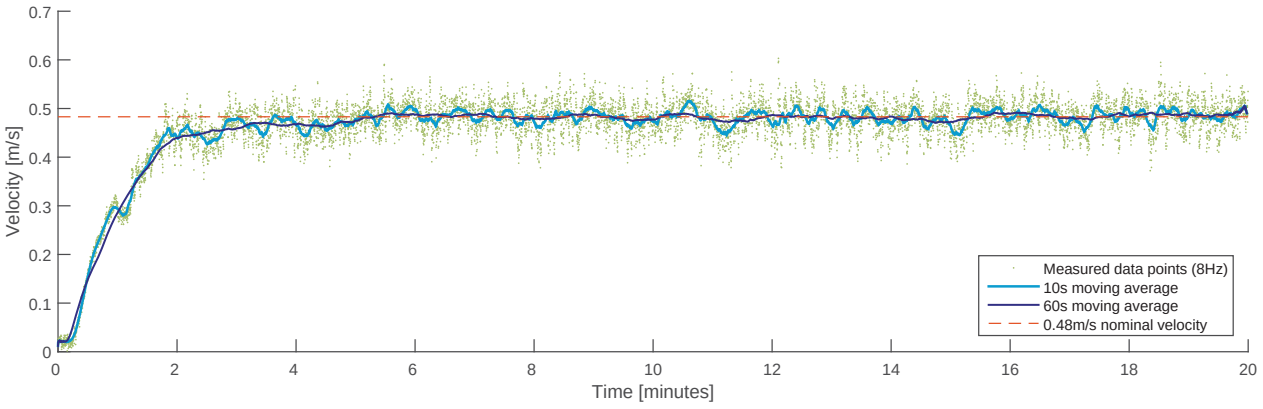

Fig. 3. Temporal stability test, showing velocity at the centre of the tank 1.5 m above floor, over the 20 minute test duration

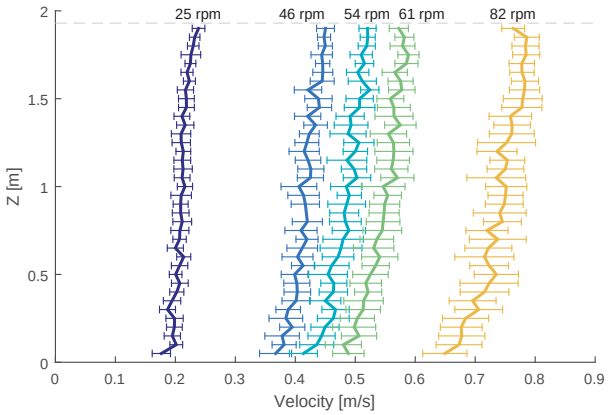

Fig. 4. Vertical velocity profiles measured at tank centre for different input drive motor rpm, with error bars showing $\pm 1\sigma$ deviation, and water surface at 1.93 m shown dashed grey

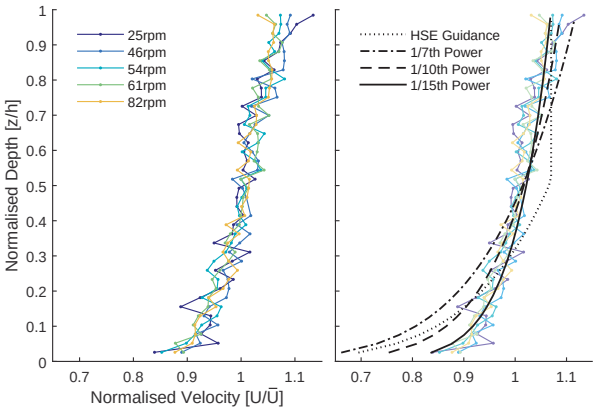

Fig. 6. Normalised vertical velocity profiles measured at tank centre, showing a) different input drive motor rpm, and b) these profiles overlain with various theoretical models

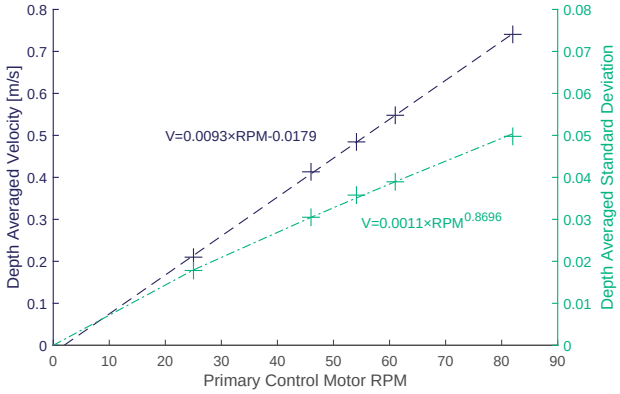

Fig. 5. Depth averaged velocity and standard deviation against primary control motor rpm, showing linear relationship

C. Development of vertical profile along flow direction

The vertical profiles across the 15 m diameter floor were used to construct a vertical slice through the tank, parallel to the direction of flow and passing through the centre, Fig. 7. This shows an increase in flow speed towards the centre of the tank, a result of the converging nature of the flow in this region that is required to create uniform flow in a circular tank, as discussed above.

There is a significant velocity deficit in the lower part of the water column at the extreme 'upstream' edge of the floor (X = -7.5 m). Above this is a jet of higher velocity flow, approximately 0.6 m to 1.0 m above the floor. Both of these features are clearly apparent in the vertical profile Fig. 8a, and are a result of the current rising at an angle from the turning vanes.

Close to the centre of the tank, in the middle of test area, is a relatively uniform section of flow. This covers approximately X = -2.5 m to X = +5.0 m in the lower part of the water column, and X = $\pm$10 m in the upper half of the water column. At the 'downsteam' edge of the floor (X = 7.5 m) the velocity throughout the water column reduces, as a result of the flow diverging into the tuning vanes around that half of the tank.

D. Spatial variability of velocity across the plan area

The spatial variation in flow across the central section of the tank is shown in Figs. 9 and 10 for three nominal velocities. This shows the velocity magnitude to be broadly symmetrical about the current flow direction. It is also relatively consistent (around $\pm$10% or $\pm$0.05 m/s) across a test area approximately 8 to 10 m wide and 6 m long, which is offset about 1 m downstream of the tank centre.

The measurements show a slight asymmetry in the velocity magnitude, with marginally faster flows ($< 5\%$) on the right hand side of the flow. There is also marginally slower flow ($\approx 5\%$) along the centreline of the current near the middle of the tank. The velocity vector plots in Fig. 11 show that an acceptable horizontally uniform flow can successfully be created in the circular tank, with only a slight directional bias around the outside of the raisable floor.

IV. Discussion

Physical model testing is a well-established practice in the development of new technologies. Experiments in a tank facility offer more control over test parameters than conducting open water testing, however this requires the facility to be well calibrated. Dedicated test facilities are also able to produce the desired conditions on demand, rather than being dependent on the vagaries of the weather.

A. Velocity Calibration and Stability

Measured velocity at a reference point in the tank needs to be calibrated against the control input, the primary drive motor rpm. Together with a transfer function based on the velocity variations measured throughout the tank, this allows a prescribed velocity to be produced at any particular location in 3D space above the test area floor.

The depth averaged velocity in the tank has been shown to vary linearly with drive motor rpm. This allows for accurate control of the reference velocity in the tank. Initial test results demonstrate that the tank can also produce a stable current over time. There are minor fluctuations around this stable current that may be due to large scale turbulent structures, and further work is required to investigate this.

B. Velocity Shear Profile and Comparison with Theory

The 1/7th power law is frequently used to describe the vertical distribution of velocities fluid flow. This was originally developed to model boundary layer effects in turbulent pipe flow, however it is often applied to tidal flow in coastal regions. Other power law profiles, such as 1/10th, are also commonly used. Guidance by the UK Health and Safety Executive [11] suggests the following discontinuous function for the velocity profile for coastal seas around the UK with a uniform velocity in the upper half of the water column.

$$U = \begin{cases} \left(\frac{z}{0.32h}\right)^{\frac{1}{7}} \bar{U}, & 0 \leq z \leq 0.5h \\ 1.07\bar{U}, & 0.5h \leq z \leq h \end{cases} \quad (1)$$

where $\bar{U}$ is the mean volumetric flow velocity, h the water depth, and z the position in the water column.

In reality, flow in highly energetic tidal flows is far more complex than a simple vertical shear profile, with significant effects from large scale turbulent eddies and bathymetry effects. Measurements undertaken at the European Marine Energy Centre (EMEC) tidal test site at the Fall of Warness as part of the ReDAPT project show complex shear profiles, with the velocity at the surface significantly less than at points lower in the water column for some states of the tide [12], [13].

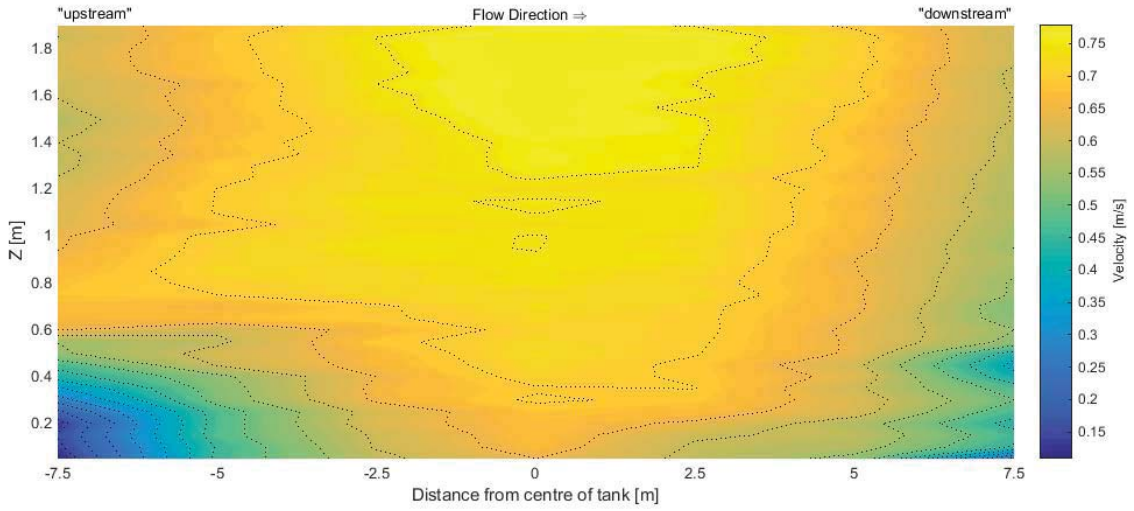

Fig. 7. Vertical section across the tank in line with flow, for nominal 0.8 m/s input velocity. Flow direction left to right.

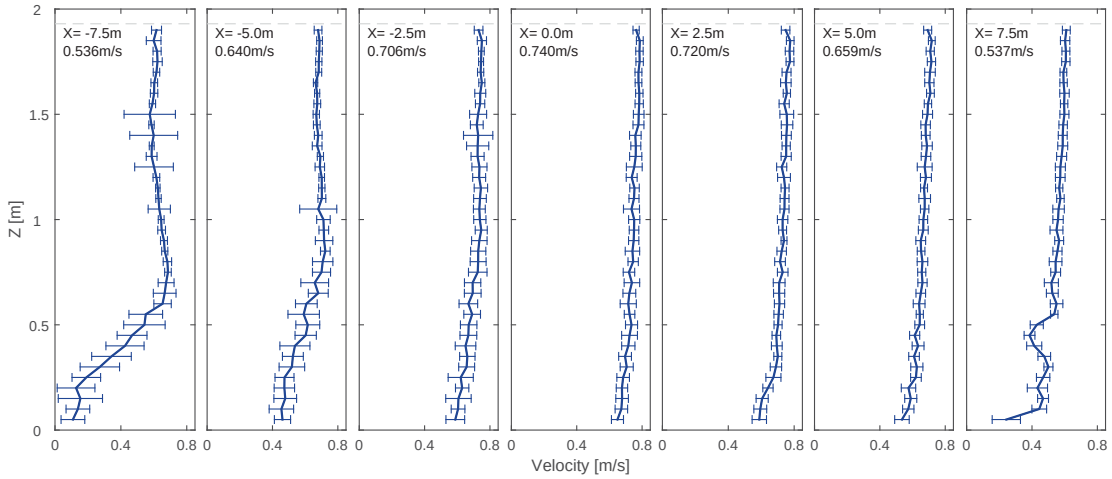

Fig. 8. Vertical velocity profiles across the tank in line with flow, at X coordinates noted. Nominal 0.8 m/s input velocity, with depth averaged velocity given for each profile location. Error bars show $\pm 1\sigma$.

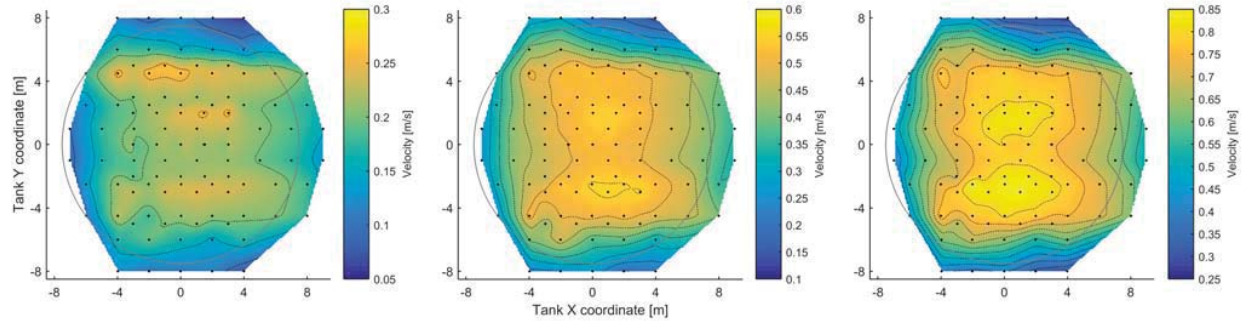

Fig. 9. Variation in velocity across test area for horizontal plane 1.5 m above floor. Three different nominal input velocities: a) 0.2 m/s b) 0.5 m/s c) 0.8 m/s, with flow direction from left to right. Measurement points indicated by + marker, 15 m diameter raisable floor shown as a grey circle

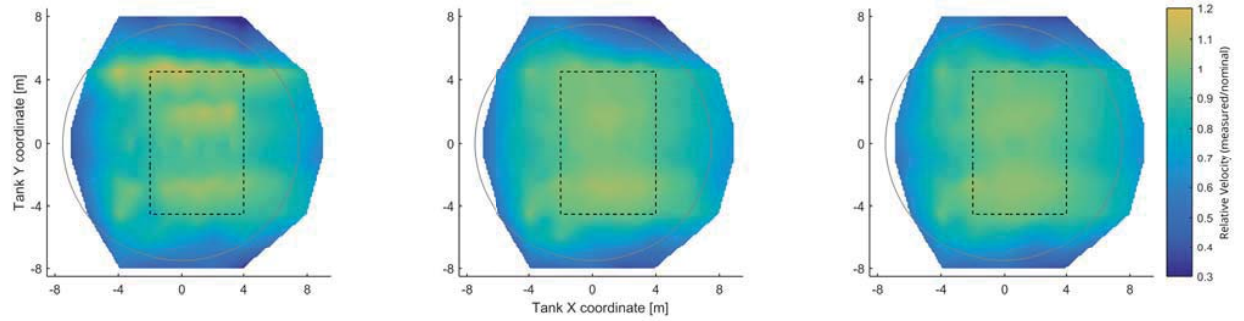

Fig. 10. Variation in velocity, relative to nominal input, across test area for horizontal plane 1.5 m above floor. Three different nominal input velocities: a) 0.2 m/s b) 0.5 m/s c) 0.8 m/s, with flow direction from left to right. Nominal test area shown by black dashed rectangle, 15 m diameter raisable floor shown as a grey circle.

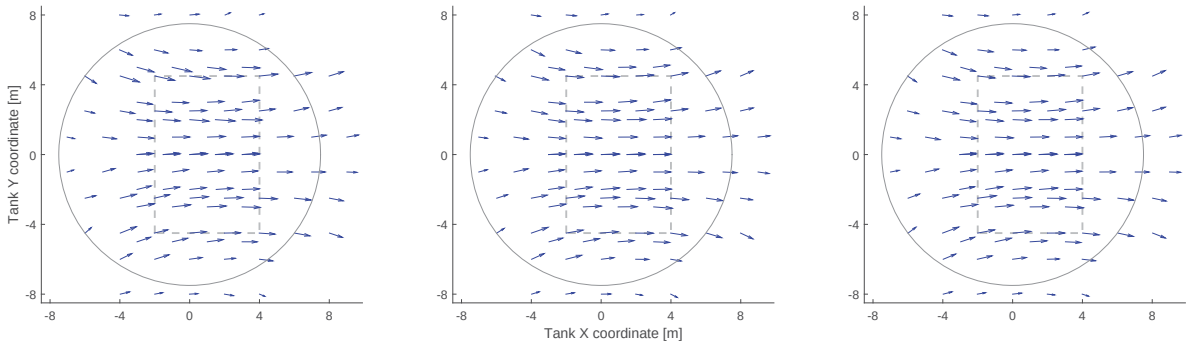

Fig. 11. Velocity vectors across test area for three different nominal input velocities: a) 0.2 m/s b) 0.5 m/s c) 0.8 m/s. Vector length is proportional to velocity at measurement point relative to input velocity. Flow direction from left to right. Nominal test area shown by grey dashed rectangle, 15 m diameter raisable floor shown as a grey circle.

The flow profile at FloWave was found to be close to a 1/15th power law, which is reasonably similar to observed and theoretical profiles. By increasing the roughness on the test floor, and/or using different spatial locations in the tank, it should be possible to model a range of different flow profiles. This offers the ability to model differential loading at varying water depths, something that is of concern for developers of tidal turbines.

The development of the shear profile across the tank, shown in Fig. 7, follows the trend of previous work on inlet design for combined wave and current test facilities [3]. This work was undertaken in a flume channel, with a range of inlet vane angles, so is not directly comparable to FloWave. However the jet of water above mid depth with a region of slower flow below was clearly present in those tests as well as the accompanying CFD model.

C. Spatial Variability and Usable Test Area

The usable test area in the tank is at least 50 m^2, which is large enough for testing small arrays of devices. Whilst there is some variation in velocity over this area, it is only around 10% in plan and in depth. Knowing this baseline variation allows a reference velocity to be calculated at any point in the tank, or device in an array. Theoretical forces can then be predicted with a computer model and compared to those measured, for example. In addition, velocity measurements are typically made at a point close to the model during testing.

D. Flow Field in a Circular Tank

The tests undertaken show that across the test area, the flow is acceptably straight and horizontally uniform. This allows consistent testing over a large area of the tank, for example, to investigate impacts between small arrays of devices. However the configuration of a circular tank, with circumferential wave-makers and impeller drive units below the floor, by necessity leads to non-uniformities in the current flow field around the turning vanes. The extent of non-uniform flow is limited through careful design of the turning vanes and drive motor control.

Full characterisation of the variation in flow field allows for a greater variety of flow conditions to be modelled in the tank, making use of the velocity gradients that exist in specific locations away from the central test area. A circular tank also has the significant advantage of being able to create complex multi-directional and multi-modal sea states, as discussed in Section I.

V. Conclusions

The FloWave facility offers the ability to test a wide variety of realistic sea conditions prior to deployment of prototype devices at sea, provided that the generation of these conditions in the tank is well understood. Results of the initial characterisation programme show that steady currents can be generated in the tank, with a large uniform test volume in the centre of the tank.

- The vertical flow profile in the tank is not particularly dependent on the input velocity, and can be approximated by a 1/15th power law. This is a more uniform flow than the 1/7th and 1/10th profiles commonly used to represent tidal flows.
- The flow over the test area is uniform within 10% or 0.05 m/s over an area greater than 50 m^2 around the centre of the tank. The shape and size of this test area is close to that predicted by the CFD modelling and experimental tests carried out during the design phase.
- The velocity is broadly symmetrical on both sides of the tank about the flow direction, although it varies along the direction of flow from ‘upstream’ to ‘downstream’. The variation in velocity across the tank is consistent between the different input velocities tested.
- Steady flows can be produced in the facility, following a ramp up period of about 5 minutes. However further work is required to better understand the turbulent nature of the flow.

Acknowledgment

The authors would like to thank the Energy Technology Institute and RCUK Energy programme for funding this research as part of the IDCORE programme (EP/J500847/1), and the UK Engineering and Physical Science Research Council for funding the FloWave facility (EP/I02932X/1).

References

[1] EquiMar, “EquiMar Protocol II.A Tank Testing,” in *Protocols for the Equitable Assessment of Marine Energy Convertors*, D. M. Ingram, G. H. Smith, C. Bittencourt Ferreira, and H. C. M. Smith, Eds., Edinburgh, 2011, ch. 3.3.

[2] D. M. Ingram, A. R. Wallace, A. Robinson, and I. G. Bryden, “The design and commissioning of the first, circular, combined current and wave test basin.” in *Proceedings of Oceans 2014 MTS/IEEE*, Taipei, Taiwan, 2014.

[3] A. Robinson, D. Ingram, I. Bryden, and T. Bruce, “The effect of inlet design on the flow within a combined waves and current flumes, test tank and basins,” *Coastal Engineering*, vol. 95, pp. 117–129, Jan. 2015.

[4] ——, “The generation of 3D flows in a combined current and wave tank,” *Ocean Engineering*, vol. 93, Jan. 2015.

[5] B. Holmes and K. Nielsen, “Guidelines for the development & testing of wave energy systems,” Hydraulics Maritime Research Centre, UCC, Cork, Ireland, Tech. Rep. June, 2010.

[6] J. C. Mankins, “Technology readiness levels,” *White Paper, April*, pp. 4–8, 1995.

[7] V. Heller, “Scale effects in physical hydraulic engineering models,” *Journal of Hydraulic Research*, vol. 49, no. 3, pp. 293–306, Jun. 2011.

[8] T. Vyzikas, D. Greaves, D. Simmonds, C. Maisondieu, H. C. M. Smith, and L. Radford, “Application of numerical models and codes Task 3.4.4 of WP3 from the MERiFIC Project A,” University of Plymouth, MERiFIC, Plymouth, UK, Tech. Rep., 2014.

[9] Valeport, “Model 801 Electromagnetic Flow Meter Datasheet,” Totnes, UK, Tech. Rep., 2011. [Online]. Available: http://www.valeport.co.uk/Portals/0/Docs/Datasheets/Valeport_Model801_v2a.pdf

[10] ——, “Model 802 Electromagnetic Flow Meter Datasheet,” Totnes, UK, 2011. [Online]. Available: http://www.valeport.co.uk/Portals/0/Docs/Datasheets/Valeport_Model802_v2a.pdf

[11] HSE, “Environmental considerations,” Health & Safety Executive, London, Tech. Rep., 2002.

[12] K. Gunn and C. Stock-Williams, “On validating numerical hydrodynamic models of complex tidal flow,” *International Journal of Marine Energy*, vol. 3-4, pp. e82–e97, Dec. 2013.

[13] ——, “Falls of Warness 3D Model Validation Report,” E.ON Technologies, Tech. Rep., 2014. [Online]. Available: http://www.eti.co.uk/redapt-full-report-falls-of-warness-3d-model-validation/

Ocean Engineering 139 (2017) 103–115

Contents lists available at ScienceDirect

Ocean Engineering

journal homepage: www.elsevier.com/locate/oceaneng

Characterisation of current and turbulence in the FloWave Ocean Energy Research Facility

Duncan R.J. Sutherland[a,*], Donald R. Noble[b], Jeffrey Steynor[b], Thomas Davey[b], Tom Bruce[a]

[a] Institute for Energy Systems, University of Edinburgh, United Kingdom
[b] FloWave Ocean Energy Research Facility, University of Edinburgh, United Kingdom

ARTICLE INFO

Keywords:
Renewable energy
Tidal energy
Physical testing
Turbulence
Acoustic sensors
Wave-current basin

ABSTRACT

Tidal energy is a developing industry and requires high precision test facilities which replicate the full-scale flows as accurately as possible to develop new technologies. In particular, the spatial and temporal variation must be well understood. FloWave is a state-of-the-art test facility with the ability to produce multi-directional waves and currents. This work investigates the mean and turbulent flow parameters throughout the tank using an ADV. The goal is to provide a comprehensive characterisation of the flow in the tank, in a robust and repeatable manner. These flow parameters are then compared to sample data from field measurements for context.

The turbulence intensities are normally distributed in the range of 5–11% and integral lengthscales were log-normally distributed over a 0.18–0.41 m range across the test area. The Reynolds stresses showed the streamwise-vertical pair were relatively constant throughout the depth, with values in the range −0.31 to 0.15 Pa, while the transverse-vertical pair show high vertical variation with values of −1.35 to 0.20 Pa. For the majority of locations the flow metrics are generally realistic compared with those measured at the Fall of Warness site. This work improves the understanding of flow behaviour in the tank, facilitating higher confidence testing of scaled devices.

1. Introduction

The FloWave Ocean Energy Research Facility allows the scale testing of marine energy extraction devices, with the ability to create realistic sea-states comprising combined waves and current. For tidal developers it is vital that the spatial and temporal variation of current is well characterised. This needs to consider variation with both depth and across the test area, as well as small scale temporal variation, i.e. turbulence.

The goal of this work is to present a comprehensive flow characterisation of the FloWave facility. This will allow developers to reference the flow metrics for their own tests at the facility and give context of how they compare to full-scale site conditions. Flow characterisation requires a robust methodology, taking into account instrument vibration, noise and repeatability of results. This work presents flow metrics which are used to characterise full-scale sites, assessing their variation with location and flow speed in the tank and providing distributions to quantify repeatability.

In giving context for the tank in relation to field data, it should be noted that tidal energy sites are hugely diverse and a full analysis of the drivers and range of the variations in flow metrics is out of scope for this work. However, it is important to give a basic overview of the similarities and differences to inform designers testing at the facility.

This work makes use of the newly available Nortek Vectrino Profiler, a 100 Hz sample rate pulse coherent Acoustic Doppler Velocimeter (ADV) to perform this characterisation. This work builds on previous studies (Noble et al., 2015) using Electro-Magnetic (EM) induction metres to measure the spatial variation of mean flow across the tank. It also makes use of field measurements collected at the EMEC tidal test site, made during the Reliable Data Acquisition for Tidal Platform (ReDAPT) project (Sellar and Sutherland, 2015).

Variation of flow over a range of scales is known to affect Tidal Energy Converters (TECs) (Clark et al., 2015). As testing at full scale in the sea is challenging in terms of expense and uncontrollable conditions, it is advantageous for device developers to learn as much about their design in small scale facilities, where tests are repeatable and modifications are more practical.

The authors are not aware of any published papers dealing specifically with the subject of characterisation of flow and turbulence in a wave-current basin. However, facility baseline flow conditions are

* Corresponding author.
E-mail addresses: D.Sutherland@ed.ac.uk (D.R.J. Sutherland); D.Noble@ed.ac.uk (D.R. Noble); Jeff.Steynor@flowave.ed.ac.uk (J. Steynor); Tom.Davey@flowave.ed.ac.uk (T. Davey)
URLS: http://www.eng.ed.ac.uk/research/institutes/ies (D.R.J. Sutherland), http://www.flowavett.co.uk/ (D.R. Noble), http://www.flowavett.co.uk/ (J. Steynor), http://www.flowavett.co.uk/ (T. Davey).

http://dx.doi.org/10.1016/j.oceaneng.2017.02.028
Received 11 February 2016; Received in revised form 4 January 2017; Accepted 22 February 2017
Available online 03 May 2017

discussed in a number of experimental studies (Park et al., 2005; Mori et al., 2007; Myers and Bahaj, 2010; Blackmore et al., 2016). The methodologies used are broadly similar to that presented here, although differ in aspects specific to the facility or measurement instruments. Flow characteristics of the Chilworth flume at Southampton were measured using a Nortek ADV (Myers and Bahaj, 2010) in order to investigate wake effects of TEC at small scale using porous disks. Results in terms of velocity defect and turbulence intensity are only presented for cases with the model installed. As part of a study investigating methods to change the level of turbulence in the IFREMER flume, flow measurements were conducted using laser Doppler velocimetry (LDV) (Blackmore et al., 2016). Velocity and turbulence metrics were calculated across a plane in the centre of the flume, forming the swept area of a model turbine being tested. Details of facility characterisation are presented in Park et al. (2005) and Mori et al. (2007), although both relate to recirculating flumes, and use LDV measurements via a window in the side of the flume, something that is not currently possible at FloWave.

2. Experimental set-up and instrumentation

2.1. The FloWave Facility

FloWave is a circular combined wave and current test tank, with wavemakers located around the entire circumference. Impellers mounted below the test area drive the current recirculation through a series of turning vanes, as shown in Fig. 1.

There is a 15 m diameter buoyant floor in the centre of the tank, which notionally represents the test area. This floor can be raised above the water level to facilitate model installation and reconfiguration as required, then submerged to the 2 m working depth. With the wavemakers powered off, the water level in the tank drops slightly, resulting in a water depth of 1.93 m, which was the configuration throughout this work. Around the circumference of the tank there are 168 active-absorbing hinged wavemakers, although they were not used in these tests.

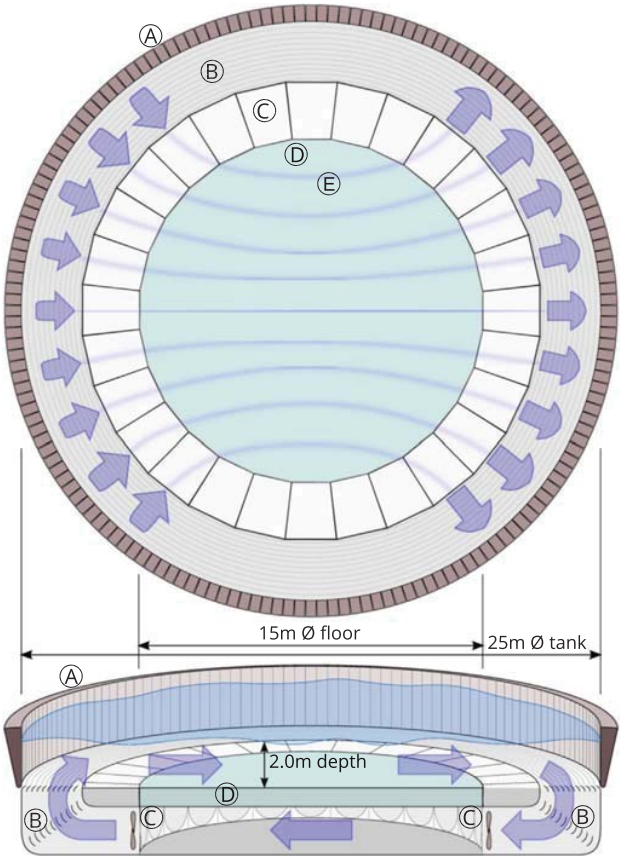

Fig. 1. Schematic of FloWave in plan and oblique section showing: (A) wavemaker paddles around circumference (168 Nr), (B) turning vanes and flow conditioning filters, (C) current drive impeller units (28 Nr), (D) buoyant raisable floor (15 mØ) below test area, (E) idealised streamlines of flow across tank floor.

The tank is capable of generating currents upwards of 1.6 m s^{-1}, using 28 drive units mounted in a plenum chamber below the test floor. Each of these contains a single 1.7 m diameter low-solidity 5-bladed symmetrical impeller, driven by a 48 kW motor. Turning vanes mounted below and in front of the wavemakers direct the current across the tank (Robinson et al., 2015), as shown in Fig. 1. These turning vanes incorporate porous screens to provide flow conditioning and prevent debris ingress to the plenum chamber.

Creating a horizontally uniform current in a circular tank requires precise control of the individual impellers (Robinson et al., 2014). In summary, the impeller units on either side of the required current direction on both the upstream and the downstream side of the tank are driven at varying speeds to produce the required current corresponding to the desired test velocity. Here, the highest of these impeller rotational speeds (ω) is used to reference the tank setting. The control system for the impellers includes the ability to change the direction of the current during the test. This capability allows for the simulation of cross-currents, or a tidal ellipse, without having to reposition the device model.

The tank is equipped with an instrumentation gantry from which sensors can be suspended into the flow, the base of which is 1 m above the water surface. The tank co-ordinate system is Cartesian, as shown in Fig. 2, with the origin at the centre of the tank on the test floor, and $+z$ vertically upwards. All tests were run with a current direction of 0°, i.e. flow in the $+x$ direction. Here co-ordinate sets are referred to in short as (x, y) or (x, y, z).

2.2. ADV

An Acoustic Doppler Velocimeter (ADV) was used to measure the flow velocities in this study. The ADV used was a Nortek Vectrino Profiler capable of sample rates of up to 100 Hz and measuring multiple depth cells (Nortek-AS, 2016). The ADV operates by emitting a single acoustic pulse into the water. This pulse is reflected by particulate (termed back-scatters) in the water, assumed to be moving with the same flow speed, and the reflected pulse is detected by four angled transducers. The pulse is Doppler shifted according to the flow velocity and the four transducers allow the measurements of four flow

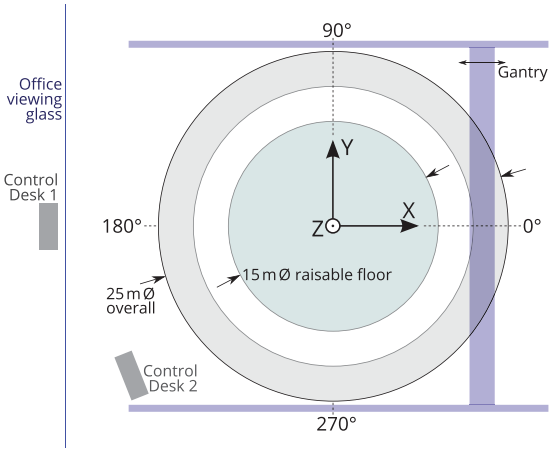

Fig. 2. Plan view of the facility including reference co-ordinates.

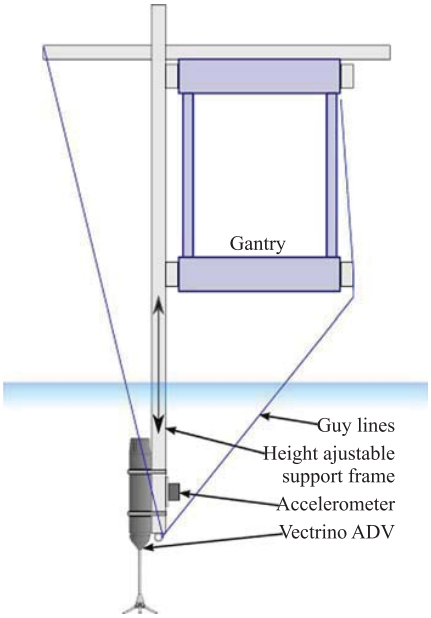

Fig. 3. Instrument set-up schematic (not to scale), showing the ADV with associated supports, accelerometer and instrumentation gantry.

components which can be transformed into a u,v,w co-ordinate system (Nortek-AS, 2016).

The ADV was attached to the gantry via an adjustable support frame, made from 45 mm square aluminium section. The support frame was mounted vertically, fixed to the gantry at two points 2 m apart. A schematic of the ADV mounting rig is provided in Fig. 3. The ADV data uses the same co-ordinate system as the tank where velocities u, v and w correspond to directional vectors x, y and z.

ADV settings are a trade off between minimising bad data and maximising resolution. One key metric in assessing data quality is the pulse to pulse correlation. Here the minimum pulse length and cell volume were selected to keep a mean correlation >95%. The velocity range was monitored in order to keep it to the minimum value without velocity wrapping occurring due to high velocity spikes. Table 1 gives the range of settings utilised for these tests.

It is a key that the water contains sufficient back-scatters for the ADV measurements to be accurate. Low particle density will result in weak signal returns with low associated correlation values and high uncertainty. For these tests the tank was tested unseeded with the correlations found to be in the ~70% range which was deemed unacceptable. Glass micro-beads of neutral buoyancy (on average given slight variation between beads) were added to the tank until the average correlation on all four beams was greater than 95%. When the facility had not been operated for an extended period, i.e., overnight, it was found that the correlations dropped. However, once the tank was run at a high velocity for a period of time the seeding was redistributed and correlation values rose back to acceptable levels. Correlation was monitored throughout testing and where correlations dropped, further seeding was added.

Table 1
Vectrino settings.

Sample rate	Velocity range ($m\,s^{-1}$)	Cell size (mm)	Pulse length (mm)	No. of cells
100	0.8–1.6	0.3	0.3	5

2.3. Vibration mitigation and measurement

When the ADV was close to the tank floor, the support frame had a maximum cantilever of ~3 m, therefore vibration was expected to be potentially significant. To reduce vibration amplitudes, three tensioned guy lines (separated by approximately 120° in plan) were attached to the base of the support frame. The vertical angle was dependent on the position of the sensor in the water column, with the two front lines angled at approximately 34–38° from vertical, and the single rear line (in the flow direction) at 37–51°, dependent on the sensor depth.

The tension in the guy lines was kept constant as far as possible between tests. However it was noted that for tests close to the water surface, high tension in the guy lines increased the vibration amplitude. Therefore a reduced tension was used for tests at $z \geq 1.4$ m.

For a subset of tests an ADXL327Z three-axis accelerometer was mounted on the reverse side of the beam to the ADV. This was included to assess the effect of vibration of the system. The accelerometer was limited to a maximum sample-rate of 50 Hz (Analog-Devices, 2016). This was done in order to compare the spectral decomposition of the accelerometer with the ADV to assess the impact of vibration on velocity measurements as discussed in Section 3.9.

3. Test methodology

3.1. Overview

The tests were divided into three categories: temporal stability, flow magnitude with impeller speed, and spatial variation throughout the test volume.

Measurement of long-term variation in velocity and turbulence was carried out at (0, 0, 1.4), in the horizontal centre of the tank. The tank was run at $\omega = 82$ rpm with the flow accelerated and allowed to stabilise prior to starting a 1 h long measurement set.

A range of flow speeds was also tested at the same location, with the primary drive motor increased in steps of 20 rpm up to a maximum of 120 rpm. A 600 s data sample was taken at each rpm step, once the velocity in the tank had stabilised. Spatial variation was then tested at a fixed impeller speed.

3.2. Measurement locations

A series of depth profiles were measured at points along and perpendicular to the current direction, with co-ordinates given in Table 2. For each profile, a 600 s data sample was taken at 11 elevations above the floor, as given in Table 3. These profiles were all measured at the tank's design specification flow, nominally 0.8 $m\,s^{-1}$ ($\omega = 82$ rpm). Two additional depth profiles were measured in the centre of the tank at nominal velocities of 0.2 and 0.5 $m\,s^{-1}$, with the velocities chosen to allow comparison with previous work (Noble et al., 2015).

3.3. Period of stationarity

In order to calculate a mean or turbulent parameter of the flow a period of stationarity must be defined. This is defined as a period over which flow measurements have stable mean ($\bar{u}$) and variance (σ_u^2) (Thomson et al., 2010). The first stage of flow parametrisation is to assess an appropriate stationarity period based on the variation of σ_u^2 and $\bar{u}$. This was done utilising the 1 h sample set at a fixed location at (0, 0, 1.4) and a fixed impeller setting of $\omega = 82$ rpm. The resulting time

Table 2
x, y co-ordinates of measured vertical profiles, relative to the tank centre.

X (m)	−5.0	−2.5	0.0	2.5	5.0	0.0	0.0
Y (m)	0.0	0.0	0.0	0.0	0.0	2.5	5.0

Table 3
z co-ordinates for each measured vertical profile (as given in Table 2), heights above the test floor.

Z (m)	0.1	0.2	0.3	0.4	0.6	0.8
	1.0	1.2	1.4	1.6	1.8	

series is then subdivided into a range of T_{stat} periods from 1 to 120 s in 1 s increments, with the mean ${\sigma_u}^2$ and $\bar{u}$ values across each sample calculated.

3.4. Mean velocity

Once the period of stationarity has been defined, the mean velocity is simply the mean value of the velocity over this period. The variation of velocity with depth is normally characterised by

$$\frac{\bar{u}(z)}{\bar{u}(z=d)} = \left(\frac{z}{d}\right)^{\frac{1}{n}} \tag{1}$$

where $\bar{u}(z)$ is the mean velocity at a given depth, $\bar{u}(z=d)$ is the velocity at the surface, z is the elevation, d is the depth and n is the power law coefficient (Cheng, 2007; Legrand, 2009).

3.5. Turbulence intensity

One of the metrics commonly used to quantify the magnitude of turbulence is the turbulence intensity (I). This term is adopted from the wind industry as a measure of the magnitude of fluctuation as a percentage of the mean flow velocity. It is defined as the Root-Mean-Square (RMS) of the velocity perturbations divided by the mean velocity over a period of stationarity (Thomson et al., 2010).

Here an anisotropic environment is assumed, and individual components of I for each Cartesian direction are calculated as per Eq. (2). Where u' is the streamwise velocity perturbation and $\bar{u}$ is the mean velocity value:

$$I_u = \frac{\sqrt{\langle u'^2 \rangle}}{\bar{u}} \times 100 \tag{2}$$

The measured velocity is a combination of the mean velocity, the turbulent fluctuation and a noise component:

$$u = \bar{u} + u' + n \tag{3}$$

Determination of n allows the correction of the measured I value for the uncertainty due to instrument noise. Eq. (13) allows the calculation of the variance due to noise (${\sigma_n}^2$) in order to make this correction to Eq. (2) resulting in Eq. (4):

$$I_u = \frac{\sqrt{\langle u'^2 \rangle - \sigma_n^2}}{\bar{u}} \tag{4}$$

3.6. Integral lengthscale

The integral lengthscale is defined qualitatively as the average size of the largest eddies in a turbulent flow (Pope, 2000). There are several methods of estimating this value. Here the temporal autocorrelation method is utilised as it was deemed the most appropriate for the measurement data (Sutherland, 2015; O'Neill et al., 2004). This method utilises the integral timescale ($\mathfrak{I}$) of turbulence which is calculated from the time based autocorrelation function given by Eq. (5). Where Δt is a temporal lag, $R(\Delta t)$ is the correlation coefficient, t is a point in time and ${\sigma_u}^2$ is the variance of the velocity (Pope, 2000). The area under the $R(\Delta t)$ curve between $\Delta t = 0$ and where $R(\Delta t)$ crosses the Δt axis gives the integral timescale. Assuming a frozen field of turbulence (Taylor, 1938), this can be multiplied by the mean streamwise velocity to give an estimate of the integral lengthscale:

$$R(\Delta t) = \frac{\langle (u_t - \bar{u})(u_{t+\Delta t} - \bar{u}) \rangle}{\sigma_u^2} \tag{5}$$

$$\ell_x = \bar{u} \cdot \mathfrak{I} = \bar{u} \cdot \sum_{\Delta t=0}^{R(\Delta t)=0} R(\Delta t) \mathrm{d}\Delta t \tag{6}$$

3.7. Reynolds stress tensors

The Reynolds stress tensors are a matrix of nine tensors which describe the stresses in the turbulent flow. Here only the two most relevant tensors are assessed: the streamwise-vertical and streamwise-transverse pairs. These are defined as:

$$\tau_{uw} = \overline{uw}\rho \tag{7}$$

$$\tau_{vw} = \overline{vw}\rho \tag{8}$$

These are calculated from the four individual beam velocities measured by the ADV (b_1, b_2, b_3 and b_4), based on the bisecting angle between the beams (θ), using Eqs. (9) and (10) (Lohrmann et al., 1990):

$$\overline{uw} = \frac{\overline{b_3'^2} - \overline{b_4'^2}}{4\sin\theta\cos\theta} \tag{9}$$

$$\overline{vw} = \frac{\overline{b_1'^2} - \overline{b_2'^2}}{4\sin\theta\cos\theta} \tag{10}$$

3.8. Data quality control and uncertainty analysis

Ensuring data quality is key to the accuracy of any experimental work. The data quality control follows the established work of Goring and Nikora (2002) along with the instrument noise (measurement uncertainty) spectral analysis technique developed for turbulence analysis by Richard et al. (2013).

Goring and Nikora propose several operations based on both physical limits and statistical likelihood when treating ADV data. As removing data points requires the interpolation (i.e., best guess but non-real data), replacement of measured data points should be carefully selected. Here two methods are used to identify spurious data points: signal correlation and measurement to measurement acceleration. Values with correlation less than 80% or with an associated acceleration greater than 9.81 m s^{-2} were removed (Goring and Nikora, 2002).

The new development of the Vectrino profiler allows multiple bins to be measured. This allows the possibility for spatial as well as temporal interpolation of points. The methodology adopted was to interpolate via a linear spatial method in a first pass then run the acceleration threshold a second time, replacing any unsatisfactory values via temporal cubic spline interpolation. Where three or more consecutive values were removed no interpolation was performed and that T_{stat} length data segment was removed.

Further data quality is assessed through the measurement of the instrument noise floor, a method developed to calculate the portions of the variance due to turbulent fluctuations and to Doppler noise or measurement uncertainty (Richard et al., 2013). The technique involves fitting a two part slope to the Power Spectral Density (PSD) of the velocity fluctuations. The method relies on two assumptions: one, that the flow measurements capture the $f^{-5/3}$ slope of the inertial subrange of turbulence; and two, that the instrument noise is white, i.e., spread evenly across the frequency range.

In order to compute the PSD, each T_{stat} length detrended velocity time series are multiplied by a hamming window and computed into a Power Spectral Density (PSD) via a Fast Fourier Transform (FFT) method and Eq. (11). Where $Y(f)$ is the FFT result, L_{FFT} the number of values in $Y(f)$, and Δt is the time step (Emery and Thomson, 2001). The PSD for all T_{stat} samples for the given measurement set are averaged

together and fitted to a two part line of best fit, following the method outlined in Richard et al. (2013). This line fit assumes the presence of two slopes, firstly of $f^{-5/3}$, following the integral sub-range of turbulence, and secondly of 0, due to white noise, see Eq. (12). This allows the calculation of the magnitude of variance in the velocity signal that is due to instrument noise ($\sigma_n{}^2$), via Eq. (13):

$$S(f) = \frac{2}{(L_{FFT}\Delta t)}|Y(f)|^2 \tag{11}$$

$$S(f)_{measured} = K \cdot f^{\frac{-5}{3}} + N \tag{12}$$

$$\sigma_n^2 \approx N \times f_{Nyquist} \tag{13}$$

Under these assumptions if the noise is white with zero mean the mean velocity values will not be affected and the turbulence intensity values can be corrected for the variance in the signal due to noise, as per Section 3.5. It is not yet clear how noise affects the integral lengthscale measurements. As a signal tends towards white noise the autocorrelation coefficient tends towards zero, thus noise is likely to bias measurements low but by what value is unknown and requires an independent study beyond the scope of this work. Conversely a vibration could create artificially high correlation values, as vibrations are cyclic and thus inherently correlated. However, if the vibrations are of suitably low amplitude and high frequency it is predicted that the effect will be minimal.

The instrument accuracy is likely to represent the highest experimental uncertainty in this work. Further measurement uncertainties include: variation in the repeatability of test conditions, which are relativity small at this facility and the variation of seeding density over the testing, which was monitored throughout.

3.9. Vibration analysis

The analysis of the accelerometer data can be used to compare with the ADV data under the assumption of a two part spectral slope, as discussed in Section 3.8. If the ADV velocity measurements show any deviation from the $f^{-5/3}$ slope it can be inferred that this is due to vibration by comparing the normalised spectra of the ADV to the accelerometer and if the frequencies of the affected regions align. Variance due to vibration can be accounted for by the same method as Doppler noise, calculating the area under the vibration affected region of the power spectrum. Vibrations are expected to be zero mean and therefore do not affect mean velocity measurements. It should be noted that the accelerometer cannot be used to verify spikes in the 25–50 Hz range of the ADV as these are beyond the Nyquist frequency of the sensor. Given the expected fundamental vibration frequency range, spikes in this region are likely to be harmonics of lower frequency vibrations and this is assessed in the analysis.

4. Results

4.1. Stationarity

The stationarity of the flow in the tank is assessed via the mean value and variance of the streamwise velocity (u) for a variety of stationarity periods as discussed in Section 3.3. Fig. 4 illustrates that the mean of $\bar{u}$ remains constant as would be expected while the standard deviation of the mean values slowly decreases with increasing T_{stat}. The standard deviations of $\bar{u}$ appear to be nearing an asymptotic value. A target value of the standard deviation of $\bar{u}$ to be less than 1.5% of the total mean value was set.

Fig. 5 shows the variance increasing towards an asymptotic value. Defining the asymptote as the mean of the values over the 100–120 s range the period at which the variance was within 1.5% of this value was found to be 43 s. The first value where both the mean and standard deviation of $\bar{u}$ were within their 1.5% thresholds was selected as the stationarity period, which was 43 s. This period relates to a standard deviation in mean values of 0.0101 m s^{-1} in Fig. 4.

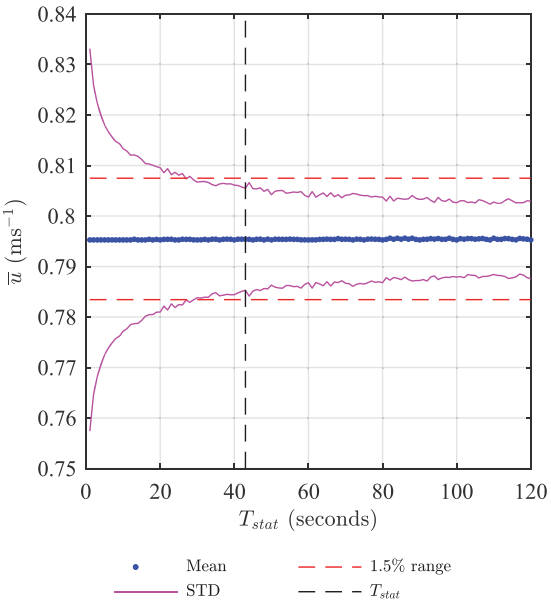

Fig. 4. Variation of mean and standard deviation of $\bar{u}$ with T_{stat}. The blue dots represent the mean values and the magenta line the standard deviation of the mean velocity around that value for a given T_{stat}. The dashed red line represents the 1.5% threshold, and the vertical black line the final T_{stat} value. (For interpretation of the references to colour in this figure caption, the reader is referred to the web version of this paper.)

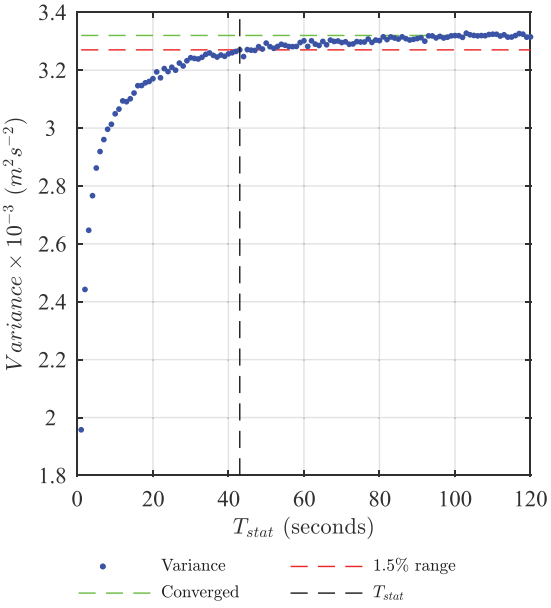

Fig. 5. Variation of streamwise velocity variance with T_{stat} showing convergence to within 1.5% of the long term mean value. The blue dots represent the mean variance over the given T_{stat}, the green dashed line the mean variance over 120 s, the red line the 1.5% threshold, and the vertical black line the final T_{stat} value. (For interpretation of the references to colour in this figure caption, the reader is referred to the web version of this paper.)

4.2. Mean velocities

The first stage in characterising the tank is to quantify the relationship between impeller rotational velocity (ω) and flow velocities.

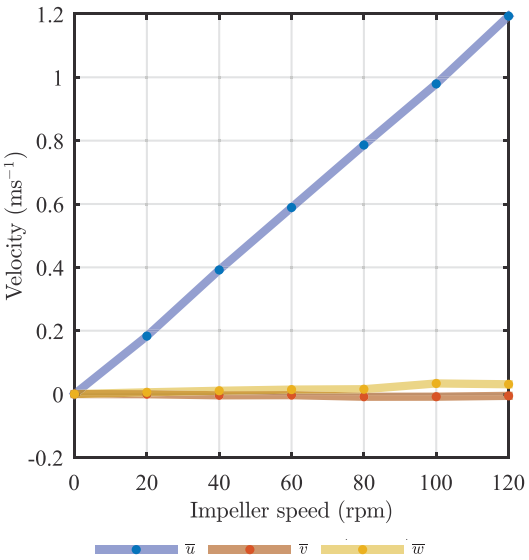

Fig. 6. Variation of $\overline{u}$ (blue), $\overline{v}$ (red), and $\overline{w}$ (yellow) at a single point (0,0,1.4) with impeller speed (ω). (For interpretation of the references to colour in this figure caption, the reader is referred to the web version of this paper.)

Table 4
Linear fits of flow velocity at a single point (0,0,1.4) with impeller speed, as given in Fig. 6.

Vector	Gradient $\times 10^{-3}$ (m s^{-1} rpm^{-1})	Y intercept $\times 10^{-3}$ (m s^{-1})	Fit R^2
$\overline{u}$	10.02	−14.06	1.00
$\overline{v}$	−0.06	−0.75	0.58
$\overline{w}$	0.28	−1.43	0.87

Measurements of u, v and w were taken for a range of impeller velocities from 0 to 120 rpm in 20 rpm increments, at the centre point of the tank at (0, 0, 1.4). The results are presented in Fig. 6 with a line of best fit to the data given in Table 4. It can be seen that there is a linear relationship between the impeller rpm and $\overline{u}$, while $\overline{v}$ shows a flat response and $\overline{w}$ a maximum increase of 0.03 m s^{-1} with increasing ω.

With the response of a single point characterised, the next stage was to assess the variation with depth of flow velocities with ω at the horizontal centre point of the tank. For this three values of ω: 25, 54 and 82 rpm were tested. The results of $\overline{u}(z)$, $\overline{v}(z)$ and $\overline{w}(z)$ are presented in Fig. 7. It shows that as ω increases so does the streamwise velocity gradient with depth. The power law fit indexes are 15.6, 16.4 and 16.6 with increasing ω, all with associated R^2 of greater than 0.95. The transverse and vertical velocities are an order of magnitude smaller and are show more complex relationship with depth. The transverse velocities are always negative and at the two faster impeller speeds the surface velocity increases relative to the mid depth. The vertical velocities follow a trend across the tested impeller speeds of negative (downward) velocities near the floor and positive velocities near the surface. The difference between the minimum and maximum velocities, at 0.4 m and 1.4 m respectively, increases with increased impeller speed. The streamwise velocity gradient would be expected to increase with increased mean streamwise flow velocity due to increasing friction at the bottom boundary, as recorded in field data at tidal sites (Sellar and Sutherland, 2015).

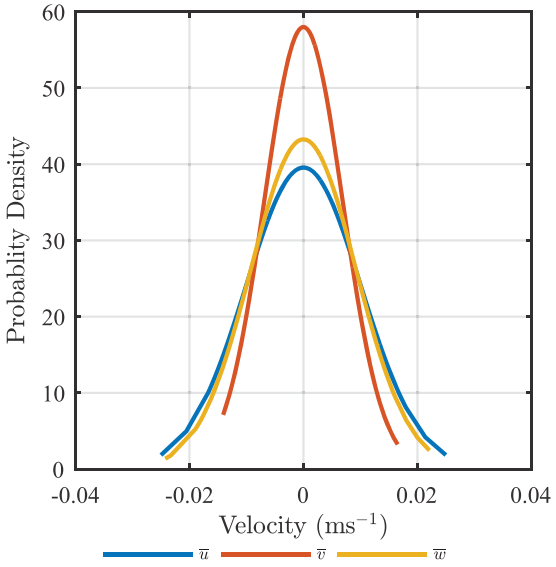

Fig. 8. Distributions of de-trended mean velocities for a single point (0,0,1.4) at 82 rpm.

A 1 h test was conducted to assess the long term variation and distribution of flow metrics in the tank, with a single measurement point at (0, 0, 1.4). The de-trended velocity in each direction is assessed for their distributions in Fig. 8. The distribution type was tested via a χ^2 distribution test. The null hypothesis for the test was that these

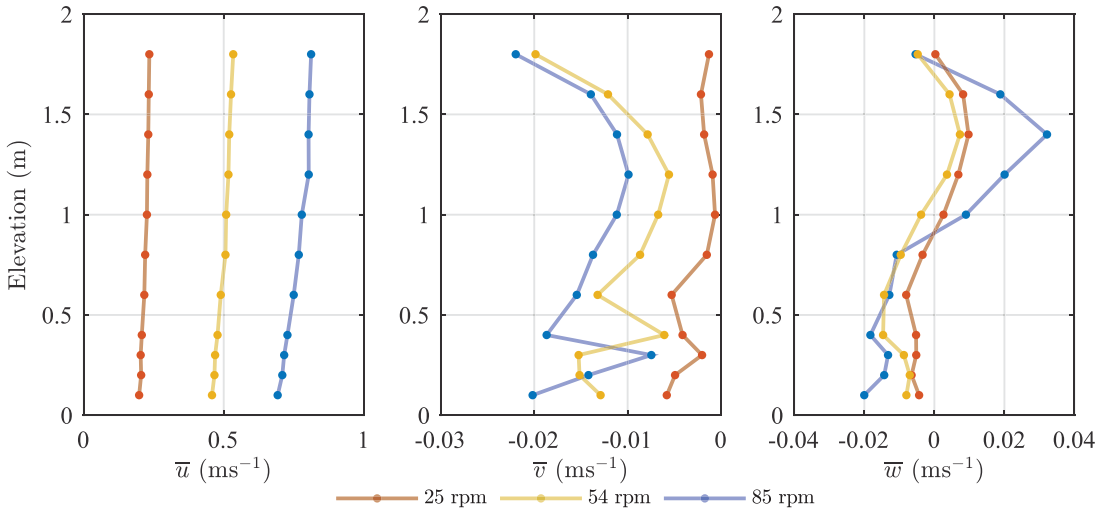

Fig. 7. Variation of $\overline{u}(z)$, $\overline{v}(z)$ and $\overline{w}(z)$ with depth for three impeller speeds.

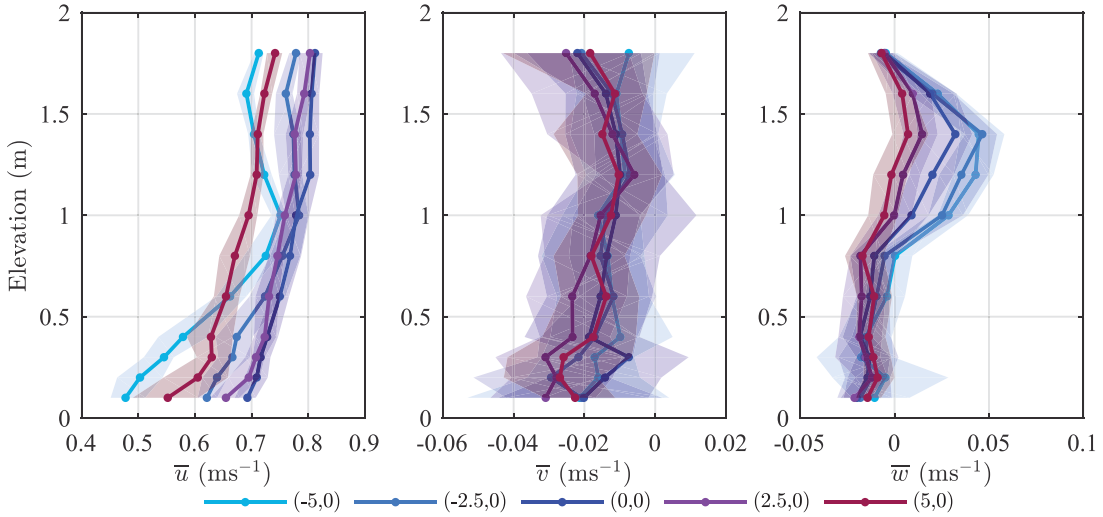

Fig. 9. Depth profiles of $\overline{u}$, $\overline{v}$ and $\overline{w}$ across the streamwise centerline of the tank at an impeller speed of 82 rpm. The solid lines represent mean values and the shaded area the range of values. (For interpretation of the references to colour in this figure caption, the reader is referred to the web version of this paper.)

parameters were normally distributed. The test failed to reject the hypothesis at the 1% significance level. The spread of the data was smallest in the transverse direction, with roughly equal spread in the streamwise and vertical. The standard deviation of mean velocities was expected to be very low as the T_{stat} was selected based on minimising this property.

The spatial variation of the three velocities (u,v and w) in the tank was assessed along the central streamwise and transverse transects, with points measured at 11 depths at 7 horizontal locations as per Table 3. Fig. 9 illustrates the depth profiles at five locations along the x-axis and Fig. 10 those along the y-axis. Each of the $\overline{u}(z)$ depth profiles is fitted to a power law line of best fit in the form of Eq. (1), with the power index (n) and respective R^2 goodness of fit values are presented in Table 5.

For the x-axis results; the depth profile at (0,0) consistently shows the fastest streamwise velocities. The two $\overline{u}$ profiles upstream are most poorly represented by this line fitting methods with $R^2 < 0.95$ and with the fastest flow at 1.0 m elevation.

The transverse and vertical velocity components vary significantly less across the streamwise axis. The $\overline{v}$ values are generally less than zero and an order of magnitude less than $\overline{u}$. As these measurements are taken in the centre of the tank a non-zero mean value probably represents a small misalignment of the sensor (in the region of ~2° if a zero mean $\overline{v}$ is assumed). However the fluctuation of $\overline{v}$ with depth is an interesting factor with the greatest values near the floor and free surface. The vertical velocities show the trends that would be expected given the flow generation method of the tank. Near the inlet there are greater upward velocities of up to 0.046 m s^{-1} with these decreasing to near zero by the furthest downstream measurement. There is generally

Table 5
Power law indices for a line of best fit of $\overline{u}(z)$ in the form of Eq. (1) for depth profiles in the x direction.

x (m)	y (m)	Power law index	Power law fit R^2
−5.0	0.0	6.7	0.84
−2.5	0.0	12.6	0.90
0.0	0.0	16.6	0.96
2.5	0.0	14.4	0.98
5.0	0.0	10.3	0.98
0.0	2.5	12.2	0.88
0.0	5.0	7.4	−0.28

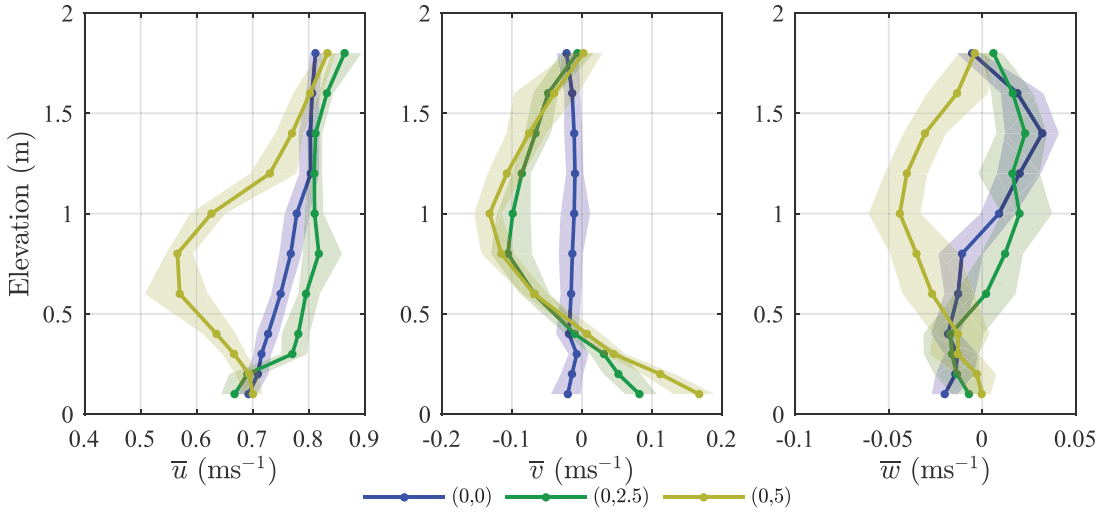

Fig. 10. Depth profiles of $\overline{u}$, $\overline{v}$ and $\overline{w}$ across the transverse direction at an impeller speed of 82 rpm. The solid lines represent mean values and the shaded area the range of values. (For interpretation of the references to colour in this figure caption, the reader is referred to the web version of this paper.)

a small (~0.02 m s^{-1}) down-welling at depths of 0.8 m and below.

The locations offset in the transverse show further complicated patterns. In the streamwise velocity there is a change in profile in the depth profile at (0,5) compared with the other two locations. It shows a velocity deficit with speeds at 0.8 m elevation only a third of those at 1.8 m. In the transverse velocities it can be seen that there are negative values at 1 m elevation indicating a flow direction away from the centre of the tank, while there are positive velocities near the floor. The transverse components are not trivial with $\bar{v} = 0.2\bar{u}$ of the mean values at the 0.8 m elevation. The profiles of $\bar{v}(z)$ are highly similar in the two outer measurement locations. The vertical components show little similarity across the transverse locations. There is a trend of higher magnitude values in the upper half of the water column. These are positive (upward) for the inner two measurements and negative (downward) for the outer measurements. These spatial variations are due to the flow generation method of the tank to accommodate the circular design and are not unexpected.

4.3. Instrument noise and vibration

The effects of vibration were assessed through the accelerometer and the ADV, the goal being to quantify the effect of the vibration on the measured velocities. The vibrations in the x and y directions were ~0 mean (as would be expected) and thus the mean velocities were not affected. The implications for turbulence metrics required analysis of the spectra of both the accelerometer and the ADV. This required the normalisation of the spectra which in this case was done by multiplication by the Nyquist frequency and divided by the variance of the signal.

Fig. 11 presents the results for the x- and y-axes for an example where the vibrations were very high and thus easily identified. In the x-axis there is a peak in both accelerometer and ADV at 20.0 Hz and a Harmonic at 40.0 Hz in the ADV (beyond the Nyquist frequency of the accelerometer). There is an additional peak at 6 Hz in the accelerometer which is not replicated in the ADV spectrum, this may be due to the amplitude being insufficient to impact velocity measurements.

In the y-axis there is a peak at 18.9 Hz in both instruments (although it is difficult to see clearly in Fig. 11 due to closely matched amplitudes). The closely matched f values of these peaks between the x and y suggest that this is a coupled motion. In the y-axis there is an additional high amplitude motion with a peak at 2.3 Hz which is affecting the v measurement in the ADV. An additional peak which is not of sufficient amplitude to affect velocity is seen at 9.9 Hz.

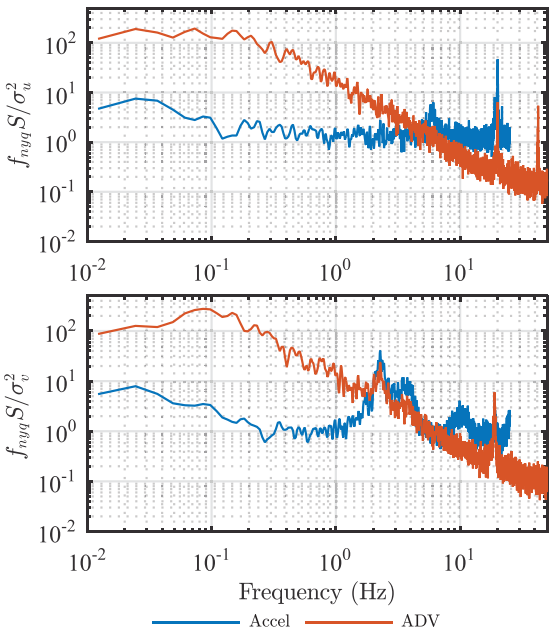

Fig. 11. Normalised power spectral densities of both the accelerometer (blue) and ADV (orange) data in the x-axis (top) and y-axis (bottom). (For interpretation of the references to colour in this figure caption, the reader is referred to the web version of this paper.)

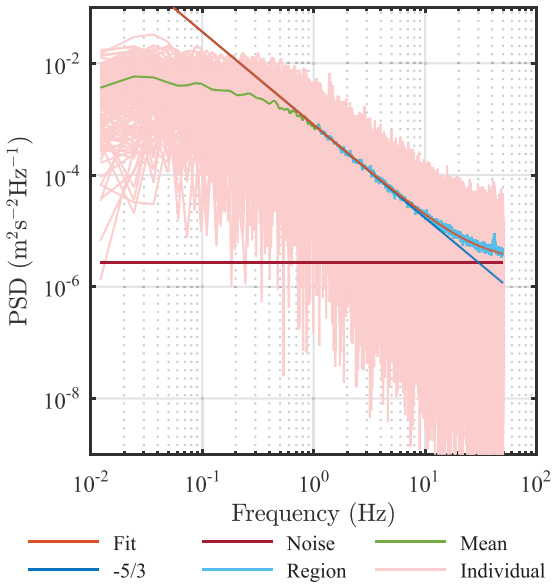

Fig. 12. Example of PSD showing individual samples and the fitting method applied to the mean. A small vibrational frequency is present at 41.7 Hz. The pink lines represent the individual PSD per T_{stat} time series, the green line is the mean PSD with the light blue highlighting the region used in the line fitting calculation. The dark blue line is the $f^{-5/3}$ slope, the dark red line the noise floor and the orange line the best fit calculated by the algorithm. (For interpretation of the references to colour in this figure caption, the reader is referred to the web version of this paper.)

The features in the ADV spectrum that are not attributable to the turbulent cascade are all accounted for as vibrations via comparison to the accelerometer. The frequency and amplitude of vibrations was different for every cantilever length (depth measured) and flow speed and the data presented in Figs. 11 and 12 are only two examples. In order to minimise this effect a mitigation strategy of losing the guy lines for near surface measurements and tightening them for longer lever, deep measurements proved very effective. In addition, the variance due to vibration, i.e., the total area under vibration induced spikes can be deducted from the I measurements in the same manner as Doppler noise, as described in Section 3.8. However, this value was found to be low (as shown in the example in Fig. 12) for all data used. Note that the data used in Fig. 11 was not used in the analysis of turbulence metrics, and is included only as an extreme example case.

Instrument noise is an important metric both to assess instrument performance and to correct measured I values. The instrument noise was assessed through the PSD line fit method developed by Richard et al. (2013). The PSD is computed for each sample then averaged before the fit method is applied. Fig. 12 illustrates an example with the raw sample PSDs, the averaged PSD with the region used for the line fit method highlighted, the integral sub-range and noise floor slopes and the line of best fit. In addition to the white Doppler noise the additional variance in the signal due to vibration of the sensor, which can be seen in Fig. 12 at 41.7 Hz. It is evident that the magnitude of the spike in this case is severely reduced compared with the extreme data given in Fig. 11.

Across the measurements taken the maximum variance due to noise in any orientation after conversion was 0.0010 m^2 s^{-2} which represents 26.2% of the total measured variance of that data-set. For each T_{stat} sample a σ^2_{noise} value is calculated, to correct the corresponding I values.

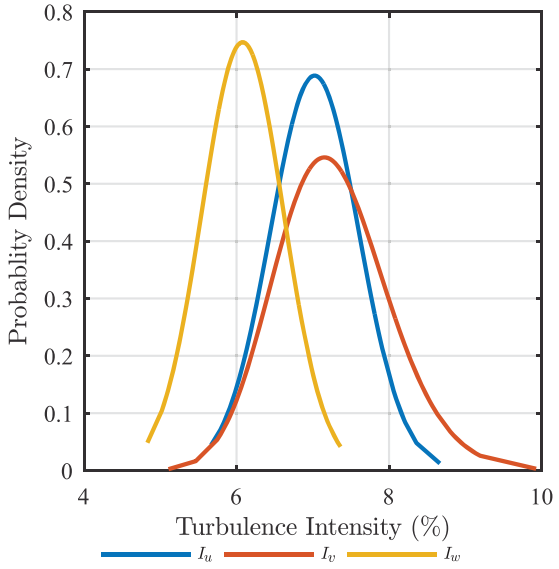

Fig. 13. Distributions of I for each velocity direction at a single point (0,0,1.4) at 82 rpm.

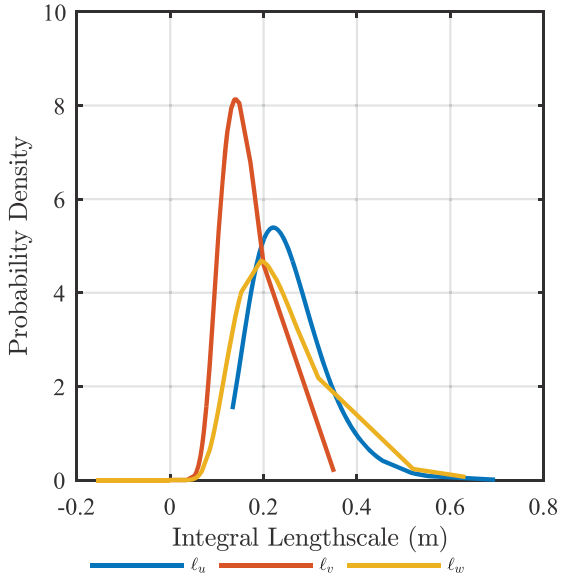

Fig. 15. Distribution of lengthscales at centre of tank at a single point (0,0,1.4) at 82 rpm.

4.4. Turbulence intensities

Fig. 13 presents the distributions of the turbulence intensity values at (0, 0, 1.4). For each direction a χ^2 distribution test with a 1% significance level was used to assess the best distribution type. The x and z components were shown to be normally distributed while the y component was log-normal. In real sea conditions (Sellar and Sutherland, 2015) found all I components to be normally distributed and thus the I_v represents an anomaly.

The variation of turbulence intensities (I_u, I_v, I_w) in the z- and x-axes is given in Fig. 14. It can be seen that the turbulent fluctuations are most prominent furthest upstream in the lower portion of the water column in all cases, this is in part due to the normalisation by the local slower $\bar{u}$ as given in Fig. 9. In the majority of locations I_u are in the 5–10% range which agrees well with field measurements from multiple sites (Sellar and Sutherland, 2015; Thomson et al., 2012). The streamwise and transverse values are approximately equal in value across the measurement range (mean values are $1.0I_u$), with the vertical being on average $0.8I_u$.

The transverse I_v and vertical values show similar patterns, with the highest values at below 1.2 m depth upstream of the horizontal centre point with a maximum value of 20%. The other measurement points showed values in the 5–10% range.

4.5. Integral lengthscales

In tidal channels the integral lengthscales (ℓ) of turbulence and the ratio between the stream-wise and normal components is a key metric in characterising the site. Fig. 15 presents the probability distribution function of the three lengthscale components at 1.4 m elevation at the horizontal centrepoint of the tank. All three showed evidence of being log-normally distributed via the χ^2 distribution test to 1% significance factor. Field measurements have also shown these metrics to follow log-normal distributions (Sellar and Sutherland, 2015).

The ratio of mean values of ℓ_u: ℓ_v: ℓ_w in the tank is 1: 0.64: 0.96. Here coherent structures are likely dominated by the direction of the water injection resulting in higher transverse and vertical values than

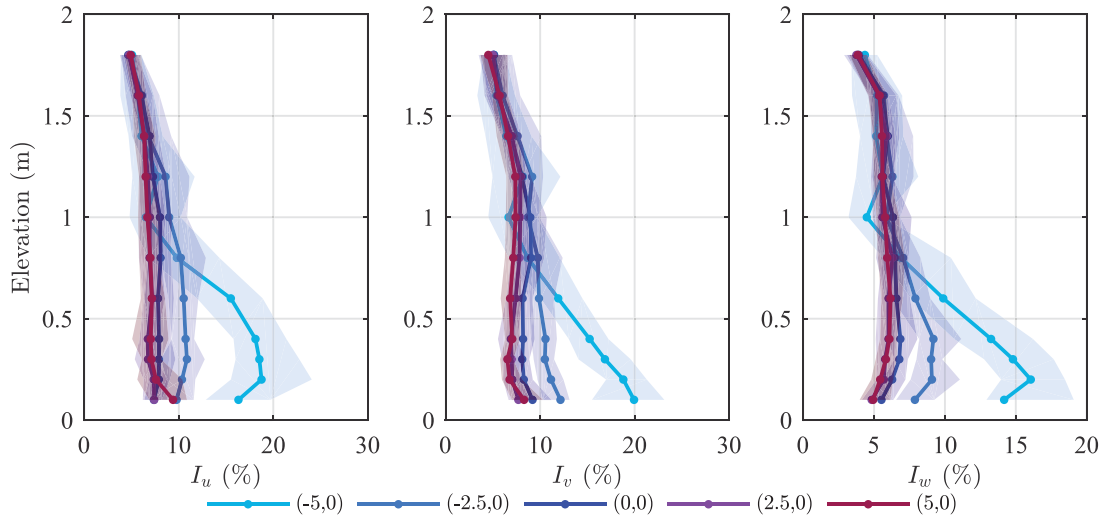

Fig. 14. Distribution of I_u, I_v and I_w, along the x- and z-axes. The solid lines represent mean values and the shaded area the range of values. (For interpretation of the references to colour in this figure caption, the reader is referred to the web version of this paper.).

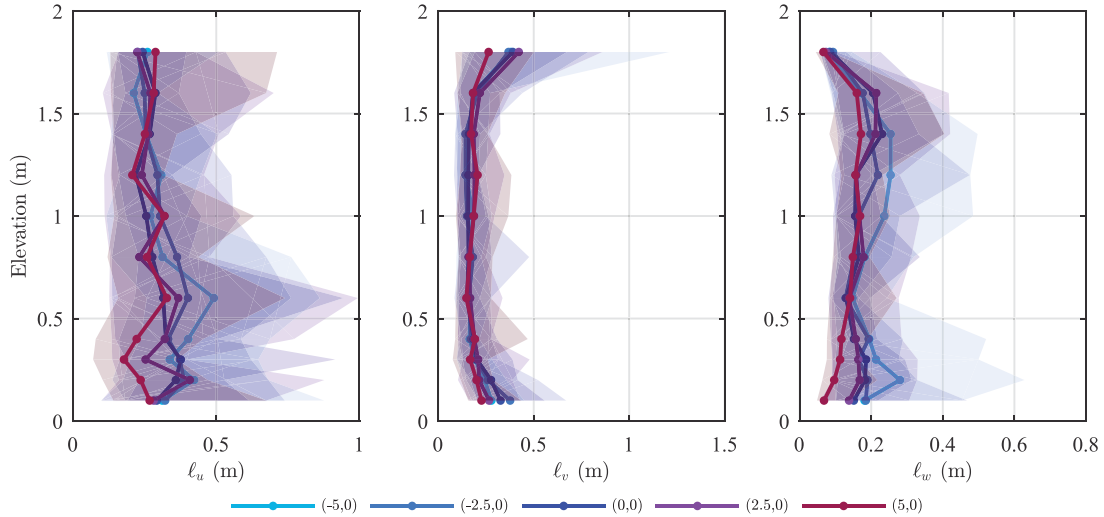

Fig. 16. Distribution of ℓ along the *x*- and *z*-axes. The solid lines represent mean values and the shaded area the range of values. (For interpretation of the references to colour in this figure caption, the reader is referred to the web version of this paper.)

found in the field where ratios are in the region of 1:0.3–0.5:0.1–0.3 have been measured (Thomson et al., 2014; Sutherland, 2015).

Fig. 16 shows the variation of these coherent structures across the *x*-axis of the tank. The streamwise values show a peak at 1.3 m depth decreasing and the flow moves downstream. The transverse profiles show largest values near the upper and lower boundaries, while the vertical component is suppressed near the surface but has a maximum at 1.6 m depth with the highest values furthest upstream.

4.6. Reynolds stresses

Two of the Reynolds stress tensors: τ_{uw} and τ_{vw} are presented in Figs. 17 and 18. τ_{uw} shows a maximum at (−5, 0, 0.3) of 0.40 Pa with other depth profiles fluctuation around 0 Pa. The same location provides the maximum in τ_{vw} but with values are an order of magnitude higher indicating that the shear in the tank is dominated by transverse-vertical fluctuations upstream. This effect is in contrast to the turbulence generation in the field where it is generally the τ_{uw} tensor that dominates turbulent production (Togneri and Masters, 2012).

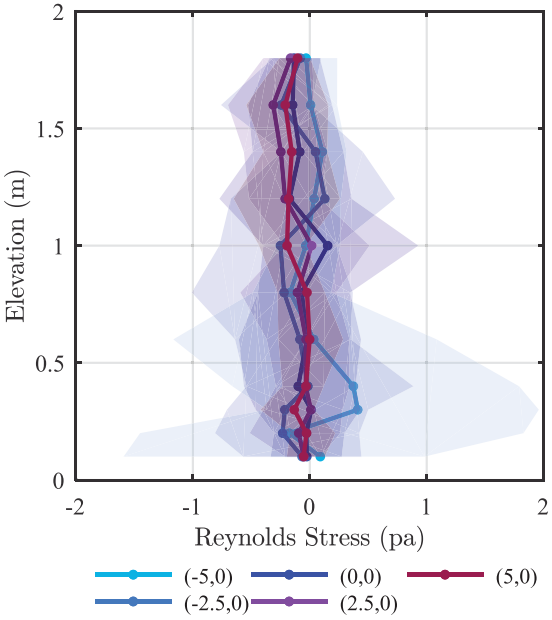

Fig. 17. Distribution of τ_{uw} along the *x*- and *z*-axes. The solid lines represent mean values and the shaded area the range of values. (For interpretation of the references to colour in this figure caption, the reader is referred to the web version of this paper.)

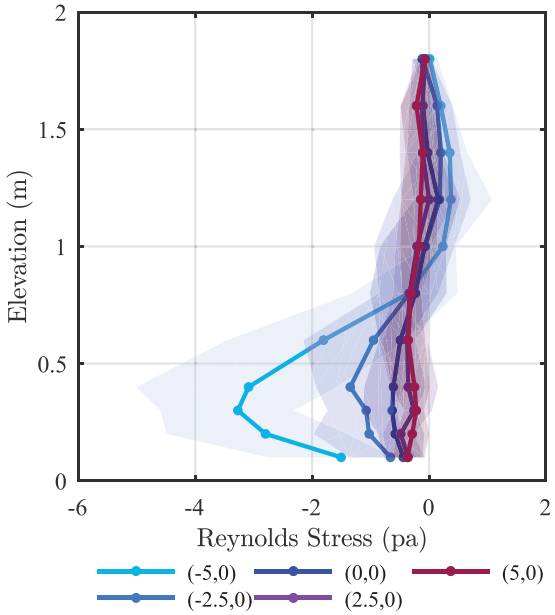

Fig. 18. Distribution of τ_{vw} along the *x*- and *z*-axes. The solid lines represent mean values and the shaded area the range of values. (For interpretation of the references to colour in this figure caption, the reader is referred to the web version of this paper.)

5. Discussion

5.1. Overview

To ensure the tank characterisation was comprehensive, the test methodology had to be robust, with the metrics covering both spatial and temporal variation. The measurement technique proved successful with the accelerometer accounting for non-turbulent fluctuations due to vibration in the ADV data. Uncertainty due to Doppler noise was quantified using an established technique. However, there remains uncertainty as to how increased variance from noise and vibration will

affect the length-scale measurements. The metrics used were chosen to be in-line with what is used in field measurement campaigns (Sellar and Sutherland, 2015; Thomson et al., 2012). The metrics were chosen over a stationarity period that was deemed stable while allowing for multiple samples to be taken in the available testing time. The distribution of metrics allows a quantification of the repeatability of tests which is important for designers.

In this section, the results are compared with previous flow measurements in the tank. Then, a discussion of the results in the context of field measurements and the differences in values is conducted.

5.2. Comparison with previous work

Previous measurements of mean flow in the tank using both single and dual axis electro-magnetic current metres were reported in Noble et al. (2015), which compares well with the results presented here. The previous depth profiles had a finer vertical resolution of 0.05 m, and generally showed little variation between points throughout the water column, which confirms the validity of interpolating between the more coarsely spaced, but higher individual measurement resolution, ADV measurements. The streamwise profiles along y=0 from both these and previous tests show the jet of water at mid-depth from the turning vanes predicted by CFD modelling (Robinson et al., 2015). As time at the facility was limited, the symmetry of the tank around the x-axis was not prioritised. The tank has 28-fold rotational symmetry and the impellers are driven to produce symmetrical flow about the mean direction. Previous measurements (Noble et al., 2015) across the entire test area of the tank at z=1.5 m confirm the velocity to be symmetrical about the flow direction. In summary, the previous study gives confidence to extrapolation in terms of symmetry and interpolation of data to the current study, which adds the temporal resolution required to process the turbulence metrics.

5.3. Comparison with Fall of Warness field measurements

In real tidal energy stream sites the flow conditions are complex with characterising metrics varying with location, tide direction, mean velocity, depth, tidal cycle and wave conditions. To make comparisons between turbulence metrics in the field and in scaled conditions, a framework for comparing metrics must be established. A developer will likely propose a single flow condition for a test based on field measurements. As a basis of this discussion a test condition, based on a data set collected from a single ADCP deployment during the ReDAPT project, was utilised. The first stage in such comparisons is to declare the representative metrics to be used. For scale model testing it is likely that these will be those that have maximum impact on devices, rather than those that define the turbulence production.

It is proposed that the next stage is to define the ratios of a given parameter in the x, y and z directions as well as the variation of each parameter with depth. As a 20th scale turbine model for a 1 MW device tested in the facility will occupy ~50% of the water column, it is important that the variation with parameters over this range is similar to those that a device will experience in a real site.

The field data used in this comparison was collected at the Fall of Warness over a 2 month period (June–July 2014), for more information see Sellar and Sutherland (2015). The data were limited to a subset of conditions, where depth averaged velocity was between 0.9 and 1.1 m s^{-1} (a representative cut-in velocity for a commercial scale tidal turbine). Surface significant wave heights were limited to a maximum of 0.5 m.

The results from the FloWave tests show a degree of variation of metrics throughout the tank as predicted. This variation can potentially be used to select an area of the tank best matched to a specific set of site conditions for a device test. However, tidal sites are hugely varied in terms of the flow conditions and it is not possible to use any facility to

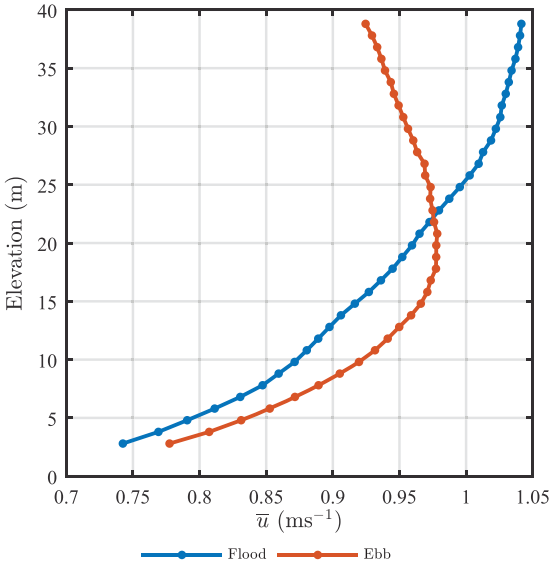

Fig. 19. Sample $\overline{u}$ depth profiles from field measurements.

recreate all possible conditions without modifying the flow. Where it is desirable to recreate a range of real sea conditions a variety of depth profile shapes are required, as some sites show a power-law relationship between velocity and depth (Legrand, 2009) and others a near surface velocity deficit (Sellar and Sutherland, 2015). Fig. 19 shows the high degree of variation in $\overline{u}(z)$ between Flood and Ebb tides at this site within these conditions. As the $\overline{u}(z)$ profiles measured in the FloWave facility do not show this near surface velocity deficit, only metrics from flood tides were used for this discussion. Fitting the streamwise velocity to a power law results in a power index of 7.8. This fits most closely with the velocity profile at (−5, 0) in Table 5, ignoring fits with $R^2 < 0.8$. The majority of depth profiles have a similar shape with the exception of the (0,5) profile, which is unlikely to be of use as a test condition given the severity of the velocity deficit.

A measurement of streamwise depth profiles in the field is normally associated with a rough surface causing a flow gradient. Thus, a depth profile near the bottom boundary would be fitted to a log-law and include a roughness-coefficient term (Cheng, 2007). In this case there is limited length over-which the bottom surface has to impede the flow and develop a gradient, in addition the facility's tank floor is relatively smooth. Here, it is likely that the driving factor of the flow gradient is the flow direction generated by the impeller and turning vanes. The new generation of ADVs do allow near surface fine spatial resolution depth profiles for this purpose. However, this was deemed out of scope for this work, whose main focus was the turbulence of flow with regard to testing tidal energy devices away from this bottom boundary.

The mean mid-depth noise corrected turbulence intensities for 1 m s^{-1} flow data from the same site in the x, y and z orientations are reported as 10%, 9% and 5% respectively (Sutherland, 2015). These are the same order of magnitude as those measured in the tank with values in the region of 6–7% in all directions. In this case the tank showed a higher degree of isotropy than the field results. The (−5.0, 0) depth profile shows the values least in keeping with those from the EMEC site.

The integral lengthscales are generally found to be in the region of 30–50% of the channel depth in field measurements (Thomson et al., 2014; Sutherland, 2015). In the tank, however, the largest scales are ~25%. As previously mentioned the lengthscales both in the tank and field followed a log-normal distribution of values.

The two measured Reynolds stress tensors τ_{uw} and τ_{vw} were found in the field to have a ratio of τ_{uw}: τ_{vw} of 5:1. with τ_{uw} values of ~15 Pa. τ_{uw} values were greatest near the bottom but τ_{vw} were greatest at

Table 6
A summary of typical mean values of turbulence parameters from the Results section.

Metric	Symbol	Typical values
Turbulence intensity	I_x	5–11%
Integral lengthscale	ℓ_u	0.18–0.41 m
Reynolds stress	τ_{uw}	−0.31–0.15 Pa
	τ_{vw}	−1.35–0.20 Pa

mid-depth (Desguers, 2016). These patterns were not well replicated in the tank environment where the causes of shear forces is the impeller generated flow angles, as opposed to natural boundary layer friction in the field. It is not clear that Reynolds Stress is a metric that directly affects device loading, thus it is a more important and more realistic goal that the lengthscales and I magnitudes be well matched.

When talking about any scale reproduction of flows the method of scaling must be discussed. There are two main ratios that are traditionally used to do this at tidal sites. These are the Reynolds number, a ratio of the momentum to viscous forces, and the Froude number, a ratio of the inertia to the gravitational effects on the flow. These ratios are defined in Eqs. (14) and (15) where ρ is the density, μ is the dynamic viscosity, l is a characteristic length and g is the gravitational field strength (Draper et al., 2013):

$$Re = \frac{\rho u l}{\mu} \tag{14}$$

$$Fr = \frac{u}{\sqrt{gl}} \tag{15}$$

As the density, viscosity and gravitational field strength have limited variability, it is the velocity and characteristic length that will dominate matching conditions. There are various options for which length to select: one is the depth, one is the stream-wise integral length-scale. The goal here is to adopt a scaling that will effectively reproduce loadings on a tidal device and thus future work must assess the effect of altered scaling parameters on lift and drag forces. As well as scaling the tank's turbulence parameter, successful testing of a small scale TEC device should consider modifying the rotor geometry, as discussed in Whelan and Stallard (2011). For a comprehensive review of the high degree of variation in metrics at tidal sites and how to characterise them see Sellar and Sutherland (2015) and Clark et al. (2015). The University of Edinburgh is a charitable body, registered in Scotland, with registration number SC005336.

6. Summary and future work

This work extends the understanding of the flow characteristics in the new FloWave facility. It defined and followed a robust methodology for measuring and processing flow metrics, detailing their variation and repeatability. As a quick reference, some typical mean values for key turbulence parameters have been selected from the results, which are given in Table 6.

Robustness of results was ensured by measuring and mitigating instrument vibration. Noise was quantified and where possible removed from turbulence metrics. The repeatability of metrics was quantified through the distributions, allowing designers to make informed decisions about the duration of a test in a given condition.

The 77 measurement locations utilised during this work still represent coarse spacings given the size of the facility, and it would be advantageous to take more detailed measurements around the centre of the tank in the main test area. In general the results show that aside from the depth profiles at $(-5, 0)$ and $(0, -5)$ the flow characteristics are relatively consistent. With downstream centreline locations in particular more consistent with the centre point. It is therefore a fair reflection to advise testing be kept within the 5 m radius for the tested flow regime. For scale device testing, it is important that the valid area over which a range of conditions are met is well defined by the user, before a definitive test area can be defined.

It should be noted that it is not necessary for the full depth of the tank replicate the full depth of field measurements. Rather, it is important that the inflow experienced by a device or devices is representative of what they would experience at the mounting depth range in the field, and that bypass and blockage effects are appropriate.

The flow regime tested shows similar turbulence intensity values to those at the EMEC tidal site for one flow condition based on a limited set of conditions. The integral lengthscales are slightly smaller as a percentage of total depth and their ratios are inconsistent. The Reynolds stress tensors being highly dissimilar in value and spatial distribution. As the real field conditions vary so wildly future work should involve a discretisation of conditions into subsets which can be compared to tank flow. This will necessitate the inclusion of waves with current and the characterisation of their interaction. This will include: high and low turbulence conditions and a variety of surface wave states based on height, period and direction. The ideal scenario being that both waves and turbulence and their interactions can be specified from any site and replicated in the tank for scale device testing. It is a significant piece of ongoing work to fully characterise the waves, current, turbulence, and their interactions in the tank.

Beyond characterising the tank as it currently operates, future work could focus on flow modification to cover a greater number of real sea conditions. This would include surface waves and concurrent flow and the effects on depth profiles and turbulence metrics. In addition, Blackmore et al. (2015) give an overview of techniques that can be used to modify tank turbulence and these could be explored in the more complex geometry of the FloWave facility. Applying these, and other methods, and then validating them in the FloWave facility is an ongoing goal to improve both understanding of turbulence and its effect on devices.

Acknowledgements

The authors would like to thank Nortek UK for supporting this work along with the Engineering and Physical Science Research Council (EPSRC) for funding the project under the Impact Accelerator Account. In addition we would like to thank the Energy Technologies Institute and RCUK Energy programme for funding this research as part of the IDCORE programme (EP/J500847/1), and the UK EPSRC for supporting the construction of the FloWave facility (EP/I02932X/1). The University of Edinburgh is a charitable body, registered in Scotland, with registration number SC005336.

References

Analog-Devices, 2016. Three-Axis Accelerometer Technical Specifications. URL ⟨http://www.analog.com/media/en/technical-documentation/evaluation-documentation/EVAL-ADXL327Z.pdf⟩.

Blackmore, T., Gaurier, B., Myers, L., Germain, G., Bahaj, A., 2015. The effect of freestream turbulence on tidal turbines. In: European Wave and Tidal Energy Conference.

Blackmore, T., Myers, L.E., Bahaj, A.S., 2016. Effects of turbulence on tidal turbines implications to performance, blade loads, and condition monitoring. Int. J. Mar. Energy 14, 1–26. http://dx.doi.org/10.1016/j.ijome.2016.04.017.

Cheng, N.S., 2007. Power-law index for velocity profiles in open channel flows. Adv. Water Resour. 30 (8), 1775–1784. http://dx.doi.org/10.1016/j.advwatres.2007.02.001.

Clark, T., Fisher, S., Minns, N., 2015. Turbulence: Best Practices for the Tidal Power Industry - Part 3: Turbulence and turbulent effects in turbine and array engineering. Technical Report. ⟨http://www.oceanarraysystems.com/publications⟩.

Desguers, T., 2016. Turbulence characterisation in energetic tidal currents.

Draper, S., Stallard, T., Stansby, P., Way, S., Adcock, T., 2013. Laboratory scale experiments and preliminary modelling to investigate basin scale tidal stream energy extraction. In: 10th European Wave and Tidal Energy Conference, Aalborg, Denmark.

Emery, W., Thomson, R., 2001. Data Analysis Methods in Physical Oceanography, 2nd edition.

Goring, D.G., Nikora, V.I., 2002. Despiking acoustic Doppler velocimeter data. J. Hydraul. Eng. 128 (1), 117–126. http://dx.doi.org/10.1061/(ASCE)0733-9429(2002)128:1(117).

Legrand, C., 2009. Assessment of tidal energy resource. Technical Report. Black and Veatch, EMEC.

Lohrmann, A., Hackett, B., Røed, L., 1990. High resolution measurements of turbulence, velocity and stress using a pulse-to-pulse coherent sonar. J. Atmos. Ocean. Technol. 7 (1), 19–37.

Mori, T., Naganuma, K., Kimoto, R., Yakushiji, R., Nagaya, S., 2007. Hydrodynamic and hydroacoustic characteristics of the Flow Noise Simulator. In: Proceedings of the 5th ASME-JSME Joint Fluids Engineering Conference, pp. 121–127. doi:10.1115/FEDSM2007-37531.

Myers, L.E., Bahaj, A.S., 2010. Experimental analysis of the flow field around horizontal axis tidal turbines by use of scale mesh disk rotor simulators. Ocean Eng. 37 (2–3), 218–227. http://dx.doi.org/10.1016/j.oceaneng.2009.11.004.

Noble, D.R., Davey, T., Smith, H.C.M., Kaklis, P., Robinson, A., Bruce, T., 2015. Spatial variation in currents generated in the FloWave Ocean Energy Research Facility. In: 11th European Wave and Tidal Energy Conference, Nantes, France.

Nortek-AS, 2016. Vectrino Profiler Technical Specifications. URL ⟨http://www.nortek-as.com/lib/brochures/vectrino-ii⟩.

O'Neill, P., Nicolaides, D., Honnery, D., Soria, J., 2004. Autocorrelation functions and the determination of integral length with reference to experimental and numerical data. In: 15th Australasian Fluid Mechanics Conference, vol. 1, pp. 1–4.

Park, J.T., Cutbirth, J.M., Brewer, W.H., 2005. Experimental methods for hydrodynamic characterization of a very large water tunnel. J. Fluids Eng. 127 (November), 1210. http://dx.doi.org/10.1115/1.2060740.

Pope, S., 2000. Turbulent Flows. Cambridge University Press, 65–73.

Richard, J.-B., Thomson, J., Polagye, B., Bard, J., 2013. Method for identification of Doppler noise levels in turbulent flow measurements dedicated to tidal energy. Int. J. Mar. Energy 3–4, 52–64. http://dx.doi.org/10.1016/j.ijome.2013.11.005.

Robinson, A., Bryden, I., Ingram, D., Bruce, T., 2014. The use of conditioned axial flow impellers to generate a current in test tanks. Ocean Eng. 75, 37–45. http://dx.doi.org/10.1016/j.oceaneng.2013.10.016.

Robinson, A., Ingram, D., Bryden, I., Bruce, T., 2015. The effect of inlet design on the flow within a combined waves and current flumes, test tank and basins. Coast. Eng. 95, 117–129. http://dx.doi.org/10.1016/j.coastaleng.2014.10.004.

Sellar, B.G., Sutherland, D.R.J., 2015. MD 3.8 – Tidal energy site characterisation at the Fall of Warness, emec, UK. Technical Report, available from: ⟨http://redapt.eng.ed.ac.uk/⟩. http://dx.doi.org/10.7488/ds/1687.

Sutherland, D.R.J., 2015. Assessment of mid-depth arrays of single beam acoustic Doppler velocity sensors to characterise tidal energy sites (Ph.D. thesis).

Taylor, G., 1938. The spectrum of turbulence. Proc. R. Soc. A: Math. Phys. Eng. Sci. 164 (919) 476–490.

Thomson, J., Polagye, B., Richmond, M., Durgesh, V., 2010. Quantifying turbulence for tidal power applications. In: MTS/IEEE Seattle, OCEANS 2010, no. 4. http://dx.doi.org/10.1109/OCEANS.2010.5664600.

Thomson, J., Polagye, B., Durgesh, V., Richmond, M.C., 2012. Measurements of Turbulence at two tidal energy sites in Puget Sound, WA. IEEE J. Ocean. Eng. 37 (3), 363–374.

Thomson, J., Kilcher, L.F., Harding, S.F., 2014. Multi-scale coherent turbulence at tidal energy sites. In: Proceedings of the 5th International Conference on Ocean Energy, Halifax, Nova Scotia, pp. 1–6.

Togneri, M., Masters, I., 2012. Comparison of marine turbulence characteristics for some potential turbine installation sites. In: 4th International Conference on Ocean Energy, pp. 6–11.

Whelan, J. I., Stallard, T.J., 2011. Arguments for modifying the geometry of a scale model rotor. In: 9th European Wave and Tidal Energy Conference, Southampton, UK.

International Journal of Marine Energy 18 (2017) 109–113

Contents lists available at ScienceDirect

International Journal of Marine Energy

journal homepage: www.elsevier.com/locate/ijome

Design diagrams for wavelength discrepancy in tank testing with inconsistently scaled intermediate water depth

Donald R. Noble [a,b,*], Samuel Draycott [a], Thomas A.D. Davey [a], Tom Bruce [b]

[a] FloWave Ocean Energy Research Facility, The University of Edinburgh, Edinburgh EH9 3BF, United Kingdom
[b] School of Engineering, The University of Edinburgh, Edinburgh EH9 3FB, United Kingdom

ARTICLE INFO

Article history:
Received 9 March 2017
Revised 13 April 2017
Accepted 17 April 2017
Available online 20 April 2017

Keywords:
Tank testing
Water depth
Froude scaling
Marine renewable energy

ABSTRACT

The well-known dispersion relation links the length and period of a water wave with the depth in which it propagates. When model testing in tanks, the water depth should be consistently scaled to correctly replicate the waves. While this is done routinely by scaling foreshore bathymetry in coastal engineering physical model studies, and is not significant for deep water scenarios, this is not always considered when testing marine renewable energy devices, which are often in intermediate depth. Where water depth is not scaled consistently there will be resulting errors in wave parameters including wavelength, steepness, celerity, group velocity, and power. Design diagrams are presented to quantify and visualise these discrepancies over a typical range for testing offshore renewable energy devices. This design tool will facilitate experimental planning, quantification of uncertainties, and correlation of model test results with field data.

1. Introduction

When re-creating waves in a tank using Froude scaling laws, it is important to consider the depth ratio between the deployment site of interest and the tank, and to scale this correctly where possible. There will of course be instances where this is not possible, for example the deployment site water depth is not known, the tank has a fixed depth, or there are other constraints on the model size.

Whilst it is common knowledge that the wavelength of a water wave is a function of water depth, there has been little published regarding the incorrect scaled reproduction of wavelength resulting from inconsistent depth scaling. This issue was mentioned in [1], and expanded upon in [2], but the authors are not aware of other published discussions.

A number of authors, including [3,4], highlight the issue of scaling water depth when tank testing in the context of modelling mooring systems. These do not, however, highlight the consequences for wavelength error. Water depth scaling in relation to distorted hydraulic models is discussed in [5], noting that these models cannot be used for the study of water waves, as wavelength depends on water depth. For similitude in waves, the horizontal and vertical scales must be the same.

This technical note highlights the potential discrepancy in wavelength, group velocity, and power by restating the relevant aspects of small-amplitude wave theory. A method for calculating and visualising the errors resulting from incorrectly scaling the water depth when testing is then presented. This is followed by a brief discussion of implications for testing, focusing on marine renewable energy converters, which may be particularly sensitive to this issue.

* Corresponding author at: FloWave Ocean Energy Research Facility, The University of Edinburgh, Edinburgh EH9 3BF, United Kingdom.
E-mail address: D.Noble@ed.ac.uk (D.R. Noble).

http://dx.doi.org/10.1016/j.ijome.2017.04.001
2214-1669/

2. Background theory

When re-creating waves in a test tank, the Froude scaling law is used to match the ratio of inertial to gravitational forces that dominate this problem. The ratio of depth at the site of interest to the tank depth is important because gravity waves in water of finite depth can only be correctly re-created when the water depth is also scaled. The wavelength, celerity, and group velocity are all influenced by water depth, which in turn affect wave steepness and power. If the depth is not correctly scaled, this will lead to frequency dependent errors in these parameters, as discussed below. This situation may arise from constraints in the test facility, or from the deployment site depth not being known or considered when the model testing was being conducted.

It is well known that the properties of water waves are related by the dispersion relation, Eq. (1)

$$\omega^2 = gk\tanh(kh) \tag{1}$$

where ω is rotational frequency, k the wavenumber, g acceleration due to gravity, and h water depth. The dispersion relation can also be expressed in terms of period T, and wavelength L, using Eq. (2) to obtain Eq. (3).

$$\omega = 2\pi/T, \quad k = 2\pi/L \tag{2}$$

$$\Rightarrow L = \frac{gT^2}{2\pi}\tanh\left(\frac{2\pi h}{L}\right) \tag{3}$$

Eq. (3) gives a unique relationship between the three quantities of wavelength, period, and depth. Therefore, if the depth is not scaled consistently, then wavelength will also be incorrect for a given Froude scaled period.

The wavelength at a site L_{site} can be calculated from wave period and depth using the dispersion relation Eq. (3), expressed here in terms of wavelength and period at the site.

$$L_{\text{site}} = \frac{gT_{\text{site}}^2}{2\pi}\tanh\left(\frac{2\pi h_{\text{site}}}{L_{\text{site}}}\right) \tag{4}$$

Using Froude scaling, where λ is the scale factor, these properties at tank scale should thus be Eq. (5) giving Eq. (6).

$$T_{\text{tank}} = T_{\text{site}}\sqrt{\lambda}, \quad h_{\text{tank}} = h_{\text{site}}\lambda, \quad L_{\text{tank}} = L_{\text{site}}\lambda \tag{5}$$

$$L_{\text{tank}} = \frac{gT_{\text{site}}^2\lambda}{2\pi}\tanh\left(\frac{2\pi h_{\text{site}}\lambda}{L_{\text{tank}}}\right) \tag{6}$$

However, if the tank depth is not correctly scaled, $h_{\text{tank}} \neq h_{\text{site}}\lambda$, the (incorrect) wavelength in the tank $L_{\text{tank}*}$ will instead be given by Eq. (7), assuming the period is correctly Froude scaled.

$$L_{\text{tank}*} = \frac{gT_{\text{site}}^2\lambda}{2\pi}\tanh\left(\frac{2\pi h_{\text{tank}}}{L_{\text{tank}*}}\right) \tag{7}$$

The error in wavelength ε_L is taken as the ratio of wavelength actually generated in the tank $L_{\text{tank}*}$ to the correctly scaled wavelength $L_{\text{tank}} = L_{\text{site}}\lambda$.

$$\varepsilon_L \equiv \frac{L_{\text{tank}*}}{L_{\text{tank}}} \tag{8}$$

The group velocity of a wave C_g is a more complex function of wavelength and water depth, given by Eq. (9).

$$C_g = \frac{1}{2}\sqrt{\frac{gL}{2\pi}\tanh\left(\frac{2\pi h}{L}\right)}\left[1 + \frac{4\pi h}{L\sinh\left(\frac{4\pi h}{L}\right)}\right] \tag{9}$$

The error in group velocity can be computed in the same manner, by calculating $C_{g,\text{tank}*}$ based on the wavelength actually generated in the tank, and $C_{g,\text{tank}}$ from the correctly scaled wavelength. The error is simply the ratio between these, Eq. (10)

$$\varepsilon_{Cg} \equiv \frac{C_{g,\text{tank}*}}{C_{g,\text{tank}}} \tag{10}$$

The speed, or celerity, of an individual wave is given by $C = L/T$, and steepness by $S = H/L$. Provided the period and height are correctly Froude scaled, the corresponding relative errors in celerity and steepness will thus equal the error in wavelength. As wave power $P = E_A C_g$, where E_A is wave energy per unit horizontal area [5], the relative error in power will equal that of group velocity. Any discrepancy in wave power is particularly important in tank testing wave energy converters, as wave power (kW/m) is scaled by $\lambda^{2.5}$, magnifying the projected full scale power discrepancy.

3. Graphical visualisation of errors

Whilst the theory covered in Section 2 is not new knowledge, a method to calculate and visualise these discrepancies has been developed in order to assist with test design and aid understanding of this potential source of error. This method utilises a new term 'scale depth discrepancy' (*SDD*), defined as Eq. (11), and shown graphically in Fig. 1.

$$SDD \equiv \lambda \frac{h_{\text{site}}}{h_{\text{tank}}} \tag{11}$$

This term aggregates the scale factor plus relative water depths between deployment site and tank into one variable. A value of *SDD* less than unity corresponds to the tank being too deep for the scaled site depth, resulting from a relatively shallower deployment site and/or a smaller model scale.

The frequency dependent errors resulting from this discrepancy can then be plotted over the range of *SDD* and non-dimensional tank-scale period, Eq. (12).

$$\tau_{\text{tank}} = T_{\text{tank}} \sqrt{g/h_{\text{tank}}} = T_{\text{site}} \lambda \sqrt{g/h_{\text{tank}}} \tag{12}$$

The non-dimensional period is only the same in the tank as at the site when the depth is scaled consistently, i.e. $SDD = 1$. Discrepancy in wavelength, steepness, or celerity is shown in Fig. 2, noting that these are of the same magnitude, whilst the discrepancy in group velocity or power is shown in Fig. 3.

A deep water simplification is often used in offshore engineering, based on the fact that $\tanh(kh) \to 1$ for large kh. This simplification is usually applied for $kh > \pi$ where the discrepancy is $< 0.4\%$ [6]. Expressed in terms of depth and wavelength, this limit equates to $h/L > 1/2$. For situations where both the deployment site and test tank can be considered deep water, i.e. below both dashed lines in Fig. 2, the error in wavelength is negligible and correct depth scaling is not required. It is interesting to note that the errors in wavelength are compounded when calculating the group velocity, resulting in a discrepancy for $C_g \approx 2\%$ at the deep water limit, although this is still likely to be acceptable when tank testing.

Wave energy converters typically operate in wave periods of 3–15 s, and depths around 20–80 m, which equates to full-scale non-dimensional periods of about 1–10. At tank scale, the non-dimensional period should be similar, providing *SDD* is close to unity. Typical model scales for testing model renewable energy devices are between 1:100 and 1:10, tested in tanks 0.5–5 m deep, although large models are unlikely to be tested in small tanks and vice versa. This may result in scaled depth discrepancies in the order of 0.3–3, obviously depending on the specifics of model, device, and tank. Therefore, errors in wavelength/steepness/celerity of up to $\pm 30\%$ may be experienced in testing. This results in a corresponding $\pm 20\%$ discrepancy in wave power and group velocity.

To facilitate understanding of Figs. 2 and 3, examples are shown on the secondary axes with a 1:25 scale model, 50 m deep site, and 2 m deep test facility. A 12 s full-scale wave of interest to a wave-energy device would have non-dimensional period $\tau_{\text{tank}} = 5.3$. If the site depth was 40 m or 100 m instead of 50 m, as shown on the lower secondary x-axis, the wavelength/steepness/celerity (Fig. 2) would be wrong by a factor ε_L of 0.95 or 1.09 respectively, and group velocity/wave power (Fig. 3) would be wrong by a factor ε_{Cg} of 1.02 or 0.88, as shown in Table 1 along with additional examples.

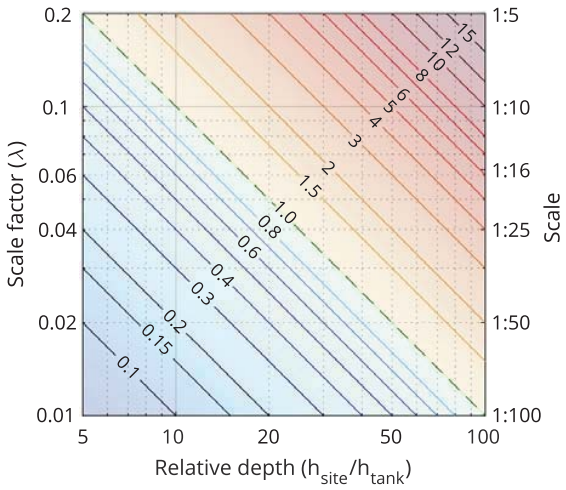

Fig. 1. Contours of scale depth discrepancy (SDD) shown for a range of relative depths (site to tank) and scale factors. A value of SDD less than unity corresponds to the tank being too deep for the scaled site depth, resulting from a relatively shallower deployment site and/or a smaller model scale.

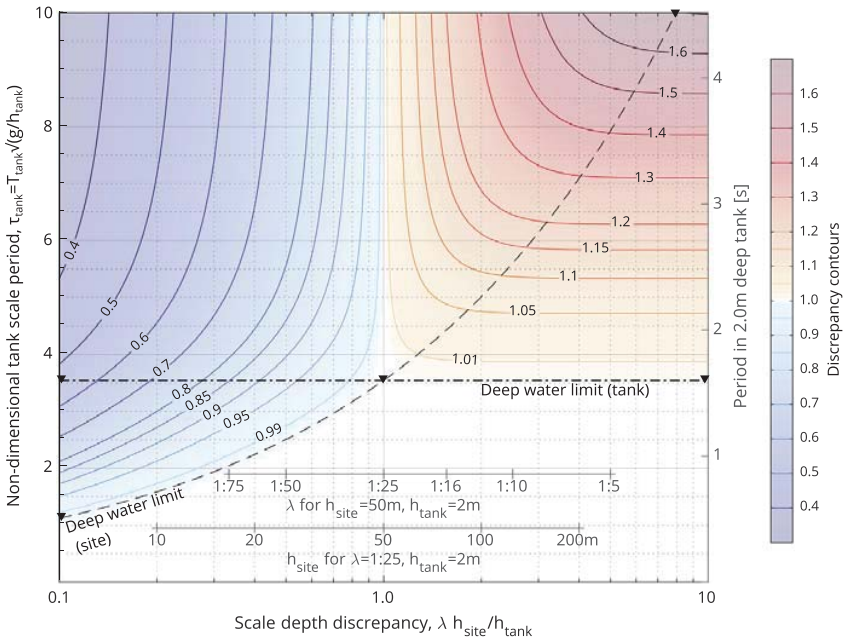

Fig. 2. Contours of relative error in wavelength or steepness or celerity for a range of scaled depth discrepancies and non-dimensional tank scale periods. Secondary axes show example scale factor and site depth for other parameters fixed. Dashed and dash-dot lines shows deep water limits for site and tank respectively.

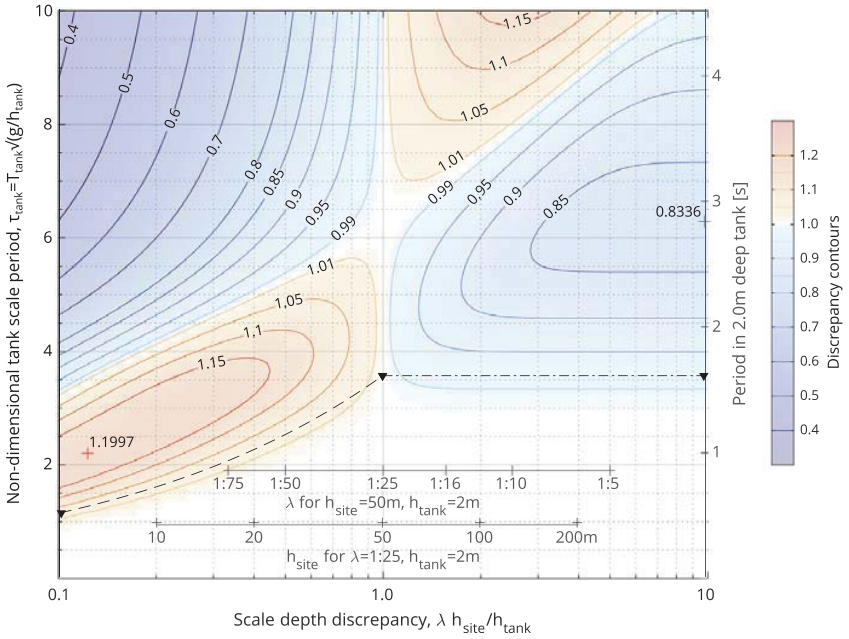

Fig. 3. Contours of relative error in group velocity or wave power for a range of scaled depth discrepancies and non-dimensional tank scale periods. Secondary axes show example scale factor and site depth for other parameters fixed. Dashed and dash-dot lines shows deep water limits for site and tank respectively.

4. Discussion

For marine renewable energy devices, such as wave energy converters or floating offshore wind turbines, wave steepness can be particularly important as this affects floating device response. It is also beneficial to understand how the power of waves is scaled and what errors may be present when modelling a device to extract this power. The method presented here is designed to be an aid to tank test planning, allowing the range of discrepancies to be quantified when selecting a facility

Table 1
Example discrepancies in a 12 s full-scale wave, for wavelength/steepness/celerity ε_L Fig. 2 and group velocity/wave power ε_{Cg} Fig. 3

Scale	h_{site}	h_{tank}	*SDD*	τ_{tank}	ε_L	ε_{Cg}
1:25	50 m	2 m	1	5.31	1	1
1:25	40 m	2 m	0.8	5.31	0.95	1.02
1:25	75 m	2 m	1.5	5.31	1.07	0.93
1:25	100 m	2 m	2.0	5.31	1.09	0.88
1:50	50 m	2 m	0.5	3.76	0.92	1.13
1:16	50 m	2 m	1.56	6.64	1.13	0.98
1:25	50 m	3 m	0.67	4.34	0.94	1.08

and model scale. It will also be of benefit when correlating tank test measurements to real site deployment where the scaled depth ratio is not unity, which is a likely scenario.

This issue of incorrect depth scaling may not have received much attention previously, as it is less critical for other applications of tank testing. For coastal models where water depth is paramount, the bathymetry is usually re-created in the test facility, removing any depth error and corresponding wavelength issues. When testing ships, there is not a unique depth in which they operate, and this can usually be classified as 'deep water' reducing the importance of understanding this depth scaling discrepancy. Oil platforms also typically operate in deep water relative to the waves experienced.

While the errors presented here have been calculated using linear wave theory, they also hold for second order Stokes waves, where although the wave shape is different the dispersion relation remains the same [6]. A correction to the dispersion relation is required for third and higher orders.

Discrepancies in wave spectra are frequency dependent, and can be visualised as vertical sections through the contoured surfaces shown in Figs. 2 and 3. For wavelength, steepness, or celerity the error has the same direction as the scale depth discrepancy, i.e. $\varepsilon_L < 1$ for $SDD < 1$. For group velocity or wave power it is possible to have both errors smaller and larger than unity for a given *SDD*.

Scale dependencies are routinely accounted for in the analysis of test results. For example, when using Froude scaling in tank testing, time is scaled by $\sqrt{\lambda}$. It is also common to test in fresh water which is approximately 2.5% less dense than typical sea water. In the same manner, the design methods presented here could also be applied to any discrepancy in the scaled water depth.

5. Conclusion

A method has been developed to quantify and visualise the errors that may arise while tank testing if the scaled water depth is not correct. This issue may be of particular relevance to marine renewable energy, where devices sensitive to wavelength and power are moored in finite depth water conditions. For typical model tests, this may result in wavelength/steepness errors of up to $\pm 30\%$, and up to $\pm 20\%$ in wave power.

Acknowledgement

The authors would like to acknowledge the Energy Technologies Institute and RCUK Energy programme for funding this research as part of the IDCORE programme (EP/J500847/1), and the UK EPSRC for supporting the construction of the FloWave facility (EP/I02932X/1).

References

[1] S. Draycott, T. Davey, D.M. Ingram, J. Lawrence, A. Day, L. Johanning, Applying site-specific resource assessment: emulation of representative EMEC seas in the flowave facility, Proceedings of the Twenty-fifth International Ocean and Polar Engineering Conference, ISOPE, Kona, Big Island, Hawaii, USA, 2015.
[2] S. Draycott, On the Re-creation of Site-Specific Directional Wave Conditions, Engineering doctorate, The University of Edinburgh, 2016.
[3] B. Holmes, Tank Testing of Wave Energy Conversion Systems, Tech. rep., European Marine Energy Centre, Orkney, 2009. url: http://www.emec.org.uk/tank-testing-of-wave-energy-conversion-systems/.
[4] B. Holmes, K. Nielsen, Guidelines for the development & testing of wave energy systems, Tech. Rep. June, Hydraulics Maritime Research Centre, UCC, Cork, Ireland, 2010.
[5] B.L. Méhauté, An Introduction to Hydrodynamics and Water Waves, Springer, New York, 1976.
[6] R.G. Dean, R.A. Dalrymple, Water Wave Mechanics for Engineers and Scientists, World Scientific, 1991.

Proceedings of the ASME 2017 36th International Conference on Ocean, Offshore and Arctic Engineering
OMAE 2017
June 25-30, 2017, Trondheim, Norway

OMAE2017-62052

TESTING MARINE RENEWABLE ENERGY DEVICES IN AN ADVANCED MULTI-DIRECTIONAL COMBINED WAVE-CURRENT ENVIRONMENT

Donald R. Noble*
IDCORE/FloWave Ocean
Energy Research Facility,
Max Born Crescent, Kings Buildings,
Edinburgh, EH9 3BF, UK.
Email: D.Noble@ed.ac.uk

Samuel Draycott
Dr. Thomas A.D. Davey
FloWave Ocean Energy Research Facility,
Max Born Crescent, Kings Buildings,
Edinburgh, EH9 3BF, UK.
Email: Sam.Draycott@flowave.ed.ac.uk
Tom.Davey@flowave.ed.ac.uk

Prof. Tom Bruce
Institute for Energy Systems,
School of Engineering,
The University of Edinburgh,
Edinburgh, EH9 3FB, UK.
Email: Tom.Bruce@ed.ac.uk

ABSTRACT

Physical scale model testing is an important development tool, used extensively to study the behaviour of marine devices, vessels and structures in a controlled environment prior to deployment at sea. Whilst specific guidance on developing and testing marine renewable energy devices has been published over the past decade, it has limitations in terms of advanced environmental conditions for testing. The body of existing guidance is reviewed, and initial suggestions offered for additional test conditions that may be considered in later stages of model testing. This focuses on testing in combined waves and currents, particularly the multi-directional aspect thereof, which is now possible in facilities such as FloWave.

NOMENCLATURE

FOWT Floating Offshore Wind Turbine
MRE Marine Renewable Energy
TRL Technology Readyness Level
TST Tidal Stream Turbine
WEC Wave Energy Converter

*Address all correspondence to this author.

1 INTRODUCTION

Physical scale model testing in dedicated facilities is an important part of the development process for marine renewable energy and other technologies. It allows the study of device behaviour and performance in a controlled environment at relatively low cost, prior to deployment at sea.

There are many aspects involved in model testing, but the focus of this paper is reproducing the environmental conditions of the sea, and potential benefits of using more complex conditions when testing in a combined wave-current basin. The behaviour and power capture of Marine Renewable Energy (MRE) devices is highly dependent on the environmental conditions present at the site. Depending on the type of device, re-creating either the wave or current conditions will be paramount. However, the interaction between waves and current may also be important. The physical form of water waves is impacted by the presence of a current, becoming shorter and higher with an opposing flow, but longer and lower on a following current. Waves will also change the velocity profile and turbulence within a tidal current, with strongest effect close to the water surface.

This paper primarily considers testing of Wave Energy Converters (WECs) and Tidal Stream Turbines (TSTs), both fixed and floating devices. Although some of this guidance will also be applicable to Floating Offshore Wind Turbines (FOWTs), the additional complexities of including the aerodynamic interface are outside the scope of this work.

The following sections first summarise structured technol-

ogy development programmes and considerations for a combined wave-current basin such as FloWave, then offer a review of published guidance on environmental conditions for testing MRE devices, and finally present some initial recommendations for conditions that may be considered by developers during the later stages of tank testing. These recommendations are based on ongoing research and lessons learnt during testing at the FloWave Ocean Energy Research Facility at the University of Edinburgh.

1.1 Scale Model Testing as Part of Device Development Programme

Model testing has become an established part of a structured development process for MRE devices, as in other technologies and processes. Similar multi-stage development plans for WECs and TSTs are outlined in published guidance, as discussed in Section 2.1. These all relate to the widely used Technology Readiness Level (TRL) concept, developed initially by NASA [1], suggesting increasingly complex testing as the device technology matures. At each stage the developer is aiming to maximise understanding of the device performance with the minimum of risk and outlay. The stages can broadly be defined as per Table 1, although there is likely to be overlap between stages in reality. The development might be an iterative process, particularly for subsequent revisions to the device concept, going back to tank test improvements to the design following open water deployment.

1.2 Considerations for Combined Wave-Current Basins, Such as FloWave

Early scale model tests were conducted by towing model ships in tanks, which later had wave-makers added to create uni-directional and then multi-directional waves. Recirculating flumes and cavitation tunnels were used for tasks such as propeller design. These facilities were only able to simulate some of the phenomena that make up the complexity of the real ocean. More recently, advanced wave basins have been constructed, able to simulate more realistic sea conditions, comprising multi-directional waves and currents, with some facilities additionally able to simulate wind forcing.

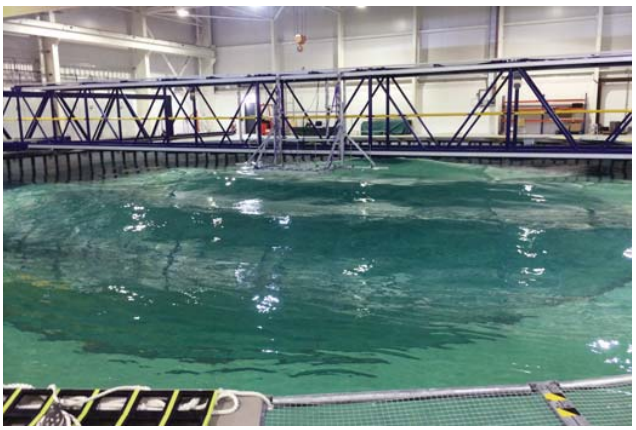

FIGURE 1. Photograph of FloWave facility, showing an observation test of regular waves combined with a following current.

FloWave is one such state-of-the-art test facility, designed to produce waves and currents from any direction in the circular tank [5], facilitating the reproduction of realistic sea conditions. It is optimised for waves around 2 s period, approximately 0.5 m high, and can produce currents in excess of 1.0 m/s, see Fig. 1. The tank was designed specifically to test MRE device at scales around 1:20, which ties in with stage 2 of the development process given in Table 1. The large size of the facility also permits the testing of small arrays of devices, including studies of the interactions between them.

As a new and novel facility, it was important to characterise and measure the performance of the generated waves and currents. The wave generation has been shown to be highly repeatable, with the ability to produce complex spectra based on recorded conditions [6, 7]. Characterisation of the current has shown that despite spatial variability across the tank, there is a large test area with acceptably uniform flow ($\pm 5\%$ at 0.8 m/s) [8].

TABLE 1. Five stages of development, for marine renewable energy devices. After [2, 3, 4]

Stage	TRL	Nominal scale*	Typical infrastructure
1. Concept validation	1-3	Small scale (circa 1:50)	Small university laboratory
2. Design validation	3-5	Larger scale (circa 1:25–1:10)	Industrial scale laboratory
3. Systems validation	5-6	Sub-prototype size (circa 1:4)	Benign test site
4. Device validation	7-8	Approaching full size (circa 1:1)	Exposed test site
5. Economics validation	9	Full size, small arrays	Commercial site

* Scales refer to WEC & TST models, for FOWT smaller scales are typically used at each stage given the larger size of the prototypes.

Work is ongoing to quantify the envelope for combined wave-current testing.

2 REVIEW OF PUBLISHED GUIDANCE

Historically, there has been only limited guidance available relating specifically to scale model testing of marine renewable energy systems. This situation has improved over the last decade however, as the offshore renewables industry has developed towards commercialisation. Device developers previously had to make use guidance for the model testing of ships and offshore structures, such as that produced by the International Tank Testing Conference (ITTC). This lack of published practice was highlighted in 2008 [10]. More recently marine renewable energy specific guidance has been published by OES IA, EMEC, ITTC and EU funded projects. These are still somewhat generic, however, as it is difficult to go into specifics for such a broad field with a very diverse range of concepts being tested. Recent technology reviews [26, 27] identify more than 100 wave and tidal energy concepts in various stages of development.

A chronological list of published guidance relating to model testing of marine renewable energy devices is given in Table 2. The published guidance is predominantly segregated by technology types, with a slight bias towards guidance on WECs. This bias may be due to similarities between tank testing of WECs to the more established testing of ships and oil platforms.

Recommendations of best practice learned from tank testing of marine renewable energy devices were published almost a decade ago by IFREMER [10] and the University of Edinburgh [11], covering TSTs and WECs respectively. Additional guidance was published after this by the European Marine Energy Centre (EMEC) [3] and Ocean Energy Systems (OES-IA) [4].

One of the key organisations involved in tank testing of ships and offshore structures is the International Towing Tank Conference (ITTC). Their established Recommended Procedures for Floating Offshore Platform Experiments [9] were extended to cover WEC model testing [14]. Three major differences from floating platforms, and challenges specific to wave energy, are given as: the inclusion of power-take-off; testing various stages from concept validation onwards; and the testing of multiple devices (or multi-body devices), including their interactions. Updated guidance covering WECs, TSTs, and FOWTs was published following the subsequent ITTC conference in 2014.

Two EU funded projects have produced a wealth of information relating to the development and testing of MRE devices, the Protocols for the Equitable Assessment of Marine Energy Converters (EquiMar) and the Marine Renewables Infrastructure Network (MARINET). The EquiMar protocols are focused primarily on procedural aspects such as the test design, and as such do not offer specific guidance on types of environmental conditions to use during testing, although wider guidance is available in the supporting work-package deliverable documentation. Similarly, a number of the MARINET work package reports are pertinent to the task of tank testing, as shown in Table 2.

The International Electro-technical Commission (IEC) is preparing guidance for wave, tidal and other water current converters at present [28, 29], due to be published later this year. It is expected that these will be consistent with existing guidance in their recommendations.

2.1 Structured Device Development Programmes

As noted in Section 1.1, scale model testing is widely used in the development of various technologies and processes. Some of the first guidance specifically relating to MRE devices outlined similar multi-stage development plans for tidal-current devices [2] and for wave energy systems [3, 4]. More recent guidance issued by ITTC [23, 24, 25] also suggests similar stages. While these are technology specific, they have commonality and wider applicability, linking back to the same TRL.

A similar process is recommended for resource assessment [30], using available data from existing atlases and wide area models for early development stages. Once projects progress further, more money can be spent on collecting actual site measurements for detailed assessment.

2.2 Increasing Complexity of Test Conditions

This incremental approach is also recommended in the selection of environmental conditions for tank testing. Initial tests should be made with simple conditions, which should be easier to interpret results from, before adding increased complexity, giving additional understanding of device performance.

2.2.1 WECs and Floating Devices The need for testing in both regular and irregular waves during WEC development was highlighted in [11]. Regular waves are useful to obtain an understanding of the device performance with a minimum of parameters to consider, just height, period, and possibly angle. They are commonly used to determine Response Amplitude Operators (RAO) and for validation of numerical models. To account for non-linear wave response, which may be easier to characterise with regular waves [11], it is also recommended that several wave heights should be checked at selected wave periods [31].

As regular waves do not capture the complexity of a real ocean, it is also important to test irregular (polychromatic) seas to better characterise device performance. This should include consideration of multi-directional seas and energy spreading, both of which may impact how much of the available energy a particular device can absorb. Even when testing more advanced models, it is good practice to use regular waves to check the response of the new model is similar to previous models [4].

For concept design stage, it is usual to test with long-crested

TABLE 2. Chronological list of published marine renewable tank testing guidance documents

Organisation	Date	Applicability	Title & Reference
ITTC	2005		Recommended Procedures for Floating Offshore Platform Experiments [9]
IFREMER	2008	TST	Marine current energy converter tank testing practices [10]
OES IA	2008	TST	Tidal-current Energy Device Development and Evaluation Protocol [2]
UoEdin	2009	WEC	Best Practice Guidelines for Tank Testing of Wave Energy Converters [11]
EMEC	2009	WEC	Tank Testing of Wave Energy Conversion Systems [3]
OES IA	2010	WEC	Guidelines for the development & testing of wave energy systems [4]
EquiMar	2009-2011	General	EquiMar Protocol II.A Tank Testing [12], plus various work package deliverable reports
ITTC (26th)	2011	General	Recommended Procedures and Guidelines Seakeeping Experiments [13]
		WEC	Recommended Guidelines, Wave Energy Converter Model Test Experiments [14]
MARINET	2012-2015	WEC	Wave Instrumentation Database [15] Collation of Wave Simulation Methods [16] Standards for Wave Data Analysis, Archival and Presentation [17] Best Practice Manual for Wave Simulation [18]
		TST	Collation of Tidal Test Options [19]
		FOWT	Collation of Offshore Wind-Wave Dynamics [20] Best Practice Protocol for Offshore Wind System Fluid-Structure Interaction Testing [21]
ITTC (27th)	2014	General	Specialist Committee on Hydrodynamic Testing of Marine Renewable Energy Devices [22]
		WEC	ITTC Recommended Guidelines - Wave Energy Converter Model Test Experiments [23]
		TST	ITTC Recommended Guidelines - Model Tests for Current Turbines [24]
		FOWT	ITTC Recommended Guidelines - Model Tests for Offshore Wind Turbines [25]

waves to simplify the test design and analysis. Initially from a single direction, then considering waves at an oblique angle to the device. Short-crested waves with directional spreading should be considered later in the development process to obtain accurate estimates of power production, especially where WEC power production may depend on incident wave direction [23].

As well as understanding device performance, it is important to test survivability limit conditions prior to sea trials [23]. This should consider the performance of both the hull(s) and moorings in extreme waves [3]. Given the limitations of facilities to generate large waves, it may be appropriate to adapt the smaller stage 1 model for testing survivability at stage 2 [4].

2.2.2 Tidal Stream Turbines

Whilst there is an obvious progression in the specification of waves for testing, this is not so straightforward when considering tidal currents, and there is little in the way of existing guidance.

An additional complexity is that the environmental conditions at tidal sites can be difficult to fully characterise, see Section 2.3.2. For early stage devices, this may be compounded by the fact that deployment sites may not have been identified or licensed [24].

During more advanced tank tests for higher TRL devices, it is recommended that extreme tidal conditions should be tested [32]. An example given is by adding large scale high intensity turbulence to the flow, although it is noted that scaling turbulence is problematic.

2.3 Specification of Environmental Conditions

A wealth of guidance exists on how environmental conditions in the ocean can be specified, both specific to the marine renewable sector [33], as well as from other related sectors [34] published by organisations such as the International Standards Organisation (ISO), American Petroleum Institute (API), and

Det Norske Veritas (DNV). These full scale conditions need to be translated and simplified to a matrix of tank scale conditions for testing.

2.3.1 Waves It is possible to accurately generate both irregular and regular wave equivalents of the desired parameters in test tanks. Historically, only uni-directional waves were possible, however most ocean basin facilities are now able to generate waves across multiple directions, providing realistic conditions for model testing.

It is common to test a matrix of regular waves, specified by height and period, which tie up with industry standard power matrices [3]. Tests with regular waves can be quite short, allowing wide range of conditions to be tested in a relatively short time. A minimum run length of 10 cycles is given in ITTC guidelines [31], however some longer tests may be considered.

When testing irregular sea states, the test duration should be long enough to give a statistically representative sample. ITTC guidelines and procedures recommend a minimum length of 20–30 minutes (at full scale), or approximately 500–1000 waves, a well-established benchmark in tank testing [32]. For survivability conditions, a three hour (full-scale) storm duration should be simulated.

For the creation of short-crested sea states, a cosine squared ($\cos^{2s}\theta$) spreading function is often used to describe the directional spread of the waves [23]. Methods to estimate the spreading parameter s from site data are given in [35].

2.3.2 Currents There is uncertainty of both the real-world flow field dynamics in energetic tidal channels where TSTs will be deployed, as well as how to reproduce these in test facilities once the flow is characterised. The local bathymetry of tidal channels can be complex and lead to localised conditions that may not be captured effectively [24].

The flow conditions that can be generated is specific to the type of facility, e.g. towing tank, cavitation tunnel, offshore basin, etc. These should be documented [24], including:

- Flow speed and direction;
- Spatial uniformity, including blockage effects and vertical flow profile;
- Steadiness and turbulence characteristics.

Turbulence is commonly described by a single 'turbulence intensity' parameter, but length scales are also important to characterise small and large scale fluctuations within the flow. Many facilities are only able to change the mean flow velocity, but cannot easily adjust turbulence or change the vertical flow profile. Generation of small scale turbulence may be possible in some facilities by introducing a grid or other structure upstream of the turbine [24].

2.3.3 Combined Conditions There is limited guidance on the specification of combined wave-current conditions, however ITTC guidance for floating platforms [9] recommends that the wave spectrum is calibrated in the presence of current, i.e. the combined conditions are re-created.

The presence of waves will alter the flow field and impact on submerged device loadings. A wave-current tank should be used to study this, although may present challenges for scaling TSTs [24]. It is possible to test with waves in a tow-tank or apply an oscillatory motion to the device foundation, however this will not produce the correct distribution of velocities across the rotor plane [24].

2.3.4 Directionality The influence of directionality of the environmental conditions should be considered for all devices that are not rotationally symmetrical. The moorings/foundation for the device should be considered when assessing symmetry as these are usually sensitive to direction. For example, the moorings of an axi-symmetric point absorbing WEC may still be sensitive to the predominant wave direction [4].

2.4 Key Limitations of Guidance

As noted above, existing published guidance does not offer detailed recommendations for testing in advanced environmental conditions now possible in facilities such as FloWave, discussed in Section 1.2. These include multi-directional multi-modal waves, as well as combined waves and currents at various relative directions.

Although the issue of directionality is mentioned in guidance, it may not be given sufficient importance when developing test plans. This may result in discrepancy between predicted and observed performance when devices are deployed at sea. Directional spectra have increased complexity in terms of documenting, generating, analysing, and interpreting model results [31], which may partially account for directionality being neglected.

The uncertainty of both measuring and re-creating complex real-world turbulent tidal flows was highlighted as an issue in 2008 [10], and this still remains an area with little published guidance. Recent studies, such as those conducted under the ReDAPT project [36], are providing promising site specific information based on spatially rich, high-resolution velocimetry, that may in future be used to define test conditions.

3 INITIAL RECOMMENDATIONS AND JUSTIFICATION FOR ADVANCED ENVIRONMENTAL CONDITIONS

A key challenge for combined wave-current basins such as FloWave is the limitations of existing guidance, specifically on testing in advanced multi-directional waves and testing with combined wave-current. Initial recommendations and justification are given in the following sections, used to inform the tests

taking place in the FloWave facility. Since opening in 2014, numerous clients have made use of the facility to test MRE devices, measurement instrumentation, and other devices. This has included several tests assessing performance and loading on WECs and TSTs with combined wave-current at multiple angles, as well as WEC performance in site specific wave conditions.

It is envisaged that these advanced environmental conditions would be used towards the end of stage 2 tank testing, for devices at mid TRL. They are offered in addition to existing guidance on developing test plans, and are based on the ongoing research as well as lessons learnt during testing conducted at FloWave.

3.1 Directional Sensitivity

When assessing the directional sensitivity of the device, this should apply to all environmental conditions being tested: wind, wave, current, and combined; unless there is strong justification not to do so. Wind is likely only to be significant for FOWT tests, as most WECs and TSTs do not protrude significantly above the sea surface. Combined wave-current effects are discussed further in Section 3.3.

- For devices that do not weathervane to face the incoming conditions, the effect of off-axis waves or currents (as appropriate) on power capture and foundation/mooring loads should be assessed.
- Some WECs are designed to face into the prevailing wave direction to maximise power capture. The presence of cross-currents or multi-modal waves could affect this orientation, potentially increasing the mooring loadings and decreasing power capture.
- Particularly for sites at headlands, the tidal flow may exhibit asymmetry rather than being purely rectilinear, with corresponding directional loading on the TST and foundation.
- TSTs are also likely to be affected by wave loading which is unlikely to always be aligned with the current direction, except perhaps in narrow channels.

Where there is symmetry in the device, either mirror or rotational, this can be used to reduce the size of the test matrix. Many devices will have bilateral symmetry although this is worth confirming with a few test cases, especially where the device has rotating turbine(s) that may impart asymmetry. Where the worst case direction(s) for mooring loads can readily be identified, this can also be used to minimise the test matrix size, as noted in [25].

3.2 Advanced Wave Conditions

Additional understanding of device performance can be obtained by testing with increased complexity sea conditions. These include multi-modal and multi-directional waves, either specified parametrically or from the characterisation and re-creation of recorded sea conditions. Multi-modal waves may be important for understanding directional performance, as discussed above.

Dynamic response of devices is dependent on spectral form [37], hence it is the frequency and directional spectral shapes that determine the device response, rather than proxy statistical parameters such as H_{m0} and T_E. It is suggested [3] that using site specific spectral shapes be used for testing in order to assess devices in more realistic wave conditions, however methodologies for extracting meaningful test cases from the vast amount of data are not detailed. This has been explored in [6, 7], and it is noted that in order to make use of recorded site data in the tank within a realistic time-frame, a small number of representative sea states are required. These should embody the various characteristics of the site, such as:

- Significant wave height H_{m0}, energy period T_E, and wavelength L;
- Wave energy frequency and directional spectra, $S(f)$ and $E(f,\theta)$ respectively;
- Mean direction $\bar{\theta}$, spectral width ν, and directional spreading e.g. s, $\bar{\sigma}_\theta$.

The relative importance of these variables is somewhat subjective, and will depend on site, device, and test purpose. Data can be partitioned using classical binning techniques applied to statistical parameters, e.g. [12,38], however more advanced clustering algorithms can be used to classify spectral and other high-dimensional data [39, 6, 7]. These sorts of clustering and binning approaches can be used to partition the data into distinct groups, from which representative sea states can be extracted and used for testing. Using such sea states will increase test realism, providing an understanding of real-world-like performance. For subsequent test plans, at higher TRL, insight may also be gained by comparing the performance of model and prototype in the 'same' sea-conditions, in order to improve future testing.

3.3 Combined Wave-current

Testing in combined wave-current conditions is important for floating and mid-water-column devices. Currents change the shape of waves and the impact of wave orbitals propagate well below the surface, particularly for longer period waves. Both waves and currents are present throughout the oceans, and they interact in a complex non-linear way. While the frequency or period of the wave remains constant, the wave height and length are altered.

3.3.1 Considerations for Floating Devices and WECs

For devices that are floating on the sea surface, and/or aim to capture the power of waves, it is important to model the combined wave-current properties correctly. Even low currents have an impact on wave height and length, changing the relationship between period and wavelength.

The dynamic response of every WEC is different, therefore the underlying change in wave length and height from interaction with a current is considered. To illustrate this, theoretical values have been calculated using linear interaction theory for a typical range of wave conditions used in the tank, as shown in Figs. 2 and 3. For waves on opposing currents, length L shortens, while height H increases, and visa-versa for following currents.

The steepness of an individual wave is given by $S = H/L$, the speed (or celerity) by $C = L/T$, and group celerity by Eq. (1),

$$C_g = \frac{1}{2}\sqrt{\frac{gL}{2\pi}\tanh\left(\frac{2\pi h}{L}\right)}\left[1+\frac{4\pi h}{L\sinh\left(\frac{4\pi h}{L}\right)}\right] \qquad (1)$$

where h is water depth and g gravitational acceleration. Wave power can be expressed as $P_w = E_A C_g$, where E_A is wave energy per unit horizontal area [40]. All of these parameters (H, L, S, C, C_g, P_w) are affected by the interaction of waves with currents. Therefore, the only way to properly test waves where a current is present at the site is to reproduce that current at scale in the test facility. The change in wave shape as a result of the interaction with a current will affect floating device motion and mooring loads, and may impact WEC power capture efficiency.

In addition to the change in wave shape, the 'apparent' power in a wave calculated ignoring wave-current interaction will be different to the true wave power [41]. This may be higher or lower than the correct value, depending on current direction. If this change in wave power is not accounted for, device performance will be misrepresented, affecting economic assessment and comparison with real-world performance.

A method has been developed to reproduce a combined wave-current field in the FloWave facility [41]. It has been shown that a linear iterative correction procedure can effectively be used to produce the desired wave conditions in the tank test area when combined with a comparatively low current (up to around 1 m/s at full scale) at an arbitrary angle to the wave direction. This method has been demonstrated for regular waves, long-crested spectra, and a complex non-parametric multi-modal sea state. The overall process is as follows:

1. Produce wave conditions in the tank, with current and measure the amplitude of each wave component $A_i(f_i, \theta_i)$.
2. Calculate linear correction factor based on discrepancy for each component using Eq. (2)

$$CF(f_i, \theta_i) = \frac{A_i^{desired}}{A_i^{measured}} \qquad (2)$$

3. Apply this correction factor to the tank input, then repeat steps 1. and 2. until the measured spectrum in the tank is acceptably correct.

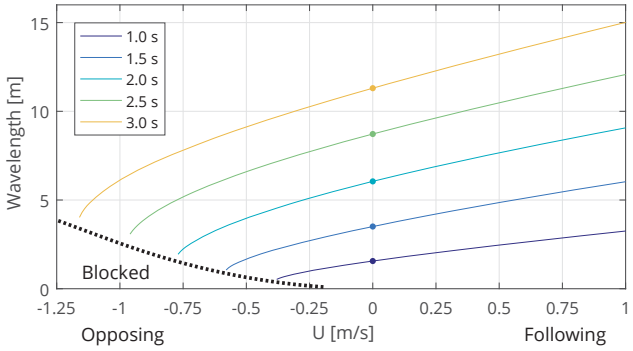

FIGURE 2. Change in wavelength with collinear current based on linear theory, for typical wave conditions at tank scale in 2 m water depth. Represents 1:25 scale test of periods from 5 s to 15 s in 50 m water depth. Wavelength without current L_0 marked by point for each period. Blocking limit shown by black dotted line.

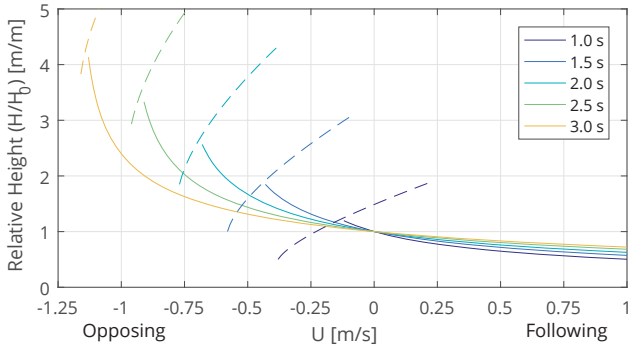

FIGURE 3. Change in relative wave height with current for typical wave conditions at tank scale, solid lines. Breaking criteria for H_0 = 0.15 m shown by dashed lines.

As well as in tank testing, it is important to consider the potential effect of tidal currents in resource assessment for wave energy sites, as the wave power will be altered. Wave-current interactions should also be included when determining the environmental conditions for floating device deployment. If the current is not included, the wave shape will not match that expected, with implications on power capture and device motion that may be significant.

3.3.2 Impact of Waves on Currents The influence of waves on a tidal current is also important for the design of near surface structures and turbine blades, as wave orbital velocities can introduce significant additional cyclic loading. Wave orbital size decreases exponentially with depth, but may still result in considerable cyclic velocities at mid depth where turbines are typically located. This is particularly true for sites that are not

'deep water' as defined by Eq. (3) where h is water depth, T wave period, and g gravitational acceleration. These waves are influenced by the bed as wave orbital size at this depth is not insignificant.

$$h > gT^2/4\pi \tag{3}$$

Surface gravity waves also impact on the flow, increasing turbulence and changing the shape of the vertical profile [42]. This may have implications for TSTs, particularly on differential blade loading for horizontal axis turbines.

Although tidal currents are predictable, and may propagate through a channel with approximately 180° between ebb and flood, potentially removing the need to assess directionality, the waves will not be predictable and might come from any direction. In narrow channels predominant wave directions may be limited, but still may not necessarily be aligned with the tidal flow. Understanding impact of off-axis waves on a device could be important for device loading and performance, and is something that has been studied in the FloWave facility on behalf of external clients.

4 CONCLUSIONS

Tank testing is an important process in the development of marine renewable energy devices. The use of structured development plans is an established part of this process, as set out in guidance, with an incremental approach recommended. Initial tank tests should be undertaken at small scale with relatively simple input conditions, before moving on to larger and more complex tank tests, then open water deployment. At each stage the developer is aiming to maximise understanding of their device and its performance, with the minimum of risk and financial outlay.

Published guidance for MRE development and testing outlines the process and, give details for general aspects of tank testing. Recommendations for advanced test conditions are more limited however. Facilities such as FloWave are currently conducting tests with more advanced conditions, and this paper aims to document procedures used in a manner consistent with existing guidance.

Realistic waves, and wave-current interactions particularly, are complex non-linear processes that can be difficult to model numerically, and thus developers may benefit from the increased learning carried out in controlled conditions on a relatively inexpensive model, prior to conducting real-world tests in the ocean.

The advanced test conditions proposed all have potential to affect both the power capture performance and loading on devices. These should therefore be considered when testing wave energy converters, tidal stream turbines, and floating offshore wind turbines, although the applicability of particular conditions will depend on the specifics of device and deployment site.

ACKNOWLEDGEMENTS

The authors would like to acknowledge the Energy Technology Institute and RCUK Energy programme for funding this research as part of the IDCORE programme (EP/J500847/1), and the UK Engineering and Physical Science Research Council for supporting the construction of the FloWave facility (EP/I02932X/1).

REFERENCES

[1] Mankins, J. C., 1995. "Technology readiness levels". *White Paper, April*, pp. 4–8.

[2] Bahaj, A. S., Blunden, L., and Anwar, A. A., 2008. Tidal-current Energy Device Development and Evaluation Protocol. Tech. Rep. August, University of Southampton, Southampton.

[3] Holmes, B., 2009. Tank Testing of Wave Energy Conversion Systems. Tech. rep., London.

[4] Holmes, B., and Nielsen, K., 2010. Guidelines for the development & testing of wave energy systems. Tech. Rep. June, Hydraulics Maritime Research Centre, UCC, Cork, Ireland.

[5] Davey, T., Brown, S., Bryden, I. G., Ingram, D. M., Robinson, A., and Wallace, A. R., 2013. "The All-Waters Test Facility The Role of a New Facility in Physical Modelling for Marine and Coastal Engineering". In ICE Breakwaters 2013.

[6] Draycott, S., Davey, T., Ingram, D. M., Lawrence, J., Day, A., and Johanning, L., 2015. "Applying Site-Specific Resource Assessment : Emulation of Representative EMEC seas in the FloWave Facility". In Proceedings of the Twenty-fifth (2015) International Ocean and Polar Engineering Conference, ISOPE, pp. 815–821.

[7] Draycott, S., 2016. "On the Re-creation of Site-Specific Directional Wave Conditions". Engineering doctorate, The University of Edinburgh.

[8] Noble, D. R., Davey, T., Smith, H. C. M., Kaklis, P., Robinson, A., and Bruce, T., 2015. "Spatial variation in currents generated in the FloWave Ocean Energy Research Facility". In 11th European Wave and Tidal Energy Conference, Nantes, France, pp. 1–8.

[9] ITTC, 2005. Recommended Procedures and Guidelines - Floating Offshore Platform Experiments. Tech. rep., International Towing Tank Conference.

[10] Germain, G., 2008. "Marine current energy converter tank testing practices". In 2nd International Conference on Ocean Energy (ICOE 2008), pp. 2–7.

[11] Payne, G. S., Taylor, J. R. M., and Ingram, D. M., 2009. "Best Practice Guidelines for Tank Testing of Wave Energy Converters". *Journal of Ocean Technology,* **4**(4), pp. 38–70.

[12] Ingram, D., Smith, G., Bittencourt-Ferreira, C., and Smith,

H., 2011. Protocols for the Equitable Assessment of Marine Energy Converters. Tech. rep., EquiMar, Edinburgh.

[13] ITTC, 2011. "Seakeeping Experiments". In Proceedings of the 26th International Towing Tank Conference, Rio de Janeiro.

[14] ITTC, 2011. Recommended Guidelines - Wave Energy Converter Model Test Experiments. Tech. rep., International Towing Tank Conference, Rio de Janeiro.

[15] Lawrence, J., Holmes, B., Bryden, I., Magagna, D., Torre-Enciso, Y., Rousset, J.-M., Smith, H., Paul, M., Margheritini, L., and Cândido, J., 2012. Wave Instrumentation Database. Tech. rep.

[16] Guillouzouic, B., 2014. Collation of Wave Simulation Methods. Tech. rep.

[17] Cândido, J., Finn, MatthewDampney, KeithAwrence, J., and Margheritini, L., 2015. Standards for Wave Data Analysis, Archival and Presentation. Tech. rep.

[18] Holmes, B., 2015. Best Practice Manual for Wave Simulation. Tech. rep.

[19] McCombes, T., Iyer, A. S., Falchi, M., Elsäßer, B., Scheijgrond, P., and Lawrence, J., 2012. Collation of Tidal Test Options. Tech. rep.

[20] Bredmose, H., Larsen, S. E., Matha, D., Marino, E., and Saettran, L., 2012. Collation of offshore wind-wave dynamics. Tech. Rep. November.

[21] Brand, A. J., Peeringa, J. M., Marino, E., Cappietti, L., and Pecora, M. L., 2015. Best Practice Protocol for Offshore Wind System Fluid Structure Interaction Testing. Tech. rep.

[22] ITTC, 2014. "Specialist Committee on Hydrodynamic Testing of Marine Renewable Energy Devices". In Proceedings of the 27th International Towing Tank Conference, Copenhagen, pp. 680–725.

[23] ITTC, 2014. "Recommended Guidelines - Wave Energy Converter Model Test Experiments". In Proceedings of the 27th International Towing Tank Conference, Copenhagen.

[24] ITTC, 2014. "Recommended Guidelines - Model Tests for Current Turbines". In Proceedings of the 27th International Towing Tank Conference, Copenhagen.

[25] ITTC, 2014. "Recommended Guidelines - Model Tests for Offshore Wind Turbines". In Proceedings of the 27th International Towing Tank Conference, Copenhagen.

[26] Falcão, A. F. d. O., 2010. "Wave energy utilization: A review of the technologies". *Renewable and Sustainable Energy Reviews,* **14**(3), apr, pp. 899–918.

[27] Yuce, M. I., and Muratoglu, A., 2015. "Hydrokinetic energy conversion systems: A technology status review". *Renewable and Sustainable Energy Reviews,* **43**, pp. 72–82.

[28] IEC. Marine energy - Wave, tidal and other water current converters - Part 103: Guidelines for the early stage development of wave energy converters: Best practices and recommended procedures for the testing of pre-prototype scale devices. Tech. rep.

[29] IEC. Marine energy - Wave, tidal and other water current converters - Part 202: Scale testing of tidal stream energy systems. Tech. rep.

[30] Davey, T., Venugopal, V., Girard, F., Smith, H., Smith, G., Lawrence, J., Caveleri, L., Bertotti, L., Prevosto, M., and Holmes, B., 2010. D2.7 Protocols for wave and tidal resource assessment. Tech. rep., EquiMar.

[31] ITTC, 2005. "Recommended Procedures and Guidelines - Laboratory Modelling of Multidirectional Irregular Wave Spectra". In Proceedings of the 24th International Towing Tank Conference, Edinburgh, pp. 1–8.

[32] McCombes, T., Johnstone, C. M., Holmes, B., Myers, L. E., Bahaj, A. S., Heller, V., Kofoed, J. P., Finn, J., and Bittencourt-Ferreira, C., 2010. D3.3 Assessment of current practice for tank testing of small marine energy devices. Tech. rep.

[33] Venugopal, V., Davey, T., Smith, H. C. M., Smith, G. H., Holmes, B., Barret, S., Prevosto, M., Maisondieu, C., Cavaleri, L., Bertotti, L., Lawrence, J., and Girard, F., 2011. D2.2 Wave and Tidal Resource Characterisation. Tech. rep., EquiMar.

[34] Ricci, P., Villate, J. L., Scuotto, M., Zubiate, L., Davey, T., Smith, G. H., Smith, H. C. M., Huertas-Olivares, C., Neumann, F., Stallard, T., Ferreira, C. B., Flinn, J., and Sorensen, H. C., 2009. D1.2 Recommendations from other sectors. Tech. rep., EquiMar.

[35] Payne, G. S., 2008. "Guidance for the experimental tank testing of wave energy converters". *SuperGen Marine*.

[36] Sellar, B., Harding, S., and Richmond, M., 2015. "High-resolution velocimetry in energetic tidal currents using a convergent-beam acoustic Doppler profiler". *Measurement Science and Technology,* **26**(8), p. 085801.

[37] Mansour, A. E., and Ertekin, R. C., 2003. "Report of technical committee I.1 environment". *Proceedings of the 15th international ship and offshore structures congress,* **1**.

[38] Pitt, E., 2009. *Assessment of Wave Energy Resource*. European Marine Energy Centre.

[39] Hamilton, L. J., 2010. "Characterising spectral sea wave conditions with statistical clustering of actual spectra". *Applied Ocean Research,* **32**(3), jul, pp. 332–342.

[40] Méhauté, B. L., 1976. *An introduction to hydrodynamics and water waves*. Springer, New York.

[41] Draycott, S., Noble, D. R., Davey, T., Bruce, T., Ingram, D. M., Johanning, L., Smith, H. C. M., Day, A., and Kaklis, P., 2016. "Re-creation of Site-Specific Multi-Directional Waves with Non-Collinear Current". *Manuscript submitted for publication*.

[42] Klopman, G., 1994. Vertical structure of the flow due to waves and currents: laser-Doppler flow measurements for waves following and opposing a current. Tech. rep., Delft Hydraulics.

Ocean Engineering 152 (2018) 391–403

Contents lists available at ScienceDirect

Ocean Engineering

journal homepage: www.elsevier.com/locate/oceaneng

Re-creation of site-specific multi-directional waves with non-collinear current

S. Draycott [a,*], D.R. Noble [a,**], T. Davey [a], T. Bruce [b], D.M. Ingram [b], L. Johanning [c], H.C.M. Smith [c], A. Day [d], P. Kaklis [d]

[a] FloWave Ocean Energy Research Facility, Max Born Crescent, King's Buildings, Edinburgh, EH9 3BF, UK
[b] Institute for Energy Systems, School of Engineering, The University of Edinburgh, Edinburgh, EH9 3JL, UK
[c] College of Engineering, Mathematics and Physical Sciences, University of Exeter, Penryn Campus, TR10 9FE, UK
[d] Naval Architecture, Ocean and Marine Engineering, University of Strathclyde, Glasgow, G4 0LZ, UK

ARTICLE INFO

Keywords:
Wave-current interactions
Site-specific wave conditions
Directional wave spectra
Directional spectrum measurement
Tank testing

ABSTRACT

Site-specific wave data can be used to improve the realism of tank test conditions and resulting outputs. If this data is recorded in the presence of a current, then the combined conditions must be re-created to ensure wave power, wavelength and steepness are correctly represented in a tank. In this paper we explore the impacts of currents on the wave field and demonstrate a simple, effective methodology for re-creating combined wave-current scenarios. Regular waves, a parametric unidirectional spectrum, and a complex site-specific directional sea state were re-created with current velocities representing 0.25, 0.5, and 1.0 m/s full scale. Waves were generated at a number of angles relative to the current, providing observations of both collinear and non-collinear wave-current interactions. Wave amplitudes transformed by the current were measured and corrected linearly, ensuring desired frequency and wavenumber spectra in the presence of current were obtained. This empirical method proved effective after a single iteration. Frequency spectra were within 3% of desired and wave heights normally within 1%. The generation-measurement-correction procedure presented enables effective re-creation of complex wave-current scenarios. This capability will increase the realism of tank testing, and help de-risk devices prior to deployment at sea.

1. Introduction

Tank testing of physical scale models is an essential element in the development of marine renewable technologies and techniques. Undertaking this testing in laboratories provides a controlled, repeatable, and low-risk environment where technological concepts and operational techniques may be developed (Ingram et al., 2011). A five-stage structured development plan for wave energy systems was outlined by Holmes and Nielsen (2010), which can be related to the widely used Technology Readiness Level (TRL) concept, developed initially by NASA (Mankins, 1995). Using scaled sea conditions based on open sea measurements at wave energy sites when tank testing renewable energy devices, particularly at mid and later stage TRL levels, can improve understanding of device performance prior to deployment at sea.

The aim of this work is to explore the impacts of currents on the wave field, and to demonstrate an effective approach to include currents in scale model testing thus representing the combined conditions appropriately. A site-specific directional sea state is used to illustrate this methodology, derived from the Billia Croo wave test site at the European Marine Energy Centre (EMEC). Experiments were carried out in the circular wave basin of the FloWave Ocean Energy Research Facility, enabling both waves and current to be generated in all directions.

Currents change the physical form of waves, as discussed by Peregrine (1976) and others. Although the wave period remains constant, waves become steeper when they encounter an opposing current; a combination of both the wave height increasing and wavelength decreasing. Wave breaking will occur as the steepness approaches a critical limit, and faster currents prevent upstream wave propagation completely, i.e. wave blocking. With a following current the converse occurs and waves become less steep. For waves at an angle to the current, there is also refraction of the wave direction to consider.

Several experimental studies have been published on the influence of

* Corresponding author.
** Corresponding author.
E-mail addresses: S.Draycott@ed.ac.uk (S. Draycott), D.Noble@ed.ac.uk (D.R. Noble).

https://doi.org/10.1016/j.oceaneng.2017.10.047
Received 8 December 2016; Received in revised form 27 September 2017; Accepted 22 October 2017
Available online 28 October 2017

currents on waves. Early studies including Thomas (1981); Kemp and Simons (1982, 1983) used hydraulic flumes to investigate collinear wave-current interaction for regular waves. The main focus was the influence of waves and bed roughness on the current profile, although modification of the waves by the current was also included. This experimental work on regular waves was extended to consider uni-directional spectra with collinear currents by Hedges et al. (1985) and Chakrabarti and Johnson (1995). Adding more complexity, Nwogu (1993) and Guedes Soares et al. (2000) looked at the influence of currents on directional spectra. Both studies were carried out in wave basins with a single bank of wavemakers with nozzles in front to generate current, so considered spectra with a predominantly following current. Mean wave directions of $0^{\circ}, 15^{\circ}, 30^{\circ}$, and 45° relative to the current were tested by Nwogu (1993), although any modification of the frequency spectra were not reported. As far as the authors are aware, the research presented below is the first comprehensive study of oblique wave-current interaction.

Measured site wave data may be used to produce scaled sea states that capture spectral complexity and directional features not effectively represented by standard parametric spectra and spreading functions (as discussed in Draycott et al. (2015)). This site data, typically gathered by a wave buoy, may have been measured in the presence of current. This current is not typically reproduced in the test tank and therefore wave power and steepness of the sea states will be misrepresented. This has potentially large implications on the assumed resource and on the validity of observed device response, as discussed in Section 2.

The rest of the paper is organised into four sections. In Section 2 we explore the impact of a current on the wave field, including implications for power and steepness if this current is omitted during testing. The experimental methodology is given in Section 3, with results in Section 4. Some discussion of these findings is then presented in Section 5.

2. The effect of current on the wave field

Currents transform the wave field, including wave height and length, as mentioned in Section1. This alters the form of the frequency and wavenumber spectra, along with the power available. The impact of tides on wave power resource has been investigated using a numerical model by Hashemi et al. (2014). This work showed the impact of tides on wave power resource could exceed 10% at sites with currents of around 1.5 m/s. Other papers such as Saruwatari et al. (2013) suggest this effect may be as large as 60% in 3 m/s currents, however current-induced wavelength and group velocity changes appear to have been ignored. This leads to an over-estimation as described in Section 2.3, analogous to the described wave buoy scenario.

Wave buoys, including the Datawell Waverider© buoys deployed by EMEC, typically measure heave, pitch, and roll. The resulting frequency spectra are calculated from the heave motions (Earle, 1996), whilst the directionality is inferred through cross-correlation of the three signals. If a current is present at the site, the sea surface elevations and hence calculated frequency spectrum will therefore be altered, but without knowing the corresponding change in wavelength.

If it is assumed there was no current, wavenumber spectra calculated for the recorded frequency spectra will be incorrect, as will steepness and power. This has potentially large implications for the assumed resource available, along with the form of the waves, as explored below. Additionally, if a spectrum is replicated in a test environment without current, this would fail to capture the true nature of the site conditions.

2.1. Calculation of available power and steepness

For waves in the absence of current the wavenumber for each frequency can be obtained from the dispersion relation Eq. (1), with corresponding wavenumber spectrum $S(k)$ and group velocities Cg calculated from Eq. (2) and the measured frequency spectrum $S(f)$.

$$\omega = \sqrt{gk \tanh kh} \tag{1}$$

$$S(k) = \frac{S(f)C_g(f)}{2\pi} \quad ; \quad C_g(f) = \frac{1}{2}\frac{\omega}{k}\left(1 + \frac{2kh}{\sinh 2\,kh}\right) \tag{2}$$

where ω is the angular frequency, k the wavenumber, and h water depth. The total power in a wave spectrum P is calculated from Eq. (3), integrating component wave power.

$$P = \int p(f)\delta f \quad \text{where} \quad p(f) = \rho g S(f) C_g(f) \tag{3}$$

Significant steepness S_p^* is calculated from the wavelength associated with the peak of the wavenumber spectrum L_p^* and Eq. (4). This version of peak wavelength has been used, rather than the wavelength associated with the peak frequency, for two reasons. Firstly, the wavelength associated with the peak of the wavenumber spectrum does not always equal that obtained from f_p, as discussed in Plant (2009). The peak energy lies at the wavelength associated with the wavenumber peak, so using this value provides a more representative figure for the true steepness of a sea state. Secondly, this definition allows for a consistent comparison of steepness between cases with and without current. H_{m0} is the significant wave height.

$$S_p^* = \frac{H_{m0}}{L_p^*} \tag{4}$$

2.2. Transformation of wave spectra in the presence of current

In the presence of current, wavelength is no longer related to frequency through the standard dispersion relation, Eq. (1). A modified relation, Eq. (5), is used instead (Jonsson, 1990). In the following equations, α is the angle between wave and current propagation directions, and subscripts 1 and 0 refer to regions with and without current respectively. Importantly, the wavenumber in the presence of a current k_1 will differ from k_0.

$$\omega - k_1 U \cos\alpha = \sqrt{gk_1 \tanh k_1 h} \tag{5}$$

Using a linear assumption, the amplitudes of each frequency component $A(f)$ are given by:

$$A(f) = \sqrt{2S(f)\Delta f} \tag{6}$$

The current modified component wave amplitudes can be calculated assuming conservation of a quantity termed 'wave action' (Jonsson, 1990) defined as:

$$\frac{\partial}{\partial x}\left(\frac{E\left(C_{gr} + U\cos\alpha\right)}{\omega_r}\right) = 0 \tag{7}$$

where E is the wave energy and x the direction of wave propagation. The subscript r denotes variables relative to the current, i.e. assuming a frame of reference moving at the same velocity as the current. The relative angular velocities ω_r and group velocities C_{gr} can be expressed as:

$$\omega_r = \sqrt{gk_1 \tanh k_1 h} \tag{8}$$

$$C_{gr} = \frac{1}{2}\frac{\omega_r}{k_1}\left(1 + \frac{2k_1 h}{\sinh 2k_1 h}\right) \tag{9}$$

Equating wave action between regions with a steady current U and with no current, Eq. (7) can be rearranged to relate the wave heights (Smith, 1997), giving component amplitudes as:

$$A_1 = A_0\sqrt{\left(\frac{C_{g,0}}{C_{gr,1} + U\cos\alpha}\right)\left(\frac{1}{1 + U\cos\alpha/C_{gr,1}}\right)} \tag{10}$$

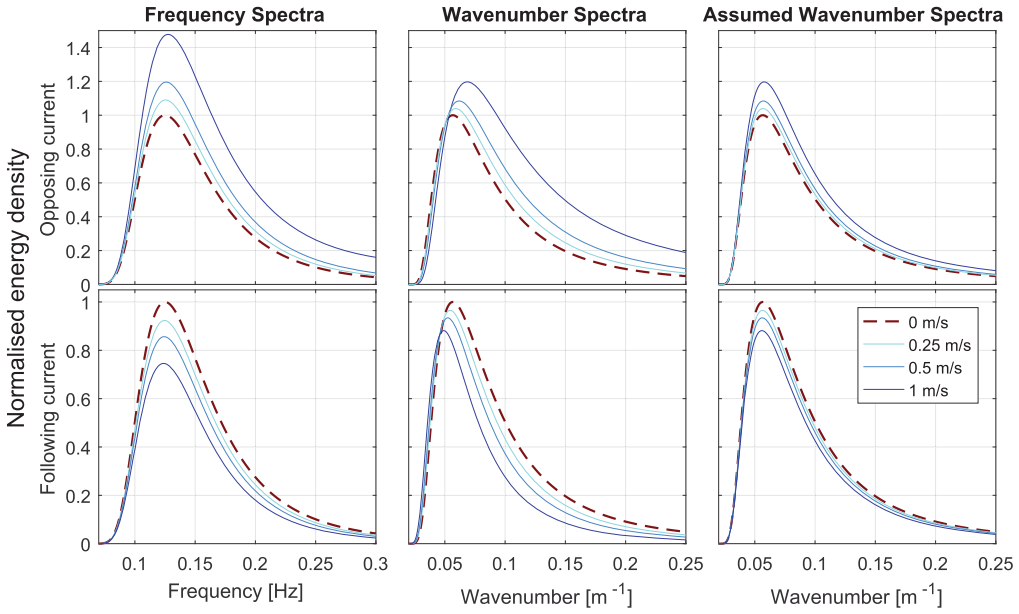

Fig. 1. Change in example PM spectrum ($H_{m0} = 5$ m, $T_p = 8$ s) in the presence of opposing and following currents. Panels show the real frequency and wavenumber spectra, along with the wavenumber spectra assumed without knowledge of the change in wavelength resulting from the interaction with current.

The transformed frequency spectrum can be reconstructed using Eq. (6), taking $A_1(f)$ to get $S_1(f)$. This results in the same transformation as that formulated in Chakrabarti and Johnson (1995). The wavenumber spectra, power available, and wave steepness in the presence of a current can be calculated via Eqs. (2)–(4), using the relevant terms with current as appropriate.

2.3. Power and steepness assumed if wavelength and group velocity change omitted

Calculating power and steepness for waves in the presence of a current using the method in Section 2.1 will give incorrect results if the wavenumber transformation described in Section 2.2 is not also included. This situation could arise when using measurements from a wave buoy where there is no knowledge of the current, and thus the wavelength change. The measured transformed spectrum $S_1(f)$ has associated wavenumbers $k_1(f)$. With the assumption of no current, wavenumbers $k_0(f)$ are calculated using Eq. (1), rather than using Eq. (5) to get $k_1(f)$. This assumption leads to incorrect calculation of group velocities and wavenumber spectra, hence the power and steepness will also be incorrect.

To demonstrate the effect of current on both the transformed and assumed spectra, a Pierson Moskowitz (PM) spectrum with H_{m0} of 5 m and T_p of 8 s is used to show the effect over a wide range of frequencies. This has been analysed with both opposing and following current velocities of 0.25, 0.5 and 1.0 m/s. The significant wave height is found to increase 27.6% with 1 m/s opposing current, and decrease 17.2% for 1 m/s following current.

The transformation of frequency and wavenumber spectra are shown in Fig. 1, along with the wavenumber spectrum that would be assumed without the knowledge of the current present. In opposing flow, waves increase in steepness and thus spectral magnitude increases, with associated reduction in wavelength shown as a shift to higher wavenumbers. The opposite is true of the following current conditions.

For the assumed case with no current there is no shift in wavenumber, and hence the steepness change will be under-estimated. In addition, the group velocity is unaltered which causes an over-estimation of the change in power. This is shown in Fig. 2, where the maximum discrepancy is the 1 m/s opposing case, under-estimating steepness by 18.6% and over-estimating power by 26.9%. This demonstrates the importance of measuring currents at a site in order to obtain a realistic resource assessment and site characterisation.

When tank testing with realistic site conditions the associated current should be included, so that conditions mimic the site, and results inferred from the testing are representative. The correct wavenumber for each frequency component cannot be attained without the current, but are implicitly correct if the current and scaled depth are accurately reproduced. It is important the frequency spectrum is correct in order to obtain the desired wavenumber spectra, power and steepness. At FloWave this requires a correction procedure as a result of the current transformation, so input amplitudes must be altered. This process is detailed in Section 3.4.3, and demonstrated for a range of combined wave-current conditions in Section 4.

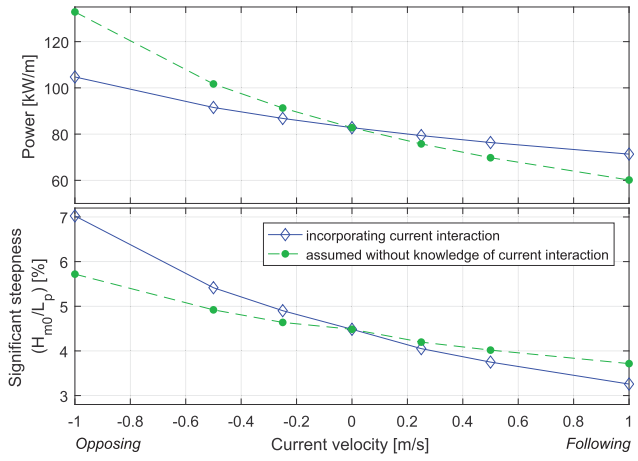

Fig. 2. Change in power and significant steepness in the presence of opposing and following currents for cases incorporating wavelength change and that assumed without knowledge of the interaction with current.

3. Experimental method

3.1. The FloWave Ocean Energy Research Facility

The experimental measurements presented here were made at the FloWave Ocean Energy Research Facility, located at the University of Edinburgh. The facility is comprised of a circular 25 m diameter combined wave and current test basin, encircled by 168 active-absorbing force-feedback wavemakers. The water depth in the test area is 2.0 m. A re-circulating flow system is created using 28 impeller units mounted in the plenum chamber beneath the floor (Robinson et al., 2015). These enable a predominantly straight flow to be achieved in any direction across the central test area (Noble et al., 2015). These unique design features remove any inherent limitation on both wave and current direction, enabling the re-creation of complex directional sea states in combination with current.

The modification of waves by a current is of particular relevance at the FloWave facility, where the waves are generated in a region of still water around the circumference of the tank, and then interact with the current which is injected through the floor (Robinson et al., 2015). In order to produce the desired wave height in the central test area of the tank with the presence of a current, a correction factor must be applied to the wave generated in still water, as discussed in Section 3.4.3.

3.2. Site characterisation and sea state choice

The European Marine Energy Centre (EMEC) is an open water test facility for wave and tidal energy devices, with both full scale and nursery sites, based in Orkney, UK. Over the last 12 years EMEC has gained vast experience in both device installation and resource measurement at these sites.

Directional wave data from the full-scale grid connected wave test site at Billia Croo have been made available, albeit without corresponding data on currents. This EMEC dataset contains multiple years of half hourly directional sea states from January 2010 to January 2014. Rather than choosing an individual spectrum for this case study, outputs from Draycott et al. (2014, 2015) have been used. The aim of this previous work was to produce a small subset of statistically representative spectra from the same dataset, whilst retaining the sea state complexity and directionality. The use of clustering algorithms was of particular interest as they enable the consideration of the whole spectral form in the classification. In Draycott et al. (2015), 40 representative spectra were created from two years of data (January 2010 to January 2012, around 35 000 sea states) using a variety of methods. A method was chosen, which maximised intra-group similarity and inter-group distinctness, utilising a combined binning-clustering approach.

One of the resulting sea states was chosen as an example for reproduction, representing approximately 0.14% of the dataset. This was chosen as it represents an interesting case of a: multi-modal sea state with reasonable directional spreading. The sea state has a significant wave height H_{m0} of 3.53 m, a peak period T_p of 20 s, and mean power P of 87.6 kW/m wave crest. The frequency and directional spectra, along with the weighted Directional Spreading Function (DSF) are shown in Fig. 3. The water depth at the wave buoy location is 52 m, relating to intermediate water depth for the majority of wave components present.

With no tidal records available for the site, the Atlas of UK Marine Renewable Energy (ABP MER, 2012) has been used to obtain the peak tidal velocity at the Billia Croo site, which is expected to be between 0.25 and 0.5 m/s (0.5–1.0 knots).

3.3. Test plan: wave-current scenarios

The wave current correction procedure was applied for wave conditions of increasing complexity. Tests were conducted with regular waves, a long-crested parametric JONSWAP spectrum, and the non-parametric directional sea state derived from the EMEC data. To facilitate comparison, the height and period of the parametric waves were chosen to roughly match the peak of the recorded sea state (see Table 1). Test lengths were specified as a power of 2 s to facilitate frequency domain analysis, with longer tests used to capture the detail of the directional spectra.

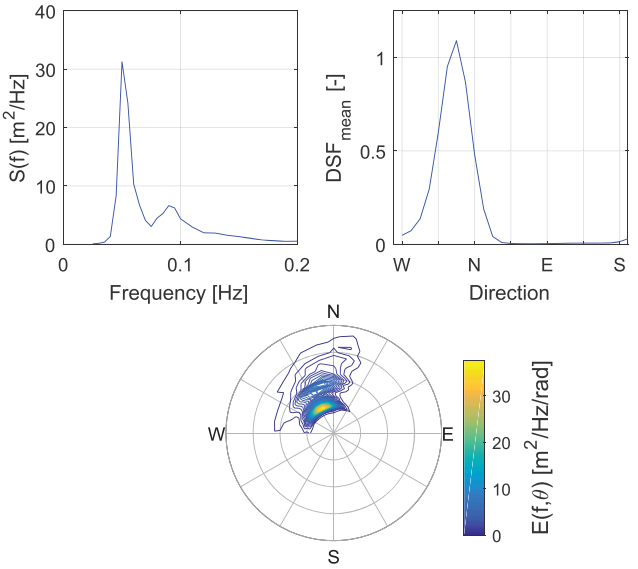

Fig. 3. Representative complex sea state from Billia Croo. Subplots show the spectral density $S(f)$, weighted mean directional spreading function DSF_{mean}, and directional spectrum $E(f,\theta)$.

The three different sea states (regular, parametric, and non-parametric) were tested at various relative angles to the current direction with three current velocities. The chosen sea states must be scaled before re-creation in the tank. Froude scaling was used to ensure the correct ratio between inertial and gravitational forces, which are dominant in free surface waves. When choosing a scale one must consider the ratio of tank to site depth along with the wave generation limits of the tank. The FloWave facility has a test water depth of 2 m and is optimised for wave generation at around 2 s period, which corresponds to scales around 1:20 to 1:40 for wave climates typically of interest to renewable energy. For waves in intermediate depth water, spectra need to be scaled by the depth ratio between tank and site. If this is not done, although the energy distribution across frequency and direction will be correct, the resulting wavenumber spectra will not. This results in a frequency dependent wavelength discrepancy. As there are no wave generation limits at the desired scale, the depth ratio of 1:26 can be used without issue. As well as scaling the wave spectra, the tidal current must also be scaled using the same relationship. At 1:26 (Froude) scale the site estimates correspond to between 0.05 and 0.1 m/s in the tank. An additional velocity of 0.2 m/s was also used to demonstrate the method effectiveness in faster currents, where the wave-current interaction is greater.

Previous published work on wave-current interactions has largely focussed on collinear cases; waves either propagating in the same direction as the current, or directly opposing it. The capability of FloWave permits the testing of non-collinear cases, with the waves at an arbitrary angle to the current direction. Waves were generated at relative angles to the current of 0 (following) $\pi/4$, $\pi/2$ (perpendicular), $3\pi/4$ and π (opposing). For the regular wave tests, an additional four intermediate angles were also measured. A range of angles were tested to demonstrate the applicability of the method, however, when considering a real site these would be chosen based on the wave fetch and tide directions.

3.4. Test method

The sea states defined in Table 1 were initially validated in the tank without the presence of a current, confirming that they have been correctly generated prior to observing and analysing the transformation with current.

Current velocities were set based on a depth averaged calibration from measurements taken in the centre of the tank. It is noted that there is some spatial variation with reduced velocity towards the outside of the basin due to the method of producing current in the circular tank (Noble et al., 2015). The potential implications of this are explored in Section 5.2. Velocity measurement using an Acoustic Doppler Velocimeter (ADV) ensured that the current had reached an equilibrium prior to wave generation.

3.4.1. Directional sea state generation

Deterministic waves are generated at FloWave, providing a very high degree of repeatability (Ingram et al., 2014). To generate a directional spectrum using this deterministic approach the single-summation, rather than double-summation method is used, depicted in Fig. 4. This avoids a phenomenon called phase-locking (Miles and Funke, 1989), whereby waves with the same frequency but different directions interact and cause spatial patterns, resulting in a non-ergodic wave field. To avoid this, the initial frequency increments ΔF can be split up further to create sub-frequency increments $\delta F = \Delta F / N_\theta$ as shown in Pascal (2012). These new frequency increments, still within the original frequency bins, now have a unique wave propagation direction associated with each of them.

The single-summation approach used also aids in both the sea state measurement and the implementation of correction factors. When analysing results in the frequency domain each measured component amplitude can be identified and operated on individually, but only if the Fast Fourier Transform (FFT) bins match the generation frequencies. This is key to the correction method, and means that the appropriate correction factors can be identified and applied, for each of the sub-frequencies. Essentially this allows different correction factors to be applied for the various relative current angles, which is vital for correcting directional seas with current.

The directional sea states presented here have a repeat time T of 2048 s, defining the sub-frequency increments δf to be 1/2048 Hz. In order to achieved the desired frequency increments, the scaled spectrum was interpolated to create 64 frequency bins between 0 and 1 Hz, and 32 directional bins from $0 - \pi$, covering the region with significant energy content in the directional spectrum ($N_f = 64, N_\theta = 32$). Re-defining the

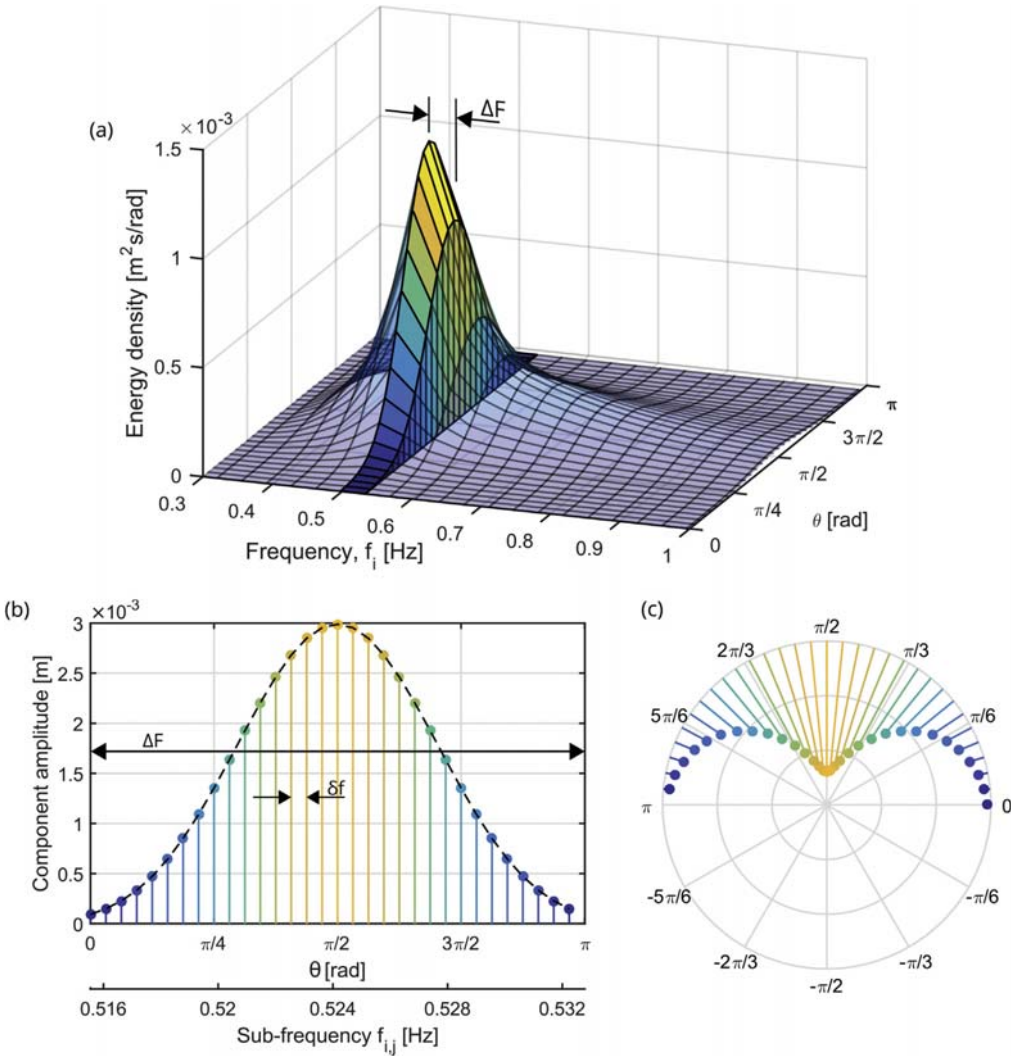

Fig. 4. Schematic of discretisation of a directional spectrum using the single summation method and subsequent re-creation in the tank. Panels show (a) the directional spectrum highlighting the frequency bins ΔF, (b) how the sub-frequency bins δf are split across direction for each ΔF frequency bin, and (c) how this directional spread is created in the tank.

Table 1
Matrix of test parameters (tank scale).

Wave parameters	Wave angles relative to current	Currents [m/s]	Test length [s]
Long crested regular waves, $T = 3.3$ s, $H = 0.130$ m	9 angles: $0 - \pi$ at $\pi/8$ increments	0.05, 0.1, 0.2	128
Long crested JONSWAP spectrum, $T_p = 3.3$ s, $H_{m0} = 0.130$ m, $\gamma = 3.3$	5 angles: $0 - \pi$ at $\pi/4$ increments	0.05, 0.1, 0.2	512
Measured EMEC directional sea, $T_p = 3.76$ s, $H_{m0} = 0.128$ m	5 angles: $0 - \pi$ at $\pi/4$ increments	0.05, 0.1, 0.2	2048

directional spectrum for use in the single-summation method gives the required frequency increments of:

$$\delta f = \frac{\Delta F}{N_\theta} = \frac{1}{(N_f \times N_\theta)} = \frac{1}{T} = \frac{1}{2048}\,[Hz] \tag{11}$$

3.4.2. Directional wave measurement

Surface elevations are measured at FloWave using multiplexed two-wire resistance type wave gauges, providing point measurements at a sample frequency of 128 Hz. In order to calculate component wave directions and infer directional spectra, these wave gauges are deployed in a carefully designed array (Draycott et al., 2016), shown in Fig. 5a. The array has been chosen to encompass desirable spacings for the analysis, and is based on optimising the co-array uniformity over the angle and magnitude range of interest. This co-array is shown in Fig. 5b, providing favourable separations for the calculation of directional spectra.

A Phase-Time-Path-Difference (PTPD) approach (Fernandes et al., 2000; Esteva, 1976) has been used to calculate component angles and directional spectra. This method uses the measured phase differences, and known separations between gauges, to infer the wave direction at each frequency, and provides a single wave angle per frequency through triangulation. Draycott et al. (2016) has shown this method to be a highly effective approach for measuring directional spectra when combined with single-summation wave generation. For measuring directional wave characteristics in currents, this approach has also found to be much more effective as discussed in Section 5.3, and as such has been applied here. In addition to reducing directional spectrum reconstruction error, the PTPD outputs provide individual component wave angles, opening up the possibility of effectively assessing wave refraction in current.

3.4.3. Correction procedure

To produce waves of a specified height in combination with a current, an amplitude based correction factor needs to be applied to the wavemaker input. For a directional spectrum, it is necessary to determine this factor for every frequency and direction component. As a result of using a single summation method, see Section 3.4.1, the amplitude of each wave component with unique frequency and direction $A_i(f_i, \theta_i)$ can be corrected. These correction factor are assumed linear, taken as the inverse of the change in component amplitude as a result of the interaction with the current field discussed in Section 2.2, and are calculated empirically. The input wave spectrum is generated in the tank with current, measured, and the resulting component amplitudes compared with those desired, Eq. (12). The correction based on observed discrepancy between the desired and measured directional spectra was multiplicatively applied to the input spectrum, and the process repeated as necessary in an iterative manner until the measured spectrum was acceptably correct, defined in this case as a mean spectral error $\varepsilon < 5\%$, Eq. (13).

$$CF_{empir}(f_i, \theta_i) = \frac{A_i^{desired}}{A_i^{measured}} \tag{12}$$

$$\varepsilon = \frac{\sum_{i=1}^{N_f} |S^{measured}(f_i) - S^{desired}(f_i)|}{\sum_{i=1}^{N_f} S^{desired}(f_i)} \tag{13}$$

4. Results

4.1. Regular waves

The observed change in wave height as a function of relative angle and current velocity can be seen in Fig. 6a. As expected the observed transformation increases with larger current velocities, and for a given current, a larger relative angle corresponds to an increase in wave height. This change has been compared to wave-current interaction theories, both linear (Smith, 1997) and non-linear second order (Baddour and Song, 1990; Zaman and Baddour, 2011). The observed transformation is

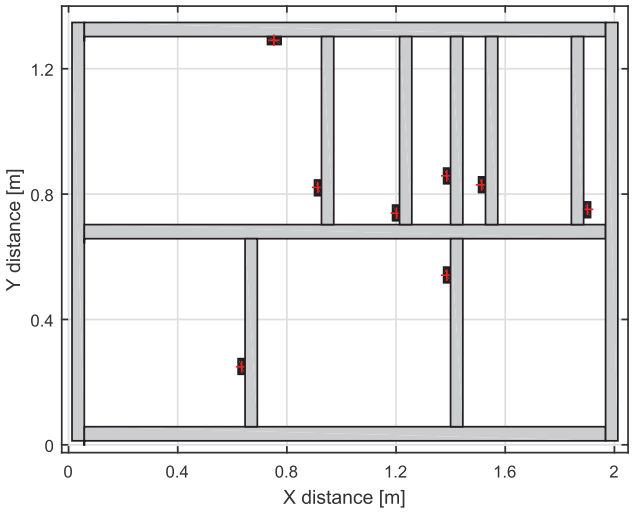

(a) Wave gauge array layout with bar positions for re-configurable FloWave rig

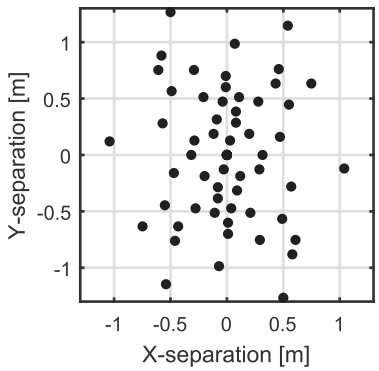

(b) Co-array separations of wave gauge array layout presented in Fig. 5a

Fig. 5. (a) Wave gauge array layout with bar positions for re-configurable FloWave rig. (b) Co-array separations of wave gauge array layout presented in Fig. 5a.

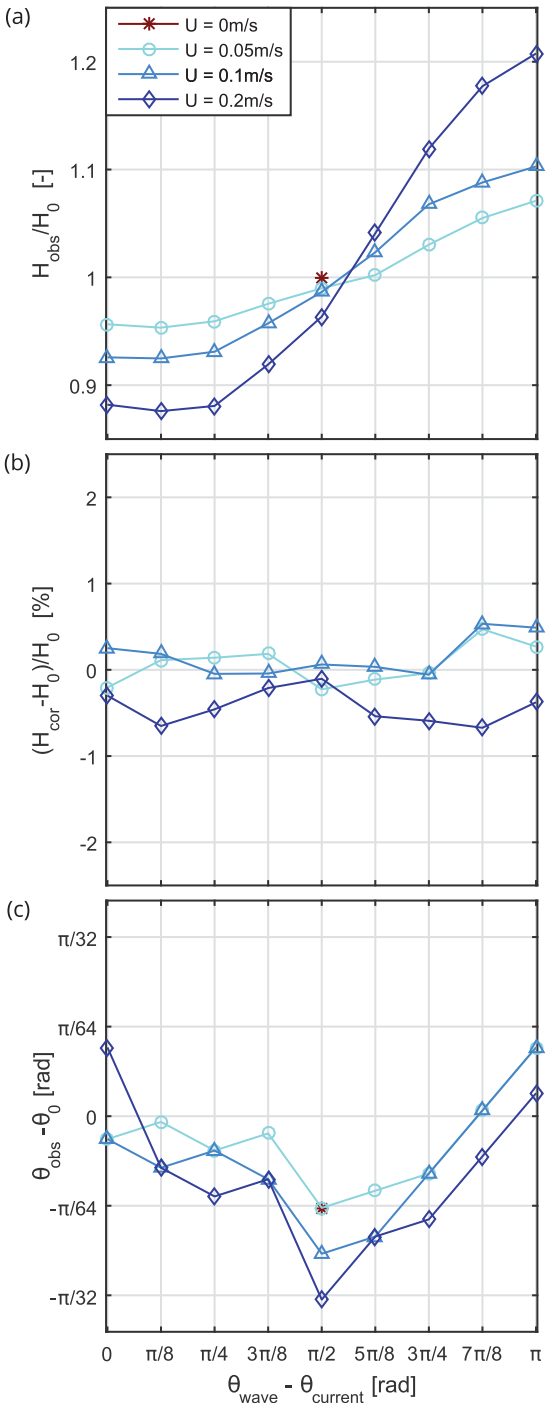

Fig. 6. Results for regular waves at nine measured angles to the current direction and three velocities. H_0 refers to wave height values obtained without the presence of current, and θ_0 refers to the input wave angle, known to be correct. Panels show (a) Observed change in wave height, (b) Observed error in wave height once corrected, (c) Observed change in wave direction.

larger than predicted by either, as can be seen in Fig. 7. This highlights that applying theoretical correction factors in this context is not particularly effective. Another interesting observation is the reduction in wave height with increasing current velocity when waves and current are perpendicular, which is discussed further in Section 5.1. From preliminary results of other regular wave cases (Noble, 2017), this under-prediction of wave transformation by theory appears to be consistent for all wave frequency–steepness combinations tested. The effect of wave steepness also appears to be fairly insignificant in terms of relative wave height change, whilst frequency dominates both measured transformations and deviations from theory.

The error in wave height following empirical correction is shown in Fig. 6b, with Fig. 6c showing the *apparent* angular change. For all velocities and relative angles, the resulting measured wave heights were within 0.7% of the desired. The measured angular change is also relatively small, yet displays no obvious pattern with respect to relative angle and current velocity. The presence of a current reduces measurement accuracy (through increased reflections, gauge vibrations, bending etc.) making it difficult to isolate small refraction effects from this increased error. It is, however, evident that any refraction effects are very small at these velocities and so have not been corrected for any of the sea states. This, along with other practical considerations, is discussed further in Section 5. Interestingly, there is an apparent angular offset when there is no current present. These calculated angles are a function of the measured phase differences and assumed gauge positions. In addition to small physical position errors of individual gauges or the array, reflections can significantly alter the measured phase differences and resulting apparent angles. These reflections, which exist with and without current present, are likely the dominant cause of this apparent angular error.

4.2. Uni-directional parametric spectrum

The observed transformation of the parametric spectra is shown in Fig. 8, along with the deviation in energy density compared to the desired before and after correction. Clearly the same trend is seen as with the regular waves, with larger transformations in the presence of larger currents, and larger wave heights with increasing angle.

Analysing this change in energy density, it can be inferred that although the majority of the change is a result of wave-current interaction, there is also significant variation due to reflections, particularly affecting the higher frequencies. The magnitude of these variations are a function of the reduced absorption effectiveness in the presence of larger currents. The reason for this 'spiky' variation at higher frequencies is due to incident and reflected wave components at a given frequency being in or out of phase at the gauge array location.

Regardless of the source of the frequency dependent variation, the corrected deviation shows that the spectrum has been effectively corrected using a linear approach in a single iteration. All wave-current-angle scenarios were corrected to give a final weighted error of less than 3%.

4.3. Non-parametric directional spectrum

Similar to the parametric outputs found in Fig. 8, the frequency spectrum transformation and correction for the non-parametric EMEC derived sea state are shown in Fig. 9. Again, only a single iteration was required to achieve these results. Despite this sea state having significant directional spreading associated, similar magnitude of transformation is observed to the parametric case, along with analogous influence of reflections. The corrected frequency spectra are also all within 3% of the desired, demonstrating that the linear correction procedure applied to the sub-frequency angular components is just as effective.

Fig. 10 shows the final corrected sea states output. Frequency spectra along with weighted DSF are shown, for the three velocities and five relative angles. The final directional spectrum output using the PTPD approach is shown for the base 0.1 m/s case, noting that the 0.05 m/s and 0.2 m/s results appear very similar.

The final sea states re-iterate that the frequency spectra have been effectively corrected for all velocity-angle combinations, and in general so have the directional spectra and mean DSF. Directional errors are larger with increasing current velocity which is clear when assessing the weighted DSF errors. With zero current the weighted DSF error was

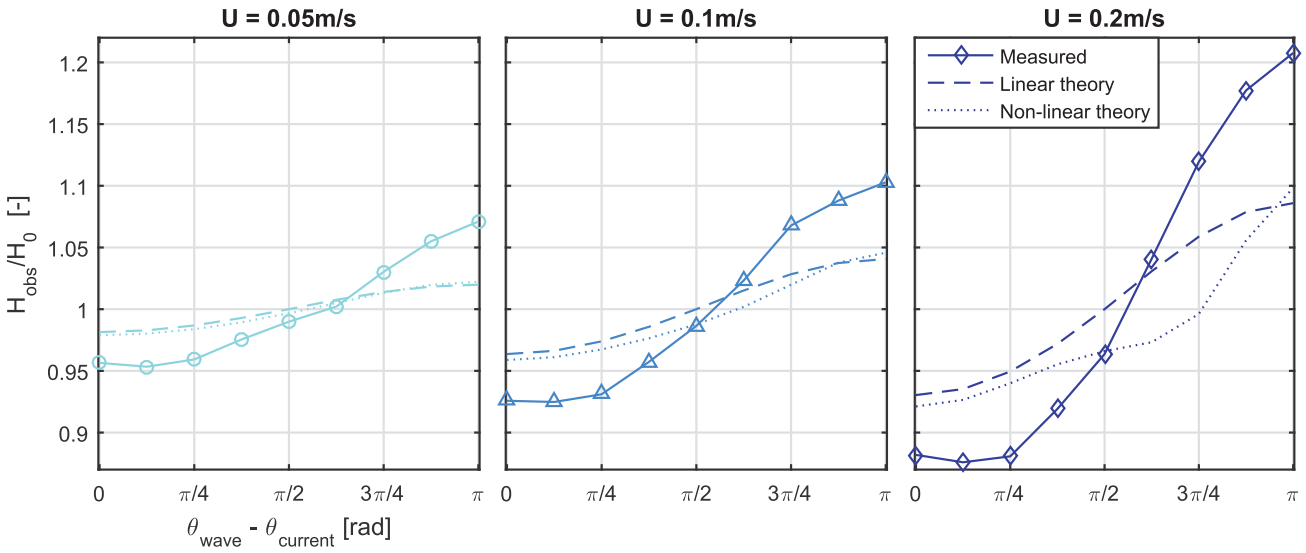

Fig. 7. Observed change in wave height for regular waves at various angles to the current direction, with comparison to theory.

6.95%, whereas in 0.05, 0.1 and 0.2 m/s current the mean errors over all angles are 13.3%, 14.3% and 18.5% respectively. Although this is a significant increase it is felt that the majority of this is not refraction induced and instead is a product of increased measurement error combined with the way the error is calculated. This is discussed further in Section 5.3.

5. Discussion

5.1. Observed change in wave height and spectra

Although the main aim of this work is to demonstrate the effective re-creation of directional spectra with current, one of the interesting

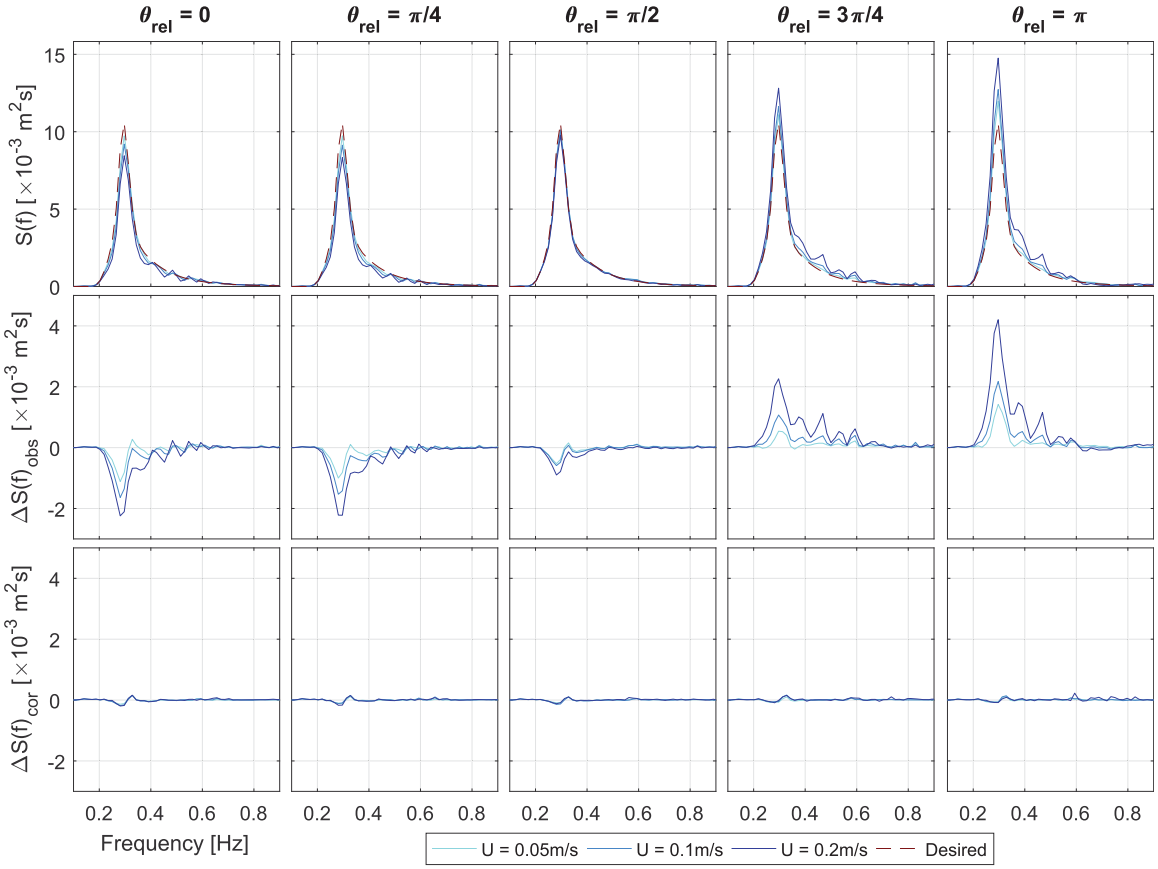

Fig. 8. Results of parametric spectrum correction procedure, at 5 relative angles to current. Top row shows observed spectral density, middle row observed deviation from desired prior to correction, and bottom row deviation following correction.

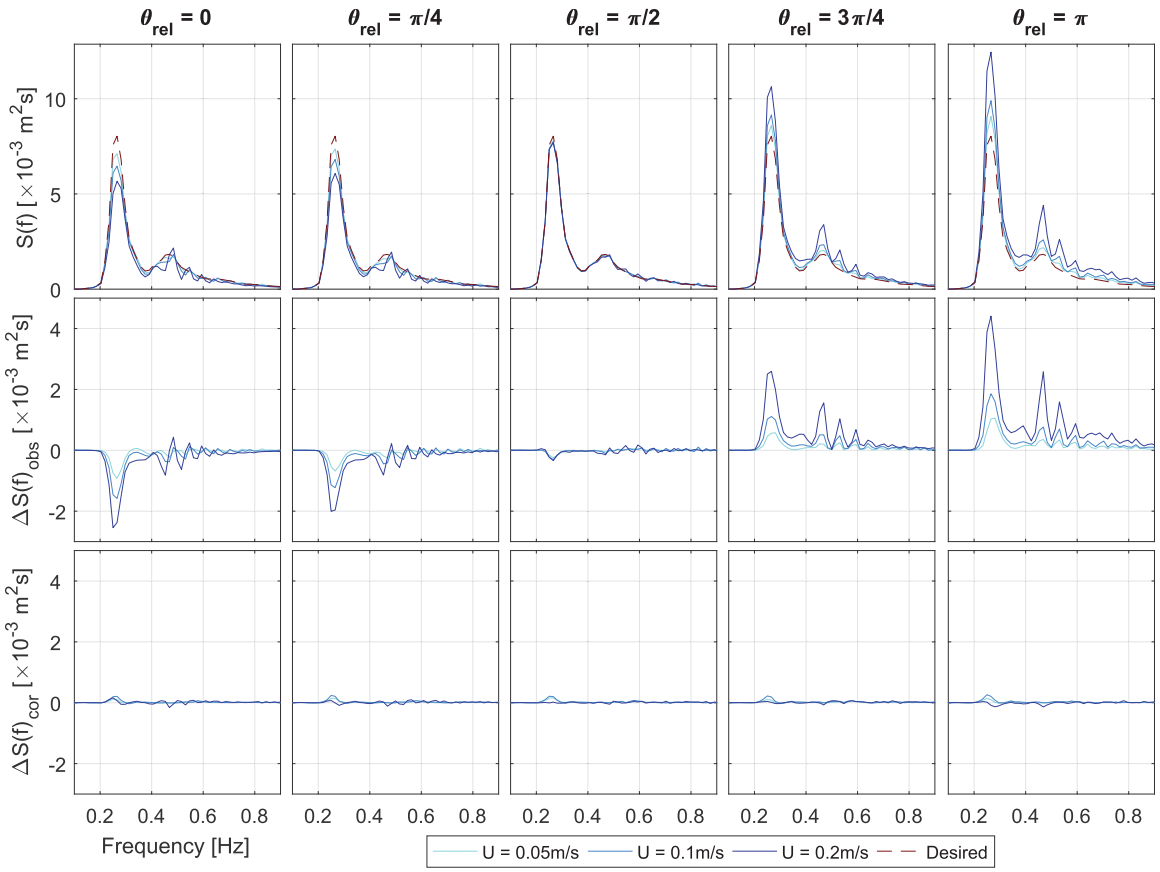

Fig. 9. Results of non-parametric EMEC spectrum correction procedure, at 5 relative angles to current. Top row shows observed spectral density, middle row observed deviation from desired prior to correction, and bottom row deviation following correction.

outcomes is the observation of non-collinear wave current interactions. All results show larger wave transformation in the presence of higher current velocities and an increase in wave amplitude with increasing relative angle, as would be expected. The magnitude of the regular wave transformation, however, was much larger than expected, as shown in Fig. 7.

The change in wave height (regular or significant) with respect to the current condition was observed to be comparable for each of the sea states. This is shown in Fig. 11, and is largely a result of all sea states having similar frequency and steepness values. It may be expected that the directional sea state would have a smaller range in measured wave heights due to different wave components propagating at different relative angles. However, this proved not to be the case, which is clear when assessing the observed wave height for the EMEC sea state in 0.2 m/s current at a relative angle of π. The cause of this is unknown, but may be a consequence of reflections causing a net constructive effect over the wave gauge array area. These reflections are dependent on frequency, flow velocity, and relative angle.

As expected from the similar wave height transformations, the spectra also display a larger transformation than predicted by linear theory (Section 2). These discrepancies may be a result of tank specific wave generation issues in the presence of a current (discussed further in Section 5.2), so caution must be used before assuming that these results are representative of pure wave-current interaction. Interestingly, however, the same effect has been observed by Nwogu (1993); Chakrabarti and Johnson (1995); Guedes Soares et al. (2000). Although this does not resolve the cause of the difference it does suggest that, at least in part, these larger transformations may be a pure wave-current interaction effect.

Interestingly, wave height was found to decrease in all cases where the mean wave angle was perpendicular to the current, with a greater reduction at higher velocities. With the current running, water passes through the turning vanes, and wave energy may be lost via the current return path under the floor. This is analogous to having a finite crest length in open water, with the perpendicular current causing wave crests to 'stretch out' along their length, thus reducing wave height. The theories considered assume plane waves with infinitely long crests, so predict no change in wave height with a perpendicular current.

5.2. Assessment of correction procedure

The amplitude correction procedure applied has proven to be effective for all sea states, providing frequency spectrum errors of less than 3% in all cases. Consequently, the resulting wave heights were found to be very close to the desired. For the regular, uni-directional parametric, and non-parametric EMEC sea states, the mean wave height discrepancy over all velocity-angle combinations were found to be 0.27%, 0.42% and 0.91% respectively (maximum errors of 0.67%, 1.11% and 1.38%).

The correction factor, although assumed linear, includes a number of different factors of which the proportional influence remains unknown. Namely:

1. Superposition of wave and current fields,
2. Energy transfer between wave and current fields,
3. Increased reflections with larger currents, which is relative to the array location,
4. Spatial variation of current in the tank, and
5. Paddle response to presence of current.

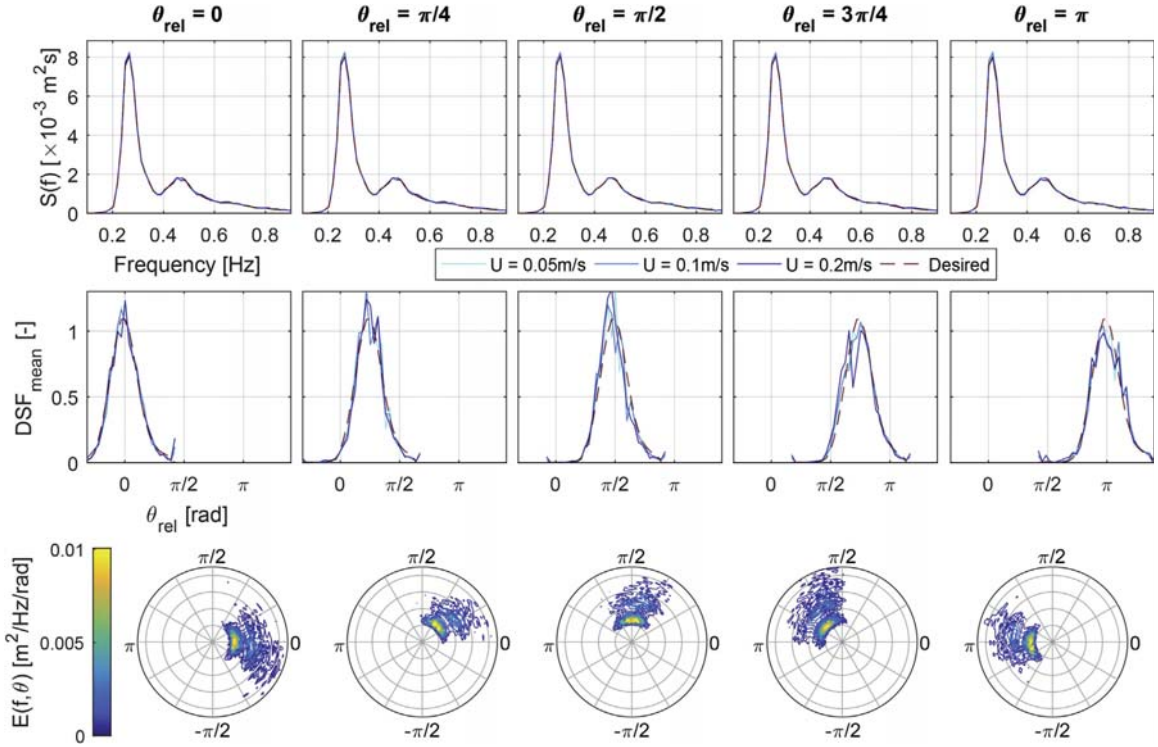

Fig. 10. Final non-parametric EMEC spectra following correction, at 5 relative angles to current. Top row shows spectral density $S(f)$, middle row weighted mean directional spreading function DSF_{mean}, and bottom row directional spectra $E(f,\theta)$ for 0.1 m/s current.

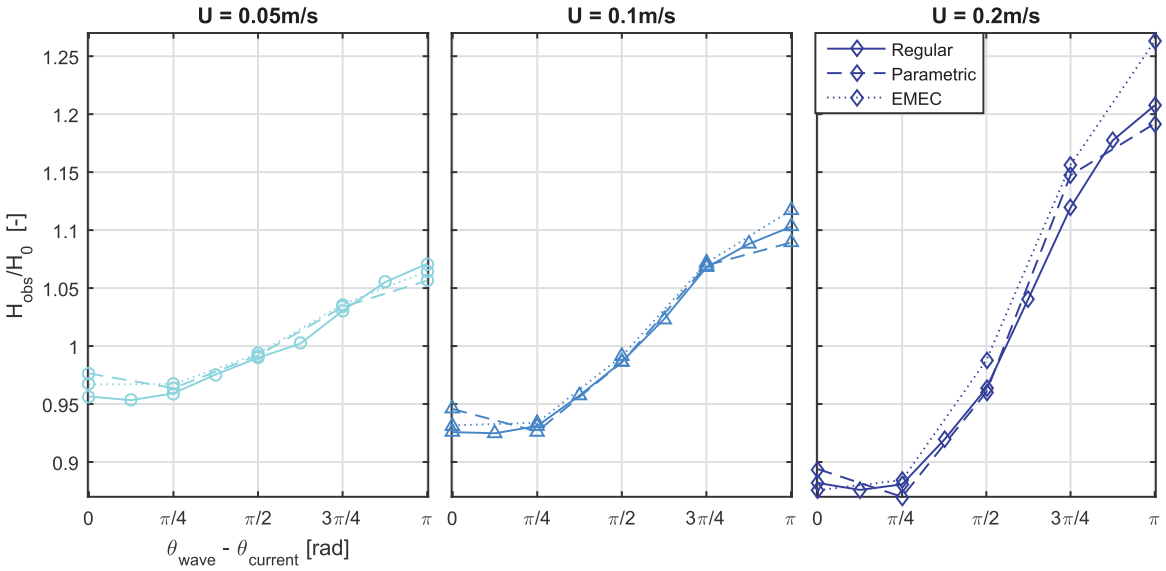

Fig. 11. Observed change in wave height by relative wave angle, for regular, parametric, and site-specific EMEC sea, for three current velocities tested.

The favourable results show that, although current effects on the wave field at FloWave are inherently complex and non-linear, the variation in relative wave deformation as a result of a modest change in input wave amplitude can effectively be approximated as a linear process. This is a useful output from this work, although limits to the validity of this will need to be identified through additional testing with steeper waves and higher current velocities. The wave-current interaction theories do not include all of these factors, which may account for the discrepancies in Fig. 7. The linear theory only accounts for the first, while the non-linear theory also partially accounts for the second. Factors 3–5 are facility specific, and thus cannot be dealt with by general theories.

5.3. Measurement of wave directionality

5.3.1. Measurement of component wave angles in current

Component angles are measured using the PTPD approach as implemented by Draycott et al. (2016). Each gauge triad provides an estimate of wave angle for each of the frequency components based on the

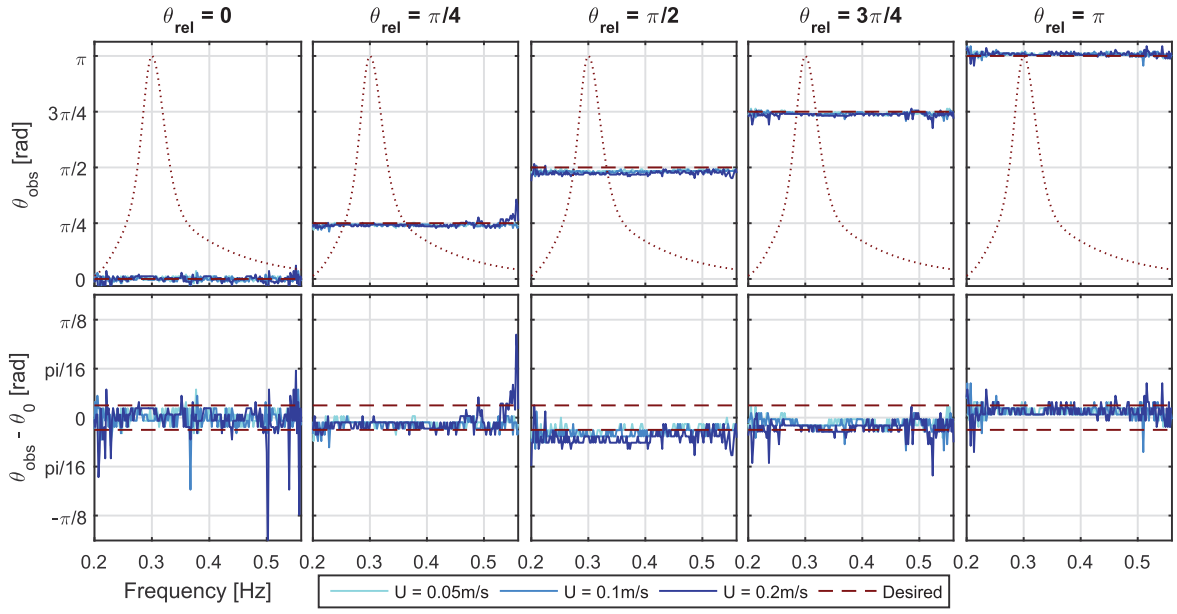

Fig. 12. Observed wave component angles at different velocities (top) and discrepancy from desired (bottom). Amplitude spectrum shown dotted in top panels to highlight where energy content lies. Spacing between dashed lines in lower panels represents directional bin size.

measured phase differences from an FFT. A circular kernel density estimate (250 bins) is then applied to the 56 individual triad estimates in an aim to identify the true incident angle for each component. This approach has been shown to provide very good estimates of incident wave angle without the presence of current, typically identifying the correct angle within $\pi/90$. Noting the directional bin widths are $\pi/32$ this usually provides good resulting spectral estimates.

In the presence of currents, estimates of wave angle are not so accurate. This is partly due to additional measurement uncertainty from a number of sources: run-up on gauges, turbulence, and Vortex Induced Vibration (VIV). The presence of the current also causes inconsistent bending to occur in the gauges meaning the assumed gauge positions are somewhat inaccurate, and importantly wire separations can be variable. Additionally, reflection levels are higher in the presence of currents, which also alter the perceived phases, particularly when the reflections are not opposing the incident components. The cumulative effect of this is increased uncertainty in the angular estimates.

Fig. 12 shows the PTPD angle calculation outputs for the unidirectional parametric spectrum, noting that it is much easier to observe and analyse than the non-parametric directional sea state. It is clear that the overall sea state direction is generally identified well. With directional bin size of $\pi/32$, a measured deviation of just $\pi/64$ from the desired angle would result in the energy being attributed to a different directional bin for that frequency component. This happens relatively frequently in the presence of current as can be seen in Fig. 12, causing apparently large errors to arise through a measurement discrepancy of less than three-degrees. This results in the DSF and $E(f,\theta)$ in Fig. 9 showing significant deviation, even though the underlying errors themselves are quite minimal. To get an error metric not related to bin size, a net weighted angular error has been defined in Eq. (14), with the observed outputs for both the parametric and non-parametric EMEC sea shown in Fig. 13.

$$\theta^*_{error} = \frac{\sum(\theta_{obs,i} - \theta_{0,i})A_i}{\sum A_i} \tag{14}$$

As refraction levels are expected to be in the order of a few degrees, isolating what is refraction and what is simply increased measurement error has proved difficult. Any significant refraction should, however, manifest itself as a negative weighted angular change in Fig. 13 for all non-collinear cases. As there is no clear indication that this is the case, it is assumed that the refraction levels in these tests are low enough that

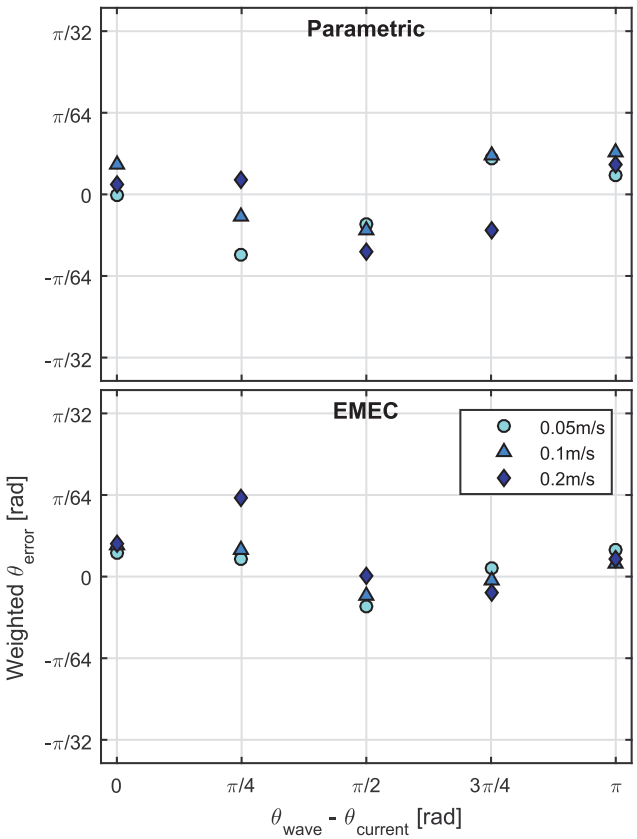

Fig. 13. Net weighted error for parametric and non-parametric sea states for the combinations of current and relative wave angle tested, showing no significant deviation.

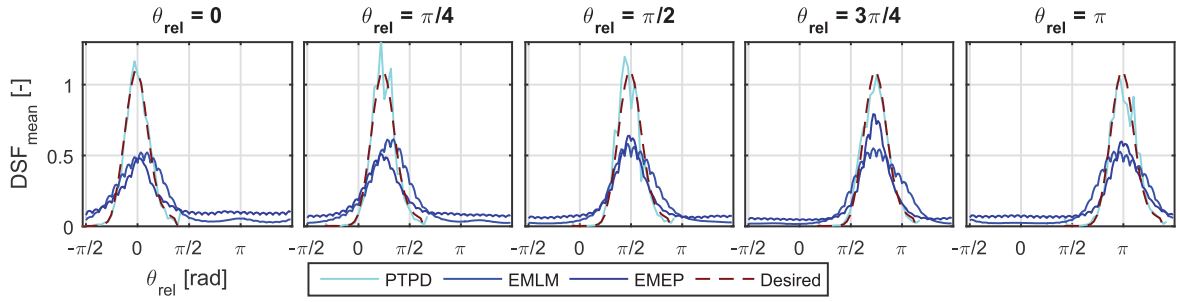

Fig. 14. Comparative performance of three directional spectrum reconstruction approaches: Phase-Time Path Difference (PTPD), Extended Maximum Likelihood Method (EMLM) and Extended Maximum Entropy Method (EMEP).

they do not need to be corrected. If this work was to be extended to tests with larger currents it may be that the refraction cannot be ignored, requiring improvements to the measurement system. This may take the form of stiffer wave gauges (or an alternative measurement system) to reduce vibration and deflection in the presence of current. This would allow the implementation of an iterative procedure to correct for the observed refraction.

5.3.2. *Relative performance of PTPD approach*

In the presence of a current, the increased measurement errors mean that the PTPD outputs have some uncertainty associated. Although it has been inferred that the actual discrepancy is likely to be small, this still means that the true directional spectrum generated remains unknown. This uncertainty, however, is still significantly smaller than if typical directional spectrum reconstruction methods were used. This is demonstrated in Fig. 14, where the DSF outputs for the base 0.1 m/s cases are shown for the PTPD, Extended Maximum Likelihood Method (EMLM) and Extended Maximum Entropy Method (EMEP) approaches. In Fig. 14 it appears that other than the EMEP reconstruction at $3\pi/4$, the EMEP and EMLM approaches fail to effectively characterise the DSFs; having a non-zero magnitude for all angles. This is clearly not the case and is likely due to the limitations of these 'curve-fitting' methods trying to fit to small reflections, along with additional reconstruction errors. As there is only significant energy within a range of $\pi/4$, and the array is in the tank centre (meaning component reflections are opposing incident), there should only be a very small DSF component (~1–4% size of incident peak corresponding to 10–20% reflection) opposing the incident, rather than the observed constant energy content.

The poor performance of the EMEP and EMLM approaches in these instances mean that the resulting reconstructions would clearly not be suitable to use as a basis for subsequent directional correction. Despite the PTPD approach reducing errors significantly, identification of refraction effects with these low velocities and wave gauges available is still error prone. It is thought, however, that using this approach with stiffer gauges will prove effective at measuring DSFs accurately in current, with the additional advantage that component angles have been calculated, and can now inform a correction procedure.

5.4. *Application and implications for physical testing*

The results of this work demonstrate that site-specific directional spectra can be re-created with current at FloWave. It also highlights the importance of including any currents present when aiming to re-create site conditions, and the value in obtaining measurements of current velocity when carrying out resource assessment, or carrying out full scale testing.

When re-creating site conditions for tank testing, including measured or representative currents can help explore the envelope of expected responses. This will in turn provide more insightful and realistic device and mooring loads, including both those incurred through the presence of the current directly as well as those resulting from the influence of the current on the wave field. If combined conditions are specified, then the input spectrum will need to be corrected so that the desired spectrum is obtained at the device location, thus appropriately representing the power available. With the current included, the correct wavenumber spectrum will also be obtained, ensuring that wave amplitudes, along with wavelength, steepness and celerity match those at the site.

Due to the significant effect current can have on the perceived power and assumed wavelengths, it is clearly advantageous to measure current velocities when carrying out resource assessment. This is also the case when carrying out full scale testing as it enables true context to be placed on the results. For example, if characterising a WEC performance by H_{m0} and T_e, a device sensitive to wavelength and steepness will respond very differently in the presence of current despite having comparable $H_{m0} - T_e$ values (in addition to the available power being misinterpreted).

The level of sea state complexity generally increases as a concept advances through Technology Readiness Levels (TRLs) (Ingram et al., 2011). Early stage testing is typically limited to regular waves of varying frequency and height before advancing to standard parametric spectra (both long and short crested). The ability to produce combined wave-current sea states, especially with non-parametric spectra, will usually apply more to devices at advanced TRLs where a particular deployment site has been identified. As such, this ability to produce site-specific combined sea states has the potential to extend and complement established development paths.

6. Conclusions

A site-specific non-parametric directional spectrum has been obtained from EMEC, and re-created at 1:26 scale at the FloWave Ocean Energy Research Facility with current velocities of 0.05, 0.1 and 0.2 m/s (representing 0.5, 1 and 2 knots full scale). The studies conducted on complex directional wave fields in combination with currents within the FloWave Ocean Energy Research Facility resulted in the following main findings:

- The transformation of waves by current has been shown to have a significant impact on both the true wave power and steepness, and on that which may be assumed without knowledge of the current field. If the current present at the site is not included in tank testing, incorrect power and wavenumber spectra will be generated, and test results will not be representative of real site conditions.
- An empirical correction procedure has been used to correct this sea state, along with equivalent regular waves and uni-directional parametric spectrum, in the presence of currents from multiple relative angles. The linear correction procedure applied proved effective after a single iteration, providing corrected frequency spectra all within 3% of the desired, and wave heights normally within 1%. Refraction effects were found to be minimal at the velocities tested. Although angle estimates prove to be error prone in current, the PTPD approach

provides much improved outputs over either the EMLM or EMEP methods.
- In this process, non-collinear wave-current interactions were observed for each of the wave cases. The measured wave transformation was larger than expected from theory, which may partially be facility specific effects resulting from the method of generating currents and absorbing waves at FloWave.

Acknowledgements

The authors would like to thank the Energy Technologies Institute and RCUK Energy programme for funding this research as part of the IDCORE programme (EP/J500847/1), the UK EPSRC for funding the FloWave facility (EP/I02932X/1), and the European Marine Energy Centre for providing buoy data for the sea state replication work.

References

ABP MER, 2012. Pentland Firth and Orkney Waters Strategic Area : Marine Energy Resources. Tech. Rep. November, The Crown Estate.
Baddour, R.E., Song, S., 1990. On the interaction between waves and currents. Ocean Eng. 17, 1–21.
Chakrabarti, S., Johnson, J., dec 1995. Random wave-current interaction – theory and experiment. In: Proceedings of the 19th International Conference on Ocean, Offshore and Arctic Engineering (OMAE2000).
Draycott, S., Davey, T., Ingram, D.M., Day, A., Johanning, L., 2016. The SPAIR method: isolating incident and reflected directional wave spectra in multidirectional wave basins. Coast. Eng. 114, 265–283.
Draycott, S., Davey, T., Ingram, D.M., Lawrence, J., Day, A., Johanning, L., 2015. Applying site-specific resource assessment : emulation of representative EMEC seas in the FloWave facility. In: Proceedings of the 25th International Offshore and Polar Engineering Conference.
Draycott, S., Davey, T., Ingram, D.M., Lawrence, J., Johanning, L., Day, A., Steynor, J., Noble, D.R., 2014. Applying site specific resource assessment: methodologies for replicating real seas in the FloWave facility. In: Proceedings of the 5th International Conference on Ocean Energy, Halifax, Canada.
Earle, M., 1996. Nondirectional and Directional Wave Data Analysis Procedures. NDBC Tech. Doc. 96 002 (January).
Esteva, D., 1976. Wave direction computations with three gage arrays. In: Coastal Engineering Proceedings.
Fernandes, A.A., Sarma, Y.V.B., Menon, H.B., 2000. Directional spectrum of ocean waves from array measurements using phase/time/path difference methods. Ocean Eng. 27 (4), 345–363.
Guedes Soares, C., Rodriguez, G., Cavaco, P., Ferrer, L., 2000. Experimental study on the interaction of wave spectra and currents. In: Proceedings of the 19th International Conference on Ocean, Offshore and Arctic Engineering (OMAE2000).
Hashemi, M.R., Neill, S.P., Davies, A.G., Lewis, M.J., 2014. The implications of wave-tide interactions in marine renewables within the UK shelf seas. In: Proceedings of the 2nd International Conference on Environmental Interactions of Marine Renewable Energy Technologies (EIMR2014). No. May 2014. Stornoway, Scotland.
Hedges, T.S., Anastasiou, K., Gabriel, D., 1985. Interaction of random waves and currents. J. Waterw. Port, Coast. Ocean Eng. 111 (2), 275–288.
Holmes, B., Nielsen, K., 2010. Guidelines for the Development & Testing of Wave Energy Systems. Tech. Rep. June, Hydraulics Maritime Research Centre, UCC, Cork, Ireland.
Ingram, D., Wallace, R., Robinson, A., Bryden, I., 2014. The Design and Commissioning of the First, Circular, Combined Current and Wave Test Basin.
Ingram, D.M., Smith, G.H., Bittencourt Ferreira, C., Smith, H.C.M., 2011. EquiMar protocol II.A tank testing. In: Protocols for the Equitable Assessment of Marine Energy Convertors. Edinburgh, Ch. 3.3.
Jonsson, I., 1990. Wave-current interactions. In: LeMehaute, B., Hanes, D.M. (Eds.), The Sea, Ocean Engineering Science, vol. 9. Wiley-Interscience publications, New York, pp. 65–120. Ch. 7.
Kemp, P.H., Simons, R.R., apr 1982. The interaction between waves and a turbulent current: waves propagating with the current. J. Fluid Mech. 116 (-1), 227–250.
Kemp, P.H., Simons, R.R., apr 1983. The interaction of waves and a turbulent current: waves propagating against the current. J. Fluid Mech. 130, 73–79.
Mankins, J.C., 1995. Technology Readiness Levels. White Paper, April, 4–8.
Miles, M.D., Funke, E.R., 1989. A Comparison of Methods for Synthesis of Directional Seas.
Noble, D.R., 2017. Combined Wave-current Scale Model Testing at FloWave. Ph.D. thesis. University of Edinburgh.
Noble, D.R., Davey, T., Smith, H.C.M., Kaklis, P., Robinson, A., Bruce, T., 2015. Characterisation of spatial variation in currents generated in the FloWave Ocean energy research facility. In: Proceedings of the 11th European Wave and Tidal Energy Conference, Nantes, France. Nantes, France.
Nwogu, O., jun 1993. Effect of steady currents on directional wave spectra. In: Proceedings of the 12th International Conference on Offshore Mechanics & Arctic Engineering (OMAE1993). ASME, Glasgow, UK.
Pascal, R., 2012. Quantification of the Influence of Directional Sea State Parameters over the Performances of Wave Energy Converters.
Peregrine, D.H., 1976. Interaction of waves and currents. In: Advances in Applied Mechanics, Vol. 16. Elsevier, pp. 9–117.
Plant, W., 2009. The ocean wave height variance spectrum : wavenumber peak versus frequency peak. J. Phys. Oceanogr. 1, 2382–2383.
Robinson, A., Ingram, D., Bryden, I.G., Bruce, T., jan 2015. The generation of 3D flows in a combined current and wave tank. Ocean Eng. 93.
Saruwatari, A., Ingram, D.M., Cradden, L., nov 2013. Wave-current interaction effects on marine energy converters. Ocean Eng. 73, 106–118.
Smith, J.M., 1997. Coastal Engineering Technical Note One-dimensional Wave-current Interaction (CETN IV-9). Tech. rep., US Army Engineer Waterways Experiment Station, Coastal Engineering Research Center, Vicksburg, MS.
Thomas, G.P., 1981. Wave-current interactions: an experimental and numerical study. Part 1. Linear waves. J. Fluid Mech. 110 (1981), 457.
Zaman, M.H., Baddour, R.E., mar 2011. Interaction of waves with non-colinear currents. Ocean Eng. 38 (4), 541–549.